ЖУРНАЛ
ЭКСПЕРИМЕНТАЛЬНОЙ И ТЕОРЕТИЧЕСКОЙ
ФИЗИКИ
Zhurnal Eksperimental'noi i Teoreticheskoi Fiziki

SOVIET PHYSICS
JETP

VOL. 13, NO. 2 AUGUST, 1961

A Translation

of the

Journal of Experimental and Theoretical Physics

of the

Academy of Sciences of the USSR

(Russian Original Vol. 40, No. 2, February, 1961)

Published by the

AMERICAN INSTITUTE OF PHYSICS
INCORPORATED

SOVIET PHYSICS
JETP

A translation of the Journal of Experimental and Theoretical Physics of the USSR.

A publication of the

AMERICAN INSTITUTE OF PHYSICS

Governing Board

Ralph A. Sawyer, *Chairman*
James G. Baker
R. H. Bolt
Wallace R. Brode
Harvey Brooks
Dirk Brouwer
J. H. Elliott
Herbert A. Erf
N. S. Gingrich
S. A. Goudsmit
W. W. Havens, Jr.
W. V. Houston
Winston E. Kock
R. Bruce Lindsay
David L. MacAdam
H. Victor Neher
Leonard O. Olsen
C. J. Overbeck
Ray Pepinsky
S. L. Quimby
Francis W. Sears
Frederick Seitz
C. G. Suits
Mary E. Warga
William R. Willets

Administration

Elmer Hutchisson
Director
Wallace Waterfall
Secretary and Treasurer
Henry A. Barton
Administrative Consultant
W. C. Kelly
Director of Education
Eugene H. Kone
Director of Public Relations
Hugh C. Wolfe
Director of Publications
Kathryn Setze
Assistant Treasurer
James E. Mills
Supervisor, Editorial Department
Sistina Greco
Circulation Manager
Edward Tober
Manager, Production and Distribution
Theodore Vorburger
Advertising Manager
Emily Wolf
Manager, Special Services

American Institute of Physics Advisory Board on Russian Translations

Robert T. Beyer, *Chairman*
J. George Adashko, Freeman Dyson, Dwight Gray,
Morton Hamermesh, David Harker, Harold F. Weaver

Editor of Soviet Physics—JETP

J. George Adashko, 25 West 81st St., New York 24, New York

Soviet Physics—JETP is a monthly journal published by the American Institute of Physics and contains a complete translation of the Journal of Experimental and Theoretical Physics of the U.S.S.R. Academy of Sciences.

This translating and publishing project was undertaken by the institute in the conviction that dissemination of the results of researches everywhere in the world is invaluable to the advancement of science. The National Science Foundation of the United States has encouraged the project initially and is supporting it in large part by a grant.

The American Institute of Physics and its translators propose to translate faithfully all the material appearing in the original articles. The views expressed in the translations are therefore those of the original authors, and not those of the translators nor of the American Institute of Physics.

Volume 1 of Soviet Physics—JETP corresponds to Russian Volume 28 (1955). Two volumes are published annually, each of six issues. Each volume contains the translation of one volume of the Journal of Experimental and Theoretical Physics.

Beginning with Vol. 9(36), the transliteration of the names of Russian authors follows British Standard 2979, which is being adopted by a large number of scientific journals in the United States. The Library of Congress transliteration is followed in the earlier volumes.

Subscription Prices

Per Year (12 issues), starting with Vol. 13, No. 1

General:	
United States and Canada	$75.00
Elsewhere	79.00
Libraries of non-profit degree-granting Institutions:	
United States and Canada	$50.00
Elsewhere	54.00
Single Copies	$ 8.00

Subscriptions should be addressed to the American Institute of Physics, 335 East 45th Street, New York 17, New York.

SOVIET PHYSICS, JETP is published monthly by the American Institute of Physics, Inc. Second Class postage paid at New York, N. Y. and Ann Arbor, Michigan.

Copyright by American Institute of Physics 1961

SOVIET PHYSICS

JETP

A translation of Zhurnal Éksperimental'noǐ i Teoreticheskoǐ Fiziki.

Vol. 13, No. 2, pp 263-501 (Russ. orig. Vol. 40, No. 2, pp 385-720, Feb., 1961) August, 1961

CHANNEL EXPANSION IN SMALL INTENSE SPARKS

B. A. DEMIDOV, Yu. F. SKACHKOV, and S. D. FANCHENKO

Submitted to JETP editor June 3, 1960

J. Exptl. Theoret. Phys. (U.S.S.R.) 40, 385-390 (February, 1961)

An electron-optical chronograph has been used to study the initial stages of channel expansion in sparks in oxygen and nitrogen (at pressures up to 10 atm), in deuterium (13 atm) and in hydrogen (up to 20 atm) produced by discharging low-inductance capacities of 30 and 6300$\mu\mu$f. The maximum rate of rise of the current is of the order of 3×10^{12} amp/sec, the calculated peak current approximately 10^3 amp, and the calculated current density $10^8 - 10^9$ amp/cm^2. The initial expansion of the spark channel is due to a cylindrical shock wave which propagates at a velocity up to 6×10^6 cm/sec in nitrogen, up to 8×10^6 cm/sec in hydrogen and up to 7×10^6 cm/sec in deuterium (in the last case the temperature at the shock wave front is approximately 8 ev). The calculated temperature in the spark channel in hydrogen is approximately 22 ev.

1. INTRODUCTION

ACCORDING to contemporary ideas, the development of a spark discharge in a high-density gas takes place in two stages. The first state is terminated when the discharge gap is bridged by the electron-photon streamers which are formed in this gap. The second stage starts with the flow of a high current through the conducting bridge which has been formed; this current causes intense Joule heating of the gas in this bridge, transforming it into a brightly emitting, thread-like channel. It has been known for a long time that rapid channel expansion starts as soon as the channel is formed and that the channel boundaries remain clearly defined throughout the expansion process. The expansion of spark channels has been studied by a number of authors,[1-10] who have generally used high-speed cameras with rotating photographic films or mirrors. The cameras used in these investigations provided continuous recording with a time resolution up to 3×10^{-8} sec.

In the work cited above, particularly that of S. L. Mandel'shtam and his colleagues,[1,3,5-7] it has been shown that the initial expansion of the spark channel, which is characterized by the highest velocity, is due to the propagation of a shock wave in the gas. This shock wave causes preliminary heating and ionization of the gas which is drawn into the channel. It has been found that the initial velocity of propagation of the channel is very sensitive to the inductance in the discharge circuit, increasing as the initial current derivative $(dI/dt)_0$ increases. For this reason we have undertaken an investigation of the initial stages of channel expansion in a discharge circuit with a higher value of dI/dt than has been available to the workers in the work indicated above.

2. DESCRIPTION OF THE APPARATUS

Discharge Circuits

a) Disc capacitor. Two discs, 7 cm in diameter, separated by a distance of 1 mm in the gas being studied, form a 30-$\mu\mu$f capacitor. The spark always occurs at the center of the discs, because of the presence of a point there (Fig. 1a). The period of the natural oscillations of this discharge circuit is determined by observation of periodic variations

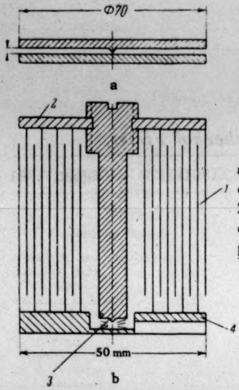

FIG. 1. Discharge circuits. a) disc capacitor, b) coaxial capacitor; 1) foil electrodes, 2) upper plate with coaxial current-conducting rod, 3) point, 4) lower plate.

in the emission intensity of the spark and is found to be 2×10^{-9} sec. An additional check is provided by measurement of the wavelength of the radio wave produced by the discharge; this check shows qualitative agreement with the results of the optical measurements of the oscillation period. The total inductance of the circuit, as computed from the period of the natural oscillations, is 3 cm.

b) Coaxial capacitor. In Fig. 1b we show a low-inductance coaxial capacitor of the type suggested by Fischer[11] which has been developed for the present work. The spark occurs between point 3 and the lower plate 4. The capacitance is 6300 $\mu\mu$f and the total inductance of the discharge circuit is 7 cm.

Method of Observation

In addition to using a camera with a rotating mirror, we have employed an electron-optical chronograph[12] which, in principle, permits a time resolution of approximately 10^{-14} sec. In the present case the time resolution was approximately 10^{-10} sec and was completely adequate for the purposes of this investigation.

The image of the spark 1 (cf. Fig. 2) is projected by the objective lens 2 on the input photocathode 4 of a multistage electron optical image converter (EOC). A narrow slit 3, is located in front of the photocathode; this slit isolates a short section of the channel image. The electron image of this portion of the channel is swept in time by the deflection plates 5, 6, to which is applied an alternating voltage at frequencies of 5, 11, and 21 Mc/sec (in certain experiments 1 Mc/sec). The sweep is along the longitudinal dimension of the channel. The time-swept image of the expanding spark channel passes through several stages of electron-optical amplification;[13,14] the intensified image on the output luminescence screen[7] can then be photographed with a conventional camera 8. In order to obtain good photographs we have used a pulsed spark supply and the EOC. In Fig. 2 we also show the voltage pulse which produces the image of the spark on the output screen at the appropriate time.

3. RESULTS

Examples of photographs obtained with the discharge circuit shown in Fig. 1a are given in Figs. 3 and 4. In most of the photographs obtained there is a periodic variation in the emission intensity from the spark channel caused by the natural oscillations of the discharge circuit (period approximately 2×10^{-9} sec). In hydrogen (Fig. 3) these brightness variations are observed over the entire range of initial pressures which has been studied, 2 – 20 atm. In nitrogen, the periodic variations in brightness are clearly visible at pressures above 6 atm (Fig. 4); at 6 atm they become weak, and at 4 atm or below cannot be observed at all.

Many cases in which the channel splits into two parts have been observed in nitrogen. In agreement with observations which have been published earlier by other authors, we have observed a noticeable repulsion between the two channels which result from

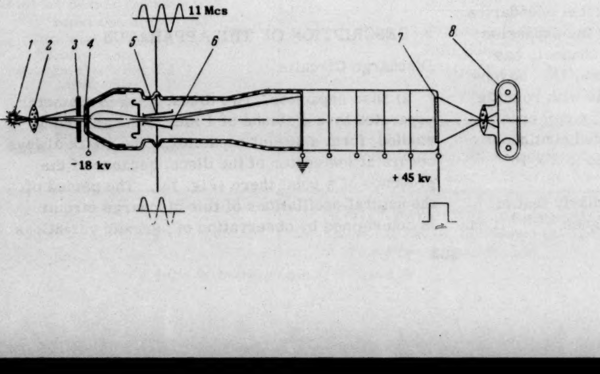

FIG. 2. Diagram of the apparatus.

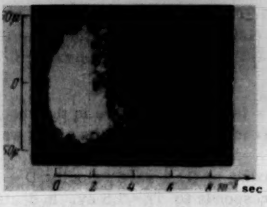

FIG. 3. Expansion of a spark channel in hydrogen at a pressure of 12 atm. Time is plotted along the abscissa axis while the spark diameter is plotted as the ordinate.

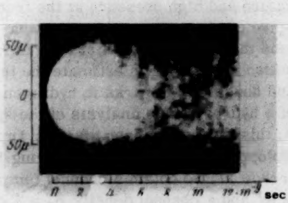

FIG. 4. Expansion of a spark channel in nitrogen at a pressure of 8 atm.

splitting. Many cases have also been observed in which channel expansion is not completely symmetric.

The general pattern of channel expansion and the order of magnitude of the expansion velocity in oxygen are the same as in nitrogen.

The highest expansion rate is observed in the first quarter of the natural oscillation period of the discharge circuit (τ). This rate is estimated by dividing the channel radius at approximately $\tau/4$ by the elapsed time from the beginning of the expansion process. It should be noted that with identical initial discharge conditions (gas pressure and gap length) the initial expansion rates vary by a factor of several times in individual cases. Special photographs of the entire channel, which were taken with slit 3 removed and with no sweep show that the channel is usually twisted and kinked and that the emission intensity is not uniform over the channel. The spread in the observed expansion rate is apparently due to the fact that images of widely different portions of the channel reach the slit 3. In considering this spread we may note that in our measurements physical significance is to be given to only the highest observed value of the initial expansion rate, which is determined with an accuracy of 10%.

In nitrogen (sweep frequency 11 Mc/sec) the observed expansion velocity is as high as 6×10^6 cm/sec. In hydrogen a faster sweep is used (21 Mc/sec); hence, in determining the rate of expansion we use a value of the channel radius corresponding to an earlier time, specifically, $\tau/8$. In this case, the highest measured expansion velocity in hydrogen is found to be 8×10^6 cm/sec. In deuterium (initial pressure 13 atm) the highest measured velocity is 7×10^6 cm/sec.

Comparative data obtained in investigations of spark channel expansion by different authors.

Literature reference	Electrical parameters of the discharge circuit				Spark parameters			
	Capacitance C, μF	Current, amp	$(dI/dt)_0$, amp/sec	Period of the natural oscillations of the discharge circuit, μsec	Gas	Pressure atm	Maximum current density, amp/cm²	Initial rate of expansion of the channel, 10^5 cm/sec
[2]	—	10^4--10^5	10^{10}*	Aperiodic pulse, t = 10–1000	Air	1	$2.7 \cdot 10^4$	2
[4]	—	500	10^9—10^{10}*	Aperiodic pulse, $t_{rise} = 0.25$ $t_{fall} = 10–28$	Air			
					Nitrogen	1	$3 \cdot 10^4$	0.93
					Oxygen	1	$3 \cdot 10^4$	
					Hydrogen	1	$3 \cdot 10^4$	
						1	$7 \cdot 10^4$	2*
[6]	0.0035—0.25	10^4—10^5	10^8--10^{10}*	0.5÷30*	Air	3		3
					Hydrogen	1	$6 \cdot 10^6$	4
					Argon	1		3
[8]	—	200	10^9—10^{10}*	Rectangular pulse, 4–10	Hydrogen	1	10^5—10^6*	10*
[9]	57	$2.65 \cdot 10^5$	$5 \cdot 10^{10}$*	30	Air	1	$7 \cdot 10^4$	3
					Argon		$9 \cdot 10^4$	9
					Hydrogen		$2 \cdot 10^5$	2
[10]	132	$2 \cdot 10^6$	$1 \cdot 10^{12}$	17*	Air	1	$9 \cdot 10^8$	20
Present work	0.00003	10^3	$3 \cdot 10^{12}$	0.002	Oxygen			60
					Nitrogen	10	10^8—10^9	60
					Hydrogen	20		80
					Deuterium	13		70
	0.0063	10^4	$2 \cdot 10^{12}$	0.04	Nitrogen	10	10^7	25
					Hydrogen	18		60

*This quantity is not given in the cited work; it is computed on the basis of other data reported in the paper.

The discharge circuit shown in Fig. 1b has been used to investigate the expansion of a spark channel in nitrogen and hydrogen at pressures from 1 to 18 atm. The maximum initial expansion velocity in nitrogen was found to be 2.5 × 10^6 cm/sec and the maximum in hydrogen, 6 × 10^6 cm/sec.

4. DISCUSSION OF THE RESULTS

Comparative data for the parameters of discharge circuits used by various authors and values of the observed expansion rates are given in the table. The data given for the present discharge circuits are computed from the known capacity, the period of the natural oscillations, and the breakdown voltage; ohmic resistance is neglected.

The table shows that in spite of its low capacity and simplicity of construction, the first discharge circuit used in our work provides the highest initial current derivative and the highest initial channel expansion rate. Comparison of the initial channel expansion rates for our first and second discharge circuits, and of our data with the data of other authors, emphasizes the dependence of the initial expansion rate on $(dI/dt)_0$.

In the present experiments the shock waves have not been recorded by the Teller method. Only the brightly illuminated region of the discharge was photographed. For this reason it was not possible to observe experimentally the time at which the shock wave breaks away from the channel. However, there is little doubt that the initial stage of expansion, which is the only one for which we estimate velocity, precedes this breaking away. If we assume that in this stage the boundary of the luminous region is a shock front and compute the temperature from the measured expansion rate, then, as is shown below, the temperature in the shock front is found to be sufficient for total ionization of the gas drawn into the discharge channel. Thus, in the present case we are not dealing with the mechanism considered by Mandel'shtam et al.[3,6] in which the shock wave breaks away from the channel because of the inadequate conductivity in its front.

On the other hand, simple estimates show that in our experiments the current and the magnetic field of the plasma itself are inadequate to constrict the channel by the pinch mechanism. This effect as has been observed in high-current discharges by Komel'kov and Parfenov.[10]

For total ionization of the gas in the shock front the temperature in the front in hydrogen is given by the following expression:[15]

$$T_f = 3.95\,(D/9\cdot 10^6)^2 \left[1 - (9\cdot 10^6/D)^2 + \sqrt{1 + \tfrac{2}{3}\,(9\cdot 10^6/D)^2} \right], \qquad (1)$$

where T_f is the temperature in the shock front in ev and D is the velocity of the shock wave in cm/sec.

According to (1) a wave velocity D = 8 × 10^6 cm/sec corresponds to T_f = 3.5 ev. In deuterium the velocity of the shock wave, 7 × 10^6 cm/sec, corresponds to a temperature T_f = 8 ev.

The gas ionization for the obtained values of temperature and high pressure at the front of the shock wave can be estimated by the Saha equation; it is found that essentially all of the gas is ionized.*

It is also interesting to estimate the temperatures and densities of sparks in hydrogen on the basis of a hydrodynamic analysis of the spark channel; this theory has been given by Drabkina[5] and developed by Braginskii.[17] Applying Eq. (3.13) of reference 17, we obtain a channel temperature T_c = 22 ev and a channel density $n_c = 3 \times 10^{20}$ cm^{-3}. It should be noted that the formulas in reference 17 are known to apply for sparks with low initial pressures; strictly speaking, this applicability has not been demonstrated in the present case. Nonetheless, it is interesting to compare the temperature which has been obtained with the data reported by Fischer,[11] who has estimated the temperature of a spark channel in helium at a pressure of 35 atm from the spectral distribution of the radiation and finds a value $T_c \sim 25$ ev.

In conclusion the authors wish to thank E. K. Zavoĭskii for valuable comments and continued interest in this work and S. I. Braginskii and S. L. Mandel'shtam for many valuable comments and discussions.

---

[1] I. S. Abramson and I. S. Marshak, JETP **12**, 632 (1942).

[2] J. W. Flowers, Phys. Rev. **64**, 225 (1943).

[3] Abramson, Gegechkori, Drabkina, and Mandel'shtam, JETP **17**, 862 (1947).

[4] J. B. Higham and J. M. Meek, Proc. Phys. Soc. (London) **B63**, 649 (1950).

---

*Because of possible relaxation processes the use of the Saha equation is not completely valid in this case. However, according to an estimate made by Mandel'shtam and Sukhodrev,[16] at an electron concentration of approximately 10^{21} cm^{-3} the time needed for establishing a steady state for ionization in the spark channel is $\tau \approx 10^{-11}$ sec, which is an order of magnitude higher than the resolution time in the present experiment.

[5] S. I. Drabkina, JETP **21**, 473 (1951).

[6] I. M. Gegechkori, JETP **21**, 493 (1951).

[7] K. S. Vul'fson and I. Sh. Libin, JETP **21**, 510 (1951).

[8] R. D. Craig and J. D. Craggs, Proc. Phys. Soc. (London), **B66**, 500 (1953).

[9] J. E. Allen and J. D. Craggs, Brit. J. Appl. Phys. **5**, 446 (1954).

[10] V. S. Komel'kov and D. S. Parfenov, Doklady Akad. Nauk SSSR **111**, 1215 (1956), Soviet Phys.-Doklady **1**, 769 (1957).

[11] H. Fischer, J. Opt. Soc. Am. **47**, 981 (1957).

[12] E. K. Zavoĭskii and S. D. Fanchenko, Doklady Akad. Nauk SSSR **100**, 661 (1955); **108**, 218 (1956) [the second article is translated in Soviet Phys.-Doklady **1**, 285 (1957)].

[13] Zavoĭskii, Butslov, and Smolkin, Doklady Akad. Nauk SSSR **111**, 996 (1956), Soviet Phys.-Doklady **1**, 743 (1957).

[14] Butslov, Zavoĭskii, Plakhov, and Smolkin, Атомная энергия (Atomic Energy) **1**, 34 (1956).

[15] A. C. Kolb, Phys. Rev. **107**, 345 (1956).

[16] S. L. Mandel'shtam and H. S. Sukhodrev, JETP **24**, 701 (1953).

[17] S. I. Braginskii, JETP **34**, 1548 (1958), Soviet Phys. JETP **7**, 1068 (1958).

Translated by H. Lashinsky
58

SOVIET PHYSICS JETP VOLUME 13, NUMBER 2 AUGUST, 1961

AN INVESTIGATION OF THE PARAMAGNETISM OF μ-MESIC ATOMS

L. B. EGOROV, G. V. ZHURAVLEV, A. E. IGNATENKO, LI HSUANG-MING, M. G. PETRASHKU, and D. CHULTÉM

Joint Institute for Nuclear Research

Submitted to JETP editor June 27, 1960

J. Exptl. Theoret. Phys. (U.S.S.R.) 40, 391-399 (February, 1961)

The nature of the paramagnetism of various mesic atoms was investigated by measuring the asymmetry of μ-e decay electrons. The experimental results indicate that in dielectrics and in normal diamagnetic and weakly paramagnetic metals the paramagnetism of mesic atoms results from the μ^--meson magnetic moment, whereas in paramagnetic transition metals, lanthanides, and actinides it is due to the magnetic moments of both the electron shell and meson. It is shown that polarized mesons can be employed to investigate the magnetic properties of the atoms and hydrides of transiton metals, actinides, and lanthanides with zero nuclear spin.

1. INTRODUCTION

THE investigation of fine structure and hyperfine structure in atomic systems and of the associated quantum electrodynamical effects is of great interest. While ordinary atoms and positronium have been studied extensively, such atomic systems as muonium and μ-mesic atoms are also attractive objects of study. An earlier paper[1] reported an investigation of the hyperfine structure of μ-mesic atoms that results from coupling of the meson and nuclear spins. The present paper is concerned mainly with the hyperfine structure due to meson-electron coupling. Some of the many reasons for practical interest in this effect will now be enumerated.

A. Polarized μ^- mesons in matter are essentially depolarized as a result of the interactions that produce fine and hyperfine structure in mesic atoms.[1] One can inquire whether it is possible to eliminate or restore meson polarization in mesic atoms. It is obvious that depolarization due to hyperfine structure resulting from meson-nucleus spin coupling can be obviated by using substances with zero nuclear spin. It would appear that depolarization due to fine structure or hyperfine structure resulting from spin coupling of the meson and electron shell could be eliminated by using a sufficiently strong magnetic field. However, the magnetic neutralization of depolarization encounters insurmountable experimental difficulties. Kinematic depolarization associated with π-μ decay in flight can also not be eliminated. The fact that the depolarization time ($\sim 10^{-12}$ sec) is many orders of magnitude shorter than the meson lifetime τ suggests that static methods of nuclear polarization be used to repolarize mesons in mesic atoms with zero nuclear spin.

For our purposes two methods are of interest, in both of which magnetic fields are applied at low temperatures. The first method uses the effect of an external magnetic field on the nuclear magnetic moment, while the second method uses the internal atomic magnetic field resulting from uncanceled electron moments. The coefficient of nuclear polarization produced directly by the external field H is given by

$$f \approx \tfrac{1}{3}\,[(I+1)/I]\,(\mu_N H/kT), \qquad (1)$$

where I is the nuclear spin, μ_N is the nuclear magnetic moment, k is the Boltzmann constant, and T is the absolute temperature.

When internal atomic magnetic fields are used, nuclear polarization is given by[2]

$$f \approx \tfrac{1}{3}\,f_e\,[(I+1)/I]\,[J_e/(2J_e+1)]\,(\Delta W/kT), \quad J_e \geqslant 1, \qquad (2a)$$

$$f \approx \tfrac{1}{3}\,f_e[(I+1)/(2I+1)]\,(\Delta W/kT), \quad J_e \leqslant 1. \qquad (2b)$$

Here f_e is the electron polarization, J_e is the electron angular momentum, and ΔW is the hyperfine splitting energy.

It follows from (1) and (2) that the greater μ_N and ΔW, and the smaller I, the easier it is to achieve a given degree of polarization.

Since a muon has spin ½, while its magnetic moment is one order of magnitude greater than the nuclear magneton, a given degree of meson polarization in mesic atoms can be produced by using temperatures that are higher or magnetic fields that are weaker by one order of magnitude than in the case of nuclei.

It must be noted that the external field method can encounter insuperable difficulties because of the large meson spin relaxation time compared with τ. These difficulties disappear when internal atomic fields are used. Indeed, the electron moments in a sample can be polarized before irradiation with mesons. The meson spin-flip time in the field of a mesic-atom shell will then be given[1] by the "interaction time" $t' \sim \hbar/\Delta W \sim 10^{-10}$ sec, which is many orders of magnitude smaller than τ.

B. At the present time one of the most effective methods of investigating the electron configurations of paramagnetic atoms is the study of the emission asymmetry of polarized nuclei. This method is obviously feasible only for elements with nonzero nuclear spin. By investigating the asymmetry of the decay electrons of polarized muons in mesic atoms it is possible to study the electronic structure of atoms in paramagnetic substances having zero nuclear spin.

C. The measurement of the gyromagnetic ratio of mesic atoms having zero nuclear spin and exhibiting electron spin paramagnetism due to a single unpaired electron makes it possible to determine μ^- spins directly.

D. The paramagnetism of mesic atoms must be investigated before the depolarization mechanism of $\mu^\pm$ mesons can be determined.

2. BASIC THEORETICAL POSTULATES

The formation of mesic atoms is associated with the destruction of the electron-shell state of the original atom. The lifetime t_0 of an excited shell state of free mesic atoms depends only on the electron configuration and degree of excitation. When mesic atoms are formed in a substance the lifetime t_0 depends greatly on the nature of the atomic bonds. In a metal the electron shell of a mesic atom returns to the ground state in a very short time ($< 10^{-12}$ sec) compared with t' and τ. On the other hand, in ionic crystals or dielectrics t_0 is greater than t' and τ. Consequently, at the instant of decay the electron state of a mesic atom depends on the kind of compound that contains the given atom and on the state of aggregation.

In the case of isolated mesic atoms with zero nuclear spin, when the electron shell has a nonzero moment the paramagnetic moment will consist of three parts:

1) the magnetic moment of the muon,

$$\mu_\mu = \sqrt{3}\, M_B/207, \tag{3}$$

2) the electron orbital magnetic moment

$$\mu_L = M_B \sqrt{L(L+1)}, \tag{4}$$

3) the electron spin magnetic moment

$$\mu_S = 2M_B \sqrt{S(S+1)}. \tag{5}$$

When mesic atoms are formed in a medium their paramagnetism will be influenced by neighboring atoms, and some magnetic moments will be canceled, depending upon the electron shells that are responsible for the magnetic moment. By analogy with the properties of the ionic magnetic moments of paramagnetic substances we can expect that when mesic atoms are formed from lanthanide or actinide atoms, where the magnetic moment is due to deep-lying electrons that are least subject to external influences, the paramagnetism of such mesic atoms in a substance will result from all magnetic moments — μ_L, μ_S, and μ_μ. In the case of the transition elements, where the electrons responsible for the atomic magnetic moment are not deep-lying and are thus more subject to external influence, mesic atoms in a substance can possess only the spin moments μ_S and μ_μ, the orbital moments being canceled, as a rule. Finally, mesic atoms of diamagnetic substances, or normal weakly paramagnetic metals can possess only μ_μ moments on the average.

In substances with uncanceled moments the electron shell can affect muon polarization only in the mesic-atom ground state. This is easily seen by comparing the lifetime t of a meson on lower levels with the time t' required for meson spin flip in the field of the shell. The inequality $t' \ll t$ is fulfilled only for the 1S level, as indicated in Sec. 1.

It must be noted that in substances with angular momentum $J_e \neq 0$ of the electron shell, mesic atoms will be formed in two hyperfine states with total spins $F = J_e \pm 1/2$. In first approximation the hyperfine interaction energy ΔW in mesic atoms will be of the same order as in muonium, that is,

$$\Delta W = -32\, \mu_\mu p_{\mathrm{eff}}/3a_{e\mu}^3.$$

Here μ_μ is the muon magnetic moment, p_{eff} is the effective magnetic moment of the electron shell, and $a_{e\mu}$ is the Bohr radius of the hydrogen atom. The hyperfine splitting of a mesic-atom ground state is much larger than $\hbar/\tau$. Therefore the states with $F = J_e + 1/2$ and $J_e - 1/2$ are incoherent in a mesic atom; each state is characterized by its own value of the gyromagnetic ratio. Thus the expressions for g are[4]

$$g_+ = (\mu_\mu + p_{\mathrm{eff}})/(J_e + 1/2), \tag{6}$$

$$g_{-} = -\left[\mu_{\mu} - \frac{(J_e + 1)}{J_e} p_{\text{eff}}\right] / (J_e - {}^{1}/{}_{2}). \qquad (7)$$

If mesic-atom paramagnetism is studied by measuring the asymmetry of decay electrons,[5] the experimentally observed precession curve will represent the superposition of the precession curves of mesons decaying from both hyperfine states. The larger the value of J_e, the more difficult it will obviously be to interpret this curve. In actuality we denote by P_0 the degree of polarization of the muon beam. According to the literature,[4,6-8] the degree of polarization P of a meson in the K shell, averaged over the two hyperfine states, will be

$$P = \tfrac{1}{6} P_0 \cdot \tfrac{1}{3} [1 + 2/(2J_e + 1)^2]. \qquad (8)$$

It follows from this formula that the polarization depends on the total moment J_e of the electron shell. Thus, for $J_e = 1/2$ polarization will be reduced to one-half, while for mesic atoms with $J_e \gg 1$ it will be reduced to one-third. All of the foregoing discussion obviously pertains to isolated mesic atoms. The presence of a surrounding medium can complicate the picture; for example, meson transitions between hyperfine levels can occur.

3. EXPERIMENTAL PROCEDURE

The following materials were investigated: 1) dielectrics (paraffin, polythene, water, and sulfur); 2) diamagnetic and normal weakly paramagnetic metals (graphite, magnesium, zinc, cadmium, and lead); and 3) paramagnetic transition metals (chromium, molybdenum, palladium, and tungsten). The results obtained for water, magnesium, sulfur, zinc, cadmium, and lead have been published in reference 9; the remaining substances were investigated in the present work.

Chromium, molybdenum, tungsten, and palladium were studied in metallic form. The carbonaceous media were graphite, polythene, and paraffin, which were selected for the following reasons. The direction of the μ^--meson spin has so far been an open question,[10] the answer to which has been sought, in one way, by investigating the asymmetry of B^{12} decay electrons in the reaction $\mu^- + C^{12} \rightarrow B^{12} + \nu$.[11] The experiments reported in reference 10 revealed an absence of asymmetry that evidently resulted from the depolarization of B^{12} nuclei in the investigated samples of hexane and pentane. According to Jackson, Treiman, and Wyld[11] there are two possible causes of B^{12} depolarization: 1) the hyperfine structure due to the spin coupling of the B^{12} nucleus and electron shell, and 2) the short relaxation time of B^{12} nuclear spin in the given materials compared with the B^{12} lifetime. We proposed to check the presence of a B^{12} depolarization mechanism due to hyperfine structure by using different carbon compounds, with the expectation that mesic carbon atoms in these substances would have the electron configuration of the boron atom.[11]

The paramagnetism of mesic atoms of carbon, chromium, molybdenum, tungsten, and palladium in the given substances was investigated by the precession technique,[5] where the nature of the paramagnetism can be determined by measuring the asymmetry of μ-e decay electrons in the following manner. The electronic circuit is tuned to register the precession frequency of the free meson spin. It follows from Eqs. (6) and (7) that in a given magnetic field H the spin precession frequency of a mesic atom possessing both an electron moment and a meson moment will be several orders of magnitude greater than the spin precession frequency of mesic atoms in which paramagnetism is due to meson spin alone. In virtue of the large frequency difference the nature of the paramagnetism can be determined by measuring the numbers of μ-e decay electrons, $N_{\max}$, and $N_{\min}$ at two field strengths ± H, using the formula

$$t_1 + \Delta t = T/2 = \pi mc/eH, \qquad (9)$$

where t_1 is the delay time, Δt is the gate width, and T is the spin precession period of a "free" muon. For mesic atoms possessing an electron moment the ratio $\xi = N_{\max}/N_{\min}$ will be unity, whereas for mesic atoms in which paramagnetism results from meson spin alone ξ will differ from unity. A control experiment that confirmed directly the existence of electronic paramagnetism by this technique was the measurement of ξ in the hydrides of paramagnetic metals having the hydrogen concentration at which the paramagnetism of the compound, such as $PdH_{0.6}$, decreases to zero. Indeed, the palladium atoms in a $PdH_{0.6}$ solution have no magnetic moment, and the hydrogen will not participate in the formation of mesic atoms.

The experiments were performed with the same apparatus, except for the electronic equipment, and under the same experimental conditions as in our earlier work.[9,12] A block diagram of the apparatus is shown in the figure. Negative muons stopped in the target 6 were registered by the anticoincidence scheme 8 (1 + 2 − 3). Pulses from 8 were amplified, shaped, and delayed for the time t_1. The delayed pulses operated the trigger 16, which opened simultaneously two identical gates 18 and 21 for

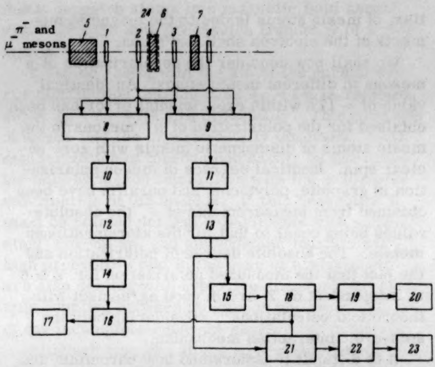

Block diagram of apparatus. 1, 2, 3, 4 – scintillation counters; 5 – copper filter; 6 – target; 7 – paraffin filter; 8, 9 – anticoincidence circuit; 10, 11 – amplifiers; 12, 13 – pulse shapers; 14 – delay t_1; 15 – delay t_2; 16 – trigger; 18, 21 – gating circuits; 19, 22 – discriminators; 17, 20, 23 – scalars; 24 – magnetizing coil.

the time Δt. The meson decay electrons and the background were registered by the anticoincidence circuit 9 (3 + 4 − 2). Pulses from 9, after passing through the amplifier 11 and the pulse shaper 13, were split, and were then fed to the gating circuit 18 after a delay $t_2 > t_1 + \Delta t$ and to the gating circuit 21 without delay. The use of two identical gating circuits and the delay t_2 made it possible for the scaler 23 to register simultaneously the number of pulses produced by decay electrons and by the background, while the scaler 20 registered only the background pulses. The count difference between scalers 23 and 20 represents the number of decay electrons. Pulses from the trigger 16 were fed through a separate output to the scaler 17, which registered the number of gate openings, and served as a monitor.

In each experiment the ratio $t_1/\Delta t$ was ~ 0.2. The axis of the electron detector and the target formed the angles 90° and 45°, respectively, with the meson beam axis. The target area was 15 × 15 cm^2, and the target thickness was 4 – 6 g/cm^2. In the experiments with graphite, polythene, and paraffin the paraffin filter 7 between counters 3 and 4 was 4 g/cm^2 thick. In the experiments with chromium, molybdenum, tungsten, and palladium, the paraffin filter 7 was replaced by a 4 g/cm^2 aluminum filter, which reduced to under 10^{-3} the registration efficiency for γ rays under 10 Mev emitted from the target as a result of μ^- absorption.[13]

Substance	$\xi = N_{max}/N_{min}$
Graphite	1.10 ± 0.02
Paraffin	1.09 ± 0.02
Polythene	1.10 ± 0.02
Palladium hydride	1.09 ± 0.02
Palladium	1.00 ± 0.02
Chromium	1.00 ± 0.02
Molybdenum	0.99 ± 0.02
Tungsten	0.99 ± 0.02

The table gives the values obtained for $\xi = N_{max}/N_{min}$, including corrections for t_1 and Δt, meson decay and the solid angle of the electron detector. The statistical errors are indicated.

4. DISCUSSION OF RESULTS

The table shows that for graphite, polythene, paraffin, and palladium hydride ($PdH_{0.6}$) identical values of ξ were obtained within the limits of statistical errors. Equal values of ξ were also obtained for chromium, molybdenum, tungsten, and palladium. However, the absolute values of ξ for graphite, polythene, paraffin and $PdH_{0.6}$ differ from those for chromium, molybdenum, tungsten, and palladium. It should be noted that for graphite a_0 — the asymmetry coefficient in the electron angular distribution $1 + a \cos \theta$, integrated over the energies — obtained from ξ agrees within error limits with the value of a_0 obtained in earlier work[1,9,12] from a large number of measured points on the precession curve.

The departure of ξ from unity for graphite, paraffin, polythene, and the agreement of the values among themselves, indicate that the paramagnetism of mesic carbon atoms in these substances is due to the meson magnetic moment alone. Let us first consider the formation of mesic atoms in metals, which, together with graphite, can be regarded in first approximation as ion aggregates immersed in an electron gas. Diamagnetic metals and normal weakly paramagnetic metals have ions with zero magnetic moment. It is therefore probable that when mesic atoms are formed in these metals, since $t_0 \ll t'$ the electron state of an ion is not actually destroyed and the ionization of atoms is accompanied only by the emission of collective conduction electrons. In view of the constant measured value of a_0 previously obtained[9] for metals in this group such as magnesium, zinc, cadmium, and lead, and also the equality of this value to a_0 for graphite, it can be asserted that electronic paramagnetism does not arise when mesic atoms are formed in diamagnetic or normal weakly paramagnetic metals.

The formation of mesic atoms in dielectrics, where $t_0 \gg t'$, presents a different picture. Mesic carbon atoms in paraffin and polythene, mesic oxygen atoms in water, and mesic sulfur atoms[9] can lack an electron magnetic moment for two possible reasons. First, the mesic atoms can be negative ions with the electron configuration of the original atoms. Secondly, the formation of mesic atoms can possibly be associated with disturbance of the original atomic electron shell. In this case, according to Dzhrbashyan,[6] the electron moment can be canceled completely by neighboring atoms.

Further investigation is required before a choice can be made between these two hypotheses. The experimental results will determine whether a B^{12} depolarization mechanism exists due to hyperfine structure arising from the spin coupling of the nucleus to the electron shell of boron atoms produced in the reaction $\mu^- + C^{12} \rightarrow B^{12} + \nu$. It would appear that mesic carbon atoms in graphite should have the electron configuration of boron atoms,[11] but experimental results indicate the absence of any electron moment. It is obvious that electronic paramagnetism cannot arise in boron atoms produced by the given reaction in graphite. Therefore a B^{12} depolarization mechanism due to hyperfine structure in graphite cannot exist, whereas for the aforementioned reasons this mechanism can exist when boron atoms are formed in dielectrics.

The experimental results obtained for palladium in $PdH_{0.6}$. furnish direct evidence that the paramagnetism of mesic palladium atoms is due to the magnetic moments of the electron shell and meson. The electrons of the magnetically active inner 4d shell are responsible for the magnetic moment of ions of the transition metal palladium. The measurements of ξ for carbon, paraffin, and polythene show that in the compound $PdH_{0.6}$ hydrogen does not affect meson depolarization.

We wish to emphasize especially that, as the experiments with Pd and $PdH_{0.6}$ have shown, polarized μ^- mesons can possibly be used to investigate the magnetic properties of atoms and hydrides, with zero nuclear spin, of the transition metals, lanthanides, and actinides. Unfortunately, no control experiment can be performed to confirm directly the existence of electronic paramagnetism in chromium, molybdenum, or tungsten, since hydrides are not formed when hydrogen is dissolved in these metals.

ξ can equal unity for these transition metals and they can agree among themselves if 1) mesons are completely depolarized, or 2) the paramagnetism of mesic atoms is due to the magnetic moments of the electron shell and muon.

We shall now consider the depolarization of μ^- mesons in different mesic atoms. An identical value of $\sim 17\%$ within experimental error has been obtained for the polarization of μ^- mesons in the mesic atoms of diamagnetic metals with zero nuclear spin. Identical degrees of meson polarization in graphite, polythene, and paraffin have been obtained from measurements of ξ, the absolute values being equal to that for the aforementioned metals. The absolute degree of polarization and the fact that the measured polarization for $Z \geq 6$ is independent of Z are in good agreement with theoretical calculations[6,7] considering only the spin-orbit interaction mechanism.

It is difficult to understand how chromium and molybdenum can differ essentially from the substances already mentioned with respect to μ^- depolarization. Ford and Mullin[14] have shown that there is practically no depolarization of mesons slowed down and captured into the higher levels of mesic atoms. The probability of mesic atom formation is known to be unity. The elements Cr and Mo consist 80 — 90% of atoms with zero nuclear spin. The nuclei of these atoms possess no properties that could result in complete meson depolarization. It is therefore unlikely that depolarization mechanisms other than spin-orbit interaction exist in mesic atoms with the corresponding values of Z. Chromium and molybdenum differ from the previously mentioned substances only in their possession of unfilled inner electron shells. Therefore the results of the experiments with palladium and $PdH_{0.6}$ show that the hyperfine structure is very probably involved in the cases of chromium and molybdenum, whose ions possess nonzero magnetic moments due to the magnetically active inner 3d and 4d shells, respectively.

The experiments with tungsten merit special attention, since tungsten, unlike palladium, chromium, and molybdenum, has mesic atoms with deformed nuclei. It has been shown by Zaretskii and Novikov[15] that the interaction of a meson with the quadrupole deformation of a nucleus can result in considerable depolarization of μ^- mesons. We shall now compare the measured values ξ_e with theoretical predictions ξ_T. If the hypothesis of the relationship between the observed depolarization of μ^- mesons and the quadrupole deformation of the nucleus is correct, then we should theoretically[15] have the relationship $a_0(W) \approx 0.4\, a_0(C)$ between the values of a_0 for carbon and tungsten. The spin precession frequency of mesic tungsten atoms in a magnetic field should agree with the spin precession frequency of a free meson.

It can be shown with the aid of the normal error distribution that the case $\xi_e = \xi_T$ is rejected, since $\xi_e < \xi_T$ with 70% probability. This provides evidence that the experimentally observed "total" depolarization of mesons can hardly be accounted for only by meson interaction with the quadrupole deformation of the nucleus. In this connection it must be pointed out that experiments with palladium, chromium, and molybdenum indicate with high probability that in the case of tungsten we are also dealing with hyperfine structure due to spin coupling between the meson and electrons of the incomplete inner 5d shell.

Although tungsten atoms have a very small effective magnetic moment compared with chromium atoms, for example, the experimental technique is sufficiently sensitive to detect this magnetic moment. Muons have a magnetic moment one order of magnitude larger than the nuclear magneton, while the spin-flip time ($\sim 10^{-10}$ sec) of a meson in the field of the mesic-atom shell is many orders of magnitude shorter than the meson lifetime. In order to arrive at more definite conclusions it is obviously necessary to observe directly the spin precession curves of mesic Cr, Mo and W atoms.

The present and earlier investigations[1,9,12] lead to the following conclusions regarding the process of μ^- depolarization:

1) The interaction between the magnetic moments of the meson and electron shell affects meson polarization only in mesic atoms of the transition elements, lanthanides, and actinides.

2) Spin-orbit interaction reduces the polarization of μ^- mesons to one-sixth. This result agrees well with the theoretical calculations of Dzhrbashyan[6] and Shmushkevich.[7]

The authors consider it a pleasure to thank V. P. Dzhelepov for his continued interest. They are also indebted to S. S. Gershtein, D. F. Zaretskii and V. M. Novikov for discussions of the results.

---

[1] Egorov, Ignatenko, and Chultém, JETP 37, 1517 (1959), Soviet Phys. JETP 10, 1077 (1960).

[2] M. E. Rose, Nucleonics 3, 23 (December, 1948).

[3] Hughes, Lurio, Malone, Lederman, and Weinrich, Bull. Am. Phys. Soc. 3, 51 (1958); McColm, Hughes, Malone, Lederman, and Lurio, ibid. 3, 229 (1958); McColm, Ziock, Hughes, Penman, and Prepost, ibid. 5, 75 (1960); R. A. Swanson, Phys. Rev. 112, 580 (1958); Cassels, O'Keeffe, Rigby, Wetherell, and Wormald, Proc. Phys. Soc. (London) A70, 543 (1957).

[4] H. Überall, Phys. Rev. 114, 1640 (1959).

[5] Garwin, Lederman, and Weinrich, Phys. Rev. 105, 1415 (1957).

[6] V. A. Dzhrbashyan, JETP 36, 277 (1959), Soviet Phys. JETP 9, 188 (1959).

[7] I. M. Shmushkevich, JETP 36, 646 (1959), Soviet Phys. JETP 9, 449 (1959).

[8] I. S. Shapiro and L. D. Blokhintsev, JETP 37, 760 (1959), Soviet Phys. JETP 10, 542 (1960); E. I. Dolinskii, Dissertation, Nuclear Physics Research Institute, Moscow State University, 1959.

[9] Ignatenko, Egorov, Khalupa, and Chultém, JETP 35, 1131 (1958), Soviet Phys. JETP 8, 792 (1959).

[10] A. I. Alikhanov, Report at the Kiev Conference on High-Energy Physics, July, 1959.

[11] Jackson, Treiman, and Wyld, Phys. Rev. 107, 327 (1957).

[12] Ignatenko, Egorov, Khalupa, and Chultém, JETP 35, 894 (1958), Soviet Phys. JETP 8, 621 (1959).

[13] D. D. Yovanovitch, Phys. Rev. 117, 1580 (1960).

[14] G. F. Ford and C. J. Mullin, Phys. Rev. 108, 477 (1958).

[15] D. F. Zaretskii and V. M. Novikov, JETP 37, 1824 (1959), Soviet Phys. JETP 10, 1287 (1960).

Translated by I. Emin
59

SOVIET PHYSICS JETP VOLUME 13, NUMBER 2 AUGUST, 1961

THE INTERACTION OF 660-Mev PROTONS WITH CARBON, NITROGEN, AND OXYGEN NUCLEI

N. A. PERFILOV and Yu. I. SEREBRENNIKOV

Radium Institute, Academy of Sciences, U.S.S.R.

Submitted to JETP editor June 28, 1960

J. Exptl. Theoret. Phys. (U.S.S.R.) 40, 400-408 (February, 1961)

Sandwich emulsions (a 2μ gelatin layer between two 100μ emulsion layers) were used to record 1044 disintegrations of C, N, and O nuclei induced by 660-Mev protons. Analysis of the disintegrations indicates that the process involves a two-stage mechanism. The excitation energy, mean charge $\overline{Z}$, and mean mass $\overline{A}$, are estimated for the residual nucleus, which is formed after the cascade stage of the disintegration. The angular distributions of the charged particles are obtained. The mean lifetime of α-particle substructures inside light nuclei is estimated.

1. INTRODUCTION

THE disintegration of carbon, nitrogen, and oxygen nuclei by protons and neutrons with energies over 100 Mev has been studied in a series of papers.[1-10] The mechanism for this phenomenon has been experimentally obtained for the energy region ~ 100 Mev. It was found that when the incident particles have such energies, the C, N, and O nuclei disintegrate in two states,[1,2] as in Serber's disintegration mechanism.[11] The first stage consists of the development of an intranuclear cascade of nucleon-nucleon collisions leading to the direct emission of nucleons with the residual nucleus being left in an excited state, and the second stage consists of the decay of the excited residual nucleus. In a number of articles[8-10] it has been shown that among the ejected particles are a significant number of complex particles: H^2, H^3, He^3, and He^4. The idea is presented in these articles that nucleons inside nuclei apparently form for a certain time groups such as quasideuterons, quasitritons, and quasialpha particles (intranuclear substructures).

Fewer articles[4-8] have dealt with the disintegration of C, N, and O nuclei by nucleons with energies over 500 Mev. These articles supply only preliminary data and are mostly of a descriptive nature.

The results available in the preceeding articles are insufficient for extrapolating the two-stage disintegration mechanism to cases where the bombarding nucleons have energies substantially greater than 100 Mev. Not all the data are reliable enough for such an extrapolation. On the other hand, it can be assumed that such factors as the participation by the nuclear substructures in the nuclear cascade process, the increase in the number of ejected particles with an increase in the energy of the incident nucleons,[12] and the increase in the role played by meson absorption within the nucleus can cause complete fission of C, N, and O nuclei in the first stage at sufficiently high energies. A suggestion of this sort was made by Hodgson in an endeavor to explain some results observed in disintegrations of these nuclei by cosmic rays.[5] Such an assumption also follows from Messel's theory for nuclear cascade showers induced in the atmosphere by cosmic rays.

The present work was concerned with obtaining more detailed experimental data on the disintegration of C, N, and O nuclei by protons with energies over 500 Mev with the object of specifying more precisely the fission mechanism.

2. EXPERIMENTAL TECHNIQUE

Sandwich emulsions[3] consisting of a thin layer of gelatin (2μ) between two layers of P-9 emulsions,* each 100μ thick, were used to detect the fission of C, N, and O nuclei. This technique permitted a more complete collection of the disintegrations than would have been possible by using other criteria[7] to differentiate the disintegrations of light nuclei from all the disintegrations occurring in the emulsion.

The P-9 emulsion used was found to be sensitive to protons with $E_p < 30$ Mev by measurements of the visible postions of π^--meson tracks. Consequently, only charged particles with so-called

---

*The P-9 emulsions and sandwich emulsions were prepared in Prof. N. A. Perfilov's laboratory in the Radium Institute, Academy of Sciences, U.S.S.R.

"black" tracks (including α-particles with energies below ~ 500 Mev) were recorded.

Sandwich emulsions were exposed to a beam of 660-Mev protons extracted from the synchrocyclotron of the Joint Institute for Nuclear Research. The proton beam was incident parallel to the surface of the emulsion (with an accuracy of 1 to 2°).

All disintegrations centered in the gelatin layer of the sandwich (stars without visible centers) were ascribed to disintegrations of C, N, and O nuclei. Among these (about 1,000 stars), not a single star with 8 or more "black" prongs was discovered. This means that any possible contamination by disintegrations of Ag and Br nuclei which have diffused from the emulsion into the layer of gelatin amounts to less than 1%, since, according to Ostroumov's data,[12] stars with eight or more "black" prongs comprise about 13% of all the stars when Ag and Br nuclei are disintegrated by 660-Mev protons.

The charged particles emitted by C, N, and O nuclei were assigned into singly-charged, doubly-charged, or multiply-charged ($Z > 2$) categories by a method previously described.[13] The singly-charged particles were considered to be protons and the doubly-charged ones α particles.

The kinetic energy E of a charged particle was determined from the particle's total range in the gelatin and emulsion by using the relation

$$E = E(R_1) + 0.6\,[E(R_1 + R_2) - E(R_1)], \qquad (1)$$

which takes into account the difference in stopping power of the emulsion and gelatin. In Eq. (1) R_1 and R_2 are the ranges in the emulsion and gelatin respectively, and $E(R)$ is the particle energy corresponding to a range R in the emulsion.

The experimental data (with the exception of angular distributions) were corrected for the loss of particle tracks within the gelatin layer and for the emergence of tracks from the emulsion into the backing and air. Corrections were computed on the basis of an isotropic distribution of particles. In our case allowance for anisotropy would have reduced the magnitudes of the corrections by no more than 3%.

When stars centered within the gelatin layer are selected, false multiple-prong stars may be recorded if the centers of two disintegrations are near each other (up to $5\,\mu$ apart). We estimate that the probability of recording such false multiple-prong stars did not exceed 1%.

3. EXPERIMENTAL RESULTS

Altogether 1,044 C, N, and O disintegrations were recorded. The corrected distribution of the number of stars with various numbers of "black" prongs, N_h, is given below. In correcting for the losses it was assumed that the number of tracks lost in the gelatin was proportional to the total number of particles for each type of star.

N_h	1	2	3	4	5	6	7
Number of stars	28	245	383	257	101	26	4

Here the mean number of "black" prongs per star is 3.25, of which 1.94 were attributed to α particles and 1.29 to protons. Thus the α/p ratio is 1.5. According to references 3, 6, and 7 the average number of charged particles emitted by C, N, and O nuclei varies slightly with the energy of the bombarding nucleons and can be assumed to be 4.0 for energies of 500 - 600 Mev. Consequently, because of the sensitivity of the photographic plates used in our experiments, an average of ~ 0.75 fast protons ($E_p > 30$ Mev) per disintegration were not recorded.

The fraction of stars having recoil nuclei with $A > 4$ amounted to 25% after correction for losses in the gelatin. In the remaining 75% of the cases the C, N, and O nuclei were completely disintegrated into their component particles with masses $A < 4$.

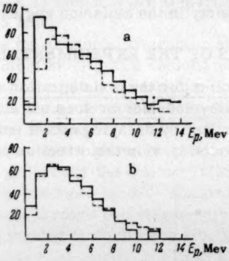

FIG. 1. Energy distribution (in l.s.) of secondary protons emitted into the forward (a) and backward (b) hemispheres measured relative to the direction of the bombarding protons (the ordinate represents the number of protons for 1 Mev energy interval). The solid lines represent the experimental distributions, $N_1(E)$ and $N_2(E)$, and the broken lines the calculated distribution $N_1'(E)$.

Figures 1 and 2 show the experimental energy distributions in the laboratory coordinate system for the secondary protons and α particles for both forward and backward hemispheres $N_1(E)$ and $N_2(E)$, measured relative to the direction of the bombarding proton beam.

The distributions of the emission angles projected on the plane of the emulsion are shown in Figs. 3 and 4. A separate distribution is given for protons with energies $0 < E_p \leq 3$ Mev, and simi-

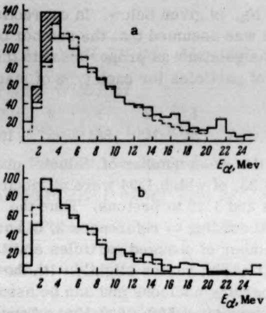

FIG. 2. Energy distributions (in l.s.) of α particles emitted into the forward (a) and backward (b) hemisphere (the ordinate represents the number of particles for 1 Mev energy interval). The solid lines represent the experimental distributions, $N_1(E)$ and $N_2(E)$, and the broken lines the calculated distribution, $N'_1(E)$. The correction for contamination by Li nuclei is indicated by the shaded area.

larly for α particles with energies $E_\alpha \leq 8$ Mev. The α particles for which $E_\alpha < 2$ Mev have not been incorporated in Fig. 4a, because of the shortness of their tracks in the emulsion and the consequent uncertainty in the emission angles.

4. ANALYSIS OF THE EXPERIMENTAL DATA

1. Mechanism for the disintegration of C, N, and O nuclei by 660-Mev protons. If all of the particles are emitted by decaying nuclei moving with some mean velocity v in the direction of the proton beam, then in the laboratory coordinate system the energy distribution of the particles in the backward hemisphere $N'_2(E)$ is related uniquely through the quantity v with the distribution in the forward hemisphere, $N'_1(E)$ and with the angular distribution of the particles $N'(\varphi)$. In other words, if v and $N'_2(E)$ are known, then $N'_1(E)$ and $N'(\varphi)$ can be uniquely computed.

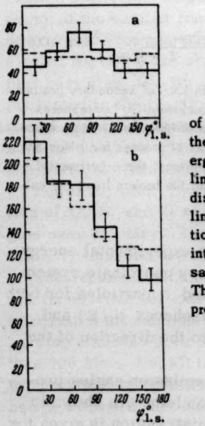

FIG. 3. Angular distributions of protons, $N(\varphi)$: a) energies in the range $0 \leq E_p \leq 3$ Mev, b) energies $E_p > 3$ Mev. The solid lines represent the experimental distributions, while the broken lines show calculated distributions, $N'(\varphi)$, for the same energy intervals and normalized to the same total number of protons. The ordinate gives the number of protons per 30° angular intervals.

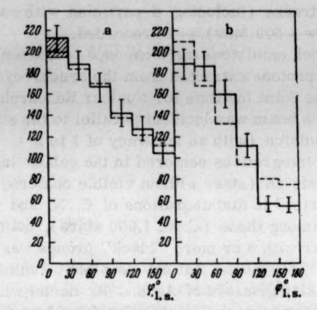

FIG. 4. The angular distributions for α particles, $N(\varphi)$: a) energies $2 \leq E_\alpha \leq 8$ Mev, b) $E_\alpha > 8$ Mev. The solid lines represent the experimental distributions, while the broken lines show the calculated distributions, $N'(\varphi)$, for the same energy intervals and normalized for $E_\alpha > 8$ Mev to the same total number of α particles; for $2 \leq E_\alpha \leq 8$ Mev, the $N'(\varphi)$ distributions have been plotted without normalization. The correction for contamination by Li nuclei is indicated by the shaded area. The ordinate gives the number of α particles per 30° angular intervals.

We have looked for such correlations in our data. From the ratio of the number of α particles with energies $E_\alpha < 4$ Mev emitted forward to those emitted backward the value of v was found to be $\sim 3.5 \times 10^8$ cm/sec. In this calculation it was assumed that for those disintegrations of the residual nuclei in which α particles occur with energies below the Coulomb barrier for C, N, and O nuclei (~ 4 Mev) the contamination by knock-on α particles must be a very slight (because of the opacity of the Coulomb barrier). From the experimental values for $N_2(E)$ and v the corresponding $N'_1(E)$ and $N'(\varphi)$ distributions were computed (within the limits of the model for the disintegrating nucleus) for both α particles and protons. In the computation it was assumed that the angular distribution of the emitted particles would be isotropic in the center-of-mass system of the decaying residual nucleus. The calculated distributions $N'_1(E)$ and $N'(\varphi)$ are shown by the broken lines in Figs. 1a, 2a, 3, and 4. In Figs. 1a, 2a, and 4a the calculated distributions are given as computed (i.e., without normalization) whereas in Fig. 3 and 4b,

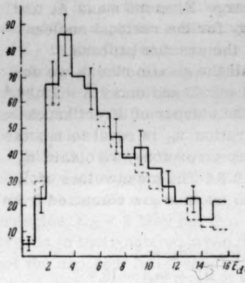

FIG. 5. The energy distribution $N_1(E)$ (in l.s.) for α particles emitted within the angles $45° \leq \theta \leq 90°$. The solid line represents the experimental distributions and the broken line the calculated distribution $N_1'(E)$ for the same angular region. The ordinate gives the numbers of α particles for 1 Mev energy interval.

for convenience in comparing form, the calculated distributions have been normalized to the same total number of particles observed experimentally.

When the $N(\varphi)$ and $N'(\varphi)$ distributions for the α particles are compared for the different energy intervals, it is found that they practically coincide for all $E_\alpha \leq 8$ Mev (Fig. 4a), i.e., when $E_\alpha \leq 8$ Mev there exists a correlation between the $N(\varphi)$ and $N_2(E)$ distributions. This fact is in conflict with the lack of correlation between $N_1(E)$ and $N_1'(E)$ for $E_\alpha < 8$ Mev (Fig. 2a). However, allowance must be made in Fig. 2a for the distortion of the experimental distribution due to contamination by tracks of Li nuclei (nuclear fragment), which, since their range in the emulsion is less than $30\,\mu$, could not be satisfactorily distinguished from α-particle tracks. To minimize this effect we made use of the fact that the probability of emission of Li fragments decreases sharply for increasing emission angles.[14] Thus the $N_1(E)$ and $N_1'(E)$ (unnormalized) distributions were formed for α particles emitted within the angle of $45° \leq \theta \leq 90°$ in the l.s. (Fig. 5). From Fig. 5, it is evident that a correlation also exists between the $N_1(E)$ and $N_2(E)$ distributions for α particles with $E_\alpha < 8$ or 9 Mev.

From Figs. 1 and 3 it is evident that such a clear partial correlation between distributions does not occur in the case of protons. Nevertheless, the comparison of the $N(\varphi)$ and $N'(\varphi)$ distributions in Fig. 3 reveals that at low proton energies these distributions have some characteristics in common (Fig. 3a).

Besides the attempt to find a correlation in the distributions in the l.s., a study was made of the energy and angular distributions of particles in a coordinate system moving in the direction of the proton beam at a velocity of 3.5×10^8 cm/sec. It was found that when the energies and angles of emission had been converted into this coordinate

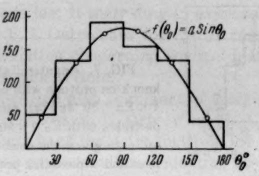

FIG. 6. The angular distribution (histogram) for α particles (with $4 \leq E_\alpha \leq 8$ Mev in the l.s.) in a coordinate system moving in the direction of the proton beam with a velocity of $3.5 \cdot 10^8$ cm/sec. The solid line shows the isotropic angular distribution, which has been normalized to the same number of particles. The ordinate gives the number of particles per 30° angular interval.

system, the angular distribution for α particles with $E_\alpha = 4$ to 8 Mev (in the l.s.) agreed quite satisfactorily with the isotropic distribution (Fig. 6). In the moving coordinate system the energy distributions for the particles in the forward $N_1(E_0)$ and backward $N_2(E_0)$ hemispheres (in relation to the direction of the proton beam) proved to be quite close to one another. Indeed, the ratios of the ordinates of these curves for the same energies E_0 are quite close to unity for proton energies $0 < E_{0p} < 11$ Mev and for α-particle energies $2 < E_{0\alpha} < 13$ Mev.

Thus, the experimental characteristics in a coordinate system moving at a velocity of 3.5 $\times 10^8$ cm/sec are in some respects like the characteristics in the center-of-mass system of the disintegrating nucleus.

On the basis of the above results it can be inferred that apparently the disintegrations of C, N, and O nuclei produced by 660-Mev protons pass, in most cases, through two stages with the residual nucleus making the main contribution to particle emission.

A different mechanism may come into play when C, N, and O nuclei are completely disintegrated into singly-charged high-energy particles (E > 30 Mev) and neutrons. Our detectors did not record these disintegrations. According to Philbert's data[6] they probably comprise no more than a few percent of the total events.

2. Characteristics of knock-on particles. As a rule the ordinates of the experimental distributions $N_1(E)$ and $N(\varphi)$ exceed those of the unnormalized calculated distributions $N_1(E)$ and $N'(\varphi)$. It is natural to attribute this to the presence of knock-on particles. After correction for contamination by Li nuclei (the shaded areas in Figs. 2a and 4a, which correspond to about 0.09 Li nuclei per disintegration), the difference between the experimental

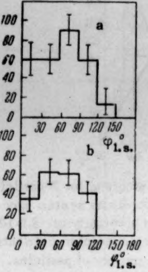

FIG. 7. Angular distribution for knock-on protons with energies $1 < E_p < 30$ Mev (a), and for α particles with $E_\alpha > 8$ Mev (b). The ordinate gives the number of protons and α particles per 30° angular interval.

and calculated distributions can be considered as characterizing the knock-on particles. Because of the small number of disintegrations, we have shown only the approximate angular distributions for knock-on particles (Fig 7). Figure 7 was obtained as the difference between $N(\varphi)$ and $N'(\varphi)$, with $N'(\varphi)$ normalized to the same number of particles as $N(\varphi)$ for the angular interval $150° < \varphi < 180°$ (it was assumed that practically no particles are knocked out at angles close to $\theta = 180°$ relative to the direction of the proton beam). From Fig. 7 we find that approximately 0.2 α particles are knocked out per disintegration, while about 0.28 protons are knocked out per disintegration with $E_p < 30$ Mev. In all about $0.28 + 0.75 = 1.03$ protons are knocked out per disintegration (here 0.75 is the number of protons per disintegration with $E_p > 30$ Mev, all of which can be considered as knock-on with negligible error).

For knock-on α particles the overall ratio of the numbers of particles emitted forward and backward was found to be 3.8; for knock-on protons with $E_p < 30$ Mev it is 2.8. Thus, even for light nuclei, 20 - 25% of the knock-on particles are emitted at angles $\theta > 90°$ relative to the direction of the proton beam.

From Figs. 1a and 3a it can be seen that knock-on protons may also have energies up to 1.5 Mev, which is somewhat less than the Coulomb barrier for C, N, and O nuclei (~2 Mev). As can be seen from Figs. 4 and 5, the knock-on α particles are emitted effectively only with energies $E_\alpha > 8$ Mev, although the Coulomb barrier of the C nucleus for α particles is $U_{\text{Coul}} \approx 4$ Mev., and does not limit their emission for energies $E_\alpha > 4$ Mev. Nevertheless, knock-on α particles with $E_\alpha < 8$ Mev are practically unnoticed in the background of α particles originating in the decay of the residual nuclei.

3. Decay characteristics of the residual nucleus. The data on the knock-on particles permits one to estimate the mean charge $\bar{Z}$, mean mass $\bar{A}$, and mean excitation energy for the residual nucleus formed as a result of the cascade process.

Weighing equally all the gelatin nuclei, we obtain a mean charge $\bar{Z} = 6.63$ and mass $\bar{A} = 13.26$.[4] Assuming that the mean number of direct knock-on neutrons per disintegration n_n is equal to n_p, the number of direct knock-on protons, we obtain $n_n = n_p = 1.03$ and $n_\alpha = 0.2$. The mean values of $\bar{Z}$ and $\bar{A}$ for the residual nucleus are computed from the obvious relations

$$\bar{Z} = \bar{Z}_0 - (n_p + 2n_\alpha) = 5.2,$$
$$\bar{A} = \bar{A}_0 - (n_p + n_n + 4n_\alpha) = 10.4.$$

The residual nucleus in turn emits an average of $N_\alpha = 1.94 - 0.09 - n_\alpha = 1.65$ α particles per disintegration (1.94 being the total number of α particles emitted per disintegration of the C, N, and O nuclei, and 0.09 being the correction for Li emission) and an average number of protons equal to $N_p = 1.29 - n_p = 1.01$. The decay of the residual light nucleus is thus characterized by a high α-particle yield ($\alpha/p = 1.65$). The excitation energy of the residual nucleus can be determined if the number of emitted particles and their mean kinetic energies in the nuclear center of mass system are known. These kinetic energies were computed and found to be $E_{0p} = 4.98$ Mev for protons and $E_{0\alpha} = 7.28$ Mev for α particles. In the case of the neutrons emitted by the nucleus, their energy E_{0n} was assumed equal to $\bar{E}_{0p}$ less the Coulomb barrier height of the B^{10} nucleus, which for protons is about 2 Mev, i.e., $\bar{E}_{0n} \sim 2.98$ Mev. The binding energy of a nucleon in the residual nucleus can be assumed to be about 6 Mev and that of an α particle about 3.3 Mev.

If it is assumed that the excited residual nucleus emits only protons, neutrons, and α particles and that the number of neutrons emitted is equal to the number of protons, then the mean excitation energy of the residual nucleus is about 35 Mev.

4. Average α-particle lifetime τ_α inside the nucleus. After considering the reasons why knock-on α particles are effectively emitted only with energies $E_\alpha > 8 \text{ Mev} > U_{\text{Coul}}$, we have assumed that this phenomenon is a consequence of α-particle instability inside the nucleus.[15]

A mathematical expression has already been proposed[15] to describe the energy spectrum of the ejected α particles, with allowance for their disintegration during the time they move through the nucleus. It is assumed that the probability of disintegration can be described by an exponential law of the form

$$N(E) = f(E)\,P(E)\exp\{-[m_\alpha/2(E+U)]^{1/2}\,l/\tau_\alpha\}, \qquad (2)$$

where f(E) is the recoil-energy distribution function of the α particle within the nucleus $(E > 0)$, P(E) is the Coulomb barrier penetration factor, l and τ_α are the shortest distance and average α-particle lifetime inside the nucleus, m_α is the mass, and U is the depth of the potential well for α particles.

With Eq. (2) and the data given in this article, one can estimate τ_α. For Eq. (2) to describe the fact that there are practically no α particles with energies $E_\alpha < 8$ Mev but that there is a rapid increase in their number when $E_\alpha > 8$ Mev, one can set the exponent in (2) equal to 3 for $E = E^* = 8$ Mev, i.e.,

$$[m_\alpha/2\,(E + U)]^{1/2} l/\tau_\alpha \approx 3. \qquad (3)$$

Then, for $E_\alpha < 8$ Mev, the exponential term will be smaller than unity, while for $E_\alpha > 8$ Mev, it will rapidly increase and approach one.

To estimate τ_α from Eq. (3), l should represent the shortest possible distance over which the α-particle structures maintain contact with the nuclear nucleons. We shall assume that α particles are most effectively knocked out from the surface layer of the nucleus. Thus, l should equal $2R_\alpha$, where R_α is the radius of a α particle. According to data in reference (16), the mean value for R_α is 1.8×10^{-13} cm. The value of U for a C^{12} nucleus can be assumed to be ~11 Mev.[9,10] Inserting these values in Eq. (3) we obtain the value $\tau_\alpha \approx 4 \times 10^{-23}$ sec.

Because of the lack of sufficient statistical accuracy in our data we cannot state emphatically that there are practically no knock-on α particles when $E_\alpha < 8$ Mev. Therefore, the value $\tau_\alpha \approx 4 \times 10^{-23}$ sec should be considered as the minimum mean lifetime of α particles inside the nucleus. On the other hand, the effect of a drop in the number of knock-on α particles with a decrease in their energy could not occur for $\tau_\alpha \geq 5 \times 10^{-22}$ sec if Eq. (2) is valid. Consequently, all we can say is that the value for τ_α must lie between 4×10^{-23} and 5×10^{-22} sec.

The authors feet it their duty to express their gratitude to V. I. Ostroumov for his extremely helpful consultation concerning several matters touched on in this article.

The authors are also cognizant of their debt to technical associates E. L. Grigor'ev, G. A. Leksin, and B. S. Neganov of the Joint Institute for Nuclear Research who cooperated in conducting the experiment at the Institute's synchrocyclotron.

---

[1] D. A. Kellog, Phys. Rev. **90**, 224 (1953).

[2] H. Muirhead and W. G. V. Rosser, Phil. Mag. **46**, 652 (1955).

[3] Blau, Oliver, and Smith, Phys. Rev. **91**, 949 (1953).

[4] P. E. Hodgson, Phil. Mag. **42**, 955 (1951).

[5] P. E. Hodgson, Phil. Mag. **43**, 190 (1952).

[6] M. G. Philbert, Compt. rend. **243**, 141 (1956).

[7] R. McKeaque, Proc. Roy. Soc. **236**, 104 (1956).

[8] Azhgireĭ, Vzorov, Zrelov, Meshcheryakov, Neganov, and Shabudin, JETP **33**, 1185 (1957), Soviet Phys. JETP **6**, 911 (1958).

[9] A. Samman, Compt. rend. **242**, 2232 (1956).

[10] A. Samman and P. Cuer, J. Phys. radium **19**, 13 (1958).

[11] R. Serber, Phys. Rev. **72**, 1114 (1947).

[12] V. I. Ostroumov, JETP **32**, 3 (1957), Soviet Phys. JETP **5**, 12 (1957).

[13] Yu. I. Serebrennikov, Научно-технический информационный бюллетень Ленинградского политехнического института (Sci.-Tech. Info. Bull. Leningrad Polytech. Inst.) No. **12**, 85 (1957).

[14] V. I. Ostroumov and Yu. P. Yakovlev, JETP **35**, 1359 (1958), Soviet Phys. JETP **8**, 949 (1959).

[15] Yu. I. Serebrennikov, JETP **35**, 789 (1958), Soviet Phys. JETP **8**, 547 (1959).

[16] I. I. Levintov, Nucl. Phys. **4**, 330 (1957); M. L. Rustgi and J. S. Levinger, Phys. Rev. **106**, 530 (1957).

Translated by A. Skumanich
60

SOVIET PHYSICS JETP VOLUME 13, NUMBER 2 AUGUST, 1961

FISSION OF ANTIMONY BY HIGH-ENERGY PROTONS

A. K. LAVRUKHINA, É. E. RAKOVSKII, SU HUNG-KUEI, and S. KHOĬNATSKII

Institute of Geochemistry and Analytical Chemistry, Academy of Sciences, U.S.S.R.

Submitted to JETP editor July 8, 1960

J. Exptl. Theoret. Phys. (U.S.S.R.) 40, 409-418 (February, 1961)

The fission of antimony nuclei induced by 660-Mev protons was studied. The fission yields as functions of A and Z are single-humped curves. The highest production probabilities are obtained for isotopes lying near the nuclear stability line. The fission is mainly symmetric, and is accompanied by the emission of a large number of charged particles. At $E_p = 660$ Mev the total fission cross section is 0.25 mb. Neutron-deficient isotopes are produced relatively more frequently by fissioning antimony than by heavy nuclei. The relative number of asymmetric fissions diminishes with decreasing incident proton energy.

The principal characteristics of fast-proton fission are shown to vary regularly with decreasing Z of the target nucleus.

1. INTRODUCTION

THE fission of medium-weight nuclei ($Z \lesssim 70$) was discovered in 1950 by Dzhelepov, Golovin, and Kazarinov,[1] using the ionization method of detection, in connection with the irradiation of ${}_{45}$Rh by 120-Mev neutrons. Radiochemical techniques were used soon afterward to detect individual fragments from the fission of ${}_{29}$Cu, ${}_{35}$Br, ${}_{50}$Sn, ${}_{56}$Ba,[2] ${}_{47}$Ag,[2,3] and ${}_{57}$La[4] by high-energy protons. However, the principal characteristics of fission in medium-weight nuclei have hitherto not been determined. Shamov's recent work,[5] in which nuclear emulsions were used to investigate Ag fission induced by 330 — 660-Mev protons cannot entirely fill the gap in our knowledge, since the acquired statistics did not provide an adequate basis for unequivocal conclusions.

The present situation results from difficulties in identifying the fission fragments of light nuclei, which are formed with considerably smaller probability than the products of competing nuclear reactions.

The present work investigates the products of the fission of antimony ($Z = 51$) induced by high-energy protons, with the aim of determining the principal characteristics of the fission process (the mass spectrum, isotopic distribution of fragments, nuclear charge distribution, and cross section).

2. EXPERIMENTAL TECHNIQUE

Special care was taken to prepare a pure target. It is known from the literature that cross sections for the production of individual fragments from fissioning medium-weight nuclei are in the range $10^{-29} - 10^{-30}$ cm^2. Therefore when the target contains as little as 10^{-3}% of the elements represented by the fission fragments or neighboring elements, the measured activities of individual radioactive fragments are considerably exaggerated. The targets were prepared from an ingot of metallic antimony after several purifications by the zone melting technique used in semiconductor technology. Spectral analysis performed by two different methods failed to detect impurity lines. The antimony was also analyzed by neutron activation. These experiments were performed by one of the present authors in collaboration with Yu. V. Yakovlev and L. A. Smakhtin. The following preliminary results show that the antimony did not contain amounts of impurities sufficient to affect appreciably the yields of its fission fragments:

Impurity element:	Mn	Cu	Zn	As	P	Cr	Ga
Content, %:	$3 \cdot 10^{-6}$	$3.5 \cdot 10^{-6}$	$8 \cdot 10^{-7}$	$4 \cdot 10^{-5}$	$8 \cdot 10^{-6}$	$5 \cdot 10^{-4}$	$3 \cdot 10^{-7}$

Samples of metallic antimony (0.5 — 1 g) were bombarded for one-half to three hours in the internal beam of the synchrocyclotron at the Laboratory of Nuclear Problems of the Joint Institute for Nuclear Research. The aluminum foil wrapping of the samples served to monitor the proton flux by the reaction $Al^{27}(p, 3pn)Na^{24}$, the cross section for which was taken to be 10 mb. Elements with atomic numbers from 11 to 37 were separated chemically. Special attention was devoted to developing in advance the most reliable techniques for separating fission fragments in

Table I. Yields of identified fragments from antimony bombarded with 660-Mev protons

Element	Mass number, A	Decay mode	$T_{1/2}$, experimental	$T_{1/2}$, experimental	$\bar{\sigma}$,* 10^{-30} cm^2
$_{11}$Na	24	β^-	14.5 hrs.	15 hrs	95 (2)**
$_{12}$Mg	28	β^-	21.5 hrs	21.2 hrs	9.0 (4)
$_{15}$P	32	β^-	14.1 days	14.3 days	3.0*
$_{16}$S	38	β^-	~ 3 hrs	2.9 hrs	0.7 (2)
$_{17}$Cl	38	β^-	~34 min	37.3 min	5.7 (3)
	39	β^-	58 min	55.5 min	1.2 (3)
$_{19}$K	43	β^-	~ 1 days	22.4 hrs	8.0 (3)
$_{20}$Ca	47	β^+	~ 6 days	~5 days	3.5 (3)
$_{22}$Ti	45	β^+, EC***	3.2 hrs	3.1 hrs	5.8 (3)
$_{23}$V	48	β^+, EC	16.7 days	16.0 days	6.8 (7)
$_{24}$Cr	48	EC	23.5 hrs	23 hrs	4.0 (5)
$_{25}$Mn	56	β^-	2.5 hrs	2.6 hrs	8.3 (3)
$_{26}$Fe	59	β^-	~46 days	45.1 days	8.0 (6)
$_{27}$Co	58^m	IT***	9.8 hrs	9 hrs	3.1 (5)
	61	β^-	~120 min	99—110 min	5.1 (5)
$_{28}$Ni	65	β^-	2.7 hrs	2.6 hrs	5.5 (2)
	66	β^-	~60 hrs	55 hrs	2.2 (2)
$_{30}$Zn	62	EC, β^+	9.3 hrs	9.3 hrs	3.9 (2)
	69^m	IT	~14.5 hrs	13.8 hrs	15 (2)
	72	β^-	48 hrs	49 hrs	1.1 (2)
$_{31}$Ga	66	β^+, EC	9.3 hrs	9.4 hrs	29 (5)
	67	EC	78 hrs	78 hrs	24 (4)
	72	β^-	14.8 hrs	14.3 hrs	3.0 (3)
$_{34}$Se	72	EC	9.8 days	~9 days	38 (2)
	73	β^+, EC	7.1 hrs	7.1 hrs	63 (2)
$_{35}$Br	75	β^+, EC	1.6 hrs	1.6 hrs	92 (2)
	76	β^+	16 hrs	17.2 hrs	32 (2)
	80^m	IT	4.3 hrs	4.4 hrs	24 (2)
$_{37}$Rb	86	β^-	18—23 days	18.7 days	440 (4)

*Average cross section for P^{32} production, taking into account certain data communicated privately by L. P. Moskaleva and V. V. Malyshev.

**The number of different determinations of the yield is given in parentheses.

***EC – electron capture; IT – isomer transition.

radiochemically pure form against the background of highly active antimony spallation products, which in many instances resemble the elements to be separated.

The activity of the samples was measured by a type MST-17 end-window counter. Individual radioisotopes were identified from their half-lives, and in some instances from the energy of emitted particles as determined by absorption in the aluminum foil.

A magnetic analyzer was used to determine the sign of the 38-minute activity observed in a chlorine fraction, which could be either β^- emission from Cl^{38} or β^+ emission from Cl^{34m}. Since positrons were not detected, it was established that the given proton bombardment of Sb produces Cl^{38} rather than Cl^{34m}.

Extremely weak radioactivities were measured by a setup consisting of type T-25 BFL back-to-back end-window counters in anticoincidence with a ring of MS-9 counters.[6] This resulted in 5 to 6 times greater efficiency than with end-window counters alone.

The cross sections for radioisotope production were corrected for self-absorption and self-scattering in the sample, for absorption in air, in the mica windows of counters, and in the wrappings of the samples, for reflection from the backing, and also for a difference in solid angle whenever this last circumstance affected counts from the sample and monitor. In the case of isotopes decaying by electron capture, corrections were also introduced for counting efficiency, absorption in the counter insensitive volume and the fluorescent yield. The accuracy of the cross sections ranged from 50 to 100%.

3. RESULTS AND DISCUSSION

Table I gives the half-lives $T_{1/2}$, the decay modes and average production cross sections $\bar{\sigma}$ of identified products from the bombardment of antimony with 660-Mev protons. Two groups of nuclides were identified (Fig. 1). The region from Rb to Zn $(Z \geq 30)$ comprises isotopes formed in antimony spallation. Here the yield diminishes sharply with increase of the difference $\Delta Z = Z_0 - Z$, where Z_0 denotes the atomic number of the original nucleus.

Fission products were found in the region $16 \lesssim Z \lesssim 28$, where the yield was observed to be

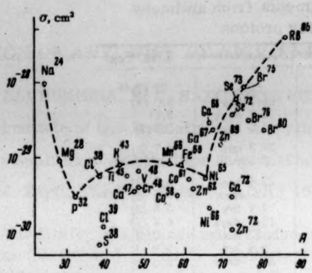

FIG. 1. Yields of identified radioactive products from antimony bombarded with 660-Mev protons.

practically independent of Z. An estimate of the excitation energy E_{exc} required to produce $_{23}V^{48}$ by antimony spallation gave ~ 700 Mev for a reaction involving both proton and neutron emission, and ~ 300 Mev for a reaction with α-particle and neutron emission (without considering cascade particles or the variation of the Coulomb barrier as a function of E_{exc}). Practically identical $_{23}V^{48}$ yields were obtained with the bombarding energies $E_p = 660$ and 220 Mev. The assignment of the given group to fission is also confirmed by nuclear-emulsion data,[5] which show a shift ΔZ between the fission-product regions of Ag and Sb representing the difference between the atomic numbers of these two target nuclei.

The yield of Na^{24}, which is considerably larger than that of Sb fission products, can be a result of fragmentation, as indicated by the angular distributions of this isotope when produced by the bombardment of several elements with 660-Mev protons.[7] Mg^{28} is also evidently formed by this kind of process. The assignment of the identified products of antimony bombardment to groups with different origins is somewhat arbitrary in view of their overlapping.

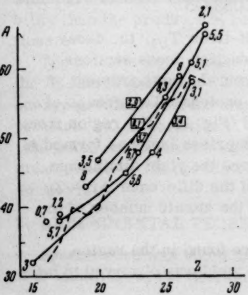

FIG. 2. Yields of radioactive fission products from antimony bombarded with 660-Mev protons. Mean values are enclosed in small boxes.

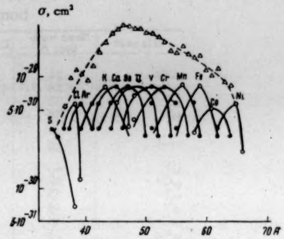

FIG. 3. Fission yields from antimony bombarded with 660-Mev protons as a function of mass number. Dashed curve – total yields; ○ – experimental; ● – interpolated; Δ – total yield for each A.

The yields of the unidentified stable, long- and short-lived radioactive fission fragments of antimony were estimated by interpolation on a plot (Fig. 2) in the coordinates A and Z, where solid lines connect nuclei formed with approximately equal yields. Most of the fission fragments lie very close to the (dashed) nuclear stability line. The cross sections for the formation of a number of unidentified isotopes were obtained by interpolation to within a factor of the order 2. The character of the distribution of antimony fission yields with respect to A and Z was determined from the combined experimental and interpolated data.

The yields are shown in Fig. 3 as a function of mass number. The single-humped curve is similar to those obtained in earlier work[8,9] for fission fragments of the heavy nuclei U, Th, and Bi. However, differences were observed in the character of the yield distribution. Antimony fission is characterized by the formation of fragments with a broad range of masses for each value of Z, from neutron-rich isotopes to those with relatively large neutron deficiencies, whereas the fission of heavy nuclei results principally in neutron-rich isotopes. The half-width of the humped curves in the latter case is considerably narrower (4 – 5 mass units) than in the case of antimony (7 – 8 units).

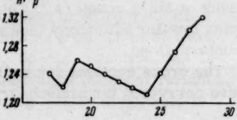

FIG. 4. Neutron-to-proton ratio of the antimony fission products with the largest yield for each Z.

Table II. Characteristics of fission induced by high-energy protons

Target nucleus	E_p, Mev	σ_{fis}, mb	$\sigma_{fis}/\sigma_{geom}$	Ratio of neutron deficient, stable, and neutron-rich fragments	Relative number of symmetric fissions, $\sigma_{sym\ fis}/\sigma_{fis}$	No. of emitted protons	No. of emitted neutrons	Reference
1	2	3	4	5	6	7	8	9
$_{92}U$	480	1650	0,73	11:21:58	0.32	—	19	[9]
$_{83}Bi$	480	100	$4.8\cdot10^{-2}$	12:28:60	0.45	—	15	[9]
$_{67}Ho$	450	2	$1.1\cdot10^{-3}$	—	0,71	4	18	[11]
$_{51}Sb$	660	0.25	$1.7.10^{-4}$	20:35:45	0.73	6—8	16	Present work

The yield peaks from the fission of antimony correspond to the isotopes $_{16}S^{34}$, $_{17}Cl^{38}$, $_{18}Ar^{40}$, $_{19}K^{43}$, $_{20}Ca^{45}$, $_{21}Sc^{47}$, $_{22}Ti^{49}$, $_{23}V^{51}$, $_{24}Cr^{53}$, $_{25}Mn^{56}$, $_{26}Fe^{59}$, $_{27}Co^{62}$, and $_{28}Ni^{65}$, most of which are stable. Figure 4 shows that the neutron-to-proton ratio N_n/N_p for most of these nuclei lies in the narrow range from 1.22 to 1.27. The only larger ratios are 1.29 for Co^{62} and 1.32 for Ni^{65}.

In the fission of heavy elements the maximum yield is found for isotopes with large neutron deficiencies.

The characteristics of the fission process in antimony result in a marked difference between the isotopic distribution of its fission fragments compared with those of heavy nuclei. Neutron-deficient, stable, and neutron-rich fission fragments of antimony are present in the ratio 20 : 35 : 45. The corresponding ratios for Bi, Th, and U,[7] given in Table II, are 12 : 28 : 60, 5 : 31 : 64, and 11 : 21 : 58, respectively. Antimony fission thus exhibits a considerably larger fraction of neutron-deficient isotopes.

An extensive literature exists on the mass distribution of fission fragments, but very little is known regarding their distribution with respect to nuclear charge. This results from the lack of data on the yields of "screened" isobars* among the fission products. Since the majority of the nuclides identified by us are "screened" isobars under the given experimental conditions, it is surely of interest to study their yields in order to determine the character of the nuclear charge distribution.

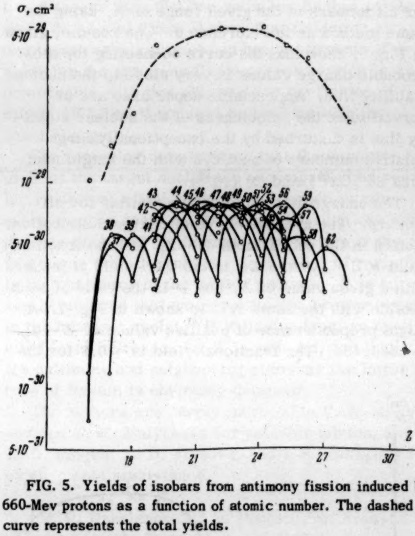

FIG. 5. Yields of isobars from antimony fission induced by 660-Mev protons as a function of atomic number. The dashed curve represents the total yields.

Figure 5 shows the charge distribution curves for isobars in the range A = 37 — 62. Yields estimated from the curves in Fig. 3 were taken into account. The charge distribution curves, like the mass distribution curves, are single-humped, with half-widths of three to four charge units. Similar curves plotted for the fission of heavy elements have considerably narrower half-widths (2 or 3 charge units).

FIG. 6. The most probable charge Z_p as a function of the mass numbers of antimony fission products. The dashed curve is the nuclear stability line.

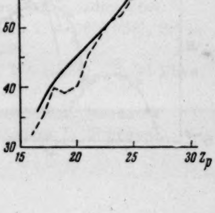

---

*"Screened" isobars are nuclides which under the given experimental conditions cannot be formed as a result of the decay of other nuclides with the same A.

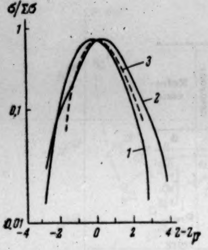

FIG. 7. Fragment charge distribution curves for the fission of (1) U and (2) Bi by 480-Mev protons, and (3) Sb by 660-Mev protons.

The most probable charge Z_p was determined for all isobars in the given range of A, using the same method as in reference 9. The results, given in Fig. 6, show that the curve connecting the most probable charge values is very close to the nuclear stability line. Appreciable departures are observed when the smoothness of the nuclear stability line is disturbed by the exceptionally large relative numbers of nuclides with the magic numbers 20 (Ca^{40}) and 28 (Ni^{58}).

The charge distributions are similar for all isobars. The average curve of charge distribution, plotted in the coordinates $Z - Z_p$ and the fractional yield $\sigma/\Sigma\sigma$ (where $\Sigma\sigma$ is the total yield of isobars with a given value of A, and σ is the yield of each nuclide with the same A), is shown in Fig. 7. A slight preponderance of positive values of $Z - Z_p$ is observed. The fractional yield is ~ 0.4 for the most probable charge, and ~ 0.05 for the least probable charge. The ratio of the maximum to the minimum fractional yield is one-seventh as large for antimony fission as for heavy-element fission. A similar reduction of the nuclear charge range is observed in heavy-element fission when the bombarding energy is increased.[10] The half-width of the charge distribution curve is 2.5 charge units for antimony fission and 3 units for U and Bi (Fig. 7).

The single-humped curve of the total yields of antimony fragments (the dashed curve in Fig. 5) indicates a large percentage of symmetric fissions, in agreement with Shamov's data.[5] Symmetric fissions and near-symmetric fissions (when $|Z_{sym} - Z| \leq 3$) comprise $\sim 73\%$. The three elements Ti, V, and Cr in the middle of the distribution contribute $\sim 34\%$. A similar result is obtained for Ho from an interpolation, like that above, using the data in reference 11. The data in column 6 of Table II show a decreasing proportion of symmetric fissions as Z of the target nucleus increases. Therefore fission asymmetry does not play as large a part in the case of medium-weight nuclei as could be expected from theoretical considerations.[12]

Figure 8 shows the distributions of total yields, with respect to Z, for fragments from Sb fission induced by 660-Mev protons and from the fission of Ho, Bi, and U induced by 450 — 480-Mev pro-

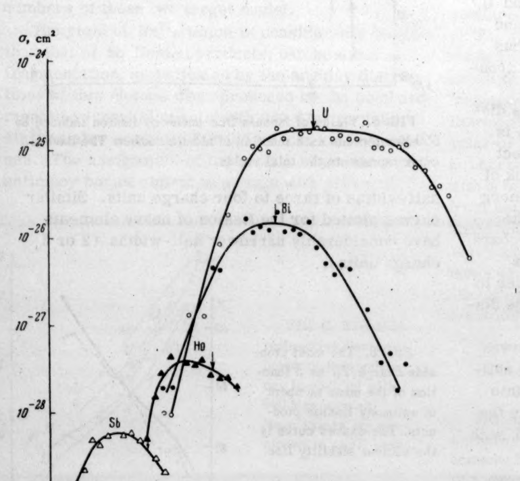

FIG. 8. Total fragment yields from the fission of U, Bi, Ho, and Sb induced by high-energy protons.

tons. The curves are gradually broadened as the target-nucleus charge increases. This is best seen from a comparison of the half-widths, which are 9, 10, 13, and 19 charge units for Sb, Ho, Bi, and U, respectively. The contribution of asymmetric fissions thus increases with Z of the fissioning nucleus. A similar effect from increased bombarding energy had been observed previously.[13-15] Special experiments showed that for antimony, as for other nuclei, the cross sections for the production of the asymmetric fission products Cl^{38}, Cl^{39}, Mn^{56}, and Co^{61} are reduced to one-tenth or less as the incident proton energy decreases from 660 to 220 Mev, whereas the yield of V^{48}, which is formed in symmetric fission, remains constant in the same proton energy range.

Figure 8 also shows that as Z of the target nucleus decreases the reduced half-widths of the fragment charge distributions are accompanied by a gradual shift of the peaks toward smaller values of Z compared with $Z' = (Z_{\text{init}} + 1)/2$. (In Fig. 8 values of Z′ are indicated by arrows.) This indicates that a considerable number of charged particles are emitted in the fission of medium-weight nuclei. The peak of the yield curve for antimony fission (Fig. 5) occurs at Ti (Z = 22) and V (Z = 23). In symmetric fission the formation of these two nuclei is accompanied by the emission of 6 to 8 protons, including the protons contained in emitted α particles and deuterons. The most probable number of emitted protons, including the incident proton, in antimony fission is therefore 7. This is in agreement with Shamov's result[5] $\bar{n}_{\alpha,p} = 6.5$ for Ag fission induced by 660-Mev protons.

Four protons are emitted in the fission of Ho (Table II, column 7). The peaks of the curves for U and Bi in Fig. 8 are located at $Z = (Z_{\text{init}} + 1)/2$. However, earlier data[16] show that $\bar{n}_{\alpha,p} = 0.8$ and 1.2, respectively, in the fission of U and Bi by 660-Mev protons.

The number of emitted charged particles is therefore enhanced with decreasing target-nucleus charge. It would appear that this circumstance should increase the probability for the formation of neutron-rich nuclei. However, as we have seen, neutron-deficient and stable isotopes play a relatively large part in antimony fission; this indicates the emission of a large number of neutrons in addition to protons. A calculation shows that the most probable antimony fission mode is accompanied by the emission of 15 to 17 neutrons.

The data in column 8 of Table II show that the number of emitted neutrons is practically independent of the target-nucleus atomic number.

It should be noted that the increased number of fission particles, especially protons, clearly indicates very high excitation energies for fissioning medium-weight nuclei.

A comparison of the curves in Fig. 8 shows that the fission yields from antimony are considerably smaller than from heavy nuclei. The total cross section for antimony fission by 660-Mev protons is 0.25 mb, which is 1.7×10^{-4} of the geometric cross section calculated from $R = r_0 A^{1/3}$, with $r_0 = 1.37 \times 10^{-13}$ cm.[17] The probability of fission increases greatly with Z of the target nucleus. Thus the cross section for uranium fission is 6600 times larger than that for antimony fission. Columns 3 and 4 of Table II show that fission is a dominant nuclear process in heavy elements. Our value for the antimony fission cross section is comparable with that obtained for the fission of silver (0.32 mb)[4] induced by protons with the same energy.

The foregoing data indicate that the variation of Z of the target nucleus is accompanied by regular variations of all fundamental fission parameters — cross sections, fragment distributions with respect to A and Z, isotopic distribution of the fragments etc., undoubtedly as a result of variation in the character of the fission process. It is currently believed that emissive fission predominates in the heaviest nuclei,[18] that fission from an excited level increases as Z is reduced, and that for antimony and neighboring elements the latter type of fission is obviously dominant.

The authors are deeply indebted to V. N. Mekhedov and T. V. Malysheva for valuable advice, and to L. D. Revina, L. D. Firsova, and I. S. Kalicheva for experimental assistance.

---

[1] V. P. Dzhelepov and B. Pontecorvo, Атомная энергия (Atomic Energy) **3**, 413 (1957).

[2] R. E. Batzel and G. T. Seaborg, Phys. Rev. **82**, 607 (1951).

[3] Kurchatov, Mekhedov, Borisova, Kuznetsova, Kurchatova, and Chistyakov, Conference of the U.S.S.R. Academy of Sciences on the Peaceful Uses of Atomic Energy, Session of the Division of Chemical Sciences, Acad. Sci. Press, 1955, p. 178.

[4] Lavrukhina, Krasavina, and Pozdnyakov, Doklady Akad. Nauk S.S.S.R. **119**, 56 (1958), Soviet Phys.-Doklady **3**, 283 (1958).

[5] V. Shamov, JETP **35**, 316 (1958), Soviet Phys. JETP **8**, 219 (1959).

[6] V. Baranov and L. Moskaleva, Заводская лаборатория (Factory Laboratory) in press.

[7] Lavrukhina, Moskaleva, Malyshev, Satarova, and Su Hung-Kuei, JETP 38, 994 (1960), Soviet Phys. JETP 11, 715 (1960).

[8] A. Lavrukhina, Doctoral Dissertaion, Institute of Geochemistry and Analytical Chemistry, U.S.S.R. Acad. Sci., 1955.

[9] A. Lavrukhina and L. Krasavina, Атомная энергия (Atomic Energy) 2, 27 (1957).

[10] Pate, Foster, and Yaffe, Can. J. Chem. 36, 1691 (1958).

[11] P. Kruger and N. Sugarman, Phys. Rev. 99, 1459 (1955).

[12] B. Geĭlikman, Collection, Физика деления атомных ядер (The Physics of Atomic Fission), Moscow, 1957, p. 4.

[13] Perfilov, Ivanova, Lozhkin, Ostroumov, and Shamov, op. cit. ref. 3, p. 79.

[14] Murin, Preobrazhenskii, Yutlandov, and Yakimov, ibid., p. 160.

[15] Lavrukhina, Revina, and Rakovskii, Doklady Akad. Nauk S.S.S.R. 125, 532 (1959), Soviet Phys.-Doklady 4, 361 (1959).

[16] A. Lavrukhina, Успехи химии (Progress in Chemistry) 22, 517 (1958).

[17] V. I. Moskalev and B. V. Gavrilovskii, Doklady Akad. Nauk S.S.S.R. 110, 972 (1956), Soviet Phys.-Doklady 1, 607 (1956).

[18] Perfilov, Lozhkin, and Shamov, Usp. Fiz. Nauk 70, 3 (1960), Soviet Phys.-Uspekhi 3, 1 (1960).

Translated by I. Emin
61

SOVIET PHYSICS JETP VOLUME 13, NUMBER 2 AUGUST, 1961

INVESTIGATION OF NUCLEAR-ACTIVE PARTICLES AND ELECTRON-PHOTON SHOWERS WITH ENERGIES $> 10^{12}$ ev *AT* 3860 m *ALTITUDE*

E. V. DENISOV, V. I. ZATSEPIN, S. I. NIKOL'SKII, A. A. POMANSKII, B. V. SUBBOTIN,
E. I. TUKISH, and V. I. YAKOVLEV

P. N. Lebedev Physics Institute, Academy of Sciences U.S.S.R.

Submitted to JETP editor July 12, 1960

J. Exptl. Theoret. Phys. (U.S.S.R.) 40, 419-425 (February, 1961)

An experimental arrangement for studying the interaction between nuclear-active particles with energies $> 10^{12}$ ev and air and carbon nuclei is described. Preliminary results on the energy spectrum of nuclear-active particles with energies $> 10^{12}$ ev are discussed.

THE present experiment was intended to study the nuclear-active and electron-photon components of high-energy cosmic radiation, in order to obtain additional data on the character of nuclear interactions at energies $\geq 10^{13}$ ev.

The measurements were carried out in the autumn of 1959 on the Pamirs, at 3860 m altitude.

The main part of the experimental array consisted of a detector of nuclear-active particles and high-energy electron-photon showers. The detector comprised four rows of ionization chambers, separated by lead and carbon (Fig. 1a). The first row contained 12, and the remaining rows 20 ionization chambers each. The chambers were 25 cm in diameter and 5 m long. The axes of the chambers of the rows 1 and 2 and also of the rows 3 and 4 were mutually perpendicular. Ten 12-counter hodoscope trays were placed above the detector. The area of each counter was 330 cm^2. The hodoscope served to determine the number of particles in the showers (Fig. 1b). To prevent the particles scattered in lead from reaching the hodoscope counters, the detector was covered by a layer of lead 3 g/cm^2 thick.

In addition to the elements of the array shown in Fig. 1b, two cylindrical chambers were placed 7 m from the center of the array, which made it possible to increase the range of detectable shower sizes. An additional hodoscope point, and a detector of the electron-photon energy density consisting of three ionization chambers covered by 2 cm of lead, were placed 28 m from the center of the array for the study of the fluctuations in the particle flux and in the energy density flux of extensive air showers (EAS).

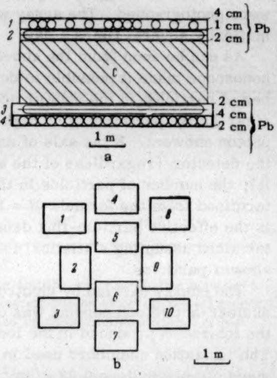

FIG. 1. a – vertical cross section through the detector of nuclear-active particles and high-energy electron-photon showers; b – position of the hodoscope points above the detector.

The electronic block diagram of the array is shown in Fig. 2. The pulses from each ionization chamber were fed to a separate amplifier. Independently, the pulses from the chambers in each row which were fed to the trigger circuit [i.e., chambers 3 – 7 of the first row, 6 – 15 of the second row, and 2 – 19 of the third and fourth rows (the chambers are counted from left to right in each row)], were added together. Whenever a coincidence of pulses from the triggering chamber groups in rows 1 and 2 or 3 and 4, greater than a certain threshold value, occured, the trigger and control circuit produced the master pulse that gated the circuits recording the pulses from the ionization chambers and initiated a scanning of the memory cells by means of a mechanical commutator. Pulses from the mechanical commutator were fed to an oscillograph with triggered sweep (one oscillograph was used for each chamber row) and were photographed. Simultaneously, the readings of the total-ionization analyzer and of the

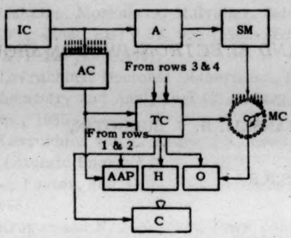

FIG. 2. Block diagram of the electronic circuitry: IC – ionization chamber, A – amplifier, SM – switch and memory cell, AC – addition circuit, TC – trigger and control circuit, AAP – analyzer of added pulses, H – hodoscope, O – oscillograph, C – camera, MC – mechanical commutator.

hodoscope, both triggered by the master pulse, were photographed. The array was tested automatically several times a day.

As can be seen from the above description, the hodoscope made it possible to determine the number of particles in the shower accompanying nuclear-active particles or in high-energy electron-photon showers. If the axis of an EAS fell upon the detector (regardless of the actual location in it), the number of particles in the shower was determined from the formula $N = 1000\rho$, (where ρ is the effective particle-flux density per m^2, determined assuming statistical independence of the shower particles.

The energy carried by electron-photon and nuclear-active components was determined from the ionization produced in the ionization chambers. The ionization chambers used in the detector were made of polyethylene 0.02 g/cm^2 thick, which practically excluded the transition effect in the chamber walls. The internal surfaces of the chambers were coated with a colloidal solution of graphite, forming a conducting layer. The chambers were filled with argon to a pressure equal to the atmospheric pressure at 3860 m altitude. Because of insufficient purity and poor seals, the argon in the chambers became gradually contaminated, which caused the electron current of the ionization pulses to change with time. The absolute calibration of the chamber sensitivity was made by comparing the spectrum of pulses obtained during short periods of time, separately for each chamber, with the spectrum obtained immediately after filling the same chamber. The sensitivity of the ionization chambers immediately after filling was assumed to equal the calculated sensitivity.

The energy carried by the electron-photon component was calculated from the number of particles measured in the two top-layers of the chambers, using cascade curves for lead and assuming that the cascade develops from a single photon.

In passing through a layer of lead equal to 14 radiation lengths, the energy of electrons and photons decreased to the order of the critical energy for lead. They were then rapidly absorbed in the carbon layer, since the critical energy for lead is much less than that for carbon.[1]

The thickness of the carbon (210 g/cm^2) was chosen so that, as a result of consecutive interactions of nuclear-active particles in the carbon, all the particle energy was transferred to the electron-photon component originating in the decay of the π^0 mesons. One can assume that the cascade multiplication and the absorption occur in lead only, if we take into account the relatively small number of radiation units in carbon and the great difference between the critical energies of electrons for carbon and lead, and if we assume that nuclear-active particles transfer their energy to a small number of π mesons.

The energy of nuclear-active particles was estimated under the assumption that nucleons and π mesons transfer one third of their energy to newly-produced π mesons in each act of interaction. The nuclear-interaction mean free path in carbon was taken as 70 g/cm^2.

The estimate results in the following relation between the number N of particles observed in one of the chambers of the lower row and the energy E of the nuclear-active particle which had interacted in the detector:

$$E = 2.3\cdot 10^8 N^{1.04} \text{ ev.}$$

The relation is correct for 10^{11} ev $\le E \le 5 \times 10^{14}$ ev. This relation was used in finding the energy spectra of the electron-photon showers in the atmosphere and of the nuclear-active particles which interacted in the array, as shown in Figs. 3 and 4.

A large fraction of bursts, produced both by electron-photon showers from the atmosphere and by nuclear-active particles which interacted in the matter of the detector, is accompanied by showers of charged particles in the atmosphere. The number of particles in the showers accompanying the ionization bursts was found from the readings of the hodoscope counters, assuming that the lateral distribution function in air is independent of the shower size. The number of ionization bursts unaccompanied by showers, or, more exactly, accompanied by showers with a total number of particles at the observation level $< 6 \times 10^3$,

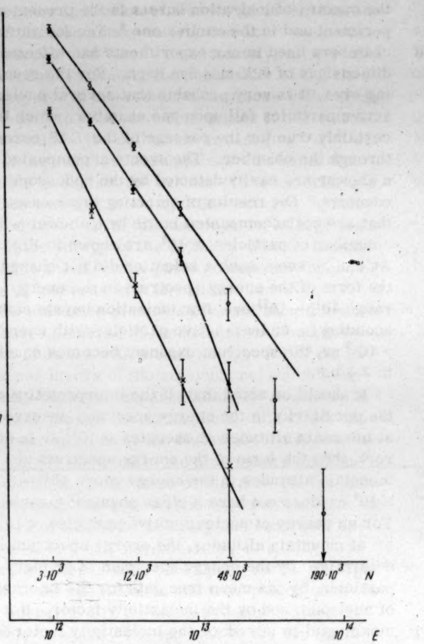

FIG. 3. Integral size distribution of ionization bursts produced by nuclear-active particles (lower scale shows the particle energy): ○ – all cases; ● – bursts unaccompanied by showers with a number of particles ≥ 10⁵; × – ionization bursts unaccompanied by showers with a number of particles ≥ 6× 10³. The y axis represents the flux of nuclear-active particles per m² per hour (logarithmic scale).

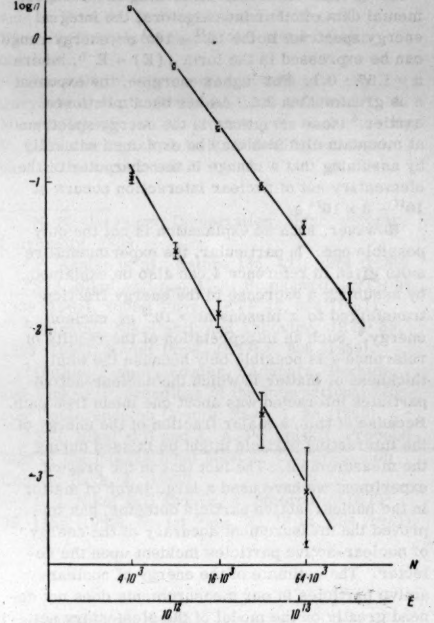

FIG. 4. Integral size distribution of ionization bursts produced by high-energy electron-photon showers: ○ – all events, × – bursts unaccompanied by showers with a number of particles ≤ 6 × 10³.

is shown in Figs. 3 and 4 by crosses. An approximately similar value of the absolute number of ionization bursts with a small density of the accompanying shower among nuclear-active particles and among electron-photon showers from the air, and also the relatively "soft" spectrum of the bursts, indicate that high-energy μ mesons may be one of the possible causes of these events. However, the comparison of our results with available data on the number of high-energy μ mesons[2] shows that not more than 15% of the events with a small accompanying density of charged particles in air can be attributed to μ mesons and, consequently, these cases should be associated with primary nucleons traversing the atmosphere with a small energy loss, or without any interaction whatsoever. The soft spectrum of the ionization bursts with a small accompanying density, as compared with the spectrum of all nuclear-active particles in the same energy range, indicates that the cross section for nuclear interactions does not decrease with increasing energy of interacting nucleons.

The high-energy electron-photon showers accompanied in air by a shower with a number of particles < 6 × 10³ may represent EAS produced in the depth of the atmosphere above the experimental array. We can calculate the contribution of such young showers to the flux of EAS observed at sea level if we compare the number of such events with the total number of electron-photon showers of the same energy. As can be seen from Fig. 4, for electron-photon showers of ~ 10¹² ev, this contribution amounts to less than 10%, which is in agreement with calculations.[3]

In measurements reported earlier,[4] a change in the energy spectrum of nuclear-active particles at mountain altitudes in the energy range 10¹³ – 3

$\times 10^{13}$ ev was observed. According to the experimental data of other investigators, the integral energy spectrum in the $10^{12} - 10^{13}$ ev energy range can be expressed in the form $f(E) \sim E^{-n}$, where $n = 1.57 \pm 0.1$. For higher energies, the exponent n is greater than 2.5. As has been mentioned earlier,[4] these variations in the energy spectrum at mountain altitudes may be explained naturally by assuming that a change in the character of the elementary act of nuclear interaction occurs at $10^{14} - 3 \times 10^{14}$ ev.

However, such an explanation is not the only possible one. In particular, the experimental results given in reference 4 can also be explained by assuming a decrease in the energy fraction transferred to π mesons at $> 10^{12}$ ev nucleon energy.[5] Such an interpretation of the results of reference 4 is possible only because the total thickness of matter in which the nuclear-active particles interacted was about one mean free path. Because of this, a major fraction of the energy of the interacting particle might be missed during the measurement. The fact that in the present experiment we have used a large layer of matter in the nuclear-active particle detector, has improved the measurement accuracy of the energy of nuclear-active particles incident upon the detector. The estimate of the energy of nuclear-active particles in our measurements does not depend greatly on the model of the elementary act, provided we assume that no nuclear-passive particles are produced.

The energy spectrum of nuclear-active particles observed in the experiment is shown in Fig. 3. The integral energy distribution of nuclear-active particles in the energy range $10^{12} - 10^{13}$ ev can be expressed as $f(>E) \sim E^{-n}$, where $n = 1.5 \pm 0.1$. In the energy range $10^{13} - 10^{14}$ ev, the exponent n becomes equal to 2.1 ± 0.4. This confirms the previous experimental data[4] and their interpretation. It does not seem reasonable to explain the observed kink in the energy spectrum of nuclear-active particles at mountain altitudes by a possible change in the energy spectrum of primary cosmic radiation, since the size spectrum of EAS in the corresponding interval does not show any peculiarities.

In the present experiment, the spectrum of ionization bursts corresponding to nuclear-active particles of $10^{13} - 10^{14}$ ev was found to be harder than that obtained in reference 4. Although large statistical errors do not permit us to consider this difference (3.5 ± 1 and 2.1 ± 0.4) as being serious, it is nevertheless necessary to point out a possible instrumental reason for the difference in the spectra of ionization bursts in the present experiment and in the earlier one.[4] The ionization chambers used in our experiments had effective dimensions of 0.25 m × 5 m each. For the resulting area, it is very probable that several nuclear-active particles fall upon one chamber, which is certainly true for the passage of the EAS cores through the chamber. The events accompanied by a shower are easily detected by the hodoscope counters. The results of selecting those cases that are not accompanied in air by a shower with a number of particles $\geq 10^5$ are shown in Fig. 3. As can be seen, such a selection did not change the form of the energy spectrum in the energy range $10^{12} - 10^{13}$ ev. For ionization bursts corresponding to nuclear-active particles with energies $> 10^{13}$ ev, the spectrum exponent becomes equal to 3 ± 0.8.

It should be noted that, if the interpretation of the peculiarity in the energy spectrum observed at mountain altitudes at energies $> 10^{13}$ ev is correct, then the form of the energy spectrum at mountain altitudes in the energy range $10^{13} - 3 \times 10^4$ ev does not have a clear physical meaning. For an energy of nuclear-active particles $< 10^{13}$ ev at mountain altitudes, the energy spectrum is determined by the energy spectrum of primary particles, by the mean free path for the interaction of nucleons, and by the inelasticity factor. If it is meaningful to introduce the inelasticity factor for nucleon energies $> 3 \times 10^{14}$ ev, then the same physical factors also determine the shape of the energy spectrum at energies $> 3 \times 10^{14}$ ev. For an inelasticity factor equal to one, the spectrum of nuclear-active particles at mountain altitudes represents the spectrum of primary cosmic-ray particles which reach the observation level without interaction.

In the intermediate range, the energy spectrum is not given by a power law and, in addition to the above factors, is determined by the fluctuations in the number of collisions and in the magnitude of the inelasticity factor, and also by the energy-measurement accuracy for each separate case of detection of a nuclear-active particle. If we attempt to estimate the value of the exponent n averaged over the whole range $10^{13} - 3 \times 10^{14}$ ev, and if we base ourselves on the interval width and assume that, for energies $> 3 \times 10^{14}$ ev, only those primary particles which passed the atmosphere without collisions are detected at the observation level, then $n \approx 2.5 - 3$. This value is in good agreement with the experiment.

Thus, the data on the energy spectrum of nuclear-active particles at mountain altitudes is yet another indication of the change in the character of the elementary interaction act of nucleons with energy > 10^{14} ev.[6] Unfortunately, all experimental data indicating the peculiarity of the elementary act of interaction of nucleons with energy > 10^{14} ev are indirect. This makes it difficult to find details of the collisions at energies > 10^{14} ev. One of the simplest assumptions which makes it possible to explain the results of the experiments on EAS was discussed by Nikol'skii and Pomanskii.[6] According to this assumption, a large fraction of the energy of the primary nucleon is transferred to the electron-photon component in collisions of nucleons with energies > 10^{14} ev.

The existence of such a process should lead to a relative increase of the number of electron-photon showers with a total energy $\gtrsim 10^{14}$ ev in the upper layers of the atmosphere, which is apparently observed experimentally.[7] However, in the lower part of the atmosphere, this effect should disappear because of the faster absorption of electron-photon showers in the atmosphere as compared with the absorption of electron-photon showers which are in equilibrium with nuclear cascade showers produced by primary nucleons with energies $\lesssim 10^{14}$ ev. Nevertheless, as can be seen from the comparison of the upper curves in Figs. 3 and 4, the spectrum of electron-photon showers with energy $\geq 10^{13}$ ev tends to become steeper, and this is exactly the opposite of the change in the spectrum of nuclear-active particles.

In conclusion, the authors express their gratitude to Prof. N. A. Dobrotin and Prof. G. T. Zatsepin for helpful comments on the results obtained.

The authors express their thanks to G. Ya. Goryacheva, G. B. Grishina, G. B. Minaeva, L. A. Miroshnichenko, A. M. Mozhaev, N. M. Nesterova, V. I. Sokolovskii, and A. E. Subbotina, who took part in the experiment.

---

[1] N. N. Goryunov, Dissertation, Moscow State University, 1959.

[2] F. Ashton et al., Nature **185**, 4710, 364 (1960).

[3] S. I. Nikol'skii and A. A. Pomanskii, JETP **39**, 1339 (1960), Soviet Phys. JETP **12**, 934 (1961).

[4] Murzina, Nikol'skii, and Yakovlev, JETP **35**, 1298 (1958), Soviet Phys. JETP **8**, 906 (1959).

[5] Duthie, Fisher, Fowler, Kaddoura, Perkins, and Pinkau, Proceedings of the International Moscow Conference on Cosmic Rays, **1**, 28 (1960).

[6] S. I. Nikol'skii and A. A. Pomanskii, Proceedings of the International Moscow Conference on Cosmic Rays, **2**, (1960).

[7] S. I. Nikol'skii and Yu. A. Smorodin, JETP **39**, 1156 (1960), Soviet Phys. JETP **12**, 804 (1961).

Translated by H. Kasha
62

SOVIET PHYSICS JETP VOLUME 13, NUMBER 2 AUGUST, 1961

MAGNETIC SPECTRUM ANALYZERS

E. K. ZAVOĬSKII and V. A. SKORYUPIN

Submitted to JETP editor July 18, 1960

J. Exptl. Theoret. Phys. (U.S.S.R.) 40, 426-432 (February, 1961)

The possibility of using paramagnetic and other magnetic resonance effects for studying radiation spectra has been investigated. The attenuation in helical and coaxial lines, sensitivity, saturation, and the limiting spectrum recording speed have been calculated. Descriptions are given of magnetic spectrum analyzers (MSA) of the following types: 1) frequency-compensated MSA, 2) "resonance" MSA, 3) induced-radiation MSA, and 4) induction MSA. The experimental results obtained with a frequency-compensated analyzer are reported; an oscillogram obtained at 3 cm with an MSA filled with the paramagnet $MnSO_4$ and an oscillogram showing the spectrum of an oscillatory spark circuit are also presented.

IN plasma investigations and certain other cases it is frequently necessary to measure a radiation spectrum over a wide frequency range in a very short period of time. The region of greatest interest is the wavelength range from 0.01 to 100 cm. In this paper we describe several methods of using paramagnetic and other magnetic resonance effects for studying radiation spectra.

PRINCIPLE OF THE METHOD

The principle of the method is the following: the radiation source is coupled to a broadband system, for example a cable or a helical line, which contains a paramagnetic material and is located in a quasi-static magnetic field. The line is terminated in its characteristic impedance and a detection device. When the frequency of the signal transmitted through the line equals the Larmor frequency of the material, the attenuation of the line increases markedly so that the signal is reduced, causing a corresponding reduction in the detector reading.

If the bandwidth of the input system and the line are both large, the range of frequencies which can be measured is determined only by the quasi-static magnetic field. For example, if the magnetic field can be varied from 10^2 to 10^5 oe, the frequency range for a paramagnetic material with a Lande factor of 2 corresponds to a wavelength range of 100 to 0.1 cm.

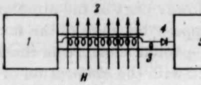

FIG. 1. Diagram of analyzer (the symbols are explained in the text).

A schematic diagram of an analyzer is shown in Fig. 1. Here, 1 is the broadband input device, which provides the coupling between the line 2 and the radiation system, 3 is the loading resistance for the line, which is made equal to the characteristic impedance, 4 is the broadband detector, 5 is the recording device (for example, an oscilloscope), and H is the quasi-static magnetic field. If an ordinary coaxial line is used, the quasi-static magnetic field must be parallel to the line. If the field is perpendicular to the axis of the line the paramagnetic-resonance attenuation factor is reduced by a factor of 2. The line 2 is filled with a paramagnetic material. The sweep in the recording device must be synchronized with the quasi-static magnetic field H.

We now consider the line parameters. The power absorbed by a cubic centimeter of paramagnetic material at paramagnetic resonance is given by the familiar relation:

$$P = \frac{\pi^2 \nu^2 g^2 \beta^2 H_\sim^2 N \delta f(\nu)}{4kTA} \frac{S(S+1) - M(M-1)}{2S+1}, \qquad (1)$$

where ν is the frequency, g is the spectroscopic splitting factor, β is the Bohr magneton, $H_\sim$ is the strength of the high-frequency magnetic field, N is the number of paramagnetic systems in a gram-molecule of the paramagnetic material, δ is the density of the paramagnetic material, k is the Boltzmann constant, T is the temperature, A is the atomic weight, $f(\nu)$ is a function which describes the shape of the paramagnetic resonance line, S is the spin and M is the magnetic quantum number.

We now consider the attenuation due to paramagnetic resonance in a long line. The velocity of propagation in the line is

$$v = c/2\pi r n_1 \sqrt{\varepsilon\mu}, \tag{2}$$

where c is the velocity of light, n_1 is the number of turns per centimeter of line, ϵ is the dielectric constant, μ is the magnetic permeability, and r is the helix radius. For a coaxial line,

$$v = c/\sqrt{\varepsilon\mu}. \tag{3}$$

First we consider a line with no ohmic losses. Dividing Eq. (1) by the energy transmitted per second through unit cross section, we find the attenuation per unit length of helical line:

$$\alpha = \frac{2\pi^4 \nu^2 g^2 \beta^2 N \delta f(\nu) r n_1 \sqrt{\varepsilon\mu}}{kTAc} \frac{S(S+1) - M(M-1)}{2S+1}, \tag{4}$$

whence, for g = 2 and s = ½, we have

$$\alpha = 3\pi^4 \nu^2 \beta^2 N \delta r_0 n_1 \sqrt{\varepsilon\mu} f(\nu)/kTAc. \tag{5}$$

Thus, at paramagnetic resonance the attenuation of the line is proportional to the square of the frequency and inversely proportional to the velocity of propagation.

Similarly, the attenuation factor for a coaxial line is

$$\alpha_c = \frac{\pi^3 \nu^2 g^2 \beta^2 N \delta f(\nu) \sqrt{\varepsilon\mu}}{kTAc} \frac{S(S+1) - M(M-1)}{2S+1}. \tag{6}$$

From Eqs. (4) and (6) we find the ratio of attenuation for a helical line and a coaxial line

$$\alpha/\alpha_c = 2\pi r n_1.$$

We now find the line attenuation due to effects other than paramagnetic resonance. The attenuation per unit length of line caused by conductor losses is denoted by α_0 while the nonresonance losses in the paramagnetic material are denoted by α_1; thus, the total attenuation per unit length of line is $\alpha + \alpha_0 + \alpha_1$.

We may estimate the minimum time in which a frequency spectrum can be analyzed in a line filled with diphenyl picril hydrazyl. Taking a relaxation time[1] $T_0 = 3 \times 10^{-8}$ sec with a half-width $\Delta H = 2$ oe, we find that the maximum rate of change of H is 7×10^7 oe/sec. Choosing a frequency range corresponding to the wavelength interval $\lambda = \infty$ to $\lambda = 0.5$ cm, we find the minimum time for a measurement to be 3×10^{-4} sec.

If the spectrum being investigated contains one or more monochromatic lines and the magnetic field is swept at a rate of 7×10^7 oe/sec the recording device 5 (Fig. 1) must have a bandwidth of 3.5×10^7 cps. If the spectrum is smoother, however, or if the paramagnetic resonance line is broader, the bandwidth requirements for the recording device can be relaxed. The conditions under which the spectrum-recording rate can be much greater than that indicated above are considered in a subsequent section.

LIMITING SENSITIVITY

We consider a line along which a traveling wave is propagated (Fig. 1). Let the power at the input of the line be P_0. The line attenuation when there is no paramagnetic resonance is denoted by $\alpha_2 = \alpha_0 + \alpha_1$ while the attenuation due to paramagnetic resonance at frequency ν is denoted by α; thus, the power at the end of a line of length L is

$$P = P_0 e^{-(\alpha_2 + \alpha)L}$$

while the change in power caused by the paramagnetic resonance is

$$\Delta P = P_0 e^{-\alpha_2 L} (1 - e^{-\alpha L}). \tag{7}$$

In order for measurements to be performed ΔP must be greater than the power due to thermal noise; i.e., in the limit

$$P_0 e^{-\alpha_2 L} (1 - e^{-\alpha L}) \approx 4 (2 P_0 e^{-\alpha_2 L} kT \Delta\nu)^{1/2}, \tag{8}$$

where $\Delta\nu$ is the frequency interval.

This relation determines the limiting sensitivity of the method: the sensitivity increases linearly with α when $\alpha L \ll 1$ and is independent of α when $\alpha L \gg 1$.

The sensitivity can be reduced considerably if the width of the paramagnetic resonance curve is very small compared with the line width of the radiation source. For this reason, sources with narrow low-intensity spectra must be investigated by means of paramagnetic materials with broad resonance lines. On the other hand, the absorption curve of the MSA at paramagnetic resonance can be broadened by inhomogeneity in the magnetic field over the volume of paramagnetic material. If the magnetic field inhomogeneity is $\Delta H'$, the frequency width of the paramagnetic resonance line in a field H is $\Delta\nu = (g\beta/h)(\Delta H' + \Delta H)$ where ΔH is the half-width of the paramagnetic resonance curve for a uniform field H. When this method of increasing the sensitivity of the MSA is used, account must be taken of the fact that the quantity $f(\nu)$ becomes $f(\nu) = h/g\beta(\Delta H' + \Delta H)$ as follows from Eq. (1); in this case it may be necessary to increase the length of the line L in order to compensate for the reduction of α due to $\Delta H'$ if the condition $\alpha L > 1$ is to be satisfied.

EFFECT OF SATURATING THE PARAMAGNETIC RESONANCE AND LIMITING SPECTRUM RECORDING RATE

When the signal amplitude is very large the paramagnetic resonance may be saturated, causing distortions in the measurements. This effect can become appreciable if the paramagnetic material is at a low temperature or if the strength of the radiation source is high.

If the line contains m grams of paramagnetic material, the maximum energy which can be absorbed within the relaxation time T_0 is

$$U = (N/A)(g\beta^2 H^2/kT)\, m, \qquad (9)$$

and if the pulse length $\tau < T_0$, the power of a pulse W which can cause saturation is $W = U/\tau$. If the recording device following the detector in the spectrum analyzer has a bandwidth $\Delta\nu$, the quantity $1/\tau\Delta\nu$ determines the "stretching" of the pulse if $\tau \ll 1/\Delta\nu$. This situation imposes a condition on the minimum power of the radiation pulse, which must yield a pulse at the recording device which is greater than noise. This power can be appreciable if $1/\tau\Delta\nu \gg 1$, and thus can cause saturation of the paramagnetic resonance. If saturation is to be avoided the condition $W < U/\tau$ must be satisfied.

If the spectrum measurement process is to be quasi-stationary, the rate-of-change of the magnetic field must be such that at any instant of time the spin system is in equilibrium with the lattice in the paramagnetic material. This requirement can be written in the form $\Delta H/\gamma > T_0$ where ΔH is the half-width of the paramagnetic resonance curve and $\gamma = dH/dt$ is the rate of change of the magnetic field. On the other hand, it is not always necessary that this requirement be satisfied. The measurement process can be a nonequilibrium process so long as the integrated radiation energy does not cause saturation of the paramagnetic resonance. Saturation effects remain unimportant so long as

$$\iint_{\nu_1\nu_2} w(\nu)\, d\nu dt \ll U_0, \qquad (10)$$

where $w(\nu)$ is the radiation energy at frequency ν applied in the measurement line,* ν_1 and ν_2 are the frequency limits of the spectrum being measured, and

$$U_0 = (N/A)(g\beta^2 H_0^2/kT)\, m, \qquad (11)$$

where H_0 is the initial magnetic field applied to the paramagnetic material.

The inequality in (10) has a simple meaning: if the total energy absorbed by the paramagnetic material in the measurement line in the frequency region between ν_1 and ν_2 in a time $t < T_0$ does not saturate the spin system, then the spectrum measurement can be carried out in a time shorter than that required to establish equilibrium between the spin system and the lattice in the paramagnetic material. In the limit, this time is comparable with the oscillation period of the spectrum.

It follows from the inequality in (10) that when $H_0 = 0$ the measurement of the spectrum requires that the variation of the magnetic field be quasi-static; on the other hand, as H_0 increases, saturation and stationarity of the field H_0 become less important. It is also apparent from (10) that at lower temperatures the spin system has a higher energy capacity and that the limitations imposed on the rate of change of the magnetic field γ are relaxed.

MILLIMETER AND SUBMILLIMETER WAVES

According to Eq. (1), at wavelengths of 1 mm and below paramagnetic absorption is so large that a thin film of paramagnetic material becomes opaque. However, it is difficult to produce the magnetic fields which correspond to this wavelength range. From the expression $\nu = g\beta H/h$ we see that a magnetic resonance is possible at high ν in weak fields if g is much greater than 2. In certain materials the g factor can be as large as 10 – 15.

We may also note that in certain semiconductors the effective mass differs considerably from unity and the cyclotron resonance is displaced toward weaker fields. For this reason, at very short wavelengths it is interesting to consider the possible utilization of cyclotron resonances. In this case the paramagnetic materials in the measurement scheme described above must be replaced by some other appropriate material.

USE OF FERROMAGNETIC RESONANCES

A ferromagnetic resonance can be used in an MSA in the same way as a paramagnetic or cyclotron resonance. For example, the absorption coefficient in ferrites is very large so that the measurement line can be very short. A shortcoming of ferrites is the nonresonant variation in loss as the fixed magnetic field is varied; this effect tends to complicate calibration of the absorption curve.

---

*We neglect line attenuation not due to paramagnetic resonance, while the attenuation due to paramagnetic resonance is assumed to be large.

Ferrites which are free of this disadvantage and which have narrow resonance lines may successfully replace paramagnetic materials in the region of relatively long wavelengths ($\lambda \geq 3$ cm). At shorter wavelengths, where the absorption coefficient in paramagnetic materials is large, ferrites show no particular advantage, especially if account is taken of the relatively long relaxation time characteristic of ferrites.

MSA SCHEMES

Four possible kinds of magnetic spectrum analyzers have been considered.

1. The frequency-compensated MSA.
2. The discrete-resonance MSA.
3. The induced-radiation MSA.
4. The induction MSA.

The various features of these versions of the MSA will now be described. In order to provide low-frequency compensation it is necessary to have two identical lines filled with paramagnetic material; these lines have a common input and a common load. The detector currents are first balanced. One of the lines is placed in a quasi-static magnetic field H. At paramagnetic resonance the signal applied to the detector in this line is reduced and a voltage pulse appears across the common load. This type of MSA is characterized by high sensitivity, large frequency-measurement range, and the greatest simplicity.

In the discrete-resonance spectrum analyzer a resonant coaxial line (or any other kind of line) is connected to a wideband input device. A detector and indicating device are connected at the other end of the line. The line is filled with paramagnetic material and placed in a field H.

The use of the resonance properties of the line allows us to reduce the required amount of paramagnetic material; by virtue of the Q of the line, its effective length is increased by a factor $Q\lambda/2\pi$. The spectrum which is obtained in this case is a line spectrum with a gain factor

$$\eta = 4Q/\pi n = cQ/\pi\nu L\sqrt{\varepsilon\mu},$$

where n is an odd integer and L is the length of the line. When $n = Q$ the gain approaches unity, $n = 4v/\pi c$, and the advantages of this system are lost accordingly.

An induced-radiation MSA can be used effectively for amplifying weak signals. An analyzer of this kind consists of a broadband input device, connected to the line filled with the paramagnetic material in the magnetic field H, the detector, and the recording device. In addition, we apply a radio-frequency signal to the input, thus increasing the population of the upper energy level of the paramagnetic material by a large factor as compared with the lower level.

Before the signal being studied is applied, the magnetic field is held at the resonance value corresponding to the rf frequency; when the signal is applied the field H is varied rapidly (compared with the relaxation time T_0) in order to traverse the entire frequency range of the spectrum being measured. Under these conditions the input signal is amplified in the line. A large population can also be obtained in the upper energy level without an rf generator if the sign of the magnetic field in the paramagnetic material is reversed rapidly when the input signal is applied.

An induction MSA can be used conveniently in the region of very short wavelengths since it eliminates the need for crystal detectors and the associated inconveniences of these devices. The features of this method are considered briefly below.

The magnetic field H in the frequency region of interest is varied rapidly from H_0 to H_1 (compared with the relaxation time T_0) where $H_0 \neq 0$ and $H_1 \neq 0$; to analyze the radiation spectrum we measure the magnetization vector in the paramagnetic material. The initial field H_0 magnetizes the paramagnetic material and the magnetization vector can be varied only under the effect of a radio-frequency field at a frequency corresponding to the instantaneous value of the resonance magnetic field $H = h\nu/g\beta$. Thus, the spin system is used here as both a memory and integrating device. The energy capacity of the spin system is $U_0 = (N/A)(g\beta^2 H_0^2/kT)\,m$ and can be rather large.

EXPERIMENTS

We have measured line attenuation due to the paramagnetic resonance and to nonresonance losses in a paramagnetic material, the sensitivity of the MSA, the dielectric permittivity of the paramagnetic material, and have verified the principles of operation of a frequency-compensated MSA. We

λ, cm	0.8	3.0	10.0
Paramagnetic resonance attenuation for a line with $L = 8.5$ cm, %			
measured	100	92	10
calculated	100	96.6	26
Measured dielectric permittivity ε	–	≈ 1.5	–
Nonresonance absorption for $L = 8.5$ cm in paramagnet, %	–	<2	–

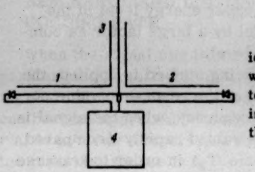

FIG. 2. 1 and 2 are identical lines, filled with paramagnetic material, 3 is a wideband input device and 4 is the detector.

have also obtained a paramagnetic resonance curve for $MnSO_4$ by rapid variation of the magnetic field as well as the spectrum of a spark discharge in an oscillatory circuit; the possibility of using a ferrite in an MSA has also been verified.

In the table we show the principal results of measurements with diphenyl picril hydrazyl [density $\delta = 1.54$ g/cm^3, $f(\nu) = 3.6 \times 10^{-7}$, $T = 300°K$] carried out with a line with $L = 8.5$ cm and a characteristic impedance of 30 ohms. It is apparent from the table that the measured attenuation for the paramagnetic resonances at $\lambda = 0.8$ cm and $\lambda = 3$ cm is in agreement with the calculated value; however, there are discrepancies at $\lambda = 10$ cm.*

The measured sensitivity of MSA is 10^{-9} watts at an amplifier bandwidth of 2 Mc/sec; however, in these experiments the sensitivity was limited by the high noise of the input stage of the amplifier rather than by detector noise. It would appear that the sensitivity can be improved considerably by modification of the input stage. A frequency-compensation scheme has been tried (cf. Fig. 2). This system uses standard demountable DKV-8 detectors; the internal resistance of these detectors can be controlled easily and it is possible to obtain signal cancellation up to 30 db. The demountable detectors have no parasitic resonances.

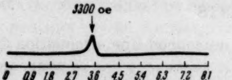

FIG. 3

In Fig. 3 we show an oscillogram obtained with an MSA filled with the paramagnetic material $MnSO_4$ using a 3-cm signal and a rate of rise $dH/dt = 2.5 \times 10^9$ oe/sec for the magnetic field. The measured half-width of the $MnSO_4$ resonance curve in the quasi-static magnetic field is 300 oe. The asymmetry and additional broadening of the curve in Fig. 3 are due to the inadequate bandwidth of the amplifier (5 Mc/sec). The tracing time for the magnetic resonance curve is 1.2×10^{-7} sec. The magnetic field is varied sinusoidally with a period of 20 μsec and an amplitude of 8.1×10^3 oe.

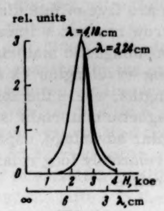

FIG. 4

In Fig. 4 we show the radiation spectrum of a small oscillatory spark circuit with a capacity of 3×10^{-12} farad and an inductance of 1.5×10^{-10} henry at a wavelength of 4.16 cm. For purposes of comparison we show the paramagnetic resonance curve for $MnSO_4$ at 3.24 cm (halfwidth, 300 oe). The halfwidth of the spectrum for the spark circuit indicates that $Q \approx 2.5$, corresponding to an oscillation period of 3.6×10^{-10} sec. This period is in good agreement with the emission time from the discharge, which has been determined earlier.[2] We have also carried out preliminary experiments with ferrites which show that these materials can be used in an MSA.

CONCLUSIONS

Both theory and experiment verify the possibility of the effective utilization of magnetic resonance effects for the static and dynamic analysis of radiation spectra over a broad wavelength region.

As compared with existing microwave devices the MSA has the advantage of extremely wide range, rapid and continuous frequency variation, and simplicity of construction.

A sensitivity of 10^{-9} watts has been obtained in the first experiments with a simple MSA. This sensitivity is far from the optimum which can be obtained and considerable improvement is to be expected.

In principle, the MSA can also be used in the millimeter and submillimeter region.

We wish to express our gratitude to Academician A. E. Arbuzov and Professor F. G. Valitova for preparation of the diphenyl picril hydrazyl and to Professor S. A. Al'tshuler for interesting discussions of this work.

---

*The origin of these discrepancies would appear to be the inaccurate determination of $f(\nu)$.

[1] Goldsborough, Mandel, and Pake, Phys. Rev. Letters 4, 13 (1960).

[2] E. K. Zavoĭskii and S. D. Fanchenko, Doklady Akad. Nauk SSSR 100, 661 (1955).

Translated by H. Lashinsky
63

SOVIET PHYSICS JETP VOLUME 13, NUMBER 2 AUGUST, 1961

THE EFFECT OF PRESSURE ON THE ELECTRICAL RESISTANCE AND GALVANOMAGNETIC EFFECT IN CHROMIUM TELLURIDE

N. P. GRAZHDANKINA, L. G. GAĬDUKOV, K. P. RODIONOV, M. I. OLEĬNIK, and V. A. SHCHIPANOV

Institute of Metal Physics, Academy of Sciences, U.S.S.R.

Submitted to JETP editor July 30, 1960

J. Exptl. Theoret. Phys. (U.S.S.R.) 40, 433-440 (February, 1961)

The temperature dependences of the electrical resistance and of the galvanomagnetic effect were measured in chromium telluride near the magnetic transition temperature at a pressure of 4,600 kg/cm^2. The shift in the Curie point under hydrostatic compression of the specimen was determined [Eq. (1)]. The variation in the exchange integral with interatomic distance in the Cr-Te system was also studied by measuring the electrical, magnetic, and galvanomagnetic properties of solid solutions of Cr-Te-Se. On the basis of the data obtained it is deduced from the thermodynamics of ferromagnetism that the nature of the change in spontaneous magnetization of CrTe is significantly different, depending on whether the reduction in the unit cell volume is produced by the hydrostatic pressure or by the introduction of selenium impurity.

INTRODUCTION

THE transition metals chromium and manganese form compounds with the elements of the subgroups V and VI-B which have the same crystal structure but different magnetic properties: ferromagnetic (CrTe, MnSb), antiferromagnetic (CrSb, CrSe, MnTe) or ferrimagnetic ($CrS_{1.17}$). There have recently been several experimental[1-3] and theoretical[4] studies of an interesting property of these compounds, which is the change in the spin ordering on substituting one of the components of these binary alloys by another of the same system, giving rise to solid solutions of the type $CrTe_{1-x}Se_x$, $CrTe_{1-x}Sb_x$, $MnCr_{1-x}Sb_x$, and $Mn_{1-x}Cr_xTe$. The change in the relative concentrations of the components of a ternary alloy leads to a change in spin ordering from ferromagnetic to antiferromagnetic (or the reverse), accompanied by a reduction in the magnetic transition temperature and a change in the lattice parameters. The transition from the ferromagnetic to antiferromagnetic state in these systems is related to the reduction in unit cell volume of the crystal.

In the present work an attempt is made to separate the influence of two factors on the spin ordering: volume changes and the change in the nature of the atomic neighbors. In order to study the change in Curie temperature Θ_f and in the spontaneous magnetization σ_s of chromium telluride under the influence of pressure, the temperature dependence of electrical resistance and the isotherms of the galvanomagnetic effect $\Delta R/R$ were measured in the region of the magnetic transition temperature at a pressure of 4,600 kg/cm^2 (we shall use $r = \Delta R/R$ for brevity). At the same time measurements on the ternary alloy $CrTe_{1-x}Se_x$ were carried out. The changes in Θ_f, σ_s, r, the resistivity ρ, and the elementary cell volume were determined as functions of selenium concentration ($0 \leq x \leq 0.1$), and the temperature dependences of σ_s, r and ρ of these alloys were investigated in the neighborhood of the Curie point.

APPARATUS AND METHOD OF MEASUREMENT

The high-pressure vessel used in the present work was made of 60G8N8Kh3V high-strength austenitic steel. A preliminary test of the vessel, by producing a hydrostatic pressure of up to 5,200 kg/cm^2 and then measuring the strength of the magnetic field inside its channel, showed that the deformation produced by this pressure in the cold state does not lead to the appearance of the ferromagnetic martensitic phase.

The specimen was contained in a 3.9 mm diameter channel in the lower part of the chamber, which in turn was 36 mm in diameter. This part of the chamber was placed between the poles of an electromagnet with a gap of 41 mm. Five conical type electrical leads were mounted on the upper part of the chamber on a special seal with copper packing rings. We used one lead for measuring the electrical resistance of a manganin manometer, in the form of a bifilar loop, laid in a groove of a special holder to which the specimen was fastened. The body of the chamber was used as the second lead for the manganin manometer.

To avoid additional electrical connections for measuring the temperature inside the chamber, the remaining four leads were used both for measuring the electrical resistance of the specimen and for temperature measurement. For this purpose, two copper-constantan thermocouples were attached to the ends of the specimen, the copper arms acting as current leads and the constantan as potential probes for the specimen. The cold junctions of the thermocouples were at atmospheric pressure and 0° C. By this simple arrangement the number of leads could be restricted to four, instead of the eight necessary for this sort of measurement.

The thermal emf of the thermocouples and the potential drop along the specimen were measured with a type PPTN-1 low resistance potentiometer and a M-21/IV mirror galvanometer with sensitivity 10^{-7}v/mm. While the thermocouple emf was being measured the primary current through the specimen was turned off so that there should be no Peltier effect at the junction of the specimen with the copper leads.

We did not take account of the effect of pressure on the thermocouple emf's since a control measurement of the emf of a "pressure thermocouple," made with arms of compressed and uncompressed metals, showed that the error introduced into the temperature determination can be neglected, for it does not exceed 0.024°. To remove errors due to extraneous effects, the measurements were made with the compensated current flowing in both directions, and the change of resistance in the magnetic field was determined for both directions of the field and of the current in the specimen. The maximum field strength was 8000 oe.

The hydrostatic pressure in the chamber was produced by a high pressure compressor using the system of L. F. Vereshchagin. Transformer oil was used as pressure transmitter. For thermostating, the chamber was surrounded by a brass case, through which was passed water from a Geppler ultra-thermostatic bath. In order to check on the absence of irreversible changes produced in the specimen by the pressure, control measurements of the temperature dependence of $\Delta R_{\perp}/R$ at atmospheric pressure and a field of 8000 oe were made at the end of a cycle of high pressure measurements.

EXPERIMENTAL RESULTS AND DISCUSSION

Figure 1 shows the results of the measurements of the effect of hydrostatic pressure on the electrical resistivity of chromium telluride at room temperature; points corresponding to increasing and decreasing pressure are shown by different symbols. It can be seen from the graph that the measurements with pressure increasing and decreasing give practically identical results: the resistivity increases with pressure, with the pressure coefficient $R_T^{-1}dR/dp$ equal to $(1 - 1.5) \times 10^{-4}$ kg^{-1}cm^2 within the range of measurement, which is two to three orders of magnitude greater than known values of $R_T^{-1}dR/dp$ for ferromagnetic metals and alloys.[5,6]

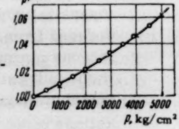

FIG. 1. The influence of pressure on the electrical resistivity of CrTe at room temperature; × – pressure increasing, ○ – pressure decreasing.

From the sign and magnitude of the pressure coefficient of resistivity it could be expected that hydrostatic compression should shift the Curie point of chromium telluride to lower temperatures, and that the magnitude of this effect should be fairly great. On this basis we tried to determine $d\Theta_f/dp$ from direct measurements of the temperature dependence of the electrical resistivity at high pressure, and not to calculate the effect from the measured temperature and pressure coefficients of resistivity in the region of the Curie point, as is usually done for small changes of Θ_f with pressure.[6]

Figure 2 shows the results of measuring the temperature dependence of resistivity at atmos-

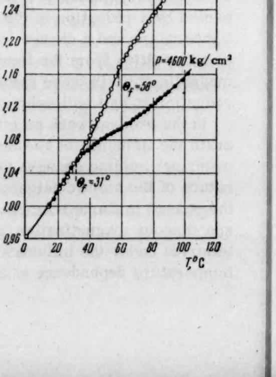

FIG. 2. The temperature dependence of the electrical resistivity of CrTe at atmospheric pressure and at p = 4,600 kg/cm².

pheric pressure and at 4600 kg/cm². It can be seen from the curves that the temperature of the Curie point, determined from the break in the R(T) curve, is +58° C at atmospheric pressure and +31° C at 4600 kg/cm². Repeated measurements showed good reproducibility of these data, giving the change in Curie point of chromium telluride under hydrostatic pressure as:

$$d\Theta_f/dp = (-5.9 \pm 0.3)\cdot 10^{-3}\ \text{deg-kg}^{-1}\text{cm}^2. \qquad (1)$$

The value of $d\Theta_f/dp$ was checked by measuring the galvanomagnetic effect $r = \Delta R/R$ at high pressures. The change in resistivity of CrTe in a magnetic field at $p = 4600$ kg/cm² was determined both above and below the Curie point. The isotherms of the galvanomagnetic effect r(H) obtained from these measurements are shown in Fig. 3. Figure 4 shows the curves of $r_\perp(t)$, representing the temperature dependence of the transverse galvanomagnetic effect at atmospheric pressure and at 4,600 kg/cm² in a magnetic field of 8000 oe. The change in Curie temperature under the influence of the hydrostatic pressure was determined in this case from the shift in the maximum of the galvanomagnetic effect $(-r)_{max}$ with the result, $d\Theta_f/dp = -6.2 \times 10^{-3}$ deg-kg⁻¹cm².

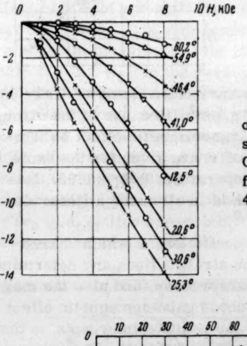

FIG. 3. Isotherms of the electrical resistivity change of CrTe with magnetic field at a pressure of 4,600 kg/cm².

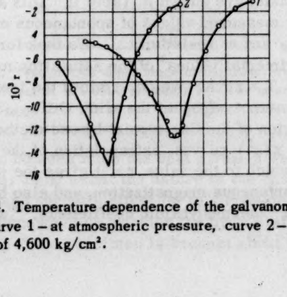

FIG. 4. Temperature dependence of the galvanomagnetic effect: curve 1 – at atmospheric pressure, curve 2 – at a pressure of 4,600 kg/cm².

We should point out that the value of $d\Theta_f/dp$ obtained is close to the magnitude of the effect in the invar alloys[7] (30% Ni, 70% Fe) and is the largest among all substances so far investigated.

Using the value of the compressibility* of chromium telluride $\kappa = (22 \pm 3) \times 10^{-7}$ cm²/kg we found $d\Theta_f/dV = 3.2 \times 10^{25}$ deg-cm⁻³.

It seemed of interest to compare the data obtained with the results of other measurements, in which the reduction in elementary cell volume is produced not by hydrostatic pressure but by introducing impurities with formation of substitutional solid solutions. The change in the Curie temperature of CrTe connected with the reduction in the interatomic distance on substituting tellurium atoms by selenium ($CrTe_{1-x}Se_x$) has been studied earlier by Tsubokawa[1] and by Lotgering and Gorter.[3] The results, while agreeing qualitatively with one another and with our data, disagree violently with one another quantitatively. For example, the values of Θ_f for chromium telluride given by different authors differ by 30° from one another and those of $d\Theta_f/dV$ differ by 37 – 40%.

We used three different methods for determining Θ_f in order to obtain more reliable data on the magnetic transition temperature of $CrTe_{1-x}Se_x$ alloys and on its variations with the elementary cell volume of the crystal: (1) from the break in the resistivity-temperature curve, (2) from the maximum in the galvanomagnetic effect r_{max}, and (3) from the disappearance of spontaneous magnetization, determined by the method of "thermodynamic coefficients" ($T = \Theta_f$ for $\alpha = 0$).[9]

The elementary cell volume of the alloys was determined by x-ray diffraction. The diffraction patterns were taken on a KROS-1 camera using a BSVL electron tube with chromium anticathode, with aluminum as the reference. The lattice parameters were calculated from the interference lines $(203)\alpha_1$, $(211)\alpha_1$ of the specimen and the lines $(113)\beta_1$ and $(222)\beta_1$ of the standard. These parameters and the elementary cell volumes of the $CrTe_{1-x}Se_x$ alloys are shown in Table I, together with the Curie temperatures determined by the three methods indicated above.

From the data of Table I, $d\Theta_f/dV$ was calculated as 3.5×10^{25} deg-cm⁻³, which agrees (within the limits of error of measuring the compressibility) with the value obtained in the pressure experiments. From this we can conclude that the interaction exchange integral in the Cr-Te

---

*The compressibility of CrTe was measured by Yu. A. Bazhin by a tensometric method.[8] We take this opportunity to thank him.

Table I. The lattice parameters a and c, the unit cell volume V and the Curie temperature Θ_f for $CrTe_{1-x}Se_x$ alloys

Composition	a, kX	c, kX	c/a	V, kX³	Θ_f, °C		
					1	2	3
CrTe	3.985	6.268	1.573	86.20	58.0	57.5	60.0
$CrTe_{0,93}Se_{0,07}$	3.974	6.241	1.570	85.35	29.5	27.0	35.0
$CrTe_{0,90}Se_{0,10}$	3.963	6.233	1.573	84.77	20.5	19.0	22.0

system changes proportionally with the reduction in elementary cell volume, independently of whether this reduction is produced by hydrostatic pressure or by the introduction of selenium impurity with the formation of solid substitutional solutions $CrTe_{1-x}Se_x$.

In order to decide whether hydrostatic pressure produces, besides a reduction in the interaction exchange integral, a change in the magnetic moment of the chromium atom in CrTe, we shall consider in more detail the isotherms of the galvanomagnetic effect which we measured at a pressure of 4,600 kg/cm². According to our measurements, the sign of the effect is negative, regardless of the relative direction of the current in the specimen and of the external field ($r < 0$ both for $H \parallel I$ and for $H \perp I$), which can be explained by the influence of the paraprocess, since the $r(H)$ curves obtained experimentally by us agree with the theoretical relations proposed by Akulov:[10]

$$r = aH^{2/3} \quad \text{for} \quad T = \Theta_f,$$
$$r = bH^2 \quad \text{for} \quad T > \Theta_f. \tag{2}$$

The law relating the galvanomagnetic effect to the magnetic field strength at the Curie point, analogous to the first equation of (2), can be obtained on the basis of the thermodynamic theory of ferromagnetism,[12] as was shown by Belov and Zaĭtseva,[11] using the relation found by Gerlach[13]

$$r_s = c\sigma_s^2, \tag{3}$$

where r_s is the value of the galvanomagnetic effect determined by the spontaneous magnetization. The coefficient a is then*

$$a = c\beta^{-2/3}\sigma_0^{8/3}. \tag{4}$$

Here β is a thermodynamic coefficient depending on pressure and temperature and σ_0 is the absolute saturation magnetization.

Figure 5 shows the variation of r with $H^{2/3}$ for chromium telluride at atmospheric pressure and at a pressure of 4,600 kg/cm², and also for the alloy $CrTe_{0.93}Se_{0.7}$, the elementary cell volume of which is equal to the elementary cell volume of CrTe at a pressure of 4,600 kg/cm². Because of the strong dependence of the galvanomagnetic effect on temperature, the values of r are given for the same values of reduced temperature $T/\Theta_f = 0.99$. It can be seen that there is in all cases a linear dependence of r on $H^{2/3}$.

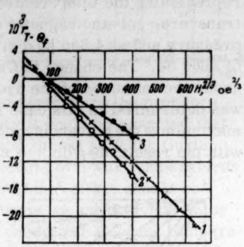

FIG. 5. The dependence of r on $H^{2/3}$: curve 1 – CrTe at atmospheric pressure, curve 2 – CrTe at p = 4,600 kg/cm², curve 3 – $CrTe_{0.93}Se_{0.07}$. at atmospheric pressure.

The values of the coefficient a which characterize the slope of the straight lines and determine the intensity of the paraprocess, and also the magnitudes of the spontaneous galvanomagnetic effect r_s, corresponding to the positive intercepts on the ordinate axis, are shown in Table II. This also gives our measured values of spontaneous magnetization σ_s and of resistivity ρ. We took for σ_0 the experimental values[3] of the saturation magnetization at T = 20° K. We determined the temperature dependence of σ_s of the alloy $CrTe_{0.93}Se_{0.07}$ in the region of the Curie point by two methods: from the $r(\sigma^2)$ curves, extrapolation of the linear parts of which to the value $r = 0$ gives the square of the spontaneous magnetization, and also by the method of "thermodynamic coefficients,"[9] which

---

*Equation (4) for the coefficient a differs from the analogous expression for a in Eq. (7) of Belov and Zaĭtseva's paper[11] in that in its derivation a term depending on the external magnetic field as σH was included in the expansion of the thermodynamic potential as a power series in the relative magnetization. In references 9 and 11 this term was included in the form ηH, which does not agree with the dimensions of thermodynamic potential, but corresponds to the energy of the magnetic field leading to saturation magnetization.

Table II

Composition	$10^{8}a$	$10^{9}r_s$	σ_s Gauss-cm³/g	σ_0 Gauss-cm³/g	$\cdot 10^{-4}\rho$, ohm-cm
			$T/\Theta_f = 0.99$	$T = 20°K$	$T = 291°K$
CrTe($p = \sim 1$ kg/cm²)	3.8	3.3	14.2	76.3	2.1
CrTe($p = 4600$ kg/cm²)	4.3	3.3	—	—	3.5
$CrTe_{0.93}Se_{0.07}$	2.6	2.3	10.1	75.0	8.2

made possible the simultaneous determination of the temperature dependence of the thermodynamic coefficient β.

Comparison of the results of measuring $CrTe_{0.93}Se_{0.07}$ with the earlier study of the temperature variation of spontaneous magnetization in CrTe[14] indicates that the magnetic transition in $CrTe_{0.93}Se_{0.7}$ is more spread out. The coefficient ξ in the well known relation $(\sigma_s/\sigma_0)^2 = \xi(1 - T/\Theta_f)$ is 1.44 for $CrTe_{0.93}Se_{0.07}$, which is considerably smaller than the value of ξ obtained for CrTe.

The dependence of the galvanomagnetic effect r on the reduced temperature T/Θ_f for CrTe at atmospheric pressure and at 4,600 kg/cm² and also for the alloy $CrTe_{0.93}Se_{0.07}$ is shown in Fig. 6. In all three cases the values of r are taken from the isotherms of the galvanomagnetic effect at a field strength H = 8000 oe. It follows that for $T < \Theta_f$, pressure leads to an increase in the absolute magnitude of the effect in CrTe, while for $T > \Theta_f$ (in the paramagnetic region) the $r(T/\Theta_f)$ curves at atmospheric pressure and at p = 4,600 kg/cm² practically coincide. This indicates that the observed change in the galvanomagnetic effect under pressure is connected with a change in magnetization produced by hydrostatic compression. The curve obtained for $CrTe_{0.93}Se_{0.07}$ lies appreciably below the first two over the whole temperature range examined.

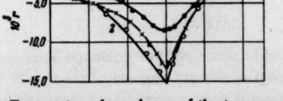

FIG. 6. Temperature dependence of the transverse galvanomagnetic effect at H = 8000 oe: curve 1 – CrTe at atmospheric pressure, curve 2 – CrTe at p = 4,600 kg/cm², curve 3 – $CrTe_{0.93}Se_{0.07}$ at atmospheric pressure.

It can be seen from the data given in Table II and Figs. 5 and 6 that the nature of the change in the galvanomagnetic effect is, to a considerable extent, dependent on whether the hydrostatic compression of the specimen is brought about by the action of pressure or by the formation of $CrTe_{1-x}Se_x$ solid solutions. The difference is seen primarily in the considerable increase in the intensity of the paraprocess produced by pressure, while the magnitude of the spontaneous galvanomagnetic effect r_s remains unchanged. Reduction of the elementary cell volume by introduction of selenium impurity leads to a reduction both in the intensity of the paraprocess, in r_s and in σ_0. The value of the electrical resistivity then increases fourfold.

If we assume that the coefficient c, which determines the relation between r and the square of the spontaneous magnetization [Eq. (3)], does not change with pressure*, then we can conclude that the whole change in spontaneous magnetization in CrTe produced by hydrostatic pressure is brought about only by a change in the exchange integral, with a constant value of the absolute saturation magnetic moment. According to (4) we can say that the observed increase in the intensity of the paraprocess under pressure is related to a decrease in the thermodynamic coefficient β with σ_0 constant. Kondorskii and Sedov[15] considered the reasons for a reduction in the absolute saturation magnetization in ferro- and ferrimagnetic substances under the influence of pressure. If we assume, according to earlier deductions,[14] that CrTe is a ferromagnetic with small s-d exchange interaction, then we may consider that the pressures employed do not bring about electron transitions from the s to the d band.

The decrease in the intensity of the paraprocess in $CrTe_{0.93}Se_{0.07}$ in contrast with CrTe (at p = 4,600 kg/cm²) is related both to a decrease in the absolute saturation magnetization σ_0 and to an increase in the thermodynamic coefficient β. We can explain the appreciable increase in ρ in the following way. Realizing that CrSe is antiferromagnetic, we can assume that substitution of tellurium atoms by selenium in the CrTe compound will lead to the existence of chromium ions with antiparallel spins; the indirect nature of the exchange interaction with the active part of the Se atoms must be dominant in this. The random distribution of ions with antiparallel spins leads to an increase in electrical resistivity of the alloy $CrTe_{0.93}Se_{0.07}$ due to scattering of conduction electrons by the fluctuations of magnetic moment.

---

*To some extent we can consider the basis for such an assumption to be the fact that there is only a small difference in the coefficient c (up to 2%) as determined by us for CrTe and for $CrTe_{0.93}Se_{0.07}$ from the $r(\sigma^2)$ curves for the same values of T/Θ_f.

The authors thank I. G. Fakidov and S. D. Margolin for making available the facilities for the magnetic measurements.

---

[1] I. Tsubokawa, J. Phys. Soc., Japan 11, 662 (1956).

[2] Hirone, Maeda, and Tsubokawa, J. Phys. Soc., Japan 11, 1083 (1956).

[3] F. K. Lotgering and E. W. Gorter, J. Phys. Chem. Solids 3, 238 (1957).

[4] T. Hirone and K. Adachi, J. Phys. Soc., Japan 12, 156 (1957).

[5] A. Michels and J. Strijland, Physica 8, 53 (1941).

[6] Michels, Jaspers, de Boer, and Strijland, Physica 4, 1007 (1937).

[7] L. Patrick, Phys. Rev. 93, 384 (1954).

[8] V. A. Gladkovskii and M. G. Kozhukhov, Физика металлов и металловедение (Phys. of Metals and Metallography) 3, 567 (1956).

[9] K. P. Belov, Usp. Fiz. Nauk 65, 207 (1958).

[10] N. S. Akulov, Ферромагнетизм (Ferromagnetism) Gostekhizdat, 1939.

[11] K. P. Belov and G. A. Zaĭtseva, loc. cit. ref. 8, 1, 404 (1955).

[12] V. G. Ginzburg, JETP 17, 833 (1947).

[13] W. Gerlach, Ann. Phys. (Leipzig) 8, 649 (1931).

[14] Gaĭdukov, Grazhdankina, and Fakidov, JETP 39, 917 (1960), Soviet Phys. JETP 12, 636 (1961).

[15] E. I. Kondorskii and V. L. Sedov, JETP 35, 845 (1958), Soviet Phys. JETP 8, 586 (1959).

Translated by R. Berman
64

SOVIET PHYSICS JETP VOLUME 13, NUMBER 2 JULY, 1961

RESONANCE OF DOMAIN WALLS IN COBALT FERRITE

T. M. PEREKALINA, A. A. ASKOCHINSKII, and D. G. SANNIKOV

P. N. Lebedev Physics Institute, Academy of Sciences, U.S.S.R.

Submitted to JETP editor August 8, 1960

J. Exptl. Theoret. Phys. (U.S.S.R.) 40, 441-447 (February, 1961)

A resonance dispersion of magnetic permeability due to domain-wall displacement processes is obtained in a monocrystal of cobalt ferrite. Resonance is observed at frequency 360 Mc/sec. A comparison is made with the theoretically calculated resonance frequency.

INTRODUCTION

THE dependence of the magnetic permeability of ferrites on the frequency at radio and microwave frequencies has two characteristic ranges, one due to motion of domain walls, and the range of natural ferromagnetic resonance. The nature of the dependence in the first of these ranges has not actually been established experimentally; however, a number of experiments[1,2] indicate that resonance dispersion occurs here.

It is known that in weak magnetic fields the magnetization is determined by ferromagnetic-domain wall-displacement processes. Döring[3] showed theoretically that a moving wall possesses an effective mass. The wall is bound to an equilibrium position by a quasi-elastic force. From the presence of a mass and an elastic bond it follows that the wall has a characteristic frequency of oscillation. Consequently, there should be observed a resonance dispersion of magnetic permeability, caused by wall-displacement processes.

In the presence of inertia $m\ddot{X}$, elastic restoring force $-\alpha X$, and frictional force $-\beta\dot{X}$, the equation of motion of a 180-degree wall under the influence of a pressure $2HI_s$ exerted by a magnetic field H, parallel to the wall, takes the form

$$m\ddot{X}+\beta\dot{X}+\alpha X=2HI_s. \tag{1}$$

On solving this equation for the case of an alternating field $H = H_0e^{i\omega t}$, we get for the magnetic permeability the well known resonance formula

$$\chi(\omega)=\chi_0\frac{1}{1-\omega^2/\omega_0^2+i\omega/\omega_1}, \tag{2}$$

where $\omega_0=\sqrt{\alpha/m}$, $\omega_1=\alpha/\beta$, and χ_0 is the initial magnetic susceptibility:

$$\chi_0=4I_s^2/\alpha l \tag{3}$$

(since $\chi = 2I_sX/Hl$, where l is the mean width of a domain).

In the present work, the resonance character of the dispersion associated with wall motion is established for cobalt ferrite.

METHOD AND EXPERIMENTAL RESULTS

The magnetic dispersion associated with wall-displacement processes was observed by Rado, Wright, and Emerson[1] in polycrystalline iron-magnesium ferrite (Ferramic A). They attributed the increase of the real part of the magnetic permeability, μ', of the specimen with increase of the frequency of the alternating magnetic field to the resonance character of this dispersion. However, they pointed out that μ' does not become less than unity, as should be the case with resonance, perhaps because of the superposition of a rotational resonance at a near frequency. Miles, Westphal, and von Hippel[2] observed the same sort of dispersion in polycrystalline nickel ferrite and nickel-zinc ferrite and in a monocrystal of nickel ferrite. They likewise obtained no values of μ' less than unity.

We constructed a coaxial line of square section. Such a line possesses all the advantages of the usual coaxial line: absence of dispersion, presence of a single TEM mode. It is important that the form of the magnetic lines of force is approximately square. Therefore if one cuts from a monocrystal a specimen in the form of a square frame, with sides along axes of easiest magnetization, then the alternating magnetic field will be parallel to the directions of the magnetization within the domains. By the same token, superposition of a natural ferromagnetic resonance is excluded, however near in frequency it may be to the resonance being observed. It is to be expected that for cobalt ferrite, because of its high magnetic anisotropy, the resonance associated with rotation of the magnetization vector in the magnetic-anisotropy field will lie in the millimeter-wave range and therefore will be in general unobservable in our experiment.

In the construction of the measuring line, we started from the specimen dimensions and as large as possible a frequency range. The outer dimensions of the coaxial were 10 × 10 mm, the inner 6 × 6 mm. The distance the probe could be moved along the line was 450 mm. The detector head was made in the form of a half coaxial resonator. Preparation of an assortment of attachments to the line, of various lengths (waveguide sections, in which the specimen is placed), made possible the measurement of the input resistances in the frequency range 200 to 300 Mc/sec. In the calculation of the input resistance, the specimen may be considered isotropic, since the magnetic lines of force of the high-frequency field are parallel to a single crystallographic direction.

To test the accuracy of performance of the apparatus, the magnetic permeability of a frame of Plexiglas was measured at several frequencies; as was to be expected, it was found equal to unity.

Monocrystals of cobalt ferrite were obtained by the method of Verneuil, in an oxyhydrogen flame. The composition of the ferrite, according to chemical analysis, was $Co_{0.94}Fe^{++}{}_{0.12}Fe^{+++}{}_{1.96}O_4$. Because of the presence of divalent iron, the crystals have a quite high electrical conductivity, which leads to difficulties in the observation of their magnetic susceptibility at high frequencies. We did not succeed in growing, by this method, crystals free from divalent iron.

To decrease the conductivity, the monocrystals were annealed in oxygen at 900° C. Divalent iron oxidized to trivalent, and the electrical conductivity decreased. By such an anneal, sufficiently prolonged, we succeeded in raising the specific resistance to 10^4 ohm cm.

Four square frames, of identical dimensions, were made. The outside dimensions of the frames were 10 × 10 mm, the inside 6 × 6 mm. (The inner opening was made by means of ultrasound.) The plane of the frames coincided to within tenths of a degree with the crystallographic plane (100), and the sides of the frames to within 2° with a direction of the type [100], i.e., with axes of easiest magnetization. The crystallographic directions were determined by x-ray diffraction ["epigrams" — Laue patterns by reflection — were taken]. The thickness of the frames was 3 mm.

Two frames made from the same crystal were annealed for six hours, two others for seven days. The resistivity of the first two frames rose to the value 10^3 ohm-cm (the chemical composition changed to $Co_{0.94}Fe^{++}{}_{0.06}Fe^{+++}{}_{2.00}O_4$), of the other two to the maximal value 10^4 ohm-cm.

For determination of the direction of magnetization and of the domain width, powder patterns on the frames were observed. For this purpose the surface of the frames was polished (mechanical polishing), and a drop of a ferromagnetic suspension was placed upon it. The powder patterns were observed under the microscope. The domain picture was photographed, and from the photographs the domain width was determined.

A photograph of the powder patterns for a frame annealed for six hours shows parallelism of the domains to the sides of the frame. The domain width (distance between walls) is from 3.7×10^{-3} to 6.4×10^{-3} cm. The domain width in frames annealed for seven days is an order of magnitude smaller, i.e., 3 to 4×10^{-4} cm. Thus in all the frames, parallelism of the alternating magnetic field to the direction of the domain magnetization was attained (with the indicated precision). An exception is the corners of the frames, where both the field and the domain configuration are more complicated. However, these corner regions occupy a small part of the whole body of the specimen, since the sides of the frames are narrow (2 mm). For this reason all the domains in the frames may be considered 180° ones, and the alternating magnetic field may be considered parallel to the domain walls.

The measurement was carried out over a range of frequencies that includes the whole region of noticeable absorption. The first two frames (with domain dimension 3.7 to 6.4×10^{-3} cm) showed a maximum of the magnetic losses at about 360 Mc/sec. Measurements on these were carried out over the range 250 to 450 Mc/sec. In the whole range of frequencies accessible to us (200 to 3000 Mc/sec), no absorption was observed for the other two frames, with the small domain dimension (2 to 3×10^{-4} cm).

The figure shows the behavior of the real (μ') and imaginary (μ'') parts of the magnetic permeability for the first two frames. The curves have a clear resonance character: μ' goes through a maximum and a minimum, in which the value of μ' is less than $\mu'(\infty)$; μ'' goes through a maximum.

We shall compare the curves obtained and formula (2). We first determine ω_0 and ω_1. This can be done by various methods: from the position of the maximum of μ'', from the intersection of

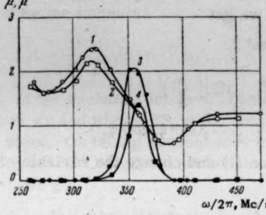

Dependence of the complex magnetic permeability $\mu = \mu' - i\mu''$ of a monocrystal of cobalt ferrite on the frequency of the alternating magnetic field: 1, μ' for frame No. 1; 2, μ' for frame No. 2; 3, μ'' for frame No. 1; 4, μ'' for frame No. 2.

μ' with the straight line $\mu'(\infty)$, from the position of the maximum and the minimum of μ'. The various methods of determination from the two curves give for the two frames, with deviation not exceeding 1%, the following values: $\omega_0 = 2\pi \times 360$ Mc/sec, $\omega_1 = 2\pi \times 2150$ Mc/sec.

On using these values and plotting the theoretical resonance curve according to formula (2), we discover that the experimental curve is narrower than the theoretical. This fact remains obscure. On the contrary, we should expect a broader experimental resonance because of different values of the parameter α for different walls, in consequence of the structure-sensitivity of this parameter.

As additional verification of the fact that the resonance obtained was not "instrumental," the measurements were repeated on the same specimens in the presence of a constant external magnetic field of intensity 10 000 oe. The magnitude of the field was sufficient to make the specimen a single domain. In this case no resonance was observed. Coaxial attachments of different length were also used. Identical results were obtained.

CALCULATION OF THE EFFECTIVE MASS OF A WALL

In order to compare the experimental values of ω_0 and ω_1 with the theoretical, it would be necessary to calculate α, β, and m. Inasmuch as we do not have sufficient quantitative information about inclusions and strains in our specimens, a calculation of the structure-sensitive parameter α according to a theoretical formula is not possible. However, it is possible by use of formula (3) to determine α from the value of the initial magnetic permeability, which we evaluated independently on one of the two frames ($\mu_0 = 2$). As regards the damping parameter β, which is a measure of the energy losses associated with wall motion, its physical nature is not yet clear, since the mechanism of losses in ferrites is not clear. Therefore we will not try to calculate ω_1 but will calculate ω_0. For this purpose we will calculate the effective mass m of the wall.

Döring[3] considered a domain wall in uniform motion in a cubic crystal and expressed its energy W in the form of a power series in the velocity v:

$$W = W_0 + mv^2/2 + \ldots \qquad (4)$$

The first term of the series is the energy of the wall at rest. The term linear in v drops out, since the energy is independent of the sign of the velocity. The quadratic term, if the remaining terms of the series are negligible, represents the kinetic energy of the moving wall. It is natural to regard the coefficient of $v^2/2$ as the effective mass of the wall.

The expansion (4) is carried out, essentially, in terms of a quantity λw^2, where $\lambda = K/2\pi I_s^2$ (K is the magnetic anisotropy constant), and w is a dimensionless velocity, $w = v\hbar n/2K\delta$ (n = number of spins in unit volume; $\delta = (Aa^2n/4K)^{1/2}$, a parameter describing the wall thickness; a = constant of the cubic lattice; A = mean value of the exchange integral). Thus for validity of the expansion (4) two conditions are necessary: $\lambda \ll 1$, which is satisfied for a whole series of materials, and $w \leq 1$. Döring assumed that the velocity was limited by damping processes.

Rado[4] extended Döring's derivation to the case of a field alternating in time, i.e., to the case of a wall in oscillatory motion. He obtained the same expression for the mass that Döring had obtained (under the condition $\lambda \ll 1$). However, the series expansion is now carried out in terms of the two dimensionless parameters

$$p = \gamma H_0/\omega \ll 1, \qquad q = \omega/\gamma(2K/I_s) \ll 1,$$

where γ is the magnetomechanical ratio and H_0 is the amplitude of the external field $H = H_0e^{i\omega t}$.

Smallness of the parameter p means that the frequency of oscillation of the external field is much larger than the frequency of the Larmor precession in the external field. Smallness of the parameter q means that the frequency of oscillation of the external field is much smaller than the Larmor resonance frequency for rotation in the internal anisotropy field. Both these conditions insure smallness of the velocity of the wall motion without allowance for damping processes, and consequently the legitimacy of neglecting terms above the quadratic in the expansion of the energy

W as a power series in the velocity v (equivalently, the mass is independent of the velocity). Rado remarked that the condition $\lambda \ll 1$ is not essential (it merely simplifies the calculation, making it possible to obtain an analytic expression for the mass) and can be dropped.

Since in our case the wall oscillates with the frequency ω of the external field, we will follow Rado[4] in the calculation of the mass. We are interested in the special case of a 180-degree wall. However, it is simpler (formally) to consider a 90-degree wall, as Rado did. The mass of a 180-degree wall is equal to twice the mass of a 90-degree wall.

The energy W of a wall layer in a cubic crystal, associated with 1 cm^2 of its surface, is given by the formula

$$W = \int_{-\infty}^{\infty} d\xi\delta \left\{ \frac{Aa^2n}{4} \left[\frac{1}{1-\alpha^2} \left(\frac{\partial\alpha}{\partial\xi} \right)^2 \frac{1}{\delta^2} + (1-\alpha^2) \left(\frac{\partial\varphi}{\partial\xi} \right)^2 \frac{1}{\delta^2} \right] \right.$$
$$+ K[(1-\alpha^2)\alpha^2 + (1-\alpha^2)^2 \cos^2\varphi \sin^2\varphi]$$
$$+ [2\pi I_s^2 (\alpha - \alpha_\infty)^2 + I_s H_0 e^{i\omega t} (1-\alpha^2)^{1/2}$$
$$\left. \times 2^{-1/2} (\sin\varphi - \cos\varphi)]\right\}, \tag{5}$$

where the first term is the exchange-interaction energy, the second is the magnetic anisotropy energy, and the third is the energy of interaction with the magnetic field. The dimensionless parameter ξ is $(x-X)/\delta$, where X is the coordinate of the center of the wall layer; φ and θ $(\alpha \equiv \cos\theta)$ are the polar angles of the direction of the mean magnetization in the wall layer, with respect to the normal to the wall as polar axis. The magnetic field is oriented as in Rado's paper[4] [Fig. 1, formula (16)].

Following Rado,[4] we seek a solution for α and φ in the form

$$\alpha(\xi, t) = \alpha_0(\xi) + \alpha_1(\xi)\, pe^{i\omega t},$$
$$\varphi(\xi, t) = \varphi_0(\xi) + \varphi_1(\xi)\, pqe^{i\omega t},$$
$$v(t) = 4\pi I_s \gamma\delta V_0 pe^{i\omega t}. \tag{6}$$

Without repeating the calculations,[4] we give the solutions for α_0 and φ_0,

$$\alpha_0(\xi) = 0, \quad \varphi_0(\xi) = \operatorname{arctg} e^{\xi} \tag{7*}$$

and the equation for α_1,

$$\left(\frac{d\alpha_1}{d\xi} \right)^2 - \alpha_1 \left(1 + \frac{1}{\lambda} - 3\sin^2\varphi_0 + 3\sin^4\varphi_0 \right)$$
$$= \frac{V_0}{\lambda} \sin\varphi_0 \cos\varphi_0. \tag{8}$$

We now substitute (6) in (5) and expand W in powers of p and q (for our ferrite, at resonance frequency $\omega = 2\pi \times 360$ Mc/sec, if we take $H_0 = 0.1$ oe, we get $p = 0.78 \times 10^{-3}$ and $q = 0.64 \times 10^{-2}$). On neglecting terms $\sim p^4$ in comparison with terms $\sim p^2$ and on neglecting q^2 in comparison with 1, we get

$$W = W_0 + mv^2/2,$$

$$m = \frac{1}{8\pi\gamma^2\delta} \frac{2\lambda}{V_0} \int_{-\infty}^{\infty} d\xi \left\{ \left(\frac{d\alpha_1}{d\xi} \right)^2 \right.$$
$$\left. + \alpha_1^2 \left(1 + \frac{1}{\lambda} - 3\sin^2\varphi_0 \cos^2\varphi_0 \right) \right\} \tag{9}$$

or, if we use (7) and change the variable of integration,

$$m = \frac{1}{8\pi\gamma^2\delta} \frac{2\lambda}{V_0} \int_0^{\pi} d(2\varphi_0) \left\{ \left(\frac{d\alpha_1}{d2\varphi_0} \right)^2 \sin 2\varphi_0 \right.$$
$$\left. + \alpha_1^2 \left(\frac{1 + 1/\lambda}{\sin 2\varphi_0} - \frac{3}{4} \sin 2\varphi_0 \right) \right\}. \tag{10}$$

In order to calculate m by this formula, it is necessary to know the solution of (8) for α_1. Rado solved this equation after setting $\lambda = 0$. In our case, however, λ is not small ($\lambda = 4$, $K = 4 \times 10^6$ erg/cm^3, $I_s = 400$ oe). Therefore it is not possible to solve (8) analytically. We use a variational method. The solution of (8) corresponds to the problem of searching for the minimum of the following functional:

$$S = \int_0^{\pi} d(2\varphi_0) \left\{ \left(\frac{d\alpha_1}{d2\varphi_0} \right)^2 \sin 2\varphi_0 \right.$$
$$\left. + \alpha_1^2 \left(\frac{1 + 1/\lambda}{\sin 2\varphi_0} - \frac{3}{4} \sin 2\varphi_0 \right) - \frac{V_0}{\lambda} \frac{d\alpha_1}{d2\varphi_0} 2\varphi_0 \right\} \tag{11}$$

(here a change of the variable of integration, as in (10), has already been introduced). Now we seek $\alpha_1(\xi)$ in the form of a series in powers of $\sin 2\varphi_0$ (since α_1 is an even function of ξ),

$$\alpha_1(\xi) = C_1 \sin 2\varphi_0 + C_2 \sin^2 2\varphi_0 + C_3 \sin^3 2\varphi_0 + \ldots \tag{12}$$

We determine the variable parameters C_1, C_2, C_3 from the condition that S be a minimum. Then on substituting (12) in (10), we get for $\lambda = 4$ the following value of the mass of a 90-degree wall (to within 1 in the third figure):

$$m_{90^\circ} = 0.24 / 8\pi\gamma^2\delta. \tag{13}$$

The value of the mass of a 180-degree wall, as has been mentioned already, is twice as large.

It is now still necessary to calculate the wall-layer thickness parameter $\delta = (Aa^2n/4K)^{1/2}$, and for this purpose it is necessary to know n and A. The number of spins in unit volume, n, can be determined according to the formula $n = I_s/\mu_B$, where μ_B is the Bohr magneton. We then get for n the value $n = 4.4 \times 10^{22}$ cm^{-3} ($I_s = 400$ oe). In this way, however, one generally gets a low value of n, since in a ferrite not all the spins are parallel.

---

*arctg = $\tan^{-1}$.

The mean value of the exchange integral A is determined by the formula

$$A = \frac{2S}{2a^2} \sum_{k \neq i} J_{ik} (x_i - x_k)^2,$$

where J_{ik} is the exchange integral of interacting atoms i and k, and where 2S is the number of spins per atom. On taking account only of interactions with nearest neighbors and on assuming them equal, we get

$$A = SJ\,(\Delta x)^2 z a^{-2},$$

where z is the number of nearest neighbors.

We estimate the exchange integral J from the condition that the kinetic energy at the Curie point is equal to the energy of exchange interaction (for one atom): $2SkT_C = 2JS^2z$. Hence

$$J = kT_c/Sz, \qquad A = kT_c\,(\Delta x)^2/a^2.$$

We take Δx in a ferrite equal to a/4. Consequently $\delta = 3.6 \times 10^{-7}$ cm ($K = 4 \times 10^6$ erg/cm^3, $a = 8.4 \times 10^{-8}$ cm, $T_C = 770$°K).

By formula (13)

$$m_{180°} = 0.48/8\pi\gamma^2\delta = 1.7 \cdot 10^{-10} \text{ g/cm}^2.$$

By formula (3)

$$\alpha_{180°} = 4I_s^2/\chi_0 l = 1{,}6 \cdot 10^9 \text{ g/cm}^2\,\text{sec}^2$$

($\chi_0 = 1/4\pi$, $l = 5 \times 10^{-3}$ cm; we take the mean value of the domain width, measured on photographs of powder patterns).

We now finally determine the value of the resonance frequency ω_0:

$$\omega_0 = \sqrt{\alpha/m} = 2\pi \cdot 500 \text{ Mc/sec}.$$

In view of the fact that some of the initial quantities in the determination of ω_0 are known only to one figure, the agreement with the experimental value $\omega_0 = 2\pi \times 36$ Mc/sec must be considered completely satisfactory.

The authors express their sincere thanks to K. V. Vladimirskii for advice and for discussion of the results of the research.

---

[1] Rado, Wright, and Emerson, Phys. Rev. **80**, 273 (1950).

[2] Miles, Westphal, and von Hippel, Revs. Modern Phys. **29**, 279 (1957).

[3] W. Döring, Z. Naturforsch. **3a**, 373 (1948).

[4] G. T. Rado, Phys. Rev. **83**, 821 (1951).

Translated by W. F. Brown, Jr.
65

SOVIET PHYSICS JETP VOLUME 3, NUMBER 2 AUGUST, 1961

PLASMA CONFINEMENT IN A TRAP WITH A MAGNETIC FIELD THAT INCREASES TOWARD THE PERIPHERY

S. Yu. LUK'YANOV, I. M. PODGORNYĬ and V. N. SUMAROKOV

Submitted to JETP editor August 24, 1960

J. Exptl. Theoret. Phys. (U.S.S.R.) 40, 448-451 (February, 1960)

The behavior of a plasma with a density of $10^{13} - 10^{14}$ cm^{-3} in a trap with a magnetic field that increases toward the periphery has been investigated. Ultrahigh-speed photographs show that plasma instabilities in such traps reduce the containment time.

THE present work is an extension of investigations which have been published earlier concerning the behavior of plasma in magnetic traps with fields which increase toward the periphery.[1,2] It has been shown in these investigations that the system can be filled with plasma by means of a coaxial electrodynamic injector which accelerates bunches of hydrogen plasma. The lifetime of the plasma formed in this way is of the order of tens of microseconds. The experiments described below have been carried out primarily for the purpose of investigating the effect of the mode of operation of the injector on the concentration of charged particles in the trap; in addition, it was desired to obtain information concerning the shape of the plasma formation in the trap as a function of time.

The first set of the experiments was carried out with a trap for accelerated bunches (TAB-1); the vacuum chamber of this system is stainless steel and is 100 cm high and 21 cm in diameter. The appropriate magnetic field configuration is obtained by connecting two solenoids, mounted on the vacuum chamber, in opposition. The maximum magnetic field in the gap between the coils is 1500 oe. The chamber pressure is $1 - 2 \times 10^{-6}$ mm Hg. The results reported below have been obtained with a 2.5-μF capacitor bank in the coaxial injector circuit[2,4]; the condenser-bank voltage was varied from 3 to 11 kv.

A Langmuir probe is used to measure the plasma parameters. The molybdenum cylindrical probe is placed at a point of zero magnetic field; the surface area of the probe is 0.6 mm^2. Various potentials (with respect to the chamber walls) are applied to the probe and the probe current as a function as time is observed by means of a pulsed oscilloscope.

In Fig. 1 we show a typical oscillogram of the saturation ion current to the probe with the solenoids in operation; the magnetic field in the gap between the coils is 1000 oe. It is apparent from this oscillogram that the plasma remains in the trap for a considerable period of time after the discharge current in the injector circuit no longer flows. The plasma containment time, i.e., the time during which the current to the probe falls off by a factor of e, is approximately 40 μsec in this case.

Conventional methods have been used to determine the electron temperature and the concentration of charged particles from the probe characteristics. In the experiments described here it was difficult to plot the probe characteristics because of the poor reproducibility of the oscillograms; hence, each point on the probe characteristic represents an average of 5 measurements.

In carrying out these experiments measures were taken to avoid arc discharges at the probes. Arcs are sometimes produced when a negative potential is applied to the probe, and these arcs cause considerably distortion of the oscillograms; in order to avoid arcs the probe is first processed for a long time in a discharge.

The probe measurements show that the charged-particle density in the trap increases rather rapidly as the injector voltage is increased. This behavior is illustrated in Fig. 2, which shows the ion saturation current at the probe J as a function of injector voltage. It is well known that J is proportional to the ion concentration if the temperature of the charged particles remains constant. Measurements carried out at two values of the injector voltage ($V_1 = 8$ kv and $V_2 = 11$ kv) indicate that the electron temperature does, in fact, remain essentially constant; in both cases the electron temperature (in energy units) is approximately 10 ev. Thus, the curve in the figure essentially represents the ion concentration in the trap as a function of injector voltage. The maximum plasma density (at V = 11 kv) is approximately 2×10^{13} cm^{-3}. It will be obvious that the absolute value of the charged-particle density quoted here must be used with

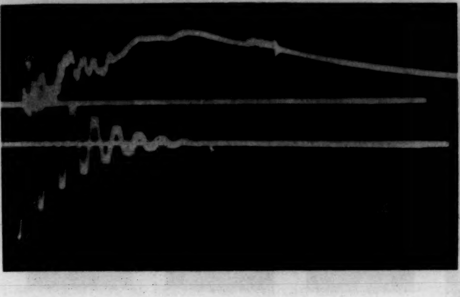

FIG. 1. The upper trace is an oscillogram of the ion probe current with the magnetic field on. The lower trace is the discharge current in the injector circuit. The sweep length is approximately 75 μsec.

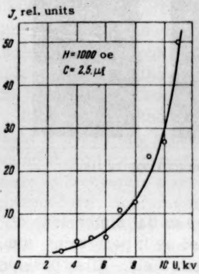

FIG. 2. The saturation ion current J as a function of the initial injector voltage U.

care. When either one or both of the solenoids are inoperative, i.e., in the absence of a trapping magnetic field, the vacuum chamber is not filled by plasma. Figure 3 shows the probe current obtained with the solenoids disconnected. In this oscillogram the gain of the system has been increased by a factor of thirty as compared with that used in the oscillogram shown in Fig. 1. A comparison of both oscillograms indicates once again that the plasma containment time in traps of this kind is of the order of tens of microseconds.

The shape of the plasma formation in the trap at different stages of the process has been investigated by taking pictures with an ultrahigh-speed movie camera. We may note that the photographic method was first used for studying the behavior of a plasma injected into a magnetic trap from a low power titanium-hydride source by Finkelstein et al.[5] In these experiments no time sweep was employed so that the behavior of the plasma as a function of time could not be investigated.

The TAB-1 system is not convenient for plasma photography because of the small size of the viewing windows in the chamber walls. For this reason, a small magnetic trap with a glass vacuum chamber (Fig. 4) was built for the ultrahigh speed photography. The magnetic field is produced by passing a current pulse through the coils shown in the diagram. The duration of the magnetic field pulse is 2000 μsec while the magnetic field in the region of

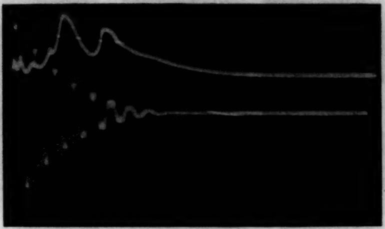

FIG. 3. The upper trace is the ion probe current with no magnetic trapping field. The lower trace is the current in the injector circuit. The sweep length is approximately 75 μsec.

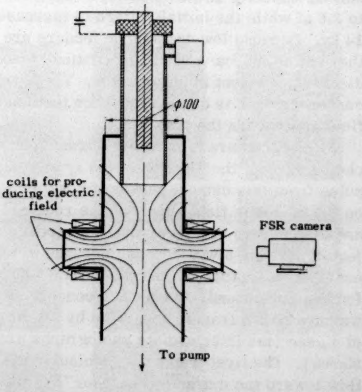

FIG. 4. Diagram of the magnetic trap designed for ultrahigh-speed movie photography of injection, capture, and plasma containment.

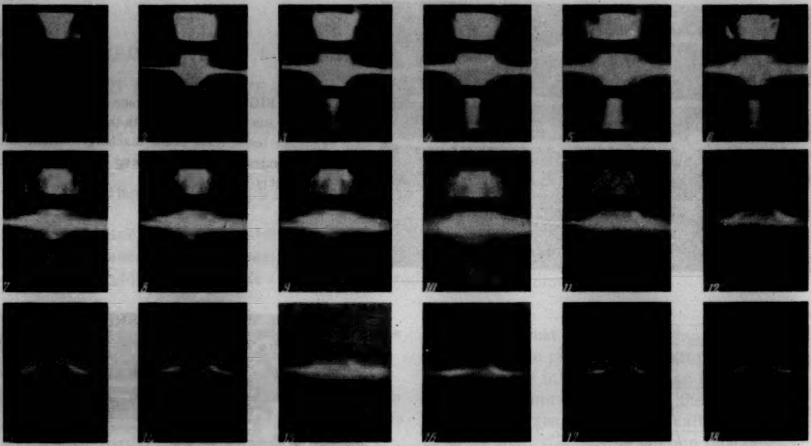

FIG. 5. Results obtained by ultrahigh-speed movie photography of the plasma with a magnetic trapping field. "Normal" plasma behavior. The time interval between frames is 4 μsec.

the magnetic gap is 6000 oe. The construction of the injector is the same as before; however, to increase the intensity of the emission in the trap the distance between the center of the trap and the injector is reduced considerably. For the same reason the capacity of the condenser bank is increased to 3.6 μf while the initial voltage is increased to 14 kv. Because low-inductance feeders are used there is no increase in the oscillation period of the discharge current in the injector. The injector condenser bank is discharged when the magnetic field approaches the peak value.

An SFR camera is used for ultrahigh-speed photography of the discharge; the synchronizing pulse from this camera makes it possible to switch on the magnetic field supply at the required time and also serves to trigger the discharge in the injector. In Fig. 5 we show photographs of injection and plasma capture in the trap obtained at 5×10^5 frames per second. In order to conserve space, we have shown frames separated by a time interval of 4 μsec (the intermediate photographs are not shown). The first frame shows clearly the plasma flow toward the magnetic "barrier"; in this frame one can also see weak emission from the surface from the lower flange of the chamber caused by the heavy fast particles which are produced in the operation of the electrodynamic injector. The energy of these particles is apparently so high that their trajectories are not affected in passing through the magnetic field of the trap.

As is to be expected, the radial dimensions of the plasma flow are reduced as it penetrates into the region of strong magnetic field. After passing through the magnetic barrier, the plasma is concentrated in the central portion of the trap; part escapes along the symmetry axis of the system. The plasma which is captured in the trap becomes a disc-shaped body of rotation. As is apparent from the photographs, this plasma formation exists stably for the entire lifetime of the plasma in the trap. The sharp boundary of the emission from the surface of the glass wall of the chamber serves as an indication of the width of the magnetic "gap" through which charged particles escape from the system.

The subsequent frames indicate that the plasma is contained in the trap for a time of the order of tens of microseconds after the injector ceases to operate. This result is in agreement with data obtained with probe and photoelectric measurements.

In an earlier work[2] the dependence of gap width on magnetic field was investigated by a calorimetric method. The results of the experiments were found to be in agreement with a classical mechanism for plasma diffusion across the magnetic field. A shortcoming of these data is the lack of information concerning the time behavior of the plasma diffusion processes. The images of the plasma formation obtained in these frames allow us to measure the width of the gap at different times.

It is reasonable to associate the experimentally observed gap expansion with the diffusion of plasma across the magnetic field. Using the formula for the width of the magnetic gap[3], we can make a rough estimate of the mean concentration of charged particles n from a knowledge (even if inaccurate) of the electron temperature in the plasma. Using the magnetic field indicated above and an electron temperature of 10 ev, we find $n \sim 3 \times 10^{14}$ cm^{-3}. This value of plasma density corresponds to an experimentally measured gap expansion of 5 mm in a time ranging from 10 to 25 μsec from the beginning of the process.

In Fig. 6 we show frames obtained under the same conditions as before but with the magnetic field switched off. The intense emission from the inner surface of the flanges and the walls observed in these photographs indicates that the plasma is able to escape to the walls easily; that is to say, the plasma is not contained.

It should be noted that stable plasma containment is not by any means observed in all cases in which there is a trapping field. On the contrary, there is frequently a marked distortion of the plasma formation; at certain stages of the process the plasma escapes via paths other than the magnetic gaps. Fig. 7 shows photographs which illustrate this anomalous plasma behavior. In this case the plasma lifetime is somewhat shorter than in the case shown in Fig. 5. It should be emphasized that both pictures were obtained under the same experimental conditions, with the same value of magnetic field and injector voltages and with the same neutral gas flow from the valve into the in-

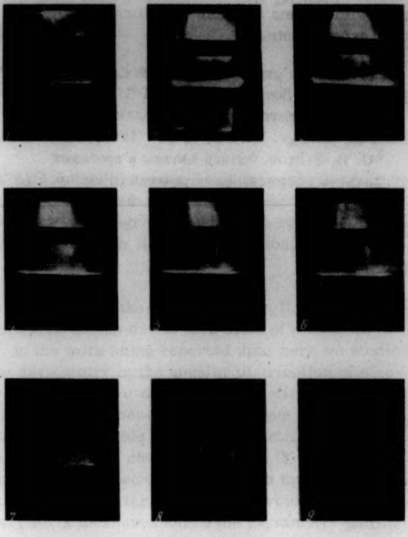

FIG. 6. Results obtained by ultrahigh-speed movie photography of the plasma with no magnetic field. The time interval between frames is 4 μsec.

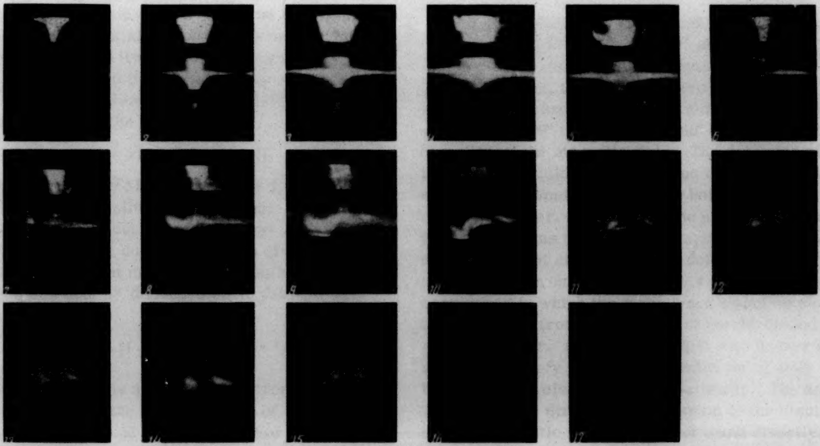

FIG. 7. Results obtained by ultrahigh-speed movie photography of the plasma with a magnetic trapping field. "Anomalous" plasma behavior. The time interval between frames is 4 μsec.

jector. Whether the observed effect is a manifestation of some kind of macroscopic instability or whether it is related to the method used to fill the trap with plasma can only be determined by further experiments.

---

[1] S. Yu. Luk'yanov and I. M. Podgnornyĭ, JETP 37, 27 (1959), Soviet Phys. JETP 10, 18 (1960).

[2] I. M. Podgornyĭ and V. M. Sumarokov, J. Nuclear Energy, Part C, 1, 236 (1960).

[3] O. B. Firsov, Физика плазмы и проблема управляемых термоядерных реакций (Plasma Physics and the Problem of a Controlled Thermonuclear Reaction) Acad. Sci. U.S.S.R. Press (1958) Vol. III, p. 327.

[4] Luk'yanov, Podgornyĭ, and Chuvatin, J. Tech. Phys. (U.S.S.R.) (in press).

[5] Finkelstein, Sawyer, and Stratton, Phys. Fluids 1, 188 (1958).

Translated by H. Lashinsky
66

SOVIET PHYSICS JETP VOLUME 13, NUMBER 2 AUGUST, 1961

ASYMMETRY IN THE ANGULAR DISTRIBUTION OF ELECTRONS FROM μ-e DECAY IN MAGNETIC FIELDS UP TO 35 000 OERSTED

S. A. ALI-ZADE, I. I. GUREVICH, and B. A. NIKOL'SKII

Submitted to JETP editor August 24, 1960

J. Exptl. Theoret. Phys. (U.S.S.R.) 40, 452-456 (February, 1961)

π-μ-e decays were observed in nuclear emulsions placed in a magnetic field, the purpose of the experiment being to study the asymmetry in the angular distribution of electrons from μ-e decays in a magnetic field. It was found that longitudinal magnetic fields up to 20 000 – 30 000 oe do not completely remove the depolarizing action of the medium (emulsion) on the μ meson.

1. INTRODUCTION

THE angular distribution of electrons from π-μ-e decays is given by the formula

$$dN = (1 - a\cos\vartheta)\,d\Omega/4\pi. \qquad (1)$$

The two-component neutrino theory, with V-A interaction, predicts that the asymmetry parameter a should have the value $\frac{1}{3}$. This prediction is difficult to check experimentally because the μ meson is depolarized upon stopping in condensed matter. The asymmetry parameter inferred from measurement of the angular distribution of the electrons is $a^* = Pa$, where P is the polarization of the μ meson after stopping in the absorber. The value of P depends on the medium and cannot be measured directly. Orear et al.[1] have considered the depolarization due to formation of muonium. The depolarization due to this process depends on the strength of the external magnetic field, directed along the spin of the muon:

$$a^* = a\,[1 - 0.5/(1 + x^2)], \qquad (2)$$

In Eq. (2), $x = \mu H/\Delta E$, where $\Delta E \sim 1.8 \times 10^{-5}$ ev is the hyperfine splitting of muonium. Ferrell et al.[2] have carried out a more detailed analysis of the depolarization due to formation of muonium, taking into account multiple electron exchange. They found that a* depended on H through the relation

$$a^* = a\,[1 - 0.5/(1 + x^2 + \tau^{-2})]^n. \qquad (3)$$

In Eq. (3), n is the number of electron exchange events, and τ is the mean lifetime of muonium in units of $\hbar/\Delta E = 3.58 \times 10^{-11}$ sec. For proper choice of the parameters n and τ, formula (3) should be good up to fields of 10 000 oe. From (3) it follows that in sufficiently strong longitudinal magnetic fields there should be negligible depolarization of muons due to formation of muonium.

In the work being reported upon here we studied the asymmetry in the angular distribution of electrons from π-μ-e decays in magnetic fields up to 35 000 oe. The dependence of a* on H was thus obtained for a wide range of magnetic field strengths. This check on formula (3) gives information on the mechanism by which muons are depolarized in matter, information which is necessary for a measurement of the asymmetry parameter a.

2. APPARATUS

Nuclear emulsions were placed in a magnetic field and irradiated with slow π^+ mesons which stopped in the emulsions. In scanning the developed emulsions, those events were selected in which the μ meson travelled in a direction making an angle β of 0° to 30° or $\beta = 180° - 150°$ with the direction of the magnetic field. The direction of the magnetic field was marked on the emulsion by exposing the emulsion to x rays before taking it out of its holder. In scanning the emulsions, particular care was taken to avoid systematic errors due to different efficiencies for detecting different π-μ-e decay events. Only those π-μ decays were considered in which the muon track ended no closer than $\Delta = 15\,\mu$ from the surface of the developed emulsion layer. Out of the 177 850 π-μ decays observed to satisfy the selection rules on β, only 66 had no visible electron from μ-e decay. The angle α between the direction of emission of the electron and the magnetic field H was not found directly; only the projection of this angle on the plane of the emulsion was measured. The value of a* was found from the relation

$$a^*_{\exp} = 2\,[N(\alpha > 90^\circ) - N(\alpha < 90^\circ)]/[N(\alpha > 90^\circ) + N(\alpha < 90^\circ)], \tag{4}$$

where the angle α was taken in the sense from the direction of the muon spin to the direction of the field H. The value of $a^*_{\exp}$ computed from (4) is a little low because the spin of the muon processes about the magnetic field. This effect can be corrected for by dividing by $\overline{\cos\beta}$

$$a^* = a_{\exp}/\overline{\cos\beta}. \tag{5}$$

where $\overline{\cos\beta}$ is the mean cosine of the angle between the direction of the field and the spin (or momentum) of the muon. The value of $\overline{\cos\beta}$ for those π-μ decays which were accepted was found experimentally.

3. RESULTS AND DISCUSSION

A total of 177 850 π-μ-e decay events satisfied the selection rules on β and Δ described in Sec. 2. These were distributed among the various values of magnetic field strength as follows:

H, oe	405	805	1610	2370	10000	20000	27000	35000
Number of cases	9705	13430	11617	10005	30331	8851	17557	17715

Table I. Asymmetry parameter a* = Pa for various values of the longitudinal magnetic field strength H

	H, oe								
	405	805	1610	2370	10 000	20 000	27 000	35 000	10 000–35 000
$a^*(\uparrow)$	0.115	0.115	0.170	0.165	0.262	0.277	0.296	0.317	0.284
$\delta a^*(\uparrow)$	0.030	0.027	0.023	0.030	0.017	0.032	0.023	0.023	0.011
$a^*(\downarrow)$	0.114	0.077	0.185	0.202	0.264	0.266	0.273	0.309	0.277
$\delta a^*(\downarrow)$	0.030	0.027	0.028	0.030	0.017	0.032	0.023	0.023	0.011
a^*	0.114	0.096	0.178	0.184	0.263	0.272	0.284	0.313	0.281
δa^*	0.021	0.020	0.020	0.020	0.012	0.023	0.016	0.016	0.008

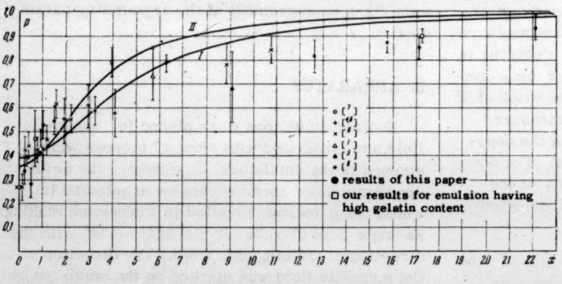

P(x) as a function of x, where P = 3a* and x = H/1580 (H in oersteds). The curves (I, II) are theoretical, while the points are experimental.

For emulsions with high gelatin content there were 58 639 cases at H = 27 000 oe.

Among all the observed π-μ-e decays we did not see one μ-3e decay, or any other anomalous decay modes of the muon. There was one case in which the muon decayed into an electron, neutrino, antineutrino and virtual γ ray, the latter being converted into an electron-positron pair[3] (Dalitz effect)

$$\mu^+ \rightarrow e^+ + \nu + \bar{\nu} + e^+ + e^-.$$

Table I shows the asymmetry coefficients calculated from (4) and corrected by (5). These results apply to emulsion with the normal amount of gelatin. The table also shows the values of a* obtained for muons going in the direction (↑) of the magnetic field ($\beta < 30^\circ$) and for those going in the opposite direction (↓) ($\beta > 150^\circ$). δa^* is the standard error ($\delta a^* = 2/\sqrt{N}$).

The data in Table I are shown in the figure, together with data obtained by other authors.[1,2,4-8] The figure also shows data obtained with emulsions having high gelatin content.

The table below gives value for the coefficient a* obtained from emulsions having a high gelatin content and in a field H = 27 000 gauss. The gelatin content is measured by the ratio of gelatin volume to total volume, $V_g/(V_g + V_{AgBr})$, and is 0.51 for normal emulsions.

$V_g/(V_g + V_{AgBr})$	0.51	0.61	0.71	0.76	0.61—0.76
a^*	0.284	0,284	0.323	0.277	0.301
δa^*	0,016	0.016	0.013	0.018	0.009

The values of a* obtained from the emulsions with high gelatin content agree with those obtained from emulsions with normal gelatin content:

$$a^* (\uparrow) = 0.297 \pm 0.013, \quad a^* (\downarrow) = 0.305 \pm 0.013.$$

Table II shows the values of a* obtained by different observers. The scatter in the values obtained by different observers is within the statistical error.

Table II. Asymmetry parameters a* = Pa from data taken by different observers

Observer	Normal emulsion H > 10000 oe	Emulsion with high gelatin content
1	0,254 ± 0,018	0.312 ± 0.022
2	0.282 ± 0.016	0.347 ± 0,020
3	0.294 + 0.017	0.283 ± 0.023
4	0.284 + 0.017	0.283 ± 0.021
5	—	0.338 ± 0,028
6	0,258 ± 0.030	0,278 ± 0.023
7	0,355 + 0,034	0.246 ± 0.029
	mean:	
	0.281 ± 0,010	0.301 ± 0.009

Two conclusions can be drawn from the above data:

1. The value of a* for muons which have stopped in matter in a magnetic field of 20 000 — 30 000 oe is less than the maximum value a* = ⅓. This result is statistically meaningful.

2. The coefficient a* tends to increase as the field is increased from 10 000 to 35 000 oe, or when the emulsion is diluted. This conclusion is not as reliable, statistically, as is the first one. The χ^2 test shows that with probability $W(\chi^2) = 0.3$ the observed dependence of a* on H in the region H = 10 000 to 35 000 oe is a statistical fluctuation.

As mentioned above, our data can be used to check the dependence of a* on H as calculated on the assumption that the depolarization is due to the formation of muonium. This comparison is made on the figure [cf. Eq. (3)]. The curves I and II correspond to parameters n and τ which have been chosen to give the best fit to the experimental data. The curves were drawn so as to minimize the quantity

$$M = \sum_i [(P_{i\,\mathrm{calc}} - P_{i\,\mathrm{exp}})/\delta P_{i\,\mathrm{exp}}]^2.$$

Curve I was calculated using the experimental data for all values of x $(0 < x < 22.15)$. The values of n and τ for this curve are $n_I = 22$, $\tau_I = 0.31$. The probability that the data would lie along this curve P(x) by accident is $W_I(\chi^2) < 0.01$. Curve II was obtained by minimizing M only for x in the range 0 to 4.09. The corresponding values of n and τ are $n_{II} = 12$, $\tau_{II} = 0.44$. The probability that curve II agree with the data by accident is $W_{II}(\chi^2) = 0.03$. It appears that the curves P(x) do not describe the experimental data $P_{\mathrm{exp}}(x)$ satisfactorily. The emulsion really consists of two components — gelatin and silver bromide; this can be roughly taken into account by replacing formula (3) by the relation

$$P = f + (1 - f)\,[1 - 0.5/(1 + \tau^{-2} + x^2)]^n. \qquad (3')$$

The assumption is made here that a certain fraction (f) of the muons stop in the gelatin and do not depolarize at all. The value of f is less than $P(x \to \infty)/P(x = 0) = 0.3$. Values of P(x) calculated from (3′), with f = 0.3, agree closely with values calculated from (3). Hence the discrepancy between the theoretical and experimental values of P(x) cannot be due to the inhomogeneity of the emulsion. The discrepancy is particularly marked for x > 10. For such values of magnetic field, the calculated values of P are practically equal to the maximum value (one), while the experimental values of P remain less than one. Hence we can finally conclude that if a = ⅓ (V-A interaction) than a comparison of theoretical values for P(x), as given by (3), with experimental ones implies that there is some mechanism for depolarization other than the formation of muonium, and that this mechanism is almost entirely responsible for the departure of P_{exp} from one for values of x greater than 10.

In conclusion, the authors would like to thank V. P. Dzhelepov for having the emulsions irradiated on the synchrocyclotron, D. M. Samoĭlovich for developing the emulsions, and V. M. Kutukov, A. M. Alpers, G. B. Pleshivtsev, S. A. Chuev, B. V. Sokolov and L. V. Surkov for their help in carrying out this research.

---

[1] Orear, Harris, and Bierman, Phys. Rev. **107**, 322 (1957).

[2] Ferrell, Lee, and Pal, Preprint (1959).

[3] Gurevich, Nikol'skii, and Surkova, JETP **37**, 318 (1959), Soviet Phys. JETP **10**, 225 (1960).

[4] Sens, Swanson, Telegdi, and Yovanovitch, Phys. Rev. **107**, 1465 (1957).

[5] Barkas, Giles, Heckman, Inman, and Smith, Phys. Rev. **107**, 911 (1957).

[6] A. O. Vaĭsenberg and V. A. Smirnit-skii,

JETP 39, 242 (1960), Soviet Phys. JETP 12, 175 (1960).

[7] Gurevich, Kutukova, Mishakova, Nikol'skii, and Surkova, JETP 34, 280 (1958), Soviet Phys. JETP 7, 195 (1958).

[8] Lynch, Orear, and Rosendorff, Phys. Rev. Lett. 1, 471 (1958); Phys. Rev. 118, 284 (1960).

Translated by R. Krotkov
67

SOVIET PHYSICS JETP VOLUME 13, NUMBER 2 AUGUST, 1961

ON THE SUPERCONDUCTIVITY OF TIN AND INDIUM UNDER PRESSURE

L. S. KAN, B. G. LAZAREV, and V. I. MAKAROV

Physical and Technological Institute, Academy of Sciences, Ukrainian S.S.R.

Submitted to JETP editor September 1, 1960

J. Exptl. Theoret. Phys. (U.S.S.R.) 40, 457-459 (February, 1961)

The shift in the critical temperature due to pressure was measured over the pressure range 0 – 1730 kg/cm² for tin and indium. A linear dependence $T_c(p)$ is observed for indium over the entire pressure range, while tin shows an appreciable deviation from linearity at pressures of 400 – 800 atm. The linearity of the function $T_c(p)$ for indium, which has a simple Fermi surface, is compared with the complicated variation of $T_c(p)$ in thallium and tin, which have complicated Fermi surfaces.

THE shifts in the critical temperatures of tin and indium have previously[1,2] been determined at pressures of 1730 and 1370 kg/cm². The values of ΔT_c obtained at these pressures were, respectively, 0.097° ± 0.002° and 0.080° ± 0.002° for tin, and 0.080° ± 0.002° and 0.063° ± 0.002° for indium.

If we assume that the effect is linear, dT_c/dp for tin amounts to $(-5.7 \pm 0.2) \times 10^{-5}$ deg/atm while for indium it amounts to $(-4.6 \pm 0.2) \times 10^{-5}$ deg/atm.

The linear dependence of $T_c(p)$ has not been questioned, and until now it has been assumed, in particular, for tin and indium. However, the completely different behavior of thallium[3,4] has forced us to consider this view with great caution. In fact, even the sign of the effect for thallium changes at pressures above 2500 atm.

A number of investigators[4,6] have studied the effect of pressure in recent years. They have obtained appreciably discrepant results for the very same metals (e.g., for tin and indium). We may find a satisfactory explanation for certain of the widely varying data. For example, the obviously low value $dT_c/dp = -3.8 \times 10^{-5}$ deg/atm given by Hatton for indium is probably associated with a considerable deformation of the metal (owing to the method of applying pressure). As is known, this leads to a rise in the transition temperature.[5] From these considerations, we should consider the highest values of the shift in T_c as being the most reliable. It is relevant that for indium the value of dT_c/dp shows only a small spread of values over the entire pressure range up to 10 000 atm [from $(-4.0 \pm 0.3) \times 10^{-5}$ to $(-4.6 \pm 0.2) \times 10^{-5}$ deg/atm]. At the same time, tin shows an appreciable discrepancy between the values of dT_c/dp at high pressures [from $(-4.3 \pm 0.4) \times 10^{-5}$ to $(-4.6 \pm 0.5) \times 10^{-5}$ deg/atm] and at pressures of 1370 and 1730 kg/cm² [$(-5.7 \pm 0.2) \times 10^{-5}$ deg/atm]. The latter values have been checked repeatedly, and it would be difficult to find a reason for the increase in the value of dT_c/dp.

It seemed essential to perform precision measurements in the pressure range 0 – 2000 atm.

The shift in T_c for tin and indium was measured using two methods for applying pressure. Pressures up to 100 atm were applied by liquid helium. A differential method was used: one sample was placed in a bomb, and the other outside. The method permitted the application and reduction of pressure at liquid-helium temperature, so that we could verify that T_c was the same before and after the application of pressure.

The results of such measurements for indium are shown in Fig. 1. The value

$$dT_c/dp = -4.4 \pm 0.3 \cdot 10^{-5} \text{ deg/atm}$$

for this pressure range agrees well within the limits of accuracy with the value in the pressure range obtained by the ice method[1,2] [$(-4.6 \pm 0.2) \times 10^{-5}$ deg/atm]. Thus, indium retains a linear dependence of $T_c(p)$ in the pressure range up to

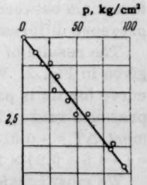

FIG. 1. The dependence of ΔT_c on p for indium in the pressure range 0–100 kg/cm².

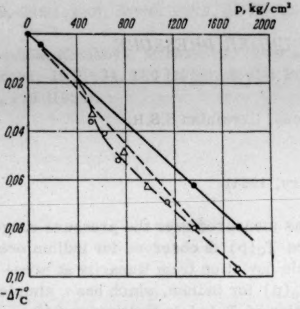

FIG. 2. The dependence of ΔT_c on p for indium (solid curve) and for tin (dotted curves). Δ and o indicate different samples of tin.

2000 atm (Fig. 2), as it does according to the data of other authors[4] at higher pressures.

Tin behaves differently. In the pressure range 0 — 100 atm, $dT_c/dp = (-4.4 \pm 0.2) \times 10^{-5}$ deg/atm, in good agreement with the results of other authors.[7] However, this value of dT_c/dp does not agree with the shift in T_c at pressures of 1730 and 1370 kg/cm². In Fig. 2, the dotted straight line corresponds to a linear variation of T_c with pressure, as was assumed in previous studies[1,2] with a value $dT_c/dp = (-5.7 \pm 0.2) \times 10^{-5}$ deg/atm.

Thus, we must conclude that for tin the curves for $T_c(p)$ have a different slope in the pressure ranges 0 — 100 and 0 — 1730 atm, i.e., the T_c of tin shows a nonlinear pressure dependence in the range 100 — 2000 atm.

In order to check this fact, measurements of T_c were made in the pressure range 500 — 1200 atm by means of the ice method using water-alcohol solutions.[8] In order to determine the pressure developed in the bomb, a sample of indium serving as a manometer was always placed in the bomb in addition to the tin sample. Supplementary measurements were made with two indium samples to establish the absence of pressure differentials between the sites of the samples (the pressure differential $\Delta p < 20$ atm).

The results of the measurements on tin are also given in Fig. 2. We see from the diagram that the curve for tin is parallel to that for indium in the pressure range 1730 — 800 atm (with a displacement $\Delta T = -0.017°$, i.e., with a value $dT_c/dp = (-4.6 \pm 0.2) \times 10^{-5}$ deg/atm).

We must consider that a transition from the one curve to the other occurs between the pressures 800 and 100 atm. Such a variation in the curve may formally be represented as a superposition of a linear variation with $dT_c/dp = (-4.6 \pm 0.2) \times 10^{-5}$ deg/atm, and a variation appearing above 100 atm, and attaining a saturation value of $-0.017°$ at about 800 atm.

We must note that something similar takes place in thallium, for which also the dependence $T_c(p)$ may be represented in the form of a linear portion of the curve having $dT_c/dp = -0.56 \times 10^{-5}$ deg/atm, superimposed on a variation showing a saturation value of $+0.03°$ above ~ 2000 atm.[4]

In spite of the fact that the behavior of thallium is a convincing example of deviation from linearity even at such low pressures as $\sim 10^3$ atm, the strange behavior of tin does not become more understandable.

In general, we must note that the effect of pressure on superconductors has not yet been explained. The new theory of superconductivity gives the following relation between the critical temperature T_c and the Debye temperature Θ and the electronic parameters (the electron-phonon interaction constant g and the electron density ν): $T_c \sim \Theta \exp(-2/g\nu)$. Uniform compression of a metal leads to an increase in the Debye temperature, and thereby to a linear increase in T_c. Apparently, we must seek an explanation for the pressure-variation of T_c in the effect of pressure on the electronic properties of the metal. In this regard, it is interesting to note that indium, which shows a linear variation of $T_c(p)$, has the simplest form of Fermi surface (closed, and almost spherical). It may be pertinent to relate the complicated variation of $T_c(p)$ for thallium to its very anisotropic Fermi surface (a system of corrugated planes). For tin, the form of the Fermi surface is also complicated (by the presence of open sections).

In order to understand the mechanism of the effect of pressure on superconductivity in general and the peculiarities of this effect in various metals, it is apparently essential to extend the studies to metals having varying electronic spectra, together with parallel studies on them of the effect of pressure on the galvanomagnetic properties. Such measurements are being carried out at present.

---

[1] B. G. Lazarev and L. S. Kan, JETP **14**, 463 (1944).

[2] Kan, Lazarev, and Sudovtsov, JETP **18**, 825 (1948).

[3] Kan, Lazarev, and Sudovtsov, Doklady Akad. Nauk SSSR **69**, 173 (1949).

[4] L. D. Jennings and C. A. Swenson, Phys. Rev. 112, 31 (1958).

[5] V. I. Khotkevich, Doctoral Dissertation, Inst. Phys. Prob., Acad. Sci. U.S.S.R. (1953).

[6] M. Garbor and D. E. Mapother, Phys. Rev. 94, 1065 (1954).

[7] N. L. Muench, Phys. Rev. 99, 1814 (1955).

[8] N. B. Brandt and A. G. Tomashchik, Приборы и техника эксперимента (Instrum. and Meas. Techn.) 4, 113 (1958).

Translated by M. V. King
68

SOVIET PHYSICS JETP VOLUME 13, NUMBER 2 AUGUST, 1961

PRODUCTION OF CHARGED MESONS BY 290 Mev π^- MESONS ON HYDROGEN

Yu. A. BATUSOV, S. A. BUNYATOV, V. M. SIDOROV, and V. A. YARBA

Joint Institute for Nuclear Research

Submitted to JETP editor September 1, 1960

J. Exptl. Theoret. Phys. (U.S.S.R.) 40, 460-463 (February, 1961)

The $\pi^- + p \rightarrow \pi^+ + \pi^- + n$ reaction is investigated. The experimental data are compared with the theoretical calculations.

THE present communication is a continuation of an investigation of the momentum and angular distribution of secondary particles in the reaction

$$\pi^- + p \rightarrow \pi^+ + \pi^- + n \tag{1}$$

at primary-meson energy of (290 ± 15) Mev.[1]

We present here an analysis of 250 cases of reaction (1) with the same primary-meson energy. The experiment was performed in the synchrocyclotron of the Laboratory for Nuclear Problems of the Joint Institute for Nuclear Research, using nuclear emulsions. The procedure for the detection of meson production and the selection criteria are described in reference 1.

The momentum spectra and the distributions of the angles between the momenta of the secondary particles are compared with the calculations based on the Fermi statistical model and on the Lindenbaum and Steinheimer isobar model. The calculations were carried out by the "random star" method,[2] using an electronic computer. The average accuracy of the theoretical histograms is 5 percent. The results of the calculations, together with the experimental data, are shown in Figs. 1 and 2.*

The comparison shows that although the statistical theory and the isobar model predict correctly the main features of the spectra and the distributions of the angles between the momenta of the secondary particles, no satisfactory quantitative agreement with experiment is observed. Thus, the maximum of the neutron spectrum (Fig. 1) is noticeably shifted towards the lower momenta. The distribution of the angles between the momenta of the secondary pions (Fig. 2) indicates that the mesons have a greater probability of diverging by larger angles than given by the theoretical calculations. We list below the average scattering angles (in degrees).

	Experiment	Statistical theory	Isobar model
$\overline{\theta}^*_{\pi^+\pi^-}$	116.7 ± 2.4	102.2	98.1
$\overline{\theta}^*_{\pi^+n}$	113.4 ± 2.5	128.6	123,9
$\overline{\theta}^*_{\pi^-n}$	129.3 ± 2.4	129.4	141.0

The angular distributions of the secondary particles relative to the direction of the primary meson are shown in Fig. 3. It should be noted that the statistical theory and the isobar model do not make it possible to calculate these distributions.

It was shown in an earlier paper[3] that the distribution over the relative momenta of the secondary particles agrees with the theoretical distribution obtained by Ansel'm and Gribov for reactions in which an additional meson is produced near threshold.[4] One can hope that this theory, which takes account of the interaction of the particles in the final state, will produce better agreement with experiment at our energy. Thus, for example, the average scattering angles between the secondary particles, calculated by the Kopylov method[5] with the aid of a matrix element of the form[4] $S^2 = 1 + ck_{12} + dk_{13}$, with parameters c and d as determined in reference 3, are

$$\overline{\theta}^*_{\pi^+\pi^-} = 109.0^\circ, \qquad \overline{\theta}^*_{\pi^+n} = 119.0^\circ, \qquad \overline{\theta}^*_{\pi^-n} = 131{,}0^\circ$$

and are in better agreement with the experimental data.

We plan to carry out calculations with variation of the coefficients c and d (within the limits of the experimental errors).

The authors express their gratitude to Prof. V. P. Dzhelepov and L. I. Lapidus for interest and attention to the work, and also to G. I. Kopylov for great help in the computations and evaluation.

---

*In comparing the experimental results with the calculations based on the isobar model it was assumed that the negative pion is always of isobaric origin, and the positive pion is always due to recoil. The momentum spectrum of the neutrons and the distribution of the angles between the meson momenta are independent of this assumption.

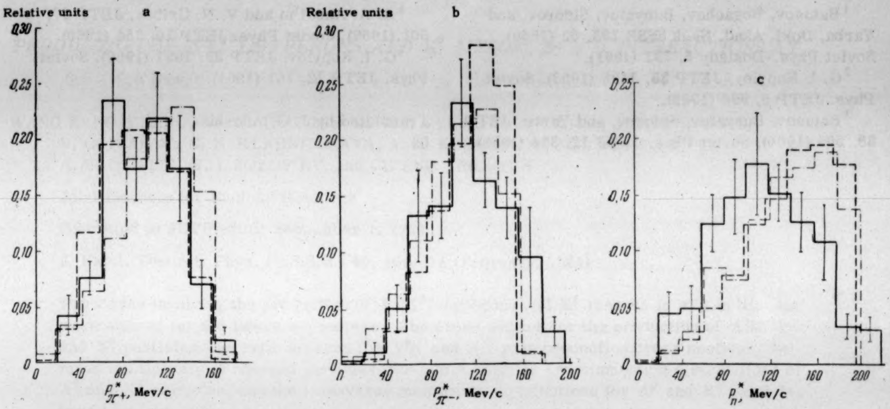

FIG. 1. Momentum distributions in the c.m.s. for secondary particles from the reaction $\pi^- + p \to \pi^+ + \pi^- + n$ (250 events); a – positive pions, b – negative pions, c – neutrons. Solid line – experiment, dotted line – calculated by the isobar model, dash-dot line – calculated by statistical theory.

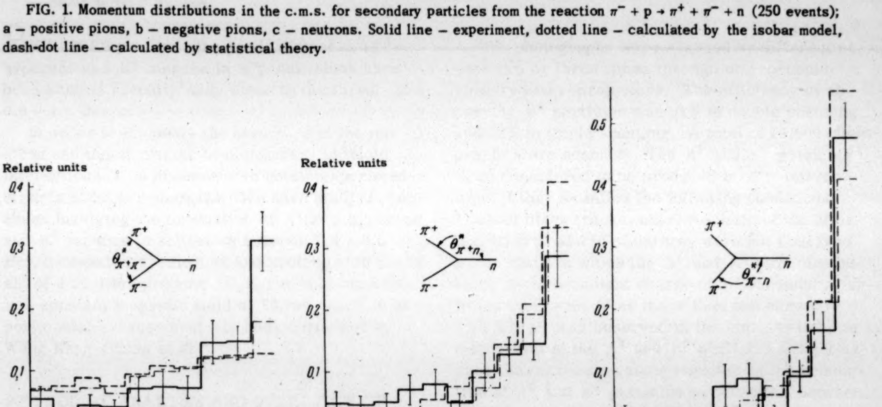

FIG. 2. Distributions of the angles between the momenta of the particles from the reaction $\pi^- + p \to \pi^+ + \pi^- + n$ in the c.m.s. (250 events). Solid line – experiment, dotted line – calculated by the isobar model, dash-dot line – calculated by the statistical theory.

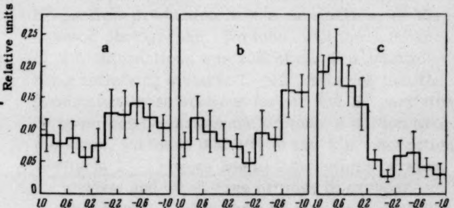

FIG. 3. Angular distribution in the c.m.s. for secondary particles from the reaction $\pi^- + p \to \pi^+ + \pi^- + n$ (250 events): a – positive pions, b – negative pions, c – neutrons.

[1] Batusov, Bogachev, Bunyatov, Sidorov, and Yarba, Dokl. Akad. Nauk SSSR **133**, 52 (1960), Soviet Phys.-Doklady **5**, 731 (1961).

[2] G. I. Kopylov, JETP **35**, 1426 (1958), Soviet Phys. JETP **8**, 996 (1959).

[3] Batusov, Bunyatov, Sidorov, and Yarba, JETP **39**, 506 (1960), Soviet Phys. JETP **12**, 354 (1961).

[4] A. A. Ansel'm and V. N. Gribov, JETP **37**, 501 (1959), Soviet Phys. JETP **10**, 354 (1960).

[5] G. I. Kopylov, JETP **39**, 1091 (1960), Soviet Phys. JETP **12**, 761 (1961).

Translated by J. G. Adashko
69

SOVIET PHYSICS JETP VOLUME 13, NUMBER 2 AUGUST, 1961

PRODUCTION OF $\Lambda^0(\Sigma^0)$ HYPERONS AND K^0 MESONS IN π^-p INTERACTIONS AT 6.8 ± 0.6 Bev/c

WANG KANG-CHANG, WANG TS'U-TSENG, V. I. VEKSLER, J. VRANA, TING T'A-TSAO,
V. G. IVANOV, E. N. KLADNITSKAYA, A. A. KUZNETSOV, NGUYEN DINH TU,
A. V. NIKITIN, M. I. SOLOV'EV, and CH'ENG LING-YEN

Joint Institute for Nuclear Research

Submitted to JETP editor September 1, 1960

J. Exptl. Theoret. Phys. (U.S.S.R.) 40, 464-474 (February, 1961)

Processes involving the production of $\Lambda^0(\Sigma^0)$ hyperons and K^0 mesons in π^-p collisions were studied for 6.8 Bev/c π^- mesons. The cross section for the production of $\Lambda^0(\Sigma^0)$ and K^0 particles, the ratio between the Y^0K and $K\bar{K}$ pair production cross sections, the mean multiplicity of charged particles, the c.m.s. angular and momentum distributions of Λ^0 and K^0 particles, and the transverse momentum distributions for Λ^0 and K^0 particles have been obtained.

PROCESSES involving the production of $\Lambda^0(\Sigma^0)$ hyperons and K^0 mesons in π^-p collisions have been studied recently[1] only close to the threshold 0.9 – 1.4 Bev/c.

In order to elucidate the structure of the nucleon and the character of elementary particle interactions, it is necessary to obtain experimental data at higher energies. We have studied processes involving the production of $\Lambda^0(\Sigma^0)$ hyperons and K^0 mesons in collisions between 6.8 ± 0.6 Bev/c negative π mesons and protons with the aid of a 24-liter propane (C_3H_8) bubble chamber in a constant magnetic field of 13,700 oe. The experimental arrangement has been described by Wang Kang-Chang et al.[2]

METHOD OF ANALYSIS AND SELECTION OF π^-p INTERACTIONS

The bubble-chamber pictures were taken with a stereoscopic camera using "Russar-plazmat" objectives with a focal length of 67 mm. The photographic film was pressed against a plane-parallel glass on which crosses were engraved (straight lines intersecting at an angle of 90°). The objectives were adjusted so that their optical axes were parallel and passed through the points of intersection of the straight lines on the glass. The stereophotographic base, determined by the distance between the crosses, was equal to 300 mm. The scale of the photograph for the median plane of the bubble chamber was 1 : 10. The camera was mounted on the upper plate of the chamber and was in a fixed position during the chamber operation.

The photographs were scanned by different persons two or three times through stereoscopic viewers and reprojectors. The efficiency of observing V^0 particles was 91% in double scanning and 96% in triple scanning. A total of 14,000 photographs were scanned. The Λ^0 and K^0 particles were considered to be produced in π^-p interactions if they satisfied the following conditions: 1) short black tracks, characteristic of the disintegration products of carbon, were not observed in the stars to which the Λ^0 and K^0 particles belong, 2) the resultant charge of all secondary particles was zero, 3) no more than one baryon (Λ^0, $\Sigma^\pm$, p) was observed in the star, 4) the c.m.s. momentum of the Λ^0 and K^0 particles did not exceed the maximum values possible in the production of Λ^0 and K^0 particles in collisions between π^- mesons and free protons.

The background of Λ^0 and K^0 particles produced in collisions with quasi-free protons was estimated from the number of Λ^0 and K^0 particles produced in collisions with quasi-free neutrons. For this purpose, we counted the cases of Λ^0- and K^0-particle production in π^-n interactions on the scanned photographs. We found that the number of π^-n interactions was 20% of the π^-p interactions satisfying criteria 1 – 4. Assuming that the production cross sections for Λ^0 and K^0 particles on quasi-free neutrons and protons of carbon are the same, we found that 20% of the π^-p interactions (criteria 1 – 4) were due to interactions between π^- mesons and quasi-free protons of carbon.

The events found in the scanning were analyzed and 233 of them satisfied all of the aforementioned criteria. We measured the events on UIM-21 microscopes by measuring the coordinates of corresponding points on both stereo frames. The space coordinates, angles, and momenta were calculated on a Ural electronic computer. The geometrical reconstruction of the track in space was calculated by the method of least squares. The curvature of the track was approximated by a parabola. The nonhomogeneity of the magnetic field over the bubble-chamber volume did not exceed ± 3%.

Owing to multiple scattering, the error in determining the momenta of relativistic particle tracks was, on the average, 13% for a track length of about 10 cm.

The kinematical relations between the angles of flight and the momenta of the decay products were used to identify the Λ^0 and K^0 particles. This made it possible to determine the Λ^0- and K^0-particle momenta to an accuracy of $\leq 10\%$.

GEOMETRICAL CORRECTION

The effective region for the production and observation of Λ^0 and K^0 particles in the chamber is less than the geometrical dimensions of the chamber ($55 \times 28 \times 14$ cm) and depends on the lifetime of the particles and their velocity.

The effective region was determined experimentally. To do this, we plotted the distribution of cases of Λ^0- and K^0-particle production in the chamber. It turned out that the distribution coincided with the distribution of primary beam tracks in the following intervals: on the x axis — from 4 to 22 cm, on the z axis — from 3 to 9 cm.* If we take the direction of the primary particle beam as the positive direction and measure y from the middle of the chamber, then 90% of all cases of Λ^0- and K^0-particle production are located in the interval between -24 and $+14$ cm. Of the 233 events, 209 lie in the effective region. It turned out that the effective regions for Λ^0 and K^0 particles practically coincide. The difference in the lifetimes is offset by the larger velocities of the K^0 mesons, which leads to a greater relativistic increase in their lifetimes, so that the K^0 lifetime becomes comparable with the lifetime of the Λ^0 particles.

In order to take into account Λ^0 and K^0 particles that decay outside the chamber, and also the difference in the probabilities of recording Λ^0 and K^0 particles emitted in the vertical and horizontal planes, we introduced a correction W_1 for the probability of Λ^0 and K^0 decay outside the chamber and a correction W_2 for the loss of Λ^0 and K^0 particles due to large azimuthal angles.

1. The probability of Λ^0 and K^0 decay within the boundaries of the chamber is determined from the well-known law $1 - \exp(-l/l_0)$, where $l_0 = \beta c \gamma \tau_0$ is the mean range and l is the potential range. By potential range we mean the distance from the point of production to the boundary of the effective region for the observation of decay. The dimensions of this region depend on the minimum length necessary for the momentum measurement of the decay products. This length was 4 cm in our experiment. Using the known values of the Λ^0- and K^0-particle lifetimes,[3] we calculated the probability f_i of observing decay in our chamber for each case. The mean values of f_i were 84% and 78% for the observation of Λ^0 and K^0 particles, respectively, and 65% and 63% for the observation of $\Lambda^0 K^0$ and $K^0 \overline{K}^0$ pairs, respectively. The reciprocal of the probability of observing decay in the chamber gives the correction W_1.

2. The chamber depth was less than its width and the probability of observing Λ^0 and K^0 particles produced in the chamber and emitted at large azimuthal angles was therefore less than that for observing Λ^0 and K^0 particles emitted at small azimuthal angles. This is what is known as the bias for unfavorable azimuthal angles Φ. We plotted the Φ distribution for Λ^0 and K^0 particles. It was found that the correction for Λ^0 decays was $W_2 = 1.48 \pm 0.1$ and $W_2 = 1.13 \pm 0.03$ for K^0 decays.

PRODUCTION CROSS SECTION FOR $\Lambda^0(\Sigma^0)$ AND K^0 PARTICLES

In this work, we did not set the task of estimating the fraction of Λ^0 hyperons resulting from the decay of Σ^0 particles for the total number of observed Λ^0 hyperons. Since only 11% of the γ quanta were converted into electron-positron pairs in our chamber, the decay of the Σ^0 hyperons into Λ^0 particles and γ quanta at practically the very point of production did not permit us to distinguish Λ^0 particles resulting from the decay of Σ^0 particles by the γ quanta. From Table I it is seen that at our energy some charged particles (n_s) are produced together with the neutral strange particles. These are mostly $\pi^\pm$ mesons. The mean number of charged particles accompanying the production of Λ^0 and K^0 particles is 2.5 ± 0.1. $K^\pm$ mesons are also present among the charged particles.

---

*x is the chamber width, y is the chamber length along the beam, and z is the depth coordinate.

Table I

Identified particles	Number of charged particles, n_s				
	0	2	4	6	Total
$\Lambda^0 + K^0$	2	8	3	0	13
Λ^0	6	47	17	3	73
$K^0 + \overline{K}^0$	0	5	1	0	6
K^0	16	62	26	3	107
Λ^0 or K^0	2	6	2	0	10
Total	26 12.5%	128 61.6%	49 23%	6 2.9%	209 100%

We recorded neutral strange particles which were produced in the following reactions:

$$\pi^- + p \rightarrow \Lambda^0 + K^0 + n\pi \tag{1}$$

$$\pi^- + p \rightarrow \Sigma^0 + K^0 + n\pi \tag{2}$$

$$\pi^- + p \rightarrow \Lambda^0 + K^+ + n\pi \tag{3}$$

$$\pi^- + p \rightarrow \Sigma^0 + K^+ + n\pi \tag{4}$$

$$\pi^- + p \rightarrow K^0 + \overline{K}^0 + N + n\pi \tag{5}$$

$$\pi^- + p \rightarrow K^0 + K^- + N + n\pi \tag{6}$$

$$\pi^- + p \rightarrow \overline{K}^0 + K^+ + N + n\pi \tag{7}$$

The following reactions with the production of K^0 mesons are also possible at our energy:

$$\pi^- + p \rightarrow \Sigma^{\mp} + K^0 + n\pi \tag{8,9}$$

$$\pi^- + p \rightarrow \Xi^- + K^0 + K^+ + n\pi \tag{10}$$

$$\pi^- + p \rightarrow \Xi^0 + K^0 + K^0 + n\pi \tag{11}$$

For the present, our problem did not involve the study of reactions (8) and (9)* The K^0-meson background from these reactions was negligible in our statistics: $\Sigma^{\pm}$ hyperons have a characteristic decay pattern, a short lifetime, and, consequently, can be reliably recorded and well separated from the reactions (1) — (7); $\Xi^{0,-}$ hyperons have a very small production cross section in the π^-p interaction.†

Ionization measurements for momenta > 1.2 Bev/c do not give a reliable separation of π^+ mesons and protons, not to mention the separation of $\pi^{\pm}$ and $K^{\pm}$ mesons. The fraction of Λ^0 hyperons produced in reactions (3) and (4), and the fraction of K^0 and $\overline{K}^0$ mesons produced in reactions (6) and (7) were estimated in the following way. We knew the fraction of Λ^0 and K^0 particles decaying into neutral particles, and also the fraction of long-lived K^0 mesons (K_2^0). Then, from the numbers of Λ^0K^0 pairs ($n_{\Lambda^0K^0}$) and $K^0\overline{K}^0$ pairs ($n_{K^0\overline{K}^0}$) that were found, we determined the true number of the pairs $N_{\Lambda^0K^0}$ and $N_{K^0\overline{K}^0}$:

$$N_{\Lambda^0K^0} = n_{\Lambda^0K^0}/(1-f_{\Lambda^0})(1-f_{K^0}),$$

$$N_{K^0\overline{K}^0} = n_{K^0\overline{K}^0}/(1-f_{\overline{K}^0})(1-f_{K^0}),$$

where f_{Λ^0} is the fraction of Λ^0 particles decaying into a neutron and π^0 meson ($f_{\Lambda^0} = 0.33$), f_{K^0} is the fraction of K^0 mesons decaying into two π^0 mesons plus the fraction of long-lived K^0 mesons [$f_{K^0} = 0.63$ (reference 4)].

Owing to the decay of K^0 mesons into neutral particles and the presence of K_2^0 mesons, part of the Λ^0K^0 pairs were recorded as single Λ^0 particles. The number of such cases is $n' = N_{\Lambda^0K^0}f_{K^0}(1 - f_{\Lambda^0})$. We subtract n' from the total number of single Λ^0 particles found after the corrections W_1 and W_2. The difference can be considered to represent production of a Λ^0 hyperon in reactions (3) and (4). A similar calculation was carried out for K^0 mesons.

We were thus able to estimate the probability of reactions (1), (2), (3), and (4), as well as (5), (6), and (7). For simplicity, we use the notation:

$$\sigma(Y^0K^0) = \sigma(1) + \sigma(2), \quad \sigma(Y^0K^+) = \sigma(3) + \sigma(4),$$

$$\sigma(K^0\overline{K}^0) = \sigma(5), \quad \sigma(K^0K^-) = \sigma(6), \quad \sigma(\overline{K}^0K^+) = \sigma(7),$$

$$\sigma(Y^0K^{0,+}) = \sigma(Y^0K^0) + \sigma(Y^0K^+),$$

$$\sigma(K^0, \overline{K}) = \sigma(K^0\overline{K}^0) + \sigma(K^0K^-) + \sigma(\overline{K}^0K^+).$$

We performed a special examination of our material with a view to observing conversion γ quanta from π^0-meson decay. From an examination of 228 cases with the production of neutral strange particles, it turned out that electron-positron pairs from conversion γ quanta were associated with primary stars in 32 cases (14%).

In order to determine the total cross section for the production of $\Lambda^0(\Sigma^0)$ and K^0 particles, we considered 7000 photographs, none of which contained more than 15 — 20 primary π^- mesons. The number of π^- mesons was counted independently by two observers. The primary particle flux was not counted on each photograph, but on every tenth frame. The difference in the number of tracks in the results of the two observers was 0.6% for about 100,000 π^- mesons. As was indicated above, the efficiency of double scanning was 91% and that of triple scanning 96%. In the determination of the total number of cases of $\Lambda^0(\Sigma^0)$- and K^0-particle production, apart from the corrections W_1 and W_2 connected with the geometrical parameters of the chamber, we introduced a correction for the neutral decay scheme of the K_1^0 particles and for long-lived K_2^0 mesons. Table II shows the results for the different reactions after all corrections have been taken into account.

---

*These reactions are studied in a separate work.

†The Ξ^- production cross section at this energy is $3.6^{+2.5}_{-2.1}$ μb/nucleon.

Table II

Reactions	(1) + (2)	(3) + (4)	(5)	(6) + (7)
Number of cases after all corrections	136±38	107±33	89±36	264±54

The total cross section for the production of $\Lambda^0(\Sigma^0)$ and K^0 particles on free protons after all the enumerated corrections and after the π^- meson contamination and scanning efficiency have been taken into account is equal to 2.0 ± 0.35 mb, where

$$\sigma(Y^0K^{0,+}) = 0.8 \pm 0.25 \text{ mb}, \quad \sigma(K^0K) = 1.2 \pm 0.3 \text{ mb},$$
$$R \equiv \sigma(Y^0K^{0,+})/\sigma(K^0K) = 0.7 \pm 0.2.$$

Λ^0- AND K^0-PARTICLE MOMENTUM AND ANGULAR DISTRIBUTIONS

In constructing the angular and momentum distributions, we took into account only the correction W_1, since the correction for Φ made no essential contribution to the character of the distributions.

Figure 1a shows the momentum distribution of the Λ^0 hyperons. In Fig. 1b, the momentum spectra of Λ^0 hyperons emitted forward and backward in the c.m.s. are compared. It is seen that the momentum of Λ^0 particles emitted backward in the c.m.s. extends from zero to 1.6 Bev/c, while for Λ^0 hyperons emitted forward, the spectrum breaks off close to 1 Bev/c.

Figure 2 shows the Λ^0-hyperon angular distribution. The character of this distribution does not depend on the multiplicity of particles produced together with the Λ^0 hyperon; the Λ^0 hyperons are emitted mainly forward.

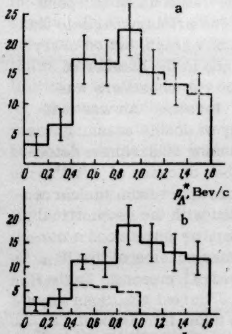

FIG. 1 C.m.s. momentum distribution of Λ^0 hyperons: a – total spectrum, b – Λ^0 hyperons emitted backward (solid line) and forward (dotted line) in the c.m.s.

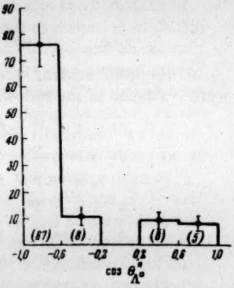

FIG. 2. C.m.s. angular distribution of Λ^0 hyperons (the number of cases is shown in parentheses).

Figure 3 shows the K^0-meson momentum distributions. It is seen from Fig. 3b that the momentum spectrum of K^0 mesons emitted forward is almost the same as for K^0 mesons emitted backward.

If the angular distribution for Λ^0 hyperons does not depend on the charged-particle multiplicity n_s, then the picture for K^0 mesons is basically changed. Figure 4a shows the K^0-meson angular distribution for $n_s \leq 2$ and Fig. 4b, for $n_s \geq 4$. For cases of low multiplicity ($n_s \leq 2$), more K^0 mesons are emitted forward than backward: $n_{\text{forward}}/n_{\text{backward}} = 2.0 \pm 0.4$. For cases of high multiplicity ($n_s = 4, 6$), the angular distribution is practically isotropic, within limits of the small statistics.

Figures 5 and 6 show the angular and momentum distributions of π^- mesons for ordinary mul-

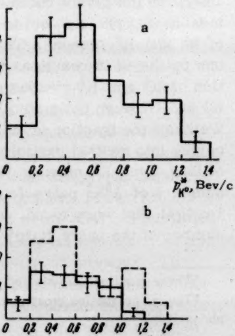

FIG. 3. C.m.s. momentum distribution of K^0 mesons: a – total spectrum, b – K^0 mesons emitted forward and backward in the c.m.s.

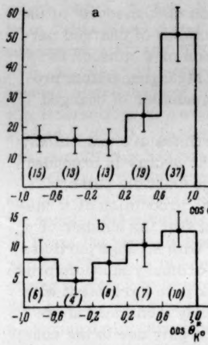

FIG. 4. C.m.s. angular distribution for K^0 mesons: a – $n_s \leqslant 2$, b – $n_s \geqslant 4$.

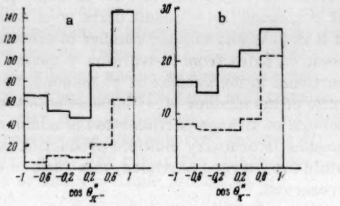

FIG. 5. C.m.s. angular distribution of π^- mesons: a – for ordinary multiple production of π^- mesons by π^- mesons, b – for π^- mesons produced together with Λ^0 hyperons. Solid line – $n_s = 2 + 4 + 6$; dotted line – $n_s = 2$.

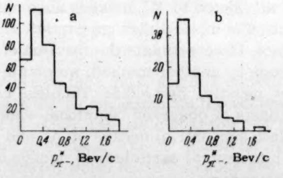

FIG. 6. C.m.s. momentum distribution of π^- mesons: a – for ordinary multiple production of π^- mesons by π^- mesons, b – for π^- mesons produced together with Λ^0 hyperons.

tiple production (a)[5] and of π^- mesons produced together with $\Lambda^0(\Sigma^0)$ hyperons (b). We compared only negative particles produced together with hyperons; this permits us to identify them uniquely as π^- mesons. In ordinary multiple production, negative particles are π^- mesons with a very large probability.

From a comparison of these distributions, it is seen that they are of the same nature.

The mean values of the transverse momenta of the Λ^0 and K^0 particles are equal to 388 ± 35 and 393 ± 35 Mev/c, respectively, i.e., they are equal within the limits of experimental error. The Λ^0-hyperon and K^0-meson transverse momentum distributions are shown in Fig. 7. The mean value of the transverse momenta does not depend on the multiplicity, as is readily seen from Table III.

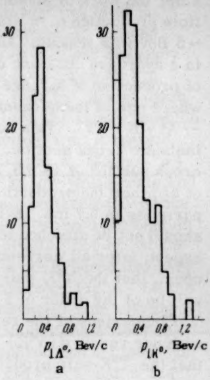

FIG. 7. Transverse momentum distribution: a – for Λ^0 hyperons, b – for K^0 mesons.

Table III

	Mean transverse momenta	
	Λ^0 particles, Mev/c	K^0 particles, Mev/c
$n_s \leqslant 2$	395±47	394±42
$n_s \geqslant 4$	367±60	386±66
$\bar{n}_s$	388±35	393±35

DISCUSSION OF EXPERIMENTAL RESULTS

1. Production cross section for $Y^0K^{0,+}$ and $K^0\bar{K}$ pairs. Our experimental results indicate that for a π^--meson energy of about 7 Bev, the production cross section for $K^0\bar{K}$ pairs is greater than the production cross section for $Y^0K^{0,+}$ pairs. The ratio of these cross sections has the value

$$R = \frac{\sigma(Y^0K^0) + \sigma(Y^0K^+)}{\sigma(K^0\bar{K}^0) + \sigma(K^0K^-) + \sigma(\bar{K}^0K^+)} = 0.7 \pm 0.2.$$

We studied only $K^0\bar{K}^0$, K^0K^-, and $\bar{K}^0K^+$ pairs. If we assume that at our energy the production cross section for charged K^+K^- pairs is the same as for $K^0\bar{K}^0$ pairs, then the ratio is reduced to 0.5:

$$R = \frac{\sigma(Y^0K^0) + \sigma(Y^0K^+)}{\sigma(K^0\bar{K}^0) + \sigma(K^0K^-) + \sigma(\bar{K}^0K^+) + \sigma(K^+K^-)} = 0.5 \pm 0.15.$$

The production cross section for Λ^0K^0 and Σ^0K^0 pairs close to the threshold was studied in detail. The total cross section for Y^0K^0 pairs has a maximum of 1.1 mb at 0.96 Bev and drops to 0.4 mb at 1.2 Bev, and then again increases to 0.6 mb at 1.3 Bev.[1]

We do not know how the cross section behaves after this. For a comparative estimate, we consider the work of Maenchen et al.,[6] where the multiple production of π^- mesons at an energy of ~5 Bev was studied. Among 106 π^-p interactions in a hydrogen diffusion cloud chamber, four cases of production of strange particles were observed, where one of these cases was identified as $\pi^- + p \rightarrow \Lambda^0 + K^+ + \pi^-$. This constitutes 4% of the total inelastic cross section. If we take a total inelastic cross section of 18 mb, as was done by Maenchen et al., then the production cross section for strange particles is 0.7 mb. Evidently, too much weight should not be attached to this result, but one may expect, after all corrections are taken into account, that the Y^0K pair production cross section will be of the order of 1 mb.

Comparison of the results of Maenchen et al.[6] with our result $\sigma(Y^0K) = 0.8 \pm 0.25$ mb indicates that the Y^0K-pair production cross section apparently remains almost constant with an increase in the π^- meson energy.

In calculations based on statistical theory[7] for the probability of the production of different pairs of strange particles, we obtain the following values relative to the total π^-p interaction cross sections: $w(\Lambda^0K) = 3.8\%$, $w(\Sigma K) = 6.8\%$, and $w(K\overline{K}) = 1.1\%$. If we take $\sigma(\Sigma^0K) = \frac{1}{3}\sigma(\Sigma K)$ and $\sigma(K^0\overline{K}) = \frac{3}{4}\sigma(K\overline{K})$, we obtain $\sigma(Y^0K) = 0.06\,\sigma_t$, or 1.5 mb; $\sigma(K^0\overline{K}) = 0.008\,\sigma_t$, or 0.2 mb.

We compare the ratios of the cross sections $\sigma(Y^0K)$ and $\sigma(K^0\overline{K})$ obtained experimentally with those calculated from statistical theory:

$$\sigma(Y^0K)_{\text{expt}}/\sigma(K^0\overline{K})_{\text{expt}} = 0.7,$$

$$\sigma(Y^0K)_{\text{theor}}/\sigma(K^0\overline{K})_{\text{theor}} = 7.5.$$

Comparison of our results with those calculated from statistical theory does not even give qualitative agreement.

If we consider the Y^0 hyperon as a bound state KN (Goldhaber's scheme), then, as was shown by Markov,[8] the production cross section for $K\overline{K}$ pairs increases with the energy of the primary π^- meson. From this viewpoint, it would be of great interest to consider the behavior of the $K\overline{K}$-pair production cross section for π^- meson energies higher and lower than ours.

2. Mean multiplicity of charged particles. Apart from strange particles, several other charged and neutral particles are produced at 6.8 Bev. We shall compare the mean multiplicities for the production of strange particles and for ordinary multiple production of π mesons[5] at the same energy. The mean number of charged particles for multiple production of π mesons is $\overline{n}_s = 3.2 \pm 0.2$. In cases of strange-particle production, the observed mean number of charged particles is $\overline{n}_s = 2.5 \pm 0.1$.

Most of the charged particles are undoubtedly π mesons. Since part of the energy is expended on the production of strange-particle pairs, less energy remains for the production of π mesons. One may then expect that the number of π mesons produced together with strange particles is less than in the case of ordinary multiple production of π mesons. This is in agreement with our results. We have already mentioned above that 14% of the cases have a pair due to the conversion of γ quanta, while for multiple production of π mesons the γ-quanta stars constitute 21%. If it is assumed that the number of electron-positron pairs from conversion γ quanta is proportional to the number of π^0 mesons, then the ratio of the number of π^0 mesons with the production of strange particles to the number of π^0 mesons in ordinary multiple production is 2 : 3, while for charged particles, this ratio is not preserved.

If we take the ratio 2 : 3 for $\pi^\pm$ mesons too, then, in the case of the production of charged particles, the mean multiplicity of the charged particles should be $\overline{n}_s = 2.0$, i.e., 0.5 less than in ordinary $\pi^\pm$-meson production. This difference can be attributed to $K^\pm$ mesons accompanying the production of neutral strange particles.

In fact, if we estimate the fraction of charged K mesons by another method, we obtain the same results, namely, $\overline{n}_{K^\pm} = 0.5$. This was estimated on the basis of observed reactions, where we have taken into account: a) decays of Λ^0 and K^0 particles into neutral particles, b) decays outside the chamber volume.

We have omitted cases in which V^0 decays were not observed, as we considered these to be ordinary multiple production of π mesons. But since we already know the probability of Λ^0- and K^0-particle decay into charged particles

$$\eta_{\Lambda^0} = (1 - f_{\Lambda^0}), \qquad \eta_{K^0} = (1 - f_{K^0}),$$

then the probability of recording decays into charged particles

$$\eta'_{\Lambda^0} = (1/W_1W_2)_{\Lambda^0}, \qquad \eta'_{K^0} = (1/W_1W_2)_{K^0}$$

can be determined as follows:

$$\overline{n}_{K^\pm} = [\eta_{\Lambda^0}\eta'_{\Lambda^0}N_{\Lambda^0K^+} + \eta_{K^0}\eta'_{K^0}N_{K^0K^\mp}]$$
$$\times [\eta_{\Lambda^0}\eta'_{\Lambda^0}N_{\Lambda^0K^+} + \eta_{K^0}\eta'_{K^0}N_{K^0K^\pm} + (\eta_{\Lambda^0}\eta'_{\Lambda^0} + \eta_{K^0}\eta'_{K^0})\,N_{\Lambda^0K^0}$$
$$- n_{\Lambda^0K^0} + 2\,(\eta_{K^0}\eta'_{K^0}N_{K^0\overline{K}^0} - \tfrac{1}{2}\,n_{K^0\overline{K}^0})]^{-1} = 0.5 \pm 0.12,$$

where $N_{\Lambda^0 K^+}$, $N_{K^0 K^\pm}$, $N_{\Lambda^0 K^0}$, and $N_{K^0 \overline{K}^0}$ are taken from Table II and $n_{\Lambda^0 K^0}$ and $n_{K^0 \overline{K}^0}$ are the observed number of $\Lambda^0 K^0$ and $K^0 \overline{K}^0$ pairs.

3. Angular and momentum distributions. The angular distribution of Λ^0 hyperons produced in $\pi^- p$ interactions close to the threshold has been studied in detail. An analysis of the S- and P-wave amplitudes has been made.[1]

Such an analysis cannot, of course, be made at 6.8 Bev. Only general ideas can be used to explain the angular distributions of the secondary particles.

From the angular distribution of single Λ^0 hyperons (Fig. 2), it is seen that they have a very strong tendency to be emitted backward in the c.m.s. Such an asymmetry can result from a background of interactions with quasi-free nucleons of carbon (in the propane molecule). In fact, even in the most unfavorable case, when the entire contamination from Λ^0 hyperons produced on quasi-free protons (about 20%) is subtracted from the distribution under the assumption that all Λ^0 are emitted backward, there still remains the asymmetry $n_{\Lambda^0 \text{forward}}/n_{\Lambda^0 \text{backward}} = 1:5$. This asymmetry was also observed in cases of $\Lambda^0 K^0$ pairs. A similar result was obtained for protons in ordinary multiple production of mesons.[5,9]

Table IV

$\cos\theta^0$	$\Lambda^0 K^0$		$K^0 \overline{K}^0$
	Λ^0	K^0	
1,0— 0.6	0.0	7.0	7.5
0.6— 0.2	5.3	0.0	4.0
0.2— —0.2	0.0	2.2	0.0
— 0.2—0.6	1.2	1.1	1.0
—0.6— —1.0	10.3	3.3	2.4

Table IV shows the c.m.s. angular distributions of $\Lambda^0 K^0$ and $K^0 \overline{K}^0$ pairs. Although the number of these pairs is small, the basic character of these distributions is evident: The Λ^0 hyperons are emitted backward, while the K^0 mesons are emitted forward, although this tendency is not so marked here. Owing to the poor statistics, we cannot consider the angular distribution of $K^0 \overline{K}^0$ pairs in greater detail. It is seen from Fig. 4 that the K^0-meson angular distribution actually extends forward to an extent depending on the multiplicity of the secondary charged particles. When $n_s = 0$ or 2, it is not symmetric, and when $n_s = 4$ or 6, the distribution is practically isotropic.

In Figure 5b, the c.m.s. angular distribution is given for π^- mesons produced together with a Λ^0 hyperon. It is seen that the π^- mesons are emitted preferentially forward in the case of low multiplicity ($n_s = 2$). The ratio $n_{\pi^- \text{forward}}/n_{\pi^- \text{backward}}$ is 1.7 ± 0.5. When $n_s \geq 4$, the anisotropy in the distribution is less marked, although the statistics here are poor and it is not possible to make a quantitative estimate. A qualitative comparison of the distribution of π^- mesons produced together with Λ^0 hyperons indicates that they are of the same character. The behavior of the π^- mesons produced in both types of interactions is of the same character as the behavior of K^0 mesons.

Birger et al.,[5] Maenchen et al.,[6] and Belyakov et al.,[9] who studied multiple production in $\pi^- p$ collisions, obtained similar results. It was established that the proton travels in the same direction as it did prior to the interaction, i.e., it travels backward in the c.m.s., while the π^- mesons are emitted forward in the case of low multiplicity and are distributed approximately isotropically as the multiplicity increases. The π^--meson momentum distributions in ordinary multiple production[5] and in production together with a Λ^0 hyperon are very similar. This is plainly seen from Fig. 6. On the basis of the similarity in the momentum and angular distributions, we can consider, as a first approximation, that the Λ^0 hyperon and nucleon (as baryons) are in one group and the K and π (as mesons) are in another group.

The character of the Λ^0-hyperon angular distribution is connected with the Λ^0 momentum distribution. Since a very small part of the Λ^0 hyperons are emitted forward, it may be expected that the probability of a large momentum transfer during the collision is small, i.e., the spectrum of Λ^0 hyperons emitted forward is soft. From Fig. 1a, it is seen that this is in agreement with our experimental results.

4. Transverse momenta. One of the interesting facts is, perhaps, that Λ^0 hyperons and nucleons in inelastic interactions without the production of strange particles have the same distributions and the same mean transverse momenta independently of the multiplicity. In references 5 and 9, the transverse momenta were measured for protons for various multiplicities. Within the limits of experimental error, the values of the transverse momenta coincide with our results.

The calculated rms transverse momentum for Λ^0 and K^0 particles is approximately equal to 400 Mev/c. Using the uncertainty relation $\Delta p \Delta r \geq \hbar$, we can estimate the radius of the region of interaction responsible for the production of strange particles: $\Delta r \geq \hbar/\Delta p \approx \hbar/3m_\pi c = 4 \times 10^{-14}$ cm.

It is interesting to note that the dimensions of the region of interaction in the case of strange-particle production and in ordinary multiple production almost coincide.

In conclusion, the authors express their profound gratitude to D. I. Blokhintsev, M. A. Markov, V. I. Ogievetskii, Chou Kuang-Chao, I. V. Chuvilo, V. S. Barashenkov, and V. G. Solov'ev for discussion of the results; to L. P. Zinov'ev, M. I. Pavlov, K. V. Chekhlov, L. N. Belyaev, and to the engineers and technicians of the accelerator group for performing the experiment; to the laboratory staff for carrying out the measurements; and to the electronic computer group for performing the calculations. We are also very grateful to T. Hofmokl and Kim Hi In for aid in checking the results.

---

[1] Eisler, Plano, Prodell, Samios, Schwartz, Steinberger, Bassi, Borelli, Puppi, Tanaka, Waloschek, Zoboli, Conversi, Franzini, Manelli, Santangelo, and Silverstrini, Nuovo cimento **10**, 468 (1958).

[2] Wang Kang-Chang, Wang Tsu-Tseng, Ting T'a-Tsao, Ivanov, Katyshev, Kladnitskaya, Kulyukina, Nguyen Dinh Tu, Nikitin, Otwinowski, Solov'ev, Sosnowski, and Shafranov, JETP **38**, 426 (1960), Soviet Phys. JETP **11**, 313 (1960).

[3] D. Glaser, Ann. Intern. Conf. on High Energy Physics at CERN, Geneva, 1958.

[4] Brown, Bryant, Burnstein, Glaser, Hartung, Kadyk, Sinclair, Trilling, and Van der Velde, Phys. Rev. Lett. **3**, 563 (1959).

[5] Birger, Wang Kang-Chang, Wang Tsu-Tseng, Ting T'a-Tsao, Katyshev, Kladnitskaya, Kopylova, Lyubimov, Nguyen Dinh Tu, Nikitin, Podgoretskii, Smorodin, Solov'ev, and Trka, JETP (in press).

[6] Maenchen, Fowler, Powell, Wright, Phys. Rev. **108**, 850 (1957).

[7] V. S. Barashenkov and V. M. Mal'tsev, Acta Phys. Polon. **17**, 177 (1958).

[8] M. A. Markov, Гипероны и К-мезоны (Hyperons and K Mesons) Gostekhizdat, 1958.

[9] Belyakov, Wang Shu-Feng, Glagolev, Dalkhazhav, Lebedev, Mel'nikova, Nikitin, Petrzilka, Sviridov, Suk, Tolstov, JETP **39**, 937 (1960), Soviet Phys. JETP **12**, 650 (1961).

Translated by E. Marquit
70

SOVIET PHYSICS JETP VOLUME 13, NUMBER 2 AUGUST, 1961

INVESTIGATION OF THE RADIATIONS FROM Zn^{63}

S. S. VASIL'EV, NO HSIENG CH'ANG, and L. Ya. SHAVTVALOV

Institute of Nuclear Physics, Moscow State University

Submitted to JETP editor September 12, 1960

J. Exptl. Theoret. Phys. **40**, 475-476 (February, 1961)

The β^+ and γ spectra of Zn^{63}, which possesses a half-life of 37.6 ± 0.3 min, were investigated. The β^+ spectrum consists of five components with end-point energies of 500, 1020, 1400, 1710 and 2360 kev. The observed 680-, 970-, 1350-, 1430- and 2300-kev γ transitions agree on the whole with the β^+ spectra.

THERE have been relatively few investigations of Zn^{63} to date.[1-4] These investigations have established the presence of three partial β^+ spectra. The Zn^{63} was investigated by using copper targets of natural isotopic composition.

We used enriched targets containing up to 98.1 percent Cu^{63} to investigate the β^+ and γ spectra of the Zn^{63} obtained from the reaction $Cu^{63}(p, n)$ Zn^{63}. The irradiation was in the 120-cm cyclotron of the Nuclear Physics Institute of the Moscow State University with 6.7 Mev protons for several minutes. The investigation of the Zn^{63} spectra began 3 — 5 minutes after the irradiation.

The β^+ spectra of Zn^{63} were investigated with a β spectrometer with a thin magnetic lens with an end-window β counter. The Fermi plot of the obtained β^+ spectrum (Fig. 1) can be resolved into five linear sections, corresponding to the individual β^+ spectra with end-point energies 500 ± 30, 1020 ± 30, 1400 ± 30, 1710 ± 30, and 2360 ± 30 kev. The relative intensities of these partial β^+ spectra are respectively 2, 10, 10, 10, and 68.

The γ spectrum of the Zn^{63} was investigated with a luminescence spectrometer. The pulses from the FÉU-1S photomultiplier with NaI(Tl) crystal were fed to the input of a 100-channel pulse-height analyzer type AI-100 ("Raduga"). Figure 2 shows the γ spectrum of Zn^{63} we obtained. In addition to the intense annihilation peak, γ lines with energies 680 ± 10, 970 ± 10, 1350 ± 20, 1430 ± 20, and 2300 ± 30 kev were observed. In all probability, a γ line with energy 1540 ± 20 kev is also present. The half-life measured by the annihilation peak was found to be 37.6 ± 0.3 minutes, the same value as obtained for the remaining γ lines, within the limits of experimental error.

Our experimental data on the β^+ transitions differ from those of Huber et al.,[1] who indicated only β^+ transitions with end-point energies 470, 1400, and 2360 kev. Recently Ricci et al.[4] proposed a probable decay scheme for Zn^{63}, starting out with the energy and relative intensity of the γ rays. In the opinion of these authors, β^+ transitions with end-point energies 950 and 1700 kev, close to those obtained by us, should exist in addition to those indicated by Huber et al. Thus, the β^+ transitions which we observed apparently confirm the decay scheme given in reference 4.

FIG. 1. Fermi plot for the positron spectrum of Zn^{63}. N – number of positrons registered by the spectrometer, F – Coulomb factor, J – current in the spectrometer lenses.

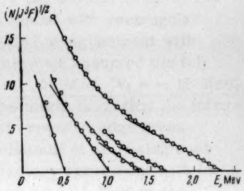

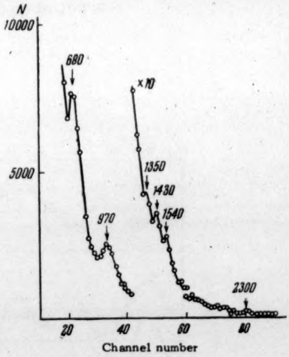

FIG. 2. γ spectrum of Zn^{63}.

[1] Huber, Medicus, Preiswerk, and Steffen, Helv. Phys. Acta 20, 495 (1947).

[2] Pasechnik, Barchuk, Totskii, Strizhak, Korolev, Gofman, Lovchikova, Koltypin, and Yan'kov, Second Geneva Conference, 1958. Papers by Soviet Scientists. 1. Nuclear Physics, M., Glavatom, 1959, p. 330.

[3] Hayward, Farrelly, Hoppes, and van Lieshout, Nuovo cimento 11, 153 (1959).

[4] Ricci, Girgis, and van Lieshout, Nuovo cimento 11, 156 (1959).

Translated by J. G. Adashko
71

SOVIET PHYSICS JETP VOLUME 13, NUMBER 2 AUGUST, 1961

ELASTIC SCATTERING OF 13.6-Mev DEUTERONS BY NUCLEI. II

Yu. V. GOFMAN and O. F. NEMETS

Submitted to JETP editor September 13, 1960

J. Exptl. Theoret. Phys. (U.S.S.R.) 40, 477-478 (February, 1961)

The angular distributions of 13.6-Mev deuterons elastically scattered on U, Bi, Cd, Zr, Nb, Zn, Ti, Si, Al and C nuclei are measured.

WE measured the angular distributions of elastically-scattered deuterons on several nuclei using the extracted 13.6-Mev deuteron beam from the cyclotron of the Physics Institute of the Academy of Sciences of the Ukrainian S.S.R. The measurement procedure and the target-preparation technique were described earlier.[1,2] The half-width of the elastic peak amounted to 2.0 — 3.0 percent (at angles up to 90°). The statistical measurement errors did not exceed one percent. Since the deviations from Rutherford scattering take place in the case of aluminum, silicon, and carbon even at small angles, we measured the absolute cross sections of these nuclei for angles 45 and 55°.

The measurement results are shown in the figure. The arrows indicate the values of $\theta = \theta_{cr}$ at which nuclear interaction begins to come into play.

An attempt to compare the angular distribution for zinc with the optical model with rectangular well (dotted curve) yielded no agreement with experiment. For this curve we assumed the following parameters: $V_0 = -50$ Mev, $W_0 = -10$ Mev, $r_0 = 1.27 \times 10^{-13}$ cm. One might think that the introduction of a potential with rounded edge gives better results, since Melkanoff et al., using such a model, obtained satisfactory agreement with experiment for aluminum at $E_d = 15$ Mev in the angle range up to 100°.[3]

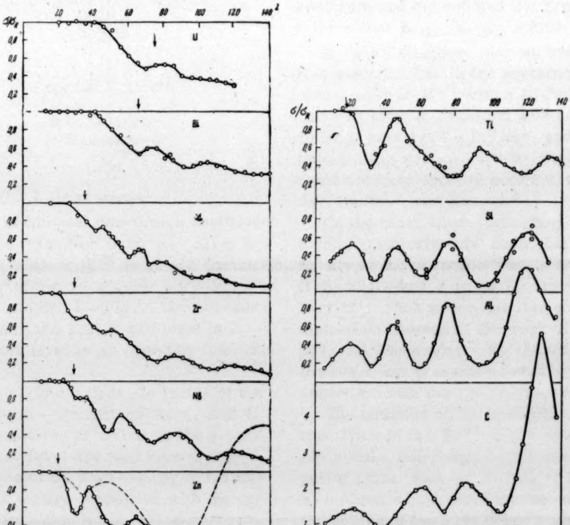

[1] N. I. Zaika and O. F. Nemets, Izv. Akad. Nauk SSSR, Ser. Fiz. 23, 1460 (1959), Columbia Technical Translations p. 1447.

[2] Yu. V. Gofman and O. F. Nemets, JETP 39, 1489 (1960), Soviet Phys. JETP 12, 1035 (1961).

[3] M. A. Melkanoff, Proc. Int. Conf. on the Nucl. Optical Model, Florida State University, 1959, p. 207.

Translated by J. G. Adashko
72

SOVIET PHYSICS JETP VOLUME 13, NUMBER 2 AUGUST, 1961

ON THE 892.4-kev GAMMA TRANSITION IN W^{182}

V. D. VITMAN, N. A. VOINOVA, B. S. DZHELEPOV, and A. A. KARAN

All-Union Metrological Institute

Submitted to JETP editor September 24, 1960

J. Exptl. Theoret. Phys. (U.S.S.R.) 40, 479-482 (February, 1961)

Results of measurements of the relative intensities of γ transitions from the 1221.8-kev level in W^{182} to the levels of the ground rotational band are presented. The intensity of the 892.4-kev transition is found to be smaller than that computed according to the theory for axial nuclei as well as that computed according to the theory for nonaxial nuclei.

1. In the decay of Ta^{182} to W^{182}, the transitions shown in Fig. 1 occur. The 1221.8-kev excited state of W^{182} is formed in most of the decays. It is a 2^+ level as shown by the following experimental data:

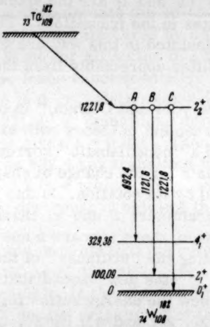

FIG. 1. Decay scheme.

a) On the basis of internal conversion coefficient measurements,[1] the transition from the 1221.8-kev level to the ground state of W^{182} is an E2 transition.

b) Investigation[2] of the $\gamma\gamma$ angular correlation in the 67.74 — 1221.8 and 67.74 — 1121.6 kev cascades shows that the spin of the 1221.8-kev level is 2.

c) The 1221.8-kev level is produced by Coulomb excitation.[3]

The 1221.8-kev state can decay to levels of the lowest rotational band — transitions A, B, and C in Fig. 1. The transitions C and B to the ground state and 100.09-kev level are well known; they are the most intense of the high-energy γ transitions. In this work we are concerned with the competing 892.4-kev transition A.

An 892-kev line was observed in 1950 by O'Meara[4] in the photoelectron spectrum. In 1955, the information[5] appeared that Fowler had also observed this line in the photoelectron spectrum. However, in the article itself to which reference had been made[6] there was no such indication. In 1959 in a study of the γ spectrum of Ta^{182} on an elotron,[7] an upper limit of 0.017 was established for the ratio of the intensities of the 892.4- and 1221.8-kev γ rays.

In the conversion spectrum of Ta^{182}, the line corresponding to this transition has never been observed. Gvozdev, Rusinov, and Khazov[8] made a special search for this line in the conversion spectrum and did not find it. From their work it follows that $K_{892.4}/K_{1221.8} \leq 0.02$.

In 1959 Gallagher, Newton, and Shirley[9] found a K-conversion line in the spectrum of Re^{182}, which also decays to W^{182} with a 13-hour half-life; this line was from a transition with nearly the same energy, $h\nu = 894.7 \pm 0.8$ kev, and had a large intensity, $K_{894.7}/K_{1221.8} = 2/3$. Such an intense line could not have escaped notice in the work of Gvozdev, Rusinov, and Khazov.[8]

On the other hand, Gallagher, Newton, and Shirley's experiments[9] show that the relative intensity of the corresponding γ transition is 0.35 if the 894.7-kev γ is an E2 transition or 0.16 if it is M1. Such an intense line could not have remained undetected in the work of Voinova, Dzhelepov, and Zhukovskii.[7] We therefore conclude that the 894.7-kev transition found by Gallagher is not connected with the 1221.8-kev level in W^{182}.

The question of the intensity of the 892.4-kev transition in the Ta^{182} decay remains unanswered. Meanwhile, knowledge of the intensities of the competing transitions A, B, and C is important both as a check on current theories and for discovering the nature of the 1221.8-kev state.

2. With the new magnetic spectrometer of the elotron type, constructed at the Metrology Institute,

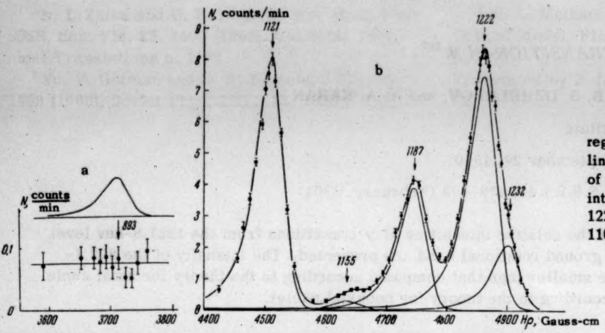

FIG. 2. Electron spectrum: a – the region which should contain the 892.4-kev line; the upper curve is the expected form of this line under the assumption that its intensity is 1% of the intensity of the 1221.8-kev line; b – the spectrum in the 1100–1250 kev region.

we have reinvestigated the portions of the γ spectrum in the energy ranges 850 – 910 kev and 1100 – 1250 kev. The higher resolution (1.2% at 1 Mev) of this spectrometer, as compared to the previous one,[7] and the lower background allowed us to lower the upper limit on the ratio of the intensities of the 892.4-kev and 1221.8-kev γ rays.

Figure 2 shows the electron spectrum in the regions studied. The background, which in the energy range 850 – 910 kev is practically constant at 0.04 count/min, has been subtracted from the experimental points. The signal that remains after subtraction of background can be attributed to the tails of the hard lines, which in this region contribute about 0.1 count/min. From our results it follows that the intensities of the γ rays satisfy

$$I(\gamma_{892.4})/I(\gamma_{1221.8}) \leqslant 0.006.$$

3. In the theory of nonaxial nuclei developed by Davydov et al.,[10,11] the intensity ratios of the transitions A, B, and C are determined uniquely.

The energy ratio of the two spin-2 rotational levels gives γ, the parameter characterizing the nonaxial nucleus, according to the formula[10]

$$E(2_2^+)/E(2_1^+) = [1+\sqrt{9-8\sin^2(3\gamma)}]/[1-\sqrt{9-8\sin^2(3\gamma)}].$$

(2_1^+ is the first 2^+ level, counting from the ground state). Setting $E(2_1^+) = 100.092$ kev[12] and $E(2_2^+) = 1221.8$ kev,[13] we find that $\gamma = 11.40°$.

Using the formula for the reduced transition probability from Davydov's review,[10] we calculated the relative intensities of the 1221.8-kev and 1121.6-kev transitions (see the table).

The formula for the reduced transition probability for the $2_2^+ \rightarrow 4_1^+$ transition is not given in the papers of Davydov et al.; only an approximate value for the reduced probability for the $4_1^+ \rightarrow 2_2^+$ transition is given.[11] However, according to a private communication from Davydov, for $\gamma = 11.4°$ the exact value is 15 per cent higher. The $2_2^+ \rightarrow 4_1^+$ transition probability is higher by a factor $(2I_f+1)/(2I_i+1) = 9/5$ (I_f and I_i are the spins of the final and initial states in the transition). The relative intensities calculated in this way are given in the table. They differ appreciably from the experimental result.

Recently Davydov and Chaban,[14] in order to obtain better agreement of theory with experiment, have proposed a "nonadiabatic" correction, i.e., one that accounts for the change of shape of the nucleus caused by its rotation. In this theory, besides the parameters β and γ, characterizing the nuclear shape, there appears a new parameter, μ, characterizing the "stiffness" of the nucleus. To determine γ' (the new "nonadiabatic" γ) and μ, one must know the energy ratios for three levels, for example, 2_1^+, 2_2^+, and 4_1^+, or 2_1^+, 2_2^+ and 6_1^+. The corrections to the reduced transition probability can be made after γ' and μ have been computed; for small μ this amounts to replacing the old "adiabatic" γ by γ'. Using the above energy values for the 2_1^+ and 2_2^+ levels and 329.36 kev for the 4_1^+ level, we found $\gamma' = 11.19°$ and $\mu = 0.186$. Using the same values for the 2_1^+ and 2_2^+ levels and 680.38 kev for the 6_1^+ level, we found $\gamma' = 11.21$ and $\mu = 0.181$. Thus the values derived from the positions of the 4_1^+ and 6_1^+ levels are in excellent agreement. For $\gamma' = 11.20°$, the relative intensities of the competing transitions are almost the same as for $\gamma = 11.40°$ (see table). The disagreement with the experiments on the 892.4-kev line is essentially unchanged.

4. In the theory of axial nuclei developed by Alaga, Alder, Bohr, and Mottelson,[15] the relative intensities of the transitions A, B, and C depend

Relative intensities of transitions from the 1221.8 kev W^{182} level

Transition energy, kev	Experimental relative value	Theoretical relative intensity					
		according to Davydov		by Alaga's rule			
						$K = 2$	
		$\gamma = 11.40°$	$\gamma' = 11.20°$	$K = 0$	$K = 1$	uncorrected	corrected
892.4	$\leqslant 0.6$	3.8	3.7	53.6	23.8	1.46	3.2
1121.6	122	131	130	93.2	23.5	93.2	122
1221.8	100	100	100	100	100	100	100

on the quantum number K of the 1221.8 kev level. The reduced relative intensities calculated according to reference 15 for K = 0, 1, and 2 are given in the table. K = 0 and K = 1 are completely excluded by the experimental data. For K = 2, the theory of axial nuclei gives results which are closer to the experimental data, but still outside the limits of error.

Not so long ago Hansen, Nielsen, and Sheline[16] proposed that the relative intensities of the transitions should be corrected by considering the mixing of K = 2 states into the K = 0 band and the mixing of K = 0 states into the K = 2 band. This mutual mixing is characterized by a parameter z, which is the same for all states in a band, and which must be found experimentally. We can determine z so that the relative intensities of the 1121.6 and 1221.8 kev transitions agree with experiment; this gives z = 0.046. Then the relative intensity of the 892.4 kev transition increases from 1.46 to 3.2 (see table). Thus, this correction increases the discrepancy between theory and experiment.

5. We should mention that the enigmatic absence of the $2_2^+ \rightarrow 4_1^+$ transition is not a general rule. For example, in the $Tb^{156} \rightarrow Gd^{156}$ and $Ho^{160} \rightarrow Dy^{160}$ decays transitions of this type are observed[11,16,17] with an intensity approximately in agreement with both theories; the experimental ratio of the reduced transition probabilities, $B(E2, 2_2^+ \rightarrow 4_1^+)/B(E2, 2_2^+ \rightarrow 2_1^+)$, are 0.12 for Cd^{156} and 0.08 for Dy^{160}; the theory of nonaxial nuclei gives 0.095 and the theory of axial nuclei gives 0.080 – 0.087 (for z = 0.04 – 0.05).

---

[1] Murray, Boehm, Marmier, and Du Mond, Phys. Rev. **97**, 1007 (1955).

[2] R. Williams and K. Roulston, Can. J. Phys. **34**, 1087 (1956).

[3] Alkhazov, Grinberg, Gusinskii, Erokhina, and Lemberg, JETP **35**, 1325 (1958), Soviet Phys. JETP **8**, 926 (1959).

[4] F. E. O'Meara, Phys. Rev. **79**, 1032 (1950).

[5] Fowler, Kruse, Keshishian, Klotz, and Mellor, Nucl. Sci. Abstr. **9**, 24B, 102 (1955).

[6] Fowler, Kruse, Keshishian, Klotz, and Mellor, Phys. Rev. **94**, 1082 (1954).

[7] Voinova, Dzhelepov, and Zhukovskii, Izv. Akad. Nauk SSSR, Ser. Fiz. **23**, 828 (1959), Columbia Tech. Transl. p. 822.

[8] Gvozdev, Rusinov, and Khazov, Izv. Akad. Nauk SSSR, Ser. Fiz. **24**, No. 12 (1960), Columbia Tech. Transl., in press.

[9] Gallagher, Newton, and Shirley, Phys. Rev. **113**, 1298 (1959).

[10] A. S. Davydov, Izv. Akad. Nauk SSSR, Ser. Fiz. **23**, 792 (1959), Columbia Tech. Transl. p. 788.

[11] A. S. Davydov and V. S. Rostovskii, JETP **36**, 1788 (1959), Soviet Phys. **9**, 1275 (1959).

[12] Müller, Hoyt, Klein, and Du Mond, Phys. Rev. **88**, 775 (1952).

[13] G. Backström, Arkiv Fysik **10**, 387 (1956).

[14] A. S. Davydov and A. A. Chaban, Nuclear Phys., in press.

[15] Alaga, Alder, Bohr, and Mottelson, Kgl. Danske Videnskab. Selskab, Mat.-fys. Medd. **29**, 9 (1955).

[16] Hansen, Nielsen, and Sheline, Nuclear Phys. **12**, 389 (1959).

[17] Voinova, Dzhelepov, and Zhukovskii, Izv. Akad. Nauk SSSR, Ser. Fiz. **24**, 852 (1960), Columbia Tech. Transl., in press.

Translated by M. Bolsterli
73

SOVIET PHYSICS JETP VOLUME 13, NUMBER 2 AUGUST, 1961

ON THE TEMPERATURE OF LIGHTNING AND FORCE OF THUNDER

Yu. N. ZHIVLYUK and S. L. MANDEL'SHTAM

P. N. Lebedev Physics Institute, Academy of Sciences, U.S.S.R.

Submitted to JETP editor June 30, 1960

J. Exptl. Theoret. Phys. (U.S.S.R.) 40, 483-487 (February, 1961)

The temperature in the lightning channel was measured by a spectroscopic method with the help of the N II and O II lines and a value T ~ 20 000° was obtained. This value is in good agreement with the results of a calculation based on the hydrodynamic theory of development of the spark channel. The hydrodynamic model was further used to calculate the force of the thunder, i.e., the pressure on the front of the shock wave. Excess pressures are obtained which in a number of cases may lead to destruction of objects located a few meters from the lightning.

WE report in this paper preliminary results of spectroscopic measurements of the temperature of a lightning channel in the high-current stage, and of calculations of the pressure on the front of the shock wave produced by the lightning.

Many papers dealing with the spectrum of lightning have been published;[1] so far, however, its temperature has not been measured nor have the pressures produced by the thunder been calculated.

The conditions under which the lightning channel is produced and the state of the plasma in it are similar to the those in the channel of a condensed spark discharge in air, which have been thoroughly investigated in our laboratory. This enables us to identify the thunder with the shock wave produced by the rapid expansion of the channel,[2] and to calculate the pressure on the front of the shock wave (thunder) in analogy with the procedure used for the spark discharge.[3]

In the ordinary laboratory spark discharge, produced at atmospheric pressure, the concentration of the electrons is $N_e \geq 10^{17}$ cm^{-3}. At these values of N_e, the excited levels of the atoms and ions have a Boltzmann distribution which sets in within ~ 10^{-7} sec. As a result, the channel plasma emits Kirchhoff-law[4] radiation practically during its entire lifetime. The gas temperature reaches the electron temperature $T_e = T_i = T$ within ~ 10^{-6} sec (reference 5), and can therefore be determined spectroscopically from the atomic lines. The same conclusions apply to lightning; the concentration of the electrons in the lightning channel, as follows from estimates based on the widths of the $H\alpha$ and $H\beta$ lines in the lightning spectra which we investigated, is of the same order of magnitude.

Let us assume that the temperature is constant over the channel section. Then, by Kirchhoff's law, the radiation intensity at a frequency ω is given within the limits of the spectral line by the expression

$$I(\omega) = I_0(\omega)(1 - e^{-k_\omega l}), \tag{1}$$

where $I_0(\omega)$ is the intensity of black-body radiation at the channel temperature, l is the channel diameter, and k_ω is the plasma absorption coefficient for the frequency ω.

In the case of a line broadened by collisions and by the Doppler effect, we have

$$k_\omega = k_0 \frac{a}{\pi} \int_{-\infty}^{+\infty} \frac{\exp(-y^2)}{a^2 + (v - y)^2} dy,$$

$$k_0 = (2\pi^{1/2}/mc)(Nf/\Delta\omega_0), \qquad v = 2(\omega - \omega_0)/\Delta\omega_d. \tag{2}$$

Here k_0 is the coefficient of absorption at the center of the line in the absence of broadening by collisions, $a = \Delta\omega_c/\Delta\omega_d$ where ω_d is the Doppler width of the line and ω_c is the line width due to the collisions.*

Let us estimate the optical thickness of the plasma for different portions of the line. The estimates given below pertain to the 3995-A line N II.

Assuming T ~ 2 × 10^4 deg K and λ ~ 4000 A, we obtain for the nitrogen ions $\Delta\lambda_d = 0.06$ A. Estimates and measurements of a laboratory spark show that $\Delta\lambda_c$ ranges from several tenths of an angstrom to several angstroms. Assuming $N_0 \sim 10^{17}$ cm^{-3} and a channel diameter $l \sim 10$ cm,

---

*When $N_e = N_i \sim 10^{17}$ cm^{-3}, the statistical line skirt can be neglected for a line with a quadratic Stark effect.

Table I.

Distance from the center of the line, $\Delta\lambda$, A	$k_\omega l$				
	$\Delta\lambda_c$ (Å) =0.05	0.1	0.15	0.5	2
0.00	104	79.5	65	31.5	6.2
0.08	55	51	45	27	6.2
0.16	11.8	17	19.6	18.4	6.1
0.23	8.8	9.2	10	11.8	5.9
0.31	2.7	2.9	5.2	8.4	5.7
0.38	1.0	2.1	3.5	6.1	5.5
0.45	0.9	1.3	2.1	4.4	5.2

Table II.

Line pair λ (Å)	Channel temperature (°K) determined from the spectrograms				
	№ 1	№ 2	№ 3	№ 4	Average
N II 5045 N II 3995	20000	31000	23000	—	25000
N II 5045 N II 4447	16000	25000	17000	22000	20000
N II 4447 O II 3857	14000	21000	—	—	18000
				Average	21000

we obtain the values of $k_\omega l$ listed in Table I. It follows from this table that, at least within ± 0.5 A and perhaps also at greater distances from the center of the line, the optical thickness of the plasma is in practice appreciably greater than unity. Consequently, the lightning channel radiates as a black body in the central portion of the line. By photographing the spectrum with a spectrograph having an apparatus function width ≤ 1 A and measuring the relative intensity at the center of the image of each of the lines with different λ, we can determine the temperature of the channel from Eq. (1).

We have photographed the lightning spectrum with the spectrographs SP-48 (operating range 3800 — 6800 A, dispersion 80 — 95 A/mm) and SP-49 (operating range 2600 — 3800 A, dispersion 76 — 80 A/mm). The slit was 0.1 mm wide. These instruments yield a strong reduction, and the width of the apparatus function, measured against the neon and mercury lines and the lines of the lightning spectrum, amounted to ~ 1 A. The lightning spectrum was photographed at night. At the beginning of the thunderstorm the spectrographs were aimed at the center of the storm area and were then made to follow the motion of the storm. Each spectrogram is thus the result of the superposition of light from several lightnings and corresponds to the entire duration of each discharge. Almost all the photographic density was produced by the direct light from the lightning channel, and not by the light scattered in the clouds; this was verified by aiming the spectrograph on a portion of the sky illuminated only by the scattered light from the lightning.

The photographs were produced with Pankhrom X and type "D" films, of sensitivity 1200 — 1500 GOST units. The film was pre-exposed prior to use to a density S = 0.2 to increase the sensitivity (by a factor 3 — 4). The density markers used were photographs of a 9-step wedge, obtained with the aid of a blue filter. To determine the spectral sensitivity of the film, the spectrum of a luminophor of known intensity distribution was photographed. The density and spectral-sensitivity markers were photographed on a section adjacent to the working section of the film and subjected to the same exposure as the working section; both sections were developed simultaneously.*

The density of the film was measured with an MF-4 recording microphotometer. The background was measured on both sides of the line and was allowed for in the usual manner. The spectrograms were calibrated against the mercury and neon spectra; the lines were identified with the aid of the Moore tables.

A total of nine spectrograms was processed. We identified and measured the positions of some 100 lines of which approximately one-half were not previously observed. The majority of the lines belongs to neutral and singly-ionized atoms of oxygen and nitrogen. The observed lines with wavelengths 5600, 5471, 4542, and 4058 A possibly belong to the ions of greater multiplicity (O III, O V, and N III). However, this identification is very unreliable. Several edges of the N_2^+ bands are also observed; the continuous spectrum is relatively intense.

Table III.

Current growth rate	Relative pressure on the front of the shock wave, kg/cm²		
	r(cm)=5	50	500
30kA/10 μsec	94	9.2	0.9
30kA/100 μsec	9.5	0.25	0.02
30kA/100 μsec	2.8	Shock wave turns into sound wave	Shock wave turns into sound wave

To determine the channel temperature we measured the lines N II 3995 A, N II 4447 A, O II 3857 A, and N II 5045 A. The measurement results are listed in Table II. The difference in the numbers should probably be attributed to the measurement error, which is very high and amounts to ~ 5000°. The value T ~ 20 000° obtained for the channel temperature apparently characterizes a certain average stage of the discharge. The final stages and the peripheral portions of the discharge have obviously a lower temperature, as evidenced by the presence of O I, N I, and N_2^+ bands in the spectrum. The initial stages of the discharge have probably a somewhat higher temperature.*

---

*The use of the average contrast factor for the entire 4000–5000 A region does not, as shown by special estimates, introduce any appreciable error in the temperature measurement. Likewise, with the types of film employed, the error due to the difference in the exposure of the lightning spectrum and the density markers, resulting from violation of the reciprocity law, is relatively small.

The temperature obtained is in good agreement with that estimated by the Braginskii formula,[7] which is based on the hydrodynamic theory of development of the channel:

$$T = 4.35\rho_0^{1/14}(Jt^{-3/4})^{2/7}.$$

Here ρ_0 is in units of 1.29×10^{-3} g/cm^3, J is in kiloamp, t is in μsec and T in ev. Taking as typical values J ~ 30 kiloamp and t = 100 — 1000 μsec,[8] we obtain T = 16,000 — 25,000°.

We can now apply the hydrodynamic theory of development of the spark-discharge channel to the calculation of the other parameters of the lightning channel, particularly the radius and the pressure of the shock wave. We assume, following Braginskii's calculations,[7] that the current in the lightning varies as J ~ $t^{3/4}$, and that the conductivity of the channel is practically constant at $\sigma = 2 \times 10^{14}$ cgs esu. Then, assuming no loss to radiation, the Drabkina formulas[3] yield the following expression for the radius and velocity of the shock-wave front:

$$r = 1{,}11\eta^{1/4}\rho_0^{-3/14}J^{5/14}t^{10/14}, \quad a = 5{,}55\cdot 10^5\eta^{1/4}\rho_0^{3/14}J^{3/14}t^{-4/14}.$$

Here r is in cm, a in cm/sec, J in kiloamp, t in μsec, and ρ_0 in units of 1.29×10^{-3} g/cm^3. The coefficient η defines the ratio of the energy required for the translational motion of the gas to the total energy released in the channel. According to Taylor's calculations for a spherical shock wave,[9] $\eta = 0.1$. Gegechkori[2] calculated $\eta = 0.2$ for a cylindrical wave from a laboratory spark discharge.

The pressure on the front of the shock wave is connected with the velocity of the front by the relation

$$p_f = \frac{2\rho_0 a^2}{\gamma+1} - \frac{\gamma-1}{\gamma+1}p_0,$$

where p_0 is the atmospheric pressure and γ the adiabatic exponent. Carrying out the calculations for a lightning with J ~ 30 kiloamp, and assuming that this value is reached within t = 10, 100, and 1000 μsec, respectively, we obtain the values of p_f listed in Table III.

Thus, at an average current growth of 30 kiloamp/100 μsec, considerable pressures are developed on the front of the shock wave, and consequently the thunder can seriously damage objects located at a distance up to several meters. By way of an example we indicate that, in accordance with the handbook data,[10] an excess pressure of 0.07 kg/cm^2 acting on the entire surface will shatter a window pane, 0.14 kg/cm^2 will damage frame buildings and telegraph poles, 0.365 kg/cm^2 produces cracks in 9-inch brick walls, etc.

The lightning spectra were obtained in the summer of 1958 at the Zvenigorod Station of the Institute of Atmospheric Physics, Academy of Sciences, U.S.S.R.

We are grateful to the associate of the station, V. S. Prokudina for help with this work, to V. I. Krasovskii for affording us the opportunity to work at this station, and also to the associate of the Physics Institute of the Academy of Sciences, I. P. Tindo, for participating in this work.

---

*The temperature of the channel of the laboratory spark discharge in air amounts to 35 000° at the initial stages of the discharge.[5] Mak's measurements[6] have shown that when the wave front of the current of the laboratory discharge is varied over a wide range, the discharge temperature remains practically constant. One can therefore assume that in spite of the considerable differences in the parameters of the discharge circuits of the lightning and of the laboratory spark, the lightning temperature in the initial stage also amounts to 30 000 – 35 000°. At the present time we are setting up experiments on the measurement of the lighting temperature with time sweep.

---

[1] Dufay, Tcheng, and Mao-Lin, Ann. de geoph. **5**, 137 (1949). M. Dufay, Ann. de geoph. **5**, 255 (1949). P. D. Jose, J. Geoph. Res. **55**, 39 (1950).

[2] Abramson, Gegechkori, Drabkina, and Mandel'shtam, JETP **17**, 862 (1947). N. M. Gegechkori, JETP **21**, 493 (1951).

[3] S. O. Drabkina, JETP **21**, 473 (1951).

[4] S. L. Mandel'shtam and N. K. Sukhodrev, Izv. Akad. Nauk SSSR, Ser. Fiz. **19**, 11 (1955), Columbia Tech. Transl. p. 7.

[5] S. L. Mandel'shtam and N. K. Sukhodrev, JETP **24**, 701 (1953).

[6] A. A. Mak, Оптика и спектроскопия (Optics and Spectroscopy) **8**, 278 (1960).

[7] S. I. Braginskii, JETP **34**, 1548 (1958), Soviet Phys. JETP **7**, 1068 (1958).

[8] J. M. Meeks and J. D. Craggs, Electrical Breakdown of Gases, Oxford Univ. Press, 1953.

[9] G. Taylor, Proc. Roy. Soc. **201**, 175 (1950).

[10] J. O. Hirschfelder, The Effects of Atomic Weapons, (1950).

Translated by J. G. Adashko

RECOIL EFFECT FOR THE TWO PARTICLE INTERACTION IN NONRELATIVISTIC QUANTUM FIELD THEORY

A. V. TULUB

Leningrad State University

Submitted to JETP editor January 17, 1960

J. Exptl. Theoret. Phys. (U.S.S.R.) 40, 488-490 (February, 1961)

The effect of the recoil on the two-particle interaction energy is considered for the case of a scalar field theory.

LET us consider a system of two nonrelativistic particles which interact with each other through a scalar boson field. The energy operator of this system can be written in the following form ($\hbar = 1$):

$$H = -\frac{1}{2M}\nabla_R^2 - \frac{1}{2\mu}\nabla_r^2 + W(r) + \sum_k \omega_k a_k^+ a_k + g\sum_k (V_k e^{i\mathbf{kR}} a_k + V_k^* e^{-i\mathbf{kR}} a_k^+), \tag{1}$$

where a_k and a_k^+ are the operators of second quantization; M and μ are the total and reduced masses; R is the coordinate of the center of mass; W(r) is a given potential as a function of the relative distance r; the function $V_k(r)$ has the form

$$V_k(r) = \gamma_k\left\{\exp\left(i\frac{m_1}{M}\mathbf{kr}\right) \pm \exp\left(-i\frac{m_2}{M}\mathbf{kr}\right)\right\}. \tag{2}$$

The problem consists in the enumeration of the eigenvalues of the operator (1) for arbitrary values of g.

We perform the canonical transformation

$$S = \exp\left\{\sum_k (a_k f_k^*(r, R) - a_k^+ f_k(r, R))\right\} \tag{3}$$

and assume that the auxiliary function f_k satisfies the supplementary condition

$$\sum_k (f_k^* \nabla f_k - f_k \nabla f_k^*) = 0,$$

which is valid in both the coordinates R and r. After averaging over the vacuum state ($a_k\Phi_0 = 0$), the transformed energy operator has the form

$$\langle\Phi_0, S^{-1}HS\Phi_0\rangle = H_0 + \sum_k \omega_k |f_k|^2 + \frac{1}{2M}\sum_k |\nabla_R f_k|^2 + \frac{1}{2\mu}\sum_k |\nabla_r f_k|^2 + \sum_k (V_k f_k e^{i\mathbf{kR}} + V_k^* f_k^* e^{-i\mathbf{kR}}), \tag{4}$$

where H_0 denotes the first three terms of the operator (1).

We shall seek the minimum of the energy for the class of functions $\Psi(r, R) = \Omega(R)\psi(r)$. Setting the functional derivative of the energy with respect to the functions f_k^* equal to zero, we obtain for the function

$$\varphi_k(r, R) = f_k(r, R)/\Omega(R)\psi(r) \tag{5}$$

the following equation

$$-\frac{1}{2M}\nabla_R^2\varphi_k - \frac{1}{2\mu}\nabla_r^2\varphi_k + \omega_k\varphi_k + \frac{1}{2M}\varphi_k\frac{\nabla^2\Omega}{\Omega} + \frac{1}{2\mu}\varphi_k\frac{\nabla^2\psi}{\psi} = -g\Omega(R)e^{-i\mathbf{kR}}\psi(r)V_k^*(r) \tag{6}$$

The solution of Eq. (6) is of the form

$$\varphi_k(r, R) = -\sum_{n, n'}\frac{u_n(R)v_{n'}(r)a_n b_{n'}}{E_n + \varepsilon_{n'} + \omega_k}, \tag{7}$$

where the coefficients a_n and b_n are given by

$$a_n = \int u_n^*(R)e^{-i\mathbf{kR}}\Omega(R)\,d\mathbf{R},$$
$$b_n = \int v_n^*(r)V_k^*(r)\psi(r)\,d\mathbf{r}, \tag{8}$$

and u_n and v_n are the eigenfunctions of the equations

$$-\frac{1}{2M}\nabla_R^2 u_n + \frac{1}{2M}\frac{\nabla^2\Omega}{\Omega}u_n = E_n u_n;$$
$$-\frac{1}{2\mu}\nabla_r^2 v_n + \frac{1}{2\mu}\frac{\nabla^2\psi}{\psi}v_n = \varepsilon_n v_n. \tag{9}$$

The indices n and n′ in the expressions (7) – (9) stand for a set of three indices: $n = (n_1, n_2, n_3)$ and $n' = (n_1', n_2', n_3')$.

Since we require the ground state of the system, we choose the functions $\Omega(R)$ and $\psi(r)$ in the form[1-3]

$$\Omega(R) = (\alpha/\pi)^{3/4}\exp(-\alpha R^2/2),$$
$$\psi(r) = (\beta/\pi)^{3/4}\exp(-\beta r^2/2). \tag{10}$$

For this choice the functions u_n and $v_{n'}$ will be eigenfunctions of the harmonic oscillator, where

$$E_n = \alpha M^{-1}(n_1 + n_2 + n_3), \qquad \varepsilon_{n'} = \beta\mu^{-1}(n_1' + n_2' + n_3').$$

The summation of the series in (7) can be easily carried out, following Gross,[2] by using the integral transformation

$$a^{-1} = \int_0^\infty \exp(-sa)\,ds.$$

With the help of the known formula for the statistical matrix of the harmonic oscillator,[4] we then obtain, using (5) and (10), the following expression for f_k:

$$f_k(r, R) = -g\gamma_k^* \int_0^\infty ds e^{-s\omega_k} F\left(\frac{k}{\sqrt{\alpha}};\ \mathbf{kR};\ \frac{\alpha s}{M}\right)$$

$$\times \left\{ F\left(\frac{k}{\sqrt{\beta}}\frac{m_1}{M};\ \mathbf{kr}\frac{m_1}{M};\ \frac{\beta s}{\mu}\right)\right.$$

$$\left. - F\left(\frac{k}{\sqrt{\beta}}\frac{m_2}{M};\ -\mathbf{kr}\frac{m_2}{M};\ \frac{\beta s}{\mu}\right)\right\},$$

$$F(x, y, z) = \exp\left\{-\frac{1}{4}x^2(1 - e^{-2z}) - iye^{-z}\right\}. \qquad (11)$$

The supplementary condition for the function $f_k(k, R)$ is satisfied. Using the equation for f_k, we can show that the energy is equal to

$$E = \langle H_0\rangle + \sum_k \langle V_k(r) e^{i\mathbf{kR}} f_k(r, R)\rangle. \qquad (12)$$

Substituting (11) in (12), we obtain, e.g., for $m_1 = m_2 = m$

$$E = \langle H_0\rangle - 2g^2 \sum_k |\gamma_k|^2 \int_0^\infty ds \exp(-s\omega_k)$$

$$\times \exp\left[-\frac{k^2}{2\alpha}(1 - e^{-\alpha s/M})\right]\left\{\exp\left[-\frac{k^2}{8\beta}(1 - e^{-\beta s/\mu})\right]\right.$$

$$\left. \pm \exp\left[-\frac{k^2}{8\beta}(1 + e^{-\beta s/\mu})\right]\right\}. \qquad (13)$$

In the case of weak coupling, expression (11) goes over into the expression obtained by Haken.[5]

As an example for the application of expression (13), we consider the problem of the interaction of an exciton with longitudinal optical phonons $[W(r) = -e^2/n^2 r$, where n is the refraction index of light]. Assuming that $\alpha \ll 1$ and $\mu\omega/\beta \ll 1$, we find (see also reference 3)

$$E = 3\beta/4\mu - 2e^2 n^{-2}(\beta/\pi)^{1/2} - 2g^2 a\omega(m\omega/\pi\beta)^{1/2}, \quad a = 0{,}76. \qquad (14)$$

In real crystals the last term of (14) is small even for $g^2 \approx 10$. The approximate value of β will therefore be equal to $16\mu^2 e^4/9\pi n^4$, which guarantees the validity of the inequality $\mu\omega/\beta \ll 1$.

If the trial functions $\Omega(R)$ and $\psi(r)$ are chosen of the form (10), the expressions (11) and (13) give the exact solution to our problem.

---

[1] V. M. Buĭmistrov and S. I. Pekar, JETP **32**, 1193 (1957), Soviet Phys. JETP **5**, 970 (1957).

[2] E. P. Gross, Ann. of Phys. **8**, 78 (1959).

[3] I. M. Dykman and I. G. Zaslavskaya, J. Tech. Phys. (U.S.S.R.) **28**, 29 (1959), Soviet Phys.-Tech. Phys. **3**, 26 (1959).

[4] A. Erdélyi, Math. Z. **44**, 201 (1938).

[5] H. Haken, Z. Physik **147**, 323 (1957).

Translated by R. Lipperheide
75

SOVIET PHYSICS JETP VOLUME 13, NUMBER 2 AUGUST, 1961

NEUTRON POLARIZATION IN THE DISINTEGRATION OF Be^9 *NUCLEI BY CIRCULARLY POLARIZED GAMMA QUANTA*

I. Sh. VASHAKIDZE, T. I. KOPALEǏSHVILI, and G. A. CHILASHVILI

Tbilisi State University and Physics Institute, Acad. Sci. Georgian S.S.R.

Submitted to JETP editor May 23, 1960

J. Exptl. Theoret. Phys. **40**, 491-492 (February, 1961)

The polarization of photoneutrons emitted in the reaction $Be^9(\gamma, n)Be^8$ is determined for circularly polarized γ quanta. It is shown that for certain neutron emission angles the polarization is as high as ~ 50 percent.

It is well known that an investigation of the polarization of photoprotons or neutrons, emitted by unpolarized nuclei, makes it possible to determine the circular polarization of the incident γ rays. Knowledge of this polarization has assumed particular importance since the discovery of parity nonconservation in weak interactions.

For low quantum energies, the most favorable target nuclei are H^2 and Be^9. However, as shown by Schopper,[1] in the case of the deuteron the protons are weakly polarized at these photon energies, so that a target of H^2 nuclei cannot be used effectively to determine the sign of the circular polarization of the gamma rays. As regards the Be^9 nucleus, the polarization of the photoneutrons released by circularly-polarized gamma quanta has not yet been determined. The present investigation concerns the polarization of photoneutrons from Be^9 nuclei.

The z component (in the direction of the incident γ quantum) of the polarization vector of photoneutrons knocked out from the Be^9 nucleus is given by the formula

$$P_z(\pm 1) = \pm \frac{0.5\left\{1.28A_2^2 - A_0^2 - [2A_0A_2\cos(\eta_0 - \eta_2) + 1.53A_2^2]P_2(\cos\theta)\right\}}{A_0^2 + 2A_0A_2\cos(\eta_0 - \eta_2)P_2(\cos\theta) + 2.14A_2^2 - 0.76A_2^2P_2(\cos\theta)},$$

$$A_0 = \int R_{0_{1/2}} R_{1_{3/2}} r^3 dr, \qquad A_2 = \int R_{2_{5/2}} R_{1_{3/2}} r^3 dr, \tag{1}$$

where $\eta_0 = \eta_{0_{1/2}}$, $\eta_2 = \eta_{2_{3/2}} = \eta_{2_{5/2}}$ are the scattering phase shifts, θ is the angle of emission of the photoneutrons. The upper and lower signs in the argument of P_z correspond to the right-hand and left-hand polarizations of the gamma quantum. In view of the arbitrariness of the choice of axis directions, the values of P_x and P_y drop out after averaging over φ.

Formula (1) contains the scattering phase shifts η_0 and η_2 as well as the radial integrals A_0 and A_2. Using the values of the parameters[2,3] of the neutron potential in the Be^9 nucleus, namely $V_{1_{3/2}} = 12.16$ Mev, $V_{0_{1/2}} = 3$ Mev, and $r_0 = 5 \times 10^{-13}$ cm, we can readily determine these quantities for a specified γ-quantum energy, and thereby determine the angular dependence of the z component of the photoneutron polarization vector. The figure shows this dependence for γ-quantum energies 2, 3, 4, and 20 Mev. The choice of these energies is dictated by the fact that at these energies the effective cross section of elastic scattering of the He^4 nucleus (which, as is well known, enables us to determine their polarization) is sufficiently large, on the order of several barns. In addition, at γ-quantum energies 2 — 4 Mev the effective cross section of the photonuclear process on the Be^9 nucleus also has a maximum, and consequently the use of such γ quanta is preferable from the point of view of increasing the overall effectiveness. As to the 20-Mev γ quantum, we know that none of the other methods of determining the sign of the circular polarization at such high energies are suitable, and only the photonuclear reaction can be used for this purpose.

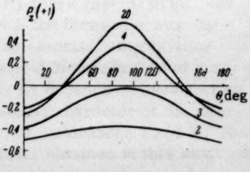

Dependence of the z component of the polarization vector of photoneutrons on the angle θ for various values of the energy of the incident gamma quantum (the numbers on the curves are the values of E_γ in megavolts).

It is seen from the figure that at some angles the polarization of the neutrons reaches almost 50 percent. We note that, depending on the direction of the circular polarization of the γ quantum, different signs are obtained for the photoneutron polarization (the curves in the figure correspond to right-hand polarization of the gamma quantum).

In conclusion, we take pleasure in thanking V. I. Mamasakhlisov and S. G. Matinyan for useful discussions.

[1] H. Schopper, Nuclear Instruments 3, No. 3, 158 (1958).
[2] V. I. Mamasakhlisov, J. of Phys. 7, 239 (1943).
[3] E. Guth and C. Mulin, Phys. Rev. 76, 234 (1949).

Translated by J. G. Adashko
76

SOVIET PHYSICS JETP VOLUME 13, NUMBER 2 AUGUST, 1961

ASYMPTOTIC BEHAVIOR OF THE SCATTERING AMPLITUDE AT INFINITE ENERGIES

L. A. KHALFIN

Submitted to JETP editor May 25, 1960

J. Exptl. Theoret. Phys. (U.S.S.R.) **40**, 493-497 (February, 1961)

The behavior of the scattering amplitude at infinite energies is investigated on the basis of the unitarity condition. A relation between the asymptotic form of the forward scattering amplitude and the derivatives of the differential cross sections for elastic scattering with respect to the angle is established.

In the present paper we investigate the asymptotic behavior of the scattering amplitude at infinite energies on the basis of the unitarity condition for all possible channels of a given reaction and the analytic properties of the scattering amplitude with respect to the momentum transfer (reference 1).* We shall investigate the general case and not just special models of interaction, as is usually done.[2,3] We shall in fact use only the most general assumptions of the quantum theory, and, in particular, the "optical" theorem,[4] which is a consequence of the unitarity condition.

The investigation of the asymptotic behavior of the scattering amplitude for $E \to \infty$, based on the most general axioms and assumptions of the quantum theory, is at present of great importance, since the application of the usual dispersion relations (between the real and imaginary parts of the scattering amplitude)[4] and Mandelstam's spectral representations[5] depends directly on the detailed asymptotic behavior of the scattering amplitude.

It is true, as has been shown earlier, that a formulation of the dispersion relations (between the modulus and the phase of the scattering amplitude) and the spectral representations is possible which does not depend directly on the exact asymptote of the scattering amplitude for $E \to \infty$; this formulation depends on information on the possible complex zeroes of the scattering amplitude,† which can be obtained from certain additional reasonable physical assumptions.[6,7]

Nevertheless, the study of the asymptotic behavior of the scattering amplitude for $E \to \infty$ is also of interest because it allows us to make predictions with regard to experimentally measurable quantities [for example, the total cross section $\sigma(E)$] in the region of high and extremely high energies. Below we shall investigate the asymptotic behavior of the forward scattering amplitude $f(E)$. The asymptotic behavior of the scattering amplitude for an arbitrary angle $f(E, \theta)$ can be investigated in an analogous manner (see also footnote on page 346).

1. Let $f(E)$ be the forward scattering amplitude. The analytic properties of $f(E)$ in the complex half-plane $\operatorname{Im} E > 0$ have been determined from the most general principles of the quantum theory [locality, relativistic covariance (causality)] and the spectral condition.[4] For the asymptotic behavior of $f(E)$ these general principles only give the result that the forward scattering amplitude $f(E)$ has no essential singularities for $E \to \infty$.[4] The detailed determination of the asymptotic form of $f(E)$ depends on assumptions with regard to the specific character of the interaction (see, for example, references 2 and 3). The asymptotic form of $f(E)$ obtained in this way, therefore, has only significance in terms of a model, especially in that region of the energy where we have no compelling reason to believe in the presently known models of interaction. Using the empirical fact that the total cross section approaches a constant value for $E \to \infty$, one usually assumes that the elastic forward scattering amplitude $f(E)$ has a simple pole at infinity.[4]

2. We shall make decisive use of the "optical" theorem,[4] which is a direct consequence of the unitarity condition for the forward scattering amplitude:

$$\operatorname{Im} f(E) = (k/4\pi)\,\sigma(E) = (k/4\pi)\,\sigma_{\mathrm{el}}(E) + (k/4\pi)\,\sigma_{\mathrm{inel}}(E), \tag{1}$$

---

*I have been informed that a similar problem has been considered independently by M. Braun and L. Prokhorov.

†There exists a definite connection between the position of the possible zeroes and the asymptotic behavior (for $E \to \infty$) of the scattering amplitude, which will be considered in a separate paper on the basis of the theory of entire functions;[9] the latter have already been used in the quantum theory of the decay of physical systems.[7,8]

where $k^2 \equiv E^2 - \mu^2$, μ is the rest mass of the scattering particles, $\sigma(E)$ is the total cross section, $\sigma_{\mathrm{el}}(E)$ is the total elastic cross section, and $\sigma_{\mathrm{inel}}(E)$ is the total cross section for the inelastic processes which include all possible inelastic channels of the reaction and, in particular, the many-particle channels. We also note the inequalities

$$\operatorname{Im} f(E) \geqslant 0, \qquad \sigma(E) \geqslant 0, \tag{2}$$

which follow from obvious physical assumptions.

To demonstrate the basic idea of our calculation, we consider first the special case, where the elastic scattering involves only s waves.* In this case

$$\sigma_{\mathrm{el}}(E) = 4\pi |f(E)|^2 \tag{3}$$

and the unitarity condition (1) takes the form

$$\operatorname{Im} f(E) = (k/4\pi)\,\sigma_{\mathrm{inel}}(E) + k\,|f(E)|^2. \tag{4}$$

We now use the elementary inequality

$$|f(E)|^2 - [\operatorname{Im} f(E)]^2 = [\operatorname{Re} f(E)]^2 \geqslant 0 \tag{5}$$

We substitute the expression (4) for Im f(E) in (5) and find

$$|f(E)|^2\,[1 - k^2 |f(E)|^2 - (k^2/2\pi)\,\sigma_{\mathrm{inel}}(E)] - (k^2/16\pi^2)\,\sigma^2_{\mathrm{inel}}(E) \geqslant 0 \tag{6}$$

Hence

$$|f(E)|^2\,[1 - k^2 |f(E)|^2 - (k^2/2\pi)\,\sigma_{\mathrm{inel}}(E)] \geqslant 0. \tag{7}$$

Then

$$1 - k^2 |f(E)^2| - (k^2/2\pi)\,\sigma_{\mathrm{inel}}(E) \geqslant 0, \tag{8}$$

since $|f(E)|$ cannot vanish in a continuous half-infinite interval because of its analyticity.

For sufficiently large $E \gg \mu$ we obtain from (8) with the help of (2)

$$|f(E)| \leqslant E^{-1}, \tag{9}$$

i.e., if only s waves participate in the elastic scattering, the elastic scattering amplitude cannot decrease faster than $|E|^{-1}$. We note that Eq. (8) also leads to the following restriction on the asymptotic form of σ_{inel}:

$$\sigma_{\mathrm{inel}}(E) \leqslant 2\pi / |E|^2. \tag{10}$$

The basic idea of the above-mentioned method of obtaining asymptotic restrictions of the type (9) is to make use of the fact that Im f(E) in the basic inequality (5) is itself determined by $|f(E)|$ through the unitarity condition. This leads us to the important conclusion that the contribution of the inelastic processes to the unitarity condition is, in general, not essential for the derivation of restrictions on the asymptotic behavior of f(E).

3. Let us now turn to the general case. The total elastic scattering cross section $\sigma_{\mathrm{el}}(E)$ is, evidently, given by the expression

$$\sigma_{\mathrm{el}}(E) = 2\pi \int_0^{\pi} \sin\theta\, |f(E,\theta)|^2\, d\theta, \tag{11}$$

where $f(E, \theta)$ is the amplitude for elastic scattering into the angle θ. At the first glance it seems impossible to carry over the method described in Sec. 2 to the general case, since Im f(E) is given by an integral of $|f(E, \theta)|^2$, which is insensitive to a change of the integrand at the isolated point $\theta = 0$, especially since the integrand contains $\sin\theta$. However, if we assume certain analytic properties of $f(E, \theta)$ with respect to θ, we can evidently hope that the above-mentioned method for studying the asymptotic behavior of f(E) on the basis of the unitarity condition will remain applicable.

As a preliminary, we note that the basic inequality (5) will hold a fortiori if we discard the positive definite terms in Im f(E). Using (2) and (11), we then obtain, instead of (5), the following basic inequality:*

$$|f(E)|^2 - \frac{k^2}{4}\left[\int_0^{\theta_1} \sin\theta\, |f(E,\theta)|^2\, d\theta\right]^2 \geqslant 0, \qquad \theta_1 < \pi, \tag{12}$$

which is completely independent of the contribution from the inelastic processes to the unitarity condition.

Let us now make the basic assumption that $f(E, \theta)$ is analytic in θ in the neighborhood of $\theta = 0$. This assumption is equivalent to the fact, proved by Lehmann[1] (we admit that Lehmann's proof is valid only under severe restrictions on the masses of the scattering particles), that the scattering amplitude is analytic in the momentum transfer in a region which includes the physical scattering region.

We expand $|f(E, \theta)|^2$ into a series about $\theta = 0$,

$$|f(E,\theta)|^2 = |f(E)|^2 + \sum_{k=1}^{\infty} \frac{\theta^k}{k!} \frac{\partial^k |f(E,0)|^2}{\partial\theta^k} \tag{13}$$

---

*This special case of the scattering of scalar mesons was considered in the work of Castillejo, Dalitz, and Dyson[10] and also by Ter-Martirosyan.[11]

*According to the mean value theorem, we can use this inequality to carry over some of the results regarding the asymptotic behavior of the forward scattering amplitude f(E) to the asymptotic behavior of the scattering amplitude for an arbitrary angle f(E, θ).

and substitute (13) in (12):

$$|f(E)|^2 - \frac{k^2}{4}\left[A(\theta_1)|f(E)|^2 + \sum_{k=1}^{\infty}\frac{B_k(\theta_1)}{k!}\frac{\partial^k|f(E,0)|^2}{\partial\theta^k}\right] \geqslant 0, \tag{14}$$

where $A(\theta_1)$ and $B_k(\theta_1)$ are positive functions of θ_1. A stronger inequality is

$$|f(E)|^2 - \frac{k^2}{4}\left[A^2(\theta_1)|f(E)|^4 + 2A(\theta_1)|f(E)|^2\sum_{k=1}^{\infty}\frac{B_k(\theta_1)}{k!}\right.$$
$$\left.\times\frac{\partial^k|f(E,0)|^2}{\partial\theta^k} + 2\sum_{k\neq j}\frac{B_kB_j}{k!j!}\frac{\partial^k|f(E,0)|^2}{\partial\theta^k}\frac{\partial^j|f(E,0)|^2}{\partial\theta^j}\right] \geqslant 0. \tag{15}$$

It is clear that for every finite E we can choose such a small $\theta_1(E) > 0$ that we can write down the following inequality instead of (15):

$$|f(E)|^2 - \frac{k^2}{4}\left[A^2(\theta_1)|f(E)|^4\right.$$
$$\left. + 2A(\theta_1)B(\theta_1)|f(E)|^2\frac{\partial|f(E,0)|^2}{\partial\theta}\right] \geqslant 0. \tag{16}$$

The inequalities (15) and (16) are completely rigorous for finite E, for the results of Lehmann[1] imply the analyticity of the scattering amplitude in the momentum transfer for finite energies $E < \infty$. However, the possible asymptotic behavior of $f(E, \theta)$ for $E \to \infty$ does not follow from the Lehmann theorem.[1] But if we make certain assumptions with respect to the behavior of $\partial^k|f(E, 0)|^2/\partial\theta^k$ for $E \to \infty$, we can use (15) to find the required asymptotic behavior of $f(E, 0)$.

Let us give the result in the form of a theorem:

If the derivatives of the differential elastic cross section with respect to the angle at $\theta = 0$ are finite for $E \to \infty$ as functions of the energy, the elastic forward scattering amplitude $f(E)$ cannot increase for $E \to \infty$; moreover,

$$|f(E)| < A/|E| + B, \qquad A, B > 0. \tag{17}$$

The proof follows from the basic inequality (15) by going to the limit.

Other restrictions on the possible asymptotic behavior of $f(E)$ can be obtained in an analogous way from the inequality (15), by making different assumptions with regard to the behavior of $\partial^k|f(E, 0)|^2/\partial\theta^k$ as $E \to \infty$. In fact, the basic inequality (15) allows us, by explicit use of the unitarity condition, to replace the assumption with regard to the asymptotic behavior of $f(E)$ by an equivalent assumption with regard to the behavior of the derivatives $\partial^k|f(E, 0)|^2/\partial\theta^k$, which have a direct physical meaning.

It clearly follows from the above-mentioned theorem that the usual assumption that $f(E)$ has a simple pole for $E \to \infty$ can only be correct if the derivatives of the differential elastic cross section with respect to the angle have a discontinuity at $\theta = 0$ for $E \to \infty$. This gives us a new experimental possibility to verify the hypothesis with regard to the asymptotic behavior of the forward scattering amplitude $f(E)$ at high and extremely high energies.

We also note that, together with the above-mentioned estimate of the asymptotic form of $f(E)$, we can also derive a lower limit for the asymptotic form of $f(E)$, by using "the criterion of physical realizability,"[12] which is also based on the most general assumptions of the quantum theory:

$$|f(E)| \geqslant A\exp\{-\gamma|E|^q\},$$
$$A > 0, \qquad \gamma > 0, \qquad q < 1. \tag{18}$$

Thus we see that very general restrictions on the possible behavior of the scattering amplitude at infinite energies can be derived from the most general assumptions of the quantum theory, including the unitarity condition. To determine the detailed behavior of the asymptotic scattering amplitude at infinite energies, we must, of course, supplement the general assumptions of the quantum theory (necessary for the derivation of the analytic properties and the spectral representations of the scattering amplitude) with specific assumptions about the interactions in the chosen model. In this connection the following problem is of interest: what are the minimal characteristics of the interaction model necessary for the determination of the detailed behavior of the scattering amplitude at infinite energies?

In conclusion I express my gratitude to Acad. I. E. Tamm, Prof. V. L. Ginzburg, Prof. E. L. Feĭnberg, and the participants of the theoretical seminar of the Institute of Physics of the Academy of Sciences for a discussion of this work and comments.

---

[1] H. Lehmann, Nuovo cimento **16**, 579 (1958).

[2] K. Symanzik, Nuovo cimento **5**, 659 (1957).

[3] R. Arnowitt and G. Feldman, Phys. Rev. **108**, 144 (1957).

[4] N. N. Bogolyubov and D. V. Shirkov, Introduction to the Theory of Quantized Fields, Interscience, New York (1959). Bogolyubov, Medvedev, and Polivanov, Вопросы теории дисперсионных соотношений (Problems of the Theory of Dispersion Relations) Gostekhizdat (1958).

[5] S. Mandelstam, Phys. Rev. **112**, 1344 (1958).

[6] L. A. Khalfin, JETP **36**, 1088 (1959), Soviet Phys. JETP **9**, 774 (1959).

[7] L. A. Khalfin, Dissertation, Institute of Physics, Academy of Sciences (1960).

[8] L. A. Khalfin, Doklady Akad. Nauk SSSR 132, 1051 (1960), Soviet Phys.-Doklady 5, 515 (1960).

[9] B. Ya. Levin, Распределение корней целых функций (Distribution of the Zeroes of Entire Functions), Gostekhizdat (1956).

[10] Castillejo, Dalitz, and Dyson, Phys. Rev. 101, 453 (1956).

[11] K. A. Ter-Martirosyan, JETP 37, 1005 (1959), Soviet Phys. JETP 10, 714 (1960).

[12] L. A. Khalfin, Doklady Akad. Nauk SSSR 111, 345 (1956), Soviet Phys.-Doklady 1, 671 (1957).

Translated by R. Lipperheide
77

SOVIET PHYSICS JETP VOLUME 13, NUMBER 2 AUGUST, 1961

ON THE THREE-BODY PROBLEM WITH SHORT-RANGE FORCES

G. S. DANILOV

Leningrad Physico-Technical Institute, Academy of Sciences, U.S.S.R.

Submitted to JETP editor May 28, 1960

J. Exptl. Theoret. Phys. (U.S.S.R.) 40, 498-507 (February, 1961)

It is shown that the scattering amplitude for the scattering of a particle on the bound state of two other particles can be expressed in terms of the parameters of the two-particle problem and the energy of the bound state of the three particles.

SKORNYAKOV and Ter-Martirosyan[1] have derived equations for the determination of the wave function of a system of three identical particles in the limiting case of zero-range forces. These equations allow one to express the scattering amplitude for the scattering of a neutron on a deuteron with the total spin $S = 3/2$ for the system in terms of the parameters of the two-particle problem. Analogous calculations for the case $S = 1/2$, however, have not been successful.[2]

For the total spin $S = 1/2$ the wave function of the system does not vanish when the distances between all particles become zero, as in the case when $S = 3/2$. It will be shown in the present paper that the above-mentioned equations have a non-unique solution in this case.* We shall also see that the wave functions for different energies are proportional to one another in the region where the three particles are sufficiently close to each other. We must therefore choose that solution of the equations of Skornyakov and Ter-Martirosyan which guarantees that the wave functions for different energies are proportional to each other in the above-mentioned region. This requirement allows us to choose a unique solution for an arbitrary energy if the wave function for a single value of the energy is known. For this wave function one can, for example, take the wave function of tritium. The determination of this wave function requires the knowledge of the binding energy of tritium. To solve the three-body problem with short-range forces, we thus require one more parameter in addition to the parameters of the two-body problem, as for example, the binding energy of tritium.

The idea that the non-uniqueness of the solution of the equations of Skornyakov and Ter-Martirosyan can be removed by introducing an experimental parameter is due to V. N. Gribov.

In Sec. 1 of the present paper we explain why the equation of Skornyakov and Ter-Martirosyan for three identical spinless particles has no unique solution. We also determine the behavior of the wave function in the region where the distances between all particles are close to zero. The rigorous proof of the non-uniqueness of the solution of the equation of Skornyakov and Ter-Martirosyan is given in the Appendix. In Sec. 2 we prove that the wave functions for different energies are proportional to one another in the region where the distances between all particles are close to zero. In Sec. 3 we derive for the wave function of three identical spinless particles an equation with a unique solution. In this form the equation of Skornyakov and Ter-Martirosyan can be solved numerically. In Sec. 4 we consider the same problem, but take into account the spin and the isotopic spin of the particles.

1. NON-UNIQUENESS OF THE SOLUTION OF THE EQUATION FOR A SYSTEM OF THREE IDENTICAL SPINLESS PARTICLES AND THE ASYMPTOTIC FORM OF THE WAVE FUNCTION

It was shown in reference 1 that it is sufficient for the solution of the scattering problem to know the wave function in the region $\rho_{23} \leq r_0$, $\rho_1 \gg r_0$, where ρ_{23} and ρ_1 are the Jacobi coordinates and r_0 is the range of the forces. In this region the wave function $\Psi_E(\rho_{23}, \rho_1)$ can be written in the form of a product of the deuteron wave function $\varphi_0(\rho_{23})$ and some function $U_E(\rho_1)$. In the problem of the scattering of a particle with relative momentum $\mathbf{k}_0$ on a bound state of two other particles, the Fourier component $\chi_E(\mathbf{k})$ of the function $U_E(\rho_1)$ is equal to

$$\chi_E(\mathbf{k}) = (2\pi)^3\delta(\mathbf{k} - \mathbf{k}_0) + 4\pi a(\mathbf{k}, \mathbf{k}_0)/(k^2 - k_0^2 - i\delta);$$

$$a(\mathbf{k}, \mathbf{k}_0) = \sum_l (2l + 1)\, a_l(k, k_0)\, P_l(\cos\theta). \qquad (1)$$

The square of the momentum k_0^2, the energy of the system E, and the binding energy of the deuteron α^2 are connected through the relation (we assume $\hbar = M = 1$, where M is the mass of the nucleon)

---

*This question was raised by Skornyakov.[3] He demonstrated the non-uniqueness of the solution of equations of similar type with the help of various examples.

$$E = {}^3/_4 k_0^2 - \alpha^2. \tag{2}$$

The functions $a_l(k, k_0)$ satisfy the equations (b) of the Appendix of reference 1.

We shall be interested in the equation for $a_0(k, k_0)$, since it is this equation which has a non-unique solution. The index 0 of the function a_0 will be omitted in the following.

The equation for $a(k, k_0)$ has the following form:

$$a(k,k_0) = \frac{8}{3}(\gamma_{k_0}(k) + \alpha) L_E(k, k_0) + \frac{16}{3\pi}(\gamma_{k_0}(k) + \alpha)\int_0^\infty \frac{a(k', k_0) k'^2}{k'^2 - k_0^2 - i\delta} L_E(k, k')\, dk', \tag{3}$$

where

$$L_E(k, k') = \frac{1}{2kk'} \ln \frac{k^2 + k'^2 + kk' - E}{k^2 + k'^2 - kk' - E},$$

$$\gamma_{k_0}(k) = \sqrt{{}^3/_4 k^2 - E}$$

[$\gamma_{k_0}(k) = -i\,|\gamma_{k_0}(k)|$ if $({}^3/_4) k^2 - E < 0$; for the choice of the branch of the logarithm, see reference 1]. We note that in the problem of the bound state of the three particles

$$\chi_{E_0}(k) = 4\pi a_{E_0}(k)/(k^2 - k_0^2), \tag{4}$$

where k_0^2 is given by formula (2) and E_0 is the energy of the bound state. The function $a_{E_0}(k)$ satisfies Eq. (3) without the free term.

As will be shown in the Appendix, the homogeneous equation corresponding to Eq. (3) has a solution for arbitrary values of E. The solution to this equation is well-defined except for a normalization factor. Therefore, the solution of the inhomogeneous equation (3) (if it exists) contains an arbitrary constant. The existence of a solution to Eq. (3) will also be shown in the Appendix.

Let us determine the asymptotic form of $a(k, k_0)$ for large k. It is easily shown that, up to terms which decrease as k^{-1}, the function $a(k, k_0)$ has the form

$$a(k, k_0) \sim \sum A_i(k_0)\, k^{s_i}, \tag{5}$$

where the s_i are the roots of the equation

$$1 - 4L(s)/\sqrt{3} = 0, \tag{6}$$

with

$$L(s) = \frac{2\sin(\pi s/6)}{s\cos(\pi s/2)}. \tag{7}$$

The summation in (5) goes over all roots of Eq. (6) which lie in the strip $|\mathrm{Re}\, s| < 1$.

To prove formula (5), we must substitute it in Eq. (3) and use the fact that for large k the integral is essentially determined by the region of large k′.

It can be shown that Eq. (6) has two roots in the strip $|\mathrm{Re}\, s| < 1$:

$$s = \pm i s_0, \quad s_0 \approx 1.$$

Except for terms which decrease as k^{-1}, the asymptotic form of $a(k, k_0)$ is therefore of the following form:*

$$a(k, k_0) \sim A_1(k_0)\, k^{is_0} + A_2(k_0)\, k^{-is_0}. \tag{8}$$

We can also compute the next term in the asymptotic expression for $a(k, k_0)$. For this purpose we must separate the integral in Eq. (3) into two parts, one of which includes the region of large k′ and the other, the region of small k′. For large k the integral over the region of small k′ and the free term decrease as $\mathrm{const}\cdot k^{-1}$. However, the asymptotic form of $a(k, k_0)$ cannot contain such terms, for their substitution in the integral in Eq. (3) would lead to the appearance of terms in the asymptotic expression which decrease as $\mathrm{const}\cdot k^{-1}\ln k$ for large k.† Therefore, the terms proportional to k^{-1} coming from the free term of Eq. (3) and from the integral over the region of small k′, and similar terms coming from the integral over the region of large k′, must sum out to zero. Thus, except for terms which decrease faster than k^{-1}, only the integral over the region of large k′ gives a contribution to the asymptotic form of $a(k, k_0)$. It is easily shown that, with this accuracy, the asymptotic expression for $a(k, k_0)$ is

$$a(k, k_0) = A_1(k_0)\,\varphi(k, s_0) + A_2(k_0)\,\varphi(k, -s_0), \tag{9}$$

where

$$\varphi(k, s_0) = k^{is_0}[1 + B(s_0)/k], \tag{10}$$

$$B(s_0) = 2\alpha/\sqrt{3}\,[1 - 4L(is_0 - 1)/\sqrt{3}]. \tag{11}$$

In principle, one of the two arbitrary constants $A_1(k_0)$ and $A_2(k_0)$ is determined by the other when this solution is joined to the solution in the region of small k. Thus it is already clear from the form of the asymptotic expression for $a(k, k_0)$ that the solution of (3) depends on a single arbitrary parameter. The asymptotic expression for $\tilde{a}(k, k_0)$, the solution of the homogeneous equation corresponding to (3), is evidently of the same form.

---

*Since $a(k, k_0)$ does not vanish as $k \to \infty$, the derivation of the equation for $\chi_E(k)$ given in reference 1 is not very convincing. Nevertheless, these equations are correct.[3]

†The absence of terms of the form $k^{-1}\ln k$ in the asymptotic expression for $a(k, k_0)$ can be rigorously shown with the help of the formulas derived in the Appendix.

The asymptotic form of $a(k, k_0)$ for large k determines the behavior of the function $U_E(\rho_1)$ for small ρ_1. Then we have for $\rho_{23} \sim r_0$ and $r_0 \ll \rho_1 \ll (|E|^{-1/2}, \alpha^{-1}, k_0^{-1})$

$$\Psi_E(\rho_{23}, \rho_1) \sim \varphi_0(\rho_{23})$$

$$\times\left[d_1 \frac{\sin\xi}{\rho_1}(1 + d_2\rho_1) + d_3 \frac{\cos\xi}{\rho_1}(1 + d_4\rho_1)\right], \qquad (12)$$

where $\xi = s_0 \ln(\rho_1\sqrt{|E|})$ and $\varphi_0(\rho_{23})$ is the deuteron wave function. The constants d_1, d_2, d_3, and d_4 are functions of A_1 and A_2.

In the following we shall require the leading term in the asymptotic expression for the wave function in the region

$$r_0 \ll \rho_{23} \ll (|E|^{-1/2}, \ \alpha^{-1}, \ k_0^{-1}),$$
$$r_0 \ll \rho_1 \ll (|E|^{-1/2}, \ \alpha^{-1}, \ k_0^{-1}).$$

To compute this term, we must substitute the main term of (12) in the integral of the equation which determines the wave function of the system in terms of the Green's function and use the fact that the principal contribution to the integral comes from the region where all three particles are close to one another. The calculation shows that in this region the wave function is proportional to the expression

$$\Psi_E(\rho_{23}, \rho_1) \sim [d_1(k_0) \sin\tilde{\xi} + d_3(k_0) \cos\tilde{\xi}]\, Q(\rho_{23}, \rho_1), \qquad (13)$$

where

$$\tilde{\xi} = s_0 \ln(\sqrt{|E|}R), \qquad R = \tfrac{2}{3}(\rho_{12}^2 + \rho_{23}^2 + \rho_{13}^2) = \rho_{23}^2 + \tfrac{4}{3}\rho_1^2,$$

$$Q(\rho_{23}, \rho_1) = \frac{1}{\rho_1\rho_{23}} f\left(\frac{\rho_{23}}{\rho_1}\right) + \frac{1}{\rho_2\rho_{13}} f\left(\frac{\rho_{13}}{\rho_2}\right) + \frac{1}{\rho_3\rho_{12}} f\left(\frac{\rho_{12}}{\rho_3}\right),$$

where ρ_{12}, ρ_{23}, and ρ_{13} are the distances between the particles and ρ_1, ρ_2, and ρ_3 denote the distance of a given particle from the center of mass of the two others. The function $f(x)$ is equal to*

$$f(x) = \mathrm{sh}\frac{s_0}{2}[\pi - \vartheta(x)], \quad \vartheta(x) = \arccos\frac{4/3 - x^2}{4/3 + x^2}.$$

2. CHOICE OF SOLUTION

In order to select the correct solution from the set of solutions to Eq. (3), we may avail ourselves of the assertion, which will be proved below, that the wave functions for different energies are proportional to each other if ρ_1 and ρ_{23} are small. In particular, the wave functions of the continuous spectrum $\Psi_E(\rho_{23}, \rho_1)$ must be proportional to the wave function of tritium $\Psi_{E_0}(\rho_{23}, \rho_1)$:

$$\Psi_E(\rho_{23}, \rho_1) = C(E)\,\Psi_{E_0}(\rho_{23}, \rho_1). \qquad (14)$$

Condition (14) determines uniquely the arbitrary constant in the solution to Eq. (3). Indeed, it follows from (14) that for $k \to \infty$

$$a(k, k_0) = C(E)\, a_{E_0}(k). \qquad (15)$$

For a given function $a_{E_0}(k)$, Eq. (15) can be satisfied only with a definite value of the arbitrary constant entering in the solution to Eq. (3). If the binding energy of tritium E_0 is known, we can find the function $a_{E_0}(k)$ from the solution of the homogeneous equation corresponding to Eq. (3) for $E = E_0$.

Let us prove Eq. (14). The wave functions $\Psi_E(\rho_{23}, \rho_1)$ and $\Psi_{E_0}(\rho_{23}, \rho_1)$ are orthogonal, i.e.,

$$\int \Psi_E(\rho_{23}, \rho_1)\,\Psi_{E_0}(\rho_{23}, \rho_1)\, d^3\rho_{23}\, d^3\rho_1 = 0. \qquad (16)$$

This integral can be written in the form of a sum of an integral over the region $R < R_0$, where $R^2 = \rho_{23}^2 + (4/3)\rho_1^2$, and an integral over the remaining portion of space. We shall assume here that R_0 and the range of the forces r_0 both go to zero in such a way that $r_0 \ll R_0$. Then the integral over the region $R < R_0$ will go to zero. The other integral can be transformed into an integral over the surface $R = R_0$ with the help of the Schrödinger equation:

$$(E - E_0)\int \Psi_E(\rho_{23}, \rho_1)\,\Psi_{E_0}(\rho_{23}, \rho_1)\, d^3\rho_{23}\, d^3\rho_1$$
$$= R^5 \int d\Omega \Big[\Psi_{E_0}(\rho_{23}, \rho_1)\frac{\partial}{\partial R}\Psi_E(\rho_{23}, \rho_1)$$
$$- \Psi_E(\rho_{23}, \rho_1)\frac{\partial}{\partial R}\Psi_{E_0}(\rho_{23}, \rho_1)\Big]\Big|_{R\to 0}, \qquad (17)$$

the integration in (17) goes over the angles in the six-dimensional space formed by the vectors $(\rho_{23}, \sqrt{4/3}\,\rho_1)$. Substituting the expression (13) for the wave functions in (17), we find that the right hand side of (17) does not depend on R for small R and is proportional to the expression

$$[d_1(k_0)d_3(E_0) - d_3(k_0)\, d_1(E_0)] \int d\Omega\, Q^2(\mathbf{n}_{23}, \mathbf{n}_1), \qquad (18)$$

where $\mathbf{n}_{23}$ and $\mathbf{n}_1$ satisfy the relation $n_{23}^2 + (4/3)\,n_1^2 = 1$.

We see* that the right-hand side of (17) goes to zero for $R \to 0$ only if

$$d_1(k_0)\, d_3(E_1) - d_3(k_0)\, d_1(E_0) = 0, \qquad (19)$$

---

*sh = sinh.

***If one attempts to verify the orthogonality condition for the wave function with the help of formula (12) of reference 1, it may appear that all solutions of the equation of Skornyakov and Ter-Martirosyan are orthogonal to each other. However, this result is the consequence of an illegitimate interchange of the orders of integration. The correct procedure leads to a formula which agrees with formula (18) of our paper.**

i.e., if the wave functions $\Psi_E(\rho_{23}, \rho_1)$ and $\Psi_{E_0}(\rho_{23}, \rho_1)$ are proportional to each other.

3. WAVE EQUATION FOR A SYSTEM OF THREE PARTICLES WITH A UNIQUE SOLUTION

We shall show now how one obtains an integral equation by which $a(k, k_0)$ is determined uniquely. Let us introduce the function

$$\omega(k, k_0) = a(k, k_0) - C(E)\, a_{E_0}(k), \tag{20}$$

which, according to our earlier discussion, has the property

$$k\omega(k, k_0) \to 0 \quad \text{for } k \to \infty. \tag{21}$$

The function $\omega(k, k_0)$ satisfies the equation

$$\frac{3}{8}\frac{\omega(k, k_0)}{\gamma_{h_0}(k) + \alpha} = f_E(k) + \frac{2}{\pi}\int_0^\infty \frac{L_E(k, k')\, k'^2}{k'^2 - k_0^2 - i\delta}\, \omega(k', k_0)\, dk', \tag{22}$$

where

$$f_E(k) = -\frac{3}{8}\frac{C(E)\, a_{E_0}(k)}{\gamma_h(k) + \alpha} + L_E(k, k_0) + \frac{2}{\pi}\int_0^\infty \frac{L_E(k, k')\, k'^2}{k'^2 - k_0^2 - i\delta}\, a_{E_0}(k')\, dk'. \tag{23}$$

It has been shown in Sec. 1 that Eq. (22) has an infinite number of solutions. We must find that solution which satisfies condition (21). It will be evident from the following discussion that the condition that Eq. (22) have such a solution determines the constant C(E) uniquely.

It follows from (22) that for $k \to \infty$

$$\omega(k, k_0) \sim \frac{4}{\sqrt{3}k}\Big\{1 + \frac{2}{\pi}\int_0^\infty \frac{\omega(k', k_0)\, k'^2}{k'^2 - k_0^2 - i\delta}\, dk' + \frac{2}{\pi} C(E) \times \int_0^\infty a_{E_0}(k')\left[\frac{k_0^2}{k'^2 - k_0^2 - i\delta} - \frac{4(E_0 + \alpha^2)/3}{k'^2 - 4(E_0 + \alpha^2)/3}\right] dk'. \tag{24}$$

On the other hand, the asymptotic form of $\omega(k, k_0)$ does not contain terms which decrease as k^{-1}. The right-hand side of (24) must therefore be equal to zero. It follows from (22) and (24) that $\omega(k, k_0)$ satisfies the equation

$$\tfrac{3}{8}\,\omega(k, k_0)/(\gamma_{k_0}(k) + \alpha) = \varphi_E(k) + \frac{2}{\pi}\int_0^\infty \frac{\omega(k', k_0)\, k'^2}{k'^2 - k_0^2 - i\delta}\,[L_E(k, k') - L_E(k, k_0)]\, dk', \tag{25}$$

where

$$\varphi_E(k) = \beta(k_0)\, L_E(k, k_0) - \frac{3}{8}\frac{C(E)\, a_{E_0}(k)}{\gamma_{k_0}(k) + \alpha} + \frac{2}{\pi}\int_0^\infty \frac{a_{E_0}(k')\, k'^2}{k'^2 - k_0^2 - i\delta}\, L_E(k, k')\, dk';$$

$$\beta(k_0) = -\frac{2C(E)}{\pi}\int_0^\infty a_{E_0}(k)\left[\frac{k_0^2}{k^2 - k_0^2 - i\delta} - \frac{4(E_0 + \alpha^2)/3}{k^2 - 4(E_0 + \alpha^2)/3}\right] dk.$$

Equation (25) can be used for the determination of $\omega(k, k_0)$, since it does no longer contain any nondecreasing solutions.

Let us now determine the constant C(E). For this purpose we multiply both sides of (25) by $\tilde{a}(k, k_0)\, k^2 (k^2 - k_0^2 - i\delta)^{-1}$, where $\tilde{a}(k, k_0)$ is the solution of the homogeneous equation corresponding to Eq. (3), and integrate over k from zero to infinity:

$$\frac{3}{8}\int_0^\infty \frac{\omega(k, k_0)\, \tilde{a}(k, k_0)\, k^2\, dk}{[\gamma_{h_0}(k) + \alpha](k^2 - k_0^2 - i\delta)} = \int_0^\infty \frac{f_E(k)\, \tilde{a}(k, k_0)\, k^2}{k^2 - k_0^2 - i\delta}\, dk + \frac{2}{\pi}\int_0^\infty \frac{\tilde{a}(k, k_0)\, k^2\, dk}{k^2 - k_0^2 - i\delta}\int_0^\infty \frac{\omega(k', k_0)\, L_E(k, k')\, k'^2\, dk'}{k'^2 - k_0^2 - i\delta}. \tag{26}$$

Since $\omega(k, k_0)$ vanishes for large k while $\tilde{a}(k, k_0)$ is bounded, we can change the order of integration in the second term on the right-hand side of (26), which evidently leads to

$$\int_0^\infty \frac{f_E(k)\, \tilde{a}(k, k_0)\, k^2}{k^2 - k_0^2 - i\delta}\, dk = 0. \tag{27}$$

From (22) and (27) we obtain the equation for the determination of C(E):

$$C(E)\int_0^\infty \left[\frac{3}{8}\frac{a_{E_0}(k)}{\gamma_{k_0}(k) + \alpha} - \frac{2}{\pi}\int_0^\infty \frac{L_E(k, k')\, k'^2}{k'^2 - k_0^2 - i\delta}\, a_{E_0}(k')\, dk'\right] \times \frac{\tilde{a}(k, k_0)\, k^2}{k^2 - k_0^2 - i\delta}\, dk = \frac{3\pi}{16}\frac{\tilde{a}(k_0, k_0)}{2\alpha}. \tag{28}$$

From formula (28) we can obtain a relation between C(E) and the coefficients $\tilde{A}_1(k_0)$, $\tilde{A}_2(k_0)$, $\tilde{A}_1(E_0)$, and $\tilde{A}_2(E_0)$ in the asymptotic form (9) for $\tilde{a}(k, k_0)$ and $a_{E_0}(k)$:

$$\frac{3\pi}{16}\frac{\tilde{a}(k_0, k_0)}{2\alpha} = 2C(E)\frac{d}{ds_0}\frac{\operatorname{sh}(\pi s_0/6)}{s_0 \operatorname{ch}(\pi s_0/2)}\,[A_1(E_0)\, \tilde{A}_2(k_0) - A_2(E_0)\, \tilde{A}_1(k_0)]. \tag{29}^*$$

Formulas (25) and (28) therefore give the solution to our problem.

4. EQUATIONS INCLUDING SPIN AND ISOSPIN OF THE PARTICLES

The preceding discussion is immediately generalized to the case of particles with spin and isotopic spin. We shall give only the results of the investigation of the equations of Skornyakov and Ter-Martirosyan, since all calculations are trivial generalizations of the corresponding calculations for a system of spinless particles.

To determine the wave function in the case of real nucleons, we must, according to reference 1, solve the following system of equations for the two quantities $a_1(k, k_0)$ and $a_2(k, k_0)$:

---

*ch = cosh; sh = sinh.

$$\frac{[\gamma_{k_0}(k)\,\delta_{ij} - R_{ij}]\,a_j(k, k_0)}{k^2 - k_0^2 - i\delta}$$

$$= L_E(k, k_0)\,\eta_i + \frac{2}{\pi}\int_0^\infty \frac{L_E(k, k')}{k'^2 - k_0^2 - i\delta} M_{ij}a_j((k, k_0)\,dk', \quad (30)$$

where

$$\{R_{ij}\} = \begin{pmatrix} \alpha_t & 0 \\ 0 & \alpha_s \end{pmatrix}, \quad k_0^2 = \tfrac{4}{3}(E + \alpha_t^2),$$

where E is the energy of the system, α_t^2 is the binding energy of the deuteron, and α_s^2 is the energy of the virtual singlet state of the deuteron;

$$\{M_{ij}\} = \begin{pmatrix} {}^1\!/_2 & {}^3\!/_2 \\ {}^3\!/_2 & {}^1\!/_2 \end{pmatrix}, \quad \{\eta_i\} = \begin{pmatrix} {}^1\!/_2 \\ {}^3\!/_2 \end{pmatrix}.$$

Summation over repeated indices is understood in formula (30) and all following formulas.

The wave function of the system in the bound state of the three particles is determined by the quantities $b_1(k)$ and $b_2(k)$, which satisfy the equations (31) without the free term for $E = E_0$, where E_0 is the energy of the bound state of the three particles.

Just as in the case of spinless particles, we can show that the equations (30) have a non-unique solution. For large k the asymptotic forms of $a_j(k, k_0)$ and $b_j(k, k_0)$ and the asymptotic form of the solution $\widetilde{a}_j(k, k_0)$ of the homogeneous equations corresponding to the equations (30) are determined by a formula which is analogous to (9) with the same s_0, and we have, up to terms which vanish as $k \to \infty$,

$$a_1(k, k_0) = a_2(k, k_0),$$

$$b_1(k, k_0) = b_2(k, k_0), \quad \widetilde{a}_1(k, k_0) = \widetilde{a}_2(k, k_0). \quad (31)$$

As before, it is necessary for the orthogonality of the wave functions for different energies that $a_j(k, k_0)$ satisfy for large k the condition

$$a_j(k, k_0) = C(E)\,b_j(k, k_0). \quad (32)$$

By the method discussed in Sec. 3 we can transform the system (30) to a system which has a unique solution. For this purpose let us introduce the function

$$\omega_j(k, k_0) = a_j(k, k_0) - C(E)\,b_j(k), \quad (33)$$

which has the property that

$$k\omega_j(k, k_0) \to 0 \text{ for } k \to \infty. \quad (34)$$

The function $\omega_j(k, k_0)$ satisfies the equation

$$\frac{[\gamma_{k_0}(k)\,\delta_{ij} - R_{ij}]\,a_j(k, k_0)}{k^2 - k_0^2 - i\delta} = \varphi_E^{(i)}(k)$$

$$+ \frac{2}{\pi}\int_0^\infty \frac{k'^2}{k'^2 - k_0^2 - i\delta}\,[L_E(k, k')$$

$$- L_E(k, k_0)]\,M_{ij}\omega_j(k', k_0)\,dk', \quad (35)$$

where

$$\varphi_E^{(i)}(k) = \beta_i(k_0)\,L_E(k, k_0) - \frac{[\gamma_{k_0}(k)\,\delta_{ij} - R_{ij}]\,b_j(k)}{k^2 - k_0^2 - i\delta}$$

$$+ \frac{2}{\pi} C(E)\int_0^\infty \frac{L_E(k, k')\,k'^2}{k'^2 - k_0^2 - i\delta} M_{ij}b_j(k')\,dk',$$

$$\beta_i(k_0) = -\frac{2}{\pi} C(E)$$

$$\times \int_0^\infty \left[\frac{k_0^2}{k^2 - k_0^2 - i\delta} - \frac{{}^4\!/_3(E_0 + \alpha_t^2)}{k^2 - {}^4\!/_3(E_0 + \alpha_t^2)}\right] M_{ij}b_j(k)\,dk. \quad (36)$$

The constant C(E) is determined by the equation

$$\frac{\widetilde{a}_i(k, k_0)}{2\alpha_t} = C(E)\int_0^\infty \frac{\widetilde{a}_j(k, k_0)\,k^2}{k^2 - k_0^2 - i\delta}\left[\frac{(\gamma_{k_0}(k)\,\delta_{ji} - R_{ji})\,b_i(k)}{k^2 - k_0^2 - i\delta}\right.$$

$$\left. - \frac{2}{\pi}\int_0^\infty \frac{L_E(k, k')\,k'^2}{k'^2 - k_0^2 - i\delta} M_{ji}b_i(k')\,dk'\right] dk. \quad (37)$$

I express my deep gratitude to V. N. Gribov for suggesting this topic and his constant attention, and also to A. A. Ansel'm and Yu. V. Petrov for their interest in this work.

APPENDIX

In order to demonstrate the non-uniqueness of the solution to Eq. (3), we rewrite it in the following form:

$$a(k, k_0) = \Phi(k) + \int_0^\lambda K(k, k')\,a(k', k_0)\,dk'$$

$$+ \int_\lambda^\infty K(k, k')\,a(k', k_0)\,dk', \quad (A.1)$$

where $K(k, k')$ and $\Phi(k')$ are the kernel and the free term of (3), and λ is an arbitrary parameter. We shall assume in the following that

$$\lambda \gg (k_0, \sqrt{|E|}, \alpha).$$

To prove the non-uniqueness of the solution to (A.1), it is sufficient to show that the solution to (A.1) for $k > \lambda$ can be expressed in terms of the value of $a(k, k_0)$ for $k < \lambda$:

$$a(k, k_0) = \int_0^\lambda K_1(k, k')\,a(k', k_0)\,dk' + \Phi_1(k) + C\varphi(k, k_0), \quad (A.2)$$

where the kernel $K_1(k, k')$ and the function $\Phi_1(k)$ can be computed in principle, C is an arbitrary constant, and $\varphi(k, k_0)$ is some solution of the homogeneous equation:

$$\varphi(k, k_0) = \int_{\lambda}^{\infty} K(k, k')\,\varphi(k', k_0)\,dk'. \qquad \text{(A.3)}$$

Indeed, substituting (A.2) in the second integral on the right-hand side of (A.1), we obtain an integral equation for $a(k, k_0)$ for $k < \lambda$. The limits of integration in this equation are finite, and the equation is therefore known to have a solution. We conclude that there exists a solution to (A.1) which depends on a single arbitrary parameter, if Eq. (A.2) is satisfied.

Let us prove formula (A.2). We rewrite (A.1) in the following form:

$$a(k, k_0) = \Phi_2(k) + \int_{\lambda}^{\infty} \Delta(k, k')\,a(k', k_0)\,dk' + \int_{\lambda}^{\infty} K_0(k, k')\,a(k', k_0)\,dk', \qquad \text{(A.4)}$$

where $\Phi_2(k)$ is the sum of the two first terms on the right-hand side of (A.1),

$$\Delta(k, k') = K(k, k') - K_0(k, k'), \qquad \text{(A.5)}$$

$$K_0(k, k') = \frac{4}{\pi\sqrt{3}}\frac{1}{k'}\ln\frac{k^2 + k'^2 + kk'}{k^2 + k'^2 - kk'}. \qquad \text{(A.6)}$$

For large k and k′ the kernel $\Delta(k, k')$ goes to zero faster than $K(k, k')$.

For convenience, let us replace the variables k and k′ by $y = \lambda^{-1}k$ and $y' = \lambda^{-1}k'$. Then (A.4) takes the form

$$a(y) = \Phi_\lambda(y) + \int_1^{\infty} \Delta_\lambda(y, y')\,a(y')\,dy' + \frac{4}{\pi\sqrt{3}}\int_1^{\infty}\frac{1}{y'}\ln\frac{y^2 + y'^2 + yy'}{y^2 + y'^2 - yy'}\,a(y')dy'. \qquad \text{(A.7)}$$

The functions $\Phi_\lambda(y)$ and $\Delta_\lambda(y, y')$ go to zero as $\lambda \to \infty$.

In solving (A.7) we shall regard the first two terms of this equation as being responsible for the non-uniqueness. For the solution we make use of the Mellin transform. Let us introduce the function

$$\tilde{a}(s) = \int_0^{\infty} y^{s-1} a_1(y)\,dy, \qquad \text{(A.8)}$$

where $a_1(y) = 0$ for $y < 1$ and $a_1(y) = a(y)$ for $y > 1$. Then

$$a_1(y) = \frac{1}{2\pi i}\int_{-i\infty}^{i\infty} y^{-s}\tilde{a}(s)\,ds. \qquad \text{(A.9)}$$

The contour in formula (A.9) is supposed to pass possible poles of the function $\tilde{a}(s)$ on the left.

To obtain an equation for $\tilde{a}(s)$, we multiply both sides of (A.7) by y^{s-1} and integrate from one to infinity. Then

$$\tilde{a}(s) = \tilde{\Phi}_\lambda(s) + \frac{1}{2\pi i}\frac{4}{\sqrt{3}}\int_{-i\infty}^{i\infty}\frac{L(s')\,\tilde{a}(s')}{s' - s}\,ds', \qquad \text{(A.10)}$$

where $L(s)$ is determined by formula (7) and $\Phi_\lambda(s)$ is the sum of the first two terms on the right-hand side of (A.7) integrated in the indicated manner. Equation (A.10) is valid for $\operatorname{Re} s \to -0$. The function $\tilde{a}(s)$ must go to zero as $|\operatorname{Im} s| \to \infty$. Otherwise the integral (A.9) has no meaning.

The solution to (A.10) can be readily obtained by known methods. It turns out that the homogeneous equation corresponding to (A.10) has a decreasing solution. It can be conveniently written in the form

$$\tilde{a}_0(s) = \frac{s - d}{s^2 + s_0^2}\exp\left(\frac{1}{2\pi i}\int_{-i\infty}^{i\infty}\frac{\ln\varkappa(s')}{s - s'}\,ds'\right),$$
$$\varkappa(s) = \frac{s^2 - d^2}{s^2 + s_0^2}\left[1 - \frac{4}{\sqrt{3}}L(s)\right], \qquad \text{(A.11)}$$

where the quantity s_0 is defined in Sec. 1 and d is an arbitrary parameter satisfying the condition $|\operatorname{Re} d| > 1$. It can be shown that in this case the expression (A.11) is independent of d.

The function $\kappa(s)$ is analytic in the strip $|\operatorname{Re} s| < 1$. The branch of the logarithm in (A.11) is chosen in such a way that $\log\kappa(s) \to 0$ in this strip when $|\operatorname{Im} s| \to \infty$. The general solution of (A.10) is written in the form of a sum of some particular solution of the inhomogeneous equation and the function $\tilde{a}_0(s)$ multiplied by an arbitrary constant:

$$\tilde{a}(s) = C\tilde{a}_0(s) + \frac{\tilde{a}_0(s)}{2\pi i}\int_{-i\infty}^{i\infty}\frac{\tilde{\Phi}_\lambda(s')\,ds'}{(s' - s)(s' - d)\,\tilde{a}_0(s')\,[1 - 4L(s')/\sqrt{3}]} \qquad \text{(A.12)}$$

It is easily verified that a change in the parameter d leads to a redefinition of the constant C.

Let us apply the inverse Mellin transformation to (A.12). Instead of (A.7), we obtain then

$$a(y) = u(y) + \Phi'_\lambda(y) + \int_1^{\infty}\Delta'_\lambda(y, y')\,a(y')\,dy', \qquad \text{(A.13)}$$

where $u(y)$ is the solution of (A.7) with $\Delta_\lambda(y, y') = 0$, and $\Phi'_\lambda(y)$ and $\Delta'_\lambda(y, y')$ are certain known functions with the property

$$\Phi'_\lambda(y) \to 0, \qquad \int_1^{\infty}|\Delta'_\lambda(y, y')|\,dy' \to 0 \qquad \text{(A.14)}$$

for $\lambda \to \infty$. Since, moreover, the functions $u(y)$

and $\Phi'_{\lambda}(y)$ are bounded, Eq. (A.13) can, in principle, be solved by the method of iterative approximations. This leads to formula (A.2). Since u(y) contains an arbitrary constant, the solution of Eq. (A.13) will, obviously, also contain an arbitrary constant.

The asymptotic form of a(k k_0) can be obtained from Eq. (A.13). The resulting expression is in agreement with formula (9).

---

[1] G. V. Skornyakov and K. A. Ter-Martirosyan, JETP 31, 775 (1956), Soviet Phys. JETP 4, 648 (1957).

[2] G. V. Skornyakov, Report at the Conference on the Problems of Nuclear Forces and the Properties of Systems with a Small Number of Nucleons, London (1959).

[3] V. N. Gribov, JETP 38, 553 (1960), Soviet Phys. JETP 11, 400 (1960).

Translated by R. Lipperheide
78

SOVIET PHYSICS JETP VOLUME 13, NUMBER 2 AUGUST, 1961

ON THE PHYSICAL MEANING OF NEGATIVE PROBABILITIES

J.-P. VIGIER and Ya. P. TERLETSKII

Institute Henri Poincaré, Paris, France

Submitted to JETP editor June 27, 1960

J. Exptl. Theoret. Phys. (U.S.S.R.) 40, 508-512 (February, 1961)

It is shown that the calculation of the statistical averages of a series of physical quantities can be carried out with the help of the distribution function instead of the probability density. The distribution function is the mathematical expectation of the particle density and is proportional to the probability density for a single particle only if all particles are absolutely identical. For a set of particles and antiparticles (with respect to some single property) the distribution function can also assume negative values. In this case it is no longer proportional to the probability, but it can be used to compute the averages of a number of physical quantities. It is shown that in the field theory of elementary particles the average values of some quantities characterizing the entire field (energy, momentum, charge, etc.) can be computed with the help of the corresponding distribution function.

1. INTRODUCTION

It is known that many attempts at a generalization or a new interpretation of the apparatus of quantum mechanics have led to negative or even complex "probabilities." Thus, for example, the density matrix in the mixed (coordinate-momentum) representation, which plays the role of the quantum mechanical probability density in the phase space, must either be complex[1,2] or a real quantity which can assume negative values.[3,4] Negative "probability" densities appeared to be inevitable in relativistic quantum mechanics which includes states with negative energies.[5,6] Finally, quantum mechanics in Feynman's functional representation[7] involves complex (or real, but sometimes negative) "probability" densities in the functional space of the particle paths.[8]

The problem of the physical meaning of complex or negative "probabilities" also turns up in the new interpretation of quantum theory as the classical statistical theory of systems which interact with an "imaginary" thermostatic oven, i.e., with a thermostatic oven that has an imaginary temperature, as has been proposed by one of us.[9] Since it is possible, in all cases known to us, to avoid the appearance of imaginary parts in the "probabilities" by an appropriate reformulation, the question of principal interest is that of the meaning of "probabilities" which can have negative as well as positive values. The discussion of this question forms the subject of the present paper.

If "probability" is understood as a quantitative measure of the possibility of the presence of some object or of the occurrence of some process, where probability one implies certainty and probability zero corresponds to impossibility, negative values of the probability have no real meaning whatsoever. Thus, if the quantity which plays the role of a probability in a physical theory is not positive definite, it cannot be an actual "probability"; it only fulfills the function of the genuine probability in the computation of certain average values. This quantity is more accurately called the formal probability or quasiprobability.

The quasiprobability (more precisely, the density of the quasiprobability) is, in general, a distribution function, i.e., the mathematical expectation of the particle density. If the particles are completely identical and indistinguishable, the probability density function for a single particle differs from the distribution function only by normalization factor. However, for a set of positive and negative (with respect to some property, e.g., the charge) particles which otherwise have identical properties, the distribution function can take positive as well as negative values, since it represents the average "charge" density. This distribution function does not coincide with the probability density; however, it can be used in place of the probability density for the computation of certain average values.

The appearance of negative "probabilities" in a physical theory may therefore mean that we are actually not dealing with a probability density but with a distribution function which plays the role of a probability density in the computation of average values of certain quantities. Let us now consider these questions in more detail.

2. PROBABILITY DENSITY AS MATHEMATICAL EXPECTATION

In every physical theory one always ignores some physical quantities and only focusses attention on certain chosen ones, namely, the observables for which the theory has been formulated. Let X denote the set of observable quantities and Y, the set of ignored quantities. We can introduce a probability density $W(X, Y)$ for the whole set of physical quantities (X, Y) in such a way that $W\,dX\,dY$ has all the properties of a probability. With the help of this probability density we can also compute the probability density for the observed quantities

$$W(X) = \int_{(Y)} W(X, Y)\,dY. \tag{1}$$

On the other hand, expression (1) can also be written in the form

$$W(X) = \int_{(X', Y')} \delta(X - X')\,W(X', Y')\,dX'dY', \tag{2}$$

where $\delta(X - X')$ stands for the corresponding product of δ functions if X denotes more than one variable. Now the last integral is the mathematical expectation of the quantity

$$F = \delta(X - X'). \tag{3}$$

The probability density of the observed quantities can therefore be regarded as the average value of a quantity of the type (3).

In the above-mentioned example $W(X)$ cannot take negative values, since $W(X, Y) \geq 0$ and $F \geq 0$; W, therefore, has all the properties of a probability density.

3. DISTRIBUTION FUNCTION AND PROBABILITY DENSITY

If the physical system under consideration consists of a set of N identical particles (i.e., the matter density is distributed over the three-dimensional space in the form of a set of N δ-function-like maxima), its statistical behavior is sufficiently, completely described by a distribution function defined as the average of the particle density.

In the classical statistical theory of gases the distribution function is defined as the average of

$$\sigma = \sum_{k=1}^{N} \delta(\mathbf{r}_k - \mathbf{r})\,\delta(\mathbf{p}_k - \mathbf{p}), \tag{4}$$

in the six-dimensional phase space of coordinates and momenta; $\mathbf{r}_k$ and $\mathbf{p}_k$ are the coordinates and momenta of the individual mass points. This means we have

$$f(\mathbf{r}, \mathbf{p}) = \bar{\sigma} = \int \sigma W(\mathbf{r}_1, \mathbf{p}_1; \mathbf{r}_2, \mathbf{p}_2; \ldots; \mathbf{r}_N, \mathbf{p}_N)\,d\mathbf{r}_1 \ldots d\mathbf{p}_N, \tag{5}$$

where $W(\mathbf{r}_1, \ldots, \mathbf{p}_N)$ is the probability density in the (6N)-dimensional phase space. If all particles are identical, the function W must be symmetric under the interchange of the particles, and therefore

$$f(\mathbf{r}, \mathbf{p}) = N \int \delta(\mathbf{r} - \mathbf{r}_1)\,\delta(\mathbf{p} - \mathbf{p}_1)\,W(\mathbf{r}_1, \ldots, \mathbf{p}_N)\,d\mathbf{r}_1 \ldots d\mathbf{p}_N, \tag{6}$$

i.e., the distribution function is, according to (2), equal to N times the probability density that a single particle has the given coordinates $\mathbf{r}$ and momenta $\mathbf{p}$. Thus the average value of any physical quantity which is the sum of identical functions of the coordinates and momenta of the individual particles can with equal success be computed either with the help of f or with the help of W, for obviously

$$\overline{\sum_{k=1}^{N} \varphi(\mathbf{r}_k, \mathbf{p}_k)} = N \int \varphi(\mathbf{r}_1, \mathbf{p}_1)\,W(\mathbf{r}_1, \ldots, \mathbf{p}_N)\,d\mathbf{r}_1 \ldots d\mathbf{p}_N$$
$$= \int \varphi(\mathbf{r}, \mathbf{p})\,f(\mathbf{r}, \mathbf{p})\,d\mathbf{r}d\mathbf{p}. \tag{7}$$

In the computation of average values of physical quantities of a certain form, the distribution function can therefore fulfill the same function as the probability density. It is clear that this result holds not only for the distribution function in the theory of gases, but also in all other cases (for example, for the distribution function in configuration space).

4. DISTRIBUTION FUNCTION FOR A SYSTEM OF OPPOSITELY CHARGED IDENTICAL PARTICLES

In the preceding example the distribution function, just like the probability density, cannot take negative values, since always $\sigma \geq 0$. It can therefore replace the probability density in all respects, as it differs from the latter only by a normalization factor. The situation is different for a set of identical but oppositely charged particles. Here "charge" must be understood in the widest sense, i.e., as a certain property which distinguishes between particles and antiparticles which are identical to each other in all other respects. The "charge" can thus be interpreted as the electric charge in the case of electrons and positrons, as the baryon number in the case of nucleons and antinucleons, and, finally, as the rest mass in the case of Dirac particles with positive and negative masses.

Let us consider the case of a system of oppositely charged particles. Let it contain N^+ positive and N^- negative particles. Together there are $N = N^+ + N^-$ particles described by a set of generalized coordinates $x_1, x_2, \ldots x_{N^+}, x_{N^++1}, \ldots, x_N$. The first N^+ coordinates, which can also be denoted by $x_k = x_k^+$, are the coordinates of the positive particles, and the remaining N^- coordinates $x_{N^++i} = x_i^-$ are the coordinates of the negative particles. The total probability density describing the statistical behavior of the total ensemble of particles must be a function of all coordinates:

$$W(x_1, \ldots, x_N) = W(x_1^+, x_2^+, \ldots, x_{N+}^+, x_1^-, x_2^-, \ldots, x_{N-}^-). \tag{8}$$

Since the particles are indistinguishable, the function (8) is evidently symmetric with respect to interchanges of particles of the same sign, but may not, in general, be symmetric with respect to interchanges of a positive and a negative particle. Hence

$$W_+(x) = \int \delta(x - x_h^+)\, W(x_1^+, \ldots, x_{N-}^-)\, dx_1^+ \ldots dx_{N-}^- \neq W_-(x) = \int \delta(x - x_i^-) \times W(x_1^+, \ldots, x_{N-}^-)\, dx_1^+ \ldots dx_{N-}^-. \tag{9}$$

i.e., the probability density for a positive particle is not equal to the probability density for a negative particle.

The role of the distribution function for the considered system of oppositely charged particles will, obviously, be played by the average "charge" density, i.e., by the average value of the quantity

$$\rho = \sum_{h=1}^{N} \varepsilon_k \delta(x - x_k). \tag{10}$$

If we set $|\epsilon_k| = 1$, this expression can also be written in the form

$$\rho = \sum_{h=1}^{N+} \delta(x - x_k^+) - \sum_{i=1}^{N-} \delta(x - x_i^-). \tag{11}$$

The average value of ρ is, according to (9) — (11), equal to

$$\bar\rho = N_+ W_+(x) - N_- W_-(x). \tag{12}$$

Because of (9), this quantity can take both positive and negative values.

It is easy to see that we can use the average density to compute the average values of quantities of the form

$$F = \sum_{k=1}^{N} \varepsilon_k \varphi(x_k) \tag{13}$$

with the help of the usual formula for the mathematical expectation. Indeed,

$$\bar F = \int \sum_{h=1}^{N} \varepsilon_k \varphi(x_h)\, W(x_1, \ldots, x_N)\, dx_1 \ldots dx_N = \int \varphi(x)\, [N_+ W_+(x) - N_- W_-(x)]\, dx = \int \varphi(x)\, \bar\rho(x)\, dx \tag{14}$$

hence, if we substitute the quantity $N\varphi(x)$ instead of $\bar F$, the quantity $\bar\rho(x)/N$ will play the role of the probability density in x space.

One might think that the situation is analogous in those cases where negative "probabilities" appear. If the formal apparatus of the theory leads to a negative probability for some particle coordinate, this may indicate that we are actually dealing with an ensemble of particles and antiparticles (with respect to some property) and that we are actually computing the average value of a quantity of the type (13), and not a function of the coordinate of a single particle.

5. AVERAGE VALUES IN THE FIELD THEORY OF PARTICLES

If the elementary particles are regarded as particular solutions of nonlinear field equations (for example, as the particle-like solutions of references 9 — 11), only quantities characterizing the whole field, not those referring to the individual particles, have a physical meaning.

In the example considered above, such a quantity is the "charge" of a given volume. A theory which uses the distribution function instead of the probability allows us to calculate the average "charge" of the unit volume, but says nothing about the average "charge" of a given particle. In the case of a set of Dirac particles with positive and negative masses, we can compute the average energy and momentum in a given volume with the help of the distribution function. Many basic average values in the field theory of elementary particles can thus be computed with the help of the corresponding distribution function, using the same rules that apply if the probability density is used. The distribution function may take negative values; but it is not correct to interpret this as the appearance so to speak of negative probabilities.

---

[1] Ya. P. Terletskii, JETP 7, 1290 (1937).

[2] D. I. Blokhintsev, J. of Phys. 2, 71 (1940).

[3] E. P. Wigner, Phys. Rev. 40, 749 (1932).

[4] J. E. Moyal, Proc. Cambr. Phil. Soc. 45, 99 (1949).

[5] P. A. M. Dirac, Proc. Roy. Soc. A180, 1 (1942).

[6] W. Pauli, Revs. Modern Phys. 15, 175 (1943).

[7] R. P. Feynman, Revs. Modern Phys. 20, 367 (1948).

[8] G. V. Ryazanov, JETP 35, 121 (1958), Soviet Phys. JETP 8, 85 (1959).

[9] Ya. P. Terletskii, Doklady Akad. Nauk 133, 568 (1960), Soviet Phys.-Doklady 5, 812 (1961).

[10] Louis de Broglie, J. Phys. rad. 20, 963 (1959).

[11] Glasko, Leryust, Terletskii, and Shushurin, JETP 35, 452 (1958), Soviet Phys. JETP 8, 312 (1959).

Translated by R. Lipperheide

79

SOVIET PHYSICS JETP VOLUME 13, NUMBER 2 AUGUST, 1961

THEORY OF MOLECULAR DISSOCIATION INDUCED BY NEUTRONS.

I. DIATOMIC MOLECULES

Yu. S. SAYASOV and G. K. IVANOV

Institute of Chemical Physics, Academy of Sciences, U.S.S.R.

Submitted to JETP editor June 26, 1960

J. Exptl. Theoret. Phys. (U.S.S.R.) **40**, 513-523 (February, 1961)

A theory based on the Fermi pseudopotential method is developed for the dissociation of diatomic molecules. It is assumed that the neutron energy is of the order of the dissociation energy, and that during disintegration the molecule remains in the ground electron state. Under these assumptions, simple final formulas can be obtained for the cross sections of the processes.

1. INTRODUCTION

THE collision of a neutron with a chemically bound nucleus can be accompanied by transfer to it of momentum that is sufficient for breaking the bond, i.e., for dissociation of the molecule. This process which has not been investigated before, is of undoubted interest in radiation chemistry and biology, and also for the theory of slowing down of neutrons. Moreover, calculations of the dissociation probability of molecules by neutrons are necessary in connection with the development now being carried on of the method proposed by Gol'danskii of molecular neutronoscopy,[1] which has as its purpose the study of the different characteristics of molecules by recording neutrons scattered by them.

We shall assume that the neutrons have an energy E of the order of the molecular dissociation energy, i.e., $E \sim 10$ ev. Such energies correspond to a wavelength $\lambda_n \sim 10^{-9}$ cm. This means that the relations $\lambda_n \gg A$, $a \gg A$ hold among λ_n, the range of nuclear forces $A \sim 10^{-13}$ cm, and the characteristic molecular dimension, by which one should mean the amplitude of vibrations of nuclei in the molecule, $a \sim 10^{-9}$ cm. These relations make it possible to use the method of the Fermi pseudopotential in the case under discussion.[2]

In other words, by introducing the interaction V between neutrons and the nuclei of a molecule of type

$$V = 2\pi\hbar^2 \sum_i \frac{1}{\mu_i} A_i \delta(\mathbf{r}_n - \mathbf{r}_i) \tag{1}$$

(here $\mu_i = m_i m/(m_i + m)$ is the reduced mass of the neutron (m) and the i-th nucleus in the molecule (m_i), $A_i = a_i + b_i(\mathbf{i}\cdot\mathbf{s})$ is the amplitude of scattering of the neutron (spin $\mathbf{s}$) by the free nucleus (spin i), $\mathbf{i}\cdot\mathbf{s}$ is the eigenvalue of the operator $\hat{\mathbf{i}}\cdot\hat{\mathbf{s}}$), we can compute the dissociation cross section $d\sigma$ in the first Born approximation relative to V, according to the usual formulas of perturbation theory, for the probability of transition from the states of the discrete spectrum to the continuous:

$$d\sigma = \frac{k'}{k}\overline{|W|^2}\,d\varkappa_1 \ldots d\varkappa_n do. \tag{2}$$

Here k, k′ are the wave numbers of the neutron before and after collision, $\kappa_1 \ldots \kappa_n$ are the wave vectors of particles which appear as products of the dissociation of the molecule, and do is the element of solid angle in which the neutron is scattered,

$$W = \frac{\mu}{2\pi\hbar^2}\int e^{i(\mathbf{k}-\mathbf{k}')\mathbf{r}_n}\psi_0 V \psi_\varkappa^* d\mathbf{r}_n d\mathbf{r},$$

μ is the reduced mass of neutron and molecule; ψ_0 is the wave function of the initial state of the molecule, ψ_κ is the wave function of the final state of the molecule which corresponds to the process of its decay of a definite type (continuous spectrum); the symbol dr denotes integration over all molecular coordinates; in (2), the averaging is carried out over all the energetically degenerate states.

For the neutron energies of interest to us, the formula (2) immediately admits a certain simplification, which is connected with the fact that in such cases the motion of the nuclei both in the initial and in the final state can be regarded as slow in comparison with electronic motion. Therefore, for the functions ψ_0, ψ_κ, the adiabatic approximation is valid, i.e., one can represent them in the form of a product of electron wave functions and wave functions describing the motion of nuclei in a certain potential field which depends on their mutual distance.

Inasmuch as the operator V acts only on the coordinates of the nuclei, then, in accord with (2), in the adiabatic approximation, the dissociation cross section of the molecule, which is accompanied by a change in its electron state, will generally be equal to zero. Thus, it is permissible to limit ourselves to an investigation of dissociation processes for which the electron state of the molecule does not change, i.e., generally to exclude from consideration the electronic functions, considering ψ_0 and ψ_K in (2) as the wave functions of the relative motion of the nuclei corresponding to the main electron term. Nevertheless, even under these simplifying assumptions, the functions ψ_K in the general case of monatomic molecules possess a very complicated character. Therefore, we shall initially limit ourselves to the study of dissociation of diatomic molecules for which the functions ψ_K have a comparatively simple form.

2. GENERAL FORMULAS FOR THE DISSOCIATION CROSS SECTIONS OF DIATOMIC MOLECULES

For simplicity we shall assume that the electron state of the molecules is $^1\Sigma$. Then the Hamiltonian of the relative motion of the nuclei of the molecule is identical in the adiabatic approximation with the Hamiltonian of the relative motion of two particles whose interaction is centrally symmetric; consequently, the functions ψ_K in the given case are identical with the functions $\psi_{\bar{K}}$ defined in reference 3, Sec. 113, whose asymptote for $r \rightarrow \infty$ ($\mathbf{r} = \mathbf{r}_1 - \mathbf{r}_2$) is itself the superposition of a plane wave and a converging spherical wave:

$$\psi_{\varkappa}^{-} = \frac{1}{4\pi\varkappa r} \sum_{l=0}^{\infty} i^l (2l+1) e^{-i\delta_l} \chi_{\varkappa l}(r) P_l\left(\frac{\varkappa \mathbf{r}}{\varkappa r}\right), \tag{3}$$

where $\chi_{\kappa l}$ are the wave functions of the equation

$$\frac{d^2\chi_{\varkappa l}}{dr^2} + \left(\varkappa^2 - \frac{2\mu_m U}{\hbar^2} - \frac{l(l+1)}{r^2}\right)\chi_{\varkappa l} = 0, \tag{4}$$

U is the molecular potential and μ_m the reduced mass of the molecule. The functions $\chi_{\kappa l}$ are regular for r = 0 and have the asymptote

$$\chi_{\varkappa l} \sim \sqrt{2/\pi} \sin(\varkappa r - \pi l/2 + \delta_l) \quad \text{for} \quad r \rightarrow \infty.$$

The initial state of the molecule, which has a vibration number n and rotational number K can be determined in the following way:

$$\psi_0 = \frac{1}{r}\left(\frac{2}{\pi}\right)^{1/4} a^{-1/2} e^{-\xi^2} H_n(\xi) Y_{KM_K}(\theta, \varphi), \tag{5}$$

where $\xi = (r - r_0)/a$, r_0 is the point of minimum U, $a = \sqrt{2\hbar/\mu_m\omega}$ is the amplitude of the vibrations of the nuclei in the molecule, $H_n(\xi)$ are Hermite functions, M_K is the projection of the moment of inertia of the molecule K on the axis of the molecule, θ and φ are angles which define the orientation of the molecule in the center-of-mass system (c.m.s.) of the neutron-molecule, to which all our discussions refer. Equation (2) in the case under discussion is rewritten in the following form:

$$d\sigma = \frac{k'}{k}\frac{1}{2K+1}\sum_{M_K=-K}^{K} \overline{|W_{M_K}|^2}\, d\varkappa\, do, \tag{6}$$

where

$$W_{M_K} = \frac{\mu}{2\pi\hbar^2}\int e^{i(\mathbf{k}-\mathbf{k}')\mathbf{r}_n} \psi_0 V \psi_{\varkappa}^{-*}\, d\mathbf{r}_n\, d\mathbf{r},$$

$$V = 2\pi\hbar^2\left(\frac{A_1}{\mu_1}\delta(\mathbf{r}_n - \mathbf{r}_1) + \frac{A_2}{\mu_2}\delta(\mathbf{r}_n - \mathbf{r}_2)\right). \tag{7}$$

In (6) the averaging is carried out over orientations of the spins of the nuclei and the neutron which are assumed to be distributed randomly.

We note that the wave numbers of the neutron k, k′ and the wave number of the molecule κ are connected by a relation which follows from the law of conservation of energy:

$$k^2/2\mu - k'^2/2\mu = D_{nK}/\hbar^2 + \varkappa^2/2\mu; \tag{8}$$

D_{nK} is the dissociation energy

$$D_{nK} = U_m - \left(n + \frac{1}{2}\right)\hbar\omega - K(K+1)\hbar^2/2\mu_m r_0^2,$$

$$U_m = -U(r_0).$$

One can transform Eq. (6) in such a way that only the characteristics of a finite state of the system are contained in it – the scattering angle of the neutron θ and the wave number of the molecule in the final state κ (see Appendix 1):

$$d\sigma_{nK} = \sqrt{\frac{\pi}{2}}\frac{k'}{k}\frac{1}{a}\left[\sum_{l=0}^{\infty}(2l+1)\sum_{L=|l-K|}^{l+K}(C_{l0K0}^{L0})^2 F_{lL}\right] d\varkappa\, do,$$

$$F_{lL} = \overline{A_1^2}\frac{1}{g_1^2}\left(\frac{\mu}{\mu_1}\right)^2 J_{g_1}^2 + \overline{A_2^2}\frac{1}{g_2^2}\left(\frac{\mu}{\mu_2}\right)^2 J_{g_2}^2 + (-1)^L \overline{2A_1A_2}\frac{\mu^2}{\mu_1\mu_2} J_{g_1} J_{g_2}\frac{1}{g_1 g_2}, \tag{9}$$

where

$$J_g = \int_0^{\infty}\frac{1}{r} e^{-\xi^2} H_n(\xi)\chi_{\varkappa l}(r)\psi_{L+1/2}(gr)\, dr,$$

$$\psi_{L+1/2}(x) = \sqrt{x} J_{L+1/2}(x), \qquad g = g_{1,2} = \frac{m_{2,1}}{m_1 + m_2}|\mathbf{k} - \mathbf{k}'|, \tag{10}$$

C_{l0K0}^{L0} are the Clebsch-Gordan coefficients.

The averaging in (9) is carried out over the directions of spins of the nuclei and of the neutron. If the nuclei in the molecule are different (see reference 3, Sec. 123), then

$$\overline{A^2_{1,2}} = a^2_{1,2} + \tfrac{1}{4} i_{1,2}(i_{1,2}+1)\, b^2_{1,2}, \qquad \overline{A_1 A_2} = a_1 a_2,$$

$i_{1,2}$ are the nuclear spins. Now if the nuclei are identical, then, as is easy to show,

$$\overline{A^2_{1,2}} = a^2 + \tfrac{1}{4}\, i\,(i+1)\, b^2,$$

$$\overline{A_1 A_2} = a^2 + \tfrac{3}{8}\, b^2\, [2i\,(i+1) - I\,(I+1)],$$

I is the total spin of the system of two nuclei.

3. DISSOCIATION CROSS SECTION UNDER QUASICLASSICAL CONDITIONS

For neutron energies of interest to us, its wavelength ($\lambda_n \sim 10^{-9}$ cm) is much less than the dimensions of the molecule. Therefore, a quasiclassical approximation is generally valid for the functions $\chi_{\kappa l}$, $\psi_{L+1/2}$:

$$\chi_{\varkappa l} = \left(\frac{2}{\pi}\frac{\varkappa}{\tilde{\varkappa}}\right)^{1/2} \sin\left(\int_{r_1}^{r} \tilde{\varkappa}\, dr + \frac{\pi}{4}\right),$$

$$\tilde{\varkappa}^2 = \varkappa^2 - \frac{2\mu_m}{\hbar^2} U - \frac{l\,(l+1)}{r^2}, \qquad (11)$$

$$\psi_{L+1/2} = \left(\frac{2}{\pi}\frac{g}{\tilde{g}}\right)^{1/2} \sin\left(\int_{r_2}^{r} \tilde{g}\, dr + \frac{\pi}{4}\right), \quad \tilde{g}^2 = g^2 - \frac{L\,(L+1)}{r^2}, \qquad (12)$$

where r_1 and r_2 are the turning points for the functions $\widetilde{\kappa^2}$ and $\widetilde{g^2}$. Using (11) and (12), we can calculate J_g (10) by the method of steepest descents. We rewrite J_g in the form

$$J_g = \frac{1}{2} \operatorname{Re} \mathcal{Y}, \qquad \mathcal{Y} = \int_0^\infty b\,(r)\, e^{S(r)}\, dr,$$

where

$$b\,(r) = \frac{2}{\pi}\left(\frac{\varkappa g}{\tilde{\varkappa}\tilde{g}}\right)^{1/2} \frac{1}{r},$$

$$S = \frac{-(r-r_0)^2}{a^2} + i\left(\int_{r_1}^{r} \tilde{\varkappa}\, dr - \int_{r_2}^{r} \tilde{g}\, dr\right).$$

$S(r)$ is a quantity of large magnitude which has a saddle point defined by the equation

$$-2\,(r_n - r_0)/a^2 + i\,(\tilde{\varkappa} - \tilde{g}) = 0. \qquad (13)$$

In the general case, calculation of J_g by the method of steepest descents leads to formulas that are difficult to handle. It is easy to note, however, that in the region of values of κ and θ where the cross section $d\sigma$ is largest, the expressions for r_n and J_g are greatly simplified. We shall carry out these simplifications, assuming that the molecule is found in the ground state (i.e., $n = 0$, $K = 0$). We note that r_n is close to the point of minimum potential of U, r_0. Then, as follows directly from Eq. (13), we obtain the following expression for r_n:

$$r_n - r_0 = i\eta,$$

$$\eta = \tfrac{1}{2} a^2\, (\tilde{\varkappa}\,(r_0) - \tilde{g}\,(r_0)) = \tfrac{1}{2} a^2 \left(\sqrt{\varkappa'^2 - l^2/r_0^2} - \sqrt{g^2 - l^2/r_0^2}\right),$$

$$\varkappa'^2 = \varkappa^2 - 2\mu_m \hbar^{-2} U\,(r_0) = \varkappa^2 + 2\mu_m \hbar^{-2} U_m. \qquad (14)$$

As is easy to show, Eq. (14) is valid under the condition $\eta/r_0 \ll 1$ [where η is determined in (14)]. Inasmuch as

$$a^2 = \sqrt{2\hbar^2/\mu_m U''(r_0)} \sim \hbar\, r_0 / \sqrt{\mu_m U_m} \sim r_0/\varkappa',$$

then the condition $\eta/r_0 \ll 1$ is equivalent to the inequality $(\kappa' - g)/\kappa' \ll 1$. Then (14) can be rewritten in the form

$$\eta \approx \frac{a^2}{4} \frac{\varkappa'^2 - g^2}{\sqrt{g^2 - l^2/r_0^2}} \approx \frac{a^2}{2} \frac{\varkappa' - g}{\sqrt{1 - l^2/l_0^2}}, \quad l_0 = g r_0. \qquad (15)$$

Simplifying the quantities $S(r_n)$, $S''(r_n)$, $b\,(r_n)$ in similar fashion, and assuming that $(\kappa' - g)/\kappa' \ll \sqrt{1 - l^2/l_0^2}$, we get

$$J_g = \frac{1}{\sqrt{\pi}} \frac{a}{r_0} \sqrt{\frac{\varkappa}{\varkappa'}} \frac{1}{\sqrt{1 - l^2/l_0^2}} \exp\left[-\frac{\rho^2}{2\,(1 - l^2/l_0^2)}\right] \cos\tau,$$

$$\rho^2 = \frac{a^2}{2}(\varkappa' - g)^2, \qquad \tau = \int_{r_1}^{r_0} \tilde{\varkappa}\, dr - \int_{r_2}^{r_0} \tilde{g}\, dr. \qquad (16)$$

Upon substituting J_g in the series (9), we note that the interference terms, which contain the product of rapidly oscillating factors $\cos\tau\,(g_1) \cos\tau\,(g_2)$, vanish in the summation, i.e., the dissociation cross section is composed additively of the cross sections corresponding to the collision of the neutron with the first ($d\sigma^{(1)}$) or second nucleus ($d\sigma^{(2)}$).* Therefore, it suffices to investigate, for example, the cross section $d\sigma^{(1)}$, which is determined by the formula

$$d\sigma^{(1)} = \sqrt{\frac{\pi}{2}} \frac{k'}{k} \frac{1}{a} \overline{A_1^2} \frac{1}{g_1^2} \left(\frac{\mu}{\mu_1}\right)^2 \left[\sum_{l=0}^{\infty} (2l+1)\, J^2_{g_1}\right] d\varkappa\, do. \qquad (17)$$

Substituting (16) therein, and replacing the summation over l by an integration, and $\cos^2\tau'$ by its mean value $1/2$, we get

$$d\sigma = \frac{1}{2\sqrt{2\pi}} \frac{k'}{k}\, a \frac{1}{\varkappa'} \frac{\mu^2}{\mu_1^2} \operatorname{Ei}(-\rho^2)\, \varkappa\, d\varkappa\, do. \qquad (18)$$

Equation (18) is evidently applicable under the condition that the region of large values of l for which $(\kappa' - g)/\kappa' \sim \sqrt{1 - l/l_0^2}$ does not make an important contribution in the integration over l. Obviously, for this to happen it is necessary that for $(\kappa' - g)/\kappa$

---

*If the nuclei in the molecule are identical, then $g_1 = g_2$, so that $\cos^2\tau(g)$ enters into the interference terms. Nevertheless, the interference series $\Sigma(-1)^l(2l+1)\, J_g^2/g^2$, as is easy to see, is equal to zero in this case in view of its sign alternation.

$\sim \sqrt{1-l^2/l_0^2}$ the inequality $\rho^2/(1-l^2/l_0^2) > 1$ be satisfied, which is possible only when $a^2\kappa'^2 \gg 1$. In Eq. (18), consequently, both large values of ρ^2, consistent with the condition $\eta/r_0 \sim (\kappa' - g)/\kappa' \ll (1-l^2/l_0^2)^{1/2}$ and small values of ρ^2, consistent with the condition $a^2\kappa'^2 \gg 1$ can enter. For $\rho^2 > 1$, Eq. (18) has the asymptotic form

$$d\sigma = \frac{1}{2\sqrt{2\pi}} \frac{k'}{k} a \left(\frac{\mu}{\mu_1}\right)^2 \overline{A_1^2} \frac{1}{\varkappa'} \frac{e^{-\rho^2}}{\rho^2} \varkappa d\varkappa do, \tag{19}$$

while for $\rho^2 < 1$

$$d\sigma = \frac{1}{2\sqrt{2\pi}} \frac{k'}{k} a \left(\frac{\mu}{\mu_1}\right)^2 \overline{A_1^2} \frac{1}{\varkappa'} \ln(\gamma/\rho^2) \varkappa d\varkappa do \tag{20}$$

(γ is Euler's constant).

Equations (18) and (20) are inapplicable for $\rho \to 0$. Nevertheless, the difference of (20) for $\rho \to 0$ from the correct equation, in which $\ln(\gamma/\rho^2)$ must approach some finite value,* possesses only a logarithmic character; consequently, Eq. (18), having been integrated over θ and κ, must yield the correct total cross section. Actually, making use of the well-known integral

$$\int_{-\infty}^{\infty} \mathrm{Ei}(-\rho^2)\, d\rho = 2\sqrt{\pi},$$

we find that the energy spectrum of the scattered neutrons has the form

$$d\sigma^{(1)} = \pi\overline{A_1^2} \frac{\mu\mu_m}{\mu_1^2} \frac{2k'\, dk'}{k^2}, \tag{21}$$

i.e., the total cross section σ is

$$\sigma = \pi\overline{A_1^2} \frac{\mu\mu_m}{\mu_1^2} \frac{E-D}{E}. \tag{22}$$

In particular, if the neutron collides with a proton in a heavy molecule, then $\mu_1 = m/2$, $\mu = \mu_m = m$ and, consequently, $\mu\mu_m/\mu_1^2 = 4$, i.e.,

$$\sigma = \sigma_0 (E-D)/E, \tag{23}$$

where $\sigma_0 = 4\pi\overline{A}_1^2$ is the cross section of scattering of the neutron by a free proton. In accord with (23), σ at $E \gg D$, as was to have been expected, is identical with σ_0. We now consider the angular distribution of the scattered neutrons from the basis of Eqs. (18) and (19). The maximum of $d\sigma$ is evidently obtained for the angle $\theta = \theta_0$ for which $\rho = 0$, i.e., $\kappa' = g$. We assume that $ak' \gg 1$. Then, as is easy to see, the angle θ_0 is determined from the relation

$$\varkappa' \approx \sqrt{\frac{\mu_m}{\mu}(k^2 - k'^2)} = g_1$$
$$= \frac{m_2}{m_1 + m_2}\sqrt{k^2 + k'^2 - 2kk'\cos\theta},$$

with accuracy up to a quantity of order $1/a^2k'^2$, i.e.,

$$\cos\theta_0 = [(\nu+1)p'^2 - (\nu-1)p^2]/2pp',$$
$$p = k\hbar, \quad p' = k'\hbar, \quad \nu = m_1(m_1 + m_2 + m)/mm_2. \tag{24}$$

It can be shown that θ_0 has the meaning of the angle at which the neutron will be scattered by a free nucleus initially at rest with mass m, in the set of coordinates which we have used, i.e., one connected with the center of mass of the neutron-molecule system. It is very easy to establish this by the example of the collision of a neutron with a proton in a heavy molecule, i.e., for $m_2 \gg m_1 = m$. Then $\nu \approx 1$ and, in accord with (24), $\cos\theta_0 = p'/p$ in correspondence with the given determination of θ_0 (the set of coordinates in this case is identical with the laboratory set).

We shall assume that the angle θ is close to θ_0, i.e., $\theta = \theta_0 + \vartheta$, $\vartheta \ll \theta_0$. Then (for $\nu = 1$) we have, in first approximation in ϑ, $\rho = \vartheta/\vartheta_0$, $\vartheta_0 = \sqrt{2}/ak' \ll 1$. In this case Eq. (18) is simplified:

$$d\sigma = \frac{\sigma_0}{\sqrt{2\pi}} \left(\frac{p'}{p}\right)^2 \mathrm{Ei}\left(-\frac{\vartheta^2}{\vartheta_0^2}\right) \frac{1}{p_0}\, dp'\, d\vartheta. \tag{25}$$

It is important to emphasize that in accord with (25) the cross section for the neutron scattering accompanied by dissociation of the molecule does not depend on the detailed form of the molecular potential, but only on the frequency of vibration of the nuclei in the molecule, ω. Moreover, inasmuch as for $\vartheta > \vartheta_0$, $\mathrm{Ei}(-\rho^2)$ is proportional to $\exp(-\vartheta^2/\vartheta_0^2)$, then one can show that all the scattered neutrons with final momentum p′ are contained in the small range of angles

$$\vartheta \sim \vartheta_0 = \sqrt{2}\, p_0/p_1, \qquad p_0 = \sqrt{m\hbar\omega}.$$

The angle ϑ_0 is in order of magnitude the difference of the scattering angles of the neutron by a free proton initially at rest and by a free proton possessing a momentum p_0 before the collision. This means that the dissociation process of the molecules by the neutrons can be described in general terms by means of a very simple model, in which the chemically associated nuclei are considered as free but possessing the same scatter of momenta as nuclei in the molecule.*

We now note that for scattering of the neutron not by a proton but by a heavy nucleus, $\nu \gg 1$, i.e., in accord with (24), $\cos\theta_0 \sim -\nu D/E$ and, consequently, the region of the maximum of the angular distribution $\theta \sim \theta_0$ in this case, with neutron energies on the order of the dissociation energy D, is generally not achieved. Therefore the dissociation total cross section, which corresponds to collision with this nucleus, should be exponentially small.

---

*As can be shown, as $\rho \to 0$, $\ln(\gamma/\rho^2)$ must be replaced by a finite quantity of the order of $\ln(ak')$.

*This model of the dissociation process, which is undoubtedly valid even in the case of the collision of a neutron with a polyatomic molecule, was pointed out to us by V. I. Gol'danskiĭ.

In conclusion, attention should be called to the fact that all the results obtained here, which are introduced under the assumption that K = 0, are valid also for K ≠ 0, if only K is not too large (K ~ 1). Actually, the summation in the series (9) is carried out over a large number of terms corresponding essentially to the largest values of l, but for $l \gg 1$ and K ~ 1, the difference between L and l can be neglected, i.e., $d\sigma_K \approx d\sigma_0$.

4. THE DISSOCIATION CROSS SECTION CLOSE TO THRESHOLD

If the wave number κ is very small, so that $\kappa r_0 < 1$, then the quasiclassical approximation (11) for the function $\chi_{\kappa l}$ is not applicable over the whole region of variation of r. This fact, which holds for energies of the neutron close to the dissociation D, requires special consideration, which will be given below.

For low energies of the scattering molecule $\hbar^2\kappa^2/2\mu_m$, the dissociation cross section should depend essentially on whether the molecule has a discrete level ϵ close to zero. We shall first assume that this level is sufficiently deep that $E - D \ll \epsilon$. In this case, one can investigate the behavior of the functions $\chi_{\kappa l}$ by a method similar to that used in the investigation of slow collisions (see reference 3, Sec. 108), i.e., in the region $r \sim r_0$, (where $\kappa^2 \ll -2\mu_m U/\hbar^2$ and which gives the principal contribution to the integrals $J_{g_{1,2}}$) $\chi_{\kappa l}$ is represented in the form $\chi_{\kappa l} = C_l(\kappa)\,\chi_l$; χ_l is the solution of the equation

$$\frac{d^2\chi_l}{dr^2} - \left(\frac{2\mu_m}{\hbar^2}U + \frac{l(l+1)}{r^2}\right)\chi_l = 0,$$

for which the quasiclassical approximation is valid. The coefficient $C_l(\kappa)$ is chosen under the condition that, for $r \to \infty$, the correct transition is obtained to the asymptote

$$\chi_{\kappa l} \sim \sqrt{2/\pi}\,\sin(\kappa r - \pi l/2 + \delta_l).$$

Thus we find that $C_l \sim \kappa^{l+1}$ (see reference 3, Sec. 108), i.e., in the series (9), only terms can be left corresponding to $l = 0$:

$$d\sigma_{nk} = \sqrt{\frac{\pi}{2}}\,\frac{k'}{k}\,\frac{1}{a}\,(C_{00K0}^{K0})^2\,F_{0K}\,d\varkappa\,do,$$

$$F_{0K} = \overline{A_1^2}\frac{\mu^2}{\mu_1^2}\frac{1}{g_1^2}J_{g_1}^2 + \overline{A_2^2}\frac{\mu^2}{\mu_2^2}\frac{1}{g_2^2}J_{g_2}^2 + (-1)^K\,2\overline{A_1A_2}\,\frac{\mu^2}{\mu_1\mu_2}\,\frac{1}{g_1g_2}\,J_{g_1}J_{g_2}. \tag{26}$$

The coefficient $C_0(\kappa)$ entering into $J_{g_{1,2}}$ is essentially independent of the form of the potential U, in particular, independent of its behavior at infinity.

As shown in Appendix 2, if $U \sim U_0 e^{-\alpha r}$ for $r \to \infty$, then

$$\chi_0 = \frac{\varkappa}{\alpha\cos q}\left(\frac{2\alpha}{\tilde{\varkappa}_0}\right)^{1/2}\sin\left(\int_{r_1}^{r}\tilde{\varkappa}_0\,dr + \frac{\pi}{4}\right), \tag{27}$$

where

$$\tilde{\varkappa}_0^2 = -\frac{2\mu_m U}{\hbar^2}, \qquad q = \int_{r_1}^{\infty}\tilde{\varkappa}_0\,dr, \qquad U(r_1) = 0$$

(it is assumed that U depends on r through the variable αr). Substituting (27) in the integrals $J_{g_{1,2}}$, and finding them as before by the method of steepest descents, we obtain the threshold formula for the dissociation cross section of a heavy hydrogen-bearing molecule in the ground state (n = K = 0), which is valid for $\sqrt{2\mu_m(E-D)}/\hbar\alpha \ll 1$:

$$d\sigma = \frac{1}{\sqrt{2\pi}}\,\sigma_0\,\frac{a}{r_0^2\alpha}\,\frac{\cos^2\tau}{\cos^2 q}\,\frac{k'\varkappa^2}{k^4}\,d\varkappa\,do, \tag{28}$$

where

$$\tau = \int_{r_1}^{r_0}\tilde{\varkappa}_0\,dr - gr_0.$$

The total dissociation cross section corresponding to (28) is given by the formula

$$\sigma = \frac{1}{2}\left(\frac{\pi}{2}\right)^{3/2}\sigma_0\,\frac{a}{\alpha r_0^2}\left(\frac{E-D}{D}\right)^2\frac{\cos^2\tau}{\cos^2 q}. \tag{29}$$

We note that the quadratic dependence of the cross section close to the threshold D on the excess energy E − D is the general property of reactions accompanied by the production of three slow particles the interaction among which bears a short-range character[4] (in our case these are the neutron and the two atoms which are produced upon decay of the molecule).

Equation (29) is clearly found to be inapplicable if q is close to $\pi(n + 1/2)$, with n an integer. But the equality

$$q = \frac{1}{\hbar}\int_{r_1}^{\infty}\sqrt{-2\mu_m U}\,dr = \pi\left(n + \frac{1}{2}\right)$$

is identical with the quasiclassical condition for the existence of a discrete level very close to zero (see reference 3, Sec. 48). Thus the inapplicability of (29) is connected with the fact that in this case (in the decay of the molecule) resonance phenomena take place which arise from the fact that the dissociating molecule decays into a state which, even though it refers to the region of continuous spectra, is quasi-stationary because of its nearness to the level ϵ. We limit ourselves to the study of these phenomena for a special choice of potential

$$U = U_0 \left[\exp\{-2\alpha(r - r_0)\} - 2\exp\{-\alpha(r - r_0)\}\right]$$

(the Morse potential). The function χ_0, having the correct asymptote as $r \to \infty$ and $r \to 0$ can be determined now by the formula

$$\chi_0 = \frac{2\sqrt{2\pi\varkappa}}{[\cos^2(\pi\lambda) + \pi^2\varkappa^2/\alpha^2]^{1/2}\,\alpha(\lambda - 1/2)\,\Gamma(\lambda - 1/2)}\,\xi^{-1/2}\,W_{\lambda,\mu}(\xi),$$

$$\lambda = \sqrt{2\mu_m U_0}/\alpha\hbar, \qquad \mu = i\varkappa/\alpha, \; \xi = 2\lambda\exp\{-\alpha(r - r_0)\}, \tag{30}$$

$W_{\lambda,\mu}$ is the Whittaker function. In the region $r \sim r_0$, (30) is simplified

$$\chi_0 = \varkappa\left[\cos^2(\pi\lambda) + \pi^2\frac{\varkappa^2}{\alpha^2}\right]^{-1/2}\sqrt{\frac{2\alpha}{\tilde{\varkappa}_0}}\sin\left(\int_{r_1}^{r}\tilde{\varkappa}_0\,dr + \frac{\pi}{4}\right),$$

$$\pi\lambda = \int_{r_1}^{\infty}\tilde{\varkappa}_0\,dr = q. \tag{31}$$

For $\cos(\pi\lambda) \gg \pi\kappa/\alpha$, (31) is identical with (29). In accord with (31), the dissociation cross section corresponding to the same assumptions as in the derivation of (29) has the form

$$d\sigma = \frac{1}{\sqrt{2\pi}}\sigma_0\frac{a}{r_0^2\alpha}\frac{\cos^2\tau}{\cos^2 q + \pi^2\varkappa^2/\alpha^2}\frac{k'\varkappa^2}{k^4}d\varkappa do. \tag{32}$$

If $\cos q = 0$ (such an assumption corresponds, as is easy to see, to the condition $E - D \gg \epsilon$), then in accord with (32) the total cross section is

$$\sigma = \frac{1}{\sqrt{2\pi}}\sigma_0\frac{a\alpha}{r_0^2 k_m^2}\frac{E - D}{D}\cos^2\tau, \qquad k_m^2 = \frac{2\mu_m D}{\hbar^2}. \tag{33}$$

Thus in this case the cross section increases linearly with the energy of the neutron E. As was pointed out to us by A. I. Baz', such a growth of the threshold cross section with energy is a general law for processes in which two slow particles arise in the collision of two particles, one of which slow particles (in our case the dissociating molecule) is in a quasi-stationary state.

We take this opportunity to thank V. I. Gol'danskii who suggested the theme of this research, and also A. I. Baz', A. S. Kompaneets, and F. L. Shapiro for discussion of the results and a number of useful hints.

APPENDIX 1

Integrating in (7) over the coordinate of the neutron r_n, we have

$$W_{M_K} = A_1\frac{\mu}{\mu_1}J_1 + A_2\frac{\mu}{\mu_2}J_2,$$

$$J_{1,2} = \int\exp\{\pm i\mathbf{g}_{1,2}\mathbf{r}\}\,\psi_0\psi_{\varkappa}^{-*}\,d\mathbf{r}, \qquad \mathbf{g}_{1,2} = \frac{m_{2,1}}{m_1 + m_2}(\mathbf{k} - \mathbf{k}'). \tag{1a}$$

We choose the z axis so that its direction in the set of coordinates which we have used for the neutron-molecule coincides with the fixed direction of the vector $\mathbf{g}$, i.e., $\mathbf{g}_1$ or $\mathbf{g}_2$. The direction $\mathbf{r}$ in the set of coordinates specialized in this fashion is defined by the angles θ, φ and the direction κ by the angles γ, 0. The angle between κ and $\mathbf{r}$ is denoted by θ'. The elements of volume in $\mathbf{r}$ and κ space will be, respectively,

$$d\mathbf{r} = r^2\,dr\sin\theta d\theta\,d\varphi, \qquad d\boldsymbol{\varkappa} = \varkappa^2\,d\varkappa\,do_{\varkappa}.$$

The Legendre polynomials entering into (3), $P_l(\cos\theta')$, can be transformed by means of the well-known theorem for the superposition of spherical functions (see reference 3, Sec. 113).

In the calculation of the integrals $J_{1,2}$, one can use the fact that in the products $P_l^*(\cos\theta') \times Y_{KM_K}(\theta, \varphi)$ only those terms make a non-vanishing contribution which contain the product $Y_{lM_K}^*(\theta, \varphi)\,Y_{KM_K}(\theta, \varphi)$, which with the aid of well-known formulas of the vector superposition of moments (see reference 2, p. 614) can be written in the form

$$Y_{lM_K}^* Y_{KM_K} = (-1)^{M_K}\sum_{L=-(l-K)}^{l+K}\left[\frac{(2l+1)(2K+1)}{4\pi(2L+1)}\right]^{1/2} \times C_{l0K0}^{L0}C_{l-M_K\,KM_K}^{L0}Y_{L0}(\theta), \tag{2a}$$

C_{l0K0}^{L0}, $C_{l-M_K K0}^{L0}$ are Clebsch-Gordan coefficients. Substituting (2a) in J_1, and making use of the well-known formula

$$\int_0^{\pi}P_L(\theta)\exp\{ig_1 r\cos\theta\}\sin\theta d\theta = \sqrt{2\pi}\frac{i^L}{g_1 r}\psi_{L+1/2}(g_1 r),$$

we get

$$J_1 = \left(\frac{2K+1}{2}\right)^{1/2}\frac{1}{2\varkappa g}\sum_l(2l+1)\,e^{i\delta_l}(-i)^l\left[\frac{(l-M_K)!}{(l+M_K)!}\right]^{1/2} \times P_l^{M_K}(\cos\gamma)\sum_{L=|l-K|}^{l+K}C_{l0K0}^{L0}C_{l-M_K\,KM_K}^{L0}\,i^L J_{g_1}, \tag{3a}$$

where

$$J_{g_1} = \int_0^{\infty}\frac{1}{r}e^{-\xi^2}H_n(\xi)\,\chi_{\varkappa l}(r)\,\psi_{L+1/2}(gr)\,dr.$$

The integral J_{g_2}, which is transformed in similar fashion, differs from J_{g_1} only in that the sum in it

$$\sum C_{l0K0}^{L0}C_{l-M_K\,KM_K}^{L0}\,i^L J_{g_1}$$

is replaced by

$$\sum C_{l0K0}^{L0}C_{l-M_K KM'_K}^{L0}\,i^{-L}J_{g_2}.$$

Making use in Eq. (6) of the expression (3a) for J_{g_1} which is similar to the expression for J_{g_2}, and the well-known property of the orthogonality of the Clebsch-Gordan coefficients, we get Eq. (9) shown in the text.

APPENDIX 2

To find the correct form of the function χ_0, which is determined by the equation

$$d^2\chi_0/dx^2 + f(x)\chi_0 = 0, \quad f(x) = -2\mu_m U/\hbar^2, \quad x = \alpha r$$

in the region $r \sim r_0$, we make use of the method of standard equations.[5] Let $f(x) \to de^{-x}$ as $x \to \infty$. We choose as a standard equation

$$d^2\varphi/ds^2 + de^{-s}\varphi = 0,$$

i.e.,

$$\varphi = Z_0(\eta), \quad \eta = 2d^{1/2}e^{-s/2}.$$

According to the general formula we have

$$\chi_0 = (de^{-s}/f(x))^{1/4} Z_0(\eta),$$

where the variable s is connected with x by the expression

$$\eta = \int_s^\infty d^{1/2}e^{-s/2}\,ds = 2d^{1/2}e^{-s/2} = \int_x^\infty f^{1/2}\,dx,$$

i.e., $s \to x$ as $x \to \infty$. If $Z_0(\eta)$ is chosen in the form

$$Z_0(\eta) = C\,[e^{-i\eta_0}H_0^{(1)}(\eta) - ie^{i\eta_0}H_0^{(2)}(\eta)],$$

$$\eta_0 = \int_{x_1}^\infty f^{1/2}\,dx, \qquad f(x_1) = 0$$

and we use the asymptote $H_0^{(1),(2)} \sim \sqrt{2/\pi\eta} \times \exp\{\pm i(\eta - \pi/4)\}$, then in the region where $\eta \gg 1$, χ_0 is reduced to the form

$$\chi_0 = \frac{2i}{\sqrt{\pi}}Cf^{-1/4}\sin\left(\int_{x_1}^x f^{1/2}\,dx + \frac{\pi}{4}\right).$$

On the other hand, $x \to s$ and $\eta \to 0$ as $x \to \infty$, and, by using the asymptote $Y_0(\eta) \to (2/\pi)\ln(2/\eta)$, we get $\chi_0 \approx \pi^{-1}C\,2xi\cos\eta_0$. In order that this asymptote go over into $\chi_0 \sim \sqrt{2/\pi}\,\sin(\kappa r + \delta_0)$ for $\kappa r < 1$, it is necessary to choose C by the formula

$$C = \sqrt{\pi/2}\,i\varkappa/\alpha\cos\eta_0,$$

which also gives in the region $r \sim r_0$

$$\chi_0 = \frac{2^{1/2}\varkappa}{\alpha\cos\eta_0}f^{-1/4}\sin\left(\int_{x_1}^x f^{1/2}\,dx + \frac{\pi}{4}\right).$$

---

[1] V. I. Gol'danskii, JETP 31, 717 (1956), Soviet Phys. JETP 4, 604 (1957).

[2] J. Blatt and V. Weisskopf, Theoretical Nuclear Physics (Russian translation IIL, 1954).

[3] L. D. Landau and E. M. Lifshitz, Квантовая механика (Quantum Mechanics) Gostekhizdat, 1948.

[4] W. H. Guer and R. W. Hart, Phys. Rev. 106, 296 (1956).

[5] S. Miller and R. Good, Phys. Rev. 91, 174 (1953).

Translated by R. T. Beyer
80

SOVIET PHYSICS JETP VOLUME 13, NUMBER 2 AUGUST, 1961

ATTENUATION OF MAGNETOHYDRODYNAMIC AND MAGNETOACOUSTIC WAVES IN A PLASMA WITH ANISOTROPIC CONDUCTIVITY AND VISCOSITY

R. V. DEUTSCH

Moscow State University

Submitted to JETP editor June 28, 1960

J. Exptl. Theoret. Phys. (U.S.S.R.) **40**, 524-526 (February, 1961)

Attenuation of weak magnetohydrodynamic and magnetoacoustic waves in an anisotropic plasma located in an external magnetic field is considered for the case where the wave frequency is smaller than the particle collision frequency and the wave length is larger than the mean free path.

A plasma in a magnetic field has anisotropic properties. The electric conductivity, the dielectric constant, the viscosity, etc., of the plasma are represented as tensors of the second rank. We shall consider the attenuation of magnetohydrodynamic and magnetoacoustic waves in an anisotropic plasma. We assume that the wave frequency is smaller than the collision frequency of the particles ($\omega \ll \nu_{\text{eff}}$) and that the mean free path is smaller than the wave length ($l \ll \lambda$).

The conductivity tensor is hermitian. It can be written in the matrix form (the index 3 corresponds to the direction of the vector **H**)[1]

$$(\sigma_{ik}) = \begin{pmatrix} \sigma_1 & i\sigma_2 & 0 \\ -i\sigma_2 & \sigma_1 & 0 \\ 0 & 0 & \sigma_3 \end{pmatrix}. \tag{1}$$

According to the elementary theory*

$$\sigma_1 = \sum_i \frac{\omega_0^2 \, \nu_{i\,\text{eff}}}{4\pi} \frac{1}{\omega_{Hi}^2 + \nu_{i\,\text{eff}}^2},$$

$$\sigma_2 = \sum_i \frac{\omega_{0i}^2 \, \nu_{i\,\text{eff}}}{2\pi} \frac{\omega\omega_{Hi}}{(\omega_{Hi}^2 + \nu_{i\,\text{eff}}^2)^2}, \qquad \sigma_3 = \sum_i \frac{\omega_{0i}^2}{4\pi\nu_{i\,\text{eff}}}, \tag{2}$$

where

$$\omega_{0i}^2 = \frac{4\pi e_i^2 N_i}{m_i}, \qquad \omega_{Hi} = \frac{|e_i| H}{m_i c},$$

e_i is the charge, N_i is the concentration, m_i is the mass, and $\nu_{i\,\text{eff}}$ is the effective number of collisions of the particles. The index $i = 1$ refers to the electrons and $i = 2, 3, \ldots,$ to the various ions. We assume, for simplicity, that the plasma consists of ions of a single type and electrons.

The sums in (2) depend on the density and temperature of the plasma and on the strength of the magnetic field. For high temperatures, low density, and strong magnetic fields, the electric conduction by the ions is more important than the electric conduction by the electrons, so that the latter can be neglected. In the opposite case, the electric conduction by the ions can be neglected in comparison with the electric conduction by the electrons. Comparing the various terms in (2), we see that the electric conduction by the ions must be included if $\omega_{H_1} \gtrsim \nu_{2\,\text{eff}}$. It follows that the electric conduction by the ions in a two-component plasma becomes important when*

$$H \gtrsim 10^{-7}\, nT^{-3/2}, \tag{3}$$

where $n = N_2$ is the number of ions in 1 cm^3, T is the temperature in °K, and H is measured in oersteds. If $\omega_{H_1} \gg \nu_{2\,\text{eff}}$, we can neglect the electric conduction by the electrons.

The equations of motion of the plasma also contain the viscosity tensor Π. This tensor is symmetric. Its components are given in the monograph of Chapman and Cowling[3] and also (with more exact values of the coefficients) in the paper of Braginskii.[4]

We must start with the system of equations of motion of the plasma in the electromagnetic field containing both of the aforementioned tensors. According to the preceding discussion, the basic system of equations is

---

*Gurevich[2] has given expressions for the tensor σ_{ik} (with only the electrons taken into account) derived from kinetic theory. He showed that, for $\omega \ll \nu_{\text{eff}}$, the expressions obtained from the kinetic theory differ relatively little from the corresponding expressions derived with the help of the elementary theory. Owing to the symmetry of the equations (2) with respect to the characteristics of the ions and electrons, one can assume that this remains true also in the case when only the electric conduction of the ions (with $\omega \ll \nu_{\text{eff}}$) is taken into account. We are therefore justified in using formula (2).

*In deriving this relation we have assumed that ν_{eff} is determined by the collisions of the electrons with the ions.

$$\frac{\partial \mathbf{H}}{\partial t} = \operatorname{rot}[\mathbf{vH}] - \frac{c^2}{4\pi}\operatorname{rot}\mathbf{G},$$

$$\rho\left[\frac{\partial \mathbf{v}}{\partial t} + (\mathbf{v}\nabla)\mathbf{v}\right] = \frac{-1}{4\pi}[\mathbf{H}\operatorname{rot}\mathbf{H}] - \operatorname{div}\mathbf{\Pi},$$

$$\operatorname{div}\mathbf{H} = 0, \qquad \frac{\partial \rho}{\partial t} + \operatorname{div}(\rho\mathbf{v}) = 0, \qquad \delta p = u_0^2\delta p, \qquad (4)^{*}$$

where

$$G_i = \alpha_{ik}[\operatorname{rot}\mathbf{H}]_k, \qquad \alpha_{11} = \alpha_{22} = \sigma_1/(\sigma_1^2 - \sigma_2^2) = \alpha_1,$$

$$\alpha_{33} = 1/\sigma_3 = \alpha_3, \qquad \alpha_{12} = -\alpha_{21} = i\sigma_2/(\sigma_1^2 - \sigma_2^2) = -\alpha_2,$$

$\alpha_{13} = \alpha_{31} \sim \alpha_{23} \sim \alpha_{32} = 0$, and $u_0^2 = (\partial p/\partial\rho)_S$ is the square of the ordinary velocity of sound.

In order to determine the attenuation of waves, we consider the wave solutions of the linearized system (4), as is usually done in isotropic magnetohydrodynamics.[5] The dissipative terms are retained only up to first order. This corresponds to comparatively weak attenuation ($\gamma \ll \omega$).

As a result we find that the anisotropy has no effect on the velocity of propagation of the waves, i.e., we find the same expressions for the velocities of the Alfvén and magnetoacoustic waves as in the isotropic case.

The attenuation coefficient for Alfvén waves is in first approximation[†]

$$\gamma = \left\{\frac{c^2}{8\pi}(\alpha_1\cos^2\beta + \alpha_3\sin^2\beta) + \frac{\mu}{1{,}92\,\rho}[b'(2\omega_{H_2})\sin^2\beta + b'(\omega_{H_2})\cos^2\beta]\right\}\frac{\omega^2}{u^2}, \qquad (5)$$

where μ is the viscosity coefficient in the absence of a magnetic field; β is the angle between **H** and the wave vector **k**, and u is the phase velocity of the wave. The expressions for the coefficients $b'(\omega_{H_2})$ and $b'(2\omega_{H_2})$ are given by Braginskii.[4]

The first term in (5) is related to the electric conductivity and the second term to the viscosity. Comparing these two terms, we find that the second term can be neglected for $T^4n^{-1} < 10^4$. In the opposite case, the second term can have a larger value only for comparatively weak fields. In the limit of very strong fields (considering the fact that the electric conduction by the ions plays the essential role) we can therefore write for γ

$$\lim_{H\to\infty}\gamma = \frac{\omega^2}{2\nu_{2\,\mathrm{eff}}} = C. \qquad (6)$$

It is seen from (5) and (6) that the attenuation of the Alfvén waves becomes weaker as the strength of the magnetic field increases, and approaches a limiting value which depends only on the wave frequency and on the effective collision frequency of the particles, but not on H. In this limiting case, the attentuation is independent of β; for finite H the dependence of γ on β can be easily obtained from (5).

For the magnetoacoustic waves we find from (4)

$$\gamma = \Bigl(\frac{c^2}{8\pi}(u^2 - u_0^2) + \frac{\mu}{1.92\rho}\Bigl\{[b'(\omega_{H2})\sin^2\beta + 1.28\cos^2\beta] \times [u^2 - u_0^2\sin^2\beta - u_H^2] + [0.32\sin^2\beta + b'(2\omega_{H2})\sin^2\beta + b'(\omega_{H2})\cos^2\beta][u^2 - u_0^2\cos^2\beta] + 2[b'(\omega_{H_2}) - 0.64]u_0^2\sin^2\beta\cos^2\beta\Bigr\}\Bigr)\frac{\omega^2}{u^2}(2u^2 - u_0^2 - u_H^2)^{-1}, \qquad (7)$$

where

$$u_H = H/\sqrt{4\pi\rho}.$$

Here we must include the effect of the viscosity both for $T^4n^{-1} < 10^4$ for accelerated waves in weak fields ($H < \sqrt{4\pi\rho}\,u_0$) and for decelerated waves in strong fields ($H > \sqrt{4\pi\rho}\,u_0$). This is due to the fact that near $\beta = 0$, $u \sim u_0$ in both these cases, so that the first term in (7) reduces to zero. This interval near $\beta = 0$ becomes wider for decelerated waves as the strength of the magnetic field increases (in the limit $H \to \infty$ it approaches the interval $-45° < \beta < 45°$). Thus the viscosity is an important effect for decelerated waves, at least for $H > \sqrt{4\pi\rho}\,u_0$. In the limit of strong fields we have

$$\lim_{H\to\infty}\gamma = C\,\mathrm{tg}^2\beta + C_1, \qquad C_1 = \frac{2}{3}\frac{\mu}{\rho}\frac{\omega^2}{u_0^2}. \qquad (8)^{*}$$

An accelerated magnetoacoustic wave becomes similar to an Alfvén wave as the strength of the magnetic field increases, and γ approaches the same limit (6). If $T^4n^{-1} \gtrsim 10^4$, the second term of formula (7) here becomes important even for $H \gtrsim \sqrt{4\pi\rho}\,u_0$ (notwithstanding the fact that the second term decreases as the magnetic field is increased).

In conclusion the author expresses his gratitude to V. P. Silin for his guidance in this work and for numerous comments and advice.

[1] Al'pert, Ginzburg, and Feinberg, Распространение радиоволн (Propagation of Radio Waves), Gostekhizdat, p. 326 (1953).

[2] A. V. Gurevich, JETP **30**, 1112 (1956), Soviet Phys. JETP **3**, 895 (1956).

[3] S. Chapman and T. G. Cowling, The Mathematical Theory of Non-Uniform Gases, Cambridge (1939).

[4] S. I. Braginskii, JETP **33**, 459 (1957), Soviet Phys. JETP **6**, 358 (1958).

[5] L. D. Landau and E. M. Lifshitz, Электродинамика сплошных сред (Electrodynamics of Continuous Media), Fizmatgiz (1959).

Translated by R. Lipperheide
81

---

[*] rot = curl, $[\mathbf{vH}] = \mathbf{v} \times \mathbf{H}$, tg = tan.

[†] In deriving expressions (5) and (7), we have assumed that the ions, and not the electrons, play the essential role in the viscosity tensor.

SOVIET PHYSICS JETP VOLUME 13, NUMBER 2 AUGUST, 1961

INSTABILITY OF LOW-FREQUENCY ELECTROMAGNETIC WAVES IN A PLASMA TRAVERSED BY A BEAM OF CHARGED PARTICLES

M. S. KOVNER

Gorkiĭ State University

Submitted to JETP editor July 5, 1960

J. Exptl. Theoret. Phys. (U.S.S.R.) 40, 527-536 (February, 1961)

The stability of low-frequency longitudinal waves and transverse waves in a magnetoactive plasma traversed by a beam of charged particles is considered. The plasma and beam are both assumed to be uniform and infinite. We consider plane-wave perturbations that propagate in the direction of the fixed external magnetic field. Stability criteria for the system are derived and the gain factors are found for a number of cases.

THE interaction of a beam of charged particles with a plasma has been considered by many authors (cf. references 1—13 etc.). In most of the work which has been published, consideration has been given to instabilities with respect to high-frequency perturbations, that is to say, waves in which the effect of the ion motion on the distribution can be neglected. It is also of interest to consider the stability of such systems with respect to low-frequency waves, i.e., waves characterized by frequencies which are much lower than the electron gyromagnetic frequency and which are comparable to, or even appreciably smaller than, the ion gyromagnetic frequency or ion plasma frequency.

It is well known that low-frequency longitudinal waves and transverse waves can propagate in the direction of the fixed external magnetic field $\mathbf{H}_0$. The stability of low-frequency magnetohydrodynamic waves in the presence of a quasi-neutral particle flux, with thermal motion neglected, has been considered by Dokuchaev.[14] The magnetic field has no effect on the propagation of longitudinal waves. The stability of low-frequency longitudinal waves in a non-equilibrium plasma has also been considered by a number of authors.[5,12]

In the present work we present a kinetic analysis of the stability of a plasma traversed by a beam of charged particles with respect to low-frequency transverse perturbations. In addition, we describe briefly certain aspects of the stability of longitudinal waves which have not been considered in references 5 and 12. The plasma and beam are both assumed to be uniform, infinite, and singly ionized. The particle beam moves along the fixed external magnetic field $\mathbf{H}_0$. Perturbations in the form of plane waves are assumed to propagate along the magnetic field $\mathbf{H}_0$.

In Sec. 1 we present the general dispersion equations which describe the propagation of transverse waves and longitudinal waves. In Sec. 2 we consider instabilities against transverse perturbations when the thermal motion of the particles in both the beam and plasma can be neglected. The effect of thermal motion on wave propagation is considered in Sec. 3. Finally, in Sec. 4 we consider longitudinal-wave propagation.

1. DISPERSION EQUATIONS

We start with a system consisting of the linearized kinetic equations for the plasma and the charged-particle beam and the electrodynamic equations (with self-consistent fields). Expanding all physical quantities F in plane waves and carrying out the calculations as in references 15—17 (cf. also reference 8), we obtain the following dispersion equations for the longitudinal and transverse waves:[18]

$$\frac{1}{\sqrt{2\pi}}\sum_{\gamma=1}^{4}\frac{\omega_{0\gamma}^2}{\omega v_{T\gamma}^3}\int\frac{u\,(u-v_\gamma)\exp\left[-\frac{1}{2}\left(\frac{u-v_{0\gamma}}{v_{T\gamma}}\right)^2\right]}{\omega-ku+i\nu_\gamma}\,du-1=0, \tag{1.1}$$

$$\frac{1}{\sqrt{2\pi}}\sum_{\gamma=1}^{4}\frac{\omega_{0\gamma}^2(\omega-kv_{0\gamma})}{v_{T\gamma}}\int\frac{\exp\left[-\frac{1}{2}\left(\frac{u-v_{0\gamma}}{v_{T\gamma}}\right)^2\right]}{\omega-ku\pm\omega_{H\gamma}+i\nu_\gamma}\,du$$
$$=c^2k^2-\omega^2. \tag{1.2}$$

In Eqs. (1.1) and (1.2), physical quantities denoted by the subscripts $\gamma = 1, 2, 3, 4$ refer to the plasma ions, the plasma electrons, the beam ions, and the beam electrons in that order. Further,

$$\omega_{H1}=\omega_{H3}\equiv-\Omega_H=-eH_0/Mc,$$

where e and M are the charge and mass of the ion;

$$\omega_{H2} = \omega_{H4} \equiv \omega_H = eH_0/mc,$$

where e and m are the charge and mass of the electron; $v_{0\gamma}$ is the mean velocity for a given kind of particle in the laboratory coordinate system; N_γ, v_γ, T_γ are the concentration, the effective number of collisions, and the temperature of the corresponding particle, where the temperature is written in energy units. In writing Eqs. (1.1) and (1.2) we have assumed that the equilibrium distribution function is Maxwellian in the coordinate system in which the mean velocity of particles of a given kind is zero; ω is the frequency and **k** is the wave vector for the perturbation. In Eqs. (1.1) and (1.2) we have also used the conventional notation:

$$\omega_{0\gamma}^2 = 4\pi N_\gamma e^2/m_\gamma, \qquad v_{T\gamma}^2 = T_\gamma/m_\gamma.$$

Neglecting collisions and using the Fock transformations,[4,19,20] we can write the dispersion equations which have been obtained in the following form: longitudinal waves

$$1 + \sum_{\gamma=1}^{4} \frac{\omega_{0\gamma}^2}{k^2 v_{T\gamma}^2} \left[1 - \frac{\omega - kv_{0\gamma}}{kv_{T\gamma}} B(\beta_\gamma) \right] = 0, \tag{1.3}$$

transverse waves

$$1 + \sum_{\gamma=1}^{4} \frac{\omega_{0\gamma}^2 (\omega - kv_{0\gamma})}{(c^2k^2 - \omega^2)\, kv_{T\gamma}} B(\beta_\gamma) = 0, \tag{1.4}$$

where

$$B(\beta_\gamma) = e^{-\beta_\gamma^2/2} \int_{i\infty}^{\beta_\gamma} e^{x^2/2}\, dx, \qquad \beta_\gamma = \frac{\omega - kv_{0\gamma} \mp \omega_{H\gamma}}{kv_{T\gamma}}. \tag{1.5}$$

In the limiting cases[4]

$$B(\beta_\gamma) \approx -i\sqrt{\pi/2}\; e^{-\beta_\gamma^2/2} + \beta_\gamma - \frac{1}{3}\beta_\gamma^3 + \ldots \quad (|\beta_\gamma| \ll 1),$$

$$B(\beta_\gamma) \approx -i\sqrt{\pi/2}\, e^{-\beta_\gamma^2/2} + \beta_\gamma^{-1} + \beta_\gamma^{-3} + \ldots \quad (|\beta_\gamma| \gg 1). \tag{1.6}$$

2. INVESTIGATION OF TRANSVERSE-WAVE INSTABILITY FOR $|\beta_\gamma| \gg 1$

1. Following the usual approach, we analyze stability in the following manner. We assume that the wave vector **k** is real. Then, if in solving the dispersion equation we find that the frequency ω is complex, the wave must be a growing (damped) wave. If we write ω in the form

$$\omega = \omega_1 + i\mu, \tag{2.1}$$

where ω_1 and μ are real, since a plane wave is proportional to $\exp(-i\omega t + i\mathbf{k}\cdot\mathbf{r})$, an instability arises when $\mu > 0$.

Using Eq. (1.4) and the asymptotic expansion (1.6) for $|\beta_\gamma| \gg 1$ (this condition means that the effect of thermal motion of the particles on wave propagation can be neglected), we obtain the dispersion equation

$$\frac{\omega_{01}^2 \omega}{\omega \pm \Omega_H} + \frac{\omega_{02}^2 (\omega - kv_{02})}{\omega \mp \omega_H - kv_{02}} + \frac{\omega_{03}^2 (\omega - kv_{03})}{\omega \pm \Omega_H - kv_{03}} + \frac{\omega_{04}^2 (\omega - kv_{04})}{\omega \mp \omega_H - kv_{04}} = \omega^2 - c^2k^2. \tag{2.2}$$

In writing Eq. (2.2) we have taken the mean velocity of the ions in the main plasma to be zero, $v_{01} = 0$; this can always be done by making a simple transformation of coordinates. Eq. (2.2) will be the subject of investigation of this section.

2. Suppose that an ion beam moves through a fixed plasma. We assume that the system as a whole is quasi-neutral:

$$N_2 = N_1 + N_3. \tag{2.3}$$

Under these conditions an uncompensated electric current is produced in the plasma; in general, it is necessary to take account of the azimuthal magnetic field H_φ produced by this current, in which case the plasma is not uniform. However, the condition that the total current must vanish can be satisfied if there is an electron current in the plasma, i.e.,

$$-eN_2 v_{02} = eN_3 v_{03}. \tag{2.4}$$

When $N_3 \ll N_2$ the velocity of these electrons is obviously small compared with v_{03}. Then, assuming that there is no electron flow and that $N_4 = 0$, the dispersion equation (2.2) for the ordinary wave, given by the upper sign in Eq. (2.2), can be written in the form

$$(\omega + \Omega_H - kv_{03}) \left[\frac{\omega_{01}^2 \omega}{\omega + \Omega_H} + \frac{\omega_{02}^2 (\omega - kv_{02})}{\omega - \omega_H - kv_{02}} + c^2k^2 - \omega^2 \right] = -\omega_{03}^2 (\omega - kv_{03}). \tag{2.5}$$

Because $N_3 \ll N_2$, in the solution of Eq. (2.5) we can neglect the term containing ω_{03}^2 in the zeroth approximation. Then Eq. (2.5) is satisfied either for

$$\omega^{(0)} + \Omega_H - kv_{03} = 0, \tag{2.6}$$

or

$$\frac{\omega_{01}^2 \omega^{(0)}}{\omega^{(0)} + \Omega_H} + \frac{\omega_{02}^2 (\omega^{(0)} - kv_{02})}{\omega^{(0)} - \omega_H - kv_{02}} + c^2k^2 - \omega^{(0)2} = 0 \tag{2.7}$$

(the superscript "0" indicates the order of the approximation). It is easily seen from Eqs. (2.5)—(2.7) that in the next approximation an instability arises only if (2.6) and (2.7) are both satisfied.

We also show that the following inequalities hold:

$$\omega^{(1)} + \Omega_H - kv_{03} = \varepsilon \ll \omega, \qquad |\omega| \ll \omega_H, \tag{2.8}$$

where $\epsilon = \omega^{(1)} - \omega^{(0)}$ is the frequency correction in the first approximation. The first inequality in (2.8) means that we are interested in an instability associated with magnetic bremsstrahlung (cyclotron radiation) of ions in the frequency region corresponding to the anomalous Doppler effect. Then, expanding the left-hand side of Eq. (2.5) in a series about the frequency $\omega = kv_0 - \Omega_H$ and limiting ourselves to the first nonvanishing term, $\mu = -i\epsilon$, we obtain the following expression for the growth (attenuation) factor

$$\mu = \pm[N_3\Omega_H^2(\omega^{(0)} + \Omega_H)^2/N_2\omega^{(0)}(\omega^{(0)} + 2\Omega_H)]^{1/2}, \quad (2.9)$$

according to which $\mu \sim (N_3/N_2)^{1/2}$. It is apparent from Eq. (2.9) that the inequality in (2.8) is satisfied if

$$N_3 \ll N_2\omega^3(\omega + 2\Omega_H)/\Omega_H^2(\omega + \Omega_H)^2. \quad (2.10)$$

For the extraordinary wave, which corresponds to the lower sign in Eq. (2.2), there is no instability in the region of the normal Doppler effect.

If we assume that the following conditions are satisfied rather than the inequality in (2.8):

$$\omega - kv_{03} \ll \Omega_H, \quad \omega \ll \Omega_H, \quad \omega_{01}^2/\Omega_H^2 \gg 1, \quad (2.11)$$

then, from Eq. (2.2) we obtain the dispersion equation

$$\omega_{01}^2\omega^2/\Omega_H^2 + \omega_{03}^2(\omega - kv_{03})^2/\Omega^2{}_H - c^2k^2 = 0, \quad (2.12)$$

and an instability arises when

$$v_{03} > H_0/\sqrt{4\pi MN_{\mathrm{eff}}}, \quad N_{\mathrm{eff}} = \sqrt{N_1N_3/(N_1+N_3)}. \quad (2.13)$$

3. We consider the case in which there is a weak electron current in the plasma $N_2 \gg N_4$ and $N_3 = 0$. We also assume that the system as a whole is quasi-neutral:

$$N_1 = N_2 + N_4, \quad (2.14)$$

and that the total current in the system vanishes:

$$eN_2v_{04} = eN_4v_{04}. \quad (2.15)$$

Assuming further that $\omega \ll \omega_H$, from Eq. (2.2) we have

$$\frac{\omega_{01}^2\,\omega}{\omega \pm \Omega_H} + \frac{\omega_{02}^2(\omega + kv_{02})}{\omega \mp \omega_H - kv_{02}} + \frac{\omega_{04}^2(\omega - kv_{04})}{\omega \mp \omega_H - kv_{04}} = \omega^2 - c^2k^2. \quad (2.16)$$

Then, proceeding as before, we find that it is possible to have a growing extraordinary wave [lower sign in Eq. (2.16)] associated with the coherent magnetic bremsstrahlung of the electron current. The wave increment (decrement) is

$$\mu = \pm[N_4\omega_H^2(\omega - \Omega_H)^2/N_2\omega(2\Omega_H - \omega)]^{1/2}, \quad (2.17)$$

where $-i\mu = \omega^{(1)} + \omega_H - kv_{04} \ll \omega$. It is clear from Eq. (2.17) that an instability arises when $\omega < 2\Omega_H$. On the other hand, an investigation of the dispersion equation in the zeroth approximation shows that the extraordinary wave can propagate only when $\omega < \Omega_H$ because the square of the refractive index is negative when $\omega > \Omega_H$.

When there is an electron current in the plasma an instability does not arise if $\omega < \Omega_H$ and $|\omega_H - k_{04}| \ll \Omega_H$.

4. If a quasi-neutral beam of charged particles passes through a quasi-neutral plasma, i.e.

$$N_1 = N_2 \equiv N, \quad N_3 = N_4 \equiv N_s,$$
$$v_{01} = v_{02} = 0, \quad v_{03} = v_{04} = v_0, \quad (2.18)$$

then, when

$$\omega \ll \Omega_H, \quad |\omega - kv_0| \ll \Omega_H \quad (2.19)$$

the dispersion equation coincides with Eq. (2.12). This equation has been obtained by Dokuchaev,[14] who has shown that an instability arises if the conditions in (2.13) are satisfied.

From Eq. (2.12), in addition to obtaining the instability conditions in (2.13), we find that an instability can arise at very high beam densities

$$N_s > Nv_{1A}^2/(v_0^2 - v_{1A}^2), \quad (2.20)$$

(where $v_{1A}^2 = c^2\omega_{02}^2/\Omega_H\omega_H$). For nonrelativistic beams ($v_0^2 \ll c^2$) the lower density limit is given by the inequality

$$N_s \gg Nv_{1A}^2/c^2.$$

If, however, we assume that the following inequalities are satisfied rather than (2.19):

$$|\omega| \ll \omega_H, \quad |\omega - kv_0 + \Omega_H| \ll \omega$$

or

$$|\omega| \ll \omega_H, \quad |\omega - kv_0 + \omega_H| \ll \omega,$$

that is, if we investigate the instability associated with coherent magnetic bremsstrahlung due to ions or electrons in the beam, from Eq. (2.2) it follows that the wave grows for arbitrarily small beam densities and that the growth (attenuation) factors are given by expressions coinciding with (2.9) and (2.17).

3. EFFECT OF THERMAL MOTION ON THE GROWTH OF TRANSVERSE WAVES

1. In the present section we consider the stability of a system consisting of a quasi-neutral plasma which is traversed by an infinite quasi-neutral beam of charged particles. We assume that the distribution functions are isotropic in the corresponding coordinate systems. The growth (attenuation) of the waves is determined basically by

the effect of thermal motion of the particles. In accordance with the considerations given above, in Eq. (1.4) we write

$$v_{01} = v_{02} = 0, \qquad v_{03} = v_{04} \equiv v_0,$$
$$N_1 = N_2 \equiv N, \qquad N_3 = N_4 \equiv N_s, \tag{3.1}$$

and this equation assumes the form

$$\frac{\omega}{k}\left[\frac{\omega_{01}^2}{v_{T1}} B(\beta_1) + \frac{\omega_{02}^2}{v_{T2}} B(\beta_2)\right] + \frac{(\omega - kv_0)}{k}\left[\frac{\omega_{03}^2}{v_{T3}} B(\beta_3) + \frac{\omega_{04}^2}{v_{T4}} B(\beta_4)\right] + c^2k^2 - \omega^2 = 0. \tag{3.2}$$

An investigation shows that in the case being considered wave amplification is possible only in the frequency region corresponding to the anomalous Doppler effect.

Because a general analysis of Eq. (3.2) is extremely difficult, we shall limit ourselves to two particular cases.

2. We consider the region in which the following inequality is satisfied:

$$|\omega + \Omega_H| \gg kv_{T1}. \tag{3.3}$$

We assume that the following conditions are also satisfied:

$$|\omega - \omega_H| \gg kv_{T2},\ kv_{T4}, \qquad |\omega - \omega_H - kv_0| \gg kv_{T4},$$
$$\omega \ll \omega_H, \qquad |\omega + \Omega_H - kv_0| \ll kv_{T3}. \tag{3.4}$$

The last inequality means that the phase velocity of the waves is of the order of the maximum velocity for the particle distribution function in the beam, shifted by an amount Ω_H/k; we shall be interested in the magnetic bremsstrahlung of beam ions outside the "light cone." Using the asymptotic expansions (1.6) we have

$$-\frac{\omega_{02}^2\omega^2}{\omega_H(\omega + \Omega_H)} + \omega_{03}^2(\omega - kv_0)\left[\frac{\omega - kv_0 + \Omega_H}{(kv_{T3})^2} - \frac{1}{\Omega_H}\right] + c^2k^2 - \omega^2 = i\sqrt{\frac{\pi}{2}}\left\{\frac{\omega_{01}^2\omega}{kv_{T1}}\left[\exp\left\{-\frac{1}{2}\left(\frac{\omega + \Omega_H}{kv_{T1}}\right)^2\right\} + \sqrt{\frac{T_1M}{T_2m}}\exp\left\{-\frac{1}{2}\left(\frac{\omega - \omega_H}{kv_{T2}}\right)^2\right\}\right] + \frac{\omega_{03}^2(\omega - kv_0)}{kv_{T3}}\left[1 + \sqrt{\frac{T_3M}{T_4m}}\exp\left\{-\frac{1}{2}\left(\frac{\omega - \omega_H - kv_0}{kv_{T4}}\right)^2\right\}\right]\right\}. \tag{3.5}$$

Eq. (3.5) can be simplified if the following inequalities hold:

$$\sqrt{\frac{T_3M}{T_4m}}\left|\exp\left\{-\frac{1}{2}\left(\frac{\omega - \omega_H - kv_0}{kv_{T4}}\right)^2\right\}\right| \ll 1,$$
$$\frac{\omega_{03}^2|\omega - kv_0|}{v_{T3}} \gg \frac{\omega_{01}^2}{v_{T1}}\left|\omega\left\{\exp\left[-\frac{1}{2}\left(\frac{\omega + \Omega_H}{kv_{T1}}\right)^2\right] + \sqrt{\frac{T_1M}{T_2m}}\exp\left[-\frac{1}{2}\left(\frac{\omega - \omega_H}{kv_{T_2}}\right)^2\right]\right\}\right|. \tag{3.6}$$

Taking account of the inequalities in (3.6) and separating the real and imaginary parts in Eq. (3.5), we have

$$\frac{\mu}{\omega_1}\left\{\frac{\omega_{02}^2}{\omega_H}\frac{\omega_1^2 + \mu^2 + 2\omega_1\Omega_H}{\mu^2 + (\omega_1 + \Omega_H)^2} + \omega_{03}^2\left[\frac{1}{\Omega_H} - \frac{2\omega_1 - 2kv_0 + \Omega_H}{(kv_{T3})^2}\right]\right\} = -\sqrt{\frac{\pi}{2}}\frac{\omega_{03}^2(\omega_1 - kv_0)}{\omega_1 kv_{T3}}, \tag{3.7}$$

where $\mu = \mathrm{Im}\ \omega$, $\omega_1 = \mathrm{Re}\ \omega$.

Whence it is apparent that amplification obtains $(\mu > 0)$ when

$$\omega_1 - kv_0 < 0. \tag{3.8}$$

In this case, when the growth factor (attenuation) is small, i.e., when

$$|\mu/\omega| \ll 1 \tag{3.9}$$

from Eq. (3.5) we have

$$\frac{\mu}{\omega^{(0)}}\left[\frac{\omega_{02}^2}{\omega_H}\frac{\omega^{(0)2} + 2\omega^{(0)}\Omega_H}{(\omega^{(0)} + \Omega_H)^2} + \frac{\omega_{03}^2\Omega_H}{(kv_{T3})^2}\right] = -\sqrt{\frac{\pi}{2}}\left\{\frac{\omega_{01}^2\omega^{(0)}}{kv_{T1}}\left[\exp\left\{-\frac{1}{2}\left(\frac{\omega^{(0)} + \Omega_H}{kv_{T1}}\right)^2\right\} + \sqrt{\frac{T_1M}{T_2m}}\exp\left\{-\frac{1}{2}\left(\frac{\omega^{(0)} - \omega_H}{kv_{T2}}\right)^2\right\}\right] + \frac{\omega_{03}^2(\omega^{(0)} - kv_0)}{kv_{T3}} \times\left[1 + \sqrt{\frac{T_3M}{T_4m}}\exp\left\{-\frac{1}{2}\left(\frac{\omega^{(0)} - \omega_H - kv_0}{kv_{T4}}\right)^2\right\}\right]\right\}, \tag{3.10}$$

where $\omega^{(0)}$ satisfies Eq. (3.5) with the right-hand side set equal to zero. If the conditions in (3.6) are also satisfied, we obtain the following expression for the growth factor:

$$\mu = \sqrt{\frac{\pi}{2}}\frac{\omega_{03}^2\Omega_H}{kv_{T3}}\left[\frac{\omega_{02}^2}{\omega_H}\frac{\omega^{(0)2} + 2\omega^{(0)}\Omega_H}{(\omega^{(0)} + \Omega_H)^2} + \frac{\omega_{03}^2\Omega_H}{(kv_{T3})^2}\right]^{-1}. \tag{3.11}$$

It can be easily shown from Eq. (3.11) that (3.9) is satisfied if any one of the following inequalities holds:

$$\omega^{(0)} \gg kv_{T3} \tag{3.12}$$

or

$$N_s \ll N\frac{M}{m}\frac{\omega^{(0)}kv_{T3}(\omega^{(0)2} + 2\omega^{(0)}\Omega_H)}{\omega_H\Omega_H(\omega^{(0)} + \Omega_H)^2}. \tag{3.13}$$

When (3.9) is taken into account the second inequality in (3.6) can be written in the form

$$N_s \gg N\sqrt{\frac{T_3}{T_1}}\frac{\omega}{\Omega_H}\left\{\exp\left[-\frac{1}{2}\left(\frac{\omega + \Omega_H}{kv_{T_1}}\right)^2\right] + \sqrt{\frac{T_1M}{T_2m}}\exp\left[-\frac{1}{2}\left(\frac{\omega_H}{kv_{T2}}\right)^2\right]\right\}. \tag{3.14}$$

3. Finally, we consider the case of gyromagnetic resonance in the plasma, i.e. the case in which

$$|\omega-\Omega_H|\ll kv_{T1}. \tag{3.15}$$

In this case, the wave is strongly damped in the absence of a beam.[21] However, growing waves are possible if a charged particle beam moves through the plasma. Suppose that the following inequalities are satisfied:

$$|\omega+\omega_H|\gg kv_{T2},\quad |\omega-kv_0-\Omega_H|\gg kv_{T3}, \quad |\omega+\omega_H-kv_0|\ll kv_{T4}. \tag{3.16}$$

Using the asymptotic expressions (1.6), from Eq. (3.2) we have

$$\frac{\omega_{01}^2\,\omega}{kv_{T1}}\left\{-i\sqrt{\frac{\pi}{2}}+\frac{\omega-\Omega_H}{kv_{T1}}\right\}+\frac{\omega_{02}^2\,\omega}{kv_{T2}}\left\{-i\sqrt{\frac{\pi}{2}}\,e^{-\beta_2^2/2}+\frac{kv_{T2}}{\omega+\omega_H}\right\}+\frac{\omega_{03}^2(\omega-kv_0)}{kv_{T3}}\left\{-i\sqrt{\frac{\pi}{2}}\,e^{-\beta_3^2/2}+\frac{kv_{T3}}{\omega-\Omega_H-kv_0}\right\}+\frac{\omega_{04}^2(\omega-kv_0)}{kv_{T4}}\left\{-i\sqrt{\frac{\pi}{2}}+\frac{\omega+\omega_H-kv_0}{kv_{T4}}\right\}+c^2k^2-\omega^2=0. \tag{3.17}$$

For simplicity we assume that the following relations are satisfied:

$$\sqrt{\frac{MT_1}{mT_2}}\,|e^{-\beta_2^2/2}|\ll 1,\qquad \sqrt{\frac{mT_4}{MT_3}}\,|e^{-\beta_3^2/2}|\ll 1 \tag{3.18}$$

Then, assuming that ω is real while the wave vector k is complex,[21] we find from Eq. (3.17) that when Im k ≪ Re k, wave amplification is possible if

$$N_4>N_1\left|\frac{\omega}{\omega-kv_0}\right|\sqrt{\frac{mT_4}{MT_1}}. \tag{3.19}$$

In the present case the energy supplied by magnetic bremsstrahlung of the beam electrons in the region of the anomalous Doppler effect is greater than the energy dissipated in the plasma; hence growing waves are possible.

4. INVESTIGATION OF THE LONGITUDINAL WAVE EQUATION

1. We consider the case in which both the beam and plasma are quasi-neutral. Neglecting collisions, in this case we can write (1.3) in the form

$$k^2+\sum_{\gamma=1}^{4}\frac{\omega_{0\gamma}^2}{v_{T\gamma}^2}-\frac{\omega}{k}\sum_{\gamma=1}^{2}\frac{\omega_{0\gamma}^2}{v_{T\gamma}^3}B(\beta_\gamma)-\frac{\omega-kv_0}{k}\sum_{\gamma=3}^{4}\frac{\omega_{0\gamma}^2}{v_{T\gamma}^3}B(\beta_\gamma)=0. \tag{4.1}$$

As was first pointed out by Gordeev,[22] in the absence of a beam the longitudinal wave is weakly damped only if the following condition is satisfied:

$$v_{T1}\ll|\omega/k|\ll v_{T2}. \tag{4.2}$$

If this condition is not satisfied the wave is highly damped. However, if a beam of charged particles passes through a plasma, growing waves are possible even when (4.2) is not satisfied (cf. for example reference 12). Everywhere below, however, we shall assume that the inequality in (4.2) is satisfied.

2. At the outset we neglect the effect of thermal motion on the stability of the system. We introduce the notation

$$\varepsilon=\omega-kv_0. \tag{4.3}$$

($\mu \equiv \mathrm{Im}\ \epsilon$) and let $|\epsilon| \ll \omega^{(0)}$, where $\omega^{(0)} = kv_0$ is a solution of Eq. (4.1) in the zeroth approximation, i.e. for $N_S \to 0$. Then, from Eq. (4.1) we have

$$\varepsilon=\left(\frac{1}{2}\right)^{1/3}kv_0\left[\frac{N_sM}{Nm\,(1+6v_{T1}^2/v_0^2)}\right]^{1/3}. \tag{4.4}$$

It follows from Eq. (4.1) that for the acoustic wave

$$k=(\omega/v_{T1})\sqrt{T_1/T_2}\qquad (v_{\mathrm{ph}}=\sqrt{T_2/M}). \tag{4.5}$$

For the ion oscillations (ion plasma waves)

$$k=(\omega/v_{T1})\sqrt{(\omega^2-\omega_{01}^2)/3\omega_{01}^2}. \tag{4.6}$$

It is apparent from Eq. (4.4) that there is always an instability in the case being considered since $(1)^{1/3} = 1,\ (-1 \pm i\sqrt{3})/2$. In writing Eq. (4.6) and everywhere below, for simplicity we omit the superscript which indicates the order of the approximation because the approximation being considered is clear in any actual case.

3. Finally, when the thermal motion in the beam is important, so that the following inequality is satisfied:

$$|(\omega-kv_0)/kv_{T3}|\ll 1,\qquad |(\omega-kv_0)/kv_{T4}|\ll 1, \tag{4.7}$$

Eq. (4.1) assumes the form

$$1-\frac{\omega_{01}^2}{k^2v_{T1}^2}\left(\frac{k^2v_{T1}^2}{\omega^2}+3\,\frac{k^4v_{T1}^4}{\omega^4}\right)+\sum_{\gamma=2}^{4}\frac{\omega_{0\gamma}^2}{k^2v_{T\gamma}^2}+i\sqrt{\frac{\pi}{2}}\left\{\frac{\omega}{k^3}\left[\frac{\omega_{01}^2}{v_{T1}^3}\exp\left\langle-\frac{1}{2}\left(\frac{\omega}{kv_{T1}}\right)^2\right\rangle+\frac{\omega_{02}^2}{v_{T2}^3}\right]+\frac{\omega-kv_c}{k^3}\left(\frac{\omega_{03}^2}{v_{T3}^3}+\frac{\omega_{04}^2}{v_{T4}^3}\right)\right\}=0. \tag{4.8}$$

Whence, it is easy to show that a sufficient condition for the production of an instability is

$$N_s>N\left(\frac{T_3}{T_1}\right)^{3/2}\frac{\omega}{kv_0-\omega}\left(1+\sqrt{\frac{mT_3^3}{MT_4^3}}\right)^{-1}\times\left[e^{-\omega^2/2k^2v_{T1}^2}+\left(\frac{mT_1^3}{MT_2^3}\right)^{1/2}\right|. \tag{4.9}$$

The growth (damping) factor is given by a relatively simple expression if

$$|\mu/\omega|\ll 1. \tag{4.10}$$

Then,

$$\frac{\mu}{\omega} = -\sqrt{\frac{\pi}{8}}\,\frac{\omega^3}{\omega_{01}^2}\left\{\frac{\omega_1}{k^3}\left[\frac{\omega_{01}^2}{v_{T1}^3}e^{-\omega^2/2k^2v_{T1}^2} + \frac{\omega_{02}^2}{v_{T2}^3}\right]\right.$$

$$\left. + \frac{\omega - kv_0}{k^3}\left[\frac{\omega_{03}^2}{v_{T3}^3} + \frac{\omega_{04}^2}{v_{T4}^3}\right]\right\}.$$

We can obtain the condition for wave amplification ($\mu > 0$) from the last expression. We may note that the inequality in (4.10) is satisfied if

$$N_s \ll N\frac{\omega}{kv_0 - \omega}\,\frac{T_3^{3/2}}{T_1^{3/2}}\left[1 + \left(\frac{mT_3^3}{MT_4^3}\right)^{1/2}\right]^{-1}$$

$$\times\left[\sqrt{\frac{8}{\pi}}\,\frac{k^3v_{T1}^3}{\omega^3}\left(\frac{mT_1^3}{MT_2^3}\right)^{1/2} + e^{-\omega^2/2k^2v_{T1}^2}\right].$$

In conclusion, the author wishes to express his gratitude to B. N. Gershman and V. V. Zheleznyakov for a reading of the manuscript and for valuable discussions.

---

[1] A. I. Akhiezer and Ya. B. Faĭnberg, JETP 21, 1262 (1951).

[2] R. Q. Twiss, Phys. Rev. 84, 448 (1951).

[3] V. L. Ginzburg and V. V. Zheleznyakov, Астрономический журнал (Astronomical Journal) 35, 694 (1958), Soviet Astronomy 2, 653 (1959).

[4] V. V. Zheleznyakov, Изв. Высш. уч. зав., Радиофизика (News of the Universities, Radiophysics) 2. 14 (1959).

[5] L. M. Kovrizhnykh and A. A. Rukhadze, JETP 38, 850 (1960), Soviet Phys. JETP 11, 615 (1960).

[6] G. G. Getmantsev and V. O. Rapoport, JETP 38, (1960), Soviet Phys. JETP 11, 871 (1960).

[7] P. J. Kellogg and H. Liemohn, Phys. Fluids 3, 40 (1960).

[8] M. S. Kovner, op. cit. ref. 4 3, 631 (1960).

[9] M. S. Kovner, op. cit. ref. 4 3, 746 (1960).

[10] B. B. Kadomtsev, Сб. физика плазмы и проблема управляемых термоядерных реакций (Plasma Physics and the Problem of a Controlled Thermonuclear Reaction) Acad. Sci. U.S.S.R. Press (1958) Vol. IV.

[11] Demirkhanov, Gevorkov and Popov, J. Tech. Phys. (U.S.S.R.) 30, 315 (1960), Soviet Phys. Tech. Phys. 5, 290 (1960).

[12] G. V. Gordeev, JETP 27, 24 (1954).

[13] A. A. Vedenov and V. Z. Sagdeev, op. cit. ref. 10 (1958) Vol. III.

[14] V. F. Dokuchaev, JETP 39, 413 (1960), Soviet Phys. JETP 12, 292 (1961).

[15] L. D. Landau, JETP 16, 571 (1946).

[16] A. I. Akhiezer and L. E. Pargamanik, Уч. зап. ХГУ (Science Notes of Kharkov State University) 27, 75 (1948).

[17] B. N. Gershman, JETP 24, 659 (1953).

[18] V. V. Zheleznyakov, op cit. ref. 4 3, 57 (1960).

[19] V. A. Fock, Дифракция радиоволн (Diffraction of Radiowaves) Acad. Sci. U.S.S.R. Press (1946).

[20] G. V. Gordeev, JETP 24, 445 (1953).

[21] P. H. Doyle and J. Neufeld, Phys. Fluids 2, 390 (1959).

[22] G. V. Gordeev, JETP 27, 19 (1954).

Translated by H. Lashinsky
82

SOVIET PHYSICS JETP VOLUME 13, NUMBER 2 AUGUST, 1961

DETERMINATION OF THE PARITIES OF STRANGE PARTICLES BY MEANS OF DISPERSION RELATIONS

Ya. I. GRANOVSKII and V. N. STARIKOV

Institute of Nuclear Physics, Academy of Sciences, Kazakh S.S.R.

Submitted to JETP editor August 9, 1960

J. Exptl. Theoret. Phys. (U.S.S.R.) 40, 537-545 (February, 1961)

The set of dispersion relations of Matthews and Salam, Igi, and Amati for the scattering of K mesons by protons is regarded as an (overdetermined) system of equations for the parities and the coupling constants of the proton with the K-Y pair. The condition for consistency leads to the result that the parities of Λ and Σ hyperons are opposite. The sign of the real part of the amplitude for scattering of a K^- meson by a proton turns out to be positive, so that there are attractive forces in the Kp system.

1. INTRODUCTION

At present a number of methods are used for determining the parities of strange particles from the phenomenological analysis of reactions in which they are created or destroyed. Various difficulties are, however, inherent in all of these methods. The point is that the strong interactions conserve not only parity but also strangeness, so that the reactions in question involve the strange particles in pairs. Therefore one cannot determine the parity of one particle without knowing the properties of the nuclear interactions of the partner particle. At present these properties are as a rule unknown, and this hinders the determination of parities.

On the other hand, the phenomenological method for determining parities, which operates only with initial and final states, cannot be applied to reactions of elastic scattering, since in this case the intrinsic parity drops out of the argument. Conversely, any theory that contains the idea of intermediate states can give an answer to the question. In particular, such ideas are contained in the method of dispersion relations, and owing to this it can be used for the determination of the parities of strange particles.[1]

The basic idea of this method is that the sign of the pole term that appears on account of the transition to an intermediate state which contains one hyperon depends on the parity of the system Kp relative to this hyperon.[2] For the calculation of the pole terms one must know the dispersion integral and the real part of the scattering amplitude. The experimental data now available[3] enable us to determine these quantities.

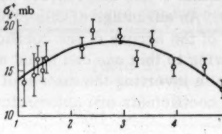

FIG 1.

Our work differs from a number of previous papers[2] in that we have avoided the simplest approximations for the energy dependence of the cross sections and have made a complete treatment of all the data by the method of least squares. This has made it possible to estimate the actual precision of the calculations, and in particular to answer a number of questions raised in the papers of Islam and Selleri.[2]

2. THE ANALYSIS OF THE EXPERIMENTAL DATA

The required experimental information on the cross sections for the interaction of K mesons

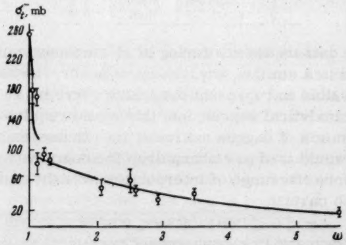

FIG. 2

with nucleons is contained in the report of Alvarez at the Kiev Conference.[3] These data are shown in Figs. 1 and 2, together with the smoothed curves obtained by treatment of the experimental data by the method of least squares.

In the obtaining of the smoothed curves it was convenient to use this method in the Chebyshev form (cf., e.g., reference 4), in which the curve is represented as an expansion in terms of polynomials

$$\sigma(\omega)=\sum_{k=1}^{n} C_k\varphi_k(\omega), \tag{2.1}$$

which are orthogonal with the weights p_i when summed over a discrete set of points ω_i:

$$\sum_{i=1}^{N} p_i\varphi_k(\omega_i)\varphi_l(\omega_i)\equiv[\varphi_k,\varphi_l]=A_k\delta_{kl}. \tag{2.2}$$

As the weights p_i one takes a set of quantities inversely proportional to the dispersions of the cross sections $\sigma(\omega_i)$. An advantage of this procedure is that the matrix of the errors of the coefficients C_k is diagonal. Owing to this one can avoid much computational labor in inverting the matrix of the errors, since the coefficients are automatically uncorrelated.

In the choice of the degree of the approximating polynomial one must confine oneself to the value of n for which the quantity

$$\eta=[(\sigma-\sum C_k\varphi_k),(\sigma-\sum C_k\varphi_k)]/(N-n) \tag{2.3}$$

first becomes close to unity.[5] The cross section $\sigma_+(\omega)$ is approximated by polynomials of degree no higher than the second. Table I shows the coefficients C_k, their dispersions $D(C_k)$, and the values of η.

Table I

k	C_k^+	$D(C_k^+)$	η
0	16,553	0.09	3,4
1	—0,745	0,08	3.1
2	—1,277	0.06	0,96

The data on the scattering of K^- mesons were treated in a similar way. Here, however, it was not possible to represent the entire curve by a single analytical expression; this would require polynomials of degree not lower than the seventh, which would lead to a sharp drop in accuracy. Therefore the range of interpolation was divided into two parts:

$$m\leqslant\omega\leqslant 1.1m,\qquad 1.1m\leqslant\omega\leqslant 5m.$$

(Both here and in all subsequent numerical calculations energies are expressed in terms of the rest energy of the K^- meson; m = 494 Mev.) In the first interval the total cross section σ_{tot}^- was divided into two parts:

$$\sigma_{tot}^-=\sigma_{sc}^-+\sigma_{ab}^-,$$

where the cross sections for elastic scattering and for charge transfer were assumed constant,

$$\sigma_{sc}^-=90\pm17\text{ mb} \tag{2.4}$$

and the absorption cross section was approximated by the formula

$$|k|\sigma_{ab}^-=(7\pm1)m^{-1}. \tag{2.5}$$

This same expression was also used in the unphysical region $\omega\leq m$. The more exact extrapolation proposed by Dalitz and Tuan[6] is not necessary, since the entire contribution of the unphysical region is small.

Table II

k	C_k^-	$D(C_k^-)$	η
0	48.9	6.4	14.2
1	—13.8	3.1	3.4
2	3.65	1,27	1.4

In the second range the curve of the total cross section was smoothed. The data for this are shown in Table II. The approximating curve is taken as a polynomial of the second degree. In the region $\omega > 5m$ the cross sections are unknown. We have assumed that they remain constant and equal to each other:

$$\sigma_{tot}^-=\sigma_{tot}^+. \tag{2.6}$$

This contradicts the direct experimental data at $\omega = 5m$

$$\sigma_{tot}^+=13\pm1\text{mb},\quad\sigma_{tot}^-=20\pm5\text{ mb}. \tag{2.7}$$

Evidently the equalizing of the cross sections occurs at somewhat higher energies. An estimate of the error introduced by the assumption (2.6) shows that in any case it is not more than 5 percent. Of course it would be very desirable to have direct data on the cross sections in this region.

3. CHOICE OF THE DISPERSION RELATIONS

The dispersion relations for the scattering of $K^\pm$ mesons by protons are given in the paper by Matthews and Salam:[1]

$$D_\pm(\omega)=B_\pm(\omega)+\frac{1}{4\pi^2}\int_m^\infty k'd\omega'\left[\frac{\sigma_+(\omega')}{\omega'\mp\omega}+\frac{\sigma_-(\omega')}{\omega'\pm\omega}\right]$$

$$+\frac{1}{\pi}\int_{\omega_{\Lambda\pi}}^{m}\frac{A_-(\omega')\,d\omega'}{\omega'\pm\omega}, \tag{3.1}$$

where

$$D(\omega) = \operatorname{Re} M(\omega), \qquad A(\omega) = \operatorname{Im} M(\omega), \tag{3.2}$$

$$\omega_{\Lambda\pi} = [(M_\Lambda + \mu)^2 - M^2 - m^2]/2M,$$

$$\omega_Y = [M_Y^2 - M^2 - m^2]/2M, \tag{3.3}$$

$$B_\pm(\omega) = \frac{g_\Lambda^2}{4\pi}\frac{\omega_\Lambda + M + M_\Lambda p_{\Lambda K}}{2M(\omega_\Lambda \pm \omega)} + \frac{g_\Sigma^2}{4\pi}\frac{\omega_\Sigma + M + M_\Sigma p_{\Sigma K}}{2M(\omega_\Sigma \pm \omega)}. \tag{3.4}$$

The term $B_\pm(\omega)$ has a pole at $\omega = \mp\omega_Y$, i.e., at the energy at which a transition to an intermediate state involving a hyperon is possible. The residue at the pole depends on the coupling constant between the system Kp and this hyperon and on the parity p_{KY} relative to the proton. The numerical values of the threshold energies are

$$\omega_{\Lambda\pi} = 0.474\ m, \qquad \omega_\Lambda = 0.129\ m, \qquad \omega_\Sigma = 0.320\ m. \tag{3.5}$$

From the relations (3.1) one can obtain other formulas which have better convergence in the region of large ω':

$$D_-(\omega) - D_+(\omega) = B_-(\omega) - B_+(\omega) + \frac{2\omega}{4\pi^2}\int_m^\infty \frac{\sigma_- - \sigma_+}{\omega'^2 - \omega^2}\,k'd\omega' + \frac{2\omega}{\pi}\int_{\omega_{\Lambda\pi}}^m \frac{A_-d\omega'}{\omega'^2 - \omega^2} \tag{3.6}$$

(the Matthews-Salam relation[1]);

$$D_+(\omega) - \frac{\omega + m}{2m}D_+(m) + \frac{\omega - m}{2m}D_-(\omega) = \frac{k^2}{4\pi^2}\int_m^\infty \frac{d\omega'}{k'}\left[\frac{\sigma_+}{\omega' - \omega} + \frac{\sigma_-}{\omega' + \omega}\right] + \frac{k^2}{\pi}\int_{\omega_{\Lambda\pi}}^m \frac{A_-d\omega'}{k'^2(\omega' + \omega)} + 2F\frac{k^2}{\omega} \tag{3.7}$$

(the Igi relation[1]);

$$\frac{D_+(\omega) - D_+(m)}{\omega - m} = \frac{B_+(\omega) - B_+(m)}{\omega - m} + \frac{1}{4\pi^2}\int_m^\infty k'd\omega'\left[\frac{\sigma_+}{(\omega' - \omega)(\omega' - m)} - \frac{\sigma_-}{(\omega' + \omega)(\omega' + m)}\right] - \frac{1}{\pi}\int_{\omega_{\Lambda\pi}}^m \frac{A_-d\omega'}{(\omega' + \omega)(\omega' + m)} \tag{3.8}$$

(the Amati relation[2]).

We shall use Eqs. (3.6) and (3.7) at the energy m, and Eq. (3.8) at $\omega = 1.22m$ (for convenience of comparison with Selleri's paper[2]). Introducing the scattering lengths a and b by the formulas

$$D_+(\omega) = -\ ak/k_c, \quad D_-(\omega) = \pm\ bk/k_c \tag{3.9}$$

(k_c is the momentum in the center-of-mass system), we then get

$$\pm b + a = B_1 + \frac{M}{M + m}\frac{2m}{4\pi^2}\left[\int_m^\infty \frac{\sigma_- - \sigma_+}{k'}\,d\omega' + \int_{\omega_{\Lambda\pi}}^m \frac{|k'|\sigma_{ab}^- d\omega'}{\omega'^2 - m^2}\right], \tag{3.10}$$

$$\pm b + a + \frac{2Mm}{M + m}D_+'(m) = B_2 + \frac{M}{M + m}\frac{m^2}{\pi^2}\left[\int_m^\infty \frac{d\omega'}{k'}\left(\frac{\sigma_+}{\omega' - m} + \frac{\sigma_-}{\omega' + m}\right) + \int_{\omega_{\Lambda\pi}}^m \frac{|k'|\sigma_{ab}^- d\omega'}{k'^2(\omega' + m)}\right], \tag{3.11}$$

$$r_+(1.22m) = B_3 + \frac{1}{\pi}\int_m^\infty k'd\omega'\left[\frac{\sigma_+}{(\omega' - 1.22m)(\omega' - m)} - \frac{\sigma_-}{(\omega' + 1.22m)(\omega' + m)}\right] - \frac{1}{\pi}\int_{\omega_{\Lambda\pi}}^m \frac{|k'|\sigma_{ab}^- d\omega'}{(\omega' + 1.22m)(\omega' + m)}. \tag{3.12}$$

The factor $M/(M+m)$ has arisen from k/k_c after passage to the limit $\omega \to m$, and

$$r_+ = 4\pi\,[D_+(1.22\ m) - D_+(m)]/0.22\ m. \tag{3.13}$$

The explicit expressions for the pole terms B_i in terms of the coupling constants are of the following form:

$$B_i = a_{i\Lambda}g_\Lambda^2/4\pi + a_{i\Sigma}g_\Sigma^2/4\pi.$$

The coefficients $a_{i\Lambda}$ and $a_{i\Sigma}$ are given in Table III, where the upper values are for positive parity $p_{KY} > 0$.

Table III

i	$a_{i\Lambda}$	$a_{i\Sigma}$
1	−2.296 0.123	−2.717 0.114
2	−2.663 0.143	−2.697 0.113
3	−9.305 0.498	−7.540 0.316

4. CALCULATION OF THE POLE TERMS

By means of the dispersion equations (3.10) – (3.12) the pole terms can be expressed in terms of the scattering lengths and the dispersion integrals. The problem is reduced to the calculation of these quantities and of their standard errors.

1. The scattering lengths. By definition [cf. Eq. (3.9)]

$$a = [\sigma_{sc}^+(m)/4\pi]^{1/2}, \qquad b = [\sigma_{sc}^-(m)/4\pi - [k_c\sigma_{ab}^-(m)/4\pi]^2]^{1/2}, \tag{4.1}$$

with the positive sign of $D(\omega)$ corresponding to attraction of the K meson to the proton. At the present time only the sign of $D_+(m)$ has been determined; it is negative,[3] i.e., the K^+ meson is repelled from the proton. The sign of $D_-(m)$ has not yet been determined, but there are certain indications (interference between Coulomb and nuclear scattering) that this sign is positive.[3] We shall investigate both possibilities.

Let us show how the scattering length a was calculated. According to Eq. (4.1) it can be expressed in terms of the coefficients C_k of the polynomial which approximates $\sigma_+(\omega)$. These coefficients are independent random variables distributed according to the normal law. Since their dispersions are small, we can use the simple differential formula

$$a = \bar{a} + \sum \frac{\partial a}{\partial C_k} \Delta C_k. \tag{4.2}$$

Substituting all the necessary data and making the calculation, we find

$$a = (0.8389 \pm 0.0268)\ m^{-1}. \tag{4.3}$$

The quantity b is calculated in a similar way, but is expressed in terms of different random quantities (σ_{sc}^-, σ_{ab}^-):

$$b = (2.046 \pm 0.330)\ m^{-1}. \tag{4.4}$$

The other quantities associated with the scattering lengths are found in just the same way. Thus the derivative $D'_+(m)$, which appears in the Igi relation (3.11), is given by

$$D'_+(m) = \frac{Mm}{M+m} a^3 - \frac{M+m}{M} \frac{\partial a}{\partial \omega} - \frac{a}{M+m}. \tag{4.5}$$

After substitution of the numerical data this formula gives

$$D'_+(m) = (-0.26 \pm 1.65)\ m^{-2}. \tag{4.5a}$$

Finally, the Amati relation (3.12) involves the effective radius r_+ [see Eq. (3.13)]. Its value is

$$r_+ = (-0.22 \pm 1.04)\ m^{-2}. \tag{4.6}$$

2. The dispersion integrals. All of the integrals that it is necessary to calculate can be divided into four types, which differ from each other by the ranges of integration:

$$\omega_{\Lambda\pi} \leqslant \omega' \leqslant m, \qquad m \leqslant \omega' \leqslant 1.1\,m,$$
$$1.1\,m \leqslant \omega' \leqslant 5m, \qquad 5m \leqslant \omega' < \infty.$$

The only contribution in the first interval is that from the absorption cross section σ_{ab}^-, which is taken from Eq. (2.5). In the second interval σ_{ab}^-, σ_{tot}^+, and σ_{sc}^- come in. The value of σ_{sc}^- is taken from Eq. (2.4), and for σ_{tot}^+ we use the approximating polynomial (2.1). In the next interval we need data on the total cross sections σ_{tot}^- and σ_{tot}^+, which we have in the form of smoothed polynomials. In the last interval we use the equality of the cross sections [cf. Eq. (2.6)]

$$\sigma_{tot}^- = \sigma_{tot}^+ = 13 \pm 1 \text{ mb},$$

which is necessary for the convergence of the integrals in the relations of Salam and Amati. In the Igi relations, where the integrals converge even without this condition, we have taken the direct experimental values of the cross sections [cf. Eq. (2.7)]. We recall that in this region all of the cross sections have been assumed independent of the energy.

In all cases the integration can be done by elementary methods, and the result is that all of the dispersion integrals are expressed in terms of the 10 independent random quantities

$$C_0^+,\ C_1^+,\ C_2^+,\ C_0^-,\ C_1^-,\ C_2^-,\ \sigma_{sc}^-,\ \sigma_{ab}^-,\ \sigma^-(\infty),\ \sigma^+(\infty). \tag{4.7}$$

Some of them have already been encountered above in the calculation of the scattering lengths.

3. The pole terms. Equations (3.10) – (3.12) serve for the determination of the pole terms B_i in terms of the dispersion integrals, the scattering lengths, and related quantities. Substituting everything in Eqs. (3.10) – (3.12), we get

$$B_i = \bar{B}_i + \sum_{k=1}^{10} b_{ik} \Delta C_k, \tag{4.8}$$

where

$$\overline{\Delta C_k} = 0, \qquad \overline{\Delta C_k \Delta C_l} = \delta_{kl} D(C_k), \tag{4.9}$$

$$b_{ik} = \begin{pmatrix} 0.073 & -0.105 & 0.132 & -0.039 & 0.025 & -0.006 & \begin{smallmatrix}0.010\\-0.029\end{smallmatrix} & \begin{smallmatrix}0.030\\0.036\end{smallmatrix} & & 0 \\ 1.773 & -4.034 & 6.362 & -0.025 & 0.024 & -0.017 & \begin{smallmatrix}0.010\\-0.029\end{smallmatrix} & \begin{smallmatrix}0.037\\0.043\end{smallmatrix} & -0.008 & -0.009 \\ 0.662 & -3.235 & 7.213 & 0.123 & -0.008 & -0.104 & -0.002 & 0.057 & -0.001 & -0.031 \end{pmatrix}. \tag{4.10}$$

The columns of the matrix b_{ik} are numbered in the order of the quantities in the list (4.7), and the rows correspond to i = 1, 2, 3. In the rows in which two values are given, the upper corresponds to attraction of K^- to the proton (i.e., to the positive sign of b).

Since the number of terms in Eq. (4.8) is rather large, we can apply the limit theorem of probability theory and assume that the value of a pole term is distributed around its average value $\bar{B}$ according to the normal law, the dispersion of this distribution being a linear function of the $D(C_k)$. By means of the formula (4.8) we can convince ourselves that the three pole terms B_i are statistically independent quantities. Substituting the numerical values, we get the data shown in Table IV, which gives the values of the pole terms with their standard errors (the diagonal elements of the error matrix).

Table IV

i	B_i
1	0.799 ± 0.211 -3.293 ± 0.503
2	0.531 ± 2.055 -3.561 ± 2.108
3	1.410 ± 2.097

The largest dispersion is obtained by the use of the Igi relations (3.7). In doing the calculation one finds that the main contribution (90 percent) to the dispersion comes from the uncertainty in the quantity $D'_+(m)$. Therefore although the subtraction method used by Igi gives convergent quantities, it at the same time leads to large ambiguities. In fact, it has been shown in a paper by Islam[2] that the different ways of interpolating the experimental data on K^+p scattering in the energy range up to 100 Mev can lead to the negative sign for the pole term, independently of the sign of the potential of the K^-p interaction.

In our case, owing to the use of the method of least squares, there are no ambiguities in the interpolation. It can be seen from Table IV, however, that although the average value $\overline{B}_2$ is indeed positive (for $b > 0$), there is a considerable probability (40 percent) that $B_2 < 0$. Thus in this case we cannot reliably indicate the sign of the pole term.

In their paper Karplus and others[2] used a dispersion relation of the same type as Eq. (3.7), but with a variable point of subtraction. In the light of what we have found, it is clear why the standard deviations in their paper were as large as 150 percent and the sign of B_2 remained completely uncertain.

Thus the subtraction used by Igi depresses the pole term too much and does not allow us to determine the necessary quantities with enough accuracy. On the other hand, the relation used by Amati (the effective-radius approximation) is less sensitive to experimental errors. This is because in this relation the main part is played by the dispersion integrals, which are determined with high accuracy. The ambiguities that arise here turn out to be very slight. Thus the probability that the sign of the pole term is opposite to that shown in the table is only 20 percent.

Of all the relations we have considered, the one that gives the most reliable data on the pole terms is the Matthews-Salam relation. The reason is that no subtraction procedure was used in the derivation of this relation, and owing to this the effects of experimental errors on the value of the pole term are reduced to a minimum. The accuracy obtained in this case is in fact the best. At any rate the sign of the pole term is determined with a probability very close to unity.

5. THE PARITIES AND COUPLING CONSTANTS OF THE STRANGE PARTICLES

The results of the treatment of the experimental data are presented in Table IV, which shows the values of the pole terms. In Table III these same terms are expressed in terms of the (unknown) parities and coupling constants of the strange particles. Combining the data of the two tables, we get an equation of the form

$$a_\Lambda g_\Lambda^2/4\pi + a_\Sigma g_\Sigma^2/4\pi = B, \tag{5.1}$$

in which the coefficients a_Y are taken from Table III and depend on the parities of the strange particles, and the quantity B is from Table IV and depends on the sign of the potential of the K^-p interaction.

In all previous papers[1,2] devoted to this problem attempts have been made to determine both parities from a single equation (5.1). For example, if we use the Amati relation, in which $B > 0$, it is clear that the parities of the Λ and Σ hyperons cannot both be positive at the same time, since then $a_\Lambda < 0$, $a_\Sigma < 0$ and Eq. (5.1) cannot be satisfied by positive values of $g_Y^2/4\pi$. If, on the other hand, both hyperons have negative parities, the equation can be satisfied. This still leads to no conclusion, however, since it remains completely obscure what the situation is if the parities of the hyperons are opposite to each other.

The point is, of course, that one equation is not enough for the determination of the parities. Therefore one must make additional assumptions to make up for the lack of information. Such an approach naturally cannot be accepted as correct. We prefer to consider not a single dispersion relation, but the entire set, and to treat it as a system of equations for the unknown coupling constants. We have

$$a_{1\Lambda} g_\Lambda^2/4\pi + a_{1\Sigma} g_\Sigma^2/4\pi = B_1, \qquad a_{2\Lambda} g_\Lambda^2/4\pi + a_{2\Sigma} g_\Sigma^2/4\pi = B_2,$$
$$a_{3\Lambda} g_\Lambda^2/4\pi + a_{3\Sigma} g_\Sigma^2/4\pi = B_3. \tag{5.2}$$

Positive definite solutions of this system do not exist in all cases, but only with a definite choice of the parities. This enables us to find them. Moreover, since we have three equations for two unknowns, the additional condition for their consistency

$$\begin{vmatrix} a_{1\Lambda} & a_{1\Sigma} & B_1 \\ a_{2\Lambda} & a_{2\Sigma} & B_2 \\ a_{3\Lambda} & a_{3\Sigma} & B_3 \end{vmatrix} = 0 \tag{5.3}$$

is a very severe one.

If we assume that attractive forces act between the K^- meson and the proton at small energies, the system (5.2) is consistent, and its solutions are positive only with the following choice of the parities:

$$p\,(K^+\Lambda_0) > 0, \qquad p\,(K^+\Sigma_0) < 0. \tag{5.4}$$

The most probable values of the coupling constants are then

$$g_\Lambda^2/4\pi = 0{,}28 \pm 0.67, \quad g_\Sigma^2/4\pi = 12{,}7 \pm 13.6. \quad (5.5)$$

Let us now consider the solutions that are obtained with a choice of the parities different from that of Eq. (5.4), for example for $p_{K\Lambda} > 0$, $p_{K\Sigma} > 0$. There is then just a change of the coefficients $a_{i\Sigma}$ in the system (5.2), with the new values proportional to the old ones. The proportionality constant can be found from Eq. (3.4), and is

$$k = (\omega_\Sigma + M + M_\Sigma)/(\omega_\Sigma + M - M_\Sigma) = -23.9. \quad (5.6)$$

Since the coefficients $a_{i\Sigma}$ are proportional to their previous values, the condition of consistency, Eq. (5.3), is not disturbed. The new solution will differ from the old one only in the quantity $g_\Sigma^2/4\pi$; it is now negative and smaller by a factor 23.9. We have an analogous situation if we change the assumption about the parity of the Λ hyperon, but in this case $k = -18.7$. Thus among the four choices for the parities only one is physically possible. With each of the other three choices at least one constant is negative. Of course, owing to the presence of the dispersions there is a nonvanishing probability of getting positive values of $g_Y^2/4\pi$ in these cases also, but this probability is not larger than 20 percent, whereas for the choice (5.4) it is 65 percent. These figures show the degree of uniqueness of the result expressed by the equations (5.4) and (5.5).

If we assume that the K^- meson is repelled from the proton ($b < 0$), the right members of the equations (5.2) take different values (see Table IV). In this case a direct calculation shows that the condition of consistency (5.3) is violated. Therefore there is no choice of the parities for which one can satisfy the system of equations with positive coupling constants. Naturally this result also is only a probable one. Knowing the dispersions and correlations of the right members, we have calculated the probability that the condition (5.3) can be satisfied. It is 3 percent, whereas in the previous case ($b > 0$) we had ~ 65 percent.

Thus owing to our use of the system of dispersion relations we are able to exclude the a priori possible case of K^-p repulsion. This means that the sign of this scattering length is determined by the very structure of the dispersion equations. We note that the conclusion that the K^- meson and proton attract each other does not contradict the data on the interference of the Coulomb and nuclear scatterings of the K^- meson.[3]

6. CONCLUSION

Our analysis of the dispersion relations for the scattering of $K^\pm$ mesons by protons leads to the following conclusions:

1. In the determination of the parities one must not use only the sign of the pole term, as has been done in all previous papers,[1,2] but must regard the dispersion relations as equations in the unknowns g_Y^2.

2. The most probable result is that the hyperons have opposite parities, which has the consequence that the constants g_Y^2 differ by a factor of about 40.

3. There is no need to make any assumptions about the sign of the scattering length of the K^- meson, since it is determined by the very structure of the dispersion relations.

4. The Igi dispersion relation leads to a broad distribution of the quantities being studied, which makes it hard to get an unambiguous answer.

5. The contribution of the absorption to the dispersion integral is small, and owing to this we can use the simplest extrapolations in the unphysical region.

We express our gratitude to Professor Zh. S. Takibaev for his interest in this work, to Professor L. Alvarez and A. Rosenfeld for furnishing experimental data before its publication, and to A. Akhmedshina for help in the calculations.

Note added in proof (January 16, 1961). The linear combinations $g_\Lambda^2/4\pi = 0.028 \pm 0.71$ and $g_\Sigma^2/4\pi - 20.6\, g_\Lambda^2/4\pi = 6.93 \pm 1.84$ have no correlation between them, and their dispersions give an optimal characterization of the accuracy attained in the present paper. Inclusion of new data[7] leads to the values $g_\Lambda^2/4\pi = 0.89$, $g_\Sigma^2/4\pi = 25.0$, with the same relative accuracy as before.

---

[1] P. T. Matthews and A. Salam, Phys. Rev. **110**, 565 (1958). K. Igi, Progr. Theoret. Phys. **19**, 238 (1958). C. Goebel, Phys. Rev. **110**, 572 (1958).

[2] Karplus, Kerth, and Kycia, Phys. Rev. Letters **2**, 510 (1959). M. M. Islam, Nuovo cimento **13**, 224 (1959). E. Galzenati and B. Vitale, Phys. Rev. **113**, 1365 (1959). D. Amati, Phys. Rev. **113**, 1692 (1959). F. Selleri, Nuovo cimento **15**, 986 (1960).

[3] L. Alvarez, Report at the International Conference on High-energy Particle Physics, Kiev, 1959.

[4] Yu. V. Linnik, Метод наименьших квадратов и основы теории обработки наблюдений (The Method of Least Squares and the Foundations of the Theory of the Treatment of Observations), Fizmatgiz, 1958.

[5] M. E. Rose, Phys. Rev. **91**, 610 (1953).

[6] S. F. Tuan, Phys. Rev. **113**, 1375 (1959). R. Dalitz and S. F. Tuan, Ann. Phys. **8**, 100 (1959).

[7] von Dardel, Frisch, Mermod, Milburn, Piroué, Vivargent, Weber, and Winter, Phys. Rev. Letters **5**, 333 (1960).

Translated by W. H. Furry
82

SOVIET PHYSICS JETP VOLUME 13, NUMBER 2 AUGUST, 1961

DOUBLE DISPERSION RELATIONS FOR POTENTIAL SCATTERING

V. I. MAL'CHENKO

Dnepropetrovsk State University

Submitted to JETP editor July 16, 1960

J. Exptl. Theoret. Phys. (U.S.S.R.) **40**, 546-548 (February, 1961)

We study the analytic properties of the scattering matrix $T(k^2, t)$ as a function of t for real k^2, where t is the square of the momentum transfer, and k^2 is the square of the momentum. The potentials treated are of the form $F(r)r^{-1}e^{-\alpha r}$.

In this article we study the analytic properties in the complex t plane of the quantum mechanical amplitude $T(k^2, t)$ for elastic potential scattering, for real k^2. Here t is the square of the momentum transfer, and k^2 is the square of the momentum. In particular, for a potential of the form

$$V(r) = F(r)r^{-1}e^{-\alpha r}, \qquad \alpha > 0 \tag{1}$$

we are able to prove the following assertion: the scattering amplitude $T(k^2, t)$ can be extended analytically into the complex t plane for all real values of k^2, and the existence, location, and types of singularities are all determined by $F(r)$. Further, $T(k^2, t) \to 0$ as $t \to \infty$ in any direction other than along the positive real axis.

The restrictions on $F(r)$ depend both on our method of proof and on whether the scattering is nonrelativistic or relativistic (determined by the Klein-Gordon equation). In the nonrelativistic case it is sufficient to choose $F(r)$ such that the Fourier transform $\widetilde{V}(k)$ of $V(r)$ exists, and such that if one writes

$$F(r) = \int_0^\infty e^{-rs}f(s)\,ds \tag{2}$$

then

$$\widetilde{V}(k) = \int e^{i\mathbf{kr}}V(r)\,d\mathbf{r} = 4\pi\int_0^\infty \frac{f(s)\,ds}{(\alpha+s)^2+k^2}. \tag{3}$$

In the relativistic case, in addition to (3) we require the existence of $\widetilde{V}^2(k)$, where

$$\widetilde{V}^2(k) = \int e^{i\mathbf{kr}}V^2(r)\,d\mathbf{r} = 4\pi\int_0^\infty \frac{f_1(s)\,ds}{(2\alpha+s)^2+k^2}, \tag{4}$$

$$f_1(s) = \int_0^s dp\int_0^p d\tau\, f(\tau)f(p-\tau). \tag{5}$$

Henceforth the $f(s)$ and $f_1(s)$ functions of Eqs. (2) – (5) shall be restricted by the additional condition that $\lim rF(r) = 0$ in the nonrelativistic case and $\lim F(r) = 0$ in the relativistic case as $r \to 0$. We may remark, however, that the results we obtain would seem to be valid also for a wider class of functions. In the nonrelativistic case one may, in addition, include $F(r)$ functions whose transforms are the $\delta(s)$ function or its derivatives $\delta^{(n)}(s)$. In the relativistic case the $\delta^{(n)}(s)$ are admissible.

As an illustration of our method of proof we proceed with the case of relativistic scattering. The configuration-space representation of the scattering matrix $T_1(\mathbf{k}', \mathbf{k})$ has been obtained elsewhere.[1] The momentum space representation is

$$\begin{aligned} T_1(\mathbf{k}', \mathbf{k}) = T(k^2, t) = \widetilde{W}(|\mathbf{k}'-\mathbf{k}|) & - \frac{1}{8\pi^3}\int \widetilde{W}(|\mathbf{k}'-\mathbf{k}_1|)\frac{d\mathbf{k}_1}{k_1^2-k^2-i\varepsilon}\widetilde{W}(|\mathbf{k}_1-\mathbf{k}|) \\ & + \frac{1}{64\pi^6}\int \widetilde{W}(|\mathbf{k}'-\mathbf{k}_1|)\frac{d\mathbf{k}_1}{k_1^2-k^2-i\varepsilon}G_1(k;\mathbf{k}_1,\mathbf{k}_2) \\ & \times \frac{d\mathbf{k}_2}{k_2^2-k^2-i\varepsilon}\widetilde{W}(|\mathbf{k}_2-\mathbf{k}|) - \frac{1}{64\pi^6}\int W(|\mathbf{k}'-\mathbf{k}_1|) \\ & \times \frac{d\mathbf{k}_1}{k_1^2-k^2-i\varepsilon}G_2(k;\mathbf{k}_1,\mathbf{k}_2)\frac{d\mathbf{k}_2}{k_2^2-k^2-i\varepsilon}\widetilde{W}(|\mathbf{k}_2-\mathbf{k}|). \end{aligned} \tag{6}$$

Explicit expressions for G_1 and G_2 can be obtained by the Fredholm solution of the scattering problem.[2] For instance, G_1 is given by

$$G_1(k;\mathbf{k}_1,\mathbf{k}_2) = \frac{1}{\Delta(k)}\Bigg[\widetilde{W}(|\mathbf{k}_1-\mathbf{k}_2|) + \sum_{n=1}^{\infty}\frac{(-1)^n}{n!}\int \begin{vmatrix} \widetilde{W}(|\mathbf{k}_1-\mathbf{k}_2|) & K_2(\mathbf{k}_1,\mathbf{x}_1) & \ldots & K_2(\mathbf{k}_1,\mathbf{x}_n) \\ K_2(\mathbf{x}_1,\mathbf{k}_2) & K_2(\mathbf{x}_1,\mathbf{x}_1) & \ldots & K_2(\mathbf{x}_1,\mathbf{x}_n) \\ \ldots & \ldots & \ldots & \ldots \\ K_2(\mathbf{x}_n,\mathbf{k}_2) & K_2(\mathbf{x}_n,\mathbf{x}_1) & \ldots & K_2(\mathbf{x}_n,\mathbf{x}_n) \end{vmatrix} d\mathbf{x}_1,\ldots d\mathbf{x}_n\Bigg], \tag{7}$$

where

$$\widetilde{W}(|\mathbf{k}_1-\mathbf{k}_2|) = 2\sqrt{k^2+m^2}\,\widetilde{V}(|\mathbf{k}_1-\mathbf{k}_2|) - \widetilde{V}^2(|\mathbf{k}_1-\mathbf{k}_2|),$$

$$K_2(\mathbf{k}_1,\mathbf{x}_i) = \int d\mathbf{z}\, e^{-i\mathbf{k}_1\mathbf{z}}W(z)\frac{e^{ik|\mathbf{z}-\mathbf{x}_i|}}{4\pi|\mathbf{z}-\mathbf{x}_i|}W(x_i),$$

$$K_2(\mathbf{x}_i,\mathbf{k}_2) = \int d\mathbf{z}\,\frac{e^{ik|\mathbf{x}_i-\mathbf{z}|}}{4\pi|\mathbf{x}_i-\mathbf{z}|}W(z)e^{i\mathbf{k}_2\mathbf{z}},$$

and $\Delta(k)$ is a certain function of k. The G_2 function has the same properties as G_1, and we therefore refrain from writing it out.

We have now reduced our study of the analytic properties of $T(k^2, t)$ to the study of Eqs. (6) and (7). Proceeding with Klein,[3] we write

$$\mathbf{k}' = k\,(\cos(\theta/2),\, -\sin(\theta/2),\, 0),$$

$$\mathbf{k}_1 = k_1\,(\sin\gamma\sin\varphi,\ \cos\gamma\sin\varphi,\ \cos\varphi),$$

where θ is the scattering angle, and make use of (3) – (5). It can then be shown, for example, that for potentials of the form

$$e^{-\alpha r}, \quad re^{-\alpha r}, \ldots, r^n e^{-\alpha r} \tag{8}$$

$T(k^2, t)$ can be analytically extended, for all real k^2, into the t-plane cut along the real axis from $4\alpha^2$ to ∞ with poles of different orders at $t = \alpha^2$ and $t = 4\alpha^2$.

We now write down the usual dispersion relation for $T(E, t)$ in the absence of bound states (with $E = k^2 + m^2$):

$$T(E, t) = \frac{(E-m)(E-E_0)}{\pi}\,\mathrm{P}$$
$$\times \int_m^\infty dE' \Big[\frac{\operatorname{Im} T(E', t)}{(E'-m)(E'-E_0)(E'-E-i\varepsilon)}$$
$$+ \frac{\operatorname{Im} T_a(E', t)}{(E'+m)(E'+E_0)(E'+E)} \Big]$$
$$+ \frac{m-E}{m-E_0}\operatorname{Re} T(E_0, t) + \frac{E-E_0}{m-E_0}\,T(m, t). \tag{9}$$

For potentials satisfying (8) this relation was obtained[1] for $-t < 4\alpha^2$. But both sides of (9) are analytic functions of t (for $E_0 > m$) for all t except the poles and the cut mentioned above. Hence (9) is valid for all t. Further, since the right side of (9) can be extended analytically into the complex E plane with cuts from $\pm m$ to $\pm\infty$, this equation establishes the analytic properties of $T(E, t)$ for complex E and complex t.

From these results we may now write the double dispersion relation

$$T(E, t) = \frac{(E-m)(E-E_0)}{\pi}$$
$$\times \Big[\mathrm{P} \int_m^\infty \frac{dE'}{(E'-E_0)(E'-m)(E'-E)} \int_{(2\alpha)^2}^\infty \frac{\rho_1(E', t')}{t'-t}\,dt'$$
$$+ \int_m^\infty \frac{dE'}{(E'+E_0)(E'+m)(E'+E)} \int_{(2\alpha)^2}^\infty \frac{\rho_2(E', t')}{t'-t}\,dt' \Big]$$
$$+ \frac{m-E}{m-E_0}\operatorname{Re} T(E_0, t) + \frac{E-E_0}{m-E_0}\,T(m, t), \tag{10}$$

where $\rho_{1,2}(E', t')$ are real functions describing respectively, scattering of particles and antiparticles.

Several results can be obtained from Eq. (10). First, one can establish the analytic properties of the partial wave amplitudes by using the formula

$$A_l(E) = \frac{1}{2}\int_{-1}^{+1} P_l(\cos\theta)\,T(E, t)\,d\cos\theta,$$

$$t = -2k^2(1-\cos\theta).$$

Further, by comparing the analytic properties of $\operatorname{Im} T(E, t)$ with those that would have been obtained for the imaginary part of the meson-nucleon scattering amplitude if Lehmann's[4] procedure had been used, one finds (letting the nucleon mass approach infinity) that the radius of the meson-nucleon interaction is $\rho = \alpha^{-1} = 0.86 \times 10^{-13}$ cm. We have obtained this result elsewhere[5] in a somewhat different way.

---

[1] V. I. Mal'chenko, Ukr. matem. zhurn. 11, 3 (1959).

[2] N. N. Khuri, Phys. Rev. 107, 1148 (1957).

[3] A. Klein (Preprint).

[4] H. Lehmann, Nuovo cimento 10, 578 (1958).

[5] V. I. Mal'chenko, Ukr. matem. zhurn. 4, 4 (1959).

Translated by E. J. Saletan
84

SOVIET PHYSICS JETP VOLUME 13, NUMBER 2 AUGUST, 1961

ON THE MECHANISM OF PHOTONUCLEAR REACTIONS

A. M. BADALYAN and A. I. BAZ'

Submitted to JETP editor July 18, 1960

J. Exptl. Theoret. Phys. (U.S.S.R.) 40, 549-552 (February, 1961)

A number of empirical laws cannot be explained by the statistical mechanism of photonuclear reactions if the energy of the gamma quantum is less than or equal to 10 Mev. The facts can be explained only by assuming that a few single-particle states of the target nuclei contribute significantly to the cross section of the photonuclear reaction. The nature of these states is discussed.

In the investigation of photonuclear reactions in heavy and medium-weight nuclei, a statistical model of the nucleus is usually employed, in which such general quantities as the level density $\rho(E)$, the nuclear temperature T, and the average values of various partial widths ($\overline{\Gamma}_\gamma$, $\overline{\Gamma}_n$, etc.) enter as parameters. The application of the statistical approach physically amounts to the assertion that a very large number of levels of the intermediate nucleus take part in the reaction, so that the cross sections become significant in spite of the fact that the contribution of each single level is small (since the average widths $\overline{\Gamma}$ are small).

However, another situation may also be considered, by which the reaction goes basically only via a small number of levels having large widths, for example, single-particle levels, the widths of which are close to the Weisskopf values. It is well known that the experimental values of the integral elastic and inelastic cross sections ($\sigma_{\gamma\gamma}$ and $\sigma_{\gamma\gamma'}$) for medium-weight and heavy nuclei seem to be of the order of 10 — 20 mb-Mev for energies in the interval 5 — 15 Mev. At the same time the integral cross section for elastic scattering ($\pi\Gamma\sigma_{\max}/2$) arising from a single single-particle level of width $\Gamma_\gamma \sim \Gamma \sim 100$ ev is also equal to ~ 10 mb-Mev for gamma-quantum energies of the order of 10 Mev. Thus, if single particle levels were located at a distance from each other of approximately 1 Mev, then they alone might explain the order of magnitude of the observed values of the cross sections.

There have been few experiments in which the interaction of gamma rays with nuclei in the energy range 5 — 15 Mev has been studied. These include measurements of the elastic scattering of gamma quanta,[1] inelastic scattering with the formation of isomers,[2] and the first information about nuclear absorption.[3] From the data available it is possible to arrive at the following conclusions.

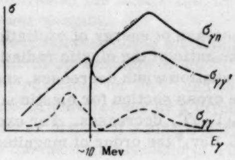

1. For the majority of elements there are definite peaks in the cross sections $\sigma_{\gamma\gamma}$ and $\sigma_{\gamma\gamma'}$ close to the thresholds for the reactions (γ, n) and (γ, p). The peak height is of the order of several millibarns, and its half-width $\Gamma \sim 1-3$ Mev. Usually in the medium weight nuclei the resonance in the cross section is associated with the (γ, p) threshold, and in heavy nuclei it is associated with the (γ, n) threshold.

2. The height and width of the peak vary irregularly from element to element[1] (see also the table).

3. A resonance in the absorption cross section has been observed. Data on nuclear absorption in the region below the threshold of (γ, n) reactions is available only for P, S, and Ca.[3]

Let us compare these results with the predictions of the statistical theory of nuclear reactions, which can be formulated as follows.

1. Nuclear reaction cross sections should be smooth functions of the atomic weight. However, the work of Fuller and Hayward[1] (see also the table) shows that in the scattering of gamma rays the individuality of nuclei appears very distinctly and cannot be explained on the basis of statistical considerations.

2. The cross section for elastic scattering ought to have the form of energy dependence schematically represented in the diagram. At first the cross section increases. However, on account of the rapid increase of the number of inelastic channels

Elastic scattering*				Inelastic scattering with the formation of isomers*			
Element	Threshold of the reaction: for (γ, n), E_n and for (γ, p), E_p	σ_{max}, mb	Position of the peak, Mev	Element	Threshold of the reaction (γ, n), Mev	σ_{max}, mb	Position of the peak, Mev
Mn	$E_n = 10.14, E_p = 9$	6	9				
Ni	$E_n = 12.8$	2.8	9.5	Y^{89}	11.8	1.3	10.5
Cu	$E_p = 6.13$	1.6	8	Rh^{103}**	9.35	5	9.3
Sn	$E_n = 6.1-9.2$	12	7	Ag^{107}	9.4	2.3	9
I	$E_n = 9.14$	2	7	In^{115}	9	1.9	8.9
Au	$E_n = 7.96$	3	—	Au^{197}	7.96	3.5	7.5
Pb	$E_n = 7.4$	17	7.4	Pb^{207}	6.9	Not observed	

*Experimental errors in the determination of the magnitude of the cross section (~1 mb) and the position of the maximum (~1 Mev) are not indicated in the table.

**Data from O. V. Bogdankevich and L. E. Lazareva.

with the increase of energy of excitation of the nucleus, the ratio of the elastic radiation width to the total radiation width decreases, and consequently the cross section for elastic scattering, $\sigma_{\gamma\gamma} = \sigma_{capt}\Gamma_\gamma/\Gamma$, decreases. For excitation energies $\gtrsim$ 5 Mev,[4] the order of magnitude of this quantity is:

$$\Gamma_\gamma/\Gamma = (\hbar\omega)^3/6\tau^4\rho(\hbar\omega) \sim 1\%$$

$[\rho(\hbar\omega) = \rho_0 e^{\hbar\omega/\tau}$ is the level density, and $\tau \approx 0.9$ Mev$]$.

In the energy range above 5 Mev the cross section for elastic scattering varies approximately as $(\hbar\omega)^4 e^{-\hbar\omega/\tau}$ (we assume that dipole absorption is taking place, that is,[5] $\sigma_{capt} \sim \hbar\omega$) with a maximum in the energy range ~4 Mev. The statistical theory is unable to explain the appearance of a maximum in $\sigma_{\gamma\gamma}$[1] in the immediate neighborhood of the nucleon threshold. A rapid decrease of the cross section with energy, correlated with the threshold for the formation of photoneutrons, is explained by the fact that the emission of nucleons is far more probable than the emission of gamma quanta.

3. The total cross section for inelastic scattering $\sigma_{\gamma\gamma'} = \sigma_{abs}\Gamma^{-1}\Sigma\Gamma_{\gamma'}$ ought to practically coincide with the absorption cross section for large excitation energies (below the neutron threshold), $\Sigma\Gamma_{\gamma'} \approx \Gamma$, and it ought to increase with increasing energy. Just above the nucleon threshold, $\sigma_{\gamma\gamma'}$ (see reference 6) falls rapidly at the expense of the appearance of the competing processes involving the ejection of nucleons. The sizes of the energy regions ΔE where the cross section is decreasing (refer to the figure) may be evaluated from the equation

$$\Gamma_n(\Delta E) \gtrsim \Gamma_\gamma(E_{thresh} + \Delta E).$$

For neutron thresholds we obtain from this $\Delta E \approx (\hbar^2/2MR^2)(\Gamma_\gamma/\gamma_n^2)^2$ (where R is the radius of the nucleus, and γ_n^2 is the reduced width for neutron emission). If, for example, one sets $\gamma_n^2 = 0.01\hbar^2/2MR^2$, then $\Delta E \sim 10$ kev. In the case of proton thresholds, the maximum of the cross section is located above the threshold, on account of the Coulomb barrier. Calculations show that for Z = 30 the maximum of the cross section ought to lie approximately 1 to 2 Mev above the proton threshold.

Thus, according to the statistical model, the maximum of the cross section for inelastic scattering ought to lie practically on the neutron threshold or a little above the proton threshold, and in any case, not below the thresholds. At present the accuracy in the determination of E_{max} is not great (± 1 Mev), and within these limits E_{max} usually coincides with E_{thresh}. However, in certain cases a displacement of the maxima into the region below the threshold is observed.[1] For example, in Y^{89}, $E_{max} \sim 10.5$ Mev, but $E_{thresh} = 11.8$ Mev.

4. The estimates given above show that in the statistical model, for $E \gtrsim 5$ Mev, the cross section $\sigma_{abs} \approx 100\sigma_{\gamma\gamma}$. Experiments[2] indicate, however, that $\sigma_{\gamma\gamma}$ is only a few times (2 to 10 times) smaller than the total absorption cross section, which is estimated by means of an extrapolation of the results on (γ, n) reactions.

Thus, the simple statistical model is incapable of explaining the results on photonuclear reactions in the range of excitation energy 5 to 10 Mev.

The contradiction between theory and experiment is, however, removed, if photonuclear reactions in the energy range considered are assumed to proceed fundamentally through only a few levels with large radiation widths. The strong levels near (γ, n) and (γ, p) thresholds observed in the cross sections of elastic and inelastic scattering correspond most closely to the so-called "threshold states," the existence of which has been predicted by one of us.[1] These states ought to have a single particle structure, and consequently, large radiation widths. A few "threshold" states with different moments and parities may be located close to the threshold for two-particle breakup of the nucleus.

This hypothesis explains in a natural manner a number of observations.

1. First, the very fact of the appearance of peaks in the cross sections of various photonuclear processes ($\sigma_{\gamma\gamma}$, $\sigma_{\gamma\gamma'}$, and σ_{abs}) near the thresholds of the reactions (γ, n), (γ, p), etc. The resonances observed[8] in the reactions $Zn^{64}(\gamma, d)Cu^{62}$ and $Zn^{66}(\gamma, d)Cu^{64}$ near the (γ, d) threshold may have such a "threshold" origin. According to reference 7, the threshold states may be shifted from the threshold on either side within an interval $E_{thresh} \pm (1 \text{ to } 2)$ Mev. Therefore, if further measurements confirm that the maxima in the cross sections are displaced relative to the neutron threshold, this will be a strong argument against the statistical model and for single-particle "threshold" states.

2. The irregular variation of the parameters (σ_{max}, Γ) as functions of the atomic weight. According to the results given in reference 7, the properties of "threshold states" depend strongly on the concrete structure of the nucleus.

3. The ratio of the magnitudes of elastic and inelastic scattering. This ratio is determined by the quantity $\Gamma_\gamma / \Sigma \Gamma_{\gamma'}$, and is, generally speaking, specific for each single particle (threshold) level. Thus $\sigma_{\gamma\gamma}$ may be of the order of $\sigma_{\gamma\gamma'}$ and in special cases may even exceed the cross section for inelastic scattering. (It is possible that such a situation, with $\Gamma_\gamma = \Gamma_{tot}$, was encountered in (γ, γ') scattering on Pb^{207}, when inelastic scattering was not observed at all.[9])

4. The absolute magnitudes of the cross sections $\sigma_{\gamma\gamma}$. Calculations by Kalinkin[10] based on the hypothesis that elastic scattering proceeds through separate single nucleon levels (nuclear fluorescence) led to satisfactory quantitative agreement with experiment.

Thus, the hypothesis presented above explains at least qualitatively the experimental results available at present.

The following should also be taken into consideration. The statistical model encounters difficulties in the attempt to explain the results on radiative capture of thermal neutrons.[11] Recently the idea of direct capture of the impinging neutron in the final level of the intermediate nucleus has become more and more attractive. Only in this way is it possible to understand why the spectrum of capture gamma rays contains exclusively strong lines corresponding to the capture of thermal neutrons in shell-model p-states in the final nucleus.

The presence of threshold states allows one to give another interpretation to the results on radiative capture. If these states actually exist, then the reaction (n, γ) would go basically through two stages: first the impinging neutron is captured in a single particle threshold state, and only after that a transition is made to lower levels, predominantly p-states. In the conception of "direct capture," the neutron, bypassing the first stage, immediately goes to the lower p-state.

The difference between these mechanisms is especially clear in the example of Pb^{208}. The results on (n, γ) reactions on Pb^{207} can be explained from two points of view: either by a direct process,[12] or by the existence of a single-particle s-state right on the neutron threshold of Pb^{208}. The results on $\gamma\gamma$-scattering prove directly the existence of such a level [$\sigma_{\gamma\gamma}$ has a strong peak at the threshold of the reaction $(\gamma, n)^1$]. In the conception of direct capture this level is absent.

We can conclude that in the energy range 5 — 10 Mev one statistical theory cannot explain satisfactorily the results of experiment, which indicate that in the course of reactions in this energy range an important role is played by a small number of very strong levels of the intermediate nucleus. Basically these levels are concentrated close to the threshold and appear to be "threshold" states. For example, in the light nuclei, such states ought to be found in the energy range 6.5 — 7.5 Mev in Li^7, 11 — 11.5 Mev in B^{11}, 18.3 — 18.9 Mev in C^{12}, 15 — 16 Mev in O^{16}, 6 — 6.4 Mev and 8 — 8.4 Mev in O^{18}, 5 — 5.6 Mev in Ne^{20}, etc.

---

[1] E. G. Fuller and E. Hayward, Phys. Rev. 101, 692 (1956).

[2] E. Silva and J. Goldemberg, Phys. Rev. 110, 1102 (1958). L. Schutzmeister and V. L. Telegdi, Phys. Rev. 104, 185 (1956). Bogdankevich, Lazareva, and Nikolaev, JETP 31, 405 (1956), Soviet Phys. JETP 4, 320 (1957).

[3] Dular, Kernel, Dregar, Mihailovič, Pregl, Rosina, and Zupančič, Nucl. Phys. 14, 131 (1959).

[4] Strutinskii, Groshev, and Akimova, JETP 38, 598 (1960), Soviet Phys. JETP 11, 430 (1960).

[5] J. Blatt and V. Weisskopf, Theoretical Nuclear Physics, Wiley 1952, Chapter 12.

[6] H. A. Bethe and J. Ashkin, Experimental Nuclear Physics, Vol. 1 (ed. E. Segre) Wiley (1953), Part 2.

[7] A. I. Baz', Adv. Phys. 8, 349 (1959).

[8] J. Goldemberg and L. Marquez, Nucl. Phys. 7, 202 (1958).

[9] Farinelli, Ferrero, Malvano, Menardi, and Silva, Phys. Rev. 112, 1994 (1958).

[10] B. N. Kalinkin, JETP 36, 1438 (1959), Soviet Phys. JETP 9, 1022 (1959).

[11] A. M. Lane and J. E. Lynn, Nucl. Phys., (to be published).

[12] A. V. Shut'ko and D. F. Zaretskii, JETP 29, 866 (1955), Soviet Phys. JETP 2, 769 (1956); D. F. Zaretskii, JETP 37, 1084 (1959), Soviet Phys. JETP 10, 772 (1960).

Translated by C. S. Littlejohn
85

SOVIET PHYSICS JETP VOLUME 13, NUMBER 2 AUGUST, 1961

BREMSSTRAHLUNG FROM A LONGITUDINALLY POLARIZED ELECTRON WITH ACCOUNT OF THE FINITE SIZE OF THE NUCLEUS

B. K. KERIMOV and F. S. SADYKHOV

Moscow State University

Submitted to JETP editor July 20, 1960

J. Exptl. Theoret. Phys. (U.S.S.R.) 40, 553-560 (February, 1961)

The effect of the finite size of the nucleus on the angular distribution of circularly-polarized bremsstrahlung emitted by a longitudinally polarized high-energy electron is considered. An expression for the angular distribution of external bremsstrahlung is derived by taking into account the mean square radius $\langle r^2 \rangle$ of the nuclear charge distribution and the longitudinal spin correlation between the initial electron state and emitted γ quantum. A formula is deduced for the effect of the finite nuclear size on the angular dependence of the degree of circular polarization of the bremsstrahlung.

1. INTRODUCTION

THE polarization correlation between the electron and the γ quantum in the bremsstrahlung of an electron in the Coulomb field of a point nucleus was considered in several papers.[1-7] It was shown that the bremsstrahlung quanta from a high-energy electron polarized in (or opposite to) the direction of motion have circular polarization, the degree of which may reach almost 100 percent near the upper limit of the spectrum.[1-5] It has been established experimentally that for a longitudinally polarized electron with kinetic energy ~ 2 Mev the degree of circular polarization of the bremsstrahlung reaches a maximum value ~ 95 percent in the upper end of the spectrum.[8-11] Thus, the theoretical results[1-5] on the polarization properties of the bremsstrahlung have proved to be in satisfactory agreement with the experimental data.

As shown by Olsen and Maximon,[5] the degree of circular polarization of bremsstrahlung quanta from a polarized high-energy electron is practically independent of the screening of the field of the nucleus and of the Coulomb corrections. Biel and Burhop[12] considered the bremsstrahlung of a relativistic electron in the Coulomb field of an extended nucleus without allowance for the polarized states of the incident electron and the emitted γ quantum, in the Born approximation. They have shown that when the electron has high energy ($E \gg m_0c^2$) the influence of the density of nuclear charge distribution on the angular distribution of the bremsstrahlung becomes appreciable in the region of γ-quantum emission angles $\theta > 10°$. An analysis of the influence of the finite dimensions of the nucleus on the polarization of the electrons in double scattering is the subject of a paper by Kerimov and Arutyunyan.[13]

In the present article we calculate in the Born approximation the angular dependence of the external bremsstrahlung of a relativistic electron with allowance for the finite dimensions of the nucleus and for the polarized states of the initial electron and of the emitted γ quantum. Formulas are derived for the dependence of the ratio of the cross section of circularly polarized bremsstrahlung from an extended nucleus to the cross section for a point nucleus on the angle of emission of the γ quantum and the mean square radius of the nucleus for a given value of energy of the longitudinally polarized electron. It can be expected that the experimental investigation of the formulas for the cross section of bremsstrahlung from polarized electrons in the region of high energies and angles can also yield definite information on the form factor and on the mean square radius of the distribution of the nuclear charge.

2. ANGULAR DISTRIBUTION OF POLARIZED RADIATION WITH ALLOWANCE FOR THE DIMENSION OF THE NUCLEUS

To take account of the finite dimensions of the nucleus, we shall use the form factor F(q) of the charge density distribution, for which we have, for not too high energies,

$$F(q) = \int_0^\infty \rho(r) \frac{\sin qr}{qr} 4\pi r^2 \, dr \approx 1 - \frac{1}{6} q^2 \langle r^2 \rangle. \qquad (1)$$

Here $\rho(r)$ is the density, $\langle r^2 \rangle$ is the mean square radius of the nuclear charge distribution, and $\hbar\mathbf{q}$ is the momentum transferred to the nucleus ($\mathbf{q} = \mathbf{k} - \mathbf{k}' - \boldsymbol{\kappa}$, $\boldsymbol{\kappa}$ is the photon wave vector). At electron energies from 20 to 100 Mev we can confine ourselves to the first two terms of the expansion of $F(q)$ (see reference 14) and obtain a bremsstrahlung cross section that depends only on the mean square of the nuclear radius. At very high electron energies it is necessary to take into account the higher moments of the nuclear charge density.

The longitudinal polarization of an electron with momentum $\mathbf{p} = \hbar\mathbf{k}$ is described by the eigenvalue $s = \pm 1$ of the projection operator $(\boldsymbol{\sigma} \cdot \mathbf{p}/p)\psi = s\psi$ (see references 15 and 1). When $s = 1$ we have a right-hand polarized electron (the spin is in the direction of the motion), and when $s = -1$ the polarization is left hand (spin opposite to the direction of motion). Circular polarization of the bremsstrahlung is characterized by a photon field polarization vector (see references 15 and 1)*

$$\mathbf{a} = \frac{1}{\sqrt{2}} \sum_{l=\pm 1} (\boldsymbol{\beta} + il\,[\boldsymbol{\varkappa}^0 \boldsymbol{\beta}]).$$

Here

$$\boldsymbol{\beta} = [\boldsymbol{\varkappa}^0 \mathbf{j}] / \sqrt{1 - (\boldsymbol{\varkappa}^0 \mathbf{j})^2},$$

$\boldsymbol{\kappa}^0 = \boldsymbol{\kappa}/\kappa$ is a unit vector in the direction of emission of the bremsstrahlung photon, $\mathbf{j}$ is a unit vector of arbitrary direction, $l = \pm 1$ describes the circular polarization of the radiated γ quantum; $l = 1$ for a γ quantum with right-hand polarization and -1 for left-hand polarization.

In the Born approximation we obtain from reference 1, with the aid of formulas (2) — (10), the following expression for the differential cross section of the external bremsstrahlung of the electron, with allowance for the form factor of the nucleus and the longitudinal polarizations of the electron (in the initial and final states) and of the emitted γ quantum

$$d\sigma_{lss'}(\theta, \theta')\, d\Omega\, d\Omega' = |F(q)|^2 \Big\{ \frac{1}{4}\, d\sigma_{\mathbf{B-H}}(\theta, \theta') + \frac{a_T}{8q^4} [ss' f_1(\theta, \theta') + ls f_2(\theta, \theta') + ls' f_3(\theta, \theta')] \Big\}\, d\Omega\, d\Omega'. \tag{2}$$

Here

$$f_1(\theta, \theta') = \frac{1}{2kk'} \Big\{ [2(k_0^2 + KK')(4K'^2 - q^2) - 4k_0^2(3K'^2 + K^2)] \frac{k^2 \sin^2\theta}{\Delta^2} + [2(k_0^2 + KK')$$

$$(4K^2 - q^2) - 4k_0^2(3K^2 + K'^2)] \frac{k'^2 \sin^2\theta'}{\Delta'^2}$$

$$- 2[2(k_0^2 + KK')(4KK' + 2\varkappa^2 - q^2) - 4k_0^2(K + K')^2] \frac{kk' \sin\theta \sin\theta' \cos(\varphi' - \varphi)}{\Delta\Delta'}$$

$$+ 16k_0^2\varkappa^2 \frac{KK'}{\Delta\Delta'} + 4\varkappa^2 KK' \frac{k^2 \sin^2\theta + k'^2 \sin^2\theta'}{\Delta\Delta'}$$

$$+ 4\varkappa k_0^2 (K + K') \Big(\frac{1}{\Delta^2} - \frac{1}{\Delta'^2} \Big) kk' \sin\theta \sin\theta' \cos(\varphi' - \varphi)$$

$$+ 4\varkappa k_0^2 \frac{K + K'}{\Delta\Delta'} (k^2 \sin^2\theta - k'^2 \sin^2\theta') - 4\varkappa^2 k_0^2 \Big(\frac{K'}{\Delta'} + \frac{K}{\Delta} \Big)$$

$$- 4\varkappa^2 k_0^2 \Big[\frac{K'(K' + k' \cos\theta')}{\Delta^2} + \frac{K(K + k\cos\theta)}{\Delta'^2} \Big] \Big\},$$

$$f_2(\theta, \theta') = \frac{2}{k} \Big\{ [\varkappa K(k\cos\theta + k'\cos\theta') - \varkappa^2 K + \varkappa k_0^2] \frac{k^2 \sin^2\theta}{\Delta^2} + [\varkappa K(k\cos\theta + k'\cos\theta')$$

$$+ \varkappa^2 K - \varkappa k_0^2] \frac{k'^2 \sin^2\theta'}{\Delta'^2}$$

$$- 2\varkappa K(k\cos\theta + k'\cos\theta') \frac{kk' \sin\theta \sin\theta' \cos(\varphi' - \varphi)}{\Delta\Delta'}$$

$$+ \varkappa(\varkappa K - k_0^2) \frac{k^2 \sin^2\theta - k'^2 \sin^2\theta'}{\Delta\Delta'}$$

$$- \varkappa^2 k_0^2 \frac{k^2 \sin^2\theta - k'^2 \sin^2\theta'}{\Delta^2\Delta'}$$

$$- \varkappa k_0^2 \Big(\frac{1}{\Delta^2} - \frac{1}{\Delta'^2} \Big) kk' \sin\theta \sin\theta' \cos(\varphi' - \varphi) \Big\},$$

$$f_3(\theta, \theta') = \frac{2}{k'} \Big\{ [\varkappa K'(k'\cos\theta' + k\cos\theta) - \varkappa^2 K' - \varkappa k_0^2] \times \frac{k^2 \sin^2\theta}{\Delta^2} + [\varkappa K'(k'\cos\theta' + k\cos\theta) + \varkappa^2 K'$$

$$+ \varkappa k_0^2] \frac{k'^2 \sin^2\theta'}{\Delta'^2}$$

$$- 2\varkappa K' \frac{(k\cos\theta + k'\cos\theta')}{\Delta\Delta'} kk' \sin\theta \sin\theta' \cos(\varphi' - \varphi)$$

$$+ \varkappa k_0^2 \Big(\frac{1}{\Delta^2} - \frac{1}{\Delta'^2} \Big) kk' \sin\theta \sin\theta' \cos(\varphi' - \varphi)$$

$$- \varkappa(\varkappa K' + k_0^2) \frac{k^2 \sin^2\theta - k'^2 \sin^2\theta'}{\Delta\Delta'}$$

$$- \varkappa^2 k_0^2 \frac{k^2 \sin^2\theta - k'^2 \sin^2\theta'}{\Delta\Delta'^2} \Big\}; \tag{3}$$

$$\Delta = K - k\cos\theta, \qquad \Delta' = K' - k'\cos\theta',$$

$$K = \sqrt{k^2 + k_0^2}, \qquad K' = \sqrt{k'^2 + k_0^2},$$

$$q^2 = k^2 + k'^2 + \varkappa^2 - 2k\varkappa\cos\theta + 2k'\varkappa\cos\theta' - 2kk'(\cos\theta\cos\theta' + \sin\theta\sin\theta'\cos(\varphi' - \varphi)),$$

$$\cos\theta = \frac{\mathbf{k}\boldsymbol{\varkappa}}{k\varkappa}, \qquad \cos\theta' = \frac{\mathbf{k}'\boldsymbol{\varkappa}}{k'\varkappa}, \qquad a_T = Z^2\alpha^3 \frac{k'\,d\varkappa}{2\pi^2 k\varkappa}. \tag{4}$$

Here $E = c\hbar K$, $p = \hbar k$ and $E' = c\hbar K'$, $p' = \hbar k'$ are the total energy and momentum of the electron before and after radiation, respectively; $\epsilon_\gamma = c\hbar\kappa = c\hbar(K - K')$ and $\mathbf{p}_\gamma = \hbar\boldsymbol{\kappa}$ are the energy and momentum of the radiated γ quantum; $k_0 = m_0 c/\hbar$ is the rest mass of the electron; α is the fine-structure constant; $d\Omega$ and $d\Omega'$ are the solid angles of the direction of the electron momentum before and after radiation; $s' = \pm 1$ is the eigenvalue of the projection operator $\boldsymbol{\sigma}\cdot\mathbf{p}'/p'$, which characterizes the longitudinal polarization of the electron in the final state.

---

*$[\boldsymbol{\varkappa}^0 \boldsymbol{\beta}] = \boldsymbol{\varkappa}^0 \times \boldsymbol{\beta}$.

In Eq. (2), $d\sigma_{\mathrm{B-H}}(\theta, \theta')$ is the known cross section of the unpolarized bremsstrahlung, given by formula (25.13) of Heitler's book,[16] the terms proportional to ls and ls' define the longitudinal spin correlation between the radiated γ quantum and the electron in the initial and final states, respectively, and the term proportional to ss' characterizes the correlation between the longitudinal polarizations of the electron in the initial and final states.

Summing (2) over the final spin states of the electron, we obtain a formula for the differential bremsstrahlung cross section with allowance for the form factor and the spin correlation between the electron and the γ quantum $(\sim ls)$:

$$d\sigma_{ls}(\theta, \theta')\, d\Omega\, d\Omega' = |F(q)|^2 \left\{\frac{1}{2}\, d\sigma_{\mathrm{B-H}}(\theta, \theta') + ls\, \frac{a_T}{4q^4} f_2(\theta, \theta')\right\} d\Omega\, d\Omega'. \tag{5}$$

Integrating (5) over the solid angle $d\Omega'$ of the scattered electron with allowance of (1), we obtain the following expression for the angular distribution of the circularly-polarized bremsstrahlung from the longitudinally-polarized electron, with allowance for the finite dimensions of the nucleus:

$$\begin{aligned} d\sigma_{ls}(\theta, \langle r^2\rangle)\, d\Omega &= d\sigma^T_{ls}(\theta)\, d\Omega \\ &- 2\pi a_T \{\langle r^2\rangle [\Phi_2(\theta) + ls\, \Phi_3(\theta)] \\ &- \langle r^2\rangle^2 [\Phi_4(\theta) + ls\, \Phi_5(\theta)]\}\, d\Omega. \end{aligned} \tag{6}$$

Here

$$\begin{aligned} \Phi_2(\theta) = \frac{1}{3}\Bigg\{ & \frac{k_0^2(k^2 + 2K^2)}{2k^2\Delta^2} - [\varkappa^2 k^2 K' \\ & + 2T^2 K(k^2 + K^2)]\, \frac{1}{2k^2 T^2 \Delta} \\ & + \frac{3T^2 + \varkappa^2}{2T^2} - \frac{\varepsilon^T}{2k'T}\left(\frac{2k_0^2 K'^2}{\Delta^2} + \frac{\varkappa^3\Delta}{T^2} + \frac{\varkappa^2}{T^2}(\varkappa K' + k'^2)\right) \\ & + \frac{\varepsilon}{2k'}\left(\frac{K^2 + K'^2}{\Delta} - K'\right) \\ & + \frac{L_0}{2kk'}\left[\frac{k_0^2 K}{k^2\Delta^2}(\varkappa k_0^2 + k^2 K') - \frac{\varkappa k_0^2 K^2}{k^2\Delta} - \frac{\varkappa^2}{2}\right]\Bigg\}, \end{aligned}$$

$$\begin{aligned} \Phi_3(\theta) = \frac{1}{6k}\Bigg\{ & \frac{\varkappa^2 K}{T^2} - \frac{\varkappa^2 K K'}{T^2\Delta} - \frac{4\varkappa K^3}{k^2\Delta} + \varkappa k_0^2\, \frac{2K^2 + k^2}{k^2\Delta^2} \\ & + \frac{\varkappa(K^2 + k_0^2)}{k^2} + \frac{\varkappa\varepsilon^T}{k'T}\left[\frac{2k_0^2 K'}{\Delta} - \frac{2k_0^2 K K'}{\Delta^2} - \frac{\varkappa^2 K\Delta}{T^2} \right. \\ & \left. - \varkappa K(\varkappa K' + k'^2)\, \frac{1}{T^2}\right] + \frac{L_0}{2kk'}\left[\frac{2k_0^2 K(\varkappa k_0^2 + k^2 K')\varkappa}{k^2\Delta^2} \right. \\ & \left. - \frac{2k_0^2(2\varkappa K^2 + k^2 K)\varkappa}{k^2\Delta} + \frac{\varkappa^2 K(K^2 + k_0^2)}{k^2}\right] \\ & + \frac{\varepsilon\varkappa}{k'}\left[\frac{K}{\Delta}(K + K') - K\right]\Bigg\}, \end{aligned}$$

$$\begin{aligned} \Phi_4(\theta) = \frac{1}{36}\Bigg\{ & k_0^2\left[\frac{1}{2}(T^2 + k'^2) - 2K'^2\right]\frac{1}{\Delta^2} + [KK'(K + 2K') \\ & - \varkappa k'^2 - T^2(\varkappa + K' \sin^2\theta)]\, \frac{1}{\Delta} + (K + K')\,\Delta \\ & - (k_0^2 + 2(2K^2 + K'^2)) + \frac{\varepsilon}{k'}[k_0^2(2KK' - K^2 - K'^2 \\ & + T^2 \sin^2\theta)\, \frac{1}{\Delta} - \frac{1}{2}(K^2 + K'^2 + k_0^2)\,\Delta \\ & + K(K^2 + K'^2) + \frac{3}{2} k_0^2 K']\Bigg\}, \end{aligned}$$

$$\begin{aligned} \Phi_5(\theta) = \frac{1}{72k}\Bigg\{ & - \varkappa k_0^2(4k_0^2 + k'^2 + T^2)\, \frac{1}{\Delta^2} \\ & + 2\varkappa K[4k_0^2 + K'(K + K')]\, \frac{1}{\Delta} \\ & + 6\varkappa\Delta K - 2\varkappa(2KK' + 6K^2 - k_0^2) + \frac{\varepsilon}{k'}\left[- \frac{2k_0^2\varkappa^2 K}{\Delta} \right. \\ & \left. - \varkappa(k^2 + KK')\,\Delta + \varkappa(2K^3 + K'(2k^2 - k_0^2))\right]\Bigg\}; \end{aligned} \tag{7}$$

$$\begin{gathered} d\sigma^T_{ls}(\theta) = \tfrac{1}{2}\, d\sigma_{\mathrm{B-H}}(\theta) + ls\cdot 2\pi a_T \Phi_1(\theta), \\ d\sigma_{\mathrm{B-H}}(\theta) = 4\pi a_T \Phi_0(\theta); \\ T = |\mathbf{k} - \boldsymbol{\varkappa}|, \qquad \varepsilon = \ln\frac{K' + k'}{K' - k'}, \qquad \varepsilon^T = \ln\frac{T + k'}{T - k'}, \\ L_0 = \ln\frac{KK' + kk' - k_0^2}{KK' - kk' - k_0^2}. \end{gathered} \tag{8}$$

$d\sigma^T_{ls}(\theta)$ is the cross section of the circularly-polarized bremsstrahlung, emitted by the longitudinally-polarized electron in the field of the point nucleus, and given by formula (17) of reference 1. The functions $\Phi_0(\theta)$ and $\Phi_1(\theta)$, which are included in (8), are determined by formulas (18) and (19) of reference 1; $d\sigma_{\mathrm{B-H}}(\theta)$ is the Bethe-Heitler bremsstrahlung cross section integrated over the angles of the scattered electron [see reference 1, formula (18)]. The terms proportional to $\langle r^2\rangle$ and $\langle r^2\rangle^2$ represent the corrections to the cross section of the bremsstrahlung from the longitudinally-polarized electron, due to the finite dimensions of the nucleus. These corrections account for the influence of the finite dimensions of the nucleus on the polarization correlation $(\sim ls)$ and the usual angular correlation $[\sim \Phi_2(\theta)$ and $\Phi_4(\theta)]$ between the electron and the γ quantum in bremsstrahlung. If only one correction term, corresponding to the region of not very large energies $(qr < 1)$ is taken into account in the form factor, it is possible to neglect the Coulomb effect in the circular polarization of the bremsstrahlung.

After averaging over the polarizations of the incident electron and summing over the polarizations of the emitted γ quantum, we obtain from (6)

$$\begin{aligned} d\sigma(\theta, \langle r^2\rangle)\, d\Omega = d\sigma_{\mathrm{B-H}}(\theta)\, d\Omega - 4\pi a_T\, \{\langle r^2\rangle\, \Phi_2(\theta) \\ - \langle r^2\rangle^2\, \Phi_4(\theta)\}\, d\Omega. \end{aligned} \tag{9}$$

Formula (9) describes the angular distribution of the unpolarized bremsstrahlung with allowance for the mean square radius $\langle r^2 \rangle$ of the distribution of the nuclear charge. As $\langle r^2 \rangle \to 0$ (Coulomb center concentrated in a point), formula (6) goes into $d\sigma_{\text{B-H}}(\theta)$. Thus, the cross section (6) obtained is a generalization of the known bremsstrahlung of an electron on a point nucleus with allowance for the longitudinal polarization of the spins of the electron and of the emitted γ quantum for finite nuclear dimensions.

3. DEGREE OF POLARIZATION OF RADIATION WITH ALLOWANCE FOR THE DIMENSIONS OF THE NUCLEUS

According to (6) and (8), the cross section of the circularly polarized bremsstrahlung emitted by a longitudinally-polarized electron in the field of a nucleus of finite dimensions is connected with the cross section in the field of a point nucleus $d\sigma_{ls}^T(\theta)$ by the relation

$$d\sigma_{ls}(\theta, \langle r^2 \rangle) = d\sigma_{ls}^T(\theta)\left\{1 - \langle r^2 \rangle \frac{\Phi_2(\theta) + ls\,\Phi_3(\theta)}{\Phi_0(\theta) + ls\,\Phi_1(\theta)} + \langle r^2 \rangle^2 \frac{\Phi_4(\theta) + ls\,\Phi_5(\theta)}{\Phi_0(\theta) + ls\,\Phi_1(\theta)}\right\}. \tag{10}$$

In the case of unpolarized bremsstrahlung we have in lieu of (10)

$$d\sigma(\theta, \langle r^2 \rangle) = d\sigma_{\text{B-H}}(\theta)\left\{1 - \langle r^2 \rangle \frac{\Phi_2(\theta)}{\Phi_0(\theta)} + \langle r^2 \rangle^2 \frac{\Phi_4(\theta)}{\Phi_0(\theta)}\right\}. \tag{11}$$

If the longitudinal polarization of the electron is fixed ($s = 1$ or -1), the degree of polarization of the bremsstrahlung, corresponding to the two types of circular polarization ($l = \pm 1$) of the radiated quantum, can be determined from the formula

$$P(\theta, \langle r^2 \rangle) = (\{d\sigma_{ls}\}_{l=1} - \{d\sigma\ _s\}_{l=-1}) / (\{d\sigma_{ls}\}_{l=1} + \{d\sigma_{ls}\}_{l=-1}). \tag{12}$$

From this, using (10), we obtain for the degree of circular polarization of the bremsstrahlung on a nucleus of finite dimensions

$$P(\theta, \langle r^2 \rangle) = sP^T(\theta) \frac{1 - \langle r^2 \rangle d_3(\theta) + \langle r^2 \rangle^2 d_5(\theta)}{1 - \langle r^2 \rangle d_2(\theta) + \langle r^2 \rangle^2 d_4(\theta)}, \tag{13}$$

where

$$d_3(\theta) = \Phi_3(\theta)/\Phi_1(\theta), \qquad d_5(\theta) = \Phi_5(\theta)/\Phi_1(\theta),$$
$$d_2(\theta) = \Phi_2(\theta)/\Phi_0(\theta), \qquad d_4(\theta) = \Phi_4(\theta)/\Phi_0(\theta),$$
$$P^T(\theta) = \Phi_1(\theta)/\Phi_0(\theta). \tag{14}$$

Here $P^T(\theta)$ is the degree of circular polarization of the bremsstrahlung produced by a longitudinally-polarized electron in the Coulomb field of a point nucleus [see reference 1, formula (20)].

Formulas (10), (11), and (13) describe, at high energies, the influence of the finite dimensions of the nucleus on the angular dependence of the cross section, and also the influence of the degree of circular polarization of the bremsstrahlung from a longitudinally-polarized electron in the Born approximation. We can use here for the mean square radius $\langle r^2 \rangle$ of the nucleus the value obtained from experiments on the scattering of high-energy electrons by nuclei.[14] In the extreme relativistic case (e.r.) of high energies, when $E, E' \gg m_0c^2$, the functions $\Phi_i(\theta)$, which determine the angular dependence of the cross section and of the polarization, become much simpler and we obtain for them the following expressions

$$\Phi_2^{\text{e.r.}}(\theta) = \frac{1}{6}\left\{3 + \frac{a^2b^2k_0^2}{T^2} - \left[4 + a^2b^2(1-a)\frac{k_0^2}{T^2}\right]\frac{1}{\Delta_0} - \frac{\varepsilon^T a^2 b^3 k_0^3}{T^3(1-a)}(1 - a\cos\theta) - \frac{a^2\varepsilon'}{2(1-a)} + \varepsilon\left(\frac{1}{\Delta_0} - \frac{1}{2}\right)\frac{2 - 2a + a^2}{1-a}\right\},$$

$$\Phi_3^{\text{e.r.}}(\theta) = \frac{a}{6}\left\{1 + \frac{ab^2k_0^2}{T^2} - \left[4 + a(1-a)\frac{b^2k_0^2}{T^2}\right]\frac{1}{\Delta_0} - \frac{\varepsilon^T ab^3k_0^3}{T^3(1-a)}\left(1 - a\cos\theta\right) + \frac{a\varepsilon'}{2(1-a)} + \frac{\varepsilon}{1-a}\left[\frac{2-a}{\Delta_0} - \left(1 - \frac{a}{2}\right)\right]\right\},$$

$$\Phi_4^{\text{e.r.}}(\theta) = \frac{1}{36}\Big\{-2k_0^2b^2(3 - 2a + a^2) + b^2k_0^2(2-a)\Delta_0 + [b^2k_0^2(1-a)(3 - 3a + a^2) - T^2(a + (1-a)\sin^2\theta)]\frac{1}{\Delta_0} - k_0^2\frac{(1-a)^2}{\Delta_0^2} + \frac{\varepsilon}{b^2(1-a)}\Big[(T^2\sin^2\theta - a^2b^2k_0^2)\frac{1}{\Delta_0} - k_0^2b^4(2 - 2a + a^2)\left(\frac{\Delta_0}{2} - 1\right)\Big]\Big\},$$

$$\Phi_5^{\text{e.r.}}(\theta) = \frac{abk_0}{36}\left\{-2\,bk_0(4-a) + 3bk_0\Delta_0 + bk_0(2 - 3a + a^2)\frac{1}{\Delta_0} - \frac{k_0(1-a)}{b\Delta_0^2} - \frac{\varepsilon k_0}{2(1-a)}\left[\frac{2a}{b\Delta_0} - (2-a)(1 + \cos\theta)\right]\right\};$$

$$a = \frac{\varepsilon_\gamma}{E}, \qquad b = \frac{E}{m_0c^2}, \qquad \varepsilon^T = \ln\frac{T + (1-a)}{T - (1-a)},$$
$$\varepsilon = 2\ln[2b(1-a)], \quad \varepsilon' = -2\ln a, \qquad \Delta_0 = 1 - \cos\theta,$$
$$T = k_0 b\sqrt{1 + a^2 - 2a\cos\theta},$$
$$1/k_0 = \hbar/m_0c = 3.86 \cdot 10^{-11}\ \text{cm}.$$

Here $E = cp$ is the kinetic energy of the extreme-relativistic electron, ϵ_γ is the energy of the bremsstrahlung quantum. We do not give here the functions $\Phi_0^{\text{e.r.}}(\theta)$ and $\Phi_1^{\text{e.r.}}(\theta)$ for a point-like center, since these are readily derived from (18) and (19) of reference 1 by assuming ϵ_γ, E, and $E' \gg m_0c^2$.

To illustrate the derived formulas (10), (11), and (13), let us estimate the role of finite nuclear dimensions in the case of bremsstrahlung of both a polarized and an unpolarized electron on the nucleus of Ag^{108}. The mean-square radius of Ag^{108}, determined from electron-scattering experiments, is (see reference 14)

$$\langle r^2 \rangle = 19.594 \cdot 10^{-26} \ \text{cm}^2.$$

It was observed experimentally that the left-polarized electron of high energy ($s = -1$) from β emitters radiates predominantly bremsstrahlung quanta with left-hand circular polarization ($l = -1$, quantum spin opposite to quantum direction).[8–11] For a right-polarized high-energy electron ($s = 1$) the emitted bremsstrahlung quanta should have right-hand circular polarization ($l = 1$, quantum spin parallel to the direction of motion).

Figure 1 shows the dependence of the cross section ratios

$$I_1 = d\sigma_{ls}(\theta, \langle r^2 \rangle)/d\sigma_{ls}^T(\theta),$$
$$I_2 = d\sigma(\theta, \langle r^2 \rangle)/d\sigma_{\text{B-H}}(\theta) \qquad (15)$$

on the angle of emission θ of the bremsstrahlung quanta for the incident-electron and radiated-photon energies $E = 50$ Mev and $\epsilon_\gamma = 25$ Mev, and for $s = 1$ and $l = 1$ (or $s = -1$, $l = -1$). Figure 2 shows the dependence of the degree of circular polarization of the bremsstrahlung for an extended nucleus, $P(\theta, \langle r^2 \rangle)$ and for a point nucleus $P^T(\theta)$ on the angle of emission θ of the bremsstrahlung quanta with $E = 50$ Mev, $\epsilon_\gamma = 25$ Mev, and $s = 1$.

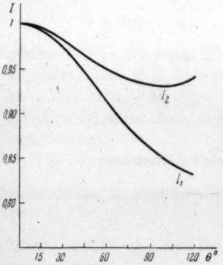

FIG. 1. Dependence of the cross-section ratios (15) on the angle of emission θ of the bremsstrahlung quanta, for Ag^{108} with $E = 50$ Mev, $\varepsilon_\gamma = 25$ Mev, $s = 1$, and $l = 1$.

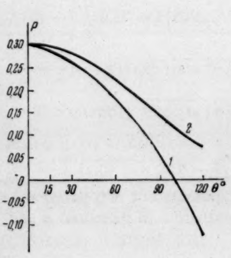

FIG. 2. Dependence of the degree of circular polarization of radiation, P, on the angle of emission θ of bremsstrahlung quanta with $E = 50$ Mev, $\varepsilon_\gamma = 25$ Mev, and $s = 1$: curve 1 – $P(\theta, r^2)$ for Ag^{108}, curve 2 – $P^T(\theta)$.

It is seen from Fig. 1 that allowance for the finite dimensions of the nucleus exerts a greater influence on the angular distribution of the circularly-polarized bremsstrahlung (curve I_1) than on the angular distribution of unpolarized bremsstrahlung (curve I_2). For small values of the angle, $\theta < 10°$, the cross section of the bremsstrahlung on an extended nucleus, $d\sigma_{ls}(\theta, \langle r^2 \rangle)$, coincides with the cross section for a point-like center $d\sigma_{ls}^T(\theta)$. When the angle θ exceeds 10°, the cross section ratio for the extended and point-like centers is greatly reduced.

As can be seen from Fig. 2, allowance for the finite dimensions of the nucleus leads to a noticeable reduction in the degree of circular polarization of the bremsstrahlung. In the range of larger angles of emission of the bremsstrahlung quanta ($\theta > 10°$) the deviations of the polarization $P(\theta, \langle r^2 \rangle)$ for an extended nucleus from the polarization $P^T(\theta)$ for a point-like nucleus are quite noticeable. In view of the lack of experimental data on bremsstrahlung of polarized high-energy electrons, we cannot as yet estimate the accuracy of the resultant formulas. However, the result obtained can serve as an indication that the effects of the finite dimensions of the nucleus may contribute greatly to the cross section and to the circular polarization of the bremsstrahlung produced by longitudinally-polarized high-energy electrons.

In conclusion, we thank Prof. A. A. Sokolov for continuous interest in this work.

---

[1] B. K. Kerimov and I. M. Nadzhafov, Izv. Akad. Nauk SSSR, Ser. Fiz. **22**, 886 (1958), Columbia Tech. Transl. p. 879.

[2] K. W. McVoy, Phys. Rev. **110**, 1484 (1958) and **111**, 1333 (1958).

[3] H. Banerjee, Phys. Rev. **111**, 532 (1958).

[4] C. Fronsdal and H. Überall, Phys. Rev. **111**, 580 (1958).

[5] H. Olsen and L. C. Maximon, Phys. Rev. **110**, 589 (1958) and **114**, 887 (1959).

[6] A. A. Kresin, JETP **37**, 872 (1959), Soviet Phys. JETP **10**, 621 (1960).

[7] Vysotskiĭ, Kresin, and Rozentsveĭg, JETP **32**, 1078 (1957), Soviet Phys. JETP **5**, 883 (1957).

[8] Goldhaber, Grodzins, and Sunyar, Phys. Rev. **106**, 826 (1957).

[9] S. Galster and H. Schopper, Phys. Rev. Lett. **1**, 330 (1958).

[10] A. Bisi and L. Zappa, Phys. Rev. Lett. 1, 332 (1958); Nucl. Phys. 10, 331 (1959).

[11] L. A. Page, Revs. Modern Phys. 31, 759 (1959).

[12] S. J. Biel and E. H. Burhop, Proc. Phys. Soc. A68, 165 (1955).

[13] B. K. Kerimov and V. M. Arutyunyan, JETP 38, 1798 (1960), Soviet Phys. JETP 11, 1294 (1960).

[14] R. Hofstadter, Revs. Modern Phys. 28, 214 (1956). Ann. Rev. Nucl. Sci. 7, 231 (1957).

[15] A. A. Sokolov, Введение в квантовую электродинамику, (Introduction to Quantum Electrodynamics), Fizmatgiz, 1958, Secs. 20 and 21.

[16] W. Heitler, The Quantum Theory of Radiation, Oxford, 1954, Sec. 25.

Translated by J. G. Adashko
86

SOVIET PHYSICS JETP VOLUME 13, NUMBER 2 AUGUST, 1961

THE DOPPLER WIDTH OF EMISSION AND ABSORPTION LINES

M. I. PODGORETSKII and A. V. STEPANOV

Joint Institute for Nuclear Research and P. N. Lebedev Physics Institute,
Academy of Sciences, U.S.S.R.

Submitted to JETP editor, August 3, 1960

J. Exptl. Theoret. Phys. (U.S.S.R.) 40, 561-566 (February, 1961)

We give a classical and quantum mechanical treatment of the influence of the Doppler effect on line shape. We consider the possibility of experimental observation of resonance absorption of γ rays in liquids.

THE purpose of the present work is to discuss certain features of the resonance absorption of γ rays and slow neutrons in liquids, where, since we have as our purpose only the formulation of the problems, we consider a highly idealized model of the liquid.

For a more pictorial description of the fundamental features of the phenomenon, it is logical to begin the treatment from the classical point of view. Let us assume that a certain system (an atom, nucleus, or other object) is part of a macroscopic system, and that it radiates electromagnetic waves of frequency ω_0. Then if the projection of its radius vector on the direction of emission changes as $x = x(t)$, the electromagnetic field can be written as

$$A \sim \exp[-i\omega_0 t - \lambda t/2 + i\varkappa x(t)], \qquad (1)$$

where $1/\lambda$ is the mean life, and κ is the wave number. Here it is assumed that a collision of the radiating atom with other atoms does not change its internal state, i.e., does not lead to collision broadening.

The corresponding Fourier component is

$$B \sim \int_0^\infty dt \exp\left[i\Omega t + i\varkappa x(t) - \frac{\lambda t}{2}\right],$$

where $\Omega = \omega - \omega_0$, and the spectral intensity is

$$J(\Omega) \sim \int_0^\infty\int_0^\infty dt\,dt' \exp\Big\{i\Omega(t-t') - \frac{\lambda}{2}(t+t')\Big\}\,\overline{\exp\{i\varkappa[x(t)-x(t')]\}}.$$

The quantity $\overline{\exp\{i\kappa[x(t) - x(t')]\}}$ is given by

$$\overline{\exp\{i\varkappa[(x(t)-x(t')]\}} = 1 + i\varkappa\,\overline{[x(t)-x(t')]} - \frac{\varkappa^2}{2!}\overline{[x(t)-x(t')]^2} - \frac{i\varkappa^3}{3!}\overline{[x(t)-x(t')]^3} + \cdots.$$

Assuming that the stochastic quantity $x(t) - x(t')$ has a Gaussian distribution, we obtain

$$\overline{\exp\{i\varkappa[x(t)-x(t')]\}} = 1 - \frac{\varkappa^2}{2!}\overline{[x(t)-x(t')]^2} + \frac{\varkappa^4}{4!}\overline{[x(t)-x(t')]^4} - \ldots = 1 - \left[\frac{\varkappa^2\sigma^2(|t-t'|)}{4}\right] + \frac{1}{2!}\left[\frac{\varkappa^2\sigma^2(|t-t'|)}{4}\right]^2 - \ldots = \exp\{-\varkappa^2\sigma^2(|t-t'|)/4\},$$

where

$$\sigma^2(|t-t'|)/2 = \overline{[x(t)-x(t')]^2}.$$

For the spectral intensity, we have the expression

$$J(\Omega) \sim \int_0^\infty\int_0^\infty dt\,dt' \exp\Big\{i\Omega(t-t') - \frac{\lambda}{2}(t+t') - \frac{\varkappa^2}{4}\sigma^2(|t-t'|)\Big\},$$

which, after some simple transformations, can be written as

$$J(\Omega) \sim \operatorname{Re}\int_0^\infty d\tau \exp\Big\{-i\Omega\tau - \frac{1}{2}\lambda\tau - \frac{1}{4}\varkappa^2\sigma^2(\tau)\Big\}. \qquad (2)$$

This relation describes the shape of the absorption line. In the classical case in which we are interested, it also follows immediately from Kirchhoff's theorem.* Relations like (2) can not only be used for the emission, absorption and scattering of photons, but also are applicable to particles, for example neutrons. However at this point it is more appropriate to go over to a quantum treatment, which we shall carry through for the case of absorption.†

It is well known[1] that the probability, per nucleus, for resonance absorption of a neutron (or γ quantum) can be written in the following form:

---

*In the quantum treatment one must take into account the fact that the emission of a photon, in general, results in a recoil which changes the state of motion of the radiating system and thus destroys the thermodynamic equilibrium (cf. later on p. 395). Under these conditions Kirschhoff's theorem is no longer valid.

†Emission can be treated analogously.

$$W(E) \backsim \sum_i q_i \sum_m \frac{|(m|V|i)|^2}{(E - E_0 + \varepsilon^i - \varepsilon^m)^2 + \Gamma^2/4}. \quad (3)$$

Here $E = p^2/2m$ is the energy of the incident neutron; E_0 and Γ are the energy and width of the resonance level of the absorbing nucleus; $V = V(\mathbf{r}_n - \mathbf{r}_N)$ is the operator for the interaction between the neutron and the nucleus, and depends on the difference $\mathbf{r}_n - \mathbf{r}_N$ between the radius vectors of the neutron and nucleus; ϵ^i and $E_0 + \epsilon^m$ are the initial and final energies of the absorbing system. The summation over i corresponds to an averaging over initial states, each of which is taken with weight q_i.

Assuming that the motion of the incident neutron is described by the plane wave

$$\Psi_n(r_n) \backsim \exp(i\mathbf{p}\mathbf{r}_n/\hbar)$$

and using the standard representation of the δ function

$$\delta(\rho) = \frac{1}{2\pi}\int_{-\infty}^{+\infty} e^{i\tau\rho}\,d\tau,$$

we can transform the expression for W(E) as follows:

$$W(E) \backsim |M_0|^2 \sum_i q_i \sum_m \frac{1}{2\pi}\int_{-\infty}^{+\infty} \frac{d\rho}{(E - E_0 + \hbar\rho)^2 + \Gamma^2/4}$$

$$\times \int_{-\infty}^{+\infty} d\tau \exp\left\{i\tau\left[\rho + \frac{\varepsilon^m - \varepsilon^i}{\hbar}\right]\right\} \left|\int d\mathbf{r}\,\varphi_i(\mathbf{r})\,\varphi_m^*(\mathbf{r})\,e^{i\varkappa\mathbf{r}}\right|^2,$$

where $\kappa = \mathbf{p}/\hbar$, M_0 is the matrix element of the interaction of the neutron with an isolated nucleus, and the functions $\varphi_i(\mathbf{r})$ and $\varphi_m(\mathbf{r})$ determine the "molecular" states of the absorbing system.

Writing the operator for the coordinate of the nucleus in the Heisenberg representation, and carrying out the summation over m, we obtain

$$W(E) \sim \int_{-\infty}^{+\infty} d\tau \int_{-\infty}^{+\infty} \frac{e^{i\tau\rho}\,d\rho}{(E - E_0 + \hbar\rho)^2 + \Gamma^2/4}\,F_s(\varkappa, \tau),$$

where

$$F_s(\varkappa, \tau) = \sum_i q_i\,(i|\exp\{-i\varkappa\mathbf{R}_N(0)\}\exp\{i\varkappa\mathbf{R}_N(\tau)\}|i).$$

The quantity $F_s(\kappa, \tau)$ can be expressed in terms of the function introduced by Van Hove:[2]

$$G_s(\mathbf{r}, \tau) = \left\langle \int d\mathbf{r}'\,\delta(\mathbf{r} - \mathbf{R}_N(0) - \mathbf{r}')\,\delta(\mathbf{r}' - \mathbf{R}_N(\tau)) \right\rangle,$$

which has the significance of a self-diffusion function.* Namely

$$F_s(\varkappa, \tau) = \int d\mathbf{r}\,e^{i\varkappa\mathbf{r}}\,G_s(\mathbf{r}, \tau).$$

For the majority of isotropic dynamical systems, the function $G_s(\mathbf{r}, \tau)$ has a Gaussian shape with a dispersion which depends on the time.[3] Then

$$F_s(\varkappa, \tau) = \pi^{-3/2}\sigma^{-3}(\tau)\int d\mathbf{r}\exp\left\{i\varkappa\mathbf{r} - \frac{r^2}{\sigma^2(\tau)}\right\} = \exp\left\{-\frac{\varkappa^2\sigma^2(\tau)}{4}\right\},$$

which gives

$$W(E) \backsim \int_{-\infty}^{+\infty} \frac{d\rho}{(E - E_0 + \hbar\rho)^2 + \Gamma^2/4} \int_{-\infty}^{+\infty} d\tau \exp\left\{i\rho\tau - \frac{\varkappa^2\sigma^2(\tau)}{4}\right\}.$$

Calculating the integral over ρ, and using the relation[2] $\sigma^*(\tau) = \sigma(-\tau)$, which guarantees the reality of the expression for W(E), we finally obtain

$$W(E) \backsim \mathrm{Re}\int_0^\infty d\tau \exp\left\{i\,\frac{E_0 - E}{\hbar}\,\tau - \frac{\Gamma\tau}{2\hbar} - \varkappa^2\,\frac{\sigma^2(\tau)}{4}\right\}. \quad (4)$$

For $\Gamma = 0$, the expression analogous to (4) determines the angular and energy distribution of neutrons in incoherent scattering. Computing W(E) in the semiclassical approximation, i.e., treating the motion of the atoms of the material classically, one can show that formula (4) is identical with the result (2) of the consistently classical computation.

The information concerning the nature of the motion of the absorbing nuclei is contained in the quantity $\sigma^2(\tau)$, which can, in particular, be determined from experimental data on potential scattering of neutrons and from the shape of the resonance absorption line for neutrons and γ quanta. It is also not difficult to compute $\sigma^2(\tau)$ for certain simple models of the material.[3,4] Thus for an ideal gas,

$$\sigma^2(\tau) = v_0^2(\tau^2 - i\hbar\tau/kT), \quad (5)$$

where $v_0^2 = 2kT/M$, where M is the mass of the atom, k is the Boltzmann constant and T is the temperature.

For a harmonic oscillator of frequency Ω,

$$\sigma^2(\tau) = \frac{2\hbar}{M\Omega}\left\{\frac{\exp\{\hbar\Omega/kT\} + 1}{\exp\{\hbar\Omega/kT\} - 1}(1 - \cos\Omega\tau) - i\sin\Omega\tau\right\} \quad (6)$$

and finally, for an atom in a crystal lattice with cubic symmetry,

$$\sigma^2(\tau) = \frac{2\hbar}{M}\int_0^\infty \frac{\nu(\Omega)\,d\Omega}{\Omega}\left\{\frac{\exp\{\hbar\Omega/kT\} + 1}{\exp\{\hbar\Omega/kT\} - 1}(1 - \cos\Omega\tau) - i\sin\Omega\tau\right\}, \quad (7)$$

where $\nu(\Omega)$ is the normalized spectrum of eigenfrequencies of the crystal. Formulas (5) – (7) were obtained quantum mechanically.

The classical calculation[3] gives a somewhat different result in each of these cases:

---

*We should remind the reader that the argument of the δ function contains the quantum mechanical operator $\mathbf{R}_N(\tau)$ in the Heisenberg representation; since these are taken at different times, they do not commute with one another.

$$\sigma_{\mathrm{cl}}^2(\tau) = v_0^2\tau^2, \qquad (5')$$

$$\sigma_{\mathrm{cl}}^2(\tau) = (2v_0^2/\Omega^2)(1 - \cos\Omega\tau), \qquad (6')$$

$$\sigma_{\mathrm{cl}}^2(\tau) = 2v_0^2\int_0^\infty \frac{\nu(\Omega)\,d\Omega}{\Omega^2}(1 - \cos\Omega\tau). \qquad (7')$$

The main difference between the quantum mechanical and classical formulas is the appearance in the former of an imaginary part, which arises as a result of the noncommutativity of the operators. Physically, as it is not difficult to show for the example of the ideal gas, the imaginary part takes account of the recoil of the atom, i.e., the back reaction of the radiation on the matter. From their physical meaning, the classical expressions must be real ($\sigma_{\mathrm{cl}}^2(\tau) \sim \overline{|\mathbf{r}(\tau) - \mathbf{r}(0)|^2}$).

It is not difficult to show that at high temperatures and after long times ($\tau \gg \hbar/kT$ in the case of a gas, and $\tau \gg 1/\Omega_{\mathrm{av}}$ for the case of a crystal) the imaginary part is small. It should be mentioned that in the case of the oscillator and the crystal, the quantum effects do not disappear completely for $\tau \to \infty$, since formulas (6) and (7) contain the effective temperature

$$T_{\mathrm{eff}}(\Omega) = \frac{\hbar\Omega}{2k}\frac{\exp\{\hbar\Omega/kT\} + 1}{\exp\{\hbar\Omega/kT\} - 1}.$$

At short times, the imaginary part dominates in $\sigma^2(\tau)$.

Substituting in (4) the values of $\sigma^2(\tau)$ for the gas and the crystal, we arrive at the well known expressions for the probability of absorption of slow neutrons which were obtained by Bethe and Placzek[5] and Lamb.[6] These same formulas are also suitable for describing the resonance absorption of γ quanta in gaseous and crystalline samples.[7,8]

Let us now consider an absorbing system which is diffusing inside a compressed gas or a liquid (which for simplicity we treat as a highly compressed gas). Because of the complexity of a consistent quantum mechanical approach, we shall compute the quantity $\sigma^2(\tau)$ classically, using the Langevin equation

$$\ddot{\mathbf{r}} + \eta\dot{\mathbf{r}} = \mathbf{f},$$

where $\mathbf{f}$ is the random force, $\eta = kT/MD$, and D is the diffusion coefficient. Then, as shown by Chandrasekhar,[9]

$$\sigma^2(\tau) = 4D\,[\tau - (1 - e^{-\eta\tau})/\eta]. \qquad (8)$$

Substituting (8) in (2), we get

$$J(\Omega) \backsim \operatorname{Re}\int_0^\infty d\tau \exp\left\{i\Omega\tau - \lambda\tau/2 - \varkappa^2 D\left[\tau - \frac{1 - e^{-\eta\tau}}{\eta}\right]\right\}. \qquad (9)$$

If collisions are not important, formula (9) leads to the usual formula, which is valid for an ideal gas. In the opposite limiting case, the condition

$$kT/MD^2\varkappa^2 \approx (\Lambda/2\pi L)^2 \gg 1 \qquad (10)$$

is satisfied, where Λ is the wave length and L is the mean free path. Then (9) goes over into

$$J(\Omega) \backsim \operatorname{Re}\int_0^\infty d\tau \exp\left\{i\Omega\tau - \left(\frac{\lambda}{2} + \varkappa^2 D\right)\tau\right\},$$

which leads to*

$$J(\Omega) \backsim [\Omega^2 + (\lambda/2 + \varkappa^2 D)^2]^{-1}. \qquad (11)$$

If the damping is weak, the width of the line is of the order of κ^2D, which differs from the usual Doppler width κ (kT/M) by the small factor L/Λ.

Under conditions where collisions are unimportant, the absorbing atom can be assumed to be free, and the absorption of the γ quantum is accompanied by a recoil

$$\Delta\omega = \hbar\omega_0^2/2Mc^2. \qquad (12)$$

If the absorption takes place in the presence of an interaction between the absorbing system and some other body, the recoil momentum is distributed over the two bodies, which results in an increase of the effective mass and a consequent reduction of the shift $\Delta\omega$.

As the ratio L/Λ decreases, the collisions become more important, and the absorbed photon interacts effectively with more and more of the atoms in the material, which results in a further increase in the effective mass M_{eff}. The latter in turn is associated with a reduction in the Doppler width, which is of order $M_{\mathrm{eff}}^{1/2}$, and with a much more rapid drop in the shift due to recoil, which is of order M_{eff}^{-1}. One may therefore expect that when condition (10) is satisfied the recoil leads to practically no shift of the center of the line.

For soft γ rays, condition (10) may be satisfied in liquids, if we assume that the diffusion model of the liquid gives any sort of description of the situation.[12] It then follows that it may be possible to observe resonance absorption of γ rays when working with a liquid source and absorber. We may expect that the conditions for observing resonance absorption in this case will be much more favorable than in a gas, disregarding for the moment the fact that it will be possible to use much stronger sources. First of all, in working with gases one must somehow compensate the recoil, which makes the experiment more difficult. This is not necessary in liquids. Secondly the intensity of resonance absorption in liquids should be considerably stronger than in gases, since the line width is much smaller.

---

*For the case of $\lambda = 0$ this formula was given in the paper of Wittke and Dicke,[10] A more detailed analysis of the limiting cases of formula (9) was given by Podgoretskiĭ and Stepanov.[11]

The resonance absorption of γ quanta and neutrons can be used to study the mechanism of transfer in the liquid. Of particular interest in this connection are experiments of the type of resonance absorption of γ quanta in Kr^{83} ($E_\gamma = 9.3$ kev, $N_e/N_\gamma \sim 10$, $T_b = -151°C$, $T_m = -157°C$). The fact that the boiling point is close to the melting point enables us to eliminate temperature effects and to investigate the dependence of resonance absorption on the state of aggregation.

The authors thank F. L. Shapiro for many stimulating discussions, and also M. V. Kazarnovskii and I. I. Sobel'man for help in this work.

Note added in proof (January 16, 1961). After this paper was sent to press, we saw a preprint of the paper of Singwi and Sjölander, which contains similar results. [See Phys. Rev. 120, 1093 (1960); transl. note.]

---

[1] W. Heitler, The Quantum Theory of Radiation, Oxford University Press, 1954.

[2] L. Van Hove, Phys. Rev. **95**, 249 (1954).

[3] G. H. Vineyard, Phys. Rev. **110**, 999 (1958).

[4] A. C. Zemach and R. J. Glauber, Phys. Rev. **101**, 118 (1956).

[5] H. Bethe and G. Placzek, Phys. Rev. **51**, 450 (1937).

[6] W. Lamb, Phys. Rev. **55**, 190 (1939).

[7] R. L. Mössbauer, Z. Physik **151**, 124 (1958).

[8] R. L. Mössbauer, Z. Naturforsch. **14a**, 211 (1959).

[9] S. Chandrasekhar, Stochastic Problems in Physics and Astronomy, Revs. Modern Phys. **15**, 1 (1943).

[10] J. P. Wittke and R. H. Dicke, Phys. Rev. **103**, 620 (1956).

[11] M. I. Podgoretskii and A. V. Stepanov, Preprint, Joint Institute for Nuclear Research.

[12] K. S. Singwi and A. Sjölander, Bull. Am. Phys. Soc. **5**, 168 (1960).

Translated by M. Hamermesh
87

SOVIET PHYSICS JETP VOLUME 13, NUMBER 2 AUGUST, 1961

THEORY OF INELASTIC SCATTERING OF NEUTRONS BY IMPERFECT CRYSTALS

M. A. KRIVOGLAZ

Institute of Metal Physics, Academy of Sciences, Ukrainian S.S.R.

Submitted to JETP editor August 6, 1960

J. Exptl. Theoret. Phys. (U.S.S.R.) 40, 567-584 (February, 1961)

We consider inelastic one-phonon scattering of neutrons by solid solutions or by crystals containing defects. Phonon scattering by static inhomogeneities in a crystal results in broadening of the peaks in the energy distribution of coherently scattered neutrons. This broadening depends strongly on the degree of order in the arrangement of the atoms of the solution and becomes anomalously large near critical points on the decomposition curve and near points of second-order phase transitions. We consider the peculiarities of the broadening in the scattering by vibrations corresponding to extrema of the vibration spectrum. It is shown that including the effects of defects and correlations in the solution results in the appearance of an angular dependence of the intensity of incoherent scattering, and that imperfection of the crystal leads to a smearing out of singularities in the energy spectrum of this scattering and in the distribution function of the vibration frequencies. The incoherent scattering increases sharply near critical points on the decomposition curve. We consider the scattering of neutrons by local vibrations.

IT is known that in the elastic scattering of neutrons by imperfect crystals (where the imperfection of the crystal may be related to the presence of atoms of different sorts, or of defects at the sites of some sublattice, or of distortions of the crystal), in addition to the allowed Bragg reflections which are characteristic of the ideal crystal, there appears a diffuse scattering. The fact that the crystal is not ideal should also lead to important peculiarities in the inelastic scattering of neutrons by the thermal vibrations of the atoms, resulting in a change not only in the angular distribution but also in the energy distribution after scattering. The scattering of neutrons by vibrations of an ideal crystal have been studied in detail, for the harmonic approximation, in many papers (cf., for example, references 1 — 3, where references are given to other work). It was found that, in addition to a smooth distribution, the energy spectrum of the scattered neutrons contains terms proportional to δ functions which correspond to the case where the energy and momentum conservation laws are satisfied in the processes of absorption or emission of a phonon during the scattering. The investigation of the location of these peaks in the energy distribution at various scattering angles is the basis of the widely used method for determining the energy distribution of the crystal vibrations.

It is obvious that the δ functions are associated with perfectly monochromatic waves propagating in an ideal crystal. The presence of inhomogeneities in the crystal, or interaction of phonons with one another or with other elementary excitations, leads to scattering and damping of the waves and to a smearing of the δ function distribution in the energy spectrum. Since the determination of the vibration spectrum is possible only when the distribution is sufficiently sharp, it is of interest to investigate theoretically the width and shape of the distribution (for the scattering of neutrons by superfluid He, this problem was studied in references 4 and 5).

Moreover, the study of the broadening may give new and valuable information concerning the interaction of phonons with crystal inhomogeneities and with one another, concerning their relaxation times, concerning singularities in the vibration spectrum, concerning order in the arrangement of atoms in solution, etc. In addition to a broadening of the peaks, corresponding to one-phonon coherent scattering, imperfection of the crystal may also cause a smearing out of the singularities in the spectrum of incoherent scattering and the appearance of an angular dependence of this scattering. We shall also consider these questions.

In this paper we consider effects associated with the influence of the interaction of phonons with static inhomogeneities in the crystal on the nuclear scattering of neutrons (effects associated with anharmonicity and with phonon-magnon interaction in ferromagnets will be discussed elsewhere[6]). Nonideal crystals include solid solutions (including solutions of isotopes) and crystals containing vacancies, interstitial atoms, etc. Since the scattering depends strongly on the order in the arrangement of the atoms of different types, we shall not assume that the solutions are ideal, and will explicitly include correlations. In particular, we shall investigate the important special phenomena which must occur near critical points on the decomposition curve and near points of second order phase transition. In most cases the interaction of phonons with static inhomogeneities will be assumed to be small, which permits us to use perturbation theory and to disregard local vibrations. We shall consider separately the case where defects have a strong influence on the vibrations and lead to the appearance of new local frequencies.

1. GENERAL FORMULAS FOR THE DIFFERENTIAL SCATTERING CROSS SECTION

For simplicity of presentation, we shall carry through the treatment for the case of a binary solution A-B. The differential cross section, $d^2\Sigma/d\Omega\, dE = \sigma(\mathbf{q}_1, \omega)$, for the nuclear scattering of monochromatic neutrons by a single crystal, per unit solid angle and per unit energy, is given by the expression:[3,4]

$$\frac{d^2\Sigma}{d\Omega\, dE} = \sigma(\mathbf{q}_1, \omega) = \frac{m^2}{8\pi^3\hbar^5}\frac{k_2}{k_1}\operatorname{Sp}\Big\{\sum_{ss'\gamma\gamma'}(A_{s\gamma}A_{s'\gamma'} + \delta_{ss'}\delta_{\gamma\gamma'}B^2_{s\gamma})$$

$$\times\exp(i\mathbf{q}_1, \mathbf{R}_{s\gamma} - \mathbf{R}_{s'\gamma'})\exp(i\mathbf{q}_1, \delta\mathbf{R}_{s\gamma} - \delta\mathbf{R}_{s'\gamma'})$$

$$\times\int_{-\infty}^{\infty} dt\, e^{-i\omega t}\exp[i\mathbf{q}_1, \mathbf{u}_{s\gamma}(t)]\exp[-i\mathbf{q}_1, \mathbf{u}_{s'\gamma'}(0)]\,e^{-\lambda H}\Big\}$$

$$\times(\operatorname{Sp} e^{-\lambda H})^{-1}. \qquad (1)$$

Here m is the neutron mass; $\mathbf{q}_1$ is the difference of the wave vectors $\mathbf{k}_2$ and $\mathbf{k}_1$ of the scattered and incident waves; $\mathbf{q} = \mathbf{q}_1 - 2\pi\mathbf{K}_n$, where $\mathbf{K}_n$ is the vector of the reciprocal lattice which is closest to the end of the vector $\mathbf{q}_1/2\pi$; s is the number labelling the elementary cell; γ is the number of the site in the lattice; $\mathbf{R}_{s\gamma}$ is the radius vector to a site in the "average" periodic lattice; $\delta\mathbf{R}_{s\gamma}$ is the static displacement of the atom from this site; $A_{s\gamma}$ and $B_{s\gamma}$ are constants in the expression for the interaction of the neutron with the nucleus at the site labelled $s\gamma$:

$$V_{s\gamma}(\mathbf{r}) = \{A_{s\gamma} + 2B_{s\gamma}(\mathbf{s}\mathbf{S}_{s\gamma})[S_{s\gamma}(S_{s\gamma}+1)]^{-1/2}\}\,\delta(\mathbf{r})$$

($\mathbf{s}$ and $\mathbf{S}_{s\gamma}$ are the operators for the spin of the neutron and the spin of the nucleus $s\gamma$); $A_{s\gamma}$ and $B_{s\gamma}$ take on the values A_1, A_2, B_1, B_2, depending on the sort of atom which is located at the $s\gamma$ site;

$$E = \hbar\omega = \hbar^2(k_2^2 - k_1^2)/2m$$

is the change in energy of the neutron in the scattering; $\lambda = (kT)^{-1}$; H is the Hamiltonian for the vibrations of the atoms;

$$\mathbf{u}_{s\gamma}(t) = \exp(iHt/\hbar)\,\mathbf{u}_{s\gamma}(0)\exp(-iHt/\hbar)$$

is the operator for the thermal displacement of the $s\gamma$ atom, in the Heisenberg representation. In taking the trace in (1), it is understood that we also average over all configurations corresponding to the given values of the order and correlation parameters.

In the case of a nonideal crystal, the normal vibrations are no longer described by plane waves, which complicates the computation of the trace in (1). Making use of the fact that the imperfection is small, we can carry out the computation in two ways. First, by using perturbation theory we can find the approximate normal coordinates of the problem, as was done by I. Lifshitz[7] in treating the problem of the absorption of light by imperfect crystals, and then evaluate the trace in these coordinates. However it is more convenient to solve the problem by expanding the displacements, not in the normal coordinates of the nonideal crystal, but rather in plane waves, and to use perturbation theory directly for computing the trace. This method is more general, and is also applicable, for example, to the treatment of anharmonicity.

We expand the thermal displacement vector in plane waves describing the normal vibrations in the zero'th approximation, which corresponds to an ideal crystal consisting of atoms with the average (for sites of the particular type) reciprocal masses and force constants:

$$\mathbf{u}_{s\gamma} = \sum_{\mathbf{k}j}\sqrt{\frac{\hbar}{2\rho N v\omega_{\mathbf{k}j}}}\,\mathbf{e}_{\mathbf{k}j\gamma}\exp(i\mathbf{k}\mathbf{R}_{s\gamma})(a_{\mathbf{k}j} - a^{+}_{-\mathbf{k}j}),$$

$$\mathbf{e}^{*}_{-\mathbf{k}j\gamma} = -\mathbf{e}_{\mathbf{k}j\gamma},$$

$$\frac{\partial}{\partial\mathbf{u}_{s\gamma}} = \sum_{\mathbf{k}j} M_\gamma\sqrt{\frac{\omega_{\mathbf{k}j}}{2\rho N v\hbar}}\,\mathbf{e}_{\mathbf{k}j\gamma}\exp(i\mathbf{k}\mathbf{R}_{s\gamma})(a_{\mathbf{k}j} + a^{+}_{-\mathbf{k}j}),$$

$$[a_{\mathbf{k}j}(0)\,a^{+}_{\mathbf{k}'j'}(0)] = \delta_{\mathbf{k}\mathbf{k}'}\delta_{jj'}. \qquad (2)$$

Here ρ is the density of the crystal, N the number of elementary cells, v the volume of a cell; $\omega_{\mathbf{k}j}$ is the vibration frequency for the j-th branch with wave number $\mathbf{k}$; the values $\mathbf{k}/2\pi$ lie inside a unit cell of the reciprocal lattice; $\mathbf{e}_{\mathbf{k}j\gamma}$ are polarization vectors satisfying the normalization condition

$$\sum_{s\gamma} \mathbf{e}_{\mathbf{k}j\gamma}\mathbf{e}^{*}_{\mathbf{k}'j'\gamma}M_{\gamma}\exp\left(i(\mathbf{k}-\mathbf{k}'),\mathbf{R}_{s\gamma}\right)=MN\delta_{\mathbf{k}\mathbf{k}'}\delta_{jj'},$$

M_{γ} are the masses of the atoms at the γ sites, and M is the mass of a cell.

The Hamiltonian for the vibrations of the nonideal crystal has the following form, when expressed in terms of the operators $a_{\mathbf{k}j}$ and $a^{+}_{\mathbf{k}j}$:[8]

$$H=\sum_{\mathbf{k}j}\hbar\omega_{\mathbf{k}j}a^{+}_{\mathbf{k}j}a_{\mathbf{k}j}+\sum_{\mathbf{k}j\mathbf{k}'j'}V_{\mathbf{k}j\mathbf{k}'j'}a^{+}_{\mathbf{k}j}a_{\mathbf{k}'j'}$$

$$-\frac{1}{2}\sum_{\mathbf{k}j\mathbf{k}'j'}\left(V'_{\mathbf{k}j\mathbf{k}'j'}a^{+}_{\mathbf{k}j}a^{+}_{\mathbf{k}'j'}+V'^{*}_{\mathbf{k}j\mathbf{k}'j'}a_{\mathbf{k}j}a_{\mathbf{k}'j'}\right). \tag{3}$$

The quantities V and V′, which characterize the probability of scattering of phonons by static inhomogeneities, are determined by the values of the differences in masses of the atoms, by the force constants of the interaction and by the static imperfections. Explicit expressions for these quantities were obtained earlier[8] and are given below for various cases. Here we mention only that $V_{\mathbf{k}j\mathbf{k}'j'} = V^{*}_{\mathbf{k}'j\mathbf{k}j'}$, that $V_{\mathbf{k}j\mathbf{k}j'} = 0$, and that the average of $V_{\mathbf{k}j\mathbf{k}'j'}$ over the configurations of the atoms is also equal to zero.

The thermal vibrations result in a weakening of the intensity of the allowed Bragg reflections and the appearance of inelastic diffuse scattering. The reduction in intensity of allowed reflections and the multiphonon diffuse scattering by nonideal crystals will be treated elsewhere. Here we shall consider only processes which are accompanied by the absorption or emission of one (real or virtual) phonon, so that in the expansion of $\exp(i\mathbf{q}_1\cdot\mathbf{u}_{s\gamma})$ we need keep only the linear terms. In addition we shall treat the case when there are no static imperfections present $(\delta\mathbf{R}_s = 0)$ or when both $\delta\mathbf{R}_s$ and $A_1 - A_2$ can be treated as small quantities, and we can neglect cubic terms in these quantities. We split the quantities $B^2_{s\gamma}$ and $A_{s\gamma} = \bar{A}_{\gamma} + (c_{s\gamma} - c_{\gamma})(A_1 - A_2)$ into an average value (for the particular sublattice), $\bar{A}_{\gamma} = c_{\gamma}A_1 + (1 - c_{\gamma})A_2$, and a fluctuating part, $(c_{s\gamma} - c_{\gamma}) \times (A_1 - A_2)$ (where $c_{s\gamma}$ take on the values one or zero, depending on whether the atom at the $s\gamma$ site is of type A or type B; c_{γ} is the concentration of atoms A at the γ sites). Expanding in $\delta\mathbf{R}_{s\gamma}$ and $\mathbf{u}_{s\gamma}$, we find the expression for the differential inelastic scattering of neutrons

$$\sigma(\mathbf{q}_1,\omega)=\sigma_1(\mathbf{q}_1,\omega)+\sigma_2(\mathbf{q}_1,\omega)+\sigma_3(\mathbf{q}_1,\omega), \tag{4}$$

$$\sigma_1(\mathbf{q}_1,\omega)=CN\frac{k_2}{k_1}\sum_{jj'}\frac{Q_{j\mathbf{q}_1}Q^{*}_{j'\mathbf{q}_1}}{\sqrt{\omega_{\mathbf{q}j}\omega_{\mathbf{q}j'}}}\varphi_{\mathbf{q}j/\mathbf{q}j'}(\omega), \tag{5}$$

$$\sigma_2(\mathbf{q}_1,\omega)=CN\frac{k_2}{k_1}\sum_{jj'}\left\{-2\,\mathrm{Re}\sum_{\mathbf{k}}\frac{Q_{j\mathbf{q}_1}S^{*}_{j'\mathbf{q}_1}(\mathbf{k})}{\sqrt{\omega_{\mathbf{q}j}\omega_{\mathbf{k}j'}}}\varphi_{\mathbf{q}j/-\mathbf{k}j'}(\omega)\right.$$

$$\left.+\sum_{\mathbf{k}\mathbf{k}'}\frac{S_{j\mathbf{q}_1}(\mathbf{k})S^{*}_{j'\mathbf{q}_1}(\mathbf{k}')}{\sqrt{\omega_{\mathbf{k}j}\omega_{\mathbf{k}'j'}}}\varphi_{\mathbf{k}j/\mathbf{k}'j'}(\omega)\right\}, \tag{6}$$

$$\sigma_3(\mathbf{q}_1,\omega)=C\frac{k_2}{k_1}\sum_{jj'}\left\{\sum_{\mathbf{k}}\frac{b_{jj'\mathbf{q}_1}(\mathbf{k})}{\sqrt{\omega_{\mathbf{q}j}\omega_{\mathbf{k}j'}}}\varphi_{\mathbf{k}j/\mathbf{k}j'}(\omega)\right.$$

$$\left.+(B_1^2-B_2^2)\sum_{\mathbf{k}\mathbf{k}'}\sum_{\gamma}\frac{(\mathbf{q}_1\mathbf{e}_{\mathbf{k}j\gamma})(\mathbf{q}_1\mathbf{e}^{*}_{\mathbf{k}'j'\gamma})c_{\mathbf{k}-\mathbf{k}'\gamma}}{\sqrt{\omega_{\mathbf{k}j}\omega_{\mathbf{k}'j'}}}\varphi_{\mathbf{k}j/\mathbf{k}'j'}(\omega)\right\}. \tag{7}$$

We have introduced the notation

$$C=\frac{m^2}{8\pi^2\hbar^4\rho v},\qquad c_{\mathbf{k}\gamma}=\frac{1}{N}\sum_{s}(c_{s\gamma}-c_{\gamma})\exp(i\mathbf{k}\mathbf{R}_{s\gamma}),$$

$$\mathbf{R}_{\mathbf{k}\gamma}=-\frac{i}{N}\sum_{s}\delta\mathbf{R}_{s\gamma}\exp(i\mathbf{k}\mathbf{R}_{s\gamma}),$$

$$Q_{j\mathbf{q}_1}=\sum_{\gamma}\bar{A}_{\gamma}\,\mathbf{q}_1\mathbf{e}_{\mathbf{q}j\gamma}\exp(2\pi i\,\mathbf{K}_n\mathbf{R}_{s\gamma}),$$

$$S_{j\mathbf{q}_1}(\mathbf{k})=\sum_{\gamma}\left[(A_1-A_2)c_{\mathbf{q}+\mathbf{k}\gamma}\right.$$

$$\left.-\bar{A}_{\gamma}\mathbf{q}_1\mathbf{R}_{\mathbf{q}+\mathbf{k}\gamma}\right]\mathbf{q}_1\mathbf{e}_{\mathbf{k}j\gamma}\exp(2\pi i\,\mathbf{K}_n\mathbf{R}_{s\gamma}),$$

$$b_{jj'\mathbf{q}_1}(\mathbf{k})=\sum_{\gamma}\bar{B}^2_{\gamma}(\mathbf{q}_1\mathbf{e}_{\mathbf{k}j\gamma})(\mathbf{q}_1\mathbf{e}^{*}_{\mathbf{k}j'\gamma}),$$

$$\varphi_{\mathbf{k}j/\mathbf{k}'j'}(\omega)=\varphi'_{\mathbf{k}j/\mathbf{k}'j'}(\omega)+\varphi''_{\mathbf{k}j/\mathbf{k}'j'}(\omega),$$

$$\varphi'_{\mathbf{k}j/\mathbf{k}'j'}(\omega)=\frac{1}{2\pi}\int_{-\infty}^{\infty}dt\,e^{-i\omega t}\mathrm{Sp}\left[e^{-\lambda H}a_{\mathbf{k}j}(t)\,a^{+}_{\mathbf{k}'j'}(0)\right](\mathrm{Sp}\,e^{-\lambda H})^{-1},$$

$$\varphi''_{\mathbf{k}j/\mathbf{k}'j'}=\frac{1}{2\pi}\int_{-\infty}^{\infty}dt\,e^{-i\omega t}\,\mathrm{Sp}\left[e^{-\lambda H}a^{+}_{\mathbf{k}j}(t)\,a_{\mathbf{k}'j'}(0)\right](\mathrm{Sp}\,e^{-\lambda H})^{-1}. \tag{8}$$

In expressions (5) – (7) it is understood that we average over all configurations of the atoms.

As we see from these formulas, the problem of determining the energy distribution of the scattered neutrons has been reduced to the computation of the spectral representations $\varphi_{\mathbf{k}j\mathbf{k}'j'}(\omega)$ for the product of two single-particle operators. These quantities are most simply found by using the method of temperature Green's functions.[9] In the following we shall use a variant of this method, based on the use of spectral representations of two-time retarded and advanced Green's functions[9e] $G(\omega)$. For a system with the Hamiltonian (3), these functions are given in the Appendix. Remembering that (cf. reference 9e):

$$\varphi''_{\mathbf{k}j/\mathbf{k}'j'}(\omega)=\varphi'_{\mathbf{k}'j'\mathbf{k}j}(-\omega)\,e^{-\lambda\hbar\omega},$$

$$\varphi''_{\mathbf{k}'j'\mathbf{k}j}(\omega)=i\,(e^{\lambda\hbar\omega}-1)^{-1}\lim_{\varepsilon\to 0}\left[G_{\mathbf{k}j/\mathbf{k}'j'}(\omega+i\varepsilon)\right.$$

$$\left.-G_{\mathbf{k}j/\mathbf{k}'j'}(\omega-i\varepsilon)\right],$$

and also using the relation $(x + i\epsilon)^{-1} = Px^{-1} - i\pi\delta(x)$ (where P denotes the principal value), we can obtain the expressions for the functions φ' and φ'' from formulas (A.4) – (A.7) of the Appendix:

$$\varphi''_{\mathbf{k}j\mathbf{k}j}(\omega) = \varphi''_{\mathbf{k}j}(\omega) = \varphi'_{\mathbf{k}j}(-\omega)\frac{n(\omega)}{n(\omega)+1} = \frac{1}{\pi}\frac{\Gamma_{\mathbf{k}j}(\omega)\,n(\omega)}{[\omega - \omega_{\mathbf{k}j} - P_{\mathbf{k}j}(\omega)]^2 + \Gamma^2_{\mathbf{k}j}(\omega)}, \tag{9}$$

$$\varphi''_{\mathbf{k}j'\mathbf{k}j}(\omega) = \varphi''_{\mathbf{k}j'j}(\omega) = \frac{P_{\mathbf{k}jj'}\varphi''_{\mathbf{k}j'}(\omega)}{\omega - \omega_{\mathbf{k}j}} + \frac{1}{\pi}\frac{\Gamma_{\mathbf{k}jj'}n(\omega)}{\omega - \omega_{\mathbf{k}j}}\frac{\omega - \omega_{\mathbf{k}j'} - P_{\mathbf{k}j'}}{[\omega - \omega_{\mathbf{k}j'} - P_{\mathbf{k}j'}]^2 + \Gamma^2_{\mathbf{k}j'}} \quad (\text{for } \omega \approx \omega_{\mathbf{k}j'}), \tag{10}$$

$$\varphi'_{\mathbf{k}'j'\mathbf{k}j}(\omega) = \frac{V_{\mathbf{k}j\mathbf{k}'j'}}{\hbar}\varphi'_{\mathbf{k}'j'}(\omega)\,\mathrm{P}\frac{1}{\omega - \omega_{\mathbf{k}j}} \quad (\text{for } \omega \neq \omega_{\mathbf{k}j}), \tag{11}$$

where

$$n(\omega) = [e^{\lambda\hbar\omega} - 1]^{-1},$$

$$P_{\mathbf{k}jj'}(\omega) = \frac{1}{\hbar^2}\mathrm{P}\sum_{\mathbf{k}''j''}\left[\frac{V_{\mathbf{k}j\mathbf{k}''j''}V_{\mathbf{k}''j''\mathbf{k}j'}}{\omega - \omega_{\mathbf{k}''j''}} - \frac{V'_{\mathbf{k}j\mathbf{k}''j''}V'^{*}_{\mathbf{k}''j''\mathbf{k}j'}}{\omega + \omega_{\mathbf{k}''j''}}\right],$$

$$\Gamma_{\mathbf{k}jj'}(\omega) = \frac{\pi}{\hbar^2}\sum_{\mathbf{k}''j''}[V_{\mathbf{k}j\mathbf{k}''j''}V_{\mathbf{k}''j''\mathbf{k}j'}\delta(\omega - \omega_{\mathbf{k}''j''}) - V'_{\mathbf{k}j\mathbf{k}''j''}V'^{*}_{\mathbf{k}''j''\mathbf{k}j'}\delta(\varphi + \omega_{\mathbf{k}''j''})]. \tag{12}$$

From (9) and (12) we see that, in the second approximation of perturbation theory, the quantity $P_{\mathbf{kj}} = P_{\mathbf{kjj}}$ determines the displacement of the $(\mathbf{kj})$ vibration frequency associated with the imperfection of the crystal, while $\Gamma_{\mathbf{kj}} = \Gamma_{\mathbf{kjj}}$ determines the damping.

In the limiting transition to the ideal crystal, when V and $V' \to 0$, $\varphi''_{\mathbf{kj}}(\omega)$ goes over into the δ function, while the other functions $\varphi''_{\mathbf{kjk'j'}}(\omega)$ vanish. At the same time, the expression (5) for σ_1 goes over into the usual formula for coherent inelastic scattering, and the expressions (6) and (7) for σ_2 and σ_3 into the formulas for incoherent scattering. We shall continue to use the convention, even for the case of nonideal crystals, of calling the scattering corresponding to σ_1 coherent scattering, and the scattering corresponding to the sum $\sigma_2 + \sigma_3$, incoherent scattering. Let us now separately consider the coherent and incoherent scattering.

2. COHERENT INELASTIC SCATTERING

As we see from (5), (9) and (10), the main contribution to the coherent scattering comes from the diagonal terms σ_{1jj} in the sum (5), which correspond to absorption of a phonon,

$$\sigma'_{1jj}(\mathbf{q}_1, \omega) = CN\frac{k_2}{k_1}\frac{|Q_{j\mathbf{q}_1}|^2}{\pi\omega_{\mathbf{q}j}}\frac{\Gamma_{\mathbf{q}j}(\omega)\,n(\omega)}{[\omega - \omega_{\mathbf{q}j} - P_{\mathbf{q}j}(\omega)]^2 + \Gamma^2_{\mathbf{q}j}(\omega)}, \tag{13a}$$

or to its emission:

$$\sigma''_{1jj}(\mathbf{q}_1, -\omega) = CN\frac{k_2}{k_1}\frac{|Q_{j\mathbf{q}_1}|^2}{\pi\omega_{\mathbf{q}j}}\frac{\Gamma_{\mathbf{q}j}(\omega)\,[n(\omega)+1]}{[\omega - \omega_{\mathbf{q}j} - P_{\mathbf{q}j}(\omega)]^2 + \Gamma^2_{\mathbf{q}j}(\omega)}. \tag{13b}$$

For each $\mathbf{q}_1$, these terms determine the intensity of the series of peaks in the energy distribution of the scattered neutrons whose maxima lie at $\pm\omega \approx \omega_{\mathbf{q}j} + P_{\mathbf{q}j}$, and which correspond to the different branches of the vibration spectrum. The peak intensities are proportional to the squares of the "structure amplitudes" $Q_{j\mathbf{q}_1}$ [cf. Eq. (8)], which are different for the different peaks, and depend on the temperature through the factors $n(\omega)$ and $n(\omega) + 1$. The peak widths $\Gamma_{\mathbf{q}j}$, according to (12), do not depend explicitly on the temperature, and are essentially determined by the magnitude of the inhomogeneities and the amount of order in the arrangement of the atoms. The temperature dependence of $\Gamma_{\mathbf{q}j}$ shows itself when we include the effects of anharmonicity.[6] If the peaks are sufficiently narrow, and $\Gamma(\omega)$ does not depend very strongly on frequency, so that $d\Gamma_{\mathbf{q}j}/d\omega \ll 1$, the shape of each peak is described by a symmetric Lorentz curve. In the general case, because of the dependence of Γ on ω, the shape of the curve is more complicated.

The nondiagonal terms in (5) correspond to more complicated scattering processes, in which phonons belonging to two different zones participate. As we see from (10), they are also most important when $\pm\omega \approx \omega_{\mathbf{q}j'} + P_{\mathbf{q}j'}$, and vanish for $V = V' = 0$. These terms lead to a slight change in the peak intensities [the first term in Eq. (10)] and to the appearance of an asymmetry of the distribution, which is associated with the second term in (10). (Analogous effects also occur in the exciton absorption spectrum.[10]). The degree of asymmetry is of order $\Gamma_{\mathbf{q}jj'}(\omega_{\mathbf{q}j'} - \omega_{\mathbf{q}j})^{-1}$ (if all the $Q_{j\mathbf{q}_1}$ are of the same order) and increases rapidly when the vibration frequencies of different branches approach one another. For sufficiently small values of $|\omega_{\mathbf{q}j'} - \omega_{\mathbf{q}j}|$, the expression (10) ceases to be applicable to the most important part of the frequency range, around $\omega \approx \omega_{\mathbf{q}j'}$. In this case the function $\varphi_{\mathbf{q}j\mathbf{q}j'}(\omega)$ can be gotten by starting from the more exact expression (A.8) for the Green's function. Without giving the resulting very complicated formulas, we merely remark that the values of the displacements and broadenings of the levels are determined in this case not only by $P_{\mathbf{q}j}$ and $\Gamma_{\mathbf{q}j}$, but also by $P_{\mathbf{q}jj'}$ and $\Gamma_{\mathbf{q}jj'}$, and depend strongly on the frequency difference $\omega - \omega_{\mathbf{q}j}$

(since the energy bands begin to "interact" strongly as they approach one another).

Now let us compute the $\Gamma_{\mathbf{q}j}$. To do this we must have explicit expressions for the $V_{\mathbf{k}j\mathbf{k}'j'}$. We shall assume that quantities like the density of the crystal and the elastic moduli depend linearly on the concentrations c_γ. Then the $V_{\mathbf{k}j\mathbf{k}'j'}$ will depend linearly on the Fourier components of the fluctuations of these concentrations. In the following we shall, for the most part, treat solutions in which the atoms of the two types can only be at the sites of one of the sublattices, while there are identical atoms at the sites of the other sublattices (for example, crystals with one site per unit cell, solutions like NaKCl with two sites per unit cell, etc). In this case the quantity $c_{\mathbf{k}'-\mathbf{k},\gamma} = c_{\mathbf{k}'-\mathbf{k}}$ is different from zero for only one value of γ (so that we can drop the index γ), and

$$V_{\mathbf{k}j\mathbf{k}'j'} = h_{\mathbf{k}j\mathbf{k}'j'}c_{\mathbf{k}'-\mathbf{k}},\ V'_{\mathbf{k}j\mathbf{k}'j'} = h_{\mathbf{k}j\mathbf{k}'j'}c_{\mathbf{k}'+\mathbf{k}} \tag{14}$$

(the expressions for h are given below). Substituting (14) in formula (12) for the $\Gamma_{\mathbf{q}j}$, dropping the second term in this formula (which is important only for negative ω, when the scattering is very small), and going over from a sum to a surface integral over the surfaces $S_{j'}$ on which the conditions $\omega = \omega_{\mathbf{k}j'}$ are satisfied, we get

$$\Gamma_{\mathbf{q}j}(\omega) = \frac{vN}{8\pi^2\hbar^2}\sum_{j'}\int_{S_{j'}}\frac{dS_{j'}}{|\nabla_{\mathbf{k}}\omega_{\mathbf{k}j'}|}h^2_{\mathbf{q}j\mathbf{k}j'}\overline{|c_{\mathbf{k}-\mathbf{q}}|^2}. \tag{15}$$

If the $c_{\mathbf{k}\gamma}$ are different from zero for several sublattices, we must replace $h^2_{\mathbf{q}j\mathbf{k}j'}|c_{\mathbf{k}-\mathbf{q}}|^2$ in (15) by $\left|\sum_\gamma h^\gamma_{\mathbf{q}j\mathbf{k}j'}c_{\mathbf{k}-\mathbf{q},\gamma}\right|^2$.

The average values of the $|c_{\mathbf{k}-\mathbf{q}}|^2$, and consequently $\Gamma_{\mathbf{q}j}$, are essentially related to the degree of order of the atomic arrangement. We shall therefore treat separately the cases of different types of correlation in the solid solution.

Ideal solutions. In ideal solutions there is no correlation, and the atoms of different types are distributed completely at random over the sites of the particular sublattice. Then the $\overline{|c_{\mathbf{k}}|^2}$ are given by the simple formula:

$$\overline{|c_{\mathbf{k}}|^2} = c(1-c)/N \tag{16}$$

(where c is the concentration in the particular sublattice). As we see from (16), in this case $|c_{\mathbf{k}}|^2$ does not depend on $\mathbf{k}$, which greatly simplifies the integration in (15). The integral (15) can be calculated explicitly for the long wave acoustical and optical vibrations.

In the case of the acoustic vibrations, in the approximation of an elastic isotropic continuum, the quantities $h_{\mathbf{k}j\mathbf{k}'j'}$ and $\omega_{\mathbf{k}j}$, according to reference 8a, are given by the formulas

$$h_{\mathbf{k}j\mathbf{k}'j'} = \frac{\hbar}{2\rho\sqrt{\omega_{\mathbf{k}j}\omega_{\mathbf{k}'j'}}}$$

$$\times\Big\{\mathbf{e}_{\mathbf{k}j}\mathbf{e}_{\mathbf{k}'j'}\omega_{\mathbf{k}j}\omega_{\mathbf{k}'j'}\rho' + (\mathbf{e}_{\mathbf{k}j}\mathbf{k})(\mathbf{e}_{\mathbf{k}'j'}\mathbf{k}')\left(K' - \frac{2}{3}\mu'\right)$$

$$+ [(\mathbf{e}_{\mathbf{k}j}\mathbf{e}_{\mathbf{k}'j'})(\mathbf{k}\mathbf{k}') + (\mathbf{k}\mathbf{e}_{\mathbf{k}'j'})(\mathbf{k}'\mathbf{e}_{\mathbf{k}j})]\mu'\Big\},$$

$$\omega_{\mathbf{k}1} = c_1k = \sqrt{\frac{K+4\mu/3}{\rho}}\,k, \qquad \omega_{\mathbf{k}2} = c_2k = \sqrt{\frac{\mu}{\rho}}\,k. \tag{17}$$

Here $j = 1$ corresponds to longitudinal vibrations ($\mathbf{e}_{\mathbf{k}_1} \parallel \mathbf{k}$), while $j = 2, 3$ correspond to transverse vibrations ($\mathbf{e}_{\mathbf{k}j} \perp \mathbf{k}$); K and μ are the bulk and shear moduli; ρ', K' and μ' are the derivatives of the corresponding unprimed quantities with respect to c; c_j is the velocity of propagation of the vibrations. Substituting (16) and (17) in (15) and carrying out the integration, for $j = 1$ and $j = 2$, over the surfaces of the three spheres $S_{j'}$ (for the three vibration branches), we find the widths $\Gamma_{\mathbf{q}_1}$ and $\Gamma_{\mathbf{q}_2}$ of the energy distributions for the longitudinal and transverse acoustic vibrations:

$$\Gamma_{\mathbf{q}1}(\omega) = \frac{vc_1q^4}{24\pi}\left(\frac{\omega}{\omega_{\mathbf{q}}}\right)^3\left[(1+2\varkappa^3)\left(\frac{\rho'}{\rho}\right)^2\right.$$

$$\left.+\frac{45K'^2 + 8(2+3\varkappa^5)\mu'^2}{15\varkappa^4\mu^2}\right]c(1-c)$$

$$\sim 10\left(\frac{q}{q_m}\right)^3\omega\varepsilon_1^2c(1-c), \tag{18}$$

$$\Gamma_{\mathbf{q}2}(\omega) = \frac{vc_2q^4}{12\pi}\left(\frac{\omega}{\omega_{\mathbf{q}}}\right)^3\left[\frac{1+2\varkappa^3}{2\varkappa^3}\left(\frac{\rho'}{\rho}\right)^2 + \frac{2+3\varkappa^5}{5\varkappa^5}\left(\frac{\mu'}{\mu}\right)^2\right]c(1-c)$$

$$\sim\left(\frac{q}{q_m}\right)^3\omega\varepsilon_1^2c(1-c). \tag{19}$$

Here $\kappa = c_1/c_2$; $\omega_{\mathbf{q}}$ is the frequency of the $\mathbf{q}$-th vibration (and, if we can neglect the dependence of Γ on ω, $\omega/\omega_{\mathbf{q}} \approx 1$); q_m is the maximum value of the phonon wave vector; ϵ_1 is the largest of the quantities ρ'/ρ, K'/K, μ'/μ; the last equalities in (18) and (19) determine the order of magnitude of $\Gamma_{\mathbf{q}}$. For frequencies of longitudinal vibrations which are greater than the maximum frequency of transverse vibration $\omega_{\perp\,\mathrm{max}}$, those scattering processes are excluded in which a longitudinal phonon is annihilated and a transverse phonon is created, and we must replace the square bracket in (18) by the expression $(\rho'/\rho)^2 + (45K'^2 + 16\mu'^2)/15\kappa^4\mu^2$ [and also drop the factor 10 in the estimate given in Eq. (18)].

It is obvious that, except for singular points in the vibration spectrum, (cf. below) formulas (18) and (19) give the correct order of the widths $\Gamma_{\mathbf{q}}$ of the distribution for ideal solutions. As we see from these formulas, for large q ($q \sim q_m$), for components which differ markedly in their properties ($\epsilon_1 \sim 1$), and for high concentrations ($c \sim 1/2$), $\Gamma_{\mathbf{q}}$ is of the same order of magnitude as ω, i.e., the peak in the energy distribution is almost completely smeared out. In solutions of isotopes (except for the lightest elements) usually $\epsilon_1 < 1/10$, and the broadening of the peaks due to the presence of different isotopes is usually small ($\Gamma_{\mathbf{q}} < 1/100\,\omega$) and less than the broadening due to anharmonicity. Since for low frequencies $\Gamma_{\mathbf{q}} \sim q^4$, for the scattering by the low frequency vibrations, one should in all cases observe sharp peaks.

A different dependence of $\Gamma_{\mathbf{q}}$ on q is obtained for the case of long-wave optical vibrations. To avoid giving very involved formulas, we shall restrict ourselves to the usually occurring case where the effects due to the mass difference of the atoms of the solution are considerably greater than the effects due to differences in force constants and to imperfections. We then have for all the vibration branches and all **k** and **k′** (cf. reference 8b):

$$h_{\mathbf{k}j\mathbf{k}'j'} = \frac{1}{2}\hbar\sqrt{\omega_{\mathbf{k}j}\omega_{\mathbf{k}'j'}}\,e_{\mathbf{k}j\gamma}e_{\mathbf{k}'j'\gamma}\,\varepsilon, \qquad \varepsilon = \frac{\rho'}{\rho} = \frac{M_1 - M_2}{M} \tag{20}$$

(where M_1, M_2 and M are the masses of the component atoms and the average mass per cell).

Let us consider the case when there is an analytic minimum or maximum of $\omega_j(\mathbf{k})$ at the point $\mathbf{k} = 0$ and the other branches have no vibrations with this frequency. Then for cubic crystals $\omega_j(\mathbf{k}) = \omega_0 + 1/2\,\omega_2 k^2$ (we neglect retardation effects, which are important only for very small k) and, according to (15), (16) and (20), $\Gamma_{\mathbf{q}\parallel}$ and $\Gamma_{\mathbf{q}\perp}$ for the longitudinal and transverse optical vibrations are equal to:

$$\Gamma_{\mathbf{q}\parallel}(\omega) = \frac{v\omega_{\mathbf{q}}\omega q(\omega)}{24\pi|\omega_2|}n^4\varepsilon^2 c(1-c) \sim \frac{\omega_0^2}{\Delta\omega}\frac{q}{q_m}\varepsilon^2 c(1-c),$$

$$\Gamma_{\mathbf{q}\perp}(\omega) = \frac{v\omega_{q}\omega q(\omega)}{12\pi|\omega_2|}n^4\varepsilon^2 c(1-c), \tag{21}$$

where the quantity $n = n_j$ is equal to the length of the polarization vector $e_{\mathbf{k}j\gamma}(k \to 0)$ for the particular sublattice (in which the atoms are arranged at random), $q(\omega)$ is the wave vector corresponding to the frequency ω (for narrow peaks $\omega \approx \omega_{\mathbf{q}}$, $q(\omega) \approx q$), $\Delta\omega \sim 1/2\,|\omega_2|q_m^2$ is the width of the particular frequency band. According to (12), expressions for the $\Gamma_{\mathbf{q}jj'}(\omega)$, for frequencies ω corresponding to optical vibrations can be obtained from (21) by replacing $\omega_{\mathbf{q}}n_j^2$ by $\sqrt{\omega_{\mathbf{q}j}\omega_{\mathbf{q}j'}}\,n_j n_{j'}$, if the two branches j and j′ both describe longitudinal or transverse (optical or acoustical) vibrations. If one of the branches is longitudinal and the other transverse, then $\Gamma_{\mathbf{q}jj'}(\omega) = 0$.

As we see from (21), now as q decreases the quantity $\Gamma_{\mathbf{q}}$ falls off not like q^4 but like q, i.e., the broadening may be sizable even for small q. For a given ϵ, the broadening is especially large for narrow zones (small $\Delta\omega$), for example for optical vibrations in molecular crystals. The same type of formula for the $\Gamma_{\mathbf{q}}(\omega)$ is also valid for other minima and maxima in the dependence of $\omega_j(\mathbf{k})$ (including the case of the maximum frequency of acoustic vibration), so long as only this one branch occurs near the frequency ω. Then q in (21) denotes the distance to the extremal point in **k** space. If other branches have this same frequency, then in evaluating $\Gamma_{\mathbf{q}}$ for small q the terms corresponding to these branches are very important. Their order of magnitude is given by formulas (18) or (19).

As Van Hove[11] has shown, for each vibration branch there must exist critical points (c.p.) of the vibration spectrum, i.e., minima, maxima and saddle points, at which $\nabla_{\mathbf{k}}\omega_{\mathbf{k}} = 0$. As follows from (15), the occurrence of such an analytic c.p. for one of the branches at the frequency ω_1 leads to the appearance of a singularity in the dependence of Γ on ω of the form $|\omega - \omega_1|^{1/2}$ for all the other vibration branches (whose frequencies coincide with ω_1). Here the term proportional to $|\omega - \omega_1|^{1/2}$ appears only for those frequencies ω which lie on that side of the point ω_1 for which new poles appear on the surface $\omega_j(\mathbf{k}) = \omega$. The same kind of singularity also occurs if a nonanalytic c.p. is a minimum or maximum for not one but two vibration branches, and $\nabla_{\mathbf{k}}\omega_{\mathbf{k}} = 0$ at the point. If however the c.p. is singular, i.e., if some of the components $\nabla_{\mathbf{k}}\omega_{\mathbf{k}}$ do not vanish at it but instead have discontinuities, then the singularity of the function $\Gamma_{\mathbf{q}}(\omega)$ is weaker.

It should be emphasized that the singularity of $\Gamma_{\mathbf{q}}(\omega)$ was found only in this particular approximation of perturbation theory. The next approximation leads to a smearing out of the singularity over a frequency interval $\sim \Gamma_{\mathbf{q}}$, analogous to the smearing of the singularity in the spectrum of incoherently scattered neutrons (cf. Sec. 3). For small values of $\Gamma_{\mathbf{q}}$, the singularity will still manifest itself in experimental studies of the dependence of $\Gamma_{\mathbf{q}}(\omega)$, which can be used as an independent method for locating the frequencies of c.p.'s.

It is easy to show that for multicomponent ideal solutions we should make the following replacements in formulas (18), (19), and (21):

$$c(1-c)\,\varepsilon^2$$

$$= c(1-c)\,\frac{(M_1-M_2)^2}{M^2} \to \sum_{\mu_1<\mu_2} c_{\mu_1}c_{\mu_2}(M_{\mu_1}-M_{\mu_2})^2/M^2,$$

where c_μ is the concentration of the μ-th component, whose atoms have mass M_μ.

Nonideal solutions. In nonideal solutions the correlation between positions of atoms is important. In this case the expression for $|c_{\mathbf{k}}|^2$ becomes more complicated, and its dependence on k becomes important. A simple formula for $|c_{\mathbf{k}}|^2$ can be given only for small values of k. In this case, as it follows from the thermodynamic theory of fluctuations, for disordered solutions

$$\overline{|c_{k'}|^2} = kT/Nv\,(\varphi_{cc} + \beta k'^2). \tag{22}$$

Here k is the Boltzmann constant, T is the temperature at which short range order is established in the solution (and is not necessarily the same as the temperature at which the experiment is done), $\varphi_{cc} = \partial^2\varphi/\partial c^2$ is the second derivative of the thermodynamic potential per unit volume, β is a quantity of order kTr_0^2/v (where r_0 is the interatomic separation). From a comparison of (16) and (22), we see that in the case of long wave acoustical or optical vibrations, when $\beta q^2 \ll \varphi_{cc}$, the formulas obtained above for $\Gamma_{\mathbf{q}}$ can also be applied to nonideal solutions, if we replace $c(1-c)$ by $kT/v\varphi_{cc}$. Since φ_{cc} is usually greater for ordering nonideal solutions (which go over into the ordered state at low temperatures) than for ideal solutions, whereas it is smaller in dissociating solutions, the establishment of short range order leads to a reduction of $\Gamma_{\mathbf{q}}$ in the first case and to its increase in the second case.*

A marked decrease in the value of $\Gamma_{\mathbf{q}}$ should occur when a high degree of long range order is established in the solution. In almost completely ordered solutions having two types of sites, just as in ideal solutions, the atoms are distributed chaotically over the sites of each sublattice, and in the expressions for $|c_{\mathbf{k}}|^2$ and $\Gamma_{\mathbf{q}}$ we must simply replace $c(1-c)$ by $c(1-c) - \nu(1-\nu)\eta^2$, where ν is the ratio of the number of sites of the first type to the total number of sites and η is the long range order parameter, which is equal to unity in an alloy having stoichiometric composition and complete order. In particular, for this composition $(c = \nu)$, $\Gamma_{\mathbf{q}} \sim (1-\eta^2)$, i.e., $\Gamma_{\mathbf{q}}$ actually falls off rapidly in the transition from a disordered to an almost completely ordered solution.

Solutions near a critical point on the decomposition curve. Characteristic features of the energy distribution of the scattered neutrons should appear near a critical point on the decomposition curve (d.p.), i.e., a point at which the decomposition curve has a maximum. It is known^{12} that $\varphi_{cc} = 0$ at a d.p. Therefore, near such a point, as we see from (22), the probability for scattering of phonons with a small change in momentum increases markedly, so that $\Gamma_{\mathbf{q}}$ should decrease markedly. It follows from (15), (17) and (22) that for long wave acoustical vibrations, in the case where $K' = \mu' = 0$, the $\Gamma_{\mathbf{q}}$ are equal to:

$$\Gamma_{q1}(\omega) = \frac{c_1 q^2}{32\pi}\frac{kT}{\beta}\varepsilon^2\left[\ln\frac{2}{ae^2} + \varkappa(1+\varkappa^2) - \frac{1}{2}(\varkappa^2-1)^2\ln\frac{\varkappa+1}{\varkappa-1}\right] \sim \frac{q}{q_m}\,\omega\varepsilon^2\ln\frac{2}{ae^2}, \tag{23}$$

$$\Gamma_{q2}(\omega) = \frac{c_2 q^2}{32\pi}\frac{kT}{\beta}\varepsilon^2\left[\ln\frac{2}{ae} + \frac{1}{2}\frac{1+\varkappa^2}{\varkappa^3} - \frac{(\varkappa^2-1)^2}{4\varkappa^4}\ln\frac{\varkappa+1}{\varkappa-1}\right] \sim \frac{q}{q_m}\,\omega\varepsilon^2\ln\frac{2}{ae}. \tag{24}$$

Here e is the base of the natural logarithms, and

$$a = \{\varphi_{cc} + \beta\,[q - q(\omega)]^2\}/2\beta q q(\omega), \tag{25}$$

$q(\omega)$ is the wave vector for the same branch that contains q corresponding to the frequency ω, and we have used the fact that $\omega \approx \omega_{\mathbf{q}}$, $\varphi_{cc}/\beta q^2 \ll 1$. (For $\omega > \omega_{\perp\,\max}$, only the first term in the square brackets in (23) should be kept.)

Comparison of (23), (24) and (18), (19) shows that the transition from the ideal solution to the solution in the neighborhood of the d.p. leads to a considerable increase in $\Gamma_{\mathbf{q}}$ (by a factor of $\sim (q_m/q)^2 \ln a^{-1}$). This effect makes itself felt more strongly for long waves, since then, as q decreases, $\Gamma_{\mathbf{q}}$ falls off not like q^4, but almost like q^2. For a given q, and for $\omega = \omega_{\mathbf{q}}$, the value of $\Gamma_{\mathbf{q}}$ goes to infinity logarithmically as we approach the d.p. (while $\varphi_{cc} \to 0$).

An especially sharp rise in $\Gamma_{\mathbf{q}}$ near the d.p. should occur for values of $\mathbf{q}$ which are in the neighborhood of a c.p. For example, for the minimum or maximum points of long wave optical vibrations, we obtain from (15), (20) and (22) the following expressions in place of (21):

---

*A very sharp increase in Γ_q should be observed when large groups of impurity atoms are formed, for example when particles of a new phase separate out in the crystal. According to reference 8b, when n atoms are joined into a group, then for long wave oscillations whose wavelength $\lambda_0 > r$ (where r is the linear size of the particles), Γ_q increases by a factor ~n, i.e., it may increase by several orders of magnitude. For shorter waves, for which $\lambda_0 \ll r$ and $(\varepsilon r/\lambda)^2 \ll 1$, Γ_q increases by a factor $\sim n^{1/3}(q_m/q)^2$ compared to the case of individual impurity atoms. Finally, for vibrations of such short wave length that $\lambda_0 \ll r$ and $(\varepsilon r/\lambda_0)^2 \gg 1$, Γ_q changes by a factor $\sim (q_m/q)^4 n^{-1/3}$ and falls off with increasing n. The transition from the $\Gamma_q \sim q^4$ law to the q^2 law (or to $\Gamma_q \sim q^0$) for $\lambda_0 \sim r$ may make it possible to determine experimentally the dimensions of the particles which separate out.

$$\Gamma_{\mathbf{q}\parallel}(\omega) = \frac{\omega_{\mathbf{q}}\omega}{32\pi\,|\omega_2|\,q(\omega)}\frac{kT}{\beta}n^4\varepsilon^2(1+a) \times\left[(1+a)\ln\left(1+\frac{2}{a}\right)-2\right],$$

$$\Gamma_{\mathbf{q}\perp}(\omega) = \frac{\omega_{\mathbf{q}}\omega}{34\pi\,|\omega_2|\,q(\omega)}\frac{kT}{\beta}n^4\varepsilon^2\left[(2+2a+a^2)\ln\left(1+\frac{2}{a}\right) - 2(1+a)\right];$$

$$\Gamma_{\mathbf{q}\parallel} \sim \Gamma_{\mathbf{q}\perp} \sim \frac{\omega_0^2}{\Delta\omega}\varepsilon^2\frac{q_m}{q}\ln\frac{1}{a} \text{ for } a \ll 1,$$

$$\Gamma_{\mathbf{q}\parallel} \sim \Gamma_{\mathbf{q}\perp} \sim \frac{\omega_0^2}{\Delta\omega}\varepsilon^2\frac{q_m}{q}\frac{1}{a} \text{ for } a \gg 1. \tag{26}$$

From (26) we see that for $\omega = \omega_{\mathbf{q}}$ and for very small q, when $a \gg 1$ ($\varphi_{cc} \gg \beta q^2$), just as in ideal solutions, $\Gamma_{\mathbf{q}}$ is proportional to q, but the coefficient of proportionality is increased by a factor $\sim \beta q_m^2/\varphi_{cc}$, and tends to infinity as we approach the d.p. Thus, even for small ϵ, near the d.p. the peaks in the energy distribution which correspond to values of q in the neighborhood of the c.p. are smeared out badly. For somewhat larger values of q (but still small compared with q_m), when $a \ll 1$, $\Gamma_{\mathbf{q}}$ varies inversely with q instead of being proportional to it.

As we see from (26) and (25), in this case $\Gamma_{\mathbf{q}}$ depends strongly on ω, i.e., the curve describing the energy distribution may differ markedly from the Lorentz shape. Since $\Gamma_{\mathbf{q}jj'}$, just as for formula (21), differs from $\Gamma_{\mathbf{q}j'}$ only by the replacement of $n^2\omega_{\mathbf{q}j'}$ by $\sqrt{\omega_{\mathbf{q}j}\omega_{\mathbf{q}j'}}\,n_j n_{j'}$, the value of $\Gamma_{\mathbf{q}jj'}$ should also increase sharply, i.e., the role of two-zone processes becomes more important, leading to an asymmetry in the energy distribution.

Near a d.p. there should also be a considerable shift of the vibration frequencies (or of the energy levels of conduction electrons). In the case of minimum or maximum points of long wave longitudinal optical vibrations, the value of the shift $P_0(\omega_0)$ as given by (12), (14), (20) and (22), is

$$P_0(\omega_0) = -\frac{\omega_0^2}{24\pi\omega_2}\frac{kTn^4}{\sqrt{\varphi_{cc}\beta}}\varepsilon^2 \sim -\frac{\omega_0^2}{\Delta\omega}\sqrt{\frac{kT}{v\varphi_{cc}}}\varepsilon^2 \tag{26a}$$

(and twice this for transverse vibrations), and increases like $\varphi_{cc}^{-1/2}$ as we approach the d.p. It should be emphasized that near the d.p. the perturbation expansion is actually not in powers of the small quantity ϵ, but in the quantity $\epsilon^2\sqrt{kT/v\varphi_{cc}}$; i.e., right near the d.p. the method we are using, which is based on the application of perturbation theory, ceases to be valid. In the case of small ϵ, we can however approach sufficiently close to the d.p.

The same type of expression for $\Gamma_{\mathbf{q}}(\omega)$ is obtained for any analytic minimum or maximum point (at which $\nabla_{\mathbf{k}}\omega_{\mathbf{k}} = 0$), where q denotes the distance from this point in the reciprocal lattice space, and an additional factor of order unity appears in the expression for $\Gamma_{\mathbf{q}}$ for the case of nonspherical isofrequency surfaces. In the case of analytic c.p.'s which are saddle points, again $\nabla_{\mathbf{k}}\omega_{\mathbf{k}} = 0$, and $\Gamma_{\mathbf{q}}$ increases sharply near the d.p. In the two limiting cases $a \ll 1$ and $a \gg 1$, the formulas for $\Gamma_{\mathbf{q}}$ then have the form

$$\Gamma_{\mathbf{q}} = \frac{\omega^2 kTn^4\varepsilon^2}{32\pi q\omega_{2q}\beta\cos\psi}\ln\frac{\zeta}{a} \text{ for } a \ll 1,$$

$$\Gamma_{\mathbf{q}} = \frac{\omega^2 DkT\varepsilon^2}{32\pi^2\sqrt{\beta\varphi_{cc}}} \text{ for } a \gg 1. \tag{27}$$

Here $\omega_{2\mathbf{q}} = |\nabla_{\mathbf{q}}\omega_{\mathbf{q}}|/q$; ψ is the angle between $\nabla_{\mathbf{q}}\omega_{\mathbf{q}}$ and **q**; $\zeta \sim 1$; the constant $D \sim \omega_2^{-1}$ is defined by the relation

$$Ddk = \int(\mathbf{e}_{\mathbf{q}j\gamma}\mathbf{e}_{\mathbf{k}j\gamma})^2\frac{dS}{|\nabla_{\mathbf{k}}\omega_{\mathbf{k}}|},$$

where the integral extends over the belt on the surface S which is cut out by two spheres with radii k and k+dk. Thus, in this case, for very small q ($\beta q^2 \ll \varphi_{cc}$) $\Gamma_{\mathbf{q}}$ increases like $\varphi_{cc}^{-1/2}$ as we approach the d.p.

As one can show by using the formula which relates the mean square fluctuations at high temperatures to the corresponding susceptibility at zero frequency (see Chap. XIII of reference 13), the integral of the coherent scattering intensity over frequency near the d.p. has a singularity of the type $\sqrt{\varphi_{cc}}$.

Solutions near a point of second-order phase transition. A marked increase in $\Gamma_{\mathbf{q}}$ for certain values of **q** may also occur near points where there is a second-order phase transition (t.p.). To be specific, we shall consider processes of ordering in solutions which in the disordered state have one sublattice, while in the ordered state there are two sublattices with the same number of sites (for example solutions of the type of β-brass). Effects of anomalously large scattering of phonons are related to the anomalously large fluctuations of the degree of long range order, η, near the t.p.

First let us treat disordered solutions. In the neighborhood of values $\mathbf{k}' = 2\pi\mathbf{K}_1$, where $\mathbf{K}_1$ is a vector of the reciprocal lattice of the ordered crystal which is absent in the disordered crystal, according to references 14 and 15,

$$\overline{|c_{\mathbf{k}'}|^2} = \frac{kT}{4Nv}\left[\varphi_{\eta\eta} + \alpha\,(\mathbf{k}' - 2\pi\mathbf{K}_1)^2\right]^{-1},$$

where $\varphi_{\eta\eta} = \partial^2\varphi/\partial\eta^2$. Since $\varphi_{\eta\eta} = 0$ at the t.p.,[12] $|c_{\mathbf{k}'}|^2$ increases markedly near these values of $\mathbf{k}'$. As we see from (14) and (15), such a marked increase in $|c_{\mathbf{k-q}}|^2$ manifests itself in the value of $\Gamma_{\mathbf{q}}$ if vibrations with vectors $\mathbf{q}$ and $\mathbf{k}$, such that $\mathbf{q} - \mathbf{k} \approx 2\pi\mathbf{K}_1$, have the same energy. Such a situation can occur in two cases: first, if the vector $\mathbf{q}/2\pi$ lies near the surface of a new Brillouin zone which appears when ordering occurs, and secondly if the optical and acoustical vibration branches, which are obtained in the reduction of the vibration spectrum to the cell of the reciprocal lattice of the ordered solution, intersect, and $\mathbf{q}$ lies near the surface of intersection of these branches. In both cases, after integration we obtain for $\Gamma_{\mathbf{q}}$ an estimate of the type of (23) and (24):

$$\Gamma_{\mathbf{q}} \sim \frac{c_1 q^2}{100}\frac{kT}{\alpha}\varepsilon^2 \ln\frac{\zeta}{a'} \sim \frac{q}{q_m}\,\omega\varepsilon^2 \ln\frac{\zeta}{a'}, \qquad a' = \frac{\varphi_{\eta\eta} + \zeta' q'^2}{2\alpha q^2}, \tag{28}$$

where ζ and $\zeta' \sim 1$, and q' is the distance to the surface of the new Brillouin zone or the surface of intersection of the branches. If there is a c.p. near such a surface, then in the neighborhood of such a point there occurs an even greater broadening as we approach the t.p., and $\Gamma_{\mathbf{q}}$ is given by formulas like (26). The expression (28) is also valid for certain points and lines in the reciprocal lattice space which lie on isofrequency surfaces and are connected by the vector $2\pi\mathbf{K}_1$; however, in contrast to the case of a d.p., there will not be a sizable increase of $\Gamma_{\mathbf{q}}$ at arbitrary points of the reciprocal lattice.

A similar picture exists near a t.p. in an ordered solution. Since in this case the ratio $|\mathbf{e}_{\mathbf{k}j\gamma}| : |\mathbf{e}_{\mathbf{k}j\gamma'}|$ for different γ and γ' is not equal to unity, but differs from it by an amount $\sim \epsilon^2\eta^2$, the probability of scattering of a phonon will contain a term proportional to $[\varphi_{\eta\eta} + \alpha\,(\mathbf{q}-\mathbf{k})^2]^{-1}$ not just when the momentum change $\mathbf{q}-\mathbf{k}$ is $2\pi\mathbf{K}_1$, but in general (for example, for $\mathbf{k} \approx \mathbf{q}$). However this term contains a factor $\epsilon^2\eta^2$ which is small in just that region where $\varphi_{\eta\eta}^{-1}$ is large. Therefore, in this case, when ordering occurs $\Gamma_{\mathbf{q}}$ changes only somewhat, without changing its order of magnitude. In the case of a second-order phase transition near a critical point on the curve of t.p.'s, η^2 can already take on sizable values when $\varphi_{\eta\eta}$ is still small,[16] and there may be a considerable increase in $\Gamma_{\mathbf{q}}$, especially near a c.p., if the factor η^2 which appears in formulas (26) (in which φ_{cc} is replaced by $\varphi_{\eta\eta}$) is not small.

As Landau has shown,[16] at the critical point, at which the curve of t.p.'s changes into the decomposition curve, we have $\varphi_{cc} = 0$ and $\varphi_{\eta\eta} = 0$ for the ordered phase, while for the disordered phase only $\varphi_{\eta\eta} = 0$. Therefore in this case, in the ordered phase, as we approach the critical point there should occur a sharp rise in $\Gamma_{\mathbf{q}}$, just as in the case of an ordinary d.p. In the disordered phase, the rise in $\Gamma_{\mathbf{q}}$, as it occurs in the neighborhood of an ordinary t.p., will occur only near the surfaces of new Brillouin zones and the surfaces of intersection of the acoustical and optical branches. We also note that in certain cases, for example in Rochelle salt crystals, near a t.p. the frequencies of certain vibration branches (the transverse optical branches) become extremely small.[17,18a] Then, as we see from formulas (5) – (7), the intensity of inelastic scattering of neutrons by these frequencies increases sharply.

3. INCOHERENT INELASTIC SCATTERING

The cross section $\sigma_2 + \sigma_3$ for incoherent scattering of neutrons is given by expressions (6) and (7). These expressions contain terms of zeroth, first, and second order in the constant V of interaction of the phonons with inhomogeneities. Here we shall consider only the leading terms of zeroth order (since the first and second order corrections can easily be obtained from the formulas given). As we see from formulas (A.4) – (A.7) of the Appendix, we may retain in the sums of (6) and (7) only those terms which contain functions $\varphi_{\mathbf{k}j\mathbf{k}'j}$ with $\mathbf{k} = \mathbf{k}'$, $j = j'$. The expressions for σ_2, σ_3 simplify considerably in this case, and take the form

$$\sigma_2(\mathbf{q}_1, \omega) = CN\frac{k_2}{k_1}\sum_j\sum_{\mathbf{k}}\omega_{\mathbf{k}j}^{-1}\left[A_1 - A_2 - \overline{A}\,(\mathbf{q}_1\mathbf{B}_{\mathbf{k+q}})\right]^2 \times (\mathbf{q}_1\mathbf{e}_{\mathbf{k}j})^2\,\overline{|c_{\mathbf{k+q}}|^2}\,\varphi_{\mathbf{k}j}(\omega), \tag{29}$$

$$\sigma_3(\mathbf{q}_1, \omega) = C\frac{k_2}{k_1}\overline{B^2}\sum_j\sum_{\mathbf{k}}\omega_{\mathbf{k}j}^{-1}\,(\mathbf{q}_1\mathbf{e}_{\mathbf{k}j})^2\,\varphi_{\mathbf{k}j}(\omega), \tag{30}$$

where we have used the assumption that the lattice constant is linearly dependent on composition, i.e., that $\mathbf{R}_{\mathbf{k}}$ depends linearly on $c_{\mathbf{k}}$: $\mathbf{R}_{\mathbf{k}} = \mathbf{B}_{\mathbf{k}} \cdot c_{\mathbf{k}}$. Explicit expressions for the $\mathbf{B}_{\mathbf{k}}$ were obtained earlier.[15] In particular, in the approximation of an isotropic elastic continuum,

$$\mathbf{B}_{\mathbf{k}} = b\frac{\mathbf{k}}{k^2}, \qquad b = \frac{1+\sigma}{3(1-\sigma)}\frac{1}{v}\frac{\partial v}{\partial c}$$

(where σ is the Poisson ratio).

The inclusion of defects and imperfections of the solution and the scattering of phonons by inhomogeneities leads to two effects which were not previously considered in treating incoherent scattering. First of all, imperfection of the solution and defects lead to a change in the value of σ_2 and to the appearance of a dependence on q. Secondly, the broadening of the levels results in a smearing out of the singularities which, according to Placzek and Van Hove,[2] should be present in the energy distribution of $\sigma_2 + \sigma_3$.

Let us begin by treating the first effect for ideal solutions, where $|c_\mathbf{k}|^2$ is given by formula (16). For sufficiently small $V_{\mathbf{k}j\mathbf{k}'j'}$ and $\Gamma_\mathbf{q}$, the functions $\varphi'_{\mathbf{k}j\mathbf{k}'j'}$ and $\varphi''_{\mathbf{k}j\mathbf{k}'j'}$ can, according to (9), be replaced by δ functions (except at the singular points of the frequency distribution function). We shall further restrict ourselves to treating a cubic crystal in the isotropic continuum approximation. We denote by $g_j(\omega)$ the distribution function for the vibration frequencies of the j-th branch (normalized to $1/3$), and by $q_{\omega j}$ the length of the wave vector of the j-th branch which corresponds to the frequency ω. The expression for σ_2 simplifies in the two limiting cases when $q \gg q_{\omega j}$ and $q \ll q_{\omega j}$. Then for processes in which a phonon is absorbed,

$$\sigma_2(\mathbf{q}_1, \omega) = CN\frac{k_2}{k_1}\frac{n(\omega)}{\omega} q_1^2 c(1-c)\sum_j g_j(\omega) \times\left[A_1 - A_2 - \overline{A}b\frac{\mathbf{q}_1\mathbf{q}}{q^2}\right], \qquad q \gg q_{\omega j};$$

$$\sigma_2(\mathbf{q}_1, \omega) = CN\frac{k_2}{k_1}\frac{n(\omega)}{\omega} q_1^2 c(1-c)\sum_j g_j(\omega) \times\left[(A_2 - A_1)^2 + \chi_j\overline{A}^2 b^2\frac{q_1^2}{q_{\omega j}^2}\right], \qquad q \ll q_{\omega j}, \tag{31}$$

where $\chi_j = 3/5$ for longitudinal vibrations and $\chi_j = 2/5$ for transverse vibrations. For arbitrary q, the expression for σ_3 has the form

$$\sigma_3(\mathbf{q}_1,\omega) = CN\frac{k_2}{k_1}\frac{n(\omega)}{\omega} g(\omega)\, q_1^2 \overline{B}^2, \qquad g(\omega) = \sum_j g_j(\omega). \tag{32}$$

In the case of processes in which a phonon is emitted, one should replace $n(\omega)$ by $n(\omega)+1$ in (31) and (32).

Thus, inclusion of defects leads to the result that σ_2 depends not only on the vibration frequency but also on q. The effects associated with defects are especially large if the change in energy of the neutron, $\hbar\omega$, in the scattering is very small or close to the energy of the long wave optical vibrations, and if the end of the vector $\mathbf{q}_1/2\pi$ lies near a point of the reciprocal lattice. Then, if q and and $q_{\omega j}$ are sufficiently small, even in slightly distorted crystals (small b) the terms in (31) caused by defects become dominant, and as $q, q_{\omega j} \to 0$ the value of σ_2 goes to infinity like q^{-2} or $q_{\omega j}^{-2}$. This characteristic dependence of σ_2 on q and ω can be used for the experimental determination of the limiting frequencies of optical vibrations. As we see from (32), σ_3 is independent of defects.

It follows from a comparison of (16) and (22), and from (29), that for small q and $q_{\omega j}$ the formulas (31) for σ_2 can also be applied to nonideal solutions, if we replace $c(1-c)$ by $kT/v\varphi_{cc}$. Thus, in this range of values of q and $q_{\omega j}$, σ_2 changes when short range order is established in the solution, increasing in solutions which decompose and decreasing in solutions which become ordered. When long-range order is established in an almost completely ordered solution, we must replace $c(1-c)$ in (31) by $c(1-c) - \nu(1-\nu)\eta^2$, i.e., σ_2 decreases sharply. In the case of solutions, close to a d.p. we must keep the second term in the denominator of (22) even for small k′. It follows from (29) and (22) that we have (for the case of absorption of the phonon)

$$\sigma_2(\mathbf{q}_1,\omega) = CN\frac{k_2}{k_2}\frac{n(\omega)}{\omega} g(\omega)\, q_1^2 \frac{kT}{v(\varphi_{cc}+\beta q^2)}\left(A_1 - A_2 - \overline{A}b\frac{\mathbf{q}_1\mathbf{q}}{q^2}\right)^2, \qquad q \gg q_{\omega j};$$

$$\sigma_2(\mathbf{q}_1,\omega) = CN\frac{k_2}{k_1}\frac{n(\omega)}{\omega} q_1^2 \sum_j g_j(\omega)\frac{kT}{v(\varphi_{cc}+\beta q_{\omega j}^2)} \times\left[(A_1 - A_2)^2 + \chi_j\overline{A}^2 b^2\frac{q_1^2}{q_{\omega j}^2}\right], \qquad q \ll q_{\omega j}. \tag{33}$$

From (33) we see that for small q and $q_{\omega j}$, the cross section σ_2 increases markedly when we approach the d.p., when $\varphi_{cc} \to 0$. From the results obtained above it follows that anomalous changes should occur not only in the intensity distribution of the elastic scattering of x-rays and neutrons near t.p.'s[14,15,18] and d.p.'s,[15,18] and in the magnetic scattering of neutrons near the Curie and Neel points,[19] but one should also observe singularities in the energy distribution of neutrons coherently scattered by thermal vibrations near d.p.'s and t.p.'s, and in the energy and angular distributions of incoherent scattering near a d.p.

Now let us consider the smearing out of singularities in the energy spectrum of the incoherent scattering by ideal solutions. If we replace the $\varphi_{\mathbf{k}j}(\omega)$ in (29) and (30) by δ functions, then for frequencies ω_1 corresponding to c.p.'s, at which $\nabla_{\mathbf{k}}\omega_{\mathbf{k}} = 0$, the quantities $g(\omega)$, σ_2 and σ_3 will, according to the results of Placzek and Van Hove,[2] have singularities of the type $|\omega - \omega_1|^{1/2}$. The change from the δ functions to the smoothed functions (9) obviously leads to a smearing out of these singularities. Except for cases where there are no vibrations of other branches at the frequency ω_1 corresponding to the minimum or maximum for a particular branch, we can neglect the change in $\Gamma_{\mathbf{q}}(\omega)$ over the narrow frequency range $\omega - \omega_{\mathbf{q}} \sim \Gamma_{\mathbf{q}}$. Integrating with respect to $\mathbf{k}$ in (29) and (30), and using (9), we find that the term $A(\omega - \omega_1)^{1/2}$, which describes the singularity near a minimum, must when we include damping be replaced by

$$A(\omega-\omega_1)^{1/2} \rightarrow A\Gamma_{\mathbf{q}}/2\,[(\omega-\omega_1)^2+\Gamma_{\mathbf{q}}^2]^{1/4}\sin\frac{\theta}{2},$$

$$\operatorname{tg}\theta = \frac{\Gamma_{\mathbf{q}}}{\omega-\omega_1}, \quad 0<\theta<\pi. \qquad (34)^*$$

Here ω_1 is the frequency at the particular c.p. when we include the shift by an amount $p(\omega_1)$ and drop terms of the form $P(\omega_1)/\omega_1$. For $\omega - \omega_1 \gg \Gamma_{\mathbf{q}}$ the expression (34) goes over into $A(\omega - \omega_1)^{1/2}$, i.e., the damping is unimportant. For $\omega - \omega_1 = 0$, the right side is however equal to $A\sqrt{\Gamma_{\mathbf{q}}/2}$, and does not vanish. For negative $\omega - \omega_1$, when $\omega_1 - \omega \gg \Gamma_{\mathbf{q}}$, the right side of (34) is equal to $A\Gamma_{\mathbf{q}}/2\sqrt{\omega_1 - \omega}$, i.e., it falls off like $(\omega_1 - \omega)^{1/2}$. Thus the singularity in $g(\omega)$ and in the spectrum of incoherent scattering is smeared out over an interval of frequencies $\sim \Gamma_{\mathbf{q}}$. Obviously such a smearing may also be associated with anharmonicity, electron-phonon interaction, etc. If other branches have no vibrations at the frequency of the minimum or maximum ω_1, then according to (21), $\Gamma_{\mathbf{q}}(\omega) \rightarrow 0$ for $\omega \rightarrow \omega_1$, and in this approximation $g(\omega)$ has a singularity of the type $|\omega - \omega_1|^{1/2}$.

In the discussion given above it was assumed that no local oscillations occur in the crystal. For small ϵ, local vibrations in the neighborhood of impurity atoms actually do not occur.[20] However, no matter how small ϵ, if a sufficiently large group of impurity atoms is formed which are located close to one another, such levels must necessarily appear. As a result of the concentration fluctuations in the large crystal, there is a finite (though small) probability of formation of large groups of impurity atoms. Since the groups differ from one another in the number and location of the impurity atoms, and since the local vibrations of the different groups interacting with one another are split up in a very complicated way, the local levels associated with the different groups will give a resultant continuous spectrum which lies either below or above the point of minimum or maximum frequency ω_1 (and has a very rapidly decreasing level density). Thus, in concentrated solutions the smearing out of extremal points occurs because of fluctuational deviations from the average concentration, and because of the local levels which appear in regions where there are such concentration changes. It can be shown that the smearing associated with this effect in ideal solutions leads to a smearing out of the singularity $|\omega - \omega_1|^{1/2}$ over a very narrow range (for small ϵ) of frequencies $\sim \lambda'\omega_1$, where

$$\lambda' = c^2(1-c)^2\varepsilon^4(\omega_1/\omega_2 q_m^2)^3.$$

As we move away from the point ω_1, at large distances the level density first falls off exponentially according to the law $\exp[-(\omega - \omega_1)^2/\lambda'^2\omega_1^2]$, and then even faster. This level density goes to zero only at the frequency ω' which is equal to the frequency of vibration of a crystal containing only the atoms of the heavier element (in the case of a minimum frequency) or of the lighter element (in the case of a maximum frequency). The same argument is obviously equally applicable to the energy levels of conduction electrons in a crystal.

4. SCATTERING OF NEUTRONS BY LOCAL VIBRATIONS

Now let us consider the case when the impurity atoms (or other defects) strongly perturb the crystal vibrations and lead to the appearance of local levels.[7,20] We shall assume that the concentration of defects is small. For determining the scattering cross section from formula (1), it is more convenient in this case to expand not in plane waves but in exact normal coordinates. We shall denote by

$$\sqrt{\hbar/2\rho v\omega_\varkappa}\,\mathbf{e}_{\varkappa s\gamma}\,(a_\varkappa - a^{+}_{-\varkappa})$$

the term in the expansion of the displacement of the $s\gamma$ atom corresponding to the local vibration κ. Then the cross section for scattering with absorption or emission of a phonon κ is equal to

$$\sigma_\varkappa(\mathbf{q}_1,\omega) = C\frac{k_2}{k_1}\frac{1}{\omega_\varkappa}\Big[\Big|\sum_{s\gamma}A_{s\gamma}\exp(i\mathbf{q}_1\delta\mathbf{R}_{s\gamma})\exp(i\mathbf{q}_1\mathbf{R}_{s\gamma})\mathbf{e}_{\varkappa s\gamma}\mathbf{q}_1\Big|^2$$

$$+\sum_{s\gamma}B_{s\gamma}^2(\mathbf{e}_{\varkappa s\gamma}\mathbf{q}_1)^2\Big]\varphi_{\varkappa\varkappa}(\omega), \qquad (35)$$

where $A_{s\gamma}$ and $B_{s\gamma}$ are now fixed, $\varphi_{\kappa\kappa}(\omega)$ is given by formula (8) with $a_{\mathbf{k}j}$ replaced by a_κ, and we have dropped the small terms corresponding to $\varphi_{\kappa\kappa'}(\omega)$ with $\kappa \neq \kappa'$. In the harmonic approximation, the Hamiltonian is diagonal in the variables a_κ, a_κ^+, so that $\varphi_{\kappa\kappa}(\omega)$ reduces to $\delta(\pm\omega - \omega_\kappa)$ (and $\varphi_{\kappa\kappa}^{(\omega)} = 0$). However, because of anharmonicity, there is an interaction between the vibrations which leads to a broadening of the distribution. We shall assume that the frequency ω_κ is such that processes are possible in which a local phonon κ is annihilated and two phonons $\mathbf{k}j$ and $\mathbf{k}'j'$ are created. The Hamiltonian describing such processes can be written in the form

---

*tg = tan

$$H = \hbar\omega_\varkappa a_\varkappa^+ a_\varkappa + \frac{1}{2}\sum_{\mathbf{k}j\mathbf{k}'j'} (V_{\varkappa\mathbf{k}j\mathbf{k}'j'} a_\varkappa^+ a_{\mathbf{k}j} a_{\mathbf{k}'j'} + V^*_{\varkappa\mathbf{k}j\mathbf{k}'j'} a_\varkappa a^+_{\mathbf{k}j} a^+_{\mathbf{k}'j'})$$

$$+ \sum_{\mathbf{k}j} \hbar\omega_{\mathbf{k}j} a^+_{\mathbf{k}j} a_{\mathbf{k}j}. \tag{36}$$

Setting up the equations for the Green's function corresponding to this Hamiltonian and breaking off the chain of equations in the second approximation of perturbation theory, as is done in the Appendix for the Hamiltonian (3), we find that $\varphi_{\kappa\kappa}(\omega)$ is given by a formula of the type of (9), in which $\Gamma_{\mathbf{k}j}$ and $P_{\mathbf{k}j}$ must be replaced by Γ_κ and P_κ, where

$$\Gamma_\varkappa = \frac{\pi}{\hbar^2} \sum_{\mathbf{k}j\mathbf{k}'j'} |V_{\varkappa\mathbf{k}j\mathbf{k}'j'}|^2 \delta(\omega - \omega_{\mathbf{k}j} - \omega_{\mathbf{k}'j'})$$

$$\times [1 + n(\omega_{\mathbf{k}j}) + n(\omega_{\mathbf{k}'j'})],$$

$$P_\varkappa = \frac{1}{\hbar^2} \mathrm{P} \sum_{\mathbf{k}j\mathbf{k}'j'} \frac{|V_{\varkappa\mathbf{k}j\mathbf{k}'j'}|^2}{\omega - \omega_{\mathbf{k}j} - \omega_{\mathbf{k}'j'}} [1 + n(\omega_{\mathbf{k}j}) + n(\omega_{\mathbf{k}'j'})]. \tag{37}$$

From (35), (9), and (37), it follows that the width of the distribution in this case depends on temperature (and is proportional to T for high temperatures). It can be shown that as ω_κ approaches the edge of the frequency band, Γ_κ increases rapidly and the distribution is smeared out. On the other hand, with increasing ω_κ the processes treated here, in which one local vibration is changed into two crystal vibrations, cease to be possible, and broadening can occur only because of multiphonon thermal transitions, whose probability is small and very strongly dependent on temperature (cf., for example, reference 21). The essential point is that when the scattering angle changes the position of the coherent scattering peaks changes in general, while the position of peaks associated with local vibrations remains unchanged.

APPENDIX

According to reference 9e, the retarded Green's function for the operators $a_{\mathbf{k}j}$, $a^+_{\mathbf{k}'j'}$ is given by the expression

$$G_{\mathbf{k}j\mathbf{k}'j'}(t, 0) = -i\theta(t)\,\mathrm{Sp}\,\{e^{-\lambda H}\,[a_{\mathbf{k}j}(t)\, a^+_{\mathbf{k}'j'}(0)$$

$$- a^+_{\mathbf{k}'j'}(0)\, a_{\mathbf{k}j}(t)]\}\,(\mathrm{Sp}\, e^{-\lambda H})^{-1} \tag{A.1}$$

(where $\theta(t) = 1$ for $t > 0$ and $\theta(t) = 0$ for $t < 0$), while the advanced Green's function differs in sign and has $-t$ in place of t. Similarly we can introduce a Green's function $F_{\mathbf{k}j\mathbf{k}'j'}$ for $a^+_{\mathbf{k}j}$ and $a^+_{\mathbf{k}'j'}$. If the Hamiltonian is given by formula (3), the equations of motion for these functions have the form

$$i\frac{dG_{\mathbf{k}j\mathbf{k}'j'}}{dt} = \delta(t)\,\delta_{\mathbf{k}\mathbf{k}'}\delta_{jj'} + \omega_{\mathbf{k}j} G_{\mathbf{k}j\mathbf{k}'j'}$$

$$+ \frac{1}{\hbar}\sum_{\mathbf{k}''j''} (V_{\mathbf{k}j\mathbf{k}''j''} G_{\mathbf{k}''j''\mathbf{k}'j'} - V'_{\mathbf{k}j\mathbf{k}''j''} F_{\mathbf{k}''j''\mathbf{k}'j'}),$$

$$i\frac{dF_{\mathbf{k}j\mathbf{k}'j'}}{dt} = -\omega_{\mathbf{k}j} F_{\mathbf{k}j\mathbf{k}'j'} - \frac{1}{\hbar}\sum_{\mathbf{k}''j''} (V_{\mathbf{k}''j''\mathbf{k}j} F_{\mathbf{k}''j''\mathbf{k}'j'}$$

$$- V'^*_{\mathbf{k}j\mathbf{k}''j''} G_{\mathbf{k}''j''\mathbf{k}'j'}). \tag{A.2}$$

For the Fourier components we get the integral equations

$$(\omega - \omega_{\mathbf{k}j})\, G_{\mathbf{k}j\mathbf{k}'j'}(\omega) - \frac{1}{\hbar}\sum_{\mathbf{k}''j''} [V_{\mathbf{k}j\mathbf{k}''j''} G_{\mathbf{k}''j''\mathbf{k}'j'}(\omega)$$

$$- V'_{\mathbf{k}j\mathbf{k}''j''} F_{\mathbf{k}''j''\mathbf{k}'j'}(\omega)] = \frac{1}{2\pi}\delta_{\mathbf{k}\mathbf{k}'}\delta_{jj'},$$

$$(\omega + \omega_{\mathbf{k}j})\, F_{\mathbf{k}j\mathbf{k}'j'}(\omega) + \frac{1}{\hbar}\sum_{\mathbf{k}''j''} [V_{\mathbf{k}''j''\mathbf{k}j} F_{\mathbf{k}''j''\mathbf{k}'j'}(\omega)$$

$$- V'^*_{\mathbf{k}j\mathbf{k}''j''} G_{\mathbf{k}''j''\mathbf{k}'j'}(\omega)] = 0. \tag{A.3}$$

These equations can be solved by the method of successive approximations, assuming that V and V′ are small quantities. The result is

$$G_{\mathbf{k}j\mathbf{k}'j'}(\omega) = \frac{V_{\mathbf{k}j\mathbf{k}'j'}}{\hbar(\omega - \omega_{\mathbf{k}j})} G_{\mathbf{k}'j'}(\omega), \quad \mathbf{k} \neq \mathbf{k}', \quad j \neq j', \tag{A.4}$$

$$G_{\mathbf{k}j\mathbf{k}j'}(\omega) = G_{\mathbf{k}jj'}(\omega) = \frac{R_{\mathbf{k}jj'}(\omega)}{\omega - \omega_{\mathbf{k}j}} G_{\mathbf{k}j'}(\omega), \quad j \neq j', \ \omega \approx \omega_{\mathbf{k}j'}, \tag{A.5}$$

$$G_{\mathbf{k}j\mathbf{k}j}(\omega) = G_{\mathbf{k}j}(\omega) = 1/2\pi\,[\omega - \omega_{\mathbf{k}j} - R_{\mathbf{k}jj}(\omega)], \tag{A.6}$$

where

$$R_{\mathbf{k}jj'}(\omega) = \frac{1}{\hbar^2}\sum_{\mathbf{k}''j''} \left[\frac{V_{\mathbf{k}j\mathbf{k}''j''} V_{\mathbf{k}''j''\mathbf{k}j'}}{\omega - \omega_{\mathbf{k}''j''}} - \frac{V'_{\mathbf{k}j\mathbf{k}''j''} V'^*_{\mathbf{k}''j''\mathbf{k}j'}}{\omega + \omega_{\mathbf{k}''j''}}\right]. \tag{A.7}$$

If the levels $\omega_{\mathbf{k}j}$ and $\omega_{\mathbf{k}j'}$ are close to one another, perturbation theory is no longer applicable. The convergence can be improved in the same way as one does in ordinary perturbation theory when there are two close levels, by treating both $G_{\mathbf{k}j}$ and $G_{\mathbf{k}jj'}$ as zeroth order quantities. We then obtain

$$G_{\mathbf{k}j}(\omega) = \frac{1}{2\pi}\,\frac{\omega - \omega_{\mathbf{k}j'} - R_{\mathbf{k}j'j'}}{(\omega - \omega_{\mathbf{k}j} - R_{\mathbf{k}jj})(\omega - \omega_{\mathbf{k}j'} - R_{\mathbf{k}j'j'}) - R_{\mathbf{k}jj'} R_{\mathbf{k}j'j}},$$

$$G_{\mathbf{k}jj'}(\omega) = R_{\mathbf{k}jj'} G_{\mathbf{k}j'}(\omega) / (\omega - \omega_{\mathbf{k}j} - R_{\mathbf{k}jj}). \tag{A.8}$$

[1] A. I. Akhiezer and I. Ya. Pomeranchuk, Некоторые вопросы теории ядра (Some Problems of Nuclear Theory), Gostekhizdat, 1948.

[2] G. Placzek and L. Van Hove, Phys. Rev. 93, 1207 (1954).

[3] A. C. Zemach and R. J. Glauber, Phys. Rev. 101, 118, 129 (1956).

[4] M. Cohen and R. P. Feynman, Phys. Rev. 107, 13 (1957).

[5] L. P. Pitaevskii, JETP 36, 1168 (1959), Soviet Phys. JETP 9, 830 (1959).

[6] V. N. Kashcheev and M. A. Krivoglaz, Физика твердого тела Soviet Phys.-Solid State, in press.

[7] I. M. Lifshitz, JETP 12, 117, 137, 156 (1942).

[8] M. A. Krivoglaz, Физика твердого тела 2, 168 (1960) [sic!]; Физика металлов и металловедение (Phys. of Metals and Metallography), in press.

[9] a) T. Matsubara, Progr. Theoret. Phys. 14, 351 (1955); b) L. D. Landau, JETP 34, 262 (1958), Soviet Phys. JETP 7, 182 (1958); c) P. C. Martin and J. Schwinger, Bull. Am. Phys. Soc. 3, 202 (1958); Phys. Rev. 115, 1342 (1959); d) Abrikosov, Gor'kov, and Dzyaloshinskii, JETP 36, 900 (1959), Soviet Phys. JETP 9, 636 (1959); e) E. S. Fradkin, JETP 36, 951, 1286 (1959), Soviet Phys. JETP 9, 672, 912 (1959); f) N. N. Bogolyubov and S. V. Tyablikov, Doklady Akad. Nauk SSSR 126, 53 (1959), Soviet Phys.-Doklady 4, 589 (1959); g) V. L. Bonch-Bruevich, Doklady Akad. Nauk SSSR 126, 539 (1959), Soviet Phys. Doklady 4, 596 (1959); h) Sh. M. Kogan, Doklady Akad. Nauk SSSR 126, 546 (1959), Soviet Phys.-Doklady 4, 604 (1959); i) D. N. Zubarev, Usp. Fiz. Nauk 71, 71 (1960), Soviet Phys.-Uspekhi 3, 320 (1960).

[10] J. Toyozawa, Progr. Theoret. Phys. 20, 53 (1958).

[11] L. Van Hove, Phys. Rev. 89, 1189 (1953). J. C. Phillips, Phys. Rev. 104, 1263 (1956).

[12] L. D. Landau and E. M. Lifshitz, Статистическая физика (Statistical Physics) Gostekhizdat, 1951 [transl. Pergamon, 1958].

[13] L. D. Landau and E. M. Lifshitz, Электродинамика сплошных сред (Electrodynamics of Continuous Media), Gostekhizdat, 1957 [transl. Pergamon, 1960].

[14] L. D. Landau, JETP 7, 1234 (1937).

[15] M. A. Krivoglaz, JETP 34, 204 (1958), Soviet Phys. JETP 7, 139 (1958).

[16] L. D. Landau, JETP 7, 19 (1937).

[17] V. L. Ginzburg and A. P. Levanyuk, JETP 39, 192 (1960), Soviet Phys. JETP 12, 138 (1961).

[18] M. A. Krivoglaz, JETP 31, 625 (1956), 32, 1368 (1957), 34, 405 (1958); Soviet Phys. JETP 4, 293 (1957), 5, 1115 (1957), 7, 281 (1958).

[19] L. Van Hove, Phys. Rev. 95, 1374 (1954). M. A. Krivoglaz, Doklady Akad. Nauk SSSR 118, 51 (1958), Soviet Phys. Doklady 3, 61 (1958). R. J. Elliot and W. Marshall, Revs. Modern Phys. 30, 75 (1958).

[20] I. M. Lifshitz, JETP 17, 1017, 1076 (1947).

[21] M. A. Krivoglaz, JETP 25, 191 (1953).

Translated by M. Hamermesh
88

SOVIET PHYSICS JETP VOLUME 13, NUMBER 2 AUGUST, 1961

SPIN-ACOUSTIC RESONANCE IN PARAMAGNETIC METALS

V. I. GERASIMENKO

Physico-Technical Institute, Academy of Sciences, Ukrainian S.S.R.

Submitted to JETP editor August 10, 1960

J. Exptl. Theoret. Phys. (U.S.S.R.) 40, 585-589 (February, 1961)

The resonance absorption of ultrasonic energy is found for paramagnetic metals, brought about by the interaction of acoustic vibrations of the lattice with the characteristic magnetic moments of the conduction electrons.

1. In a paramagnetic metal placed in a constant magnetic field H_0 and subjected to the action of ultrasonic vibrations of frequency $\hbar\omega = g\mu H_0$, resonance transitions will take place between two spin sub-levels ($+\mu H_0$ and $-\mu H_0$) as a result of the interaction of the spin magnetic moments of the conduction electrons with the acoustic vibrations of the lattice. Such a resonance phenomenon in the rare earth metals and in paramagnetic salts was first investigated by Al'tshuler.[1] In these substances, particles possessing a characteristic magnetic moment were fixed at certain points in the crystalline lattice, and the breadth of the resonance was therefore determined only by the time of paramagnetic relaxation.

In the case of a metal, it is natural to expect a broadening of the resonance line as a consequence of the high mobility of the conduction electrons. Primary interest in this phenomenon was aroused by the existence of the effect of polarization of the nuclei which accompanies paramagnetic resonance in metals (the Overhauser effect).[2] It should be expected that in spin-acoustic resonance such polarization of nuclei will take place that it would be possible to create polarized nuclear targets of arbitrary dimensions.[3] However, as will be seen from what follows, for those conditions for which resonance exists, polarization of nuclei is absent. It is shown below under what conditions spin-acoustic resonance is possible and the order of magnitude of the resonance magnetization of the metal is estimated; the absorption coefficient of ultrasonic energy is also computed.

2. It is evident that the mechanism of interaction of the spin magnetic moments of the electrons with the sound vibrations of the lattice, which leads to resonance, is the same as the mechanism of paramagnetic relaxation which is caused by the thermal vibrations of the lattice. Investigations have shown that among relaxation mechanisms, the most important is the mechanism which takes into account the spin orbit coupling of the electrons with the field of the lattice.[2,4]

In order to estimate the magnitude of the magnetic interaction of the conduction electrons with the acoustic vibrations, it is necessary to know the wave function of the electron in the lattice with account of spin-lattice interaction. For the case of alkali metals, to which we limit our considerations, such functions were found by Yaffet:[5]

$$\psi_{1,2} = e^{i\mathbf{kr}} u_{1,2}(\mathbf{k}, \mathbf{r}),$$

$$u_{1,2} = \{u_0(r) + i\mathbf{kr}u_1(r) \pm C_1 [\mathbf{kr}]_z u_2(r)\} \chi_{1/2,\,-1/2} + C_2 [\mathbf{kr}]_{x\pm iy} u_3(r)\, \chi_{-1/2,\,1/2}, \qquad (1)^*$$

where the indices 1 and 2 refer to the electron whose spin is directed along and against the constant magnetic field H_0, respectively; the direction of the field is taken as the z axis; $u_1(\mathbf{r}) \sim u_2(\mathbf{r}) \sim u_3(\mathbf{r})$; $C_1 \sim C_2 \sim \Delta g$, where Δg is the difference between the g factors of the electron in the lattice and the free electron; **k** is the wave vector of the electron; $\chi_{1/2}$ and $\chi_{-1/2}$ are the eigenfunctions of the Pauli operator $\hat{\sigma}_z$; the expression for $u(\mathbf{k}, \mathbf{r})$ is reduced to a single cell.

It is clear that in turning on the interaction of the electron with the sound

$$\hat{U} = \sum_n \nabla V(\mathbf{r} - \mathbf{R}_n)\, \mathbf{A} \exp\{iq\mathbf{R}_n + i\omega t\} \qquad (2)$$

there will occur transitions between states 1 and 2. The state of the electron gas described by the one-particle density operator $\hat{f}$ satisfying the equation

$$\partial\hat{f}/\partial t - [\hat{\mathscr{H}}_0 + \hat{U}, \hat{f}] + (\partial\hat{f}/\partial t)_{\text{collis}} = 0,$$

can, if we use the function (1) in the transition to the matrix representation, determine the resonance magnetization of the electron gas.

We note that in place of the interaction potential

---

*$[\mathbf{kr}] = \mathbf{k} \times \mathbf{r}$.

(2) we can use another potential $\hat{U}'$, which is so defined that the matrix elements of the commutator $[\hat{U}', \hat{f}]$ in the plane wave representation $(\psi_{1,2} = e^{i\mathbf{k}\cdot\mathbf{r}}\chi_{1/2,-1/2})$ are identical with the matrix elements of the previous representation. It is not difficult to show that

$$\hat{U}' = 4C_2A\hat{\sigma}_n k_l q_i e_j \lambda_{mij}\varepsilon_{lmn} \exp\{i\mathbf{q}\mathbf{r} + i\omega t\},$$

$$\lambda_{mij} = \int d\mathbf{r}\, u_0(r)\, u_1(r)\, r_m \sum_n (\mathbf{R}_n - \mathbf{r})_i \nabla_j V(\mathbf{R}_n - \mathbf{r}), \quad (3)$$

where ϵ_{lmn} is the asymmetric unit tensor, A the amplitude of the sound wave, e the polarization vector of the sound, $q = \omega/s$ the wave vector of the sound, s the sound velocity, and λ a quantity of the order of the product of the lattice constant by the mean energy of the electron in the lattice; the integral is taken over the volume of the elementary cell. It is clear from (3) that the contribution to resonance will be made both by longitudinal and transverse components of the sound wave. As will be shown from what follows, inasmuch as the resonance will exist only in weak fields H_0, when one can neglect the quantization of the electron orbits for the determination of the resonance magnetization of the metal, one can use the density operator which is quantized only in the spin of the electrons.

3. The kinetic equation which $\hat{f}$ satisfies is then written in the form[6]

$$\partial\hat{f}/\partial t + \mathbf{v}\nabla_r\hat{f} + \dot{\mathbf{p}}\nabla_p\hat{f} + [\mu\hat{\sigma}(\mathbf{H}_0 + \mathbf{H}), \hat{f}] + (\partial\hat{f}/\partial t)_{\mathbf{collis}} = 0, \quad (4)$$

where the effective magnetic field **H** is introduced with the components determined from (3) (since we can write formally $\hat{U}', = \mu\hat{\sigma}\cdot\mathbf{H}$):

$$H_n(\mathbf{r}, t) = \alpha_n A \exp\{i\mathbf{q}\mathbf{r} + i\omega t\},$$
$$\alpha_n = 4\mu^{-1}C_2 k_l q_i \lambda_{mij} e_j \varepsilon_{lmn}. \quad (5)$$

The collision integral, as in reference 6, will be assumed to be equal to $(\hat{f} - \bar{\hat{f}})/\tau + (\hat{f} - f_0)/T_{ff}$, where τ is the time of free flight of the electron in the lattice, T_{ff} is the paramagnetic relaxation time, $\bar{\hat{f}}$ is the average of the operator $\hat{f}$ over the bounding Fermi surface and

$$\hat{f}_0 = \begin{pmatrix} f_0^+ & 0 \\ 0 & f_0^- \end{pmatrix}, \qquad f_0^{\pm} = \left[\exp\left\{\frac{\varepsilon \pm \mu H_0 - \varepsilon_0}{T}\right\} + 1\right]^{-1}.$$

The magnetization is determined by the expression

$$\mathbf{M} = \mu(2\pi\hbar)^{-3}\int d\mathbf{p}\,\mathrm{Sp}\,(\hat{\sigma}\hat{f}).$$

Decomposing $\hat{f}$ over the complete set of matrices consisting of the matrices $\hat{\sigma}$ and the unit matrix $\hat{I}$ $(\hat{f} = \hat{f}_I\hat{I} + \hat{\mathbf{f}}\cdot\hat{\sigma})$ and making the substitution $\mathbf{f} = -\mu H_0 f_0'(\epsilon)(\mathbf{n} - \mathbf{w})$, we get for $\mathbf{w}$ the equation

$$\dot{\mathbf{w}} + \mathbf{v}\nabla_r\mathbf{w} + (e/c)[\mathbf{v}\mathbf{H}_0]\nabla_p\mathbf{w} + \mathbf{w}/\tau^* = \overline{\mathbf{w}}/\tau + [(\mathbf{n} - \mathbf{w})(\Omega_0 + \Omega)],$$
$$\mathbf{M} = \chi H_0(\mathbf{n} - \bar{\mathbf{w}}). \quad (6)$$

Here $1/\tau^* = 1/\tau + 1/T_{ff}$, $\mathbf{n} = \mathbf{H}_0/H_0$, $\Omega_0 = \hbar^{-1}g\mu\mathbf{H}_0$, $\Omega = \hbar^{-1}g\mu\mathbf{H}(\mathbf{r}, t)$, and χ is the paramagnetic susceptibility of the metal.

We can neglect the term $(e/c)[\mathbf{v} \times \mathbf{H}_0]\nabla_p\mathbf{w}$ in Eq. (6) since in weak fields H_0 (when the radius of the Larmor orbit is much greater than the mean free path of the electron) the character of the motion of the electron is determined only by the collisions. Transforming to the combinations $w = w_x + iw_y$ and $\Omega = \Omega_x + i\Omega_y$, we get from (6)

$$\dot{w} + \mathbf{v}\nabla w + w/\tau^* - i\Omega_0 w = \overline{w/\tau} + i\Omega(1 - w_z), \quad (7)$$
$$\dot{w}_z + \mathbf{v}\nabla w_z + w_z/\tau^* = \bar{w}_z/\tau - \mathrm{Im}(w^*\Omega). \quad (8)$$

If the resonance is far from saturation, then $w_z \ll 1$, and, consequently, we can neglect the value of w_z in Eq. (7). The solution of Eq. (7) is sought in the form $w(\mathbf{r}, t) = w\exp\{i\mathbf{q}\cdot\mathbf{r} + i\omega t\}$. Here w_z is obviously independent of $\mathbf{r}$ and t. We then get from (7) and (8)

$$w = \left\{\overline{\frac{i\Omega\tau_1}{1 + i\mathbf{q}\mathbf{v}\tau_1}}\left(\frac{\tau}{\tau_1} - \overline{\frac{1}{1 + i\mathbf{q}\mathbf{v}\tau_1}}\right)^{-1} + i\Omega\tau_1\right\}\frac{1}{1 + i\mathbf{q}\mathbf{v}\tau_1}, \quad (9)$$

$$\bar{w} = \overline{\frac{i\Omega\tau}{1 + i\mathbf{q}\mathbf{v}\tau_1}}\left(\frac{\tau}{\tau_1} - \overline{\frac{1}{1 + i\mathbf{q}\mathbf{v}\tau_1}}\right)^{-1}, \quad (10)$$

$$\bar{w}_z = T_{ff}\,\mathrm{Im}\,\overline{(w^*\Omega)}, \qquad 1/\tau_1 = 1/\tau + 1/T_{ff} + i(\omega - \Omega_0). \quad (11)$$

The bar denotes averaging over the bounding Fermi surface.

It is obvious that the resonance will exist only under the condition $\mathbf{q}\cdot\mathbf{v}\tau \ll 1$ (we note that $\tau_1 \approx \tau$, since $\Delta\omega\tau \ll 1$). Here

$$\overline{(1 + i\mathbf{q}\mathbf{v}\tau_1)^{-1}} \approx 1 - \tfrac{1}{2}\overline{(\mathbf{q}\mathbf{v}\tau)^2} \text{ and } \overline{i\Omega\tau(1 + i\mathbf{q}\mathbf{v}\tau_1)^{-1}} \approx \overline{\Omega\tau(\mathbf{q}\mathbf{v}\tau)}$$

since $\bar{\Omega} = M0$ by virtue of the linear dependence of Ω on the momentum of the electron). Thus, by neglecting the nonresonant term in (9), we get

$$w = [\overline{\Omega\mathbf{q}\mathbf{v}}\tau/(i\Delta\omega + \Gamma)][1 + i\mathbf{q}\mathbf{v}\tau]^{-1}, \quad (12)$$

$$\bar{w} = \overline{\Omega\mathbf{q}\mathbf{v}}\tau/(i\Delta\omega + \Gamma), \quad (13)$$

$$\bar{w}_z = |\overline{\Omega\mathbf{q}\mathbf{v}}|^2 T_{ff}\tau^2\Gamma/(\Delta\omega^2 + \Gamma^2). \quad (14)$$

Here $\Gamma = 1/T_{ff} + \frac{1}{2}\overline{(\mathbf{q}\cdot\mathbf{v})^2}\tau$ = width of the resonance line.

The resonance will be significant if $\Gamma \ll \omega$ or $1/\omega T_{ff} + \omega(v/s)^2\tau \ll 1$ (since $\overline{(\mathbf{q}\cdot\mathbf{v})^2}\tau \sim \omega^2(v/s)^2\tau$), i.e., the resonant frequencies should satisfy the equation

$$T_{\mathrm{ff}}^{-1} \ll \omega \ll \tau^{-1}\,(s/v)^2.$$

It then follows that we need as large a T_{ff} as possible and as small a τ as possible for the existence of resonance. For example, in lithium and beryllium, where T_{ff} depends only on the presence of impurities, for proper purity of the metal one can obtain $T_{\mathrm{ff}} \gtrsim 10^{-7}$ sec. At higher temperatures (when $\tau \sim 10^{-13} - 10^{-14}$ sec) a resonance in these metals will be observed in a region of frequencies $\omega \sim 10^{8} - 10^{9}\ \mathrm{sec}^{-1}$.

From what has been said, the impossibility of polarization of nuclei in spin acoustic resonance immediately follows, inasmuch as strong magnetic fields and low temperatures are required for the existence of polarization, which contradicts the conditions of resonance. Moreover, as is easily established by numerical estimation, $w_z \ll 1$ always, while it is necessary that $w_s \sim 1$ to achieve appreciable polarization.

4. The coefficient of absorption of ultrasonic energy in spin acoustic resonance is determined in the usual way:

$$\gamma = |T\dot{S}|_{\mathrm{ff}}/sE_{\mathrm{so}},$$

where T is the temperature of the specimen; $E_{\mathrm{SO}} = \frac{1}{4}\rho\omega^2 A$ is the energy of the sound wave;

$$S = (2\pi\hbar)^{-3}\int d\mathbf{p}\ \mathrm{Sp}\,\{(1-\hat{f})\ln(1-\hat{f}) + \hat{f}\ln\hat{f}\}$$

is the entropy of the electron gas. In order to carry out the operation Sp, we transform to the diagonal representation of the matrix of the operator f:

$$\hat{f} = \begin{pmatrix} f_{11} & f_{12} \\ f_{21} & f_{22} \end{pmatrix} \rightarrow \begin{pmatrix} f_1 & 0 \\ 0 & f_2 \end{pmatrix},$$

$$f_{1,2} = f_{11} \mp \left\{\frac{f_{11}-f_{22}}{2} + \left[\left(\frac{f_{11}-f_{22}}{2}\right)^2 + |f_{12}|^2\right]^{1/2}\right\}.$$

Noting $\mathrm{f} = \mathrm{f_I}\hat{\mathrm{I}} + \mathbf{f}\cdot\boldsymbol{\sigma}$, we obtain the result that $f_{11} + f_{22} = 2f_I$, $f_{11} - f_{22} = 2f_z$ and $f_{12} = f_x + if_y$. Therefore, $f_{1,2} = f_I \mp f$, where $f = |\mathbf{f}|$. Solution of the equation for f_I is usually sought in the form $f_0 + f'$, where f' is the addition to the equilibrium distribution function. Taking this fact into account, we get

$$T\dot{S} = T\,(2\pi\hbar)^{-3}\int d\mathbf{p}\left[(\dot{f} - \dot{f}')\ln\frac{1-f_I+f}{f_I-f}\right.$$
$$\left. + (\dot{f} + \dot{f}')\ln\frac{f_I+f}{1-f_I-f}\right].$$

Thence, after expansion in f and f′, we have for the spin part of the dissipation function

$$(T\dot{S})_{\mathrm{ff}} = 2T\,(2\pi\hbar)^{-3}\int d\mathbf{p}\, f\dot{f}\left[\frac{\ln(1-f_0)}{1-f_0} + \frac{\ln f_0}{f_0}\right].$$

Close to the bounding Fermi surface, $\ln f_0 \approx \ln(1-f_0)$. Noting that $T^{-1}(1-f_0)f_0 = \partial f_0/\partial\epsilon$, we get [after substitution $\mathbf{f} = -\mu H_0 f_0'(\mathbf{n} - \mathbf{w})$],

$$(T\dot{S})_{\mathrm{ff}} = 2\ln 2\cdot\chi H_0^2\left(\frac{\overline{w}_z - \overline{|w|^2}}{T_{\mathrm{cn}}} + \frac{|\overline{w}|^2 - \overline{|w|^2}}{\tau}\right),$$

where $\overline{w}_z$, w and $\overline{w}$ are the solutions of Eqs. (7) and (8).

Making use of Eqs. (12) — (14), we obtain the following expression for the coefficient of absorption of ultrasonic energy at spin acoustic resonance:

$$\gamma = 12\ln 2\cdot\frac{\Omega_0^2}{\omega^2}\,\frac{\chi\tau^3\,\overline{(\mathbf{qv})^2}}{\rho s}\,\frac{|\overline{\alpha\mathbf{qv}}|^2}{\Delta\omega^2 + \Gamma^2},$$

where α is determined by Eq. (5). In order of magnitude, $\alpha\mathbf{q}\cdot\mathbf{v} \sim 4\mu^{-1}\Delta g q^2 k a \epsilon v$ (a is the lattice constant, ϵ and v are the energy and velocity of the electron on the bounding Fermi surface, $\Delta g \sim 10^{-3} - 10^{-4}$). Numerical estimates under conditions in which there is resonance lead to values $\gamma \lesssim 10^{-5}\ \mathrm{cm}^{-1}$ close to resonance.

---

[1] S. A. Al'tshuler, JETP 28, 38 and 49 (1955), Soviet Phys. JETP 1, 29 and 37 (1955).

[2] A. Overhauser, Phys. Rev. 92, 411 (1953); 89, 689 (1953).

[3] A. Kastler, J. phys. radium 15, 300 (1954).

[4] R. J. Elliott, Phys. Rev. 96, 266 (1954).

[5] Y. Yaffet, Phys. Rev. 85, 478 (1952).

[6] Azbel', Gerasimenko, and Lifshitz, JETP 32, 1212 (1957), Soviet Phys. JETP 5, 986 (1957).

Translated by R. T. Beyer
89

SOVIET PHYSICS JETP VOLUME 13, NUMBER 2 AUGUST, 1961

DISPERSION FORMULAS WHICH TAKE INTO ACCOUNT THE OPTICAL INTERACTION

V. I. SERDOBOL'SKII

P. N. Lebedev Physics Institute, Academy of Sciences, U.S.S.R.

Submitted to JETP editor August 12, 1960

J. Exptl. Theoret. Phys. (U.S.S.R.) 40, 590-596 (February, 1961)

A formal theory of nuclear reactions is developed which is more adequate for treating nuclear problems than the Wigner R-matrix theory. The approximate orthogonality between the wave functions of the compound nucleus and the unexcited ground state functions is used to separate the compound nucleus resonances. The theoretical treatment leads to specific dispersion formulas which take into account the overlapping levels and the interaction between the particles and the optical potential of the nucleus.

1. A large number of articles have appeared recently in which it is attempted to describe, within the framework of a single mathematical scheme, nuclear reactions involving the production of a compound nucleus, direct nuclear reactions, and optical scattering. Previously,[1,2] we developed a variant of a formal theory in which the compound nucleus resonances were isolated by separation of the polar part of the wave function and the S matrix for complex energies.

It turned out that such a method separates correctly only those levels whose width is considerably less than the distance to the nearest threshold of a nuclear reaction. Undoubtedly, the approach suggested by Feshbach[3] is more successful. Feshbach's formalism, however, does not describe nuclear collisions accompanied by a redistribution of the particles (nuclear reactions in a narrow sense) Moreover, the dispersion formulas obtained by Feshbach were left in very general form, and their application was not discussed. Feshbach's theory is improved and developed in the present article as regards these two aspects.

It is shown in Sec. 2 that the smallness of the parameter (1) (see below) suggested by us[1] makes it possible to establish the property of approximate orthogonality of the wave functions of the compound nucleus to the functions of the reaction channels. This property permits the extension of the procedure suggested by Feshbach for the separation of compound nucleus resonances to nuclear reactions accompanied by a redistribution of particles (Secs. 3 and 4).

It is suggested in Sec. 5 that direct nuclear interactions play a minor role, and that the optical potential is energy independent. Under these assumptions, the resonance half-widths split into the products of the penetration factors, which take into account the optical interaction and the amplitudes depending only on the level. The dispersion formula (22) describing the compound nucleus resonances is found for the energy region in which the influences of the optical interaction and nuclear reaction thresholds are important. In Sec. 6, the general formula is applied to the special case in which only one of the compound nucleus levels makes an essential contribution.

2. It is known that optical interactions and direct nuclear reactions take place without a rearrangement of the internal structure of the nucleus. In contrast to these processes, the production of a compound nucleus is accompanied by the transfer of excitation to all or, at least, several nucleons. The physical difference between these states requires that the wave functions of the compound nucleus be (at least, approximately) orthogonal to the wave functions of the channels open at medium energies. It is convenient to introduce numerical criteria which make it possible to consider the accuracy to which this orthogonality is fulfilled.

Let χ_λ denote the wave function of a compound nucleus and $c_1, \ldots, c_P$ the indices for the channels open at medium energies. We shall consider the ratio η of the mean square of the wave function of the compound nucleus on parts of the hypersurface corresponding to channels $c_1, \ldots, c_P$ which can be open at medium energies to the mean over the volume. This ratio can be written in the form

$$\eta = \frac{\sum_c^P |\langle c|\chi_\lambda\rangle_R|^2}{\frac{1}{\tau}\int |\chi_\lambda|^2 d\tau = \frac{1}{3}\sum_c^P \frac{|\gamma_{\lambda c}|^2}{E_R}}. \qquad (1)$$

Here τ is that part of configuration space in which the nucleus is situated, R is the radius of the nucleus in channel c. The integrals over the internal variable $\langle c \mid \chi_\lambda \rangle$ taken for r = R are related to the amplitudes of the reduced half-widths $\gamma_{\lambda c}$. The energy E_R, which is equal to $\hbar^2/2mR$, varies from 0.1 to 1 Mev for different nuclei.

It was shown by the present author[1] that the parameter η is the ratio of the mean time of free flight of the particles from the space in which the unstable compound nucleus is situated to the lifetime of the compound nucleus. We now note that at the same time, relation (1) indicates what part of the wave function χ_λ lies in the functional subspace which is filled by the wave functions of the channels. The smallness of η means that, in a first approximation, the subspace P of the wave functions $c_1, \ldots, c_P$ is orthogonal to the subspace $\{\chi_2\}$ of the wave functions describing the states of the compound nucleus. The property of approximate orthogonality of the functions $|c\rangle$ and χ_λ permits us to exclude formally the intermediate nucleus states and introduce an effective interaction whose smooth part describes the direct and optical processes.

3. We denote by P and $P_\perp$ the projection operators in subspace P and in subspace $P_\perp$ complementary to it; $P_\perp$ is equal to 1 – P, where by the symbol 1 we have in mind the entire configuration space of the coordinates of the nucleons of the system. Schrödinger's equation with infinitesimal imaginary additional terms which automatically separate the outgoing wave solution at infinity has the form

$$(E - H + i\varepsilon)\,\psi^{(+)} = i\varepsilon\varphi. \tag{2}$$

Here φ is the incident plane wave, $\psi^{(+)}$ is the solution, and $\epsilon \to +0$.

For brevity, we introduce the notation:

$$\Gamma = P_\perp HP, \qquad \Gamma^+ = PHP_\perp, \qquad H_\perp = PHP_\perp. \tag{3}$$

The projections of Eq. (2) in the subspaces P and $P_\perp$ have the form

$$(E - PHP + i\varepsilon)\,P\psi^{(+)} = i\varepsilon\varphi + \Gamma^+\psi^{(+)},$$
$$(E - H_\perp + i\varepsilon)\,P_\perp\psi^{(+)} = \Gamma\psi^{(+)}, \tag{4}$$

from which we obtain the equation in subspace P equivalent to (2):

$$(E - H_P + i\varepsilon)\,P\psi^{(+)} = i\varepsilon\varphi, \tag{5}$$

where the "effective Hamiltonian" is

$$H_P = PHP + \Gamma^+(E - H_\perp)^{-1}_\perp\Gamma. \tag{6}$$

The subscript ⊥ after the parenthesis in (6) denotes that the inverse operator acts in the complementary space. The quantity $i\epsilon$ is omitted, since the operator $H_\perp$ has only discrete, real eigenvalues in the energy region under consideration.

The eigenfunctions of $H_\perp$ describe stationary states of the compound nucleus whose decay is artificially forbidden. The part PHP of the total Hamiltonian H_P corresponds to processes not connected with the rearrangement of the internal structure of the nucleus and which occur within a relatively small time interval. The second term of the right-hand part of (6) describes the production and decay of the compound system. We denote by χ_λ the eigenfunctions of the Hamiltonian $H_\perp$ corresponding to the eigenvalue E_λ. In the medium energy region, the operator $H_\perp$ does not have a continuous spectrum; therefore the energy E_λ is real and the wave functions χ_λ satisfy the generalized condition of realness:

$$\chi^*_\lambda = (-)^{J-M}O\chi_\lambda(-M), \tag{7}$$

where O is the time-reversal operator (spin matrix) and M is the quantum number characterizing the projection of the total angular momentum J. The minus sign in the parenthesis following χ_λ denotes that the projection of the total angular momentum in the state $\chi_\lambda(-M)$ has the opposite sign.

We write the Green's function in relation (6) in the form of a spectral expansion

$$(E - H_\perp)^{-1}_\perp = \sum_\lambda \frac{|\chi_\lambda\rangle\langle\chi_\lambda|}{E - E_\lambda}, \tag{8}$$

in which case the effective Hamiltonian takes the form

$$H_P = H_P^0 + \sum_\lambda \frac{\Gamma^+|\chi_\lambda\rangle\langle\chi_\lambda|\Gamma}{E - E_\lambda}. \tag{9}$$

It is clear that all difficulties connected with the singularities in the behavior close to the thresholds do not involve H_P. The expansion (9) is fundamental to the present theory. Further transformations are of a formal character, and, in many ways, are analogous to those presented by Lane and Thomas.[5]

4. Let $\psi_0^{(+)}$ denote the solution of Schrödinger's equation (5) in which the Hamiltonian H_P is replaced by the resonanceless operator H_P^0. Let $H = H_0 + V$, $H_P^0 = H_0 + V^0$, where H_0 is the Hamiltonian of free motion described by the wave functions φ, while V and V^0 are interaction operators in the corresponding channels. It is known[4] that the amplitude for transition from the state φ into some other state φ' is expressed by a matrix element of the form $\langle\varphi' \mid V' \mid \psi^{(+)}\rangle$. Using Eq. (2) for the functions $\psi^{(+)}$ and $\psi_0^{(+)}$, we find, after simple algebraic transformations (similar to those given by Feshbach[3]):

$$\langle \varphi' | V' | \psi^{(+)} \rangle = \langle \varphi' | V^{0'} | \psi_0^{(+)} \rangle$$

$$+ \sum_{\lambda} \frac{\langle \psi_0^{(-)'} | \Gamma^{+} | \chi_\lambda \rangle \langle \chi_\lambda | \Gamma | \psi^{(+)} \rangle}{E - E_\lambda}. \qquad (10)$$

The first term of the right-hand part of (10) gives the amplitude of optical scattering and of the direct processes.

The matrix element for transition into the state $\psi_0^{(-)'}$ is a smooth function of the energy, the matrix element for transition into the state $\psi^{(+)}$ can be expressed in terms of quantities that are smooth functions of the energy by means of the following system of equations:

$$\sum_{\lambda} [\delta_{\mu\lambda} (E - E_\lambda) - K_{\mu\lambda}] \frac{\langle \chi_\lambda | \Gamma | \psi^{(+)} \rangle}{E - E_\lambda} = \langle \chi_\mu | \Gamma | \psi_0^{(+} \rangle, \qquad (11)$$

where

$$K_{\mu\lambda} = \langle \chi_\mu | \Gamma (E - H_P^0 + i\varepsilon)^{-1} \Gamma^{+} | \chi_\lambda \rangle. \qquad (12)$$

Feshbach assumed that, in first approximation, the matrix element for transition to the state $\psi_0^{(-)'}$ and the quantity $K_{\mu\lambda}$ do not depend on the energy. This enables one to construct readily the solution (11) by means of an expansion in eigenvectors of a homogeneous equation. Of course, it is assume here that $\psi_0^{(-)}$ and $K_{\mu\lambda}$ vary little over energy intervals of the order of the width of the compound nucleus levels. If the levels overlap with the nuclear reaction thresholds, this method of treatment is known to be inapplicable.

In Eq. (11), it is easy to go over to the matrix elements of the S matrix. To do this, it is sufficient to use the formulas given in the appendix to reference 1. In place of the functions $\psi^{(+)}$ and $\psi_0^{(+)}$, we use the functions $u_c^{(\pm)}$ and $u_c^{0(\pm)}$ describing the motion with the initial quantum numbers αslJM. Schrödinger's equation for the functions $u_c^{0(\pm)}$ has the form

$$(E - H_P^0)\, u_c^{0(\pm)} = 0, \qquad (13)$$

where in the external region, in which there is no interaction,

$$| u_c^{0(-)} \rangle = \sum_{c'} \frac{\delta_{c'c} I_{c'} - S_{c'c}^{0J} O_{c'}}{v'^{1/2} r'} | c' \rangle,$$

$$\langle u_c^{0(-)} | = \sum_{c'} \frac{\delta_{c'c} I_{c'} - S_{c'c}^{0J} O_{c'}}{v'^{1/2} r'} \langle c' |. \qquad (14)$$

Here, the functions I_c and O_c are the same as those given by Lane and Thomas.[5] The matrix element $S_{c'c}^{0J}$ describes processes occurring without the formation of a compound nucleus.

5. We shall consider in detail the low-energy case, where the kinetic energy of the incident (or emitted) particles does not exceed 5 – 10 Mev. At these energies, the optical potential has only a real part, and the direct nuclear processes do not play an important role. It will be assumed that the Hamiltonian H_P^0 and the wave functions $\psi_0^{(\pm)}$ describe scattering on an optical potential.

In the approximation $E_{kin} \leq 40$ Mev, the behavior of the optical wave functions inside the potential well does not depend on the energy, and the functions $u_c^{0(\pm)}$ split into the product of two factors, one of which depends only on the energy (normalizing factor) and the other, only on the coordinates. We can then write

$$u_c^{0(+)} = k_c(E)\, g_c(r)\, | c \rangle, \qquad u_c^{0(-)*} = k_c(E)\, g_c(r)\, \langle c |. \qquad (15)$$

These relations do not hold close to the boundary of the potential well, and therefore the coefficients $k_c(E)$ cannot be found directly from the boundary conditions. We differentiate Schrodinger's equation for the function $u_c^{0(+)}$ with respect to the energy and write the conjugate equation for $u_c^{0(-)*}$:

$$(E - H_P^0)\, \partial u_c^{0(\pm)} / \partial E + (1 - \partial V^0 / \partial E)\, u_c^{0(+)} = 0,$$

$$(E - H_P^{0*})\, u_c^{0(-)*} = 0. \qquad (16)$$

Here V^0 is the optical potential in the channel c. We multiply these equations by $u_c^{0(-)*}$ and $u_c^{0(+)}$ respectively, subtract one from the other, and integrate over the internal part of the potential well. We now apply Green's theorem and, using the boundary conditions (14) for the functions $u_c^{0(\pm)}$, we obtain

$$\int_0^R \left\langle u_c^{0(-)} \left| \left(1 - \frac{\partial V^0}{\partial E}\right) \right| u_c^{0(+)} \right\rangle = 2\hbar P_c \Omega_c^2 \frac{\partial L_c^0 / \partial E}{(L_c^0 - L_c)^2}. \qquad (17)$$

Here L_c denotes, as usual, the logarithmic derivative of the function O taken at the point R and multiplied by R; similarly, L_c^0 denotes the logarithmic derivative of the optical wave functions $u_c^{0(+)}$ for r = R, multiplied by R. The quantities P_c and Ω_c are defined in the review article of Lane and Thomas.[5]

At small energies, it can be assumed that the optical potential does not depend on the energy, and the derivative in the left-hand part of (17) can be dropped. We normalize the real functions $g_c(r)$ to unity, so that the right-hand part of (17) is equal to $[k_c(E)]^2$. For convenience of notation, we introduce the energy-independent amplitudes $b_{\lambda c}$:

$$b_{\lambda c} \doteq E_R^{-1/2} \langle \chi_\lambda | \Gamma | c g_c \rangle = E_R^{-1/2} \langle c g_c | \Gamma^{+} | \chi_\lambda \rangle. \qquad (18)$$

From relation (7) for χ_λ^* and from similar relations for the functions $| c \rangle$ resulting from the properties of the time-reversal operator, it follows that $b_{\lambda c}$ is real.

We note that the logarithmic derivative L_c^0 in the minus first degree is an R function (for the definition and properties of R functions, see Lane and Thomas,[5] p. 272). This means, in particular, that the quantity $\partial L_c^0/\partial E$ is always less than zero.

We introduce the auxiliary quantity γ_c^0

$$\gamma_c^0 = +\sqrt{-(\partial L_c^0/\partial E)^{-1}}, \tag{19}$$

whose physical sense will be explained below. It can be shown that the quantity γ_c^0 weakly depends on the energy; the characteristic interval over which γ_c^0 changes is equal in order of magnitude to E_R.

We define the positive penetration factors

$$\Pi_c = E_R P_c/(\gamma_c^0)^2 |L_c^0 - L_c|^2 \tag{20}$$

and the matrix Ω_c^0 whose square gives the diagonal of the S matrix for optical scattering. From the adjointness conditions at the boundary we readily find

$$(\Omega_c^0)^2 = S_c^{\text{opt}} = \Omega_c^2 (L_c^0 - L_c^*)/(L_c^0 - L_c). \tag{21}$$

The dispersion expansion (10) taking into account resonances of the compound nucleus and optical processes takes the form

$$S_{c'c}^J = \delta_{c'c} S_c^{\text{opt}} - 2i \sum_\lambda \Omega_{c'}^0 \Pi_{c'}^{1/2} b_{\lambda c'} \Omega_c^0 \Pi_c^{1/2} x_{\lambda c}. \tag{22}$$

The energy dependence of the resonance is contained in the quantities $x_{\lambda c}$ for which the equation

$$\sum_\lambda [\delta_{\mu\lambda}(E - E_\lambda) - K_{\mu\lambda}] x_{\lambda c} = b_{\mu c} \tag{23}$$

is valid.

It is seen that the contribution of one resonance in (22) does not satisfy the reciprocity theorem. The coefficients $K_{\mu\lambda}$ in (23) are determined by (12). The imaginary part of $K_{\mu\lambda}$ contains a δ function of the energy and is readily expressed by the quantities Π_c and $b_{\lambda c}$. From the completeness relation for the functions $u_c^{0(+)}$, we find

$$\delta(E - H_P^0) = -\frac{1}{2\pi\hbar} \sum_c |u_c^{0(+)}\rangle\langle u_c^{0(+)}|,$$

$$\operatorname{Im} K_{\mu\lambda} = -\sum_c \Pi_c b_{\mu c} b_{\lambda c}. \tag{24}$$

The summation in (24) includes only channels open at a given energy.

In order to find also the real part of $K_{\mu\lambda}$, we employ the analytical character of the dependence of the quantity Λ_c on the energy. Let

$$\Lambda_c = (E_R/(\gamma_c^0)^2)(L_c^0 - L_c)^{-1}. \tag{25}$$

It is readily shown that

$$K_{\mu\lambda} = -\sum_c^P \Lambda_c b_{\mu c} b_{\lambda c}. \tag{26}$$

As a matter of fact, both parts of relation (26) represent functions which are analytical in the principal plane. The imaginary parts of (26) coincide, since $\operatorname{Im}\Lambda_e$ is equal to Π_c. As $E \to \infty$, the expression for $K_{\mu\lambda}$ in (12) tends to zero as does the quantity Λ_c. At points for which S_c^{opt} tends to infinity, both parts have poles, but the values at the poles coincide.

Far away from the optical resonances $|L_c^0| \gg 1$, Ω_c^0 goes over into Ω_c, the product $\Pi_c^{1/2} b_{\lambda c}$ goes over into $P_c^{1/2}\gamma_{\lambda c}$, where $\gamma_{\lambda c} = E_R^{-1/2} b_{\lambda c}/\gamma_c^0 |L_c^0 - L_c|$, and we obtain the same results as in R-matrix theory.

The optical resonances usually lie sufficiently far away from one another and it is necessary to take into account only one resonance. For the resonance energy E_r, the logarithmic derivative L_c^0 vanishes. Close to the resonance, we expand L_c^0 in powers of the difference $E - E_r$. Substitution of the expansion into (21) leads to the usual formula for the optical resonance with the width Γ_c^0 equal to $2P_c(\gamma_c^0)^2$. It is seen that the square of γ_c^0 has the sense of a reduced width of optical resonance. The quantity Λ_c and the penetration factor Π_c take the form

$$\Lambda_c = -\frac{E_R}{E - E_r + L_c(\gamma_c^0)^2},$$

$$\Pi_c = \frac{E_R \Gamma_c^0/2}{(E - E_r + S_c(\gamma_c^0)^2)^2 + (\Gamma_c^0)^2/4}. \tag{27}$$

6. We consider the special case in which one of the compound nucleus levels lies close to the threshold in channel c'. Let the width Γ_λ' and the shift Δ_λ' contain no contribution from channel c':

$$\Gamma_\lambda' = 2\sum_c{}' \Pi_c b_{\lambda c}^2, \qquad \Delta_\lambda' = -\sum_c^{P}{}' \operatorname{Re}\Lambda_c b_{\lambda c}^2, \tag{28}$$

where the summation in the expression for Γ_λ' is carried out only over the open channels. It is clear that these quantities vary little close to the threshold. The dispersion formula takes on the form

$$S_{c''c}^J = \delta_{c''c} S_c^{\text{opt}} - 2i \frac{\Omega_{c''}^0 \Pi_{c''}^{1/2} b_{\lambda c''} \Omega_c^0 \Pi_c^{1/2} b_{\lambda c}}{E - E_\lambda - \Delta_\lambda' + i\Gamma_\lambda'/2 + \Lambda_{c'} b_{\lambda c'}^2}. \tag{29}$$

The reaction cross section in the region below the threshold of channel c' displays an interesting behavior. If the optical interaction is of such a type that capture on a single-particle level is possible, then, at an energy corresponding to the binding energy, the quantity $\Lambda_{c'}$ in the denominator has a pole and the reaction cross section $\sigma_{c''c}$ vanishes.

In conclusion, I wish to thank Professor A. S. Davydov for his attention to this work.

---

[1] V. I. Serdobol'skii, Nuclear Phys. (in press).

[2] V. I. Serdobol'skii, JETP 38, 1903 (1960), Soviet Phys. JETP 11, 1368 (1960).

[3] H. Feshbach, Ann. Phys. 5, 357 (1958).

[4] B. A. Lippman, Phys. Rev. 102, 264 (1956).

[5] A. M. Lane and R. G. Thomas, Revs. Modern Phys. 30, 257 (1958).

Translated by E. Marquit
90

SOVIET PHYSICS JETP VOLUME 13, NUMBER 2 AUGUST, 1961

PHOTOPRODUCTION OF PIONS ON PIONS

L. D. SOLOV'EV

Joint Institute for Nuclear Research

Submitted to JETP editor August 13, 1960

J. Exptl. Theoret. Phys. 40, 597-604 (February, 1961)

An exact solution has been found for the equation that describes photoproduction of pions on pions at low energies. The condition for a unique solution is formulated. The solution is determined by the high-energy singularities of the amplitude. It has a resonant character if resonance occurs in the scattering of pions on pions in a state with J = I = 1.

1. INTRODUCTION

THE photoproduction of pions on pions

$$\gamma + \pi \rightarrow \pi + \pi \qquad (1)$$

must be taken into account if photoproduction of pions on nucleons is studied with the aid of the Mandel'stam representation,[1] just as scattering of pions on pions must be taken into consideration in an investigation of pion-nucleon scattering.

In the analysis of pion-pion scattering we introduce in the theory a new pion-pion interaction constant.[2] Should a similar constant be introduced in the analysis of the photoproduction of pions on pions? Perturbation theory answers this question in the negative. In fact, whereas a four-pion vertex with four internal nucleon lines diverges, so that it becomes necessary to introduce into the Lagrangian a corresponding counterterm and a pion-pion interaction constant (see, for example, reference 3), an analogous vertex with one photon and three pion external lines converges, so that there is no need for new counterterms and a new constant. Furthermore, such photon—three-pion counterterms cannot be introduced simply from considerations of covariance and renormalizability. Thus, from the point of view of perturbation theory, the photoproduction amplitude should be expressed in terms of the "old" constants (say, the electromagnetic, pion-pion, and pion-nucleon interaction constants).

If furthermore, after taking the electromagnetic interaction once into account on inclusion of the photon, we consider only strong interactions and disregard the πKK interaction (which cannot be stronger than the electromagnetic interaction[4]) then any diagram of process (1) should contain a nucleon or nucleon-hyperon loop (Fig. 1). Thus, the process (1) is connected in an essential manner with baryons in intermediate states and should vanish in the limits of infinitely large baryon masses.

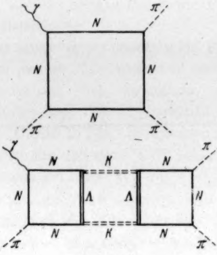

FIG. 1

It will be shown later on that these results of perturbation theory follow also from the theory of dispersion relations.

The process (1) was analyzed by Gourdin and Martin,[5] who used the double dispersion relations. They obtained a homogeneous equation for the amplitudes of this process, and obtained its solution in the approximation of sharp pion resonance. This solution depends on an indeterminate constant and has a resonant character in the limit, when the width of the pion resonance (of finite height) vanishes. From the physical point of view it is clear, however, that if the pion scattering amplitude vanishes everywhere except at one point, where it is finite, then the scattering process should not appear anywhere.

We start from the usual (one-dimensional) dispersion relations in the observable region, assuming that it is valid without subtractions. In Sec. 3 we give physical considerations from which it follows that if the dispersion relations with one subtraction are valid for scattering (as in reference 2), then the dispersion relations are valid without subtractions for photoproduction, by virtue of the gauge invariance. In order to obtain from the dispersion relations an inhomogeneous equation with a non-trivial solution, it is necessary to take into account the far singularities, primarily the singularity corresponding to the nucleon-antinucleon pair in the intermediate state in the unitarity condition.*

In Sec. 4 we obtain in explicit form a solution of the equation derived from the dispersion relations. This solution is unique if the pion phase shift tends to zero at infinity. On the other hand, if the phase shift tends to π, then the solution is not unique. However, one of the solutions at infinity tends to the inhomogeneous term faster than all others. Only this solution has the property that the entire contribution of the pion scattering vanishes from it if the width of the pion resonance (of finite height) tends to zero. We choose precisely this solution as the physical one. The diagrams of the solution are constructed for two models of pion resonance, which differ in the behavior of the phase shift at infinity.

2. KINEMATICS

Let k and e_ν be the momentum and the vector of polarization of the photon, q_1, α, and also q_2, β and q_3, γ, are the momenta and charge numbers of the initial and final pions respectively. The matrix element of the process (1) has the following form[5]

$$\langle \pi\pi | S | \pi\gamma \rangle = (2\pi)^4 \delta (k + q_1 - q_2 - q_3) \frac{\varepsilon_{mnrs} q_1^m q_2^n q_3^r e_\nu^s}{4\sqrt{q_1^0 q_2^0 q_3^0 k^0}} \varepsilon_{\alpha\beta\gamma} F(s, \bar{s}, t), \tag{2}$$

where ϵ is a completely antisymmetrical tensor, and F is a completely symmetrical function of the invariants

$$s = (q_2 + q_3)^2, \quad \bar{s} = (q_1 - q_3)^2,$$

$$t = (q_1 - q_2)^2; \quad s + \bar{s} + t = 3\mu^2. \tag{3}$$

In the center-of-mass system (c.m.s.) we have

$$\langle \pi\pi | S | \pi\gamma \rangle = (2\pi)^4 \delta (k + q_1 - q_2 - q_3) \frac{\mathbf{e}_\nu [\mathbf{qk}]}{4\sqrt{\omega_k k}} \varepsilon_{\alpha\beta\gamma} F(s, \bar{s}, t), \tag{4)†$$

$$s = (k + \omega_k)^2 = 4\omega_q^2, \quad \bar{s} = \mu^2 - 2k\omega_q - 2kq \cos\theta,$$

$$t = \mu^2 - 2k\omega_q + 2kq \cos\theta, \tag{5}$$

where μ is the pion mass, $k = |\mathbf{k}|$, $\mathbf{q} = \mathbf{q}_3$, $\omega_k = \sqrt{k^2 + \mu^2}$, $\cos\theta = \mathbf{k}\cdot\mathbf{q}/kq$, and

$$F(s, \cos\theta) = \sum_{l=0}^{\infty} f_{2l+1}(s) P'_{2l+1}(\cos\theta). \tag{6}$$

From the unitarity condition it follows that at low energies

$$f_l = |f_l| e^{i\delta_l^1}, \tag{7}$$

where δ_l^1 is the pion-pion scattering phase shift in a state with angular momentum l and isotropic spin 1. The differential cross section is

$$d\sigma / d\Omega = \tfrac{1}{8} kq^3 \sin^2\theta |F/4\pi|^2. \tag{8}$$

3. DISPERSION RELATION

We now postulate the rate of growth of the function F for fixed t and $s \to \infty$. It follows from (8) that for fixed t and $s \to \infty$ we have

$$d\sigma / d\Omega |_{\theta=0} = \text{const} \cdot |\sqrt{s}F|^2. \tag{9}$$

Were this equation to pertain to an elastic process, it would follow from it that, Im F behaves as the total cross section of this process for fixed t and at $s \to \infty$. There are theoretical grounds for assuming that the total cross section should decrease at infinity as $1/\ln^2 s$. Consequently, Im F should decrease at the same rate in (9) for an elastic process. Let us assume that this takes place also for the process considered here.

If it is assumed in general that the differential cross section forward for photoproduction and scattering of pions at infinity have the same rate of growth, then the invariant amplitudes for photoproduction should decrease more rapidly than those for scattering, since gauge invariance calls for an energy factor to stand between the invariant amplitude and the matrix photoproduction element, a factor which is absent in the case of scattering. Furthermore, if the dispersion relations are valid with one subtraction for scattering, they are valid without subtractions for photoproduction. We thus assume that the one-dimensional dispersion relations for this process, which are rigorously proved in reference 6, are valid without subtractions:

$$F(s,t) = \frac{1}{\pi} \int_{4\mu^2}^{\infty} \frac{\operatorname{Im} F(s',t)}{s' - s - i\varepsilon} + (s \to \bar{s}). \tag{10}$$

If we confine ourselves to the examination of the nearest singularities in this relation, i.e., if we consider in the unitarity condition only a two-pion intermediate state, then we obtain for the photoproduction amplitude a homogeneous equation which should have a trivial solution (the uniqueness requirement is formulated in Sec. 4). Thus, the process under consideration depends substantially on the far singularities.

---

*A similar allowance for the far singularities (for πK scattering with charge exchange) was made by A. A. Ansel'm and V. M. Shekhter and reported at the Conference on Dispersion Relations in Dubna (May 1960).

†[q k] = q × k.

Allowance for the next singularities, corresponding to four, six, etc. pions in the intermediate state, introduces into relation (10) the photoproduction amplitudes of many pions. At the present time we cannot write down a system of equations for these amplitudes. It is clear, however, that since all these amplitudes have no pole singularities, such a system should be homogeneous and its solution trivial.

The next singularity corresponds to the kaon-antikaon pair (K$\overline{\text{K}}$). If we disregard weak interactions, then the amplitude of the process $\gamma\pi \to \text{K}\overline{\text{K}}$ also has no pole singularities. It is easy to write down for it a dispersion relation [without subtraction, like (10)], which has a trivial solution if the amplitude of the pion photoproduction vanishes.

The next singularity, which introduces inhomogeneity into (10), corresponds to a nucleon-antinucleon pair (N$\overline{\text{N}}$) in the intermediate state, since the dispersion relations for the amplitude of the process $\gamma\pi \to \text{N}\overline{\text{N}}$ have an inhomogeneous pole term. Once the inhomogeneity is introduced in the equations, we can neglect the amplitudes of photoproductions of four etc. pions in the low-energy region under consideration.

Thus, the Im F· term of (10) has two parts

$$\operatorname{Im} F = (\operatorname{Im} F)_{\pi\pi} + (\operatorname{Im} F)_{N\overline{N}}, \tag{11}$$

where $(\text{Im F})_{\pi\pi}$ is expressed in terms of the amplitudes of the processes $\gamma\pi \to \pi\pi$ and $\pi\pi \to \pi\pi$ (7), while $(\text{Im F})_{\text{N}\overline{\text{N}}}$ is expressed in terms of the amplitudes of the processes $\gamma\pi \to \text{N}\overline{\text{N}}$ and $\pi\pi \to \text{N}\overline{\text{N}}$.

The term $(\text{Im F})_{\pi\pi}$ in (10) contains, generally speaking, a region of unobservable angles at low energies. There is no unobservable region when

$$t = -\mu^2/2, \tag{12}$$

and in this case relation (10) has the form

$$F\left(s, \cos\theta = \frac{q}{k}\right) = \frac{1}{\pi}\int_{4\mu^2}^{\infty} \frac{(\operatorname{Im} F(s', \cos\theta = q'/k'))_{\pi\pi}}{s' - s}\, ds'$$
$$+ \frac{1}{\pi}\int_{4m^2}^{\infty} \frac{(\operatorname{Im} F(s', \cos\theta = q'/k'))_{N\overline{N}}}{s' - s}\, ds'$$
$$+ \left(s \to \bar{s} = \frac{5}{2}\mu^2 - s\right); \tag{13}$$

here m is the nucleon mass. It is obvious that in the integrals whose lower limit is 4m^2 we can put $\cos\theta = 1$ and neglect s and $\bar{\text{s}}$ compared with s′.

4. THE INTEGRAL EQUATION AND ITS SOLUTION

At low energies in the observable region, it is sufficient to include in the expansion (6) the lower partial waves. Neglecting F and the higher waves, we have

$$F(s, \cos\theta) = f_1(s) \equiv f(s), \tag{14}$$

where f is the amplitude of the P wave. Putting $\nu = \text{q}^2/\mu^2$ we obtain from (13)

$$f(\nu) = \Lambda + \frac{1}{\pi}\int_0^{\infty} \operatorname{Im} f(\nu')\left(\frac{1}{\nu' - \nu - i\varepsilon} + \frac{1}{\nu' + \nu + {}^9/_8}\right)d\nu'. \tag{15}$$

Here

$$\Lambda = \frac{2}{\pi}\int_{4m^2}^{\infty} \frac{(\operatorname{Im} F(s', 1))_{N\overline{N}}}{s'}\, ds', \tag{16}$$

$$f(\nu) = |f(\nu)|\, e^{i\delta(\nu)}, \quad \delta \equiv \delta_1^1. \tag{17}$$

Equation (15) has crossing symmetry (under the substitution $\nu \to -\nu - {}^9/_8$) and we can write for it an exact solution (see references 7 and 8).

1) Assume that when $\nu \to \infty$

$$\delta(\nu) \to 0 \qquad (\delta(\nu) \to c\nu^{-\alpha},\ \alpha > 0). \tag{18}$$

We put

$$\Delta(z) = \frac{1}{\pi}\int_0^{\infty} \delta(\nu)\left(\frac{1}{\nu - z} + \frac{1}{\nu + z + {}^9/_8}\right)d\nu. \tag{19}$$

This function with crossing symmetry is holomorphic in the entire z plane with a cut from $-\infty$ to $-{}^9/_8$ and from 0 to ∞. Its limiting values on the cut from above (+) and from below (−) are

$$\Delta^{\pm}(\nu) = \rho(\nu) \pm i\delta(\nu), \tag{20}$$

where

$$\rho(\nu) = \frac{1}{\pi}\, \mathrm{P}\int_0^{\infty} \delta(x)\left(\frac{1}{x - \nu} + \frac{1}{x + \nu + {}^9/_8}\right)dx. \tag{21}$$

When $z \to \infty$

$$\Delta(z) \to 0. \tag{22}$$

Let us consider the function

$$\Psi(z) = \frac{1}{\pi}\int_0^{\infty} e^{\rho(\nu)} \sin\delta(\nu)\left(\frac{1}{\nu - z} + \frac{1}{\nu + z + {}^9/_8}\right)d\nu. \tag{23}$$

It has the same symmetry, the same holomorphism region, and the same cuts as $\Delta(z)$, and its jump on the cut is

$$\Psi^+ - \Psi^- = 2ie^{\rho}\sin\delta = (e^{\Delta})^+ - (e^{\Delta})^-. \tag{24}$$

Therefore the function $\Psi(z)$ should coincide with $e^{\Delta(z)}$, apart from a polynomial. Since the function $\Psi(z) \to 0$ and $e^{\Delta(z)} \to 1$ as $z \to \infty$ this polynomial is equal to unity:

$$\Psi(z) = e^{\Delta(z)} - 1. \tag{25}$$

It follows from (23), (25), and (20) that

$$f(\nu) = \Lambda \exp\{\rho(\nu) + i\delta(\nu)\} \tag{26}$$

is the solution of Eq. (15). This solution is unique, since the general solution of the corresponding homogeneous equation is of the form $Pe^{\rho+i\delta}$, where P is a polynomial (which has crossing symmetry); it should tend to zero at infinity, i.e., $P \equiv 0$.

2) Assume now that as $\nu \rightarrow \infty$

$$\delta(\nu) \rightarrow \pi, \quad (\delta(\nu) \rightarrow \pi - c\nu^{-\alpha}, \alpha > 0). \tag{27}$$

We put

$$\Delta(z) = \frac{z + {}^9/_{16}}{\pi} \int_0^\infty \frac{\delta(\nu)}{\nu + {}^9/_{16}} \left(\frac{1}{\nu - z} - \frac{1}{\nu + z + {}^9/_8}\right) d\nu. \tag{28}$$

This function has the same properties as the function in (19), but as $z \rightarrow \infty$

$$\Delta(z) \rightarrow \text{const} - 2\ln(z + {}^9/_{16}), \tag{29}$$

$$e^{\Delta(z)} \rightarrow \text{const}\,(z + {}^9/_{16})^{-2}. \tag{30}$$

As in the preceding case, we can readily show that the solution of (15) will be

$$f^{(1)}(\nu) = \Lambda A^{-1}(\nu + {}^9/_{16})^2 \exp\{\rho(\nu) + i\delta(\nu)\}, \tag{31}$$

where

$$\rho(\nu) = \frac{\nu + {}^9/_{16}}{\pi} \mathrm{P} \int_0^\infty \frac{\delta(x)}{x + {}^9/_{16}} \left(\frac{1}{x - \nu} - \frac{1}{x + \nu + {}^9/_8}\right) dx, \tag{32}$$

$$A = [\nu^2 e^{\rho+i\delta}]_{\nu=\infty} \tag{33}$$

This solution, however, is not unique since it is possible to add to it the general solution of the homogeneous equation, which in this case is

$$C \exp\{\rho(\nu) + i\delta(\nu)\}, \tag{34}$$

where C is an arbitrary constant (C cannot be a polynomial of first degree in view of the crossing symmetry requirement).

Thus, all the solutions of Eq. (15) have in this case the form

$$f^{(1)}(\nu) + C \exp\{\rho(\nu) + i\delta(\nu)\}. \tag{35}$$

They all tend at infinity to Λ as $1/\nu^2$, since as $\nu \rightarrow \infty$

$$f^{(1)}(\nu) = \Lambda\left[1 + \frac{\alpha}{\nu^2}\left(1 - 9/8\nu\right) + \frac{\beta}{\nu^4} + \ldots\right],$$
$$e^{\rho+i\delta} = \frac{\alpha_0}{\nu^2}(1 - 9/8\nu) + \frac{\beta_0}{\nu^4} + \ldots. \tag{36}$$

And the only unique solution for which

$$C\alpha_0 = -\Lambda\alpha, \tag{37}$$

tends to Λ as $1/\nu^4$ at infinity.

We shall regard as physical that solution of Eq. (15), which tends to the inhomogeneous term at infinity more rapidly than any solution of the corresponding homogeneous equation tends to zero. From (31) and (35) – (37) we obtain an expression for this solution

$$f(\nu) = \Lambda A^{-1}[(\nu + {}^9/_{16})^2 - A_1]\, e^{\rho+i\delta}, \tag{38}$$

where A is given by formula (33) and

$$A_1 = [\nu^2(A^{-1}(\nu + {}^9/_{16})^2 e^{\rho+i\delta} - 1)]_{\nu=\infty}. \tag{39}$$

At high energies the contribution from the dispersion integral vanishes rapidly from this solution, and consequently, of all the solutions (35), it is the least sensitive to the details of the behavior of the phase shift δ at infinity. Only this solution gives a physically true result when the width of the pion resonance contracts to zero. In fact, when

$$\delta = \begin{cases} 0, & \nu < \nu_k \\ \pi, & \nu > \nu_k \end{cases}, \quad e^{\rho(\nu)} = \left|\frac{(\nu_k + {}^9/_{16})^2}{(\nu_k - \nu)(\nu_k + \nu + {}^9/_8)}\right| \tag{40}$$

we have

$$f^{(1)}(\nu) = \Lambda \frac{(\nu + {}^9/_{16})^2}{(\nu - \nu_k)(\nu + \nu_k + {}^9/_8)}, \tag{41}$$

whereas in (38)

$$f(\nu) = \Lambda. \tag{42}$$

Let us give an expression for the photoproduction amplitude for two models of pion resonance (ν_k and b are certain parameters)

$$\text{I.}\ \delta = \begin{cases} 0, & \nu < \nu_k - b, \quad \nu > \nu_k + b \\ (\pi/2b)(\nu + b - \nu_k), & \nu_k - b < \nu < \nu_k \\ (\pi/2b)(\nu_k + b - \nu), & \nu_k < \nu < \nu_k + b \end{cases} \tag{43}$$

The expression (26) gives in this case

$$f(\nu) = \Lambda e^{i\delta(\nu)} \varphi(\nu),$$

$$\varphi(\nu) = \left\{\left|\frac{(\nu - \nu_k)^2}{(\nu + b - \nu_k)(\nu_k + b - \nu)}\right|^{(\nu-\nu_k)/2b} \left|\frac{\nu_k + b - \nu}{\nu + b - \nu_k}\right|^{1/2}\right\}$$
$$\cdot \{\nu \rightarrow -\nu - {}^9/_8\}. \tag{44}$$

$$\text{II.}\ \delta = \begin{cases} 0, & \nu < \nu_k - b \\ (\pi/2b)(\nu + b - \nu_k), & \nu_k - b < \nu < \nu_k + b \\ \pi, & \nu_k + b < \nu \end{cases}. \tag{45}$$

The expression (38) gives in this case

$$f(\nu) = \Lambda e^{i\delta(\nu)} \varphi(\nu),$$

$$\varphi(\nu) = [(\nu_k - \nu)(\nu_k + \nu + {}^9/_8) + b^2/3]$$
$$\times \left[\left\{\frac{e}{|\nu_k + b - \nu|} \left|\frac{\nu_k + b - \nu}{\nu_k - b - \nu}\right|^{(\nu+b-\nu_k)/2b}\right\}\right.$$
$$\left.\cdot \{\nu \rightarrow -\nu - {}^9/_8\}\right].$$

These phase shifts and solutions are shown in Figs. 2 and 3 for the resonance parameters (taken

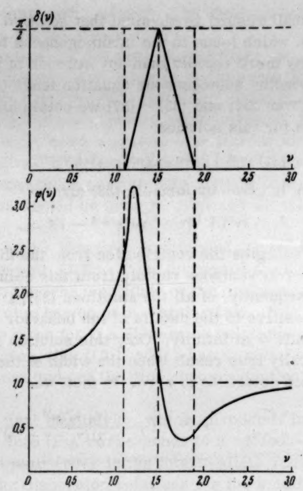

FIG. 2

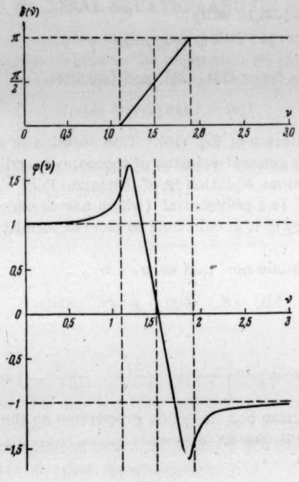

FIG. 3

from reference 9) $\nu_k = 1.5$ and $b = 0.4$. In both cases the amplitude of photoproduction has a resonant character, and its resonance is shifted somewhat relative to the pion resonance. In the first model (43) the photoproduction resonance is much sharper. In the second model (45) the photoproduction amplitude vanishes near the energy of pion resonance.

The author is grateful to G. Byalkovskii, A. Yurevich, P. S. Isaev, and M. I. Shirokov for useful discussions.

---

[1] S. Mandelstam, Phys. Rev. 112, 1344 (1958).

[2] G. F. Chew and S. Mandelstam, Theory of Low-Energy Pion-Pion Interaction, Lawrence Radiation Laboratory Reports UCRL-8728.

[3] N. N. Bogolyubov and D. V. Shirkov, Introduction to the Theory of Quantized Fields (Engl. Transl.) Interscience, 1959.

[4] A. Pais, Phys. Rev. 112, 624 (1959).

[5] M. M. Gourdin and A. Martin, Nuovo cimento 16, 78 (1960).

[6] A. A. Logunov, Dissertation, Joint Inst. Nuc. Res. 1959.

[7] N. I. Muskhelishvili, Сингулярные интегральные уравнения, (Singular Integral Equations), Gostekhizdat, 1946.

[8] K. Blankenbecler and S. Gartenhaus, Phys. Rev. 116, 1297 (1959).

[9] W. R. Frazer and J. R. Fulco, Phys. Rev. 117, 1609 (1960).

Translated by J. G. Adashko
91

SOVIET PHYSICS JETP VOLUME 13, NUMBER 2 AUGUST, 1961

COMPLETE SET OF EXPERIMENTS FOR DETERMINATION OF RELATIONS BETWEEN THE AMPLITUDES FOR PION PRODUCTION BY NUCLEONS IN VARIOUS ISOTOPIC SPIN STATES

K. S. MARISH and L. M. SOROKO

Joint Institute for Nuclear Research

Submitted to JETP editor August 16, 1960

J. Exptl. Theoret. Phys. (U.S.S.R.) 40, 605-612 (February, 1961)

A complete set of experiments for determination of the relations between the amplitudes for pion production by nucleons in various isotopic spin states is considered. The number of experiments so far performed with nucleons in the 600-Mev energy region is not sufficient to determine all the relations among the amplitudes. One of the discussed experiments may provide a sensitive test of the validity of the resonance theory of pion production by nucleons.

INTRODUCTION

THE attempts at constructing a theory for pion production by nucleons, carried out by a number of authors, have usually consisted of phenomenological considerations which would give quantitative explanations of available experimental data. Thus, for example, Watson and Brueckner[1] gave a partial analysis of the meson production process by nucleons. They supposed that only a small number of states with definite orbital angular momentum participate in the process. The matrix elements for the processes were taken to be constant, the principle of charge independence was taken into account as well as other conservation laws, and the attractive final state interaction of the nucleons was also included. On the basis of such a phenomenological approach threshold data were analyzed by Rosenfeld[2] and Gell-Mann and Watson.[3] In the analysis they have made use of a hypothesis proposed by Brueckner,[4] namely that at nucleon energies close to the threshold one of the secondary nucleons and the produced pion are predominantly in the resonant ($^3/_2$, $^3/_2$) state.

Mandelstam[5] has extended this phenomenological theory to higher energies, from 400 to 600 Mev. In his considerations the matrix elements were assumed constant, the πN resonant ($^3/_2$, $^3/_2$) interaction was introduced, all kinematic factors were taken into account, as well as the rules of composition of angular momentum and spin of the particles. According to this model, which gives the best explanation of all experimental data obtained by proton beams, there should be no significant production of pions by nucleons in isotopic spin state zero ($T_{NN} = 0$). However, recent experimental data on pion production in neutron-proton collisions[6,7] indicate that this prediction of the resonant theory of Mandelstam is in disagreement with experiment.

Can one therefore conclude that the resonant model of Mandelstam is inconsistent? In order to answer this question it is necessary to take into account not only the resonant πN interaction in the isotopic spin $T = {}^3/_2$ state, but also in the isotopic spin $T = {}^1/_2$ state. Doubtlessly both resonances should make themselves felt in the general case. However the resonant Mandelstam model is consistent only with an overwhelming preponderance of the $T_{\pi N} = {}^3/_2$ resonance. Thus the resonant theory can be directly tested if the ratio of the probabilities of the two resonant interactions could be determined. However the experiments performed so far are not sufficient to yield the desired relation. All these reasons have stimulated us anew to discuss in more detail a complete set of experiments, necessary to establish relations among the amplitudes for pion production by nucleons in various isotopic spin states.

1. REACTION CROSS SECTIONS

As is well known, in the isotopic spin space the phenomenological description of pion production by nucleons requires the introduction of three independent amplitudes. The probability of an arbitrary pion production process by a two-nucleon system can be explicitly expressed in terms of three independent amplitudes. If the amplitude for pion production in the collision of two nucleons N_1 and N_2 be denoted by $M\,(N_1N_2 \rightarrow N_1'N_2'\pi)$, where N_1' and N_2' are the secondary nucleons, then this amplitude will change under the exchange of nucleons N_1, N_2 or N_1', N_2'. When charge symmetry is taken into account the number of different pion production processes reduces to seven.[8]

The differential cross sections for these processes may be written as follows:[8,9]

$$\text{I. } d\sigma\,(pp\rightarrow np\pi^+) = \tfrac{1}{2}|F_{10}|^2 + \tfrac{1}{4}|F_{11}|^2 + \sqrt{1/2}\,|F_{11}|\,|F_{10}|\cos\Phi_{10,11} = \tfrac{3}{4}|A_{13}|^2,$$

$$\text{II. } d\sigma\,(pp \rightarrow pn\pi^+) = \tfrac{1}{2}|F_{10}|^2 + \tfrac{1}{4}|F_{11}|^2 - \sqrt{1/2}\,|F_{11}|\,|F_{10}|\cos\Phi_{10,11} = \tfrac{1}{3}\left[\tfrac{1}{4}|A_{13}|^2 + 2|A_{11}|^2 - \sqrt{2}|A_{13}|\,|A_{11}|\cos\varphi_{13}\right],$$

$$\text{III. } d\sigma\,(pp\rightarrow pp\pi^0) = \tfrac{1}{2}|F_{11}|^2 = \tfrac{1}{3}\left[\tfrac{1}{2}|A_{13}|^2 + |A_{11}|^2 + \sqrt{2}|A_{13}|\,|A_{11}|\cos\varphi_{13}\right],$$

$$\text{IV. } d\sigma\,(pn \rightarrow nn\pi^+) = \tfrac{1}{6}|F_{01}|^2 + \tfrac{1}{4}|F_{11}|^2 - \sqrt{1/6}\,|F_{01}|\,|F_{11}|\cos\Phi_{01,11} = \tfrac{1}{6}\left[\tfrac{1}{2}|A_{13}|^2 + |A_{11}|^2 + |A_{01}|^2 + \sqrt{2}|A_{13}|\,|A_{11}|\cos\varphi_{13} - 2|A_{11}|\,|A_{01}|\cos\varphi_{01} - \sqrt{2}|A_{13}|\,|A_{01}|\cos\varphi_{03}\right],$$

$$\text{V. } d\sigma\,(np \rightarrow nn\pi^+) = \tfrac{1}{6}|F_{01}|^2 + \tfrac{1}{4}|F_{11}|^2 + \sqrt{1/6}\,|F_{01}|\,|F_{11}|\cos\Phi_{01,11} = \tfrac{1}{6}\left[\tfrac{1}{2}|A_{13}|^2 + |A_{11}|^2 + A_{01}|^2 + \sqrt{2}|A_{13}|\,|A_{11}|\cos\varphi_{13} + 2|A_{11}|\,|A_{01}|\cos\varphi_{01} + \sqrt{2}|A_{13}|\,|A_{01}|\cos\varphi_{03}\right],$$

$$\text{VI. } d\sigma\,(np \rightarrow np\pi^0) = \tfrac{1}{12}|F_{01}|^2 + \tfrac{1}{4}|F_{10}|^2 - 2\sqrt{1/3}\,|F_{01}|\,|F_{10}|\cos\Phi_{01,10} = \tfrac{1}{6}\left[|A_{13}|^2 + \tfrac{1}{2}|A_{11}|^2 + \tfrac{1}{2}|A_{01}|^2 - \sqrt{2}|A_{13}|\,|A_{11}|\cos\varphi_{13} - \sqrt{2}|A_{13}|\,|A_{01}|\cos\varphi_{03} + |A_{11}|\,|A_{01}|\cos\varphi_{01}\right],$$

$$\text{VII. } d\sigma\,(np \rightarrow pn\pi^0) = \tfrac{1}{12}|F_{01}|^2 + \tfrac{1}{4}|F_{10}|^2 + 2\sqrt{1/3}\,|F_{01}|\,|F_{10}|\cos\Phi_{01,10} = \tfrac{1}{6}\left[|A_{13}|^2 + \tfrac{1}{2}|A_{11}|^2 + \tfrac{1}{2}|A_{01}|^2 + \sqrt{2}|A_{13}|\,|A_{11}|\cos\varphi_{13} + \sqrt{2}|A_{13}|\,|A_{01}|\cos\varphi_{03} - |A_{11}|\,|A_{01}|\cos\varphi_{01}\right]. \quad (1)$$

Here F_{ij} stand for the three reaction amplitudes in the representation in which in the final state the subsystem is formed out of the two nucleons; i stands for the isotopic spin of the two nucleons in the initial state, j — in the final state; A_{il} stand for the reaction amplitudes in the representation in which in the final state the subsystem is formed out of the pion and a nucleon, $l = 2T_{\pi N}$, where $T_{\pi N}$ refers to the isotopic spin of the πN subsystem.

2. METHODS FOR MEASUREMENT OF INTERFERENCE EFFECTS

In Eq. (1) the processes I and II, IV and V, as well as VI and VII differ from each other because of interference between two amplitudes. The establishment of a difference between two such processes will provide us with valuable additional data. Let us consider various methods by which this difference can be observed experimentally.

A. If the proton and neutron are exchanged in the initial state (processes IV and V), then the difference between these two processes may be determined, because of charge symmetry, by comparison of the processes $pn \rightarrow nn\pi^+$ and $pn \rightarrow pp\pi^-$ at the same pion emission angle.

B. If instead we exchange the neutron and proton in the final state (processes I and II or VI and VII), then it is necessary to observe simultaneously two particles, for example the pion and one of the nucleons, in order to detect the difference between the probabilities for the two processes. Here it becomes necessary to agree which nucleon will be referred to as the first one. We shall use the definition given by Fermi,[10] according to which the first nucleon is the one whose momentum, when projected along the direction of the pion momentum in the c.m.s. of the two colliding nucleons, is algebraically larger.

Since at this point we are interested only in relations among the amplitudes F (or A) and not in their spin and angular dependence, it is sufficient to observe the total cross sections for the appropriate processes.

If only the pion is detected in the experiment, then processes I and II, and also VI and VII, cannot be distinguished since only the sums of the probabilities of each pair of processes is measured. The corresponding total cross sections are given by

$$\sigma\,(pp\rightarrow\pi^+) = \int\frac{d\sigma}{d\Omega}(pp\rightarrow np\pi^+)\,d\Omega] + \int\frac{d\sigma}{d\Omega}(pp\rightarrow pn\,\pi^+)\,d\Omega,$$
$$\sigma\,(np\rightarrow\pi^0) = \int\frac{d\sigma}{d\Omega}(np\rightarrow np\pi^0)\,d\Omega + \int\frac{d\sigma}{d\Omega}(np\rightarrow pn\,\pi^0)\,d\Omega. \quad (2)$$

In order to distinguish between process I and II, and also VI and VII, it is necessary to measure the total cross section of each of the two processes separately: processes, when the first nucleon is a proton and when the first nucleon is a neutron.

In the general case each of the spin components of the wave functions describing the final state of the process $NN \rightarrow NN'\pi$ is a function of the pion momentum, the pion angle of emission $(\theta_\pi, \varphi_\pi)$, and also the nucleon angle of emission $(\theta_{12}, \varphi_{12})$. The angles θ_{12}, φ_{12} are here measured from the direction of the momentum of the pion in the barycentric frame of the two final state nucleons. When discussing the total cross sections it is sufficient to consider the differential cross sections averaged over the azimuth angles φ_π and φ_{12}. If we consider only contributions due to s and p waves of the pion and nucleons then the averaged cross sections may be written

$$d\sigma^{pp}_{np\pi^+}(\theta_\pi, \theta_{12};\ p_\pi) \sim a_0(p_\pi) + a_1(p_\pi)\cos\theta_{12}\cos\theta_\pi + a_2(p_\pi)\cos^2\theta_{12} + a_3(p_\pi)\cos^2\theta_\pi + a_4(p_\pi)\cos^2\theta_{12}\cos^2\theta_\pi,$$

$$d\sigma^{pp}_{pn\pi^+}(\theta_\pi, \theta_{12};\ p_\pi) \sim a_0(p_\pi) - a_1(p_\pi)\cos\theta_{12}\cos\theta_\pi + a_2(p_\pi)\cos^2\theta_{12} + a_3(p_\pi)\cos^2\theta_\pi + a_4(p_\pi)\cos^2\theta_{12}\cos^2\theta_\pi, \tag{3}$$

where $a_i(p_\pi)$ are some functions of the pion momentum.

It is seen from Eq. (3) that a measure of the difference between the probabilities for the process $pp \to np\pi^+$ and the process $pp \to pn\pi^+$ is provided by the coefficient a_1. However the total cross section for either of these processes is independent of a_1 since the difference of the differential cross sections changes sign under the transformations $\theta_\pi \to (\pi - \theta_\pi)$ and $\theta_{12} \to (\pi - \theta_{12})$. Hence it follows that the difference in the differential cross sections for these processes must be measured only for angles lying in the regions $0 < \theta_\pi < \pi/2$, $0 < \theta_{12} < \pi/2$; furthermore, one may average over relative azimuthal angles which enter into the cross section in the form[11]

$$\cos(\varphi_\pi - \varphi_{12}) \text{ and } \cos 2(\varphi_\pi - \varphi_{12}).$$

In this way the defined below difference of cross sections $\Delta\sigma$ corresponds to the difference of probabilities of the processes I and II:

$$\Delta\sigma_{10.11} = 4\int_0^{\pi/2}\int_0^{\pi/2}[d\sigma^{pp}_{np\pi^+}(\theta_\pi, \theta_{12}) - d\sigma^{pp}_{pn\pi^+}(\theta_\pi, \theta_{12})]\, d\Omega(\theta_\pi)\, d\Omega(\theta_{12}), \tag{4}$$

and, analogously, for processes VI and VII:

$$\Delta\sigma_{01.10} = 4\int_0^{\pi/2}\int_0^{\pi/2}[d\sigma^{np}_{np\pi^0}(\theta_\pi, \theta_{12}) - d\sigma^{np}_{pn\pi^0}(\theta_\pi, \theta_{12})]\, d\Omega(\theta_\pi)\, d\Omega(\theta_{12}). \tag{5}$$

The difference of cross sections for processes IV and V may be written in a simpler form

$$\Delta\sigma_{01.11} = 2\int_0^{\pi/2}[d\sigma^{pn}_{nn\pi^+}(\theta_\pi) - d\sigma^{np}_{nn\pi^+}(\theta_\pi)]\, d\Omega(\theta_\pi) = 2\int_0^{\pi/2}[d\sigma^{np}_{pp\pi^-}(\theta_\pi) - d\sigma^{np}_{nn\pi^+}(\theta_\pi)]\, d\Omega(\theta_\pi). \tag{6}$$

As in the previous two cases, the cross section (6) is a measure of the coefficient b in the angular distribution of the pions

$$d\sigma(np \to \pi^-) = a + b\cos\theta_\pi + c\cos^2\theta_\pi,$$

which, naturally, does not contribute to the usual total cross section.

3. RELATIONS AMONG AMPLITUDES WITH VARIOUS ISOTOPIC SPIN

Any six independent equations out of the following seven possible ones

$$\sigma(pp \to \pi^+) = |F_{10}|^2 + \tfrac{1}{2}|F_{11}|^2,$$
$$\sigma(np \to \pi^0) = \tfrac{1}{6}|F_{01}|^2 + \tfrac{1}{2}|F_{10}|^2,$$
$$\sigma(pp \sim \pi^0) = \tfrac{1}{2}|F_{11}|^2, \quad \sigma(np \to \pi^+) = \tfrac{1}{3}|F_{01}|^2 + \tfrac{1}{2}|F_{11}|^2,$$
$$\Delta\sigma_{10,11} = \sqrt{2}\,\Omega_{10,11}, \quad \Delta\sigma_{01,11} = \sqrt{2/3}\,\Omega_{01,11},$$
$$\Delta\sigma_{01,10} = \sqrt{1/3}\,\Omega_{01,10}, \tag{7}$$

may be used to determine the three amplitudes F_{ij} or A_{ij} – i.e., the three absolute magnitudes and three relative phases (three-dimensional case!). Here

$$\Omega_{ij,lk} = |F_{ij}||F_{kl}|\cos\Phi_{ij,kl}.$$

One of the equations relating the usual total cross sections is not independent in view of the existence of the following relation among total cross sections:

$$\sigma(pp \to \pi^+) + \sigma(np \to \pi^+) + \sigma(nn \to \pi^-) = 2[\sigma(pp \to \pi^0) + \sigma(np \to \pi^0)].$$

The amplitudes F_{ij} are obtained from experimentally observable quantities with the help of the following relations

$$|F_{10}|^2 = \sigma(pp \to \pi^+) - \sigma(pp \to \pi^0),$$
$$\Omega_{10,11} = \sqrt{1/2}\,\Delta\sigma_{10,11},$$
$$|F_{11}|^2 = 2\sigma(pp \to \pi^0), \quad \Omega_{11,01} = \sqrt{3/2}\,\Delta\sigma_{11,01},$$
$$|F_{01}|^2 = 3[\sigma(np \to \pi^+) + \sigma(np \to \pi^-) - \sigma(pp \to \pi^0)],$$
$$\Omega_{10,11} = \sqrt{3}\,\Delta\sigma_{10,01}. \tag{8}$$

Given the F_{ij}, the A_{ij} may be determined by making use of the following relations:

$$\mathbf{A}_{13} = \sqrt{2/3}\,\mathbf{F}_{10} + \sqrt{1/3}\,\mathbf{F}_{11},$$
$$A_{13}^2 = \tfrac{2}{3}F_{10}^2 + \tfrac{1}{3}F_{11}^2 + \tfrac{2}{3}\sqrt{2}\,\Omega_{10.11}$$
$$\mathbf{A}_{11} = -1/3\,\mathbf{F}_{10} + \sqrt{2/3}\,\mathbf{F}_{11},$$
$$A_{11}^2 = \tfrac{1}{3}F_{10}^2 + \tfrac{2}{3}F_{11}^2 - \tfrac{2}{3}\sqrt{2}\,\Omega_{10.11} \quad \mathbf{A}_{01} = \mathbf{F}_{01}, \quad A_{01}^2 = F_{01}^2;$$
$$\omega_{13} = \tfrac{1}{3}\sqrt{2}\,F_{11}^2 - \tfrac{1}{3}\sqrt{2}\,F_{10}^2 + \tfrac{1}{3}\Omega_{10.11},$$
$$\omega_{01} = -\sqrt{1/3}\,\Omega_{10.01} + \sqrt{2/3}\,\Omega_{11.01},$$
$$\omega_{03} = \sqrt{2/3}\,\Omega_{10.01} + \sqrt{1/3}\,\Omega_{11,01} \tag{9}$$

or, explicitly in terms of the observable quantities

$$|A_{13}|^2 = \tfrac{2}{3}\sigma\,(pp \to \pi^+) + \tfrac{2}{3}\,\Delta\sigma_{10,\,11},$$

$$|A_{11}|^2 = \sigma\,(pp \to \pi^0) + \tfrac{1}{3}\sigma\,(pp \to \pi^+) - \tfrac{2}{3}\,\Delta\sigma_{10,\,11},$$

$$|A_{01}|^2 = 3\,[\sigma\,(np \to \pi^+) + \sigma\,(np \to \pi^-) - \sigma\,(pp \to \pi^0)],$$

$$\omega_{13} = \tfrac{1}{3}\sqrt{2}\,[3\sigma\,(pp \to \pi^0) - \sigma\,(pp \to \pi^+)] + \tfrac{1}{3}\sqrt{1/2}\,\Delta\sigma_{10,11},$$

$$\omega_{01} = \Delta\sigma_{11,\,01} - \Delta\sigma_{10,01}, \quad \omega_{03} = \sqrt{2}\;\Delta\sigma_{10,01} + \sqrt{1/2}\,\Delta\sigma_{11,01}, \tag{10}$$

where $\omega_{ij} = |A_{1i}||A_{j1}|\cos\varphi_{ij}$.

4. EXPERIMENTS WITH A NEUTRON BEAM

From a study of the reactions $np \to pp\pi^-$ and $np \to nn\pi^+$ induced by 600 Mev neutrons,[7] one may conclude that $|F_{01}| \neq 0$. From the same data it follows that $\Delta\sigma_{01,11}$ is very nearly zero in this energy region. This means that the amplitudes F_{01} and F_{11} are nearly orthogonal to each other. With the neutron beam it is essential to measure the cross section $\Delta\sigma_{01,10}$. This would permit a determination of the relative phase, as well as produce a substantially more reliable value for $|F_{01}|$.

5. EXPERIMENTS WITH A PROTON BEAM

The cross sections $\sigma(pp \to \pi^+)^{12}$ and $\sigma(pp \to \pi^0)^{13}$ were measured using 600 Mev protons. From these data $|F_{10}|$ and $|F_{11}|$ may be determined. Of greatest interest are the values of $|A_{13}|$ and $|A_{11}|$ for 600 Mev protons, i.e., in the $(3/2,\ 3/2)$ resonance region where $|A_{13}|$ should dominate. However the relation between $|A_{13}|$ and $|A_{11}|$ can be found, if $\Delta\sigma_{10,01}$ is measured.

According to the resonant model of Mandelstam, $|A_{11}| = 0$, from which follows the well known relation $\sigma_+/\sigma_0 = 5$. Experimentally one observes the value $\sigma_+/\sigma_0 = 3.4$, and this is explained theoretically by introducing a somewhat artificial assumption. In fact, the explanation is simply that $|A_{11}| \neq 0$.

In order to discuss in more detail the possible values of $|A_{13}|$ and $|A_{11}|$ it is convenient to introduce the following notation: $\alpha = \sigma_+/\sigma_0$, $k = |A_{13}|/|A_{11}|$. In Fig. 1 is shown the region of permissible values of α and k, which is filled by the family of curves

$$\alpha = (4 + 5k^2 - \sqrt{8}\,k\cos\varphi_{13})/(2 + k^2 + \sqrt{8}\,k\cos\varphi_{13}) \tag{11}$$

with $\cos\varphi_{13}$ as a parameter. This region is bounded from below by the curve

$$\alpha_{\varphi_{13}=0} = (4 + 5k^2 - \sqrt{8}k)\,/\,(2 + k^2 + \sqrt{8}k), \tag{12}$$

which has the horizontal asymptotes $\alpha = 2$ $(k \to 0)$ and $\alpha = 5$ $(k \to \infty)$ and the minimum $\alpha = 1$ at $k = 1/\sqrt{2}$.

From above the region is bounded by the two branches of the curve

$$\alpha_{\varphi_{13}=\pi} = (4 + 5k^2 + \sqrt{8}\,k)\,/(2 + k^2 - \sqrt{8}\,k), \tag{13}$$

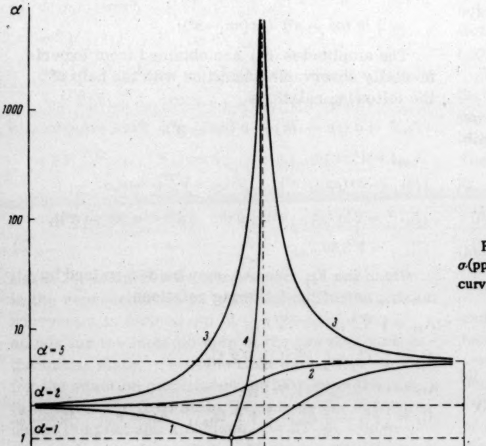

FIG. 1. Region of possible values of $\alpha = \sigma(pp \to \pi^+)/\sigma(pp \to \pi^0)$ and $k = |A_{13}|/|A_{11}|$. Curve 1 corresponds to $\varphi_{13} = 0$, curve 2 – $\varphi_{13} = \pi/2$, curve 3 – $\varphi_{13} = \pi$, curve 4 – $\Delta\sigma_{10,11} = 0$.

which has two horizontal asymptotes $\alpha = 2$ $(k \to 0)$ and $\alpha = 5$ $(k \to \infty)$ and one common vertical asymptote at $k = \sqrt{2}$.

The curves $\alpha = \alpha$ (k, cos φ_{13}) have an extremum at

$$\alpha = (5k^4 + k^2 - 4)/(k^4 - k^2 - 2), \qquad (14)$$

except for the monotonic curve

$$\alpha_{\pi/2} = 5 - 6/(k^2 + 2),$$

which corresponds to $\varphi_{13} = \pi/2$.

It is seen from Fig. 1 that for $\alpha = \sigma_+/\sigma_0 = 3.4$ the possible values of k^2 lie in the interval

$$1/20 < k^2 < 64. \qquad (15)$$

If $\sigma_+/\sigma_0 = \alpha = 5$ then the possible values of k^2 lie in the interval $1/8 < k^2 < \infty$. Therefore the equality $\sigma_+/\sigma_0 = 5$ can under no circumstances be taken as proof of validity of the resonant theory.

It should also be noted that if k is constant but the relative phase of A_{13} and A_{11} changes for some reason, then the quantity α will change. In the opinion of the authors such a process may take place in pion production on bound nucleons in a nucleus, for example in a deuteron.

In Fig. 1 we also show the curve corresponding to $\Delta\sigma_{10,11} = 0$ $[\alpha = 3k^2/(2-k^2)]$, i.e., to the case of emission of the proton and the neutron symmetrically relative to the π^+ meson.

It is interesting to note that for α very large (~ 10 and larger), as is the case for energies near threshold, one has $|A_{13}| \sim 1.5\,|A_{11}|$ and the phase difference (up to π) is very small. Precisely such a picture would follow from the assumption that for pion energies close to zero the phases of A_{13} and A_{11} should be small, and consequently their difference must be small.

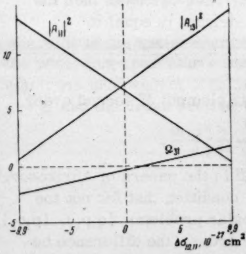

FIG. 2. Possible values of $|A_{13}|^2$, $|A_{11}|^2$ and $\Omega_{3,1}$ (in 10^{-27} cm^2) as functions of the difference of cross sections $\Delta\sigma_{10,11}$, for 660 Mev protons ($\alpha = 3.4$).

In Fig. 2 are shown the possible values of $|A_{13}|^2$, $|A_{11}|^2$ and $\Omega_{3,1}$ as a function of the difference of cross sections $\Delta\sigma_{10,11}$. It is seen from Fig. 2 that $|A_{13}|^2 \approx |A_{11}|^2$, and the amplitudes are nearly orthogonal, if $\Delta\sigma_{10,11} = 0$. For 660 Mev protons the maximum possible value of $\Delta\sigma_{10,11}$ is 9.9×10^{-27} cm^2.

CONCLUSION

Thus, in order to settle the question of the validity of the resonant theory of pion production by nucleons in the 600 Mev region it is necessary and sufficient to measure the difference of total cross sections $\Delta\sigma_{10,11}$, which is related to the asymmetry in the emission of protons and neutrons relative to the direction of flight of the π^+ meson.

The authors express their gratitude to L. I. Lapidus for interest in this work and discussions.

---

[1] K. M. Watson and K. A. Brueckner, Phys. Rev. 83, 1 (1951).

[2] A. H. Rosenfeld, Phys. Rev. 96, 139 (1954).

[3] M. Gell-Mann and K. M. Watson, Ann. Rev. Nucl. Sci. 4, 219 (1954).

[4] K. A. Brueckner, Phys. Rev. 86, 206 (1952).

[5] S. Mandelstam, Proc. Roy. Soc. A244, 491 (1958).

[6] A. F. Dunaĭtsev and Yu. D. Prokoshin, JETP 38, 747 (1960), Soviet Phys. JETP 11, 540 (1960).

[7] Dzhelepov, Kiselev, Oganesyan, and Flagin, Proceeding of the Tenth International Conference on High Energy Particle Physics, Rochester, 1960.

[8] Van Hove, Marshak, and Pais, Phys. Rev. 88, 1211 (1952).

[9] L. I. Lapidus, JETP 31, 865 (1956), Soviet Phys. JETP 4, 740 (1957).

[10] E. Fermi, Lectures on Pions and Nucleons (Russ. Transl.), IIL, 1956, p. 68.

[11] L. M. Soroko, JETP 34, 87 (1958), Soviet Phys. JETP 7, 61 (1958).

[12] B. S. Neganov and O. V. Savchenko, JETP 32, 1265 (1957), Soviet Phys. JETP 5, 1033 (1957).

[13] A. F. Dunaĭtsev and Yu. D. Prokoshin, JETP 36, 1656 (1959), Soviet Phys. JETP 9, 1179 (1959).

Translated by A. M. Bincer
92

SOVIET PHYSICS JETP VOLUME 13, NUMBER 2 AUGUST, 1961

HIGH ENERGY ELECTRON-ELECTRON SCATTERING

V. N. BAĬER and S. A. KHEĬFETS

Submitted to JETP editor August 20, 1960; resubmitted November 19, 1960

J. Exptl. Theoret. Phys. (U.S.S.R.) 40, 613-615 (February, 1961)

The cross section for large angle scattering of high energy electrons is calculated in the double logarithmic approximation.

INASMUCH as in the scattering of electrons by the electrons of a target at rest the energy of the colliding electrons in the center-of-mass system (c.m.s.) is equal to $E_{c.m.s.} = \frac{1}{2}\sqrt{2E_{l.s.}mc^2}$ (for maximum energy achieved at the present time $E_{l.s.} = 1.2$ Bev, $E_{c.m.s.} = 17$ Mev), in consequence of the noted smallness of the energy in the c.m.s. one could limit oneself in the calculation of the scattering cross section (with high degree of accuracy) to the lower orders of perturbation theory (see, for example, reference 1).

At the present time experiments are set up on the scattering of electrons in colliding beams with the purpose of testing quantum electrodynamics at small distances (see, for example, reference 2), wherein the energy of the colliding electrons will be several hundred million electron volts in the c.m.s. As is well known, the principal terms arising in the account of higher approximations of perturbation theory contain the square of a large logarithm, for example,[3] $\ln^2(E/m)$ for each power of e^2, by virtue of which it is not possible in the calculation of cross sections of electromagnetic processes to limit oneself to the lower orders of perturbation theory. At the same time it is necessary to have sufficiently correctly computed cross sections to establish any violation of quantum electrodynamics at small distances.

A method of calculation of the cross sections of electromagnetic processes at high energies was suggested by Abrikosov.[3] Within the framework of this method, only those contributions are retained which contain the maximum power of the large logarithm. We shall use this method to determine the scattering cross section of electrons by electrons for c.m.s. scattering angles $\theta \gg m/E$.

An arbitrary diagram of order $2(n+1)$ of perturbation theory (see the drawing) contains: $s+1$ virtual photon lines which connect the different electron lines ("staircase" lines); m_1 lines of virtual photons emitted and absorbed by the same electron ("overlapping" lines); similarly, m_2 overlapping lines for another electron line while $s + m_1 + m_2 + 1 = n + 1$, where $n + 1$ is the total number of lines of virtual photons.

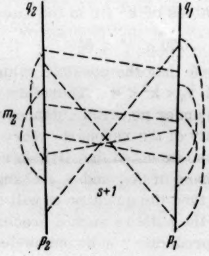

The matrix element will contain the maximum power of the logarithm $(e^2 \ln^2(E/m))^n$ under the satisfaction of two conditions: a) one of the staircase lines transfers a large momentum $l^2 \sim (q_1 - p_1)^2$, while the momenta of the remaining staircase lines $k^2 \sim 0$; b) the staircase line with the large momentum lies within all the enveloping lines. In what follows we shall consider only the class of such diagrams.

If the staircase line with the large momentum joins the r_1 and r_2 staircase vertices, then the corresponding matrix element is equal to

$$Q = (-1)^{n+r_1+r_2+s} \frac{M_0 f^n}{(r_1+m_1)!\,(r_2+m_2)!\,(s+m_1-r_1)!\,(s+m_2-r_2)!}, \tag{1}$$

where M_0 is the matrix element of second order,

$$f = \frac{e^2}{2\pi}\int \frac{du}{u}\frac{dv}{v},$$

u and v are introduced in the papers of Abrikosov.[3] Here we have used the condition that for not too small angles all the scalar problems (q_1p_1), (p_1p_2), (p_1q_2) are of the same order (the difference between them is less than the limits of accuracy of the method).

All diagrams with different topology of photon lines but with fixed s, r_1, r_2, m_1, and m_2 make the same contribution. As is easy to see, the number of such diagrams is equal to

$$N = \binom{m_1 + r_1}{m_1}\binom{m_1 + s - r_1}{m_1}\binom{m_2 + r_2}{m_2}\binom{m_2 + s - r_2}{m_2} m_1!\, m_2!\, s!. \tag{2}$$

Thus the matrix element of order 2(n+1) is equal to

$$M_{2(n+1)} = \sum_{\substack{s r_1 r_2 m_1 m_2 \\ s+m_1+m_2=n}} (-1)^{n+r_1+r_2+s}$$

$$\times \frac{M_0 f^n N}{(r_1 + m_1)!\,(r_2 + m_2)!\,(s + m_1 - r_2)!\,(s + m_2 - r_2)!}$$

$$= (-1)^n \frac{2^n f^n}{n!} M_0. \tag{3}$$

Evidently this sum differs from zero only for s = 0 (one staircase line); thus the contributions of the staircase photons are preserved and it would have been sufficient to consider only overlapping lines to obtain the cross section.

The scattering cross section of the electrons is then obtained by summation over n, which gives $d\sigma = d\sigma_0 \exp(-4f)$. It is of practical interest to know the total cross section of elastic and inelastic processes with given maximum energy of emitted quanta. Consideration of the radiation of real quanta, in view of the analogue character of the generalized diagram[3] relative to those considered above, can be carried out in the same fashion. To eliminate the infrared divergence, we limit ourselves to consideration of real quanta with momentum k, satisfying the condition $(p_{1,2}k) \gg (p_{1,2}\kappa) \sim m^2$. In the c.m.s., this momentum will be the same for all ends of electron lines. As a result we obtain an exponent whose index is added with the index of the exponent of the virtual photons. If the maximum energy of the radiated photons is equal to ω, then the total cross section is shown to be equal to

$$d\sigma = d\sigma_0 \exp\left[-\frac{8e^2}{\pi}\ln\frac{E}{\omega}\ln\frac{E}{m}\right], \tag{4}$$

where E is the initial energy of the electrons. If the recording apparatus records all the scattered electrons independent of their loss in energy, then $\omega = E$ and the cross section $d\sigma$ is identical with the cross section of Møller scattering.[3] The departure from Møller scattering is illustrated in the table for energies of 100 and 500 Mev.

ω, Mev	$d\sigma/d\sigma_0$	
	$E = 100$ Mev	$E = 500$ Mev
0.5	0.59	0.41
5	0.74	0.55
10	0,79	0.60
50	0.95	0.74

In view of the classical character of the radiation of real quanta, the distribution of the latter over angle and energy does not depend on their number. Taking this into account, and integrating over the angles of emission of the photons, we obtain the energy distribution of the radiated photons:

$$dn(\omega) = \frac{8e^2}{\pi}\frac{d\omega}{\omega}\ln\frac{E}{m}. \tag{5}$$

The probability of energy loss by the electron in the range ϵ to $\epsilon + d\epsilon$ is then equal to

$$dN(\varepsilon) = \frac{8e^2}{\pi}\ln\frac{E}{m}\frac{d\varepsilon}{\varepsilon}\exp\left\{-\frac{8e^2}{\pi}\ln\frac{E}{m}\ln\frac{E}{\varepsilon}\right\}. \tag{6}$$

In conclusion, the authors thank A. A. Abrikosov for discussions.

---

[1] A. I. Akhiezer and V. B. Berestetskii, Квантовая электродинамика (Quantum Electrodynamics), Fizmatgiz, 1959.

[2] W. K. Panofsky, Paper at the Ninth International Conference on High Energy Physics, Kiev, 1959.

[3] A. A. Abrikosov, JETP 30, 96, 386, 544 (1956), Soviet Phys. JETP 3, 71, 474, 379 (1956).

Translated by R. T. Beyer
93

SOVIET PHYSICS JETP VOLUME 13, NUMBER 2 AUGUST, 1961

ELECTROMAGNETIC PROPERTIES OF A RELATIVISTIC PLASMA, II

V. P. SILIN

Submitted to JETP editor August 24, 1960

J. Exptl. Theoret. Phys. (U.S.S.R.) 40, 616-625 (February, 1960)

We consider the reflection and absorption of electromagnetic radiation incident perpendicular to a plane surface bounding an electron plasma with relativistic particle-momentum distribution. The surface impedance of the plasma is calculated both for relativistic and nonrelativistic temperatures. Specular and diffuse reflection of the electrons from the surface of the plasma is considered.

1. The question of the transverse field in a semibounded Maxwellian plasma, and also of the reflection and absorption of electromagnetic waves by such a plasma, were considered in references 1 — 3. For the case of a degenerate electron gas in a metal, such a problem was considered in references 4 — 7. In the present communication we show that the methods used by Reuter and Sondheimer[4] can be applied directly to a plasma with relativistic electron distribution. This enables us to consider for a high temperature plasma not only the case of specular reflection, to which references 1 — 3 were confined, but also to the case of diffuse reflection of electrons from the surface of the plasma.

Under the assumption of a plane wave incident perpendicular to the surface bounding the plasma, we derive here expressions for the surface impedance for both relativistic and nonrelativistic electron temperatures. For an ultrarelativistic plasma we determine the asymptotic behavior of waves at large distances and depths from the surface of the plasma.

2. In order to describe the reflection and absorption of electromagnetic waves by the plasma, it is necessary to know the complex coefficient of reflection r, which represents the ratio of the complex amplitudes of the incident and reflected monochromatic waves ($\sim e^{-i\omega t}$). This coefficient can be written in the form[8]

$$r = \frac{(c/4\pi) Z(\omega) - 1}{(c/4\pi) Z(\omega) + 1}, \qquad (1)$$

where the surface impedance $Z(\omega)$ is determined by the ratio of the electric and magnetic fields on the surface of the plasma filling the half-space $z \geq 0$:

$$Z(\omega) = \frac{4\pi}{c} \frac{E_x(0)}{B_y(0)} = \frac{4\pi i\omega}{c^2} \frac{E_x(0)}{E_x'(+0)}. \qquad (2)$$

Here $E_x'(+0)$ denotes the derivative of the electric field with respect to the coordinate z on the surface of the plasma, corresponding to the transition to the limit from the region occupied by the plasma.

We shall use instead of the surface impedance the effective complex depth of penetration of the magnetic field[1,3]

$$\lambda = \frac{1}{B_y(0)} \int_0^\infty dz B_y(z) = -\frac{c}{i\omega} \frac{E_x(0)}{B_y(0)} = -\frac{E_x(0)}{E_x'(+0)}$$
$$= -\frac{c^2}{4\pi i\omega} Z(\omega). \qquad (3)$$

The ratio of the energy flux reflected from the surface of the plasma to the energy flux incident on the plasma is equal to $|r|^2$. Therefore the energy absorbed by the plasma is characterized by the quantity

$$A = 1 - |r|^2. \qquad (4)$$

It is clear that to determine this quantity, or in general to determine the complex reflection coefficient, it is necessary to know the impedance. We shall therefore derive expressions for the effective depth of penetration of the field, which according to (3) is equivalent to determining the surface impedance.

3. To describe the electrons we use the kinetic equation

$$\frac{\partial \delta f}{\partial t} + \mathbf{v} \frac{\partial \delta f}{\partial \mathbf{r}} + e\mathbf{E} \frac{\partial f_0}{\partial \mathbf{p}} = -\nu \delta f. \qquad (5)$$

Here f_0 is the equilibrium distribution function, δf the non-equilibrium addition, ν the collision frequency, and **E** the electric field. The assumed equilibrium distribution function is[9]

$$f_0 = \frac{N_e}{4\pi (mc)^3} \frac{\exp(-c\sqrt{m^2c^2 + p^2}/\varkappa T_e)}{(\varkappa T_e/mc^2) K_2(mc^2/\varkappa T_e)}, \qquad (6)$$

where N_e is the number of electrons per unit volume and K_2 is the MacDonald function.

Assuming the field to be incident perpendicular to the surface of the plasma, and aligning the x axis with the direction of the vector of the electric field, we can readily solve Eq. (5). Inasmuch as the time dependence for a monochromatic wave is $\sim e^{-i\omega t}$, only the dependence of E_x on the coordinate z is unknown.

Depending on the boundary conditions satisfied by the distribution function on the surface of the plasma, we obtain different laws for the absorption and reflection of the electromagnetic radiation. Thus, in the case of specular reflection of the electrons from the plasma surface, we obtain in full analogy with reference 4,

$$E_x^{(s)}(z) = \frac{E_x'(+0)}{\pi} \int_{-\infty}^{+\infty} \frac{e^{ikz}\,dk}{(\omega^2/c^2)\,\varepsilon^{tr}(\omega, k) - k^2}. \qquad (7)$$

We have left out here the periodic dependence of the field on the time. The transverse dielectric constant $\epsilon^{tr}(\omega, k)$ has the form

$$\begin{aligned}\varepsilon^{tr}(\omega, k) &= 1 + \frac{4\pi e^2}{\omega} \int d\mathbf{p}\, \frac{v_x \partial f_0 / \partial p_x}{\omega + i\nu - kv_z} \\ &= 1 - \frac{2\pi e^2 N_e}{\omega kmc}\left[K_2\left(\frac{mc^2}{\varkappa T_e}\right)\right]^{-1} \int_{-kc}^{+kc} \frac{d\omega'}{\omega + i\nu - \omega'} \sqrt{1 - \frac{\omega'^2}{c^2k^2}} \\ &\times \left\{1 + \frac{\varkappa T_e}{mc^2}\sqrt{1 - \frac{\omega'^2}{c^2k^2}}\right\} \exp\left\{-\frac{mc^2}{\varkappa T_e}\frac{1}{\sqrt{1 - \omega'^2/c^2k^2}}\right\} \\ &= 1 - \frac{2\pi e^2 N_e}{\omega mc}[K_2]^{-1}\left\{\int_{-\infty - i\nu/c}^{-(\omega + i\nu)/c} + \int_{(\omega + i\nu)/c}^{+\infty + i\nu/c}\right\} \frac{dk'}{k'(k' - k)} \\ &\times \sqrt{1 - \left(\frac{\omega + i\nu}{ck'}\right)^2}\left\{1 + \frac{\varkappa T_e}{mc^2}\sqrt{1 - \left(\frac{\omega + i\nu}{ck'}\right)^2}\right\} \\ &\times \exp\left\{-\frac{mc^2}{\varkappa T_e}\frac{\sqrt{c^2k'^2}}{\sqrt{c^2k'^2 - (\omega + i\nu)^2}}\right\}. \qquad (8)\end{aligned}$$

It must be noted that the Cauchy integral, which determines the transverse dielectric constant, yields a function which is analytic in the entire plane of complex variable k, made discontinuous by cuts that begin at the point $\pm(\omega + i\nu)/c$ and go to infinity. We note that the case of nonrelativistic distribution is to some extent more complicated in this respect, for when $c = \infty$ the cut lines join together, bisecting the entire complex variable plane.

This important property of the transverse dielectric constant permits, in the case of diffuse reflection of electrons from the plasma surface, the use of the results of references 4 and 6, according to which we can write the following expression for the field in the plasma

$$\begin{aligned}E_x^{(d)}(z) &= \frac{E_x(0)}{2\pi i} \int_{-i\delta - \infty}^{-i\delta + \infty} \frac{dk}{k} e^{ikz} \\ &\times \exp\left\{\frac{1}{2\pi i} \int_{-\infty}^{+\infty} \frac{dk'}{k - k'} \ln\left[1 - \frac{\omega^2}{c^2k'^2}\varepsilon^{tr}(\omega, k')\right]\right\}. \qquad (9)\end{aligned}$$

According to (7) and (9) (see also references 4 and 6), we have for the effective depth of penetration of the field, in the specular and diffuse cases respectively, the following formulas:

$$\lambda^{(s)} = -\frac{1}{\pi} \int_{-\infty}^{+\infty} \frac{dk}{(\omega^2/c^2)\,\varepsilon^{tr}(\omega, k) - k^2}, \qquad (10)$$

$$\lambda^{(d)} = \left\{\frac{1}{\pi}\int_0^{\infty} dk \ln\left[1 - \frac{\omega^2}{c^2k^2}\varepsilon^{tr}(\omega, k)\right]\right\}^{-1}. \qquad (11)$$

4. We consider first a case in which the effective depth of penetration of the field is much greater than both the mean free path and the average distance traversed by the particle during each cycle of oscillation of the field, the latter being proportional to v_T/ω, where v_T is the thermal velocity of the particle. Under these conditions the spatial dispersion of the dielectric constant is a small effect.

Neglecting the spatial dispersion, formula (8) assumes the form

$$\varepsilon^{tr}(\omega, 0) = \varepsilon(\omega) = 1 - \omega_0^2/\omega(\omega + i\nu), \qquad (12)$$

where

$$\omega_0^2 = \frac{4\pi e^2 N_e c^2}{\varkappa T_e}\left[K_2\left(\frac{mc^2}{\varkappa T_e}\right)\right]^{-1} \int_1^{\infty} \frac{dz}{z} K_2\left(\frac{mc^2}{\varkappa T_e} z\right). \qquad (13)$$

For nonrelativistic temperatures $(mc^2 \gg \kappa T_e)$,

$$\omega_0^2 = \omega_{Le}^2 = 4\pi e^2 N_e / m, \qquad (14)$$

and in the opposite case of ultrarelativistic temperatures[10] $(mc^2 \ll \kappa T_e)$

$$\omega_0^2 = \omega_{0r}^2 = 4\pi\, e^2 N_e c^2 / 3\varkappa T_e. \qquad (15)$$

Formula (12) yields for the effective depth of penetration the following expression

$$\lambda = ic/\omega\sqrt{\varepsilon(\omega)}. \qquad (16)$$

The root in the denominator is extracted in such a way that its imaginary part is positive.

For frequencies considerably greater than the collision frequency we have from (12) and (16)

$$\lambda = ic\,[\omega^2 - \omega_0^2 + \omega_0^2 i\nu/\omega]^{-1/2}. \qquad (17)$$

However, formula (17) cannot be employed for relativistic temperatures $(v_T \sim c)$. The point is that expression (16) came about as the result of the pole of the integrand of (10):

$$\varepsilon^{tr} = k^2c^2/\omega^2. \qquad (18)$$

In the nonrelativistic case, the expansion of the transverse dielectric constant in powers of $(kv_T/\omega)^2$ yields a term $\sim k^2$, which for small k is small compared with the right half of (18). This is caused by the presence of the small parameter

$(v_T/c)^2$. At relativistic temperatures this is no longer so, and therefore even in the limit as $k \to 0$ the role of the spatial dispersion of the dielectric constant cannot be regarded as negligibly small.

To derive a formula that generalizes (17) and is applicable to the relativistic case, let us obtain a more exact solution of (18). For this purpose we make use of the more accurate expression for the transverse dielectric constant, which differs from (12) in the terms $\sim k^2$ $(\omega \gg \nu)$:

$$\varepsilon^{tr}(\omega, k) = \varepsilon(\omega) - \alpha\frac{c^2k^2}{\omega^2} = 1 - \frac{\omega_0^2}{\omega^2}\left(1 - i\frac{\nu}{\omega}\right) - \alpha\frac{c^2k^2}{\omega^2}, \tag{19}$$

where

$$\alpha = \frac{\omega_{Le}^2}{\omega^2}\left[K_2\left(\frac{mc^2}{\varkappa T_e}\right)\right]^{-1}\int_0^1 x^2\,dx\sqrt{1-x^2}\left\{1 + \frac{\varkappa T_e}{mc^2}\sqrt{1-x^2}\right\} \times \exp\left\{-\frac{mc^2}{\varkappa T_e}\frac{1}{\sqrt{1-x^2}}\right\}. \tag{20}$$

In the case of nonrelativistic temperatures $(mc^2 \gg \kappa T_e)$

$$\alpha_{nr} = \omega_{Le}^2\frac{\varkappa T_e}{mc^2}\frac{1}{\omega^2}, \tag{21}$$

and for ultrarelativistic temperatures $(mc^2 \ll \kappa T_e)$

$$\alpha_{nr} = \tfrac{1}{5}\omega_{0r}^2/\omega^2. \tag{22}$$

In the latter case Eq. (18) assumes the form[10]

$$\omega^2 = \omega_{0r}^2(1 - i\nu/\omega) + \tfrac{6}{5}c^2k^2, \tag{23}$$

and the term containing k^2 is changed by $\frac{1}{5}$ compared with the case in which the spatial dispersion is completely neglected.

Using (19) we obtain from (10) and (11)

$$\lambda^{(s)} = \frac{ic}{\omega}\frac{1}{\sqrt{\varepsilon(\omega)}}\frac{1}{\sqrt{1+\alpha}} = \frac{ic}{\sqrt{\omega^2 - \omega_0^2 + \omega_0^2 i\nu/\omega}}\frac{1}{\sqrt{1+\alpha}}, \tag{24}$$

$$\lambda^{(d)} = \frac{ic}{\omega}\frac{1}{\sqrt{\varepsilon(\omega)}}\sqrt{1+\alpha} = \frac{ic}{\sqrt{\omega^2 - \omega_0^2 + \omega_0^2 i\nu/\omega}}\sqrt{1+\alpha}. \tag{25}$$

In order for (24) and (25) to be applicable it is necessary that we be able to confine ourselves in (19) to terms $\sim k^2$ only. This is possible if kv_T/ω is small compared with unity. In this case the corrections to formulas (24) and (25), due to the zeros of (18) are small. For nonrelativistic temperatures this takes place if

$$|\varepsilon(\omega)| \ll mc^2/\varkappa T_e, \qquad \omega^2 \gg \omega_{Le}^2 (mc^2/\varkappa T_e)^{-1}. \tag{26}$$

On the other hand, in the case of relativistic temperatures $(v_T \sim c)$ the following inequality should be satisfied

$$|\varepsilon(\omega)| \ll 1, \qquad |\omega^2 - \omega_0^2| \ll \omega_0^2. \tag{27}$$

If inequalities (26) and (27) are violated, the distance covered by the particle during one period of field oscillation is no longer small compared with the effective depth of penetration of the field.

On the other hand, we assume in this section the mean free path to be sufficiently small. This leads to the following limitations:

$$(\nu/\omega)^2 \gg |\varepsilon(\omega)|\varkappa T_e/mc^2 \text{ for } mc^2 \gg \varkappa T_e,$$

$$(\nu/\omega)^2 \gg |\varepsilon(\omega)| \text{ for } mc^2 \lesssim \varkappa T_e, \tag{28}$$

which are more stringent than (26) and (27).

5. Let us turn now to a case in which the distance covered by the particle during one period of oscillation of the field is still small compared with the effective depth of penetration, but the mean free path is greater than the depth of penetration. In this case, in addition to the contribution of the zero of (18) to expressions (10) and (11), the form of which is given in (24) and (25), it is necessary to take into account also the contribution due to the branching of ϵ^r. The latter is given by the formulas

$$\delta\lambda^{(s)} = -\frac{2i}{\pi}\frac{c}{\omega}\left(1 + \frac{\nu}{\omega}\right) \times \int_1^\infty \frac{dx\,\mathrm{Im}\,\varepsilon_+^{tr}(\omega, x(\omega+i\nu)/c)}{[\mathrm{Re}\,\varepsilon_+^{tr}(\omega, x(\omega+i\nu)/c) - (1+i\nu/\omega)^2x^2]^2 + (\mathrm{Im}\,\varepsilon_+^{r})^2}, \tag{29}$$

$$\delta\{\lambda^{(d)}\}^{-1} = \frac{i}{\pi}\frac{\omega}{c}\left(1 + \quad i\nu\right)^3 \times \int_0^1 da\int_1^\infty \frac{x^2dx\,\mathrm{Im}\,\varepsilon_+^{tr}(\omega, x(\omega+i\nu)/c)}{[a\,\mathrm{Re}\,\varepsilon_+^{tr}(\omega, x(\omega+i\nu)/c) - (1+i\nu/\omega)^2x^2]^2 + (a\,\mathrm{Im}\,\varepsilon_+^{tr})^2}. \tag{30}$$

Here

$$\mathrm{Re}\,\varepsilon_+^{tr}\left(\omega, \frac{\omega+i\nu}{c}x\right) = 1 - \frac{\omega_{Le}^2}{2\omega(\omega+i\nu)}\left[K_2\left(\frac{mc^2}{\varkappa T_e}\right)\right]^{-1}\left(\int_{-\infty}^{-1} + \int_1^{+\infty}\right)\frac{dx'}{x'}\,\mathrm{P}\,\frac{1}{x'-x} \times \sqrt{1-\frac{1}{x'^2}}\left\{1 + \frac{\varkappa T_e}{mc^2}\sqrt{1-\frac{1}{x'^2}}\right\}\exp\left\{-\frac{mc^2}{\varkappa T_e}\frac{1}{\sqrt{1-x'^{-2}}}\right\}, \tag{31}$$

$$\mathrm{Im}\,\varepsilon_+^{tr}\left(\omega, \frac{\omega+i\nu}{c}x\right) = \frac{\pi}{2}\frac{\omega_{Le}^2}{\omega(\omega+i\nu)}[K_2]^{-1}\frac{1}{x}\sqrt{1-\frac{1}{x^2}} \times \left\{1 + \frac{\varkappa T_e}{mc^2}\sqrt{1-\frac{1}{x^2}}\right\}\exp\left\{-\frac{mc^2}{\varkappa T_e}\frac{1}{\sqrt{1-x^{-2}}}\right\}. \tag{32}$$

The symbol P in (31) denotes that the singularity $1/(x'-x)$ must be taken in the sense of the principal value.

In the ultrarelativistic case with $\omega^2 = \omega_{0r}^2$ formulas (29) and (30) yield $(\nu \ll \omega)$

$$\delta\lambda^{(s)} = \frac{ic}{\omega_{0r}}\frac{3}{2}\int_1^\infty \frac{dx}{x}\left(1-\frac{1}{x^2}\right)\left\{\left[1+\frac{3}{4x}\left(-\frac{2}{x}+\left(1-\frac{1}{x^2}\right)\ln\frac{x-1}{x+1}\right)\right.\right.$$

$$\left.\left.-x^2\right]^2+(3\pi/4x)^2\left(1-\frac{1}{x^2}\right)^2\right\}^{-1} = 0.09\,\frac{ic}{\omega_{0r}}, \tag{33}$$

$$\delta\{\lambda^{(d)}\}^{-1} = -\frac{i\omega_{0r}}{c}\frac{3}{4}\int_0^1\frac{da}{a^2}\int_1^\infty x\,dx\left(1-\frac{1}{x^2}\right)\left\{\left[1+\frac{3}{4x}\left(-\frac{2}{x}+\left(1-\frac{1}{x^2}\right)\right.\right.\right.$$

$$\left.\left.\left.\times\ln\frac{x-1}{x+1}\right)-\frac{x^2}{a}\right]^2+\left(\frac{3\pi}{4x}\right)^2\left(1-\frac{1}{x^2}\right)^2\right\}^{-1} = -0.18\,\frac{i\omega_{0r}}{c}. \tag{34}$$

For nonrelativistic temperatures we can expand in (29) and (30) in powers of $(\omega_{\mathrm{Le}}^2/\omega^2)(mc^2/\kappa T_e)^{-1}$. We obtain here

$$\delta\lambda^{(s)} = i2\sqrt{\frac{2}{\pi}}\frac{c}{\omega}\,\omega_{Le}^2\left(\frac{\varkappa T_e}{mc^2}\right)^{3/2}, \tag{35}$$

$$\delta\{\lambda^{(d)}\}^{-1} = -\frac{i}{\sqrt{2\pi}}\frac{\omega}{c}\frac{\omega_{Le}^2}{\omega^2}\sqrt{\frac{\varkappa T_e}{mc^2}}. \tag{36}$$

Formulas (33) — (36) together with (24) and (25) determine the effective depth of penetration of the field subject to the satisfaction of inequalities (26) and (27).

For the case of nonrelativistic temperatures, in particular, we obtain from these formulas when $\omega_{\mathrm{Le}}^2 > \omega^2$ (with $\omega_{\mathrm{Le}}^2 - \omega^2 \gg \nu^2$)

$$A^{(s)} = \frac{2\nu}{\sqrt{\omega_{Le}^2-\omega^2}} + 4\sqrt{\frac{8}{\pi}}\frac{\omega_{Le}^2-\omega^2}{\omega^2}\left(\frac{\varkappa T_e}{mc^2}\right)^{3/2}, \tag{37}$$

$$A^{(d)} = \frac{2\nu}{\sqrt{\omega_{Le}^2-\omega^2}} + \sqrt{\frac{8}{\pi}}\sqrt{\frac{\varkappa T_e}{mc^2}}. \tag{38}$$

The dissipation, for which these formulas stand and which is independent of the collisions between particles, can be obtained, following reference 5 (see also reference 8), by considering the work performed by the field on a particle which collides with the surface of the plasma. In this case, by virtue of condition (26), the spatial dispersion of the dielectric constant is weak, and consequently we can use for the field in the plasma the following expression

$$E_x(z, t) = E_x(0)\, e^{-i\omega t} \exp\{+iz\sqrt{\varepsilon(\omega)}\,\omega/c\},$$

where it can be readily verified that when $\epsilon(\omega) < 0$ the average energy acquired by one electron is in the case of specular reflection

$$W^{(s)} = \frac{e^2}{m}\frac{\omega_{Le}^2-\omega^2}{\omega^4}\frac{v_z^2}{c^2}E_x(0)\,E_x^*(0),$$

and in the case of diffuse reflection

$$W^{(d)} = \frac{e^2}{2m\omega^2}E_x(0)\,E_x^*(0). \tag{39}$$

Accordingly, the total energy acquired per unit time by the plasma electrons, referred to unit surface, is

$$2\frac{e^2N_e}{m\omega^2}\sqrt{\frac{\varkappa T_e}{2\pi m}}\left\{\rho\,\frac{\omega_{Le}^2-\omega^2}{\omega^2}\frac{\varkappa T_e}{mc^2}+(1-\rho)\frac{1}{4}\right\}E_x(0)\,E_x^*(0), \tag{40}$$

where ρ is the fraction of the electrons specularly reflected from the surface of the plasma.

In order to obtain a formula similar to (37) and (38), expression (40) must be divided by the average flux of the electromagnetic energy of the incident wave, the value of which is $(c/8\pi)\,E_x(-\infty) \times E_x^*(-\infty)$, where $E_x(-\infty)$ is the amplitude of the incident wave. Recognizing that by the boundary condition $E_x(0) = (1+r)\,E_x(-\infty)$, and also that when $\omega_{\mathrm{Le}}^2 > \omega^2$ we have

$$r = \frac{i\omega+\sqrt{\omega_{Le}^2-\omega^2}}{i\omega-\sqrt{\omega_{Le}^2-\omega^2}},$$

we obtain

$$A = 4\rho\sqrt{\frac{8}{\pi}}\frac{\omega_{Le}^2-\omega^2}{\omega^2}\left(\frac{\varkappa T_e}{mc^2}\right)^{3/2}+(1-\rho)\sqrt{\frac{8\varkappa T_e}{\pi mc^2}}, \tag{41}$$

which is analogous to the parts of (37) and (38) independent of the collision frequency.

Since $\omega \gg \nu$, we should use in this case for the collision frequency*

$$\nu_{\mathrm{eff}} = \frac{4}{3}\frac{\sqrt{2\pi}}{\sqrt{m}}\frac{e^4N_e}{(\varkappa T_e)^{3/2}}L,$$

$$\text{where } L \approx \ln\frac{r_{\mathrm{d}}}{\rho_{min}} = \ln\left(\sqrt{\frac{\varkappa T_e}{m\omega_{Le}^2}}\frac{\varkappa T_e}{e^2}\right).$$

Therefore the dissipation characterized by formula (41) is greater in the case of specular reflection than the dissipation due to the collisions

$$A_\nu = 2\nu_{\mathrm{eff}}/\sqrt{\omega_{Le}^2-\omega^2}, \qquad \omega_{Le}^2-\omega^2 \gg \nu_{\mathrm{eff}}^2,$$

if the following condition is satisfied

$$\frac{e^2N_e^{1/3}}{\varkappa T_e}\frac{mc^2}{\varkappa T_e}L^{2/3} < \left(1-\frac{\omega^2}{\omega_{Le}^2}\right)\left(\frac{\omega_{Le}}{\omega}\right)^{4/3}.$$

In a real plasma this inequality can be realized only when $\omega \ll \omega_{\mathrm{Le}}$, where it assumes the form

$$\omega^2 \ll \omega_{Le}^2\left(\frac{\varkappa T_e}{e^2N_e^{1/3}}\right)^{3/2}\left(\frac{\varkappa T_e}{mc^2}\right)^{3/2}\frac{1}{L}.$$

It must be recalled that inequality (26) should be simultaneously satisfied.

In the case of diffuse reflection A_ν is small compared with the corresponding expression due to the collisions with the surface of the plasma, provided that

---

*In the ultrarelativistic limit $\nu_{\mathrm{eff}} \sim 13ce^4NL/15(\varkappa T)^2$.

$$(e^2 N_e^{1/3}/\varkappa T_e)^3\,(mc^2/\varkappa T_e)\,L^2 < 1 - \omega^2/\omega_{Le}^2.$$

It is easy to see that this inequality is valid over a relatively wide range. Actually, for frequencies which are not too close to ω_{Le}, this relation has the form $25\,N_e L^2 < T_e^4$, where T_e is in degrees Kelvin and N_e is the number of electrons per cm^3.

We obtain now an expression for $A^{(d)}$ in the absence of collisions when $\omega > \omega_{\mathrm{Le}}$. We note that formula (39) is independent of whether $\epsilon(\omega)$ is positive or negative. We can therefore use formula (40), setting $\rho = 0$, and use for r the ratio

$$r = \frac{1-\sqrt{\varepsilon(\omega)}}{1+\sqrt{\varepsilon(\omega)}} = \frac{1-\sqrt{1-\omega_{Le}^2/\omega^2}}{1+\sqrt{1-\omega_{Le}^2/\omega^2}}.$$

We then obtain

$$A^{(d)} = \sqrt{\frac{8}{\pi}}\sqrt{\frac{\varkappa T_e}{mc^2}}\frac{\omega_{Le}^2}{(\omega+\sqrt{\omega^2-\omega_{Le}^2})^2}. \tag{42}$$

In particular for $\omega \gg \omega_{\mathrm{Le}}$ we obtain from this

$$A^{(d)} = \frac{1}{\sqrt{2\pi}}\sqrt{\frac{\varkappa T_e}{mc^2}}\frac{\omega_{Le}^2}{\omega^2}. \tag{43}$$

6. Let us consider the case of strong spatial dispersion, when the effective depth of penetration is small compared with the mean free path, as well as with the average distance covered by the particle during one period of field oscillations. This is the case of anomalous skin effect. Under such conditions we can use in formulas (10) and (11) the following approximate expression for the transverse dielectric constant

$$\varepsilon^{tr}(\omega, k) = 4\pi i C/\omega\,|k|. \tag{44}$$

Here C, according to formula (8), has the form

$$C = \frac{\pi}{2}\frac{e^2 N_e}{m}\left\{\frac{\varkappa T_e}{mc^2}+1\right\}\frac{\exp(-mc^2/\varkappa T_e)}{K_2(mc^2/\varkappa T_e)}. \tag{45}$$

In the case of nonrelativistic temperatures

$$C_{\mathrm{nr}} = \sqrt{\frac{\pi}{2}}\frac{e^2 N_e}{m}\sqrt{\frac{m}{\varkappa T_e}}, \tag{46}$$

and in the opposite ultrarelativistic case

$$C_{\mathrm{ur}} = \frac{\pi e^2 N_e c}{4\varkappa T_e}. \tag{47}$$

Substituting expression (34) in formulas (10) and (11) we obtain

$$\lambda^{(s)} = \frac{2}{3}\left(1+\frac{i}{\sqrt{3}}\right)\left(\frac{c^2}{4\pi C\omega}\right)^{1/3}, \tag{48}$$

$$\lambda^{(d)} = \frac{3}{4}\left(1+\frac{i}{\sqrt{3}}\right)\left(\frac{c^2}{4\pi C\omega}\right)^{1/3}. \tag{49}$$

It should be noted that the last two formulas are quite analogous to those obtained by Reuter and Sondheimer[4] for a degenerate electronic plasma. Formula (48) in the nonrelativistic case is similar to that obtained by Stepanov.[3]

The condition that the effective depth of penetration be small compared with the average distance covered by the electron during one field oscillation cycle has, according to (46) – (49), the form $\omega^2 \ll \omega_{\mathrm{Le}}^2(mc^2/\kappa T_e)^{-1}$ in the nonrelativistic case, and the form $\omega^2 \ll \omega_0^2$ in the relativistic case ($v_T \sim c$), which naturally is the opposite of conditions (26) and (27).

I express my indebtedness to L. V. Pariĭskaya, who calculated the integrals in formulas (33) and (34).

APPENDIX

ASYMPTOTIC BEHAVIOR OF THE FIELD FOR LARGE z IN THE CASE OF AN ULTRARELATIVISTIC PLASMA

We now consider briefly the asymptotic behavior of the integral (7) for large z in the case of an ultrarelativistic plasma. In this case the transverse dielectric constant has the form

$$\varepsilon^{tr}(\omega, k) = 1 + \frac{3\omega_{0r}^2}{4\omega ck}\left\{-2\frac{\omega+i\nu}{ck}+\left[1-\left(\frac{\omega+i\nu}{ck}\right)^2\right]\ln\frac{\omega+i\nu-ck}{\omega+i\nu+ck}\right\}.$$

For the asymptotic behavior of the integral (7), the zeros of Eq. (18), located in the upper half-plane k are of importance, since they cause the field to fall off exponentially with increasing z. The decrement of this damping is determined here by the imaginary part of the root of Eq. (18). Near such a root, the denominator of the integral (7) can be represented in the form

$$\left\{\left(\frac{\omega^2}{c^2}\frac{\partial\varepsilon^{tr}}{\partial k}-2k\right)_{k=k_0}(k-k_0)\right\}^{-1}.$$

Here k_0 is the root of Eq. (18). The contribution made by such a pole to the asymptotic value of our integral has the form

$$\left(\frac{\omega^2}{c^2}\frac{\partial\varepsilon^{tr}}{\partial k}-2k\right)_{k=k_0}^{-1} e^{ik_0 z}.$$

In particular, for frequencies close to ω_{0r} we obtain, according to (23),

$$-\sqrt{\frac{5}{24}}\frac{c}{\left[\omega^2-\omega_{0r}^2+i\omega_{0r}^2\nu/\omega\right]^{1/2}}$$

$$\times\exp\{izc^{-1}[\omega^2-\omega_{0r}^2+i\omega_{0r}^2\nu/\omega]^{1/2}\}.$$

When extracting the square root it is necessary to choose the value with the positive imaginary part.

At frequencies $\omega \ll \omega_{0r}$ the contribution to the asymptotic value from the pole has the form

$$-\frac{1}{3k_0}e^{ik_0z}, \qquad k_0 = \left(\frac{4\pi C\omega}{c^2}\right)^{1/3}\left(-\frac{\sqrt{3}}{2}+\frac{i}{2}\right),$$

and finally, in the region $\omega \gg \omega_{0r}$ we get

$$\sim -\frac{1}{2}\frac{c}{\omega}c^{i\omega z/c}.$$

The asymptotic value is also influenced by the singular points of the dielectric constant. Our expression for $\epsilon^{tz}(\omega, k)$ has in the upper half plane a branch point $k = (\omega + i\nu)/c$. Near such a singular point the singular part of the integral (7) has the form

$$-\frac{3}{2}\frac{\omega_0^2}{(\omega+i\nu)^2}\frac{c^3}{\omega^3}\frac{[k-(\omega+i\nu)/c]\ln[k-(\omega+i\nu)/c]}{[-(\omega+i\nu)^2/\omega^2+1-3\omega_0^2/2(\omega+i\nu)^2]^2}.$$

Accordingly, the following contribution is made to the asymptotic value

$$-\frac{3}{2}\frac{\omega_0^2}{(\omega+i\nu)^2}\frac{c^3}{\omega^3}\left\{-2i\frac{\nu}{\omega}+\frac{\nu^2}{\omega^2}-\frac{3}{2}\frac{\omega_0^2}{(\omega+i\nu)^2}\right\}^{-2} z^{-2}e^{(i\omega-\nu)z/c}.$$

We note that in the original problem the presence of a branch point of the dielectric constant leads to a unique dependence on the time for a field with specified **k**, namely, a dependence of the form $\sim t^{-2}e^{-ickt}$ along with the purely exponential dependence corresponding to the damped oscillations and due to the zeros of Eq. (18).

---

[1] V. P. Silin, Тр. ФИАН (Trans. Phys. Inst. Acad. Sci.) 6, 200 (1955).

[2] V. D. Shafranov, JETP 34, 1475 (1958), Soviet Phys. JETP 7, 1019 (1958).

[3] K. N. Stepanov, JETP 36, 1457 (1959), Soviet Phys. JETP 9, 1035 (1959).

[4] G. E. H. Reuter and E. H. Sondheimer, Proc. Roy. Soc. A195, 336 (1948).

[5] T. Holstein, Phys. Rev. 88, 1427 (1952).

[6] R. B. Dingle, Physica 19, 311 (1953).

[7] R. B. Dingle, Appl. Sci. Res. B3, 69 (1953).

[8] V. L. Ginzburg and G. P. Motulevich, Usp. Fiz. Nauk 55, 469 (1955).

[9] L. D. Landau and E. M. Lifshitz, Статистическая физика, (Statistical Physics), Gostekhizdat, 1951.

[10] V. P. Silin, JETP 38, 1577 (1960), Soviet Phys. JETP 11, 1136 (1960).

Translated by J. G. Adashko
94

SOVIET PHYSICS JETP VOLUME 13, NUMBER 2 AUGUST 1961

RELATION BETWEEN THE EQUATIONS FOR PARTIAL AMPLITUDES AND FOR SPECTRAL FUNCTIONS

Yu. A. SIMONOV

Submitted to JETP editor August 31, 1960

J. Exptl. Theoret. Phys. (U.S.S.R.) 40, 626-629 (February, 1961)

It is shown how the Chew-Mandelstam equations for the partial wave amplitudes can be deduced from the equations for the Mandelstam spectral functions.

ANALYTICITY and unitarity conditions have been recently used to write equations for the amplitudes of various transitions of two particles into two particles. Several approaches are possible in this connection. On the one hand, Chew and Mandelstam[1] have constructed equations for $\pi\pi$ scattering of charged pions, which included the $l = 0$ and 1 partial wave amplitudes. On the other hand, Ter-Martirosyan[2] proposed equations which determine directly the spectral functions of the Mandelstam representation. Such equations were given by Ter-Martirosyan[3] for a few simple cases. The method of transforming to the one-dimensional representation of Cini and Fubini[4] is, in essence, equivalent to the Chew-Mandelstam approach.

When deriving the equations for the partial wave amplitude it is necessary to neglect in the integral over the left-hand cut the contributions due to partial amplitudes with large values of l. Recently a number of serious objections have been raised against this approximation. In particular, it has been shown that the integral over the left-hand cut, containing higher phase shifts with $l \geq 2$, in general diverges.[5]

We show below that the two approaches are equivalent and that it is possible to pass from the equations for the spectral functions to the Chew-Mandelstam equations. It will be seen that the divergences are absent from the equations for the spectral functions and arise solely when it is attempted to express the spectral functions in terms of the partial wave amplitudes.

In order not to complicate the formulas we shall consider scattering of neutral pions. The scattering amplitude, with its symmetry properties taken into account, can be written as follows:

$$A(s_1, s_2, s_3) = \frac{1}{\pi}\int\limits_{4\mu^2}^{\infty} f(\sigma)\,[\varphi(\sigma, s_1) + \varphi(\sigma, s_2) + \varphi(\sigma, s_3)]\,d\sigma + \frac{1}{\pi^2}\iint\limits_{4\mu^2}^{\infty} \rho(\sigma, \sigma')\,[\varphi(\sigma, s_1)\,\varphi(\sigma', s_2) + \varphi(\sigma, s_1)\,\varphi(\sigma', s_3) + \varphi(\sigma, s_2)\varphi(\sigma', s_3)]\,d\sigma\,d\sigma',$$

$$\varphi(\sigma, s) = 1/(\sigma - s) - 1/(\sigma - s_0), \quad \rho(\sigma, \sigma') = \rho(\sigma'\,\sigma). \tag{1}$$

Making use of the unitarity condition one may write

$$A_1 \equiv \operatorname{Im} A(s_1, s_2, s_3) = \sqrt{(s_1 - 4\mu^2)/s_1}\int \frac{dn_1}{4\pi}\,A(s_1, s_2', s_3')^{*}\,A(s_1, s_2'', s_3''). \tag{2}$$

By analytic continuation of Eq. (2) one may find the discontinuity in s_2 (or s_3). From here, using the method outlined by Ter-Martirosyan,[2,3] it is easy to obtain the equation for $\rho(s_1, s_2)$:

$$\rho(s_1, s_3) = \frac{2}{\pi^2}\iint\limits_{4\mu^2}^{\infty} F^{*}(\sigma)\,[\Gamma(\sigma, \sigma', s_3, s_1) + \Gamma(\sigma, \sigma', s_1, s_3)]\,F(\sigma')\,d\sigma d\sigma',$$

$$F(\sigma) = f(\sigma) + \frac{1}{\pi}\int\limits_{4\mu^2}^{\infty} \rho(\sigma, \sigma')\,[\varphi(\sigma', s_1) + \varphi(\sigma', 4\mu^2 - s_1 - \sigma)]\,d\sigma'. \tag{3}$$

From Eq. (1) we obtain for the partial wave amplitude the expression:

$$A_l(s_1) = \frac{2}{\pi}\int\limits_{4\mu^2}^{\infty} F(\sigma)\,k_l(\sigma, s_1)\,d\sigma + \Big\{\frac{1}{\pi}\int\limits_{4\mu^2}^{\infty} f(\sigma)\,\varphi(\sigma, s_1)\,d\sigma - \frac{2}{\pi}\int\limits_{4\mu^2}^{\infty}\Big[f(\sigma) + \frac{1}{\pi}\int\limits_{4\mu^2}^{\infty} \rho(\sigma', \sigma)\,\varphi(\sigma', s_1)\,d\sigma'\Big]\frac{d\sigma}{\sigma - s_0} + \frac{1}{\pi^2}\iint\limits_{4\mu^2}^{\infty}\frac{\rho(\sigma', \sigma'')\,d\sigma'\,d\sigma''}{(\sigma' - s_0)(\sigma'' - s_0)}\Big\}\,\delta_{l0}, \tag{4}$$

$$k_l(\sigma, s_1) = 2\,[s_1 - 4\mu^2]^{-1}\,Q_l\,[1 + 2\sigma/(s_1 - 4\mu^2)], \tag{5}$$

where $Q_l(z)$ is the Legendre function of the second kind. Ter-Martirosyan[3] has shown that the Chew-Mandelstam equation containing only S waves is obtained if the functions $\rho(\sigma, \sigma')$ are neglected. Below, starting from Eq. (3), we obtain the Chew-Mandelstam equation containing all partial waves.

It is easy to derive the following equalities for the function $\Gamma(\sigma, \sigma', s_3, s_1)$ defined by Ter-Martirosyan:[2]

$$\frac{1}{\pi}\int_{4\mu^2}^{\infty} \Gamma(\sigma, \sigma', \sigma_3, s_1)\, k_l(\sigma_3, s_1)\, d\sigma_3 = \sqrt{\frac{s_1-4\mu^2}{s_1}}\, k_l(\sigma, s_1)\, k_l(\sigma', s_1), \tag{6}$$

$$\sqrt{\frac{s_1-4\mu^2}{s_1}}\int \frac{1}{(\sigma-s_3')(\sigma'-s_3'')}\frac{dn_1}{4\pi} = \frac{1}{\pi}\int_{4\mu^2}^{\infty}\frac{\Gamma(\sigma, \sigma', \sigma_3, s_1)}{\sigma_3-s_3}\, d\sigma_3$$
$$= \sqrt{\frac{s_1-4\mu^2}{s_1}}\sum_{l=0}^{\infty}(2l+1)\, k_l(\sigma, s_1)\, k_l(\sigma', s_1)\, P_l(z_1). \tag{7}$$

From Eq. (4) it is easy to show that, for $s_1 \geq 4\mu^2$

$$\operatorname{Im} A_l(s_1) = \frac{2}{\pi}\int_{4\mu^2}^{\infty}\rho(s_1, \sigma)\left[k_l(\sigma, s_1) - \frac{\delta_{l0}}{\sigma - s_0}\right]d\sigma + f(s_1)\,\delta_{l0}. \tag{8}$$

Let us multiply Eq. (3) by $k_l(s_3, s_1)$ and integrate over ds_3 from $4\mu^2$ to ∞. Here s_1 lies in the interval $4\mu^2 \leq s_1 \leq 16\mu^2$. Then $\Gamma(\sigma, \sigma', s_1, s_3) = 0$, and with the help of Eqs. (7) and (6) we obtain

$$\frac{1}{\pi}\int_{4\mu^2}^{\infty}\rho(s, \sigma)\, k_l(\sigma, s_1)\, d\sigma = 2\sqrt{\frac{s_1-4\mu^2}{s_1}}\left|\frac{1}{\pi}\int_{4\mu^2}^{\infty}F(\sigma)\, k_l(\sigma, s_1)\, d\sigma\right|^2. \tag{9}$$

In order to obtain the Chew-Mandelstam equation starting from Eqs. (1) and (3) it is necessary to note in the first place that

$$\operatorname{Im} A_l(s_1) = \sqrt{(s_1-4\mu^2)/s_1}\,|A_l(s_1)|^2 \quad \text{for} \quad s_1 \geqslant 4\mu^2. \tag{10}$$

In addition, it is seen from Eq. (5) that

$$\operatorname{Im} k_l(\sigma, s_1 - i\varepsilon) = \frac{\pi}{s_1-4\mu^2}P_l\left(1+\frac{2\sigma}{s_1-4\mu^2}\right)\theta(4\mu^2 - s_1 - \sigma),$$
$$\theta(x) = 0 \quad \text{for} \quad x < 0, \qquad \theta(x) = 1 \quad \text{for} \quad x > 0. \tag{11}$$

Using Eq. (11) we obtain from Eq. (4) the value of $\operatorname{Im} A_l(s_1)$ over the left cut, which, as can be seen from Eqs. (4) and (11), runs from $s_1 = -\infty$ to $s_1 = 0$:

$$\operatorname{Im} A_l(s_1 - i\varepsilon) = \frac{2}{s_1-4\mu^2}\int_{4\mu^2}^{4\mu^2-s_1}F(\sigma)\, P_l\left(1+\frac{2\sigma}{s_1-4\mu^2}\right)d\sigma. \tag{12}$$

It is seen that the imaginary part along the left cut does not become infinite; the integral

$$\int_{-\infty}^{0} d\sigma\, [(\sigma - s_1)(\sigma - s_0)]^{-1}\operatorname{Im} A_l(\sigma)$$

also converges. In order to obtain equations involving the partial wave amplitudes we must express the integrals

$$\frac{1}{\pi}\int \rho(\sigma, \sigma')\,\varphi(\sigma', s_1)\, d\sigma',$$

$$\frac{1}{\pi}\int \rho(\sigma, \sigma')\,\varphi(\sigma', 4\mu^2 - s_1 - \sigma)\, d\sigma'$$

in terms of $A_l(\sigma)$. With the help of Eq. (3) we obtain

$$\frac{1}{\pi}\int_{4\mu^2}^{\infty}\frac{\rho(\sigma, \sigma')}{\sigma' - s_1}d\sigma' = \frac{2}{\pi^2}\iint_{4\mu^2}^{\infty}F^*(\sigma')\left[\frac{1}{\pi}\int_{4\mu^2}^{\infty}\frac{\Gamma(\sigma', \sigma'', \sigma_3, \sigma)}{\sigma_3 - s_1}d\sigma_3\right]$$
$$\times F(\sigma'')\, d\sigma'\, d\sigma'' = \frac{2}{\pi^2}\sqrt{\frac{\sigma-4\mu^2}{\sigma}}\iint_{4\mu^2}^{\infty}F^*(\tau)\, F(\tau')\sum_{l=0}^{\infty}$$
$$\times (2l+1)\, k_l(\tau, \sigma)\, k_l(\tau', \sigma)\, P_l\left(1+\frac{2s_1}{\sigma-4\mu^2}\right)d\tau\, d\tau'. \tag{13}$$

$f(\sigma)$ can be expressed in terms of $\operatorname{Im} A_0(s_1)$ and $\rho(\sigma, \sigma')$ by means of Eq. (8). In evaluating Eq. (13), the fact that we are interested only in values of σ below the threshold for production of four particles, i.e., $4\mu^2 \leq \sigma \leq 16\mu^2$, was taken into account. Then in Eq. (3) only the term involving $\Gamma(\tau, \tau', \sigma', \sigma)$ contributes, since $\Gamma(\tau, \tau', \sigma, \sigma')$ is different from zero only for $\sigma \geq 16\mu^2$.

As a result we obtain

$$f(\sigma) + \frac{1}{\pi}\int_{4\mu^2}^{\infty}\rho(\sigma, \sigma')\,[\varphi(\sigma', s_1) + \varphi(\sigma', 4\mu^2 - s_1 - \sigma)]\, d\sigma'$$
$$= \frac{1}{2}\sqrt{\frac{\sigma-4\mu^2}{\sigma}}\sum_{l=0}^{\infty}|A_l(\sigma)|^2 P_l\left(1+\frac{2s_1}{\sigma-4\mu^2}\right)(1+(-1)^l), \tag{14}$$

from where we find, for $s_1 < 0$

$$\operatorname{Im} A_l(s_1 - i\varepsilon) = \frac{2}{s_1-4\mu^2}\int_{4\mu^2}^{4\mu^2-s_1}\sum_{n=0,2,\ldots}^{\infty}\operatorname{Im} A_n(\sigma)$$
$$\times P_n\left(1+\frac{2s_1}{\sigma-4\mu^2}\right)(2n+1)\, P_l\left(1+\frac{2\sigma}{s_1-4\mu^2}\right)d\sigma. \tag{15}$$

It is now a simple matter to write dispersion relations for $A_l(s_1)$. When Eqs. (15) and (10) are taken into account it is seen that these relations yield precisely the Chew-Mandelstam equation for the scattering of neutral pions. In the integral over the left-hand cut of the quantity $\operatorname{Im} A_l(s_1)$, determined by formula (15), one may exchange the order of integration. Then every term in the summation over n, starting with n = 2, will diverge if a subtraction is performed. This circumstance was first noted by Efremov et al.[5]

We have carried out analogous considerations for the case of scattering of charged pions. Again, it is easy to obtain the Chew-Mandelstam equations[1] starting from the equations for the spectral functions. It becomes clear in the derivation how the finite expression for $\operatorname{Im} A_l^{(I)}(s_1)$ for $s_1 < 0$ is transformed into a series of divergent, after integration, terms if it is expressed in terms of partial amplitudes in the physical region. Because of the complexity of the relevant formulas we refrain from presenting here the results for the case of scattering of charged pions.

It is thus seen that if we limit ourselves to the one-dimensional spectral functions (or the first term in the expansion in the Cini and Fubini method) we obtain the Chew-Mandelstam equation for the S wave. This equation contains no divergences, but it can be correct only if all amplitudes with $l > 0$ are small in comparison with the S-wave amplitude. Inclusion of partial waves with $l > 0$ is equivalent to the taking into account of the two-dimensional spectral functions. As we have seen, this results in the Chew-Mandelstam method in the appearance of divergences. The contribution of the two-dimensional spectral functions can be taken consistently into account by solving the equations for the spectral functions, using, for example, the iteration scheme proposed by Ter-Martirosyan.[2,3]

The author is grateful to K. A. Ter-Martirosyan for suggesting this problem and for continuous interest in this work.

---

[1] G. Chew and S. Mandelstam, Phys. Rev. 119, 467 (1960).

[2] K. A. Ter-Martirosyan, JETP 39, 827 (1960), Soviet Phys. JETP 12, 575 (1960).

[3] K. A. Ter-Martirosyan, JETP, Nuclear Phys., in press.

[4] M. Cini and S. Fubini, Preprint CERN.

[5] Efremov, Meshcheryakov, Chung, and Shirkov, Preprint, Joint Inst. Nuc. Res., Nuclear Phys., in press.

Translated by A. M. Bincer
95

SOVIET PHYSICS JETP VOLUME 13, NUMBER 2 AUGUST, 1961

CALCULATION OF SOME EXTENSIVE AIR SHOWER CHARACTERISTICS WITH ALLOWANCE FOR FLUCTUATIONS

L. G. DEDENKO

Nuclear Physics Institute, Moscow State University

Submitted to JETP editor September 3, 1960

J. Exptl. Theoret. Phys. (U.S.S.R.) 40, 630-636 (February, 1961)

The size spectrum of EAS at 640 g/cm^2 altitude (the Pamirs), produced by 10^{13}, 10^{14}, and 10^{15} ev protons, is calculated with allowance for fluctuations in the number and altitude of the primary-proton collisions. The energy spectrum of protons producing showers of a given size at the observation level is determined. The size spectrum of showers produced by primary protons, α particles, and oxygen nuclei is calculated.

1. INTRODUCTION

THE probability of the production of showers with a given number of particles (shower size) at mountain altitudes (640 g/cm^2) by primary protons of various energies was calculated by the Monte-Carlo method by means of the "Strela" electronic computer. The calculations were carried out under the following assumptions:[1]

1. A proton with an arbitrary energy colliding with an air nucleus conserves a constant fraction α of its energy, and loses an energy fraction $\eta_p = 1 - \alpha$ for the production of π mesons. A proton with an initial energy E_0 will have an energy $E_j = \alpha^j E_0$ after j collisions. If we assume that the interaction mean free path for protons in air $\lambda_0 = 80$ g/cm^2, that the absorption mean free path $\lambda = 120$ g/cm^2, and that the exponent of the primary-proton energy spectrum $\gamma = 1.7$, then, from the relation[2,3] $\lambda_0/\lambda = 1 - \alpha^\gamma$, we find the inelasticity factor to be $\eta_p = 0.47$. For $\pi^\pm$ mesons, $\eta_\pi = 1$ and $\lambda_0 = 80$ g/cm^2.

2. In the collision of a proton or a $\pi^\pm$ meson of energy E with an air nucleus, the effective number of π mesons produced is equal to[4]

$$n_\pi(E) = 1.26\ (E/10^{10})^{0.25} \tag{1}$$

where E is in ev. The π^0 mesons amount to one third of the total number of mesons. The energies of all secondary mesons are assumed to be the same:

$$E_\pi(E) = \eta E / n_\pi(E), \tag{2}$$

where $\eta = 0.47$ for an incident proton and $\eta = 1$ for an incident meson.

3. The number of particles arriving at the observation level at the depth $X_0 = 8$ (nuclear lengths) in a shower produced by the collision of a proton of energy E_j with an air nucleus at a depth X_p in the atmosphere is

$$N_{j+1} = 0.47 K\ (E_\pi(E_j),\ X_0,\ X_p)\ E_j E_{\rm ph}^{-1} N\ (E_{\rm ph},\ X_0 - X_p) \tag{3}$$

where $K[E_\pi(E_j),\ X_0,\ X_p]$ is the coefficient accounting for the energy fraction transferred to π^0 mesons. The equation for calculating the coefficient K is given in reference 1. In deriving this equation, it was assumed that the atmospheric density between X_p and X_0 is equal to the density at X_p. The variation of K with the energy of the mesons produced by the protons is shown in Fig. 1 for different depths X_p of proton interactions with air nuclei in the atmosphere. $N(E_{ph},\ X_0 - X_p)$ is the number of charged particles in the pure electron-photon cascade initiated by a photon with energy $E_{ph} = 0.5\ E_\pi(E_j)$. This number was calculated from the approximate equation of Greisen[5]

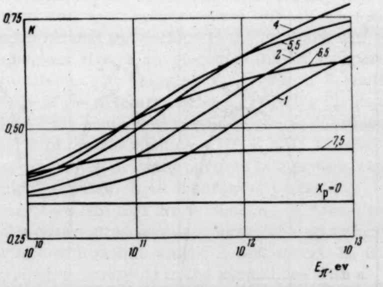

FIG. 1. Energy fraction K transferred to π^0 mesons of various energies. The numbers on the curves denote the depth of interaction X_p of the primary proton in nuclear lengths.

$$N\,(E_{\mathrm{ph}}, X_0 - X_{\mathrm{p}}) \approx 0.31\beta_0^{-0.5} \exp[t\,(1 - 1.5 \ln s)],$$

where $\beta_0 = \ln(E_{\mathrm{ph}}/\epsilon_0)$, $\epsilon_0 = 7.2 \times 10^7$ ev is the critical energy of electrons in air, $t = \rho\,(X_0 - X_{\mathrm{p}})$, $\rho = 2.34$ is the ratio of the nuclear unit to the radiation length, and $s = 3t/(t + 2\beta_0)$.

4. In the case where the proton has undergone m collisions before reaching the observation level, the total number of particles in the shower is

$$N = \sum_{j=1}^{m} N_j. \tag{4}$$

2. DISTRIBUTION FUNCTION OF THE PROBABILITY OF A GIVEN SHOWER SIZE AT THE OBSERVATION LEVEL, PRODUCED BY A PRIMARY PROTON OF A GIVEN ENERGY

In order to obtain the probability distribution function of shower sizes, a given number m of collisions of a proton with air nuclei distributed according to the Poisson law with $\overline{m} = 8$ were considered. For each m, the values of the depths of collisions between the protons in the atmosphere were played out using pseudorandom numbers.[6] The probability density of the logarithm of the number of particles $z = \ln N$ at the observation level as a function of the primary-proton energy E_0 is given by

$$\Psi(z \mid y) = \sum_{m=1}^{\infty} P_m \Psi^{(m)}(z \mid y), \tag{5}$$

where P_m is the probability of m collisions, $\Psi^{m}(z \mid y)$ is the probability density z for m collisions, and $y = \ln(E_0/10^{10})$ (E_0 being in ev).

The probability density $\Psi(z \mid y)$ was found for primary protons with energies 10^{13}, 10^{14}, and 10^{15} ev. The number of showers played for each number m of collisions was 125. Series (5) was terminated at the term for m = 15. The total number of played showers thus amounted to 1875 for each primary-proton energy. The values of the probability density $\Psi(z \mid y)$ obtained with the electronic computer are represented in Fig. 2 by the points. The solid curves represent the approximated functions.

For the approximated functions, we used the fourth-power polynomial

$$\ln \Psi(z \mid y) = \sum_{i=1}^{4} a_i (z - y)^i. \tag{6}$$

The polynomial was determined assuming a quasi-uniform dependence of the probability density $\chi(N \mid E_0)$ on the number of particles in the shower N and on the proton energy E_0. The coefficients a_i are linear functions of y. This made it possible to find the probability density $\Psi(z \mid y)$ for any proton energy in the range 10^{13}–10^{15} ev. The average values of the number of particles in showers produced by primary protons with energies 10^{13}, 10^{14}, and 10^{15} ev are equal to 2.73×10^3, 4.25×10^4, and 5.66×10^5 respectively. The double half-widths of the curves are such that protons with energies 10^{13}, 10^{14}, and 10^{15} ev produce, with a sufficiently high probability, showers whose sizes differ by factors of 5, 3.5, and 2.6 respectively from the above-given values, i.e., approximately 1/5 of the same factors at sea level.[1] With increasing primary-proton energy, the role of the fluctuations decreases. Just as at sea level, this can be explained by the increasing length of the electron-photon showers.

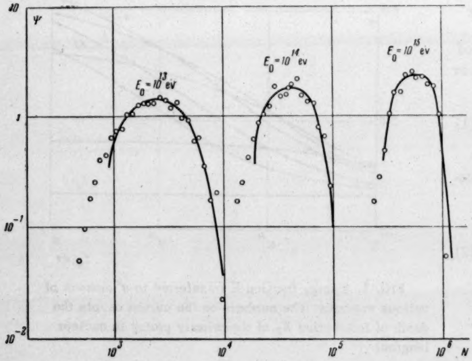

FIG. 2. Distribution function of the probability of a given shower size produced by primary protons of different energies.

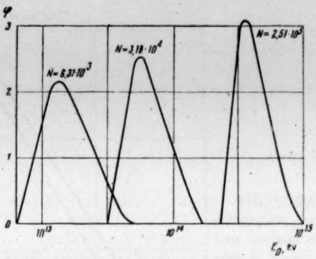

FIG. 3. Energy spectra of protons producing showers of a given size N at the observation level.

3. PROBABILITY DISTRIBUTION FUNCTION OF THE ENERGIES OF PRIMARY PROTONS PRODUCING SHOWERS OF A GIVEN SIZE AT THE OBSERVATION LEVEL

Let $\Psi(z\,|\,y)\,dz$ be the probability of a value z for a given y, and $Be^{-\gamma y}dy$ the energy spectrum of primary protons where $B = \text{const}$ and $\gamma = \text{const}$. Then, from Bayes' theorem,[7] the probability of y for a given z is

$$\varphi(y\,|\,z)\,dy = C^{-1}\Psi(z\,|\,y)\,Be^{-\gamma y}dy, \tag{7}$$

where the normalized constant C determines the total number of showers with a given value of z

$$C = \int_{y_{\min}}^{\infty} Be^{-\gamma y}\Psi(z\,|\,y)\,dy. \tag{8}$$

Figure 3 shows the functions $\varphi(y\,|\,z)$, i.e., the energy spectra of protons which, at the observation level, produce showers with a given number of particles N equal to 6.31×10^3, 3.16×10^4, and 2.51×10^5 respectively. The average values of the energy of protons producing showers with such a number of particles are equal to 1.67×10^{13}, 6.69×10^{13}, and 4.21×10^{14} ev respectively, i.e., the energy is less by a factor of 3.2, as compared to sea level.[1] Neglecting the fluctuations, the energies of protons producing showers of a given size at the Pamirs altitude and at sea level differ by a factor of 4.7, i.e., the factor is approximately 1.5 greater than in the former case. The factor $k = \overline{E}_0/N$ relating the number of particles with the average proton energy equals 2.65×10^9, 2.11×10^9, and 1.68×10^9 ev respectively. The double half-widths of the curves are such that showers with 6.31×10^3, 3.16×10^4, and 2.51×10^5 particles are produced with a sufficiently high probability by primary protons with energies differing by factors of 2.95, 2.43, and 2.05 respectively from the above-given values, i.e., approximately $1/2$ to $1/3$ of the same factors at sea level.[1]

N	Sea level			Pamirs		
	$6.3 \cdot 10^3$	$3.2 \cdot 10^4$	$2.5 \cdot 10^5$	$6.3 \cdot 10^3$	$3.2 \cdot 10^4$	$2.5 \cdot 10^5$
He^4	2.3	2.2	2	1.5	1.4	1.3
O^{16}	3.2	3	2.6	2	1.8	1.6

Under the assumptions made, it is possible to calculate the average energy of the primary nuclei with atomic weight A producing showers with a given number of particles N. The table shows the ratios of the average energies of He and O nuclei to the energy of protons which produce the same shower size N at sea level and at (640 g/cm^2) altitude.

4. SIZE SPECTRUM AND ALTITUDE DEPENDENCE OF THE SHOWERS

The number of showers with a given number of particles as determined by Eq. (8) can, as is well known, be approximately represented by a power law $C(z)\,dz \sim e^{-\kappa z}dz$, where $\kappa = \text{const}$. The number of showers with a size greater than a given one is given by

$$C(>z) = C(z)/\varkappa. \tag{9}$$

The value of κ in Eq. (9) is found from

$$\varkappa = -d\ln C(z)/dz. \tag{10}$$

On the other hand, knowing the mean shower size $\overline{N}$ produced by a primary proton of a given energy, we can determine the number of showers of a size that is, on the average, greater than a given one:

$$C(>z) = B\gamma^{-1}e^{-\gamma y}, \tag{11}$$

where $z = \ln \overline{N} = -1.28 + 1.43y - 0.015\,y^2$.

The size spectrum of the showers can also be calculated[8] for the case where the primary is a nucleus with an atomic weight A, if we accept the hypothesis that the nucleus in the collision with an air nucleus always disintegrates into A independent nucleons with energies E_0/A, where E_0 is the energy of the primary nucleus. Knowing the mean value of the number of particles $\overline{N}$ and the dispersion D of the distribution $\chi(N\,|\,E_0A^{-1})$ for the case where the primary particle is a proton, and using the central-limit theorem of probability theory,[7] we find that the number N_A of particles at the observation level produced by a primary particle with atomic weight A and energy E_0 is distributed according to the normal law with a mean value $\overline{N}_A = A\overline{N}$ and with a dispersion $D_A = AD$. Within the limits of the assumptions made, the size spectrum of showers for a primary nucleus is similarly calculated for the case where

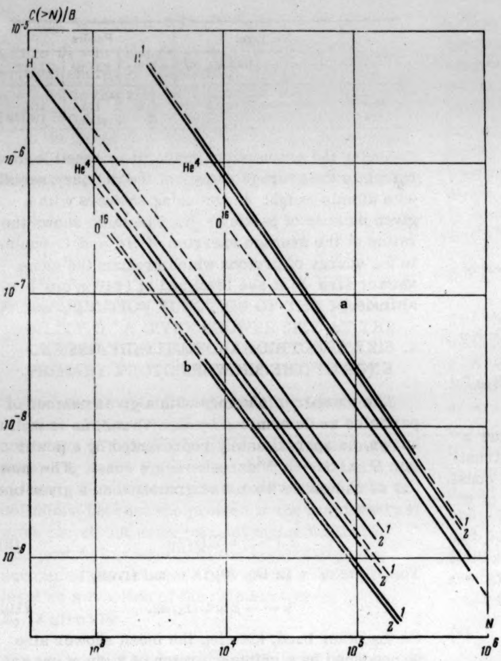

FIG. 4. Size spectra of showers (a – at the Pamirs altitude, b – at sea level) for various primary particles; 1 – taking fluctuations into account, 2 – neglecting fluctuations.

the primary particle is a proton. If the primary particle is a He nucleus, then A = 4, and the use of the central-limit theorem is not permissible. However, we are not interested in the exact shape of the function $\chi(N \mid E_0)$ but only in its integral given by Eq. (8). Therefore, small inaccuracies in the shape of the function $\chi(N \mid E_0)$ are irrelevant.

Figure 4 shows, both for sea level[1] and for the Pamirs altitude, the size spectrum of showers taking the fluctuations into account, and the average number of showers produced by primary protons, and He^4 and O^{16} nuclei. For the Pamirs altitude, the curves for primary He and O nuclei are identical whether fluctuations are considered or neglected. For primary protons at the Pamirs altitude, the curves differ by 3—5%. This difference is of the same order of magnitude as errors in the calculations. The value of the exponent κ increases from 1.45 to 1.50 with a change in the number of shower particles from 6.3×10^3 to 2.5×10^5. At sea level, the fluctuations[1] increase the number of showers of a given size by 50% for primary protons, by 16% for He nuclei, and by 5% for O nuclei. The number of showers at sea level[1] with $N > 10^4$ particles differs from that at the Pamirs altitude by factors of 11.5, 13.5, and 17 respectively for primary protons, He nuclei, and O nuclei. The altitude dependence of showers decreases by 10 to 15% with a variation of the number of particles in the showers from 10^4 to 10^5.

5. THE PRIMARY-PROTON SPECTRUM

If we compare the calculated number of showers produced by primary protons at the Pamirs altitude to the number of experimentally-observed showers,[9] we can determine the value of the constant B in Eq. (8). Knowing the value of B and γ, we can calculate the intensity of the primary protons. The primary-proton intensity calculated in such a way differs by only 5% from the proton intensity calculated by the same method from the data for sea level,[1] while it is less by a factor of approximately two than the intensity given by Greisen.[5] If, instead of the data of the Moscow group,[9] we use the experimental data for the size

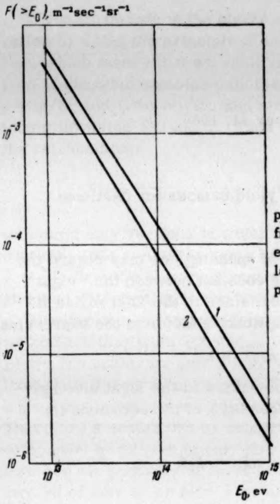

FIG. 5. Spectrum of primary protons; 1 – from the data of reference 5, 2 – as calculated in the present paper.

spectrum given in the review article of Greisen,[5] then the calculated intensity of the primary protons will be smaller yet. Figure 5 shows the intensities of primary protons as reported by Greisen and as calculated in the present paper.

6. DEPENDENCE OF SHOWER CHARACTERISTICS ON THE PROTON-ENERGY SPECTRUM EXPONENT γ

Calculations similar to those described above but for $\gamma = 1.8$ have also been carried out. For this case, in order to conserve the former value of the parameter $\alpha = 0.53$, we obtain a value of $\lambda = 117$ g/cm^2 from the relation $\lambda_0/\lambda = 1 - \alpha^{\gamma}$,[2,3] keeping the former value of $\lambda_0 = 80$ g/cm^2. The increase in γ leads to the increase in κ. The average value of κ increases from 1.47 to 1.55 at the Pamirs altitude and from 1.38 to 1.46 at sea level. With increasing γ, the role of fluctuations in the development of air showers also increases. For $\gamma = 1.8$, the difference between the number of showers calculated taking fluctuations into account and the average number of showers calculated for primary protons increases by 10% at sea level and by 6% at the Pamirs altitude, as compared to the difference for the value $\gamma = 1.7$. The altitude dependence of showers for $\gamma = 1.8$ is greater by approximately 10% than for $\gamma = 1.7$.

In conclusion, the author expresses his thanks to Prof. G. T. Zatsepin for constant help in the work. The author would also like to thank Prof. E. S. Kuznetsov, who kindly made the use of the electronic computer possible, and O. B. Moskalev for his help in programming the computer.

---

[1] L. G. Dedenko and G. T. Zatsepin, Proceedings of the Moscow International Conference on Cosmic Rays, 2, 222 (1960).

[2] G. T. Zatsepin, JETP 19, 1104 (1949), Soviet Phys. JETP.

[3] G. T. Zatsepin, Proceedings of the Moscow International Conference on Cosmic Rays, 2, 212 (1960).

[4] G. T. Zatsepin and L. I. Sarycheva, Doklady Akad. Nauk. SSSR 99, 951 (1954).

[5] K. Greisen, Progress in Cosmic Ray Physics (North-Holland Publishing Co., Amsterdam, 1956) vol. III.

[6] I. M. Sobol', Теория вероятностей и ее применения (Probability Theory and Its Application) 3, 205 (1958).

[7] B. V. Gnedenko, Курс теории вероятностей (A Course in Probability Theory), Gostekhizdat, 1950.

[8] B. Peters, Proceedings of the Moscow International Conference on Cosmic Rays, 3, (1960).

[9] Kulikov, Nesterova, Nikol'skii, Solov'eva, Khristiansen, and Chudakov, Proceedings of the Moscow International Conference on Cosmic Rays, 2, (1960).

Translated by H. Kasha
96

SOVIET PHYSICS JETP VOLUME 13, NUMBER 2 AUGUST, 1961

ON THE THEORY OF FERMION MASSES

Ya. B. ZEL'DOVICH

Submitted to JETP editor September 3, 1960; resubmitted November 11, 1960

J. Exptl. Theoret. Phys. (U.S.S.R.) 40, 637-640 (February, 1961)

It is shown that the four-fermion interaction to any order will not yield masses for particles that have no bare mass.

SEVERAL works have of late developed the point of view that the masses of particles result from their interactions with (or transformations into) other or similar particles (or fields).[1-3] The only example, however, of a definite prediction of a fermion mass is the two-component neutrino theory with an identically vanishing mass for any interaction.[4-6]

One may use the analogy with the neutrino theory to establish important restrictions on the kind of interaction which may lead to a finite particle mass. It turns out that a finite mass cannot be obtained from a theory with several different types of fermions, all with vanishing bare mass, if one uses the electromagnetic interaction and a four-fermion interaction of any kind (that is, S, V, T, A, or P, and no derivative interaction).

If some of the particles of a several-fermion theory have a finite bare mass (or a mass obtained from some other interaction), then those fermions whose bare mass vanishes can be given a finite mass by a four-fermion interaction involving those with mass. This is possible, however, only by violating the Gell-Mann—Feynman postulate,[7] which will lead to a polarization in decay differing from v/c.

Let us prove this assertion. To do this we first give a somewhat different formulation of the usual Dirac equation for a free particle possessing mass.

As is well known, a four-component wave function can be written in terms of two two-component spinors

$$\psi = \left|\begin{matrix}\varphi \\ \chi\end{matrix}\right|,$$

each of which (that is φ and $\dot{\chi}$) separately transforms by an irreducible representation of the proper Lorentz group. For vanishing mass the Dirac equation decomposes into two independent equations for φ and $\dot{\chi}$, or in other words describes separately "right" and "left" particles with mass zero and velocity equal to that of light, each of which has a fixed spin component equal to either $+\frac{1}{2}$ or $-\frac{1}{2}$ along the direction of motion.

In this manner of speaking one may regard the mass as a coupling constant between the "right" and "left" particles, since in the Lagrangian it appears as a multiplicative factor in the expression

$$m(\varphi\ddot{\chi} + \ddot{\chi}\varphi).$$

Similarly, the mass enters on the right side (giving rise to inhomogeneity) of the equations for φ and $\dot{\chi}$, namely

$$L_1\varphi = m\dot{\chi}, \qquad L_2\dot{\chi} = m\varphi,$$

where

$$L_{1,2} = i\partial/\partial t \pm \sum_{k=1,2,3} \sigma_k \partial/\partial x_k.$$

Thus, whereas in the case of vanishing mass we are dealing with independent "right" and "left" particles, a finite mass is a quantity which determines the probability for spontaneous transitions of a "right" into a "left" particle, and vice versa. This situation is reminiscent of the Pais-Piccioni scheme, in which the K^0 and $\overline{K}^0$ can be freely transformed into each other, so that the vacuum contains particles which are the linear combinations (superpositions) K_1^0 and K_2^0. In the same way particles with finite mass may be considered superpositions of right and left particles.*

In order for an interaction to lead to a particle mass, this interaction must give rise to mutual transformations of right and left particles. In other words, it must be possible with this interaction to construct Feynman diagrams with a single incoming line corresponding, for instance, to φ, and a single outgoing line corresponding to $\dot{\chi}$. Let us see whether it is possible to obtain such a result through the electromagnetic or four-fermion interaction.

---

*It should be emphasized that we are dealing with right and left particles which are not each other's antiparticles. On the contrary, we are assuming that there exist right and left particles all of whose charges (i.e., all superselection-rule quantum numbers) are the same, and such that their mutual transformation is not forbidden.

We shall introduce the electromagnetic interaction by using the principle of minimum interaction, which means that we shall assume that the free Lagrangian contains only terms of the form $\varphi^* \partial\varphi/\partial t$ and $\varphi^*\sigma_k \partial\varphi/\partial t$, and similar bilinear terms involving $\dot{\chi}^*$ and $\dot{\chi}$. Then by performing the replacements

$$\frac{\partial}{\partial t} \rightarrow ieA_4 + \frac{\partial}{\partial t}, \qquad \frac{\partial}{\partial x_k} \rightarrow ieA_k + \frac{\partial}{\partial x_k},$$

we obtain only vertices in which the incoming and outgoing lines are of the same kind ($\varphi \rightarrow \varphi$, $\dot{\chi} \rightarrow \dot{\chi}$); thus the electromagnetic interaction gives no contribution to the transformation $\varphi \rightarrow \dot{\chi}$.

Turning now to the four-fermion interaction, we remark that from φ^* and φ (as from $\dot{\chi}^*$ and $\dot{\chi}$) we can construct only a four-vector, whereas from the different spinors φ^* and $\dot{\chi}$ (or $\dot{\chi}^*$ and φ) we can construct a scalar and a tensor.* Therefore a scalar can be constructed of four two-component quantities in only five ways: three scalars are the products of pairs of four-vectors formed of four φ or four $\dot{\chi}$ or of two φ and two $\dot{\chi}$; one scalar is the product of two scalars formed of two φ and two $\dot{\chi}$; and finally one scalar is the product of two tensors (formed of two φ and two $\dot{\chi}$).

The four two-component spinors refer to different particles, but we shall not write out in detail the corresponding expressions. What is important is that in any of the versions the number of particles of each kind, that is right (undotted function) or left (dotted function), can change only by an even number, namely 0 or 2. This is obviously true to any order, no matter how many vertices we deal with. It is therefore impossible to connect any number of vertices so as to obtain a diagram in which the number of right particles changes by -1, while the number of left particles changes by $+1$. This proves the assertion. We note that this remains true when one introduces scalar form-factors depending on the (invariant) square of the momentum transfer.

We have dealt here with four-fermion expressions of the form $\psi^*\psi^*\psi\psi$, where ψ^* and ψ may refer to different kinds of right and left particles. This form corresponds to a vertex with two incoming particles and two outgoing ones; we shall call such a vertex a 2 : 2 vertex.

In addition to such vertices we must consider also those corresponding to expressions of the form $\psi^*\psi\psi\psi$ with three incoming and one outgoing particles (3 : 1 vertices), and $\psi^*\psi^*\psi^*\psi$ (1 : 3 vertices).

Since complex conjugation is equivalent to transforming from left to right particles, in 3 : 1 and 1 : 3 vertices the number of left and right particles changes by an odd number, in contradistinction from the rule we obtained for 2 : 2 vertices.

Consider a diagram with one incoming particle on the left and one outgoing one on the right, and any number of interior vertices. Any 1 : 3 vertex increases the total number of particles by two, while a 3 : 1 vertex decreases it by 2, and a 2 : 2 vertex leaves it invariant. Thus a diagram with one incoming and one outgoing line may contain any number of 2 : 2 vertices, but it is necessary that $n_{1:3} = n_{3:1}$. This means that the total number of 1 : 3 and 3 : 1 vertices, namely $n_{1:3} + n_{3:1}$, is even. Although each of these vertices changes the total number of right and left particles by an odd number, the diagram as a whole again changes the number of right and left particles by an even number, and the assertion remains valid.

In distinguishing between 1 : 3, 2 : 2, and 3 : 1 diagrams, we assume that we have decided beforehand as to what constitutes an "antiparticle" as opposed to a particle, and only then is a direction of propagation associated with each line of the diagram.

According to a remark due to B. L. Ioffe, a scalar interaction between fermions and mesons will also give no fermion mass, and this result is independent of the fermion mass. Indeed, vertices corresponding to such an interaction involve the transformation of a right fermion into a left one, or vice versa, with the simultaneous creation or annihilation of the meson. In a diagram containing a single incoming and single outgoing fermion line, the number of mesons created is equal to the number of mesons destroyed; thus the total number of meson vertices is even, and it follows thence that the total change of right or left particles is also even.

This theorem breaks down if a particular kind of meson has two different interactions (scalar and vector) with the fermions. We remark that with nonconservation of parity one need not distinguish between scalar and pseudoscalar, or vector and pseudovector.

The theorem also breaks down for three-meson vertices, in which one of the mesons is transformed into two.

If among our fermions there is at least one which has a bare mass m_0, then there exists a diagram involving this fermion in which there is

---

*We are considering only the proper Lorentz group, so that we need not differentiate between a scalar and a pseudoscalar or between a vector and a pseudovector, etc.

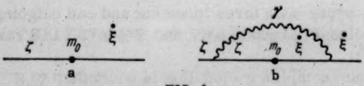

FIG. 1

an incoming right particle (ξ) and an outgoing left one ($\dot{\xi}$), as shown in Fig. 1a. The matrix element corresponding to this diagram is proportional to m_0. By combining this diagram with two electromagnetic diagrams, we obtain a correction to the mass of the particle, and at the same time we see that $\Delta m \sim m_0 e^2$ (see Fig. 1b).

By combining an m_0 diagram for one of the fermions with a four-fermion vertex, one can in principle obtain the transformation of a right particle into a left one for any pair of particles (with zero bare mass), so long as such a transformation is allowed by charge conservation. Then by perturbation theory the particle will end up with a mass $\mu \sim m_0 g^n$, where m_0 is the bare mass of the other particle, g is the four-fermion coupling constant, and n is the number of four-fermion vertices (see Fig. 2). Since g has the dimensions of m^{-2}, the form of this expression predetermines the power to which the cutoff momentum enters into μ.

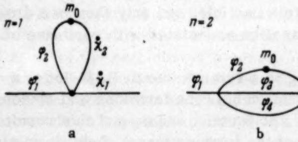

FIG. 2

Consider a given particle with wave function (φ, $\dot{\chi}$). In order that this particle have a finite mass as a result of the four-fermion interaction and the existence of some other particle with bare mass m_0, the original particle must enter into the four-fermion interaction in two ways, namely through φ and through $\dot{\chi}$. This represents a violation of the Gell-Mann—Feynman principle, which states that all particles enter into weak interactions through just a single two-component function. This violation will lead, obviously, to weak-decay production of such particles with longitudinal polarization different from v/c.

It has been remarked by L. B. Okun' that the assertion of the present article can also be proven in the more common language of four-component bispinors if one considers simultaneous γ_5-transformation of the bispinors of all particles in the Lagrangian. Any Lorentz invariant four-fermion interaction is automatically invariant under this transformation, even if any one of the fermions taken separately is not.

I take this opportunity to express my gratitude to L. D. Landau for his repeated insistence that I use two-component quantities, as well as to B. L. Ioffe, L. B. Okun', and I. Ya. Pomeranchuk for discussions.

---

[1] Dürr, Heisenberg, Mitter, Schlieder, Yamadsaki, Naturforsch. 14a, 441 (1959).

[2] Y. Nambu, Preprint.

[3] Ya. B. Zel'dovich, JETP 37, 1817 (1959), Soviet Phys. JETP 10, 1283 (1960).

[4] L. D. Landau, Nuclear Phys. 3, 127 (1957).

[5] A. Salam, Nuovo cimento 6, 299 (1957).

[6] T. D. Lee and C. N. Yang, Phys. Rev. 105, 1671 (1957).

[7] M. Gell-Mann and R. P. Feynman, Phys. Rev. 109, 193 (1959).

Translated by E. J. Saletan
97

SOVIET PHYSICS JETP VOLUME 13, NUMBER 2 AUGUST, 1961

THERMODYNAMICS OF ANISOTROPIC SUPERCONDUCTORS

V. L. POKROVSKII

Institute for Radiophysics and Electronics, Siberian Division of the Academy of Sciences of the U.S.S.R.

Submitted to JETP editor September 13, 1960

J. Exptl. Theoret. Phys. (U.S.S.R.) 40, 641-645 (February, 1961)

We have solved the Bogolyubov equation for the energy gap in a superconductor for the anisotropic case. We show that in the weak coupling approximation a change in temperature leads to a change in the magnitude of the gap by a factor which is independent of the direction. The general behavior of the change in the thermodynamic quantities is qualitatively the same as in the isotropic case. The relative jump in the specific heat turns out to be larger than 1.4. An inequality of the same kind is also obtained for the critical magnetic field near the absolute zero.

THE theory of superconductivity was developed for an isotropic model.[1,2] The isotropic theory agrees qualitatively very well with experiment, but it does not agree completely quantitatively. From this theory it follows, for instance, that the relative jump in the specific heat $\Delta C/C_n$ at the transition point should be equal to 1.4 for all superconductors, while this quantity varies in practice from metal to metal. Furthermore, the isotropic theory gives for the low-temperature behavior of the relative critical field the relation

$$H_{cr}(T)/H_{cr}(0) = 1 - \chi (T/T_{cr})^2,$$

where $\chi = 1.06$. Experimentally, χ turns also out to be different for different superconductors.

The temperature dependence of the specific heat differs rather much from that predicted by theory. Moreover, experimental results[3,4] show that the energy gap possesses a well defined anisotropy in some superconductors. It is thus of interest to develop a theory for anisotropic superconductors.

Bogolyubov et al.[2] obtained for the energy gap $\Delta(\mathbf{p})$ at absolute zero an equation which is also suitable for the anisotropic case

$$\Delta(\mathbf{p}) = g \int U(\mathbf{p}, \mathbf{p}') \frac{\Delta(\mathbf{p}')}{\varepsilon(\mathbf{p}')} d^3p'. \qquad (1)$$

Here g is the dimensionless coupling constant ($g \ll 1$), $U(\mathbf{p}, \mathbf{p}')$ the interaction potential of two pairs of electrons with momenta and spins in opposite directions, $\epsilon(\mathbf{p}) = \sqrt{\xi^2(\mathbf{p}) + \Delta^2(\mathbf{p})}$, where $\xi(\mathbf{p}) = v_F(p - p_F)$, while v_F and p_F are the velocity and momentum on the Fermi surface.

The integration in (1) is performed in such a way that the values of $\xi' = \xi(\mathbf{p}')$ lie between $\pm\omega$ where ω is the Debye frequency. We are interested in values of p and p' such that $|\xi|$, $|\xi'| \lesssim \omega$. In that region $U(\mathbf{p}, \mathbf{p}')$, $\Delta(\mathbf{p})$, and $\Delta(\mathbf{p}')$ may be assumed to depend only on the directions $\mathbf{n} = \mathbf{p}/p$ and $\mathbf{n}' = \mathbf{p}'/p'$. Taking this into account and integrating over ξ in (1) we find

$$\Delta(\mathbf{n}) = g \int U(\mathbf{n}, \mathbf{n}') \Delta(\mathbf{n}') \ln \frac{2\omega}{\Delta(\mathbf{n}')} \frac{d\sigma'}{v_F}, \qquad (2)$$

where $d\sigma'$ is an elementary area on the Fermi surface.

Taking into account that g is small, we write the solution of Eq. (2) in the form

$$\Delta(\mathbf{n}) = 2\omega\varphi(\mathbf{n}) e^{-\Lambda/g}, \qquad (3)$$

where $\varphi(\mathbf{n})$ is a dimensionless function, and Λ a constant quantity of the order of magnitude of unity. Substituting (3) into (2) we get in the first nonvanishing approximation for $\varphi(\mathbf{n})$ the equation

$$\varphi(\mathbf{n}) = \Lambda \int U(\mathbf{n}, \mathbf{n}') \varphi(\mathbf{n}') \frac{d\sigma'}{v_F}. \qquad (4)$$

Equation (4) is a homogeneous Fredholm type integral equation. One can easily symmetrize the kernel of Eq. (4). The quantity Λ is thus an eigenvalue of Eq. (4) and $\varphi(\mathbf{n})$ an eigenfunction of this equation.

We shall show that Λ is the lowest eigenvalue. Indeed, the energy of the superconducting groundstate E_s is a functional of $\Delta^2(\mathbf{n})$ and the energy of the normal state E_n is obtained from E_s by putting $\Delta(\mathbf{n}) = 0$. The difference $E_n - E_s$ is thus in first approximation a homogeneous quadratic functional of $\Delta^2(\mathbf{n})$ and is according to (3) proportional to $\exp(-2\Lambda/g)$. E_s will thus be a minimum when Λ is a minimum. We note that by virtue of a well-known theorem $\Delta(\mathbf{n})$ has no zeroes on the Fermi surface.

We denote by $\psi(\mathbf{n})$ the normalized solution of Eq. (4) which corresponds to the lowest eigenvalue. In that case $\varphi(\mathbf{n}) = Q\psi(\mathbf{n})$. To find the constant Q we must solve the next approximation. Putting $\varphi(\mathbf{n}) = Q\psi(\mathbf{n}) + \varphi_1(\mathbf{n})$ we get for $\varphi_1(\mathbf{n})$ the equation

$$\varphi_1(\mathbf{n}) = \Lambda\int U(\mathbf{n}, \mathbf{n}')\varphi_1(\mathbf{n}')\frac{d\sigma'}{v_F'} - gQ\int U(\mathbf{n}, \mathbf{n}')\psi(\mathbf{n}')\ln(Q\psi(\mathbf{n}'))\frac{d\sigma'}{v_F'}. \tag{5}$$

This is an inhomogeneous Fredholm type equation and it is known that the corresponding homogeneous equation has a solution.

The condition that (5) have a solution gives, if one takes (4) into account, an equation for Q:

$$\int\psi^2(\mathbf{n})\ln(Q\psi(\mathbf{n}))\frac{d\sigma}{v_F} = 0. \tag{6}$$

If we write the normalization condition for $\psi(\mathbf{n})$ in the form

$$\int\psi^2(\mathbf{n})\frac{d\sigma}{p_0 v_F} = 1, \tag{7}$$

where p_0 is a quantity of the order of magnitude of the momentum on the Fermi surface, we get from (6)

$$Q = \exp\left\{-\int\psi^2(\mathbf{n})\ln\psi(\mathbf{n})\frac{d\sigma}{p_0 v_F}\right\}. \tag{8}$$

We note that Eq. (8) and also the further calculations remain valid also when ω is assumed to be a function of the direction $\omega(\mathbf{n})$, so long as we substitute in (3) instead of ω a constant quantity $\tilde{\omega}$ such that

$$\ln\tilde{\omega} = \int\psi^2(\mathbf{n})\ln\omega(\mathbf{n})\frac{d\sigma}{p_0 v_F}. \tag{9}$$

In the following we shall thus assume, without sacrificing generality, that ω is constant.

We now turn to the case of finite temperatures. In that case we must solve the equation

$$\Delta(\mathbf{p}) = g\int U(\mathbf{p}, \mathbf{p}')\frac{\Delta(\mathbf{p}')}{\varepsilon(\mathbf{p}')}[1 - 2f(\beta\varepsilon(\mathbf{p}'))]\,d^3p', \tag{10}$$

where $f(x) = (e^x + 1)^{-1}$. As in the previous case, Eq. (9) leads to an integral equation on the Fermi surface:

$$\Delta(\mathbf{n}) = g\int U(\mathbf{n}, \mathbf{n}')\left[\ln\frac{2\omega}{\Delta(\mathbf{n}')} - F(\beta\Delta(\mathbf{n}'))\right]\frac{d\sigma'}{v_F'}, \tag{11}$$

where

$$F(x) = \int_{-\infty}^{\infty} dy\,(y^2+1)^{-1/2} f(x\sqrt{y^2+1}). \tag{12}$$

The function $F(x)$ was studied in great detail in the survey of Abrikosov and Khalatnikov.[5] As $x \to \infty$ it tends to zero as e^{-x}, and as $x \to 0$ it behaves asymptotically as

$$F(x) = -\ln(\gamma x/\pi) + \lambda x^2, \tag{13}$$

where $\ln\gamma$ is Euler's constant and $\lambda = (7/8\pi^2)\zeta(3)$.

We look again for a solution of Eq. (11) in the form given by (3). In zeroth approximation we get again (4) so that $\varphi(\mathbf{n}) = Q\psi(\mathbf{n})$, as before, but Q is now a function of the temperature. We can thus make the following statement: when the temperature is changed the magnitude of the energy gap in different directions will change in the same ratio. This conclusion can, apparently, be verified experimentally. We get for the function $Q(T)$ the equation

$$\ln\frac{Q(T)}{Q(0)} + \int\psi^2(\mathbf{n})F(\beta Q(T)\psi(\mathbf{n}))\frac{d\sigma}{p_0 v_F} = 0. \tag{14}$$

It is clear from Eq. (14) that $Q(T) < Q(0)$.

Equation (14) becomes unsuitable near the transition temperature where $Q(T)$ is small, because F diverges logarithmically. Using the asymptotic expression (13) for this case we get from (10)

$$\Delta(\mathbf{n}) = g\int U(\mathbf{n}, \mathbf{n}')\Delta(\mathbf{n}')\left[\ln 2\omega\beta\frac{\gamma}{\pi} - \lambda(\beta\Delta(\mathbf{n}'))^2\right]\frac{d\sigma'}{v_F'}, \tag{15}$$

from which we get in zeroth approximation in $(T - T_{cr})/T_{cr}$ a solution in the same form as (3), while the transition temperature is determined by the equation

$$T_{cr} = (\gamma/\pi)\,2\omega e^{-\Lambda/g}. \tag{16}$$

Near the transition point the equation for $Q(T)$ is of the form

$$Q^2 = A\frac{T_{cr} - T}{T_{cr}}, \qquad A = \left[\lambda\left(\frac{\pi}{\gamma}\right)^2\int\psi^4(\mathbf{n})\frac{d\sigma}{p_0 v_F}\right]^{-1}. \tag{17}$$

Comparing the results obtained here with the solution of the equation for the gap in the isotropic case, we see that the picture of the behavior of the gap as a function of the temperature is not changed qualitatively.

We consider now how the anisotropy of the superconductor affects its specific heat $C_s(T)$. Using the well-known formula for the entropy

$$S(T) = -2\sum_{\mathbf{p}}\{f(\beta\varepsilon)\ln f(\beta\varepsilon) + [1 - f(\beta\varepsilon)]\ln(1 - f(\beta\varepsilon))\} \tag{18}$$

and differentiating it with respect to the temperature, we get after some simple transformations the equation

$$C_s(T) = -\beta \frac{d}{d\beta} \frac{2}{(2\pi)^3} \int \Delta G(\beta\Delta) \frac{d\sigma}{v_F},$$

$$G(x) = 2x \int_0^\infty \operatorname{ch} 2\varphi \, f(x \operatorname{ch}\varphi) d\varphi. \qquad (19)^*$$

The asymptotic behavior of G(x) was also given in reference 5:

$$G(x) = \pi^2/3x - x/2 + 7\zeta(3)\, x^3/16\pi^2, \qquad x \to 0,$$

$$G(x) = \sqrt{2\pi x} e^{-x}, \qquad x \to \infty. \qquad (20)$$

Near the transition point we get

$$C_s(T) = \frac{2T_{\mathrm{cr}}}{(2\pi)^3} \int \frac{d\sigma}{v_F} \left(\frac{\pi^2}{3} + \frac{\pi^2 A}{2\gamma^2} \psi^2 \right), \qquad (21)$$

where A is defined by (17). The value of the specific heat of the normal phase C_n at the transition point is obtained from (21) by setting A equal to zero. We get thus for the jump in the specific heat

$$\Delta C / C_n(T_{\mathrm{cr}}) = 3A/2\gamma^2. \qquad (22)$$

(We chose p_0 by putting $\int d\sigma/p_0 v_F = 1$.)

We compare now the value of A determined by (17) with the corresponding magnitude of A_{is} in the isotropic model

$$A_{\mathrm{is}} / A = \int d\sigma \psi^4(\mathbf{n}) / p_0 v_F. \qquad (23)$$

From the normalization condition (7) follows that the integral on the right hand side of Eq. (23) is larger than unity as long as $\psi(\mathbf{n}) \neq$ const., and thus $A < A_{\mathrm{is}}$. The isotropic model gives thus too large an estimate for the ratio $\Delta C/C_n(T_{\mathrm{cr}})$.

We must now turn our attention to the discrepancy of this theoretical conclusion with experimental data[6-8] according to which for nearly all known cases $A > A_{\mathrm{is}}$ (apart from Cd, Zn, and Tl). A possible cause of this discrepancy is that the interaction is in fact not a weak one and that there occurs experimentally a stronger singularity than a finite jump.†

We consider now the behavior of the specific heat at low temperatures. Using the asymptotic behavior of G(x) as $x \to \infty$ we get from (19)

$$C_s(T) = \sigma\beta^{3/2}\Delta_{min}^{1/2} \exp\{-\beta\Delta_{min}(0)\}, \qquad (24)$$

where σ is a dimensionless constant of order of magnitude unity. We can use (3) and (16) to rewrite Eq. (24) as follows:

$$C_s(T) = \sigma\beta^{3/2} \sqrt{\Delta_{min}} \exp\{-Q(0)\psi_{min}\pi T_{\mathrm{cr}}/\gamma T\}. \qquad (25)$$

From Eq. (8) the inequality $Q(0) < 1/\psi_{\min}$ follows. The specific heat of an anisotropic superconductor is thus as function of the reduced temperature exponentially larger than the value which is predicted by the isotropic model. This result obtained already by Abrikosov and Khalatnikov[5] is well substantiated by experimental data.

In the intermediate temperature range the deviation of the specific heat from the curve obtained using the isotropic model must be large according to (19). Experimentally this deviation reaches, indeed, 30—40% (for instance,[7] for Zn and Al at $T \sim \frac{1}{2} T_{\mathrm{cr}}$).

To find the critical magnetic field we use the appropriate expression from the Bardeen-Cooper-Schrieffer (BCS) theory [see, for instance, reference 5, Eq. (3.37)] but we must replace the quantity $\nu = p_0^2/\pi^2 v_F$ in the anisotropic case by an integral operator on the Fermi surface:

$$\frac{H_{\mathrm{cr}}^2}{8\pi} = \frac{1}{2(2\pi)^3} \int \frac{d\sigma}{v_F} \Delta^2(\mathbf{n}) + \frac{T}{(2\pi)^3} \int \left[\Delta G(\beta\Delta) - \frac{\pi^2}{3} T \right] \frac{d\sigma}{v_F}. \qquad (26)$$

Using the solution of (3) for which we found for $\Delta(\mathbf{n})$ and the normalization (7) we get from (24)

$$\frac{H_{\mathrm{cr}}^2}{8\pi} = \frac{1}{2(2\pi)^3} p_0 \left(\frac{\pi}{\gamma} T_{\mathrm{cr}} \right)^2 Q^2(T) + \frac{T}{(2\pi)^3} \int \left[\Delta G(\beta\Delta) - \frac{\pi^2}{3} T \right] \frac{d\sigma}{v_F}. \qquad (27)$$

Near the absolute zero

$$\frac{H_{\mathrm{cr}}^2}{8\pi} = \frac{1}{16\pi^3} p_0 \left(\frac{\pi}{\gamma} T_{\mathrm{cr}} \right)^2 Q^2(0) - \frac{p_0 T^2}{24\pi} = \frac{H_{\mathrm{cr}}^2(0)}{8\pi} \left(1 - 2\chi \frac{T^2}{T_{\mathrm{cr}}^2} \right). \qquad (28)$$

$$\chi = \gamma^2/3Q(0). \qquad (29)$$

One sees easily from Eq. (8) that for any $\psi(\mathbf{n})$ different from unity $Q(0) < 1$ and we have thus from (29)

$$\chi > \chi_{\mathrm{is}} = 1.06. \qquad (30)$$

The data on the measurements of the critical magnetic field which are given in Shoenberg's monograph[9] are in contradiction to this result (except Sn where $\chi = 1.07$). The fact that for such anisotropic superconductors as Zn and Al the quantity χ turns out to be very nearly equal to unity seems to be especially surprising. We must note that in fact there are no measurements in the low-temperature region and the values of χ mentioned a moment ago are extrapolations, the correctness of which can, apparently, not be assumed to be established. All the same, the reasons for the discrepancy between the theoretical conclusions and the experimental data are not clear to the present author. It is, apparently, necessary to elucidate first of all how an increase of the interaction constant g would influence the results. An analysis of this problem will be the subject of a subsequent communication.

---

*ch = cosh.

†Note added in proof (February 8, 1961). According to an estimate by A. A. Abrikosov and L. P. Gor'kov (private communication) a deviation of the specific heat from its normal behavior (a finite jump) can only be manifest in a very narrow temperature range near the transition point, which is up to the present inaccessible experimentally.

---

[1] Bardeen, Cooper, and Schrieffer, Phys. Rev. 108, 1175 (1957).

[2] Bogolyubov, Tolmachev, and Shirkov, Новый метод в теории сверхпроводимости (A new Method in the Theory of Superconductivity) Acad. Sci. Press 1958, Fortschr. Phys. 6, 605 (1958).

[3] Bezuglyĭ, Galkin, and Korolyuk, JETP 39, 7 (1960), Soviet Phys. JETP 12, 4 (1961).

[4] N. V. Zavaritskii, JETP 37, 1506 (1959), Soviet Phys. JETP 10, 1069 (1960).

[5] A. A. Abrikosov and I. M. Khalatnikov, Usp. Fiz. Nauk 65, 551 (1958), Adv. in Phys. 8, 45 (1959).

[6] Brown, Zemansky, and Boorse, Phys. Rev. 92, 52 (1953).

[7] N. V. Zavaritskii, JETP 34, 1116 (1958), Soviet Phys. JETP 7, 773 (1958).

[8] H. A. Boorse, Phys. Rev. Letters 2, 391 (1959).

[9] D. Shoenberg, Superconductivity, Cambridge University Press, 1952.

Translated by D. ter Harr
98

SOVIET PHYSICS JETP VOLUME 13, NUMBER 2 AUGUST, 1961

VORTEX LINES IN AN IMPERFECT BOSE GAS

L. P. PITAEVSKII

Institute of Earth Magnetism, Ionosphere and Radio Wave Propagation,
Academy of Sciences, U.S.S.R.

Submitted to JETP editor September 14, 1960

J. Exptl. Theoret. Phys. (U.S.S.R.) **40**, 646-651 (February, 1961)

It is shown that the vortex lines possessing a thickness which is inversely proportional to the square root of the gas density and of the intensity of the interaction may exist in Bose gases with weak repulsion between the atoms. The energy of a vortex line is computed. It is also shown that in the presence of a vortex line a branch appears in the energy spectrum of the gas which corresponds to oscillations of the vortex.

1. INTRODUCTION

As is known, according to Onsager[1] and Feynman,[2] vortex lines can exist in a superfluid, i.e., certain special lines, around which the superfluid part of the liquid rotates with a velocity

$$v = s\frac{\hbar}{mr}, \tag{1}$$

where m is the mass of the atom of the liquid, r is the distance to the special line, which is known as a vortex axis, and s is an integer. A certain energy is associated with each vortex line and can be computed in general form with logarithmic accuracy. To be precise, the energy per unit length of line is equal (here and in what follows we speak only about conditions at absolute zero of temperature)

$$E = s^2\frac{\pi\hbar^2 n}{m}\ln\frac{R}{r_0}, \tag{2}$$

where n is the number of atoms of liquid per unit volume, R is the characteristic dimension of the vessel, r_0 is a quantity which has the meaning of the length of the vortex axis (it is assumed that $R \gg r_0$). In the case of real helium, r_0 has the order of interatomic distances. It is seen from (2) that the vortex lines with $s > 1$ are energetically unfavorable, inasmuch as two lines with $s = 1$ have less energy than a single line with $s > 1$. Therefore, only lines with $s = 1$ can really exist. We shall consider only such in what follows.

Vortex lines are capable of performing vibrations. In this case, when the wavelength of such vibrations is much greater than r_0, these vibrations differ in no way from the vibrations of vortices in an ordinary ideal liquid, and have the dispersion law (see references 3 — 5)

$$\omega = \frac{\hbar k^2}{2m}\ln\frac{1}{kr_0} \qquad (kr_0 \ll 1) \tag{3}$$

(ω is the frequency, k is the wave vector of the vibration). Thus the existence of vortex lines in a liquid leads to the appearance of a new "one-dimensional" branch of elementary excitations.

The existence of vortex lines in rotating helium II was shown experimentally by Hall and Vinen, and cannot be doubted today. Nevertheless, it should be kept in mind that the vortices were predicted by Onsager and Feynman on the basis of semi-qualitative considerations, inasmuch as the wave function of the liquid employed by Feynman cannot be obtained from general principles. Therefore there is definite interest in investigating vortex lines on a simple model in which calculations can be carried through to the end. Such a model is the imperfect Bose gas with weak repulsion between atoms, which has been considered in detail by Bogolyubov.[6] The purpose of the present research is the investigation of vortex lines in such a gas. The method which we shall use is a generalization of the method of Bogolyubov to a spatially inhomogeneous state.

2. THE VORTEX LINE IN AN IMPERFECT BOSE GAS

We shall consider a Bose gas with weak pair repulsions between atoms. The Hamiltonian of such a system in the second quantization representation has the form

$$\hat{H} = \int\left\{-\frac{\hbar^2}{2m}\psi^+\Delta\psi + \frac{1}{2}\int U(|\mathbf{r}-\mathbf{r}_1|)\,\psi^+\psi_1^+\psi_1\psi\,d\tau_1\right\}d\tau. \tag{4}$$

We shall assume that the potential is short range, and that the gas is sufficiently rarefied, i.e., that the range of the potential is much less than the distance between particles. In this case, we can remove the ψ operator from under the integral sign over $d\tau_1$ and obtain*

$$\hat{H} = \int\left\{-\frac{\hbar^2}{2m}\psi^+\Delta\psi + \frac{1}{2}g\psi^+\psi^+\psi\psi\right\}d\tau,$$
$$g = \int U(r)\,d\tau. \tag{5}$$

The Hamiltonian (5) corresponds to the equation of motion for the Heisenberg operator ψ

$$i\hbar\frac{\partial\psi}{\partial t} = -\frac{\hbar^2}{2m}\Delta\psi + g\psi^+\psi\psi. \tag{6}$$

Just as was done by Bogolyubov,[6] we divide the operator into two parts:

$$\psi = a_0 + \vartheta, \qquad \vartheta \ll a_0, \tag{7}$$

where a_0 is a number, and ϑ is a small operator correction. However, inasmuch as the system is no longer homogeneous in space in the presence of a vortex, we shall assume that a_0 is not a constant, but is a certain function of the coordinates.†

Substituting (7) in (6), and combining terms of zero order, we get

$$i\hbar\frac{\partial a_0}{\partial t} = -\frac{\hbar^2}{2m}\Delta a_0 + g\,|a_0|^2 a_0. \tag{8}$$

Assuming that a_0 depends on time according to the law $e^{-iE_0t/\hbar}$, we get

$$-\frac{\hbar^2}{2m}\Delta a_0 - E_0 a_0 + g\,|a_0|^2 a_0 = 0. \tag{9}$$

An equation of such a form has already been considered by Ginzburg and the author[9] in connection with the phenomenological theory of superfluidity close to the λ point. (Of course, the coefficients of the equation there have an entirely different meaning.)

The vortex lines correspond to the solution of (9) possessing a symmetry relative to some axis. Transforming to cylindrical coordinates r, φ, z, and setting

$$a_0 = e^{i\varphi}F(r).$$

we obtain the following equation for F:

$$-\frac{\hbar^2}{2m}\frac{1}{r}\frac{d}{dr}r\frac{dF}{dr} + \frac{\hbar^2}{2mr^2}F - E_0F + gF^3 = 0. \tag{10}$$

As was shown in reference 9, Eq. (10) has a solution which vanishes as $r \to 0$, and which approaches a certain constant $\sqrt{n_0}$ as $r \to \infty$; n_0 obviously has the meaning of density of particles in the condensed state and at an infinite distance from the line; with accuracy up to terms $\sim g^{3/2}$, it is identical with the total density of the gas. It follows from (10) that the constant E_0 is related to n_0 by the formula

$$E_0 = gn_0. \tag{11}$$

Taking this into account, we find that a_0 can be written in the form

$$a_0 = \sqrt{n_0}\exp i(\varphi - gn_0t/\hbar)\,\psi_0(r/r_0), \tag{12}$$
$$r_0 = \hbar/\sqrt{2mgn_0}. \tag{13}$$

$\psi_0(\xi)$ is a real function satisfying the equation

$$\frac{1}{\xi}\frac{d}{d\xi}\xi\frac{d\psi_0}{d\xi} + \left(1 - \frac{1}{\xi^2}\right)\psi_0 - \psi_0^3 = 0,$$
$$\psi_0(0) = 0, \quad \psi_0(\infty) = 1. \tag{14}$$

The graph of the function ψ_0 was given earlier by Ginzburg and the author.[9] For $\xi \to 0$, we have $\psi_0 \sim \xi$. For large $\xi \gg 1$,

$$\psi_0(\xi) \approx 1 - {}^1/_2\xi^2. \tag{15}$$

Equation (12) describes the vortex line with s = 1.

The quantity r_0 obviously has the meaning of the length of the vortex line. It is seen from (12) that the mean velocity of particles around the line is equal to $\hbar/mr$, as it ought to be.

As was shown in reference 6, the smallness of the amplitude of scattering of particles $mg/4\pi\hbar^2$, in comparison with the mean distance between particles, serves as the condition for applicability of the approximation (7):

$$mg/\hbar^2 \ll n_0^{-1/3} \approx n^{-1/3}. \tag{16}$$

n is the number density of the particles. Upon satisfaction of the conditions (16),

$$r_0 \gg n^{-1/3}. \tag{17}$$

Thus the condition for applicability of these formulas reduces to the requirement that the length of the vortex be large in comparison with the interatomic distances. This means that in the rarefied gas the vortex line is a macroscopic formation. The same condition is also necessary for applicability of the equations previously introduced.[9] However, in this case, this condition was guaranteed in reference 9 by the closeness to the λ point, while in our case it was guaranteed by the rarefied character of the gas.

The resultant formulas make it possible to compute the energy of the vortex line with nonlogarithmic accuracy. For this purpose it is necessary to substitute a_0 from (12) in (5) in place of ψ and integrate over the volume. In this case, the term proportional to the volume gives simply the energy of the homogeneous gas, while the term which depends logarithmically on the volume is the energy of the vortex. Numerical integration, results of which are taken from the work of Ginzburg and the author,[9] gives the following expression for the unit length of line located in the center of a cylindrical vessel of radius R:

---

*It is actually impossible to use Eq. (5) directly in calculations to higher orders of g. This is connected with the necessity of carrying out a renormalization of the scattering amplitude of particles (see reference 7). However, we shall not calculate terms of higher order.

†Inhomogeneous ground states of a Bose system were investigated by Gross[8] without connection to the problem of vortex lines.

$$E = (\pi\hbar^2 n_0 / m)\ln(1.46R/r_0). \tag{18}$$

3. VIBRATIONS OF THE VORTEX LINE

In the present section we shall show that there is actually a branch in the energy spectrum of the Bose gas in the presence of a vortex line with the dispersion law (3). To find the energy spectrum of a weakly perturbed state, it is necessary to substitute ψ in (6) with accuracy up to terms $\sim \vartheta$. We have

$$i\hbar\frac{\partial\vartheta}{\partial t} = -\frac{\hbar^2}{2m}\Delta\vartheta + 2g|a_0|^2\vartheta + a_0^2\vartheta^+. \tag{19}$$

We write ϑ in the form

$$\vartheta = e^{i(\varphi - E_0 t/\hbar)}\sum_{l,k} b_l(k, r)\, e^{i(kz + l\varphi)} \quad (l = 0, \pm 1, \pm 2, \ldots).$$

Further, substituting in (19) and taking (12) into account, we obtain a set of linear equations for $b_l(k)$ and $b^*_{-l}(-k)$:

$$i\hbar\frac{\partial b_l(k)}{\partial t} = -\frac{\hbar^2}{2m}\left[\frac{1}{r}\frac{\partial}{\partial r}r\frac{\partial}{\partial r} - \frac{(l+1)^2}{r^2} - k^2\right]b_l(k) + gn_0(2\psi_0^2 - 1)\,b_l(k) + gn_0\psi_0^2 b^*_{-l}(-k),$$

$$-i\hbar\frac{\partial b^*_{-l}(-k)}{\partial t} = -\frac{\hbar^2}{2m}\left[\frac{1}{r}\frac{\partial}{\partial r}r\frac{\partial}{\partial r} - \frac{(l-1)^2}{r^2} - k^2\right]b^*_{-l}(-k) + gn_0(2\psi_0^2 - 1)\,b^*_{-l}(-k) + gn_0\psi_0^2 b_l(k). \tag{20}$$

As is known, the energy levels of each linear quantum-mechanical system are determined by the characteristic frequencies of the corresponding classical problem. Therefore, in finding the energy spectrum, it suffices for us to find the characteristic frequencies of the system (20), assuming that $b_l(k)$ and $b^*_{-l}(-k)$ are simply certain classical functions of the coordinates. Among the solutions of the system (20) there are functions which decay exponentially as $r \to \infty$, and functions which oscillate as $r \to \infty$. The latter clearly describe phonons which are scattered by the vortex. The first correspond to the excited states of the vortex line itself.

A complete investigation of the characteristic values of the system (20) is very complicated, and there is scarcely any direct relation to the properties of real vortex lines in helium II. Actually, the "macroscopic" vortex in the gas probably has a much higher degree of freedom and energy levels than the vortex in helium having an atomic thickness. We therefore limit ourselves only to showing that among the solutions of (20) there are actually long wavelength vibrations with the dispersion law (3).

First of all we must determine precisely how the values of l correspond to the vibrations (3). For this purpose we note that as $k \to 0$ these vibrations simply transform into a displacement of the vortex as a whole. In this case a_0 is changed evidently by the value

$$\vartheta_0 = \delta\mathbf{r}\nabla a_0 = \delta r\left[\cos(\varphi - \varphi_0)\frac{\partial a_0}{\partial r} - \frac{1}{r}\sin(\varphi - \varphi_0)\frac{\partial a_0}{\partial\varphi}\right], \tag{21}$$

where $\delta\mathbf{r} = \delta\mathbf{r}(\delta\mathbf{r}, \varphi_0)$ = displacement vector. Therefore our equations should admit a solution of the form (21) for $k = 0$.

Equation (21) contains terms $\sim e^{i\varphi}e^{\pm i\varphi}$, i.e., terms with $l = \pm 1$. Thus the vibrations of interest to us are described by Eqs. (20) with $l = \pm 1$. We write down equations with $l = -1$, assuming that b_{-1}, $b_1^* \sim e^{-i\omega t}$, and transform to dimensionless variables. We obtain

$$\left(\frac{1}{\xi}\frac{d}{d\xi}\xi\frac{d}{d\xi} - \frac{4}{\xi^2} - \varkappa^2\right)f + (2\psi_0^2 - 1)f + \psi_0^2 f_1 = -\varepsilon f,$$

$$\left(\frac{1}{\xi}\frac{d}{d\xi}\xi\frac{d}{d\xi} - \varkappa^2\right)f_1 + (2\psi_0^2 - 1)f_1 + \psi_0^2 f = \varepsilon f_1. \tag{22}$$

Here

$$\xi = r/r_0, \quad \varkappa = kr_0, \quad \varepsilon = \hbar\omega/E_0, \quad b_1^*(k) = e^{-i\omega t}\sqrt{n_0}f,$$
$$b_{-1}(-k) = e^{-i\omega t}\sqrt{n_0}f_1.$$

It is quite simple to establish the fact that, as it should follow from (21), Eqs. (22) satisfy the regular functions

$$f^0 = (d\psi_0/d\xi - \psi_0/\xi), \qquad f_1^0 = (d\psi_0/d\xi + \psi_0/\xi) \tag{23}$$

for $\kappa = 0$ and $\epsilon = 0$ at $\xi = 0$.

We transform to a solution (22) for $\kappa \ll 1$. We initially consider distances $\xi \ll 1/\kappa$. In this case, we can neglect κ^2 in the equations and look for a solution in the form

$$f = f^0 + \varepsilon f', \quad f_1 = f_1^0 + \varepsilon f_1, \tag{24}$$

where on the right hand side of the equations, we can substitute f^0 and f_1^0 for f and f_1:

$$\left(\frac{1}{\xi}\frac{d}{d\xi}\xi\frac{d}{d\xi} - \frac{4}{\xi^2}\right)f' + (2\psi_0^2 - 1)f' + \psi_0^2 f_1' = -f^0,$$

$$\frac{1}{\xi}\frac{d}{d\xi}\xi\frac{d}{d\xi}f_1' + (2\psi_0^2 - 1)f_1' + \psi_0^2 f' = f_1^0. \tag{25}$$

We directly verify that the system (25) has a regular solution at zero of the form

$$f' = \frac{1}{2}\xi\psi_0, \quad f_1' = -\frac{1}{2}\xi\psi_0. \tag{26}$$

We shall not set forth the construction details of this solution. We only note that it is connected with the existence in Eq. (8) of solutions describing the motion of the gas as a whole together with the vortex filament, i.e., in the final analysis with Galilean invariance of the initial equations.

We now consider the region of separation $\xi \gg 1$. It is seen from (23) that at such distances

$$f - f_1 \ll f + f_1. \tag{27}$$

This inequality has a simple physical meaning. It is easy to see that the quantity $f + f_1$ is proportional to the perturbation of the density around the vortex, while $f - f_1$ is the perturbation of the velocity potential. The second perturbations fall off more rapidly than the first. We subtract the second equation of (22) from the first and everywhere write

$$f + f_1 = 0, \quad \psi_0^2 = 1 - 1/\xi^2.$$

As a result we get

$$\left(\frac{1}{\xi}\frac{d}{d\xi}\xi\frac{d}{d\xi} - \frac{1}{\xi^2} - \varkappa^2\right)(f - f_1) = 0. \tag{28}$$

The solution of Eq. (28) which vanishes at infinity has the form

$$f - f_1 = CK_1(\varkappa\xi), \tag{29}$$

where K is a modified Bessel function of second order (see, for example, reference 10, page 30).

At $\xi \ll 1/\kappa$ we find from (29), with accuracy up to terms $\sim \kappa \ln \kappa$,

$$f - f_1 \approx C\left(1/\varkappa\xi + \frac{1}{2}\xi\varkappa \ln \varkappa\right). \tag{30}$$

On the other hand, it follows from (29) and (26) that for $\xi \gg 1$

$$f - f_1 \approx -(2/\xi - \varepsilon\xi). \tag{31}$$

For $1 \ll \xi \ll 1/\kappa$, Eqs. (28) and (29) should coincide, whence we find

$$\varepsilon = -\varkappa^2 \ln \varkappa$$

for, transforming to dimensional quantities,

$$\omega = \frac{\hbar k^2}{2m} \ln \frac{1}{kr_0} = \frac{\hbar k^2}{2m} \ln \frac{\sqrt{2gmn_0}}{k\hbar},$$

which is identical with (3).

We note in closing that perturbations with the dispersion law (3) are not entirely stable in the sense that any perturbation with $k \neq 0$ possesses a finite lifetime. This is connected with the fact that an arbitrary perturbation with $k \neq 0$ can under such a dispersion law decay into three perturbations with lesser k. (Decay into two perturbations in the one-dimensional case is impossible because of the zero statistical weight of such a process.) Of course, this observation applies to the vibrations of vortices both in a gas and in a liquid.

In conclusion, the author expresses his thanks to Academician L. D. Landau for useful discussion.

---

[1] L. Onsager, Nuovo cimento 6, 249 (1949).

[2] R. P. Feynman, Progr. Low Temp. Phys., I, Amsterdam, 1955, ch. II.

[3] W. Thomson, Mathematical and Physical Papers 4, Cambridge, 1910, p. 152.

[4] L. P. Pitaevskii, Dissertation, Institute for Physics Problems, Moscow, 1958.

[5] H. E. Hall, Proc. Roy. Soc. (London) A245, 546 (1958).

[6] N. N. Bogolyubov, Izv. Akad. Nauk SSSR, Ser. Fiz. 11, 77 (1947).

[7] T. D. Lee and C. N. Yang, Phys. Rev. 105, 1119 (1957).

[8] E. P. Gross, Phys. Rev. 106, 161 (1957).

[9] V. L. Ginzburg and L. P. Pitaevskii, JETP 34, 1240 (1958), Soviet Phys. JETP 7, 858 (1958).

[10] E. Gray and G. B. Matthews, Bessel Functions and Their Application to Physics and Mathematics (Russian translation, IIL, 1953).

Translated by R. T. Beyer
99

SOVIET PHYSICS JETP VOLUME 13, NUMBER 2 AUGUST, 1961

ANTIPROTONIUM LEVEL SHIFTS FOR LARGE ORBITAL ANGULAR MOMENTA

A. F. GRASHIN

Submitted to JETP editor September 15, 1960

J. Exptl. Theoret. Phys. (U.S.S.R.) 40, 652-653 (February, 1961)

Level shifts due to a single-meson interaction are calculated for the proton-antiproton system.

STRONG interactions of particles in states with large orbital angular momentum l are determined by the exchange of the smallest possible number of mesons. An estimate of the two-meson nucleon-nucleon scattering phase shifts[1] showed that for energies of $E \lesssim 20$ Mev the interactions in states with $l \geq 1$ are quite accurately described by the single-meson interaction.* Similar estimations should be valid for the interaction between a nucleon and an antinucleon. This permits the use of the single-meson approximation for the calculation of the level shifts of the proton-antiproton system (antiprotonium) with $l \geq 1$, which are due to the nuclear interaction.

In the single-meson approximation, the peripheral interaction between the proton and antiproton coincides with the proton-proton interaction, and is described well by the tensor potential $U^{(1)}$. In the calculation of the shifts, one can use the main terms of the expansion of Coulomb functions at the origin of the coordinate system, which ensures an accuracy of $\sim me^2/\mu$ (m and μ are the masses of the nucleon and π meson, $e^2 = 1/137$, $\hbar = c = 1$). For the singlet levels and the "unmixed" triplet levels (states with $J = l$, and also $^3P_0$) we obtain

$$\Delta E_l = -\frac{1}{2}\mu f^2 \frac{(n+l)!\,(me^2/\mu)^{2l+3}}{(2l+1)!\,(n-l-1)!\,n^{2l+4}},$$

$$\Delta E_l^l = -\frac{l+1}{l}\Delta E_l, \quad \Delta E_1^0 = 3\Delta E_1,$$

where $f^2 = 0.08$ is the square of the renormalization constant of the interaction between the nucleon (antinucleon) and the π meson and n is the principal quantum number. For the "mixed" triplet levels we have

$$\Delta E_{J-1}^J = -\mu f^2 \frac{(n+J-1)!\,(me^2/\mu)^{2J+2}}{(4J^2-1)\,(2J-1)!\,(n-J)!\,n^{2J+2}} \quad \text{for } J \geqslant 2,$$

$$\Delta E_{J+1}^J = \frac{1}{4}\mu f^2 \frac{(4J^2-1)\,(n+J+1)!\,(me^2/\mu)^{2J+4}}{(2J+2)!\,(n-J-2)!\,n^{2J+6}} \quad \text{for } J \geqslant 1.$$

The largest of the calculated shifts is $E_1^0 = -0.08$ ev (for $n = 2$), and the ratio $\Delta E_1^0/E_1$ is equal to 2.5×10^{-5}.

The contribution to the level shifts from the next approximation in "degree of peripherality" (two-meson approximation) has an additional smallness of 4^{-l-1}. However, owing to the anomalous smallness of the matrix element

$$\langle J, J-1\,|\,U^{(1)}\,|\,J, J-1\rangle \sim (me^2/\mu)^{2J+2}$$

(additional power of me^2/μ) the shifts $\Delta E_{J\mp1}^J$ have an anomalous dependence on the parameter me^2/μ (ΔE_{J-1}^J is anomalously small and ΔE_{J+1}^J is anomalously large). For this reason, the two-meson approximation gives a correction to these shifts of $\sim \mu/4^{l+1}me^2$.

We shall compare the obtained shifts with the broadening due to annihilation. Since the annihilation occurs at distances $\lesssim \alpha/m$ ($1 \lesssim \alpha \leq 3$), the nuclear widths should have a smallness $(\alpha\mu/m)^{2l}$ in comparison with the nuclear shifts. This simple estimate is in agreement with the results obtained by Desai for the S- and P-level widths.[2] Thus, for comparatively small l, the widths should already be less than the shifts.

The author is grateful to A. A. Tyapkin for suggesting the problem and to I. Ya. Pomeranchuk for helpful comments.

---

*An exception are states with a total angular momentum $J = l + 1$, for which the single-meson phase shifts have an anomalous energy dependence for small momenta $\sim p^{2l+3}$ and cannot make a basic contribution.

[1] Galanin, Grashin, Ioffe, and Pomeranchuk, JETP 37, 1663 (1959), Soviet Phys. JETP 10, 1179 (1960), JETP 38, 475 (1960), Soviet Phys. JETP 11, 347 (1960).

[2] B. R. Desai, Phys. Rev. 119, 1385 (1960).

Translated by E. Marquit
100

SOVIET PHYSICS JETP VOLUME 13, NUMBER 2 AUGUST, 1961

AN INVESTIGATION OF THE PROPERTIES OF TRANSURANIUM ELEMENTS BASED ON THE SUPERFLUID MODEL OF THE NUCLEUS

V. G. SOLOV'EV

Submitted to JETP editor September 15, 1960

J. Exptl. Theoret. Phys. 40, 654-665 (February, 1961)

The properties of strongly deformed transuranic elements are investigated on the basis of the superfluid model of the nucleus. Some insignificant modifications are introduced in Nilsson's schemes by employing the experimental data and taking into account the effect of superfluidity. The pairing energies are computed and the following values for the coupling constants are obtained: $G_N = 0.020\hbar\omega_0$, $G_p = 0.022\hbar\omega_0$, where $\hbar\omega_0 = 41A^{-1/3}$ Mev. Single-particle excitation spectra are calculated for odd-mass nuclei, the calculated level density being about twice as large as that predicted by the Nilsson scheme. Single-particle excitations in even-even nuclei are computed, and in all the calculated spectra for the even-even nuclei (Th^{232}, U^{234}, Pu^{238}, Pu^{240}, Pu^{242}, Cm^{246}, Cf^{248}) the lowest levels are found to be the 1^- levels, which lie below 1 Mev. Corrections due to superfluidity of the ground and excited states are computed for the β and γ transitions. The results obtained are self-consistent: correct values for pairing energies and levels of even and odd nuclei are obtained for the same values of G, whereas variation of G by 30 — 40 percent leads to a pronounced deviation from the experimental data.

THE mathematical methods developed by Bogolyubov for the theory of superfluidity and superconductivity[1] have made it possible to account for the residual nucleon interactions leading to pair correlations in the independent-particle model. This was used by the present author as a basis to formulate[2] a superfluid model of the nucleus.

The present article is devoted to a study, based on the superfluid model, of the properties of strongly deformed transuranic elements. We use as the self-consistent field the Nilsson potential, the energy levels of which are slightly corrected in accordance with the experimental data. Under the assumption of the adiabatic approximation, we calculate the single-particle levels of both odd and even-even nuclei, the pairing energies, and also the corrections to the probabilities of the β and γ transitions.

1. FUNDAMENTAL EQUATIONS

The superfluid model of the nucleus, formulated by the author earlier,[2] being based on the self-consistent potential assumed in the shell or unified model, takes into account the interaction of the nucleons under the following assumptions.

1) The residual interactions, both between neutrons and between protons, are described by a Hamiltonian of the form

$$H = \sum_{s\sigma} \{E(s) - \lambda\} a_{s\sigma}^{+} a_{s\sigma} - G \sum_{s,\,s'} a_{s+}^{+} a_{s-}^{+} a_{s'-} a_{s'+}. \qquad (1)$$

2) The calculations are carried out for each definite nucleus, and we neglect a certain averaging connected with the conservation of the number of particles in the mean.

The states of the nucleus are described by a set of quantum numbers $s\sigma$, determined by the form of the self-consistent field; $\sigma = \pm 1$, characterizes, for example, the sign of Ω, the projection of the nucleon momentum on the symmetry axis of the nucleus; E(s) are the energy levels in the self-consistent field. A certain simplification in the physical picture is the assumption that the interaction G is constant. The chemical potential λ is determined from the condition

$$n = \sum_{s\sigma} \langle a_{s\sigma}^{+} a_{s\sigma} \rangle, \qquad (2)$$

where n is the number of particles and $\langle \ldots \rangle$ denotes averaging over a certain state. When the variational principle is used, the chemical potential plays the role of the Lagrange multiplier. We note that the Hamiltonian (1) should be considered as part of the total Hamiltonian containing, for example, collective interactions.

To solve our problem we use the variational principle proposed by Bogolyubov.[3] Operating as in reference 4, we obtain for the case of the ground state of a system consisting of an even number of particles the following equations[5,6]

$$2/G = \sum [C^2 + \{E(s) - \lambda\}^2]^{-1/2}, \tag{3}$$

$$n = \sum_s \{1 - (E(s) - \lambda)\,[C^2 + \{E(s) - \lambda\}^2]^{-1/2}\} \tag{4}$$

for the determination of C and λ. The energy of the ground state is found in the form

$$\mathcal{E} = \sum E(s)\left\{1 - \frac{E(s) - \lambda}{[C^2 + \{E(s) - \lambda\}^2]^{1/2}}\right\} - \frac{C^2}{G}, \tag{5}$$

and the wave function is

$$\Psi = \prod_s \{u_s + v_s a^+_{s+} a^+_{s-}\}\,\Psi_0, \tag{6}$$

with $a_s \Psi_0 = 0$ and

$$u_s^2 = \frac{1}{2}\left\{1 + \frac{E(s) - \lambda}{[C^2 + \{E(s) - \lambda\}^2]^{1/2}}\right\},$$

$$v_s^2 = \frac{1}{2}\left\{1 - \frac{E(s) - \lambda}{[C^2 + \{E(s) - \lambda\}^2]^{1/2}}\right\}. \tag{7}$$

The wave functions of the excited states are written in the following manner:[5]

$$\Psi(s_1, s_2) = \prod_{s \neq s_1, s_2} (u_s + v_s a^+_{s+} a^+_{s-})\, a^+_{s_1\sigma_1} a^+_{s_2\sigma_2} \Psi_0, \quad s_1 \neq s_2, \tag{8}$$

$$\Psi(s_1, s_1) = \prod_{s \neq s_1} (u_s + v_s a^+_{s+} a^+_{s-})\,(u_{s_1} a^+_{s_1+} a^+_{s_1-} - v_{s_1})\Psi_0, \tag{8'}$$

while the energy and the fundamental equations are obtained in the form

$$\mathcal{E}(s_1, s_2) = E(s_1) + E(s_2) + \frac{1}{2} G (v^2_{s_1} + v^2_{s_2})$$

$$+ \sum_{s \neq s_1, s_2} E(s)\left\{1 - \frac{E(s) - \lambda}{[C^2 + \{E(s) - \lambda\}^2]^{1/2}}\right\} - \frac{C^2}{G}, \tag{9}$$

$$\frac{2}{G} = \sum_{s \neq s_1, s_2} [C^2 + \{E(s) - \lambda\}^2]^{-1/2},$$

$$n = 2 + \sum_{s \neq s_1, s_2} \left\{1 - \frac{E(s) - \lambda}{[C^2 + \{E(s) - \lambda\}^2]^{1/2}}\right\}. \tag{10}$$

In the case of an odd shell, if the odd nucleon is in the state s_i, then the energy of the system and the equations for C and λ are found in the form

$$\mathcal{E}(s_i) = E(s_i) + \frac{G}{2} v^2_{s_i} + \sum_{s \neq s_i} E(s)\left\{1 - \frac{E(s) - \lambda}{[C^2 + \{E(s) - \lambda\}^2]^{1/2}}\right\}$$

$$- \frac{C^2}{G}. \tag{11}$$

$$\frac{2}{G} = \sum_{s \neq s_i} [C^2 + \{E(s) - \lambda\}^2]^{-1/2},$$

$$n = 1 + \sum_{s \neq s_i} \left\{1 - \frac{E(s) - \lambda}{[C^2 + \{E(s) - \lambda\}^2]^{1/2}}\right\} \tag{12}$$

These equations describe the ground state, for the most part with $E(s_i) = E_F$, as well as the excited states of a system with an odd number of particles, the wave function of which is written in the form

$$\Psi(s_i) = \prod_{s \neq s_i} (u_s + v_s a^+_{s+} a^+_{s-})\, a^+_{s_i \sigma_i} \Psi_0. \tag{13}$$

Thus, to determine C and λ of both the ground states and the superfluid excited states it is necessary to solve the corresponding system of equations. This approach differs substantially from the approach used by many authors.[7] Whereas in the case of the superfluid model of the nucleus the quantities C and λ are determined by solving suitable equations, and the interaction constant G is determined from the experimental values of the paired energy, in reference 7 the values of C are determined from the pairing energy, and λ is set equal to the energy of the Fermi surface E_F.

The advantage of the approach based on the superfluid model of the nucleus over the approach used in reference 7 lies, first, in the fact that it becomes possible to determine C and λ for excited states, to take account of the variation of C and λ with change in deformation of the nucleus, etc., something that cannot be done in the case used in reference 7. Secondly, by calculating the change of λ on going from nucleus to nucleus and from the ground state to the excited state, we take account at the same time of the change of the properties of the nucleus as a many-body system. Thirdly, our calculations are more single-valued and reliable, since we have at our disposal a single interaction constant G, which changes slowly and monotonically from nucleus to nucleus, whereas C changes abruptly, depending on the specific variation of the energy levels of the self-consistent field.

In the superfluid model of the nucleus we come upon the question of the orthogonality of the ground and excited states. It is easy to show that all the states of the odd shell are orthogoanl to each other, and that the ground and excited states given by Eq. (8) for an even shell with $s_1 \neq s_2$ are also orthogonal to each other. However, the ground and excited states given by (8′) are not orthogonal to each other when $s_1 = s_2$, namely

$$(\Psi^*(s_1, s_1)\,\Psi(s_2, s_2))$$

$$= (u'_{s_1} v''_{s_1} - u''_{s_1} v'_{s_1})\,(u'_{s_2} v''_{s_2} - u''_{s_2} v'_{s_2}) \prod_{s \neq s_1, s_2} (u'_s u''_s + v'_s v''_s), \tag{14}$$

where u'_s and v'_s pertain to the excited state $\Psi(s_1, s_2)$ while u''_s and v''_s pertain to $\Psi(s_2, s_2)$.

To estimate the error connected with the conservation of the number of particles in the mean, we calculate the mean square fluctuation Δn of the number of particles n. For the ground state of the even shell we obtain

$$(\Delta n)^2 = \sum_s C^2/(C^2 + (E(s) - \lambda^2)). \qquad (15)$$

In the case of the excited state $\Psi(s_1, s_2)$ the sum should not contain terms with $s = s_1$ and $s = s_2$. In the case of the state $\Psi(s_i)$ of the odd shell, the sum (15) should not contain the term with $s = s_i$.

2. PAIRING ENERGY AND SINGLE-PARTICLE LEVELS OF ODD NUCLEI

It is known that the Nilsson potential[8] yields neither the necessary sequence of energy levels nor the correct values of the energy differences between levels. This is due, first, to the deficiency of the Nilsson scheme itself, for although it gives the correct basic laws, it does not take sufficient account of the totality of the nuclear phenomena and, second, to the need of accounting for the residual interactions, which lead to pairing correlations. Using the experimental data[9,10] on single-particle levels of odd nuclei, let us analyze the course of the levels in the Nilsson schemes for $Z > 82$ and $N > 126$, with allowance for the influence of the superfluidity of the ground and excited states.

In reference 2 we obtain, on the basis of calculations with the superfluid model, the influence of superfluidity on the behavior of single-particle levels of odd nuclei; this influence reduces to the following: 1) superfluidity, as a rule, does not cause a change in the ground state of the nucleus as given by the Nilsson scheme; 2) the excitation energies decrease with increasing interaction constant G; 3) the hole and particle levels behave differently with increasing G, but the relative sequence of hole (particle) levels does not change.

From analysis of the experimental data on single-particle levels and equilibrium deformations, as well as from the allowance for superfluidity, we reach the conclusion that the Nilsson level schemes given in reference 9 must be modified as follows:

1. In the level scheme for nuclei with odd Z, $Z > 82$, the level $^{11}/_2{}^-[505]$, which does not appears in a single nucleus, is dropped by $0.4\hbar\omega_0$ ($\hbar\omega_0 = 41 A^{-1/3}$ Mev).

2. In the level scheme for nuclei with odd N, $N > 126$, we make the following changes: a) since the level $^{13}/_2{}^+[606]$, does not appear in any nucleus, it is dropped by $0.25\hbar\omega_0$, which is equivalent to dropping the subshell $i_{13/2}$; b) the subshell $j_{15/2}$ is raised by $0.02\hbar\omega_0$; c) the level $^1/_2{}^+[631]$ is dropped by $0.017\hbar\omega_0$, which is equivalent to dropping the subshell $d_{5/2}$.

Table I. Neutron pairing energies

N	δ	Pairing energy P_N, Mev			
		$G = 0.016\ \hbar\omega_0$	$0.020\ \hbar\omega_0$	$0.024\ \hbar\omega_0$	**Experiment**[11]
150	0.26	0.43	0.94	1.58	0.7–1.1
148	0.26	0.23	0.88	1.57	0.8–1.2
146	0.26	—	0.82	—	0.7–0.9
144	0.24	0.27	0.97	1.69	0.8–1,0

Using the corrected Nilsson schemes, we calculate the pairing energies to find G for both proton and neutron interactions. The numerical solutions of (3), (4), and (12) were obtained with an electronic computer. After calculating $\mathscr{E}(Z, N)$ by formulas (5) and (11), we obtain the pairing energies

$$P_N(Z, N) = 2\mathscr{E}(Z, N-1) - \mathscr{E}(Z, N) - \mathscr{E}(Z, N-2) \qquad (16)$$

for $G = 0.016$, 0.020, and $0.024\hbar\omega_0$. The results of the calculations are summarized in Tables I and II, from which it is seen that the pairing energies depend very strongly on G.

Comparing the calculated pairing energies with the experimental values, we find that for neutron interactions $G_N \approx 0.020\hbar\omega_0$ (more accurately, $0.018\hbar\omega_0 < G_N < 0.022\hbar\omega_0$), and for proton interactions $G_p \approx 0.022\hbar\omega_0$ (more accurately, $0.020\hbar\omega_0 < G_p < 0.024\hbar\omega_0$). From a comparison of the values of the interaction constants G, obtained above, with their values in the region $150 < A < 190$, it is seen that G decreases insignificantly on going from the rare-earth region to the transuranic region.

We now calculate the excitation spectrum of odd nuclei, solving (12) and finding the energy difference (11) for nuclei with odd N from $N = 141$ to $N = 149$, and for nuclei with odd Z from $Z = 91$ to $Z = 95$, for several deformations δ. In order to describe the behavior of the basic quantities, we list in Table III the values of C, λ and Δn for the case $Z = 93$ and $\delta = 0.26$ for the ground and two excited states, and as a comparison for the ground state with $Z = 94$. It is seen from Table III that C and λ change strongly both on going from the even to the odd nucleus and on going from the ground to the excited state. In odd-Z nuclei with $G_p = 0.016$

Table II. Proton pairing energies

Z	δ	Pairing energies P_Z, Mev			
		$G = 0.016\ \hbar\omega_0$	$0.020\ \hbar\omega_0$	$0.024\ \hbar\omega_0$	**Experiment**[11]
96	0.25	0.14	0.74	—	0.8–1.3
90	0.24	0.55	1.17	1.91	~1,4
94	0.25	0.30	0.93	—	0.8–1.4
92	0.24	0.45	1.12	1.90	0.8–1.1

Table III. Dependence of C, λ, and Δn on G
($\delta = 0.26$, $E_F = 5.628\hbar\omega_0$)

$G/\hbar\omega_0$	C	$\lambda - E_F$	Δn	$G/\hbar\omega_0$	C	$\lambda - E_F$	Δn
$Z = 94$, **ground state**				$Z = 93$, **excited state, particle, $5/2^-[523]$**			
0.016	0.027	0.005	1.2	0.016	0	−0.038	0
0.020	0.052	0.005	1.6	0.020	0.030	−0.054	1.0
0.024	0.085	0.006	2.0	0.024	0.062	−0.049	1.6
$Z = 93$, **ground state**				$Z = 93$, **excited state, hole, $1/2^-[530]$**			
0.016	0	0.009	0	0.016	0.020	0.004	1.0
0.020	0	−0.005	0	0.020	0.041	0.003	1.4
0.024	0.043	−0.031	1.1	0.024	0.069	0.001	1.7

$\hbar\omega_0$, and in individual cases with $G_p = 0.020\hbar\omega_0$, there are no pairing correlations in the ground states, and when $G_p = 0.016\hbar\omega_0$ the vanishing of superfluidity is observed in several excited states. In nuclei with odd N, no vanishing of superfluidity is observed for $G_N = 0.016\hbar\omega_0$, although C is quite small for the ground states of several nuclei. It is seen from Table III that the chemical potential fluctuates about the Fermi surface energy E_F, the value of which is $5.628\hbar\omega_0$ for $Z = 93$. We note that these changes in λ are smaller in the region $150 < A < 190$ than the changes given in reference 2.

The second assumption of the superfluid model, neglect of the conservation of the number of particles in the mean, can severely restrict the accuracy of the calculations and therefore calls for a numerical estimate. After calculating the mean square fluctuation Δn of the number of particles, it is necessary to compare it with twice the number of levels over which the summation is carried out, in our case with the number 48. From the calculated values of Δn, some of which are listed in Table III, it can be concluded that the error due to the fluctuation of the number of particles is on the order of 5 percent.

Comparing the calculated single-particle levels of the odd nuclei with the experimental data, we see that the agreement is quite crude; the best agreement occurs when $G_p = 0.024\hbar\omega_0$ for nuclei with odd Z and when $G_N = 0.020\hbar\omega_0$ for nuclei with odd N.

It must be noted that the density of the calculated low-energy levels is in good agreement with the experimental data[10] and is approximately twice the level density given by the Nilsson scheme. In Table IV we list by way of an example the low-lying energy levels of several nuclei. To obtain a more detailed agreement between the calculated and measured levels it is necessary to improve the level scheme of the self-consistent field.

We note that the effect of superfluidity on the spectra of odd nuclei is somewhat weaker in the transuranic region than the rare-earth region, although G has decreased insignificantly. Furthermore, for identical values of G the effect of superfluidity on a nucleus with odd Z is somewhat weaker in the transuranic region than in the region $150 < A < 190$, apparently owing to the change in the level density.[10]

3. EXCITATION SPECTRA OF EVEN-EVEN NUCLEI

Let us calculate the single-particle levels of the even-even nuclei on the basis of the superfluid

Table IV. Energies of excited states of odd nuclei* (Mev)

	$N = 143$		$N = 147$				$Z = 93$	
	$\delta = 0.24$		$\delta = 0.26$		$\delta = 0.27$		$\delta = 0.25$	
Ground state	0	$7/2^-$	0	$5/2^+$	0	$5/2^+$	0	$5/2^+$
Particle levels	0.18	$1/2^+$	0.18	$7/2^+$	0.26	$7/2^+$	0.08	$5/2^-$
	0.34	$5/2^+$	0.25	$9/2^-$	0.31	$9/2^-$	0.74	$3/2^-$
	0.71	$7/2^+$	1.07	$1/2^-$	0.96	$1/2^-$	0 77	$7/2^+$
Hole levels	0.26	$5/2^+$	0.20	$1/2^+$	0.30	$1/2^+$	0.27	$1/2^-$
	0.56	$3/2^+$	0.47	$7/2^-$	0.56	$7/2^-$	0.51	$3/2^+$
	0.60	$5/2^-$	0.88	$5/2^+$	0.99	$5/2^+$	0.78	$3/2^-$

*$G = 0.020\hbar\omega_0$ for odd-N nuclei and $0.024\hbar\omega_0$ for odd-Z nuclei.

Table V. Single-particle levels of U^{234} (in Mev) (for $\delta = 0.24$)

Proton levels			Neutron levels		
Ω and parity	G in $\hbar\omega_0$		Ω and parity	G in $\hbar\omega_0$	
	0.020	0,024		0.018	0.022
$2^-,3^-$	0.75	1,09	$1^-,6^-$	0.78	1.32
$2^+,3^+$	0.87	1,19	$2^+,3^+$	1.09	1,54
$1^+,4^+$	0.98	1.33	0^+	1.10	1.40
0^+	1.07	1.29	$2^-,5^-$	1.15	1.57
0^+	1.15	1.37	$1^+,6^+$	1,19	1.65
$1^-,4^-$	1.16	1.39	0^+	1.20	1.57
$0^-,5^-$	1.19	1.45	$0^+,5^+$	1.31	1,75
0^+	1.31	1.51	$3^-,4^-$	1.40	1.68
$1^-,4^-$	1.37	1.69	$1^-,2^-$	1.44	1,80
$1^-,2^-$	1.38	1.59	$1^+,4^+$	1,52	1.84
0^+	1.61	1.80	$0^-,5^-$	1.57	1.88
$1^+,2^+$	1.64	1,91	$1^-,6^-$	1,52	1.85
$1^+,2^+$	1.74	1.94	0^+	1.74	1.96
$1^-,4^-$	1.94	2,12	0^+	1.86	2,13
$0^-,3^-$	1.97	2.15	$1^-,4^-$	1,91	2.18

model of the nucleus. For this purpose we solve Eqs. (3), (4), and (10) and calculate the energy of the ground and excited states. We note that the excited states given by Eq. (8) are doubly degenerate, unlike the states given by (8′). The excitation spectrum calculated on the basis of the superfluid model of the nucleus shows, by way of a minimum, the most probable spins and parities of the lower excited states, i.e., the calculated spectra of the even-even nucleus contribute to the analysis of the experimental data at least as much as the Nilsson scheme does to the analysis of the odd nuclei.

The influence of superfluidity on the excitation spectra of the even-even nuclei is quite strong. Furthermore, whereas in the case of odd nuclei the single-particle levels condense about the ground state with increasing G, in even-even nuclei the single-particle levels shift away from the ground state with increasing G, i.e., the gap increases. The change in the behavior of the levels with increasing G is demonstrated in Table V for U^{234}.

Tables VI and VII list the values of C, λ, and Δn for Pu^{238}, for both proton and neutron interaction. In the tables the Fermi-surface level is numbered n_F, the next level is denoted $n_F + 1$, etc. Calculations show that C diminishes strongly on going from the ground state to the lowest lying excited states, vanishing in individual cases even when $G_N = 0.022\hbar\omega_0$ and $G_p = 0.024\hbar\omega_0$. The vanishing of superfluidity in the excited states with the lowest energies leads to a reduction in the gap compared with $2[C^2 + (E_F - \lambda)^2]^{1/2}$. The values of the chemical potential λ fluctuate about E_F, and the deviations of λ from E_F are greater than the deviations in odd nuclei, reaching 0.5 Mev.

Calculating in this case, too, the mean square fluctuation Δn of the number of particles and comparing it with the number 48, i.e., with twice the

Table VI. Principal characteristics of the interaction of the neutrons of Pu^{238} ($\delta = 0.26$)

	$G/\hbar\omega_0 = 0.018$			$G/\hbar\omega_0 = 0.022$		
	C	$\lambda - E_F$	Δn	C	$\lambda - E_F$	Δn
			Ground state			
—	0.063	0.029	1,87	0.108	0.030	2.42
			Excited states given by (8′)			
(n_F, n_F)	0.028	0, 76	1.07	0.057	0,070	1.50
(n_F-1, n_F-1)	0,042	0.0 1	1.44	0.076	0,076	1.93
(n_F+1, n_F+1)	0.028	−0.023	1.04	0.059	−0.011	1.53
			Excited states given by (8)			
(n_F, n_F+1)	0	0,84	0	0	0.051	0
(n_F, n_F+2)	0.0002	0.024	0	0.051	0,005	1.30
(n_F-1, n_F)	0.035	0.080	1.26	0.067	0,073	1,73
(n_F+1, n_F+2)	0.035	−0.023	1.24	0.069	−0.013	1.76

Table VII. Principal characteristics of the interaction of the protons of Pu^{238} ($\delta = 0.26$)

	$G/\hbar\omega_0=0,020$			$G/\hbar\omega_0=0,024$		
	C	$\lambda - E_F$	Δn	C	$\lambda - E_F$	Δn
	Ground state					
	0.052	0	1.60	0.085	0.01	1.96
	Excited states given by (8′)					
(n_F, n_F)	0.0004	0.09	0.01	0.027	0.07	0.78
(n_F-1, n_F-1)	0.001	0.08	0.02	0.053	0.07	1.37
(n_F+1, n_F+1)	0	−0.06	0	0.036	−0.05	1.06
	Excited states given by (8)					
(n_F, n_F+1)	0	0.10	0	0	0.08	0
(n_F, n_F+2)	0.0002	0	0.01	0.01	−0.03	0.25
(n_F-1, n_F)	0	0.09	0	0.04	0.07	1.11
(n_F+1, n_F+2)	0.018	−0.06	0.67	0.049	−0.05	1.35

number of levels, we find that $\Delta n/48$ is on the order of 5 percent. Thus, the changes in C and λ on going from the ground states to the excited states, both in even and in odd nuclei, are considerably greater than the errors due to the conservation of the number of particles in the mean.

As shown above, the excited states (8) are orthogonal neither to each other nor to the ground states (which we denote by $|0\rangle$). Let us estimate the non-orthogonality, say for Pu^{238}. For the proton interactions at $G_p = 0.024\hbar\omega_0$, we obtain

$$\langle n_F-1,\ n_F-1|0\rangle = 0.15,$$

$$\langle n_F,\ n_F|n_F-1,\ n_F-1\rangle = 0.01, \qquad \langle n_F,\ n_F|0\rangle = 0.42,$$

$$\langle n_F+1,\ n_F+1|n_F-1,\ n_F-1\rangle = 0,07,$$

$$\langle n_F+1,\ n_F+1|0\rangle = 0.40,$$

$$\langle n_F+1,\ n_F+1|n_F,\ n_F\rangle = 0.67. \qquad (17)$$

In the case of neutron interactions we obtain for $G_N = 0.022\hbar\omega_0$.

$$\langle n_F-1,\ n_F-1|0\rangle = 0.17,$$

$$\langle n_F,\ n_F|n_F-1,\ n_F-1\rangle = 0.001, \qquad \langle n_F,\ n_F|0\rangle = 0.44,$$

$$\langle n_F+1,\ n_F+1|n_F-1,\ n_F-1\rangle = 0.08,$$

$$\langle n_F+1,\ n_F+1|0\rangle = 0,31,$$

$$\langle n_F+1,\ n_F+1|n_F,\ n_F\rangle = 0.22. \qquad (17')$$

It is seen from this that the admixture of excited states (8′) is essentially large, and therefore the energy difference between the states (8) is calculated with greater accuracy than their energy relative to the ground state. The energy of the states 0^+ (8′) is calculated with considerably lower accuracy.

The calculated energies of several excited states of U^{234} with deformation $\delta = 0.24$ and of $Pu^{238,240}$ and Cm^{246} with $\delta = 0.26$ are listed in Tables V, VIII, and IX. Among the low-lying levels there are states 0^+, which enable us to treat, for example, the states 0^+ with energies 1.15 and 1.62 Mev of U^{234} as single-particle states. The values given for the level energies enable us to analyze the experimental data.

The most interesting result of the calculations is that the lowest level in all the spectra of even-even nuclei which we have calculated is the level 1^-, inasmuch as the level $\Omega = 0$ with negative parities appears as $I = 1^-$. This is the result of

Table VIII. Single-particle levels of Pu^{238} and Pu^{240} (Mev) ($\delta = 0.26$)

Pu^{238}, neutron levels		Pu^{238}, proton levels		Pu^{240}, neutron levels	
Ω and parity	$G=0.020\ \hbar\omega_0$	Ω and parity	$G=0.024\ \hbar\omega_0$	Ω and parity	$G=0.020\ \hbar\omega_0$
$3^-,4^-$	0.89	$0^-,5^-$	0.85	$2^+,3^+$	0.90
0^+	1.03	0^+	0.97	0^+	1.11
0^+	1.08	0^+	1.13	0^+	1.14
$1^-,6^-$	1.18	$2^+,3^+$	1.39	$1^-,6^-$	1.16
$2^+,3^+$	1.32	$1^-,4^-$	1.44	$3^+,4^+$	1.20
$2^+,3^+$	1.40	$1^+,6^+$	1.51	$4^-,5^-$	1.28
$1^-,6^-$	1.55	$1^+,4^+$	1.65	$3^-,4^-$	1.44
$0^+,5^+$	1.56	$2^-,3^-$	1.67	$0^-,7^-$	1.44
$0^-,7^-$	1.60	$1^-,4^-$	1.70	$1^+,6^+$	1.51
$1^+,2^+$	1.64	$1^-,6^-$	1.75	$2^-,7^-$	1.51
0^+	1.73	$1^+,2^+$	1.88	$0^+,5^+$	1.56
$3^+,4^+$	1.77	$1^+,4^+$	1.97	0^+	1.62

Table IX. Single-particle levels of Cm^{246} (Mev) ($\delta = 0.26$)

Proton levels		Neutron levels		Proton levels		Neutron levels	
Ω and parity	$G_p = 0.024\hbar\omega_0$	Ω and parity	$G_N = 0.022\hbar\omega_0$	Ω and parity	$G_p = 0.024\hbar\omega_0$	Ω and parity	$G_N = 0.022\hbar\omega_0$
$1^+,4^+$	1,00	$1^-,8^-$	0.90	$2^-,5^-$	1,57	$3^-,4^-$	1,63
$1^-,6^-$	1.10	0^+	0.91	$0^-,5^-$	1,62	$4^+,5^+$	1,64
$1^-,4^-$	1.30	0^+	0.93	0^+	1,80	$3^+,4^+$	1,70
$1^+,6^+$	1,40	$2^-,7^-$	1.25	$1^+,2^+$	1,83	0^+	1.76
0^+	1,49	$1^+,6^+$	1,34	$1^+,6^+$	1,93	$2^-,3^-$	1.80
0^+	1,47	$4^-,5^-$	1,62	0^+	2.05	$0^+,7^+$	1,96

a fortuitous combination of levels in the Nilsson scheme. It follows from our calculations that the single-particle levels 1^-, which lie lower than 1 Mev, should be observed in the nuclei Th^{232}, U^{234}, $Pu^{238,240,242,244}$, Cm^{246}, and Cf^{248}. It is possible that analogous calculations can confirm the appearance of 1^- levels in other transuranic elements, particularly in the lighter isotopes of thorium.

Actually, using the Nilsson scheme for nuclei with odd N, it can be seen that, starting with N = 130, the sequence of levels is $1/2^-$, $1/2^+$, $3/2^-$, $3/2^+$, $5/2^-$, $5/2^+$, etc., i.e., the adjacent levels have opposite parities and $|\Omega_i - \Omega_{i-1}| = 1$ or 0, which is quite favorable for the appearance of the 1^- levels. A similar picture is observed in the level scheme of nuclei with odd Z.

Thus, the calculations performed indicate that the low-lying levels with I = 1 and negative parity, which appear in many transuranic elements, can be single-particle but not collective levels.

4. CORRECTIONS TO THE PROBABILITIES OF THE BETA AND GAMMA TRANSITIONS

Let us calculate the corrections to the β and γ transitions, connected with the superfluidity of the ground and excited states. Knowing C and λ, it is easy to obtain the wave functions of the ground and excited states (6), (8), (8′), and (13). It is easy to show that the corrections to the probabilities are separated in the form of factors smaller than unity.

Calculating the corrections to the probabilities of the β decay of the odd nucleus, when the neutron from state s_1 goes into a proton in state s_2, i.e.,

$$(N = 2n_N + 1;\ Z = 2n_Z) \to (N = 2n_N;\ Z = 2n_Z + 1),$$

we obtain

$$R = (u_{s_1}^{2n_N} u_{s_2}^{2n_Z})^2 \prod_{s \neq s_1} (u_s^{2n_N} u_s^{(s_1)(2n_N+1)} + v_s^{2n_N} v_s^{(s_1)(2n_N+1)})^2$$

$$\times \prod_{s' \neq s_2} (u_{s'}^{2n_Z} u_{s'}^{(s_2)(2n_Z+1)} + v_{s'}^{2n_Z} v_{s'}^{(s_2)(2n_Z+1)})^2. \quad (18)$$

The correction to the probability of the β decay of the odd-odd nucleus, i.e., of the decay

$$(N = 2n_N + 1,\ Z = 2n_Z - 1) \to (N = 2n_N,\ Z = 2n_Z),$$

is determined in the form

$$R_0 = (u_{s_1}^{2n_N} v_{s_2}^{2n_Z})^2 \prod_{s \neq s_1} (u_s^{2n_N} u_s^{(s_1)(2n_N+1)} + v_s^{2n_N} v_s^{(s_1)(2n_N+1)})^2$$

$$\times \prod_{s' \neq s_2} (u_{s'}^{2n_Z} u_{s'}^{(s_2)(2n_Z-1)} + v_{s'}^{2n_Z} \cdot v_{s'}^{(s_2)(2n_Z-1)})^2, \quad (19)$$

where in u_s^{2n} and v_s^{2n} it is necessary to substitute C and λ for the ground state of the even shell, and in $u_s^{(s_i)(2n\pm1)}$, $v_s^{(s_i)(2n\pm1)}$ it is necessary to substitute C and λ of the ground or excited states of the odd shell, if the odd particle is in the state s_i.

In Table X we list the calculated corrections to the probabilities of the β decay of $Pu^{237,243}$ and

Table X. Correction R to the probabilities of β decay of odd nuclei for $G_p = 0.024\hbar\omega_0$ and $G_N = 0.020\hbar\omega_0$

Parent		Daughter		R
nucleus	state	nucleus	state	
Pu^{237}	$7/2$ $7/2^-$ [743]	Np^{237}	$5/2$ $5/2^+$ [642]	0.106
	$7/2$ $7/2^-$ [743]		$5/2$ $5/2^-$ [523]	0.090
Np^{239}	$5/2$ $5/2^+$ [642]	Pu^{239}	$1/2$ $1/2^+$ [631]	0.195
	$5/2$ $5/2^+$ [642]		$5/2$ $5/2^+$ [622]	0.120
	$5/2$ $5/2^+$ [642]		$7/2$ $7/2^-$ [743]	0,282
	$5/2$ $5/2^+$ [642]		$5/2$ $5/2^+$ [633]	0.326
Pu^{243}	$7/2$ $7/2^+$ [624]	Am^{243}	$5/2$ $5/2^+$ [642]	0,238
	$7/2$ $7/2^+$ [624]		$7/2$ $7/2^+$ [633]	0.613

Table XI. Corrections $R\gamma$ to the probabilities of electromagnetic transitions in odd nuclei for $G_p = 0.024\hbar\omega_0$ and $G_N = 0.020\hbar\omega_0$

Nucleus	Initial state	Final state	Energy (Mev)	Multipolarity	R_γ
Np^{237}	$^5/_2\ ^5/_2^-[523]$	$^7/_2\ ^5/_2^+[642]$	0.06	$E1$	0.46
	$^3/_2\ ^3/_2^-[521]$	$^7/_2\ ^5/_2^-[523]$	0.16	$E2$	0.65
	$^3/_2\ ^3/_2^-[521]$	$^5/_2\ ^5/_2^-[523]$	0.21	$M1$	0.93
Pu^{237}	$^1/_2\ ^1/_2^+[631]$	$^7/_2\ ^7/_2^-[743]$	0.14	$E3$	0.26
Pu^{239}	$^7/_2\ ^7/_2^-[743]$	$^5/_2\ ^5/_2^+[642]$	0.11	$E1$	$0.58 \cdot 10^{-3}$
	$^5/_2\ ^5/_2^+[622]$	$^3/_2\ ^1/_2^+[631]$	0.29	$E2$	0.207

Np^{239}. It is seen from the table that the corrections can be quite important in individual cases.

The corrections to the electromagnetic transitions are of more complicated form. For the case of an odd nucleus we obtain

$$R_\gamma = (u_{s_2}^{(s_1)} u_{s_1}^{(s_2)} - \eta v_{s_1}^{(s_2)} v_{s_2}^{(s_1)})^2 \prod_{s \neq s_1, s_2} (u_s^{(s_1)} u_s^{(s_2)} + v_s^{(s_1)} v_s^{(s_2)})^2, \quad (20)$$

where $\eta = 1$ for electric transitions and $\eta = -1$ for magnetic ones.

In Table XI we list the corrections to the γ transitions. We note that these corrections fluctuate within greater limits than the corrections for β decay.

Thus, our calculations show that in the calculation of the probabilities of β and γ transitions in strongly deformed transuranic elements it is necessary to take into account the superfluidity of the ground and excited states.

CONCLUSION

The superfluid model of the nucleus is based on the shell and unified models and is a further development of these models. At the first stage of the investigations, carried out on the basis of the superfluid model of the nucleus, we disregarded the long-range residual interactions, responsible for the main collective properties of the nucleus.

It must be noted that the results of the calculations on the basis of the superfluid model of the nucleus for specified values of G and for specified energy levels of the effective potential are single valued. In light of this single-valuedness, particular interest attaches to the mutual compatibility of the results obtained, namely: for the same values of the interaction constants G we obtain reasonable values of the pairing energies and of the levels of the even and odd nuclei, and when G is changed, say, by 30 – 40 percent to either side, a sharp discrepancy is observed with experiment, both in the level behavior and in the pairing energies.

It must also be noted that on the basis of the superfluid model of the nucleus it is possible to carry out all-out investigations of the properties of strongly deformed nuclei, for which it is necessary to calculate the moments of inertia of the ground and excited states, the probabilities of β and γ transitions, the magnetic moments, etc. On the other hand, to obtain more detailed results it is necessary to determine more accurately the behavior of the energy levels of the self-consistent field.

In conclusion I express my deep gratitude to N. N. Bogolyubov for continuous interest in the work and for fruitful discussion, I. N. Silin for setting up the program and carrying out the numerical computations, and also to N. I. Pyatov, V. I. Furman, and Liu Yu-yen for aid in the processing of the results.

---

[1] N. N. Bogolyubov, Лекции по квантовой статистике, (Lectures in Quantum Statistics), Kiev, 1947. Bogolyubov, Tolmachev, and Shirkov, Новый метод в теории сверхпроводимости, (New Method in Superconductivity Theory), AN SSSR, 1958.

[2] V. G. Solov'ev, Doklady Akad. Nauk SSSR **133**, 325 (1960), Soviet Phys.-Doklady **5**, 778 (1961).

[3] N. N. Bogolyubov, Doklady Akad. Nauk SSSR **119**, 244 (1958), Soviet Phys.-Doklady **3**, 292 (1958).

[4] V. G. Solov'ev, JETP **35**, 823 (1958), Soviet Phys. JETP **8**, 572 (1959); Nucl. Phys. **9**, 655 (1958/9).

[5] S. T. Belyaev, Mat. Fys. Medd. Dan. Vid. Selsk. **31**, No. 11 (1959).

[6] V. G. Solov'ev, JETP **36**, 1869 (1959), Soviet Phys. JETP **9**, 1331 (1959).

[7] A. B. Migdal, JETP **37**, 249 (1959), Soviet Phys. JETP **10**, 176 (1960). Grin', Drozdov, and Zaretskii, JETP **38**, 1297 (1960), Soviet Phys. JETP **11**, 936 (1960). J. J. Griffin and M. Rich, Phys. Rev. Lett. **3**, 342 (1959).

[8] S. G. Nilsson, Kgl. Dan. Vid. Selsk. Mat. Fys. Medd. **29**, No. 16 (1959).

[9] B. Mottelson and S. G. Nilsson, Mat. Fys. Skr. Dan. Vid. Selsk. **1**, No. 8 (1959).

[10] B. S. Dzhelepov and L. K. Peker, Схемы распада радиоактивных ядер, (Decay Schemes of Radioactive Nuclei), AN SSSR, 1958. F. H. Bakke, Nucl. Phys. 9, 670 (1958/9). Stephens, Asaro, and Perlman, Phys. Rev. 113, 312 (1959).

[11] V. A. Kravtsov, JETP 36, 1224 (1959), Soviet Phys. JETP 9, 871 (1959).

Translated by J. G. Adashko
101

VARIATION OF THE ADIABATIC INVARIANT OF A PARTICLE IN A MAGNETIC FIELD. II

A. M. DYKHNE and A. V. CHAPLIK

Institute of Radiophysics and Electronics, Siberian Div. Acad. Sci. U.S.S.R.

Submitted to JETP editor September 13, 1960

J. Exptl. Theoret. Phys. 40, 666-669 (February, 1961)

The change in the adiabatic invariant during passage of a charged particle through a magnetic inhomogeneity is calculated by a previously developed method.[1,2] The results significantly differ from those obtained with help of a model Hamiltonian.[2-4]

THE method of calculating the change in the adiabatic invariants, developed earlier,[1,2] makes it possible to calculate the change in the adiabatic invariant of a particle moving in an inhomogeneous magnetic field. Unlike other investigations of this topic,[2-4] we shall not use for the magnetic field a model in which the curvature of the force lines is ignored, and shall carry out a rigorous analysis of the problem.

We confine ourselves to an axially-symmetrical magnetic field. The particle energy can be represented in the form

$$E = \frac{1}{2m}(p_r^2 + p_z^2) + \frac{1}{2m}\left(\frac{M}{r} - \frac{e}{c} A_\varphi\right). \qquad (1)$$

Here $M = r(mv_\varphi + eA_\varphi/c)$ is the conserved azimuthal moment of the particle. Following reference 2, we shall solve first the quantum-mechanical problem. The Schrödinger equation for this case has the form

$$-\frac{h^2}{2m}\Delta_{r,z} + V\psi = E\psi; \quad V = \frac{1}{2m}\left(\frac{M}{r} - \frac{e}{c} A_\varphi\right)^2. \qquad (2)$$

As is well known, the motion of a particle in a strong magnetic field consists of fast Larmor rotation about the force line and motion along the force line. The equation of the force line to which the particle is "tied," as can be seen from (1), has the form

$$M = (e/c)\, r A_\varphi. \qquad (3)$$

In connection with particle motion of such nature, we shall find it convenient to replace the cylindrical coordinates r, z with new coordinates s, x, where s is the length along the force line (3), and x is the shortest distance to the force line. Obviously, these coordinates are orthogonal, and can be introduced uniquely for all x that satisfy the conditions $x < R_{min}$, where R_{min} is the least radius of curvature of the force line.

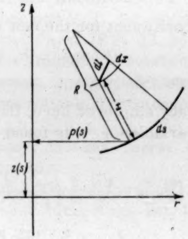

The square of the element of length in the new coordinates, as can be seen from Fig. 1, is

$$dl^2 = dx^2 + h_s^2 ds^2 + h_\varphi^2 d\varphi^2. \qquad (4)$$

Here $h_s = 1 - x/R$ and $h_\varphi = r = \rho(s) + \dot{z}(s)x$ are Lamé coefficients, $R(s)$ is the radius of curvature of the force line; the dots signify differentiations with respect to s. The equation of the force line is written in parametric form

$$r = \rho(s), \qquad z = z(s).$$

We consider the magnetic field to be sufficiently strong, meaning that the parameter of r_L/R is small (r_L is the Larmor radius). Since $x \lesssim r_L$ during the entire time of motion, we can expand the Laplacian and the potential energy in (2) in powers of s/R. In all the expansions we shall retain the terms of the first two nonvanishing orders.

We assume that the motion of the particle takes place in a region where there are no currents. In this region the magnetic field satisfies the equation

$$\frac{\partial H_x}{\partial s} - \frac{\partial}{\partial x}(h_s H_s) = 0. \qquad (5)$$

On the force line x = 0 this equation yields

$$\partial H / \partial x = H / R. \qquad (6)$$

Using (6) and the expression for H_s

$$H_s = -\frac{1}{r}\frac{\partial}{\partial x}(rA_\varphi), \tag{7}$$

we obtain an expansion for rA_φ:

$$rA_\varphi = (cM/e) - H\rho(s)\left[x + \tfrac{1}{2}x^2(1/R + \dot{z}/\rho)\right]. \tag{8}$$

Substituting (8) into expression (2) for V, we obtain

$$V = V_0 + V_1,\ V_0 = \frac{1}{2}m\omega^2(s)x^2, \tag{9}$$

$$V_1 = V_0 x(1/R - \dot{z}/\rho), \tag{10}$$

where ω is the Larmor frequency, equal to eH/mc.

We make another change of variables

$$\xi = x(m\omega(s)/\hbar)^{1/2}, \quad s = s. \tag{11}$$

The Lamé coefficient for the new variables are

$$h_\xi = (\hbar/m\omega)^{1/2},\ h_s = 1 - (\hbar/m\omega)^{1/2}\xi/R,\ h_\varphi = \rho(s) + (\hbar/m\omega)^{1/2}\xi\dot{z}. \tag{12}$$

With the accuracy employed here, the Laplace operator in the variables ξ, s is found to be $\Delta = L_0 + L_1$, where

$$L_0 = \frac{m\omega}{\hbar}\frac{\partial^2}{\partial\xi^2} + \frac{\sqrt{\omega}}{\rho}\frac{\partial}{\partial s}\left(\frac{\rho}{\sqrt{\omega}}\frac{\partial}{\partial s}\right), \tag{13}$$

$$L_1 = \left(\frac{m\omega}{\hbar}\right)^{1/2}\left(\frac{\dot{z}}{\rho} - \frac{1}{R}\right)\frac{\partial}{\partial\xi} + \left(\frac{\hbar}{m\omega}\right)^{1/2}\frac{2\xi}{R}\frac{\sqrt{\omega}}{\rho}\frac{\partial}{\partial s}\left(\frac{\rho}{\sqrt{\omega}}\frac{\partial}{\partial s}\right) + \left(\frac{\hbar}{m\omega}\right)^{1/2}\xi\left[\frac{\ddot{z}}{\rho} - \frac{\dot{z}\dot{\rho}}{\rho^2} - \frac{\dot{R}}{R^2} - \frac{1}{2}\frac{\dot{\omega}}{\omega}\left(\frac{\dot{z}}{\rho} + \frac{1}{R}\right)\right]\frac{\partial}{\partial s}. \tag{14}$$

Transforming (9) and (10) to the new variables, we get

$$V_0 = \tfrac{1}{2}\hbar\omega\xi^2,\ V_1 = (\hbar/m\omega)^{1/2}\xi(1/R - \dot{z}/\rho)V_0. \tag{15}$$

ZEROTH APPROXIMATION

The zeroth-approximation equation, as can be seen from (13) and (15), has the form

$$\left\{\frac{\hbar\omega}{2}\left(-\frac{\partial^2}{\partial\xi^2} + \xi^2\right) - \frac{\hbar^2}{2m}\frac{\sqrt{\omega}}{\rho}\frac{\partial}{\partial s}\left(\frac{\rho}{\sqrt{\omega}}\frac{\partial}{\partial s}\right)\right\}\psi = E\psi. \tag{16}$$

Separating the variables we obtain a quasi-classical solution of Eq. (16), normalized to a δ-function energy

$$\psi_{nE} = \left(\frac{m}{2\pi k_{nE}\hbar^2}\right)^{1/2}\exp\left\{i\int^{s} k_{nE}\,ds\right\}\left(\frac{m\omega}{\hbar\rho^2}\right)^{1/4}\Xi_n(\xi),$$

$$k_{nE}^2 = (2m/\hbar^2)\left[E - \left(n + \tfrac{1}{2}\right)\hbar\omega(s)\right]. \tag{17}$$

Here $\Xi_n(\xi)$ are the eigenfunctions of an oscillator with a single frequency. The wave function normalized to the unit flux differs from (17) by the factor $(2\pi\hbar)^{1/2}$.

For the sake of being definite, we have written out the solution of the "longitudinal" part of (16) under the assumption that there are no turning points. The case when turning points are present (reflection from a magnetic mirror) is considered analogously and leads to the same results.

SCATTERING MATRIX IN THE FIRST APPROXIMATION

Unlike the model considered earlier[2] for the magnetic field, the perturbing Hamiltonian (14), (15) contains odd powers of the transverse coordinate ξ and of the derivative $\partial/\partial\xi$. In this connection, the perturbation in the case of the magnetic field permits transitions to neighboring levels. Since the probabilities of transitions to more remote levels contain additional exponentially small factors, we confine ourselves to the calculation of the near-diagonal component of the scattering matrix.

In the calculation of the matrix elements, the singularities of the perturbing Hamiltonian in the complex plane come into play; these singularities coincide[2] with the zeros and the poles of the functions $\omega(s)$ and $R(s)$. [It is easy to verify that the remaining functions of s contained in (14) are expressed in terms of $R(s)$]. We assume that the main contribution to the matrix elements is made by the saddle point, which coincides with the zero s_0 of the function $\omega(s)$.

After calculating the matrix elements under this assumption, it is easy to see that the main contribution in the powers of r_L/R is made by the second term in (14). For the near-diagonal elements of the scattering matrix we have

$$S_{n,\,n-1} = C\left(\frac{m}{\hbar}\right)^{1/2}\frac{v}{R(s_0)}\frac{v^{1/4}}{[\dot{\omega}(s_0)]^{3/4}}\sqrt{\frac{n}{2}}\exp\left(i\int^{s_0}\frac{\omega}{v_\parallel}ds\right),$$

$$S_{n,\,n+1} = -C^*\left(\frac{m}{\hbar}\right)^{1/2}\frac{v}{R(s_0^*)}\frac{v^{1/4}}{[\dot{\omega}(s_0^*)]^{3/4}}\sqrt{\frac{n+1}{2}}\exp\left(-i\int^{s_0^*}\frac{\omega}{v_\parallel}ds\right). \tag{18}$$

We have introduced here

$$C = 2^{-1/4}\Gamma\left(\frac{1}{4}\right)e^{i7\pi/8},$$

$v_\parallel = [2(E - I\omega)/m]^{1/2}$ is the longitudinal velocity of the particle, and v is the total velocity.

The contribution of the next perturbation-theory approximation to the scattering matrix is estimated in complete analogy with the procedure used in reference 2. It is found to be small in r_L/R compared with the terms included.

Knowing the scattering matrix, we can calculate the change in the adiabatic invariant by going to the classical limit.[1,2] We note beforehand that the wave functions and scattering matrix have been determined only accurate to an arbitrary phase multiplier. In (17) and (18) this arbitrariness manifests itself in the absence of a lower limit in the integral. At the same time, the final result — the change in the adiabatic invariant — should be unequivocal. To eliminate this arbitrariness, a lower limit must be chosen for the integral in (18).

We proceed in the following fashion. We assume that prior to passing through the magnetic inhomogeneity ($s \to -\infty$) the particle moved in a homogeneous magnetic field. The trajectory of the particle was characterized in this case by a certain initial phase shift. The phase shifts of the wave functions must be chosen such that a wave packet built up of these functions should describe, as $s \to -\infty$, a classical particle with specified phase shift. It is easy to verify that this corresponds to the following choice of lower limit for the integral in (18):

$$\int^{s} \frac{\omega}{v_{\parallel}}\, ds = \int_{-\infty}^{s} \left(\frac{\omega}{v_{\parallel}} - \frac{\omega_{-}}{v_{\parallel}^{-}}\right) ds + \frac{\omega_{-}}{v_{\parallel}^{-}}\, s + \psi_{-}. \tag{19}$$

Here ψ_{-}, $\bar{v}_{\parallel}$, and ω_{-} are the phase, longitudinal velocity, and Larmor frequency as $s \to -\infty$.[5]

A calculation of the adiabatic invariant[2] leads to the following result:

$$\frac{I_{+} - I_{-}}{I} = \operatorname{Re}\left\{C\left(\frac{E}{I\omega_0 R_0}\right)^{1/2}\left(\frac{v}{\omega_0 R_0^2}\right)^{1/4} \exp\left[i\int_{-\infty}^{s_0}\left(\frac{\omega}{v_{\parallel}} - \frac{\omega_{-}}{v_{\parallel}^{-}}\right) ds + i\,\frac{\omega_{-}}{v_{\parallel}^{-}}\, s_0 + i\psi_{-}\right]\right\}. \tag{20}$$

We see that the change in the adiabatic invariant I, due to the motion of a particle in a magnetic field, differs from the results obtained by using the model Hamiltonian. This difference consists in the absence of the factor 2 from the exponent in (20) and the presence of a factor of order $(r_L/R)^{1/4}$ before the exponent. Thus, the results differ appreciably (in order of magnitude) from the results previously obtained,[2] and the use of the model Hamiltonian to obtain quantitative data on the motion of a charged particle in a magnetic field[3,4] must be regarded as incorrect.

---

[1] A. M. Dykhne, JETP **38**, 570 (1960), Soviet Phys. JETP **11**, 411 (1960).

[2] A. M. Dykhne and V. L. Pokrovskii, JETP **39**, 373 (1960), Soviet Phys. JETP **12**, 264 (1961).

[3] O. B. Firsov, Anthology Физика плазмы и проблема управляемых термоядерных реакций, (Plasma Physics and Controllable Thermonuclear Reactions), vol. 3, AN SSSR, p. 259, 1958.

[4] B. V. Chirkov, Атомная энергия (Atomic Energy), No. 6, 1959.

[5] A. M. Dykhne, Dissertation, Inst. of Radiophysics and Electronics, Acad. Sci. U.S.S.R., 1960.

Translated by J. G. Adashko
102

SOVIET PHYSICS JETP VOLUME 13, NUMBER 2 AUGUST, 1961

THE MAGNETIC PROPERTIES OF BERYLLIUM IN THE TEMPERATURE RANGE 300 TO 4.2°K

B. I. VERKIN, I. M. DMITRENKO, and I. V. SVECHKAREV

Physico-Technical Institute, Low Temperature Laboratory, Academy of Sciences, Ukrainian S.S.R.

Submitted to JETP editor September 14, 1960

J. Exptl. Theoret. Phys. (U.S.S.R.) 40, 670-671 (February, 1961)

The angular dependence of χ for beryllium (above 20°K) and indium is found to be described by a cosine law. The temperature dependence of the principal values of χ for beryllium is characteristic for small groups of electrons. In the case of indium, χ is found to be highly sensitive to impurities.

We have continued our investigation[1] of the magnetic properties of pure elements that show a long-period de Haas-van Alphen effect. The measurements were made by the Faraday method with a vertical gradient in fields up to 10 koe. A spring balance with photoelectric auto-compensation was used (analogous in principle to those described by Deryagin[2] and Hedgcock[3]). The accuracy of the absolute measurements was ~2%, the relative ones ~0.5%.

The angular dependence of the magnetic susceptibility of two samples of beryllium* (Be-1 and Be-2, 99.99% pure) and two samples of indium (In-1, which was studied in previous work,[1] and In-3) was measured at various temperatures in the range from 300 to 4.2°K.

Up until the appearance of the de Haas-van Alphen effect the angular dependence of χ for beryllium obeys the law (Fig. 1):

$$\chi(\theta) = \chi_{\parallel} \cos^2\theta - \chi_{\perp} \sin^2\theta. \tag{1}$$

In order not to clutter the figure the data for only a few temperatures are shown in it. The dependences calculated according to Eq. (1) are portrayed as continuous curves; the experimental points were taken every 5°, sometimes every 1°.

The principal values of the susceptibility ($\chi_{\parallel} = 2.38 \times 10^{-6}$, $\chi_{\perp} = 0.80 \times 10^{-6}$ cm³/g) and their temperature dependence agreed well for both samples of Be (Fig. 2). The character of the growth of $|\chi_{\perp}|$ with increasing temperature can be attributed to the contribution of the paramagnetism of groups containing small numbers of electrons (or holes). As in the majority of the elements studied earlier, the anisotropy decreases with increasing temperature, and the temperature-dependent component of the susceptibility tensor asymptotically approaches the independent (or weakly dependent) component. The latter probably constitutes a background for the small groups, caused by the contribution of other mechanisms and of large groups. In beryllium $\chi_{\perp}$ shows not only a temperature dependence, but also a periodic field dependence even at T ≈ 20°K, confirming, as in the other elements, the correlation of this phenomenon with the presence of small groups of mobile charges. At T ≤ 20°K the value of $\chi_{\perp}$ was determined from the average of the dependence of $\chi_{\perp}$ on the magnitude of the reciprocal of the field.

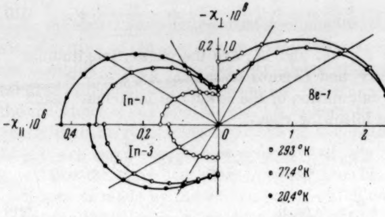

FIG. 1. The angular dependence of the magnetic susceptibility of beryllium and indium at various temperatures. The continuous curves are plots of Eq. (1).

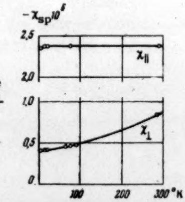

FIG. 2. Temperature dependence of the principal values of the specific susceptibility of beryllium.

---

*We express thanks to A. A. Kruglykh for the gift of the monocrystals of pure beryllium.

The curve of $\chi(\theta)$ for the indium samples also follows the cosine law (Fig. 1). However, although both samples were prepared from the very same starting material, the absolute values of χ and their dependence on temperature differ markedly. It is likely that small amounts of impurity have as significant an effect in indium as in bismuth[4] and antimony[5] (interestingly, it differs in different directions). It can be presumed that the high anisotropy of this metal is caused wholly by small groups that do not show up in the electrical and galvanomagnetic properties.

The authors express their gratitude to Prof. B. G. Lazarev for making it possible to carry out the work in the Low Temperature Laboratory of the Physico-Technical Institute of the Academy of Sciences, Ukrainian S.S.R.

[1] Aleksandrov, Verkin, and Svechkarev, JETP 39, 37 (1960), Soviet Phys. JETP 12, 25 (1961).

[2] B. V. Deryagin, Doklady Nauk SSSR 61, 275 (1948).

[3] F. T. Hedgcock, Phys. Rev. 104, 1564 (1956).

[4] A. Goetz and A. B. Focke, Phys. Rev. 45, 170 (1934); D. Shoenberg and M. Zaki Uddin, Proc. Roy. Soc. (London A156, 687 (1936).

[5] S. H. Browne and C. T. Lane, Phys. Rev. 60, 895 (1941).

Translated by L. M. Mattarese
103

SOVIET PHYSICS JETP VOLUME 13, NUMBER 2 AUGUST, 1961

ON THE PROBLEM OF COMPUTING MOMENTS OF INERTIA OF NUCLEI

S. T. BELYAEV

Submitted to JETP editor, September 15, 1960

J. Exptl. Theoret. Phys. (U.S.S.R.) 40, 672-675 (February, 1961)

By using the generalized canonical transformation method, an expression is obtained for the moment of inertia of a nucleus which takes nucleon pairing into account. The result is essentially the same as that obtained previously by Migdal using the Green's function method.

THE moment of inertia of a deformed nucleus, when we take into account superfluidity (i.e., the Cooper pairing of nucleons), was calculated earlier[1] within the framework of adiabatic perturbation theory. As was shown by Migdal[2] using the Green's function method, including the rotational energy by means of perturbation theory is not sufficient, since the rotation changes the Cooper pairs and thus gives rise to an additional term in the moment of inertia. In the present paper we shall show that a consistent application of the canonical transformation method leads to this same result.

The nucleons in the deformed self-consistent field are described by the Hamiltonian

$$H = \sum_{\nu_1} (\varepsilon_{\nu_1} - \lambda) a^{+}_{\nu_1} a_{\nu_1} + \frac{1}{2} \sum \langle 12 | G | 2'1' \rangle a^{+}_{1} a^{+}_{2} a_{2'} a_{1'}, \quad (1)$$

where $a^{+}_{\nu_1}(a_{\nu_1})$ are the operators for creation (annihilation) of a nucleon in the state $\nu_1 \equiv 1$; $\epsilon_{\nu_1} \equiv \epsilon_1$ is the energy of this single-particle state, and λ is the chemical potential for the system.

The nucleon pairing can be taken into account by introducing quasiparticles by means of the canonical transformation

$$a_{\nu} = u_{\nu} \alpha_{\nu} + v_{\nu} \alpha^{+}_{\tilde{\nu}}, \quad \alpha_{\nu} = u_{\nu} a_{\nu} - v_{\nu} a^{+}_{\tilde{\nu}}, \quad (2)$$

where $\tilde{\nu}$ denotes the state which is the time reversed state to ν (and has the same energy),* while the coefficients of the transformation satisfy the conditions

$$u_{\tilde{\nu}} = u_{\nu}, \quad v_{\tilde{\nu}} = - v_{\nu}, \quad u^2_{\nu} + v^2_{\nu} = 1 \quad (3)$$

and are chosen so that the terms with $\alpha\alpha$ and $\alpha^{+}\alpha^{+}$ in the Hamiltonian go to zero after the transformation. It is known that this requirement is equivalent to a minimization of the quasiparticle vacuum state (defined by $\alpha\Psi_0 = 0$):

$$\Psi_0 = \prod_{|\nu|} (u_{\nu} + v_{\nu} a^{+}_{\nu} a^{+}_{\tilde{\nu}}) | 0 \rangle. \quad (4)$$

Calculation of average values using the function (4) is equivalent to averaging independently over pairs of operators,* for example

$$\langle a^{+}_1 a^{+}_2 a_{2'} a_{1'} \rangle_0 = \langle a^{+}_1 a_{1'} \rangle_0 \langle a^{+}_2 a_{2'} \rangle_0 - \langle a^{+}_1 a_{2'} \rangle_0 \langle a^{+}_2 a_{1'} \rangle_0$$
$$+ \langle a^{+}_1 a^{+}_2 \rangle_0 \langle a_{2'} a_{1'} \rangle_0, \quad (5)$$

where only the "diagonal" expressions

$$\langle a^{+}_1 a_1 \rangle_0 = v^2_1, \quad \langle a^{+}_1 a^{+}_{\tilde{1}} \rangle_0 = \langle a_{\tilde{1}} a_1 \rangle_0 = u_1 v_1 \quad (6)$$

are different from zero.

To find the moment of inertia, we look for the lowest state of the system with a fixed projection of the angular momentum on an axis perpendicular to the nuclear axis. To do this, we add to the Hamiltonian the term

$$H_{\omega} = - \omega \hat{J}_x = - \omega \Sigma \langle 1 | j_x | 2 \rangle a^{+}_1 a_2, \quad (7)$$

and then determine the Lagrange multiplier ω from the condition $\langle \hat{J}_X \rangle = J_X$.

When the term H_{ω} is added to the Hamiltonian, the selection rule forbidding production of pairs of quasiparticles $\alpha^{+}\alpha^{+}$ is violated, and cannot be reestablished by simply changing the coefficients u_{ν} and v_{ν} in (2). To eliminate the terms in $\alpha\alpha$ and $\alpha^{+}\alpha^{+}$ in the total Hamiltonian $H' = H + H_{\omega}$, we make a further canonical transformation of more general form:[3]

$$\alpha_{\nu} \rightarrow \alpha_{\nu}(\omega) + \sum_{\nu'} f_{\nu\nu'} \alpha^{+}_{\tilde{\nu}'}(\omega). \quad (8)$$

The coefficients $f_{\nu\nu'}$ are related to the rotational term H_{ω} ($f_{\nu\nu'} \sim \omega$). They may be assumed to be small, and are included only in the first nonvanishing order. From the condition for the transformation (8) to be canonical, and from the symmetry with respect to change in sign of ω, it follows that

$$f_{\nu\nu'} + f_{\tilde{\nu}'\tilde{\nu}} = 0, \quad f_{\nu\nu} = 0. \quad (9)$$

For these new quasiparticles $\alpha_{\nu}(\omega)$ (corrected for rotation), the vacuum state differs from (4) and, as we find from (8), it has the form

---

*If $|\nu\rangle = |nljm\rangle$, $|\tilde{\nu}\rangle = (-1)^{j+m} |nlj-m\rangle$.

*Equation (5) shows that the canonical transformation method is equivalent to the generalized Hartree-Fock method.[3]

$$\Psi_\omega=\exp\Big\{\frac{1}{2}\sum_{\nu\nu'} f_{\nu\nu'}\alpha_\nu^+\alpha_{\tilde{\nu}'}^+\Big\}\Psi_0$$

$$=\exp\Big\{\frac{1}{2}\sum_{\nu\nu'} f_{\nu\nu'}(u_\nu a_\nu^+ - v_\nu a_{\tilde{\nu}})(u_{\nu'} a_{\tilde{\nu}'}^+ + v_{\nu'} a_{\nu'})\Big\}\Psi_0. \quad (10)$$

We note that the function (10) is not normalized:

$$(\Psi_\omega,\Psi_\omega)=\exp\Big(\frac{1}{2}\sum_{\nu\nu'}|f_{\nu\nu'}|^2\Big).$$

To determine the coefficients $f_{\nu\nu'}$, we demand that the average value of the total Hamiltonian H′ be a minimum in the state (10). Relation (5) is still valid for averages calculated with the function (10), but in addition to the diagonal quantities

$$\langle a_1^+ a_1\rangle = v_1^2 + (u_1^2 - v_1^2)\sum_2 |f_{12}|^2,$$

$$\langle a_1^+ a_{\tilde{1}}^+\rangle = \langle a_{\tilde{1}} a_1\rangle = u_1 v_1 - 2u_1 v_1\sum_2 |f_{12}|^2, \quad (11)$$

the nondiagonal expressions

$$\langle a_1^+ a_2\rangle = (u_1 v_2 - v_1 u_2) f_{12}^*,$$

$$\langle a_1^+ a_{\tilde{2}}^+\rangle = \langle a_{\tilde{2}} a_1\rangle = (u_1 u_2 + v_1 v_2) f_{12}^* \quad (12)$$

are also different from zero. In (11) and (12) we have used the relation

$$f_{12}^* + f_{21} = 0, \quad (13)$$

which can be verified by direct computation.

Calculating the average values of H and H_ω using (11) and (12), we get

$$\langle H\rangle = W_0 + \frac{1}{2}\sum_{12}(E_1+E_2)|f_{12}|^2$$

$$-\frac{1}{2}\sum\langle 1\tilde{2}|G|\tilde{2}'1'\rangle(u_1u_2+v_1v_2)(u_{1'}u_{2'}+v_{1'}v_{2'})f_{12}^* f_{1'2'}$$

$$+\frac{1}{2}\sum(\langle 1\tilde{1}'|G|\tilde{2}'2\rangle$$

$$-\langle 1\tilde{1}'|G|2\tilde{2}'\rangle)(u_1v_2-v_1u_2)(u_{1'}v_{2'}-v_{1'}u_{2'})f_{12}f_{1'2'}, \quad (14)$$

$$\langle H_\omega\rangle = -\omega\langle\hat{J}_x\rangle = -\omega\sum\langle 1|j_x|2\rangle(u_1v_2-v_1u_2)f_{12}^*, \quad (15)$$

where W_0 is the term not containing f, and E is the energy of the quasiparticles;

$$E_1 = \sqrt{(\tilde{\varepsilon}_1-\lambda)^2+\Delta_1^2},$$

$$\tilde{\varepsilon}_1 = \varepsilon_1 - \sum_2(\langle 12|G|21\rangle - \langle 12|G|12\rangle)v_2^2,$$

$$\Delta_1 = \sum_2\langle 1\tilde{1}|G|\tilde{2}2\rangle u_2 v_2. \quad (16)$$

The quantity Δ (the gap in the quasiparticle spectrum) characterizes the pairing of the particles. The parameters u and v can be expressed in terms of Δ:

$$u_1^2 = \tfrac{1}{2}[1+(\tilde{\varepsilon}_1-\lambda)/E_1], \quad v_1^2 = \tfrac{1}{2}[1-(\tilde{\varepsilon}_1-\lambda)/E_1].$$

Taking the variation of < H> + < H_ω> with respect to f_{12}^* [and using (9) and (13)], we get an integral equation for determining f_{12}:

$$(E_1+E_2)f_{12} - \sum_{1'2'}\langle 1\tilde{2}|G|\tilde{2}'1'\rangle(u_1u_2+v_1v_2)$$

$$\times(u_{1'}u_{2'}+v_{1'}v_{2'})f_{1'2'} + \sum_{1'2'}(\langle 1\tilde{1}'|G|\tilde{2}'2\rangle$$

$$-\langle 1\tilde{1}'|G|\tilde{2}2'\rangle)(u_1v_2-v_1u_2)(u_{1'}v_{2'}-v_{1'}u_{2'})f_{1'2'}$$

$$=\omega(u_1v_2-v_1u_2)\langle 1|j_x|2\rangle. \quad (17)$$

Using (17), we can rewrite (14) in the form

$$\langle H\rangle = W_0 + \frac{1}{2}\omega^2\sum(u_1v_2-v_1u_2)\langle 1|j_x|2\rangle f_{12}^*\omega^{-1} \quad (18)$$

or, eliminating ω by using (15), we get

$$\langle H\rangle = W_0 + \tfrac{1}{2}J_x^2/\mathcal{J},$$

where the moment of inertia $\mathcal{J}$ is defined by the expression

$$\mathcal{J} = \sum_{12}\langle 2|j_x|1\rangle(u_1v_2-v_1u_2)f_{12}\omega^{-1}. \quad (19)$$

It is convenient to write $\mathcal{J}$ as a sum of individual terms. From (17) and (19) we find

$$\mathcal{J} = \mathcal{J}^{(1)} + \mathcal{J}^{(2)} + \mathcal{J}^{(3)}, \qquad \mathcal{J}^{(1)} = \sum_{12}\frac{|\langle 1|j_x|2\rangle|^2}{E_1+E_2}(u_1v_2-v_1u_2)^2, \quad (20)$$

$$\mathcal{J}^{(2)} = \sum_{121'2'}\frac{\langle 2|j_x|1\rangle}{E_1+E_2}\langle 1\tilde{2}|G|\tilde{2}'1'\rangle(u_1v_2-v_1u_2)$$

$$\times(u_1u_2+v_1v_2)(u_{1'}u_{2'}+v_{1'}v_{2'})f_{1'2'}\omega^{-1}, \quad (21)$$

$$\mathcal{J}^{(3)} = -\sum_{121'2'}\frac{\langle 2|j_x|1\rangle}{E_1+E_2}(\langle 1\tilde{1}'|G|\tilde{2}'2\rangle$$

$$-\langle 1\tilde{1}'|G|2\tilde{2}'\rangle)(u_1v_2-v_1u_2)^2(u_{1'}v_{2'}-v_{1'}u_{2'})f_{1'2'}\omega^{-1}. \quad (22)$$

Taking the rotation into account by means of adiabatic perturbation theory gives only the first term $\mathcal{J}^{(1)}$.[1] This method is equivalent to including only the diagonal corrections to the average values (11), which naturally can be done without going beyond the scope of the transformation (2). The inclusion of the nondiagonal values (12) leads to the additional terms. The term $\mathcal{J}^{(2)}$ (which coincides with that found by Migdal[2]) takes account of the influence of rotation on the pairing. The additional term $\mathcal{J}^{(3)}$ describes the change in the self-consistent field of the nucleons as a result of the rotation. In the absence of pairing (Δ = 0), the term $\mathcal{J}^{(1)}$ is equal to the rigid value of the moment of inertia, and decreases with increasing Δ, going to zero for Δ → ∞. The term $\mathcal{J}^{(2)}$ goes to zero for Δ = 0, and reaches the hydrodynamic value for Δ → ∞. $\mathcal{J}^{(3)}$ gives a correction of order $A^{-1/3}$ to $\mathcal{J}$.

[1] S. T. Belyaev, Kgl. Danske Videnskab. Selskab, Mat.-fys. Medd. 31, No. 11 (1959).

[2] A. B. Migdal, JETP 37, 249 (1959), Soviet Phys. JETP 10, 176 (1960).

[3] N. N. Bogolyubov, Usp. Fiz. Nauk 67, 549 (1959), Soviet Phys. Uspekhi 2, 236 (1959).

Translated by M. Hamermesh
104

SOVIET PHYSICS JETP VOLUME 13, NUMBER 2 AUGUST, 1961

PHOTOPRODUCTION OF NEUTRINO-ANTINEUTRINO PAIRS ON ELECTRONS

WANG JUNG, J. FISCHER, I. CIULLI, and S. CIULLI

Joint Institute for Nuclear Research

Submitted to JETP editor September 30, 1960

J. Exptl. Theoret. Phys. (U.S.S.R.) 40, 676-677 (February, 1961)

The cross section for the process $\gamma + e^- \to \mu^- + \nu + \overline{\nu}$ is calculated in the extreme relativistic approximation.

TWO years ago, D. I. Blokhintsev[1] pointed out that at sufficiently high energies weak interactions can become comparable with electromagnetic interactions. According to his estimates, the process $\gamma + e^- \to \mu^- + \nu + \overline{\nu}$ has an especially large cross section, which reaches that of the Compton effect at 250 Bev. We have calculated the cross section for this process, and our result confirms this estimate.

The interaction Hamiltonian has the following form:

$$H = ie(\bar{\psi}_e \hat{A} \psi_e) + ie(\hat{\psi}_\mu \hat{A} \psi_\mu) + f(\bar{\psi}_e \gamma_\alpha (1 + \gamma_5) \psi_\mu)$$
$$\times (\bar{\psi}_\nu \gamma_\alpha (1 + \gamma_5) \psi_\nu) + f(\bar{\psi}_\mu \gamma_\alpha (1 + \gamma_5) \psi_e)(\bar{\psi}_\nu \gamma_\alpha (1 + \gamma_5) \psi_\nu).$$

In the computations, we included the two lowest order diagrams, which are similar to the corresponding diagrams for the Compton effect.

Averaging over initial polarizations and summing over final polarizations, and dropping unimportant terms which contain m_e^2 and m_μ^2, we get the following expression for the total cross section:

$$\sigma_\mu = \frac{1}{v} \frac{e^2 f^2}{(2\pi)^5} \frac{8}{\omega \varepsilon_e} \int \frac{d^3 p_\mu d^3 p_\nu d^3 p_{\bar{\nu}}}{\varepsilon_\mu \varepsilon_\nu \varepsilon_{\bar{\nu}}} \delta^4 (p_e + k - p_\mu - p_\nu - p_{\bar{\nu}})$$
$$\times \Big[- \frac{(kp_e)(p_{\bar{\nu}} k)(p_\nu p_\mu)}{[(p_e + k)^2 + m_e^2]^2} - \frac{(kp_\mu)(p_{\bar{\nu}} p_e)(p_\nu k)}{[(p_\mu - k)^2 + m_\mu^2]^2}$$
$$+ [(p_e + k)^2 + m_e^2]^{-1} [(p_\mu - k)^2 + m_\mu^2]^{-1} \{[2(p_e p_\mu)$$
$$- (p_e k) + (p_\mu k)] (p_{\bar{\nu}} p_e)(p_\nu p_\mu) + (p_e p_\mu)(p_{\bar{\nu}} k)(p_\nu p_\mu)$$
$$- (p_e p_\mu)(p_{\bar{\nu}} p_e)(p_\nu k) + (kp_\mu)(p_{\bar{\nu}} p_e)(p_\nu p_e)$$
$$- (kp_e)(p_{\bar{\nu}} p_\mu)(p_\nu p_\mu)\} \Big].$$

We have integrated this expression (in the center-of-mass system) in the following, extreme relativistic, approximation:

$$\varepsilon_e = \omega = E/2, \qquad \varepsilon_\mu = |\mathbf{p}_\mu|, \qquad \varepsilon_\mu^{max} = E/2, \ v = 2,$$

where $E = \omega + \epsilon_e$.

The final expression for the cross section, in this approximation, has the form

$$\sigma_\mu = \frac{e^2 f^2}{4\pi^3} \omega^2 \left(\ln \frac{2\omega}{m_\mu} - 0.798 \right),$$

where ω is the energy of the photon in the c.m. system.

Using the well known expression for the Compton cross section in the c.m. system, we found the following condition for satisfying the inequality $\sigma_\mu \geq \sigma_C$:

$$(e^2 f^2 / 4\pi^3) \omega^2 \geqslant \pi r_0^2 m_e^2 / \omega^2 \equiv \pi (e^2 / 4\pi)^2 \omega^{-2}.$$

This condition is satisfied for values of ω greater than 242 Bev in the c.m. system.

In conclusion, the authors express their deep gratitude to D. I. Blokhintsev for posing this problem and for valuable discussions.

---

[1] D. I. Blokhintsev, Nuovo cimento 9, 925 (1958); D. I. Blokhintsev, JETP 35, 254 (1958), Soviet Phys. JETP 8, 174 (1959); M. A. Markow, Hyperonen und K-Mesonen, Verlag der Wissenschaften, Berlin, 1960, p. 292.

Translated by M. Hamermesh
105

SOVIET PHYSICS JETP VOLUME 13, NUMBER 2 AUGUST, 1961

POSITIONS OF THE SINGULARITIES OF CERTAIN FEYNMAN DIAGRAMS

V. A. KOLKUNOV

Submitted to JETP editor September 30, 1960

J. Exptl. Theoret. Phys. (U.S.S.R.) 40, 678-683 (February, 1961)

The position of the singularity is determined for diagrams that describe the scattering of two particles.

In studying the scattering amplitude for two particles, one needs to investigate the distribution of the singularities of the Feynman diagrams. The purpose of the present paper is the determination of the positions of the singular points of certain Feynman diagrams. The position of the singular point of a diagram can be determined by the solution of the system of Landau equations, which have been investigated in a number of papers.[1-4]

Suppose we have a certain Feynman diagram (Fig. 1) with four free lines. Its singular points are determined by the system of Landau equations:

$$\sum q = p, \qquad (1)$$

$$\sum q = 0, \qquad (2)$$

$$\sum \alpha q = 0, \qquad (3)$$

$$q^2 = m^2, \qquad (4)$$

$$\sum \alpha = 1, \quad \alpha > 0, \qquad (5)$$

where q are the internal four-momenta, p are the external four-momenta, m are the masses of the internal particles, and α are the Feynman parameters.

Equations (1) and (2) express the conservation of four-momentum at the external and internal vertices of the diagram.

The solution of the system of equations for a symmetrical diagram has a remarkable property: if a replacement $q_i \rightarrow \pm q_{i'}$ takes the diagram into itself, then

$$\alpha_i = \alpha_{i'}, \quad q_i q_k = \pm q_{i'} q_{k'}, \quad q_i q_{k'} = \pm q_{i'} q_k. \qquad (6)$$

The sign of the scalar product is determined by the directions of the vectors in the diagram. As has been shown in a paper by Okun' and Rudik,[2] for diagrams with four free lines one still has to determine the values of the squares of the external four-momenta,

$$p_1^2 = M_1^2, \quad p_2^2 = M_2^2, \quad p_3^2 = M_3^2, \quad p_4^2 = M_4^2, \qquad (7)$$

after which one can determine the connection between $W^2 = (p_1 + p_2)^2$ and $Q^2 = (p_1 + p_3)^2$ at the singular point.

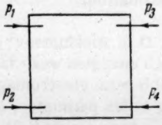

FIG. 1

Let us consider the diagram of Fig. 2. It is symmetrical with respect to the two transformations

$$q_1 \leftrightarrow -q_1, \quad q_2 \leftrightarrow -q_4, \quad q_5 \leftrightarrow q_6, \quad q_7 \leftrightarrow q_8, \quad q_3 \leftrightarrow -q_3;$$
$$q_1 \leftrightarrow -q_3, \quad q_2 \leftrightarrow -q_2, \quad q_4 \leftrightarrow -q_4, \quad q_5 \leftrightarrow q_7, \quad q_6 \leftrightarrow q_8.$$

Therefore $\alpha_1 = \alpha_3 = \alpha$, $\alpha_2 = \alpha_4 = \beta$, $\alpha_5 = \alpha_6 = \alpha_7 = \alpha_8 = 1$. The last relations can be written if we omit Eq. (5), as we shall do.

The equations (3) have the form

$$\alpha q_1 = q_5 - q_6, \quad \beta q_4 = q_7 - q_5. \qquad (8)$$

Since $q_1^2 = q_3^2 = p_1^2 = p_2^2 = p_3^2 = p_4^2 = \mu^2$ and $q_2^2 = q_4^2 = q_5^2 = q_6^2 = q_7^2 = q_8^2 = 1$, we can get from Eq. (8) the values of the scalar products by taking the squares of the equations: $q_{56} = 1 - \frac{1}{2}\alpha^2\mu^2$, $q_{57} = 1 - \frac{1}{2}\beta^2$, where $q_{ik} \equiv q_i q_k$.

If we multiply the equations (8) respectively by q_1 and q_4 and use the relations $q_{15} = -q_{16}$, $q_{47} = -q_{45}$, which follow from the symmetry of the diagram, we get $q_{15} = \frac{1}{2}\alpha\mu^2$, $q_{47} = \frac{1}{2}\beta$.

To determine the quantity q_{58} we use the equation of conservation of four-momentum at the internal vertex, which we multiply by q_5:

$$q_{58} = -1 - q_{56} - q_{57} = -3 + \tfrac{1}{2}(\beta^2 + \alpha^2\mu^2).$$

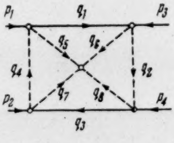

FIG. 2

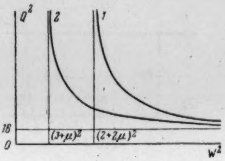

FIG. 3

The other quantities q_{ik} are determined from the equations obtained by multiplying (8) by various four-vectors q:

$$q_{18} = (2\beta^2 + \alpha^2\mu^2 - 8) / 2\alpha, \quad q_{13} = (2\beta^2 + \alpha^2\mu^2 - 8) / \alpha^2,$$
$$q_{48} = (8 - 2\alpha^2\mu^2 - \beta^2) / 2\beta, \quad q_{24} = (\beta^2 + 2\alpha^2\mu^2 - 8) / \beta^2,$$
$$q_{14} = (4 - \alpha^2\mu^2 - \beta^2) / \alpha\beta.$$

If we substitute the values of q_{14}, q_{15}, q_{45} in the equation $p_1^2 = \mu^2 = (q_1 + q_5 - q_4)^2$, we get a relation connecting α and β:

$$(2 + \alpha)\beta = 4 - \alpha^2\mu^2.$$

It is now easy to find the dependence of $W^2 = (p_1 + p_2)^2$ and $Q^2 = (p_1 + p_3)^2$ on α:

$$W^2 = \alpha^{-1}(2 + \alpha\mu^2)\,[8 + 2\alpha - (\alpha\mu)^2],$$
$$Q^2 = (8 + 2\alpha - \alpha^2\mu^2)^2/(4 - \alpha^2\mu^2), \tag{9}$$

where α varies from 0 to $2/\mu$, which follows from the fact that α and β are positive. The dependence of Q^2 on W^2 is shown in Fig. 3 (curve 1). If $\mu = 1$, the middle point $Q^2 = W^2 = 27$ is obtained for $\alpha = 1$.

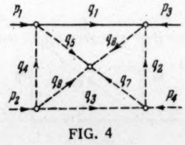

FIG. 4

Let us now study the singularities of the diagram shown in Fig. 4. It is invariant with respect to only one transformation:

$$q_1 \leftrightarrow -q_1, \quad q_2 \leftrightarrow q_4, \quad q_5 \leftrightarrow q_6, \quad q_7 \leftrightarrow q_8, \quad q_3 \leftrightarrow -q_3,$$

from which we have $\alpha_5 = \alpha_6 = \alpha$, $\alpha_7 = \alpha_8 = \beta$, $\alpha_2 = \alpha_4 = 1$. If we set $\alpha_3 = \gamma\beta$, then after some slight manipulation we can rewrite (3) as

$$q_4 = \beta q_8 - \alpha q_5, \quad \gamma q_3 = q_8 - q_7, \quad \gamma q_1 = \mu\,(q_5 - q_6). \tag{10}$$

The further solution of the system of equations is analogous to the previous case, and therefore we shall not present it. The answer is:

$$W^2 = (3 + \mu)^2 + (4 + 4\mu + 4\mu\gamma + \mu\gamma^2)\left(\frac{2}{\gamma} - 1\right),$$
$$Q^2 = \left(\frac{2+\gamma}{2-\gamma}\right)\left(\frac{4 + 4\mu + 2\mu\gamma - \mu\gamma^2}{1 + \mu + \mu\gamma}\right)^2. \tag{11}$$

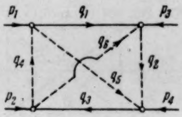

FIG. 5

From the condition that α is positive we find that γ must vary over the range from 0 to 2. For $\mu = 1$ Eq. (11) coincides with Eq. (9). The relation between W^2 and Q^2 is shown in Fig. 3 (curve 2).

Let us now go on to the diagram of Fig. 5, which admits two symmetry transformations:

$$q_1 \leftrightarrow -q_1, \quad q_4 \leftrightarrow -q_2, \quad q_3 \leftrightarrow -q_3, \quad q_4 \leftrightarrow -q_6;$$
$$q_2 \leftrightarrow -q_3, \quad q_4 \leftrightarrow -q_4, \quad q_2 \leftrightarrow -q_2, \quad q_5 \leftrightarrow q_6.$$

From these we have $\alpha_1 = \alpha_3 = \alpha$, $\alpha_2 = \alpha_4 = \beta$, $\alpha_5 = \alpha_6 = 1$. The relations (3) now reduce to a single equation:

$$\alpha q_1 + \beta q_2 = q_5. \tag{12}$$

If we multiply this equation by the various q_i, then by using the symmetry conditions we can find all the q_{ik} from the relations so obtained. Substituting the q_{ik} in W^2 and Q^2, we have

$$W^2 = 2\,(1 + 1/\alpha)^2\,(1 + \alpha^2\mu^2 - \beta^2),$$
$$Q^2 = 2\,(1 + 1/\beta)^2\,(1 - \alpha^2\mu^2 + \beta^2). \tag{13}$$

The equation that connects α and β is a cubic:

$$2\alpha\beta + \alpha^2\mu^2 + \beta^2 = 1 + \beta(\beta^2 - \alpha^2\mu^2 - 1) + \alpha\,(\alpha^2\mu^2 - \beta^2 - 1).$$

If we divide this equation by $(1 + \beta)^3$ and write

$$x = \alpha\mu/(1 + \beta), \; y = (1 - \beta)/(1 + \beta)$$

we get the simpler equation

$$\mu y^2 = (1 + \mu x - x^2)\,x.$$

Taking into account the fact that α is positive, we find that x and y can vary only over the ranges $x \geq 0$ and $|y| \leq 1$. The plot of the relation between Q^2 and W^2 is shown in Fig. 6.

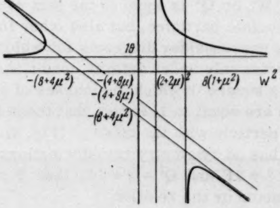

FIG. 6

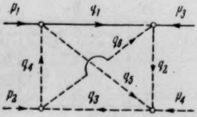

FIG. 7

Let us consider the diagram of Fig. 7. It has one symmetry transformation:

$$q_1 \leftrightarrow -q_1, \quad q_3 \leftrightarrow -q_3, \quad q_4 \leftrightarrow q_2, \quad q_5 \leftrightarrow q_6$$

and consequently $\alpha_5 = \alpha_6 = 1$, $\alpha_2 = \alpha_4 = \beta$.

The equations (3) are as follows:

$$\beta q_4 + \alpha_1 q_1 = q_6, \quad \beta q_4 + \alpha_3 q_3 = -q_5.$$

Solving this system of equations by the method presented above, we find that α_1, α_3, and β are connected by the relations

$$\alpha_1^2\mu^2(1+\beta) + \alpha_1[(1+\beta)^2 - \alpha_3^2] = (1+\beta)(1-\beta)^2,$$
$$\alpha_3^2(1+\beta) + \alpha_3[(1+\beta)^2 - \alpha_1^2\mu^2] = (1+\beta)(1-\beta)^2.$$

These equations become much simpler if we replace α_1, α_3, and β by variables x, y, z defined by

$$x = \alpha_1\mu/(1+\beta), \quad y = (1-\beta)/(1+\beta),$$
$$z = \alpha_3/(1+\beta).$$

We have

$$\mu x^2 + x(1-z^2) = \mu y^2, \; z^2 + z(1-x^2) = y^2.$$

From this we easily find that

$$z = \frac{1+\mu x}{\mu + x}\,x, \qquad y^2 = \frac{(\mu + 2x - x^3)(1+\mu x)\,x}{(\mu+x)^2}.$$

The condition that α be positive requires that $x \geq 0$, $z \geq 0$, $-1 \leq y \leq 1$. We can now find the relation between Q^2 and W^2:

$$W^2 = \left(\mu + \frac{2x}{1+y}\right)^2 + \frac{2y}{xz}\left(\mu + \frac{2x}{1+y}\right)\left(1 + \frac{2z}{1+y}\right)$$
$$+ \left(1 + \frac{2z}{1+y}\right)^2, \qquad Q^2 = 16\,\frac{1+y^2-x^2-z^2}{(1-y^2)^2}. \tag{14}$$

The curve (14) is of the same nature as the curve (13), of course with different values of the asymptotes.

We note a distinguishing feature of these diagrams: they have for the asymptotes not only lines on which W^2 or Q^2 is equal to the sum of masses of intermediate particles, but also other lines.

Let us now consider diagrams for which singularities exist only under definite conditions, for example a square in which the masses of all the particles are equal to 1, except that there is one external particle with the mass μ (Fig. 8). This diagram has no symmetry transformations. If we set $W^2 = 2 + 2F$ and $Q^2 = 2 + 2\Phi$, then F and Φ are connected by the relation

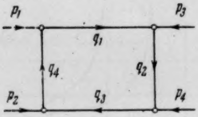

FIG. 8

$$4F(\Phi^2 - 1) = (3-\mu^2)(\Phi+1)$$
$$\pm 4\sqrt{(\Phi+1)(\Phi-0.5)(\Phi-\Phi_1)(\Phi-\Phi_2)},$$
$$4\Phi_1 = \mu^2 - 2 + \sqrt{3\mu^2(4-\mu^2)},$$
$$4\Phi_2 = \mu^2 - 2 - \sqrt{3\mu^2(4-\mu^2)}.$$

For what values of μ does the diagram have a singular point? From the condition that the Feynman parameters α be positive it follows that for $\mu^2 > 4$ there is no singular point, and for $\mu^2 < 4$ there is one. In Fig. 9 curve 1 shows the relation between Q^2 and W^2 for $\mu^2 \leq 3$, and curve 2 for $3 < \mu^2 < 4$.

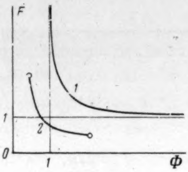

FIG. 9

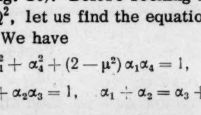

FIG. 10

Let us now consider the same square, but with a diagonal (Fig. 10). Before seeking the equations for W^2 and Q^2, let us find the equations that connect the α_i. We have

$$\alpha_1^2 + \alpha_4^2 + (2-\mu^2)\alpha_1\alpha_4 = 1,$$
$$\alpha_2^2 + \alpha_3^2 + \alpha_2\alpha_3 = 1, \quad \alpha_1 + \alpha_2 = \alpha_3 + \alpha_4. \tag{15}$$

It follows from the equations (15) that $(4-\mu^2)\alpha_1\alpha_4 = 3\alpha_2\alpha_3$, but since $\alpha > 0$, we must have $\mu^2 < 4$, which is indeed the condition for the existence of a singular point. The expressions for W^2 and Q^2 in terms of the α_i are:

$$W^2 = 1 + (1+\alpha_1+\alpha_4)(1+\alpha_2+\alpha_3)(1+\alpha_3-\alpha_2)\alpha_1^{-1}\alpha_3^{-1},$$
$$Q^2 = 1 + (1+\alpha_1+\alpha_4)(1+\alpha_2+\alpha_3)(1-\alpha_3+\alpha_2)\alpha_2^{-1}\alpha_4^{-1}.$$

The curve for this relation is shown in Fig. 11.

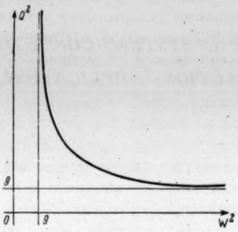

FIG. 11

The next diagram differs from that just considered in having the diagonal through different vertices (Fig. 12). We again investigate the conditions under which there is a solution with positive α. The system of equations for the α_i is more complicated:

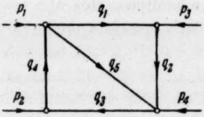

FIG. 12

$$\alpha_1^2 + \alpha_2^2 + \alpha_1\alpha_2 = 1,\ \ \alpha_3^2 + \alpha_4^2 + \alpha_3\alpha_4 = 1,$$

$$(1 + \alpha_1 + \alpha_2)(1 + \alpha_3 + \alpha_4)(\alpha_1 - \alpha_2 + \alpha_4 - \alpha_3) = (\mu^2 - 1)\,\alpha_1\alpha_4. \qquad (16)$$

It is convenient to go over to new variables x and y: $\alpha_2 = \alpha_1 x - 1,\ \ \alpha_3 = \alpha_4 y - 1.$

Then instead of Eqs. (16) we get equations for x and y:

$$\frac{2 + 2x - x^2}{1 + x + x^2} + \frac{2 + 2y - y^2}{1 + y + y^2} = \frac{\mu^2 - 1}{(1 + x)(1 + y)},$$

$$\alpha_1 = \frac{1 + 2x}{1 + x + x^2},\ \ \alpha_2 = \frac{x^2 - 1}{1 + x + x^2},$$

$$\alpha_3 = \frac{y^2 - 1}{1 + y + y^2},\ \ \alpha_4 = \frac{1 + 2y}{1 + y + y^2}. \qquad (17)$$

The condition for the α_i to be positive requires that x, y ≥ 1. With such x and y a solution of (17) exists only under the condition that $\mu^2 \leq 9$. Consequently, this diagram (Fig. 12) can have a singular point for $\mu^2 \leq 9$. The dependence of Q^2 on W^2 is of the form shown by curve 1 in Fig. 9 for $\mu^2 < 7$, and by curve 2 for $\mu^2 > 7$.

The writer expresses his deep gratitude to L. B. Okun' and A. P. Rudik for direction of this work and for their constant interest in it.

---

[1] L. D. Landau, JETP 37, 62 (1959), Soviet Phys. JETP 10, 45 (1960).

[2] L. B. Okun' and A. P. Rudik, Nuclear Physics 15, 261 (1960).

[3] Kolkunov, Okun', and Rudik, JETP 38, 877 (1960), Soviet Phys. JETP 11, 634 (1960).

[4] Kolkunov, Okun', Rudik, and Sudakov, JETP 39, 340 (1960), Soviet Phys. JETP 12, 242 (1961).

Translated by W. H. Furry
106

SOVIET PHYSICS JETP VOLUME 13, NUMBER 2 AUGUST, 1961

SINGLE PARTICLE EXCITATIONS AND SUPERFLUIDITY IN SYSTEMS CONSISTING OF FERMI PARTICLES WITH AN ARBITRARY INTERACTION. APPLICATION TO THE NUCLEUS

A. B. MIGDAL

Moscow Engineering Physics Institute

Submitted to JETP editor September 4, 1960

J. Exptl. Theoret. Phys. (U.S.S.R.) **40**, 684-697 (February, 1961)

A system of equations describing single particle excitations for excitation energies small compared to the chemical potential of the system can be obtained for an arbitrary interaction by investigating the analytic properties of the Green's function, taking pair correlation into account. Equations have been obtained which describe the excited states of a system of a finite number of particles up to terms of order $N^{-1/3}$. It is indicated how the results obtained can be applied to real nuclei.

1. INTRODUCTION

THE phenomenological approach is the only reasonable research method that yields quantitative results in the case of the many-body problem when the interaction between the particles is not small. In such an approach the problem is separated into two independent parts:

1) Derivation of the consequences of a theory into which experimentally determined constants have been introduced such as the effective mass of the particles at the Fermi surface, the depth of the effective potential well, the constant describing the Cooper pair correlation, etc. Naturally, we must first obtain for an arbitrary interaction the equations describing the behavior of the excitations of the system, and we must specify the precise meaning of the constants introduced.

2) The evaluation of these constants by some approximate method or with the aid of computers.

When the problem does not involve any small parameter, as for example in the case of the nucleus, or in the theory of metals, it is impossible to hope to obtain an analytic method of solving this second problem.

In this paper we shall be concerned only with the solution of the first problem. However, we shall specify the exact meaning of all the constants introduced, i.e., we shall indicate the set of perturbation theory graphs which corresponds to each one of the constants introduced. Unless this is done it will be impossible to find an exact approach to the solution of the second problem — the problem of the evaluation of the constants starting from a given interaction between the particles.

It is well known that systems of Fermi-particles can be divided into two classes. The first comprises systems in which the Cooper pair correlation is absent. In this case there exists a branch of excitations differing from the excitations in a Fermi-gas only by their effective mass and their effective potential well. For systems of finite size this means that there exists a spectrum of single particle excitations with energies which may be obtained from a solution of the Schrödinger equation for a single particle with an effective mass and an effective potential (when the interaction between the particles is small this effective potential reduces to the self-consistent Thomas-Fermi potential). An example of such systems are the doubly magic and their neighboring nuclei — there is no Cooper pair correlation in such nuclei.

To the second class belong systems with pair correlation. For such systems, as is shown by a study of the analytic properties of the self-energy part of the Green's function, equations may be obtained which are close to those that have been studied in the theory of superconductivity.[1] The only condition essential for obtaining these equations is that the ratio of the pair correlation energy Δ to the Fermi limiting energy ϵ_0 should be small, i.e., that the calculation is carried out to terms of order Δ/ϵ_0.

In this paper we have obtained to terms $\sim N^{-1/3}$, where N is the number of particles, a system of equations which enables us to determine the energy of the ground state and the energy of the lowest single particle excitations if we know the spectrum of single particle excitations without pair correlation. We consider a system consisting of one type of particles, but it is clear from the derivation that for two types of Fermi-particles, for example, the neutrons and the protons in a nucleus, we would obtain two independent systems of equations. Only the sets of graphs corresponding to the previously listed constants characterizing the problem become somewhat more complicated.

Application to real nuclei requires a certain development of the results obtained. First of all, the description of the single particle excitations themselves requires a more serious approach than has been adopted until now.

We shall demonstrate this on the example of a doubly magic nucleus in which there is no pair correlation. The excited state of Pb^{208} has an energy of 2.6 Mev and spin 3. If the free particle model were true the excited state of Pb^{208}, regarded as the appearance of a quasi-particle and a hole, could be obtained from the ground states of Pb^{209} and Pb^{207}. In such an approach an energy of 3.5 Mev is obtained in place of 2.6 Mev, and a spin which is not equal to 3. We shall refer to this difficulty as the "problem of the three leads." The solution of this problem requires a reasonable introduction of an interaction between excitations.

Further we must take into account the relation between the single particle states and the shape of the nucleus, and also the change in the effective potential accompanying single particle transitions. Problems of this nature have been solved in atomic mechanics and their solution within the framework of the single particle model of the nucleus presents no difficulties in principle.

The approach proposed in this paper is valid to terms of order $N^{-1/3}$. However, the fluctuating part of the neglected terms is of order $N^{-1/3}$ of their value. Therefore, the equations obtained enable us to determine the irregular variation of the masses and of the first excited states up to terms of order $N^{-2/3}$, and in the case of a nucleus this provides quite a sufficient degree of accuracy.

A further development of the technique proposed here will enable us also to determine to terms of order $N^{-1/3}$ the matrix elements for single particle transitions corresponding to the emission of γ quanta and to β decay. If comparison with experiment requires this, it will also be possible to obtain a more complicated system of equations which takes into account the possibility of pair correlation not only in a state of zero angular momentum, but also in a state with angular momentum equal to 2.

It appears to us that the completion of this program will enable us to describe quantitatively the fluctuations in the mass defects, and will enable us to give a theoretical description of the nuclear spectroscopy of single particle excitations.

2. EQUATION FOR THE GREEN'S FUNCTION

Dyson's equation for the single particle Green's function in the coordinate representation* has the form

$$(i\partial/\partial t + \mathbf{p}^2/2M)\,G(\mathbf{r},\ t;\ \ \mathbf{r}',\ t') = \delta(\mathbf{r}-\mathbf{r}')\,\delta(t-t') + \int \Sigma(\mathbf{r},\ t;\ \ \mathbf{r}_1,\ t_1)\,G(\mathbf{r}_1,\ t_1;\ \ \mathbf{r}',\ t')\,d\mathbf{r}_1\,dt_1, \tag{1}$$

where **p** is the momentum operator operating on the coordinate **r**, and Σ is the compact part of the self-energy defined by the set of graphs of the form

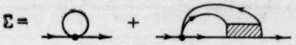

(2)

The point of intersection of the lines in this diagram corresponds to the first order in the interaction between the particles; the shaded rectangle corresponds to the set of all possible interactions between two particles.

We assume that the Hamiltonian for the system does not depend explicitly on the time. Then the quantities G and Σ will be functions only of $t-t'$. On going over to the Fourier-representation with respect to $t-t'$, we obtain

$$(\varepsilon - \mathbf{p}^2/2M)\,G(\mathbf{r},\ \mathbf{r}',\ \varepsilon) = \delta(\mathbf{r}-\mathbf{r}') + \int \Sigma(\mathbf{r},\ \mathbf{r}_1,\ \varepsilon)\,G(\mathbf{r}_1,\ \mathbf{r}',\ \varepsilon)\,d\mathbf{r}_1. \tag{3}$$

As is well known,[2] the poles of the function G in the complex plane determine the magnitude and the damping of the single particle excitations of the system. For small excitations of the system those values of ϵ play a role which lie near the Fermi limiting energy ϵ_0. It is therefore necessary to know the behavior of $\Sigma(\mathbf{r}, \mathbf{r}_1, \epsilon)$ as $\epsilon \to \epsilon_0$.

3. ANALYTICAL PROPERTIES OF THE SELF-ENERGY PART

The character of the function $\Sigma(\epsilon)$ depends in an essential manner on whether Cooper pairs can be formed near the Fermi surface. If formation of Cooper pairs is impossible, then integration over the momenta of the three lines of the second term in Eq. (2) smears out the poles contained in the Green's functions corresponding to these lines. With respect to the first term in formula (2), it may be easily seen that it is equal to

---

*The coordinate representation enables us to give a simple formulation of the boundary conditions in systems of finite size.

$$\Sigma^{(1)}(\mathbf{p}_1, \mathbf{p}_2, \varepsilon) = \sum_{\mathbf{q}} n_{\mathbf{p}_1-\mathbf{q}} V_{\mathbf{q}} \delta_{\mathbf{p}_1\mathbf{p}_2} \tag{4}$$

and does not depend on ϵ. Here $n_{\mathbf{p}}$ are the occupation numbers, $V_{\mathbf{q}}$ is the Fourier component of the interaction potential between the particles. The form of the function $\Sigma(\epsilon)$ as $\epsilon \to \epsilon_0$ can be obtained by using the methods of the theory of dispersion relations.[3]

It may be easily shown that the imaginary part of Σ as $\epsilon \to \epsilon_0$ has the form

$$\operatorname{Im} \Sigma = \alpha (\mathbf{r}, \mathbf{r}_1) |\varepsilon - \varepsilon_0| (\varepsilon - \varepsilon_0) + \beta (\mathbf{r}, \mathbf{r}_1) (\varepsilon - \varepsilon)_0^3.$$

From this by utilizing the analytic properties of Σ we can show that

$$\Sigma = \Sigma_0 (\mathbf{r}, \mathbf{r}_1, \varepsilon) + \alpha (\mathbf{r}, \mathbf{r}_1) | \varepsilon - \varepsilon_0 | (\varepsilon - \varepsilon_0)\, i$$
$$+ 2\pi^{-1}\beta (\mathbf{r}, \mathbf{r}_1) | \varepsilon - \varepsilon_0 |^3 \ln [i\varepsilon_0/(\varepsilon - \varepsilon_0)], \tag{5}$$

where Σ_0 is a function of ϵ which has no singularities as $\epsilon \to \epsilon_0$ (Σ_0 has singularities at a distance of $\sim \epsilon_0$ from the real axis).

The logarithmic singularity of Σ at $\epsilon = \epsilon_0$ makes no contribution to the quantities $(\Sigma)_{\epsilon=\epsilon_0}$ and $(\partial\Sigma/\partial\epsilon)_{\epsilon=\epsilon_0}$ which determine in an essential manner the behavior of the Green's function near the Fermi limit. Therefore, when pair correlation is absent, we can replace Σ by $(\Sigma)_{\epsilon=\epsilon_0} + (\partial\Sigma/\partial\epsilon)_{\epsilon=\epsilon_0}(\epsilon - \epsilon_0)$, and this greatly simplifies Eq. (3).

The situation is different when pair correlation is present. In this case Σ contains terms which do not involve the previously mentioned integration over the momenta of the three lines. Indeed, when two of the three lines in (2) form a Cooper pair the state of the third line is determined by the conservation laws. For example, if the pair is formed with an angular momentum equal to zero, then the angular momentum of the third line must be equal to the angular momentum of the incident line. As a result a pole with respect to ϵ appears in Σ which lies on the real axis near $\epsilon = \epsilon_0$, and it is not possible to expand Σ in a series with respect to $\epsilon - \epsilon_0$. Below we shall outline a method of separating out from Σ factors which vary slowly near $\epsilon = \epsilon_0$.

4. THE INDEPENDENT QUASIPARTICLE APPROXIMATION

When the dimensions of the system are large compared to the distance r_0 between the particles,* Eq. (3) can be greatly simplified. In an infinite homogeneous system Σ and G depend on $\mathbf{r}_1 - \mathbf{r}_2$. In a finite system, up to terms in r_0/R, where R is the size of the system, we can set $\Sigma(\mathbf{r}_1, \mathbf{r}_2, \epsilon) = \Sigma'(\mathbf{r}_1, \mathbf{r}_1 - \mathbf{r}_2, \epsilon)$. With respect to its first argument $\Sigma'(\mathbf{r}_1, \mathbf{r}_1 - \mathbf{r}_2, \epsilon)$ varies appreciably only near the surface of the system and vanishes when the second argument becomes much larger than the particle wavelength at the Fermi limit.

We shall be interested in the equation for the Green's function in those cases when all the participating quasiparticles have energies close to the Fermi limit. As will be apparent from subsequent discussion this will have the consequence that in the expansion.

$$G (\mathbf{r}, \mathbf{r}', \varepsilon) = (2\pi)^{-6} \int G (\mathbf{p}, \mathbf{p}', \varepsilon)\, e^{i\mathbf{p}\mathbf{r} - i\mathbf{p}'\mathbf{r}'} d\mathbf{p}\, d\mathbf{p}'$$

only terms with $p, p' \approx p_0$ will occur.

We denote by Σ_R the regular part of Σ' which does not contain the Cooper singularity. By utilizing the properties of Σ and G to which we have referred we can easily obtain†

$$\int \Sigma_R(\mathbf{r}, |\mathbf{r} - \mathbf{r}_1|, \varepsilon)\, G (\mathbf{r}_1, \mathbf{r}', \varepsilon)\, d\mathbf{r}_1$$
$$= (2\pi)^{-3} \int \Sigma_R (\mathbf{r}, p, \varepsilon)\, G (\mathbf{p}, \mathbf{r}', \varepsilon)\, e^{i\mathbf{p}\mathbf{r}}\, d\mathbf{p}$$
$$\approx \{\Sigma_R (\mathbf{r}, p_0, \varepsilon_0) + (\partial\Sigma_R (\mathbf{r}, p_0, \varepsilon_0)/\partial\varepsilon_0) (\varepsilon - \varepsilon_0) + (M/p_0)$$
$$\times (\partial\Sigma_R (\mathbf{r}, p_0, \varepsilon_0)/\partial\varepsilon_0) (\mathbf{p}^2/2M - p_0^2/2M)\}\, G (\mathbf{r}, \mathbf{r}', \varepsilon), \tag{6}$$

where $\mathbf{p}$ is the momentum operator operating on the coordinate $\mathbf{r}$, and $\Sigma_R(\mathbf{r}, p_0, \epsilon_0)$ is defined by the expansion

$$\Sigma_R (\mathbf{r}, |\mathbf{r} - \mathbf{r}'|, \varepsilon_0) = (2\pi)^{-3} \int \Sigma_R (\mathbf{r}; p, \varepsilon)\, e^{i\mathbf{p}(\mathbf{r} - \mathbf{r}')}\, d\mathbf{p}.$$

In the second and the third terms in the curly brackets of (6) we can again replace to terms of order r_0/R the function $\Sigma(\mathbf{r}, p_0, \epsilon_0)$ which is a slowly varying function of $\mathbf{r}$ by $\Sigma_R(0, p_0, \epsilon_0) \equiv \Sigma_R(p_0, \epsilon_0)$. As a result of these simplifications, Eq. (3) assumes the form

---

*We assume that the distance between the particles, the range of the forces, and the wavelength at the Fermi surface are quantities of the same order of magnitude.

†It may be shown[4] that the expression $(1 - \partial\Sigma_R/\partial\varepsilon_0)^{-1}$ gives the value of the discontinuity in the momentum distribution of the particles in a system without pairing, with $\partial\Sigma_R/\partial\varepsilon < 0$.

$$\{\varepsilon - \mathbf{p}^2/2M_{eff} - U(\mathbf{r})\}\,[1 - (\partial\Sigma_R(p_0, \varepsilon_0)/\partial\varepsilon_0)]\,\widetilde{G}(\mathbf{r}, \mathbf{r}', \varepsilon)$$
$$= \delta(\mathbf{r} - \mathbf{r}') + \int d\mathbf{r}_1\,\Sigma_k(\mathbf{r}, \mathbf{r}_1, \varepsilon)\,\widetilde{G}(\mathbf{r}, \mathbf{r}', \varepsilon);$$
$$M_{eff} = M\,\frac{1 - \partial\Sigma_R/\partial\varepsilon_0}{1 + (\partial\Sigma_R/\partial p_0)(M/p_0)},$$
$$U(\mathbf{r}) = \frac{\Sigma_R(\mathbf{r}, p_0, \varepsilon_0) - \varepsilon_0\partial\Sigma_R/\partial\varepsilon_0 - (p_0/2)(\partial\Sigma_R/\partial p_0)}{1 - \partial\Sigma_R/\partial\varepsilon_0}. \tag{7}$$

Here $\widetilde{G} = (1 - \partial\Sigma_R/\partial\epsilon_0)\,G$ is the renormalized Green's function; $U(\mathbf{r})$ represents the effective potential well for the quasiparticle, it varies appreciably only near the surface of the system within a layer of thickness $\sim r_0$; $\Sigma_k(\mathbf{r}, \mathbf{r}_1, \epsilon)$ is the part of the self-energy due to pair correlations.

Thus, in the absence of pairing we obtain to terms of order r_0/R the equation for the renormalized Green's function for the independent quasiparticles of effective mass M_{eff} and with the effective potential $U(\mathbf{r})$. Formula (7) represents the basis for the independent quasiparticle method in systems with a strong interaction.

Equation (7) for $\Sigma_k = 0$ determines the Green's function for the Schrödinger equation:

$$i\partial\Psi/\partial t = H\Psi, \quad H = \mathbf{p}^2/2M_{eff} + U(\mathbf{r}). \tag{8}$$

Therefore, the energies of the single particle excitations of the system may be found in this approximation as the eigenvalues of (8)

$$H\varphi_\lambda = \varepsilon_\lambda\varphi_\lambda. \tag{9}$$

In the case of a nucleus, when the quantity $r_0/R \sim A^{-1/3}$ is not very small, the independent quasiparticle approximation may turn out to be insufficient for some problems, and may have to be corrected, for example, by means of taking into account the dependence of $\partial\Sigma_R/\partial\epsilon_0$ and $\partial\Sigma_R/\partial p_0$ on $\mathbf{r}$, and this will lead to the operator $U(\mathbf{r})$ which depends on the nature of the excitation of the system. In our subsequent discussion we shall assume that the operator $U(\mathbf{r})$ includes the spin-orbit interaction.

For the solution of equation (7) for $\Sigma_k \neq 0$, it is useful to expand $\widetilde{G}$ in terms of the eigenfunctions φ_λ of Eq. (9):

$$\widetilde{G}(\mathbf{r}, \mathbf{r}', \varepsilon) = \sum_{\lambda\lambda'} G_{\lambda\lambda'}(\varepsilon)\,\varphi_\lambda(\mathbf{r})\,\varphi^*_{\lambda'}(\mathbf{r}').$$

As a result of substituting into (7) we obtain

$$(\varepsilon - \varepsilon_\lambda)\,G_{\lambda\lambda'} = \delta_{\lambda\lambda'} + \sum_{\lambda_1}\left(\varphi_\lambda \left| \frac{\Sigma_k}{1 - \partial\Sigma_R/\partial\varepsilon_0} \right| \varphi_{\lambda_1}\right) G_{\lambda_1\lambda'}. \tag{10}$$

In the absence of pairing, (10) yields

$$G^0_{\lambda\lambda'} = \delta_{\lambda\lambda'}/(\varepsilon - \varepsilon_\lambda + i\alpha\,|\varepsilon - \varepsilon_{\lambda_0}|\,(\varepsilon - \varepsilon_{\lambda_0})),$$

where ϵ_{λ_0} is the highest filled state.

For the determination of the imaginary part of the denominator we have utilized expression (5).

5. THE SELF ENERGY PART OF Σ_k ASSOCIATED WITH PAIR CORRELATION

We give a graphic representation of the term of Σ which corresponds to the formation of a Cooper pair which we denote by a wavy line:

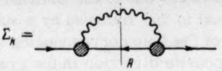

(11)

We note that a graph of the form

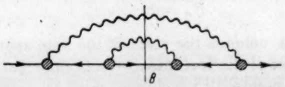

(12)

does not appear in Σ_k, since the state of the system corresponding to the point B is identical with the initial state (one pair has been added to and subtracted from the system). Therefore, a graph of the form (12) is a noncompact one, and will be obtained by a repetition of the graph of formula (11).

Both here and subsequently we assume that in our system formation of pairs of only one type is possible. By a similar method we can also obtain equations for several types of pairs. Moreover, we do not consider the excited states of the pairs, which, as may be easily seen, give corrections of the order of various powers of the small parameter Δ/ϵ_0, where Δ is the pairing energy.[*] We can also leave out of consideration graphs of the form

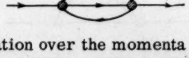

since integration over the momenta of the intermediate lines will smear out the pole due to the pairing, and the graph under consideration may be regarded as being included in the regular part of Σ_R. The analytic expression corresponding to the graph of formula (11) may be obtained in a manner analogous to the way in which this is done in the theory of dispersion relations.

If the state of the particle at the instant A is determined by the conservation laws, then the graph of formula (11) is a graph of pole type and, consequently,

---

[*] Since the maximum momentum of the center of mass of the pair is determined by the relation[5] $k_m \approx p_0\Delta/\varepsilon_0$, the volume in phase space of the possible excited states is $\approx(p_0\Delta/\varepsilon_0)^3$. The graph of the form (12), which will appear in Σ_k if one of the pairs is in an excited state, will turn out to be small, of order $(\Delta/\varepsilon_0)^3$.

$$(\Sigma_h)_{\lambda\lambda'} = \delta_{\lambda\lambda'}\,|\Delta_\lambda|^2/(\varepsilon_\lambda - E_A),$$

where Δ_λ denotes the shaded vertex which depends on the state λ of the incident particle, and E_A is the change in the energy of the system resulting from the transition to the state A.

E_A can be represented as the change in the energy of the system due to the addition of two particles (equal to 2μ) followed by a subtraction of the energy of the hole corresponding to the line going in the opposite direction in the graph of formula (11):

$$E_A = 2\mu - \varepsilon_{-\lambda},$$

where $-\lambda$ denotes the state of the hole appearing as a result of the formation of a Cooper pair. Thus, we obtain

$$(\Sigma_h)_{\lambda\lambda'} = \delta_{\lambda\lambda'}\,|\Delta_\lambda|^2/(\varepsilon_\lambda + \varepsilon_{-\lambda} - 2\mu). \qquad (13)$$

In the more general case a pair can be produced as the result of the appearance of a hole in an arbitrary state. Then we obtain from (11)

$$(\Sigma_h)_{\lambda\lambda_1} = \sum_{\lambda'} \Delta_{\lambda\lambda'}\Delta_{\lambda'\lambda_1}/(\varepsilon + \varepsilon_{\lambda'} - 2\mu). \qquad (14)$$

We shall see later that expression (13) is valid only for the potential U(**r**) in the form of a rectangular well, while in other cases expression (14) should be used.

Equation (11) can also be written in the symbolic form

$$\Sigma_h = \Delta G_0^* \Delta^*. \qquad (15)$$

G_0^* includes graphs contained in Σ_R, but, as has been shown earlier, does not include graphs of the form

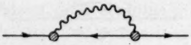

(16)

In the representation of the φ_λ the quantity G_0^* is equal to

$$(G_0^*)_{\lambda\lambda'} = \delta_{\lambda\lambda'}/(\varepsilon + \varepsilon_\lambda - 2\mu).$$

Thus, G_0 is the renormalized Green's function for the hole in the absence of pairing.

Expression (15) in the representation of the φ_λ leads to formula (14).

6. EQUATION FOR THE VERTEX PART

The equation for the vertex part Δ is of a form reminiscent of the Bethe-Salpeter equation, but with a very essential modification.

It may be easily seen that the equation for Δ is of the form

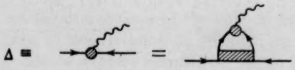

, (17)

where the shaded rectangle denotes the set Γ of the interaction graphs which are not joined by two vertical straight lines, i.e., it is the same quantity which appears in the Bethe-Salpeter equation. However, instead of the exact G and G^* we must in the following discussion substitute G and G_0^*, i.e., graphs of the form (16) are absent in one of the lines. Indeed, the expression which appears after the shaded rectangle may be represented in the following form (for the sake of simplification we do not draw the graphs corresponding to Σ_R)

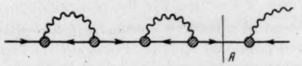

,

i.e., the outgoing pair is at the right-hand edge of the graph. The graph

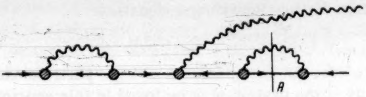

should not be taken into account, as it is identical with the one mentioned previously, since the state A is the same for both graphs. Thus, the equation for Δ has the form

$$\Delta = \Gamma G \Delta G_0^*. \qquad (17')$$

The equation for Δ^* is obtained from the graph

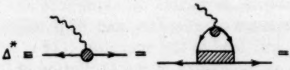

$= \Gamma^* G_0^* \Delta^* G$. (18)

Equation (18) has in the coordinate representation the form

$$\Delta^*(x_1, x_2) = \int \Gamma^*(x_1, x_2; x_3, x_4)\, F(x_3, x_4)\, dx_3\, dx_4, \qquad (19)$$

where F denotes the expression

$$F(x_1, x_2) = G_0^* \Delta^* G$$

$$= \int G_0^*(x_1, x_3)\, \Delta^*(x_3, x_4)\, G(x_1, x_2)\, dx_3\, dx_4;$$

x is the set of coordinates **r**, t. These equations are greatly simplified when the dimensions of the system are much larger than the distance between the particles. In an infinite homogeneous system the expressions $\Delta(x_1, x_2)$ and $F(x_1, x_2)$ depend only on ($\mathbf{r}_1-\mathbf{r}_2$ and t_1-t_2). Therefore, in a finite system, on going over to the Fourier components with respect to the difference variables, we obtain

$$\Delta(x_1, x_2) = (2\pi)^{-4}\int \Delta(x_1, p, \varepsilon)\, e^{i\mathbf{p}(\mathbf{r}_1-\mathbf{r}_2)}e^{i\varepsilon(t_1-t_2)}dp\, d\varepsilon,$$

where $\Delta(x_1, p, \epsilon)$ is a slowly varying function of the first argument which does not depend on the angles specifying the orientation of the vector **p**. Similarly, we can introduce the quantity $F(x_1, p, \epsilon)$ which has the same properties. To quantities of order r_0/R the interaction $\Gamma(x_1, x_2; x_3, x_4)$ depends only on three differences of the quantities x_1, x_2, x_3, x_4, with Γ appreciably differing from zero when all the differences $|\mathbf{r}_i-\mathbf{r}_k| \lesssim r_0$ and $(t_i-t_k) \leq \hbar/\epsilon_0$.

As will be shown later, the quantity $F(x, p, \epsilon)$ has a sharp maximum at $\epsilon = \epsilon_0$. By utilizing the previously mentioned properties of Γ and F, and by going over to the Fourier representation with respect to x_1-x_2 and x_3-x_4, we obtain from (19)

$$\Delta^*(x, p, \varepsilon) = (2\pi)^{-4}\int \Gamma^*(x-x', \mathbf{p}, \varepsilon, \mathbf{p}', \varepsilon_0)\, F(x, p', \varepsilon')\, dx'\, d\mathbf{p}'\, d\varepsilon'$$

We shall be interested in the value of Δ^* for $p = p_0$ and $\epsilon = \epsilon_0$. By denoting

$$\Delta^*(x) \equiv \Delta^*(x, p_0, \varepsilon_0)$$

and by utilizing the approximate lack of dependence of $\Delta^*(x, p, \epsilon)$ and $F(x, p, \epsilon)$ on the angles specifying the orientation of the vector **p**, we obtain

$$\Delta^*(x) = (2\pi)^{-4}\int \gamma^*(p')\, F(x, p', \varepsilon')\, dp'\, d\varepsilon',$$

$$\gamma^*(p') = \frac{1}{4\pi}\int \Gamma^*(x-x', p_0, \varepsilon_0, \mathbf{p}', \varepsilon_0)\, dx'\, d\omega_{\mathbf{p}'}, \qquad (20)$$

where the integral over $d\omega_{p'}/4\pi$ denotes averaging over the angles specifying the orientation of the vector $\mathbf{p}'$.

The dependence on x of $\int F(x, p', \epsilon')d\epsilon'$ is determined by the inhomogeneity of the system, or by the effect of external fields. It may be easily shown by considering a homogeneous system in an external field which varies appreciably over a distance $\sim l \gg r_0$ that the dependence of $F(x, p, \epsilon)$ on x is determined by particles with momenta lying close to p_0 in the range $\delta p \sim \hbar/l$. Because of this the difference

$$\int \{F(x, p', \varepsilon') - F(0, p', \varepsilon')\}\, d\varepsilon'$$

has a sharp maximum at $p' \approx p_0$. Therefore, we obtain from (20)

$$\Delta^*(x) - \Delta^*(0) = \gamma_0^*\{F(x, x) - F(0, 0)\}. \qquad (21)$$

where $\gamma_0^* = \gamma^*(p_0)$.

In formula (21) we have returned to the coordinate representation for F:

$$F(x, x') = (2\pi)^{-4}\int F(x, p, \varepsilon)\, e^{i\mathbf{p}(\mathbf{r}-\mathbf{r}')+i\varepsilon(t-t')}d\mathbf{p}\, d\varepsilon.$$

As $x \to x'$ this expression diverges logarithmically in the integration over $p - p_0$. Naturally, expression (21) does not contain any divergences. We shall utilize in place of (21) the simpler expression

$$\Delta^*(x) = \gamma_0^* F(x, x), \qquad (21')$$

in which the logarithmic divergence has been eliminated by cutting off the integration over p: $p_1 < p < p_2$; $p_1, p_2 \sim p_0$.

7. THE CONNECTION BETWEEN THE EQUATIONS FOR THE GREEN'S FUNCTION AND FOR THE VERTEX PART WITH THE METHOD OF TWO GREEN'S FUNCTIONS

We write in symbolic form the system of equations (7), (15), (17), and (18) which we have obtained:

$$G_0^{-1}\widetilde{G} = \mathrm{I} + \Delta G_0^*\Delta^*\widetilde{G}a,$$

$$\Delta = a\Gamma\widetilde{G}\Delta G_0^*, \qquad \Delta^* = a\Gamma^* G_0^*\Delta^*\widetilde{G}, \qquad (22)$$

where $\widetilde{G}$ is the renormalized Green's function:

$$G = a\widetilde{G}, \qquad a = (1 - \partial\Sigma_R/\partial\varepsilon_0)^{-1}. \qquad (23)$$

The factor a can be eliminated from (22) by introducing renormalized values of Δ and Γ:

$$\widetilde{\Delta} = \sqrt{a}\Delta, \qquad \widetilde{\Gamma} = a\Gamma. \qquad (24)$$

We denote

$$\widetilde{F} = -iG_0^*\Delta^*\widetilde{G}, \qquad \widetilde{F}^* = i\widetilde{G}\Delta G_0^*. \qquad (25)$$

We obtain from (22) — (25)

$$G_0^{-1}\widetilde{G} = \mathrm{I} + i\widetilde{\Delta}\widetilde{F}, \qquad (G_0^*)^{-1}\widetilde{F} = -i\widetilde{\Delta}^*\widetilde{G};$$

$$\widetilde{\Delta} = \widetilde{\Gamma}\widetilde{F}^*, \qquad \widetilde{\Delta}^* = \widetilde{\Gamma}^*\widetilde{F}. \qquad (26)$$

Equations (26) represent generalized systems of equations for the two Green's functions G and F obtained by Gor'kov[1] for weak and δ-type interaction between particles.*

The only assumption used in deriving the system (26) is the smallness of the ratio Δ/ϵ_0. A significant advantage of (26) is the natural introduction of F by means of formulas (25), while the definition of the second Green's function in Gor'kov's method

$$F(x_1, x_2) = (\Phi_0(N), \quad T\Psi(x_1)\Psi(x_2)\Phi_0(N+2)), \qquad (27)$$

---

*The method of two Green's functions was first used by Belyaev[6] in studying Bose systems.

which does not coincide with (25) leads to errors in the case of finite systems, where the addition of two particles can significantly alter the properties of the system. The same remark also applies to other methods of taking pair correlation into account developed in papers on superconductivity,[7] in which systems with N – 2, N, N + 2 particles are assumed to be the same. A particularly striking example of the breakdown of validity of such an assumption is provided by nuclei near the magic shells, when the addition of two particles signifies the transition into the next shell and is associated with a significant change in the properties of the system.

By utilizing the properties of Δ and F noted in Sec. 6 we obtain

$$(i\partial/\partial\tau - H)\widetilde{G}(x, x') = \delta(x - x') + i\widetilde{\Delta}(x)F(x, x'),$$
$$(i\partial/\partial\tau + H^* - 2\mu)\widetilde{F}(x, x') = -i\widetilde{\Delta}^*(x)\widetilde{G}^*(x, x'),$$
$$\widetilde{\Delta}^*(x) = \int \widetilde{\gamma}^*(p')\widetilde{F}(x, p', \varepsilon')\,d\mathbf{p}'d\varepsilon'/(2\pi)^4. \tag{28}$$

The second of equations (28) is a definition of the function F: H* denotes the complex conjugate of the Hamiltonian* H, which arose from the definition of the Green's function for a hole as corresponding to time reversal.

8. THE SYSTEM OF EQUATIONS. APPLICATIONS TO THE NUCLEUS

The system (28) has been utilized for the study of the properties of nonspherical nuclei, and in particular for the calculation of the moments of inertia.[8] When Eqs. (28) are applied to near-magic nuclei it is necessary to take into account the fact that the addition or subtraction of one particle may significantly alter the properties of such nuclei. Therefore, one must make a distinction between the Green's function for the particle and the Green's function for the hole.

In (28) this will affect the expressions for μ: for $\tau > 0$ we shall have $2\mu = 2\mu^+ \equiv E_0(N+2) - E_0(N)$, for $\tau < 0$ we have $2\mu = 2\mu^- \equiv E_0(N) - E_0(N-2)$, where $E_0(N)$ is the energy of the ground state of the system of N particles. We show this by means of a graph. Let $\tau > 0$ correspond to arrows pointing to the right, and $\tau < 0$ correspond to arrows pointing to the left. Then the graph of formula (11) represents $\Sigma_k = \Sigma_k^+$ for $\tau > 0$. For $\tau < 0$ we obtain in place of (11)

$\Sigma_k^- =$

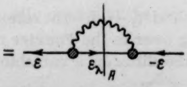

(11′)

The energy of the initial state is $W_0 = E_0(N) - \epsilon$, the energy of the state A is equal to $W_A = E_0(N-2) + \epsilon_\lambda$. By representing Σ_k^- in a form analogous to Σ_k^+ we obtain

$$\Sigma_k^- = |\Delta_\lambda^-|^2/(W_A - W_0) = |\Delta_\lambda^-|^2/(\varepsilon + \varepsilon_\lambda - 2\mu^-). \tag{13′}$$

Thus, Eqs. (28) have a different form for $\tau > 0$ and $\tau < 0$. Therefore, it is useful to introduce the Green's functions for the particle and for the hole separately:

$$\widetilde{G}(\mathbf{r}, \mathbf{r}', \tau) = G^+(\mathbf{r}, \mathbf{r}', \tau), \qquad \tau > 0,$$
$$\widetilde{G}(\mathbf{r}, \mathbf{r}', \tau) = G^-(\mathbf{r}, \mathbf{r}', \tau), \qquad \tau < 0. \tag{29}$$

We define F⁺ and F⁻ in an analogous manner.

On integrating equations (28) over an infinitesimal interval of τ near $\tau = 0$, we obtain

$$G^+(\mathbf{r}, \mathbf{r}', 0) - G^-(\mathbf{r}, \mathbf{r}', 0) = -i\delta(\mathbf{r} - \mathbf{r}'),$$
$$F^+(\mathbf{r}, \mathbf{r}', 0) = F^-(\mathbf{r}, \mathbf{r}', 0). \tag{30}$$

On the basis of (30) we obtain from the last of equations (28)

$$\widetilde{\Delta}^+(\mathbf{r}) = \widetilde{\Delta}^-(\mathbf{r}) \equiv \Delta, \tag{31}$$

and we obtain for G^+ and G^- the equations

$$(i\partial/\partial\tau - H)G^{\pm} = i\Delta F^{\pm},$$
$$(i\partial/\partial\tau + H^* - 2\mu^{\pm})F^{\pm} = -i\Delta^* G^{\pm};$$
$$\Delta^* = \gamma_1 F^{\pm}, \qquad \gamma_1 \equiv \widetilde{\gamma}_0^* \tag{32}$$

with the conditions (30). It is clear that the system (32) admits the transformation

$$\Delta = \Delta' e^{i\alpha}, \qquad F = F' e^{-i\alpha},$$

and it is therefore possible to assume that Δ(0) is real.

On going over to the representation of the φ_λ, and on assuming that $\Delta(\mathbf{r})$ does not depend on $\mathbf{r}$ and is real (for a large system $\Delta(\mathbf{r})$, and also $U(\mathbf{r})$, depend on $\mathbf{r}$ only at the surface of the system, therefore the assumption that Δ is constant introduces an error of the order of $N^{-1/3}$), we obtain

$$(i\partial/\partial\tau - \varepsilon_\lambda)G_\lambda^{\pm}(\tau) = i\Delta F_\lambda^{\pm}(\tau),$$
$$(i\partial/\partial\tau + \varepsilon_\lambda - 2\mu^{\pm})F_\lambda^{\pm}(\tau) = -i\Delta G_\lambda^{\pm}(\tau);$$
$$\Delta = \gamma_1 \sum_\lambda F_\lambda^+(0) = \gamma_1 \sum_\lambda F_\lambda^-(0). \tag{33}$$

We shall seek the solution of the system (33) in the form

In the case of the Hamiltonian (8) H = H the imaginary properties of the Hamiltonian arise, for example, as a result of the introduction of a magnetic field. If the external field depends on t, then all the quantities in (28) will be functions not only of τ, but also of t.

$$G_\lambda^{+} = -i\sum_{\nu} A_\lambda^{\nu} \exp(-iE_{1\lambda}^{\nu}\tau), \quad F_\lambda^{+} = \sum_{\nu} C_\lambda^{\nu} \exp(-iE_{1\lambda}^{\nu}\tau),$$

$$G_\lambda^{-} = i\sum_{\nu} B_\lambda^{\nu} \exp(-iE_{2\lambda}^{\nu}\tau), \quad F_\lambda^{-} = \sum_{\nu} D_\lambda^{\nu} \exp(-iE_{2\lambda}^{\nu}\tau). \tag{34}$$

From the conditions (30) we obtain

$$\sum_{\nu}(A_\lambda^{\nu} + B_\lambda^{\nu}) = 1, \quad \sum_{\nu} C_\lambda^{\nu} = \sum_{\nu} D_\lambda^{\nu}. \tag{35}$$

On substituting (34) into the system (33) we obtain

$$(E_{1\lambda}^{\nu} - \varepsilon_\lambda) A_\lambda^{\nu} = -\Delta C_\lambda^{\nu}, \quad (E_{2\lambda}^{\nu} - \varepsilon_\lambda) B_\lambda^{\nu} = \Delta D_\lambda^{\nu},$$

$$(E_{1\lambda}^{\nu} + \varepsilon_\lambda - 2\mu^{+}) C_\lambda^{\nu} = -\Delta A_\lambda^{\nu},$$

$$(E_{2\lambda}^{\nu} + \varepsilon_\lambda - 2\mu^{-}) D_\lambda^{\nu} = \Delta B_\lambda^{\nu}, \quad \Delta = \gamma_1 \sum_{\lambda\nu} C_\lambda^{\nu}. \tag{36}$$

The condition that Eqs. (36) should have a solution gives the possible values of $E_{1\lambda}^{\nu}$ and $E_{2\lambda}^{\nu}$:

$$E_{1\lambda}^{\nu} = \mu^{+} \pm \sqrt{\Delta^2 + (\varepsilon_\lambda - \mu^{+})^2},$$

$$E_{2\lambda}^{\nu} = \mu^{-} \pm \sqrt{\Delta^2 + (\varepsilon_\lambda - \mu^{-})^2}. \tag{37}$$

Thus, ν assumes two values corresponding to the two signs of the square root.

We shall show that for $E_{1\lambda}$ we should take the upper, and for $E_{2\lambda}$ the lower sign of the square root when the system is in the ground state. An exception to this rule are the states* λ_0 and $-\lambda_0$, occupied by an unpaired particle and hole in an odd nucleus. This case will be considered separately.

We note first that the branches of the square roots chosen above correspond to the values of $E_{1\lambda}$ and $E_{2\lambda}$ which reduce to ϵ_λ when $|\epsilon_\lambda - \mu| \gg \Delta$. The system (33) contains extraneous solutions since in deriving these conditions we did not impose the condition that the nucleus is in the lowest state. In order to derive the consequences of this condition we write an expansion of the Green's function similar to Lehmann's expansion in quantum field theory.[2] From the definition of the Green's function we have

$$G(x, x') = -i(\Phi_0(N), T\Psi(x)\Psi^{+}(x')\Phi_0(N)),$$

where $\Phi_0(N)$ is the exact wavefunction for the ground state of the system of N particles, T denotes the chronological product, and $\Psi(x)$ and $\Psi^{+}(x)$ are the Heisenberg operators for the annihilation and creation of particles. In the φ_λ representation on assuming, as we have done earlier, that $G_{\lambda\lambda'} = \delta_{\lambda\lambda'} G_\lambda$, we obtain

$$G_\lambda^{+}(\tau) = -i\sum_{s} |(a_\lambda^{+})_{s0}|^2 \exp\{-i[W_s(N+1) - W_0(N)]\tau\},$$

$$G_\lambda^{-}(\tau) = i\sum_{s} |(a_\lambda)_{s0}|^2 \exp\{i[W_s(N-1) - W_0(N)]\tau\}, \tag{38}$$

where $(a_\lambda^{+})_{s0} = (\Phi_s(N+1), a_\lambda^{+}\Phi_0(N))$ and $(a_\lambda)_{s0} = (\Phi_s(N-1), a_\lambda\Phi_0(N))$; $W_0(N)$, $W_s(N)$ are the energies of the ground and of the excited states of a system of N particles.

The sums over s have sharp maxima corresponding to the appearance and disappearance of quasiparticles of energies $E_{1\lambda}^{\nu}$ and $E_{2\lambda}^{\nu}$. On comparing (34) and (38) we obtain

$$E_{1\lambda}^{\nu} = W_{s\nu}(N+1) - W_0(N) > W_0(N+1) - W_0(N) \equiv \mu_1^{+},$$

$$E_{2\lambda}^{\nu} = W_0(N) - W_{s\nu}(N-1) < W_0(N) - W_0(N-1) \equiv \mu_1^{-}, \tag{39}$$

whence, on comparing with (37), we obtain

$$\pm\sqrt{\Delta^2 + (\varepsilon_\lambda - \mu^{+})^2} > \mu_1^{+} - \mu^{+},$$

$$\pm\sqrt{\Delta^2 + (\varepsilon_\lambda - \mu^{-})^2} < \mu_1^{-} - \mu^{-}. \tag{40}$$

For even nuclei due to pairing we have $\mu_1^{+} > \mu^{+}$, $\mu_1^{-} < \mu^{-}$. The empirical values of the chemical potentials always satisfy these inequalities. Therefore, for even nuclei only those solutions of (33) are possible which correspond to the values

$$E_{1\lambda} = \mu^{+} + \sqrt{\Delta^2 + (\varepsilon_\lambda - \mu^{+})^2},$$

$$E_{2\lambda} = \mu^{-} - \sqrt{\Delta^2 + (\varepsilon_\lambda - \mu^{-})^2} \tag{41}$$

and only one term remains in each of the sums (34).

With respect to the odd nuclei, it may be easily seen that for them the inequalities (40) admit both values of the square root. However, since all the quantities are altered but little when one particle is added to an even nucleus, it must be assumed that for all the values of λ with the exception of the state λ_0, occupied by the added particle, and of the state $-\lambda_0$ (which differs from λ_0 by a change in the sign of the component of the angular momentum), occupied by the hole, there exists only the solution corresponding to the values $E_{1\lambda}$ and $E_{2\lambda}$, given by (41).

Thus, for all the values of λ in even nuclei, and for the values of λ with the exception of λ_0 and $-\lambda_0$ in odd nuclei, the sums (34) contain only one term each, and the coefficients A_λ, B_λ, C_λ, D_λ can be easily obtained from (36) and (35).

---

*The symbol $-\lambda$ denotes the state which together with λ can form a Cooper pair. For a nucleus the state $-\lambda$ in our approximation differs from the state λ only by the sign of the component of the angular momentum.

We introduce the notation

$$\sqrt{\Delta^2 + (\varepsilon_\lambda - \mu^+)^2} \equiv E_\lambda, \qquad \varepsilon_\lambda - \mu^+ \to \varepsilon_\lambda;$$

$$\sqrt{\Delta^2 + (\varepsilon_\lambda - \mu^-)^2} \equiv E'_\lambda, \qquad \varepsilon_\lambda - \mu^- \to \varepsilon'_\lambda. \qquad (42)$$

Then we obtain from (36)

$$A_\lambda = (\varepsilon'_\lambda + E'_\lambda)/(E_\lambda + E'_\lambda + \mu^+ - \mu^-),$$
$$B_\lambda = (E_\lambda - \varepsilon_\lambda)/(E_\lambda + E'_\lambda + \mu^+ - \mu^-),$$
$$C_\lambda = -\Delta(E_\lambda - \varepsilon_\lambda)/(E_\lambda + E'_\lambda + \mu^+ - \mu^-)(E'_\lambda - \varepsilon'_\lambda). \qquad (43)$$

To these expressions we must add the equation for Δ:

$$\Delta = \gamma_1 \sum_\lambda C_\lambda,$$

$$1 = -\gamma_1 \sum_\lambda \{(E_\lambda - \varepsilon_\lambda)/(E_\lambda + E'_\lambda + \mu^+ - \mu^-)(E'_\lambda - \varepsilon'_\lambda)\} \qquad (44)$$

and the relation

$$N = \sum_\lambda (\Phi_0(N), \ a_\lambda^+ a_\lambda \Phi_0(N)) = -iG^-(0) = \sum_\lambda B_\lambda, \qquad (45)$$

which together with the obvious condition

$$\mu^+(N) = \mu^-(N+2) \qquad (46)$$

enables us to determine the change in the chemical potential and in the pairing energy as the shell is gradually filled, if we know the levels ϵ_λ for the single particle problem without pairing, and if the constant γ_1 has been determined.

The formulas which we have given enable us to determine the irregular variations in the nuclear masses which are superimposed on the regular variation described by the Weizsäcker formula. The quantity B_λ determines the number of particles in the state λ.

It may be easily shown that the quantity γ_1 in formula (44) is of order $\gamma_1 \sim \epsilon_0/N$. For magic nuclei and for neighboring nuclei the quantity $\mu^+ - \mu^-$ is equal to the energy gap between the shells, and is of order $\epsilon_0 N^{-1/3}$. Therefore, the denominator of C_λ contains the quantity $\epsilon_0 N^{-1/3} \gg \Delta$ and, as may be easily shown, Eq. (44) has only the zero solution $\Delta = 0$. Thus, the absence of pair correlation for magic and for neighboring nuclei appears as a natural consequence of this theory.

We now obtain the solution of the system (36) for the values λ_0, $-\lambda_0$, which determine the state of the unpaired particle and hole in an odd nucleus. The ground state of an odd nucleus should be regarded as a slightly deformed state of the preceding even nucleus with an added particle in the state λ_0 and a hole in the state $-\lambda_0$. We shall see that there exists a solution of (36) which admits such an interpretation.

If the state λ_0 is occupied by a particle, then evidently

$$G^+_{0\lambda_0} = G^+_{\lambda_0} = F^+_{\lambda_0} = 0,$$

$$-iG^-_{\lambda_0}(0) = (\Phi_0(N), \ a^+_{\lambda_0} a_{\lambda_0} \Phi_0(N)) = 1.$$

From these two relations and the conditions (35) we obtain

$$A^1_{\lambda_0} = A^2_{\lambda_0} = 0, \quad B^1_{\lambda_0} + B^2_{\lambda_0} = 1, \quad C^1_{\lambda_0} = C^2_{\lambda_0} = 0,$$
$$D^1_{\lambda_0} + D^2_{\lambda_0} = 0, \qquad (47)$$

and this, together with (36), yields in the notation of (42)

$$B^1_{\lambda_0} = (E'_{\lambda_0} + \varepsilon'_{\lambda_0})/2E'_{\lambda_0}, \quad B^2_{\lambda_0} = (E'_{\lambda_0} - \varepsilon'_{\lambda_0})/2E'_{\lambda_0},$$
$$D^1_{\lambda_0} = -D^2_{\lambda_0} = \Delta/2E'_{\lambda_0}. \qquad (48)$$

For $\lambda = -\lambda_0$ we have $G^-_{-\lambda_0} = F^-_{-\lambda_0} = 0$, $-iG^+_{-\lambda_0} = 1$.
In analogy with (48) we obtain

$$A^1_{-\lambda_0} = (E_{\lambda_0} + \varepsilon_{-\lambda_0})/2E_{\lambda_0}, \quad A^2_{-\lambda_0} = (E_{\lambda_0} - \varepsilon_{\lambda_0})/2E_{\lambda_0},$$
$$C^1_{-\lambda_0} = -C^2_{-\lambda_0} = \Delta/2E_{\lambda_0}. \qquad (49)$$

It follows from (47) and (49) that in the sum

$$\Delta = \gamma_1 {\sum_{\lambda\nu}}' C^\nu_\lambda$$

the values $\lambda = \lambda_0$ and $\lambda = -\lambda_0$ are missing in the case of an odd nucleus, and this leads to an appreciable decrease in Δ in the case of odd nuclei.[8] The theory also allows us to determine the value of λ_0. For this we must write down the energy of the system taking pairing into account, and λ_0 is determined by the requirement that the energy of the odd nucleus is a minimum. The state λ_0 determined in this manner, generally speaking, should not coincide with the state obtained from the independent particle model.

A similar procedure must be carried out to determine the energy of the excited states of even and odd nuclei; the values of λ_1 and λ_2 for the hole and for the particle describing the excitation must be determined, and formulas similar to (48) and (49) must be obtained. In the expression for $\Delta = \gamma_1 \Sigma''_\lambda C_\lambda$ the values of λ_1, $-\lambda_1$; λ_2, $-\lambda_2$, will be missing, and this will lead to a significant decrease in Δ for the excited states of nonspherical nuclei.[8]

---

[1] L. P. Gor'kov, JETP **34**, 735 (1958), Soviet Phys. JETP **7**, 505 (1958).

[2] V. M. Galitskii and A. B. Migdal, JETP **34**, 139 (1958), Soviet Phys. JETP **7**, 96 (1958).

[3] A. B. Migdal, Nuclear Phys. (in press).

[4] A. B. Migdal, JETP 32, 399 (1957), Soviet Phys. JETP 5, 333 (1957).

[5] V. M. Galitskii, JETP 34, 1011 (1958), Soviet Phys. JETP 7, 698 (1958).

[6] S. T. Belyaev, JETP 34, 417 (1958), Soviet Phys. JETP 7, 289 (1958).

[7] Bardeen, Cooper, and Schrieffer, Phys. Rev. 108, 1175 (1957). N. N. Bogolyubov, JETP 34, 58 (1958), Soviet Phys. JETP 7, 41 (1958).

[8] A. B. Migdal, JETP 37, 249 (1959), Soviet Phys. JETP 10, 176 (1960).

Translated by G. M. Volkoff
107

SOVIET PHYSICS JETP VOLUME 13, NUMBER 2 AUGUST, 1961

TRANSITIONS BETWEEN HYPERFINE LEVELS IN MESIC DEUTERIUM ATOMS

S. S. GERSHTEĬN

Joint Institute for Nuclear Research

Submitted to JETP editor September 30, 1960

J. Exptl. Theoret. Phys. (U.S.S.R.) 40, 698-707 (February, 1961)

The effective cross section for dμ mesic atom transitions to the lower (F = ½) hyperfine state in exchange collisions with deuterons is calculated. It is shown that practically complete depolarization of μ mesons should be observed in pure deuterium. It is also shown that the dμ transition to the F = ½ state increases the capture probability, $\mu^- + d \rightarrow 2n + \nu$ (by a factor of three for V-A), and the effect of the transition to the F = ½ state on the catalysis of the nuclear reaction $p + d \rightarrow He^3$, mentioned by L. Wolfenstein, is discussed.

It is known that the process, suggested by Ya. B. Zel'dovich, of μ-meson exchange between protons in liquid hydrogen leads to rapid transitions from the upper (F = 1) hyperfine state in the μ-mesonic hydrogen (pμ) atom to the lower (F = 0) state.[1] This effect produces complete depolarization of μ mesons in hydrogen and affects the $\mu^- + p \rightarrow n + \nu$ reaction, where it increases the transition probability by a factor of four (for V-A) and produces completely longitudinally polarized neutrons from the capture of μ mesons in the pμ atom[2] (for capture in ppμ see references 3 and 4).

In this note we investigate the transition between the hyperfine levels F = 3/2 → F = ½ in μ-mesonic deuterium (dμ) in collisions

$$d\mu + d \rightarrow d + d\mu \qquad (1)$$

and discuss its effects on capture

$$\mu^- + d \rightarrow 2n + \nu \qquad (2)$$

and on the catalysis of nuclear reactions by μ mesons.

1. TRANSITION CROSS SECTION[5]

The energy difference between the hyperfine F = 3/2 and F = ½ levels of dμ (**F** = **s** + **i**, where **s** is the μ-meson spin, **i** the deuteron spin) according to Fermi's formula, is

$$\Delta\varepsilon = \frac{8\pi}{3}\beta_\mu\beta_N g\,(2i+1)\,|\psi(0)|^2 = \frac{8}{3}\frac{\beta_\mu\beta_N}{a_\mu^3}g\,(2i+1)\left(1+\frac{m_\mu}{M_d}\right)^{-3} \approx 0.046\ \text{ev} \qquad (3)$$

(here g = 0.8565 is the gyromagnetic ratio of the deuteron; β_μ and β_N are the μ-meson magneton and the nuclear magneton; $a_\mu = \hbar^2/m_\mu e^2$; m_μ and M_d are the μ-meson and deuteron masses). We consider the transition between the hfs levels, due to the collision of dμ with a deuteron. Since the hfs energy can formally be obtained from the interaction

$$V = \frac{4}{3} g\beta_\mu\beta_N r^{-2}\,\delta(r)\,(\mathbf{si}) \qquad (4)$$

(where $r = |\mathbf{r}_\mu - \mathbf{R}_d|$ is the distance between the μ meson and the deuteron), the Hamiltonian for the system consisting of a μ meson and two deuterons can be written in the form (with units $e = \hbar = m_\mu = 1$)

$$H = -\frac{1}{2M_d}\Delta_{\mathbf{R}_1} - \frac{1}{2M_d}\Delta_{\mathbf{R}_2} - \frac{1}{2}\Delta_{\mathbf{r}} - \frac{1}{r_1} - \frac{1}{r_2} + \frac{1}{R} + \frac{4}{3}g\beta_\mu\beta_N\left\{\frac{\delta(r_1)}{r_1^2}(\mathbf{si}_1) + \frac{\delta(r_2)}{r_2^2}(\mathbf{si}_2)\right\}, \qquad (5)$$

where $\mathbf{R}_1$, $\mathbf{R}_2$, $\mathbf{r}$ are the positions of the deuterons and the μ meson; $r_1 = |\mathbf{r} - \mathbf{R}_1|$; $r_2 = |\mathbf{r} - \mathbf{R}_2|$; $R = |\mathbf{R}_2 - \mathbf{R}_1|$; $\mathbf{i}_1$, $\mathbf{i}_2$, $\mathbf{s}$ are the spins of the deuterons and the μ meson. The spin interaction between the deuterons is neglected in (5). Since the collisions between dμ and deuterons occur at thermal velocities, the deuterons are assumed to be in a relative S state. In this approximation the total spin of the ddμ system, which can be J = 5/2, 3/2, ½, is conserved. Obviously the F = 3/2 → ½ transition in the collision (1) can only occur for J = 3/2, ½. We shall calculate the transition cross section separately for each of these values.

1. If J = 3/2 the total spin of the two deuterons can be 2 or 1. The space part of the wave function of two identical particles must be symmetric for even and antisymmetric for odd total spin of the particles. Therefore, the wave function of the system with J = 3/2 (z projection M_J) can be written in the form

$$\Psi_{3/2,\,M_J} = G_{3/2}(R)\,\Sigma_g(r_1,\ r_2;\ R)\,S^{(2)}_{3/2,\,M_J}(1,2;\mu)$$
$$+ H_{3/2}(R)\,\Sigma_u(r_1, r_2; R)\,S^{(1)}_{3/2,\,M_J}(1,\ 2;\ \mu). \tag{6}$$

Here Σ_g and Σ_u ($1s\sigma_g$ and $2p\sigma_u$ in the usual molecular notation) are the wave functions of the muon in the field of the two deuterons with fixed separation R; Σ_g is symmetric, Σ_u is antisymmetric under interchange of the deuteron coordinates; $S^{(I)}_{J,M_J}(i,k;\,l)$ is the spin function of the system for total spin J and projection M_J; I is the spin of the particles whose indices are in the first two places; 1 and 2 as arguments of the spin functions denote the deuterons and μ denotes the meson. The explicit form of the spin function $S^{(I)}_{J,M_J}(i,k;\,l)$ can easily be written with the aid of Clebsch-Gordan coefficients. For example,

$$S^{(2)}_{3/2,\,3/2}(1,\ 2;\ \mu) = 5^{-1/2}\{2^{-1/2}[\chi_1(1)\chi_0(2) + \chi_0(1)\,\chi_1(2)]\,\varphi_{1/2}(\mu)$$
$$-\ 2\chi_1(1)\,\chi_1(2)\,\varphi_{-1/2}(\mu)\}, \tag{7}$$

where χ_m ($m = \pm 1,\ 0$) and φ_ν ($\nu = \pm 1/2$) are the spin functions of the deuteron and μ meson.

Substitution of (6) into the Schrödinger equation with the Hamiltonian (5), multiplication by the functions $\Sigma_g S^{(2)}_{3/2,M_J}$ and $\Sigma_\mu S^{(1)}_{3/2,M_J}$, and integration over the μ-meson coordinate with summation over the spin variables gives the following pair of equations for the functions $G_{3/2}(R)$ and $H_{3/2}(R)$:

$$-\frac{1}{M_d}\Delta_R G_{3/2} + U_g G_{3/2} - \Delta\varepsilon\left(\frac{1}{2}G_{3/2} - \frac{\sqrt{5}}{6}H_{3/2}\right)$$
$$= \left(\varepsilon + \frac{1}{3}\Delta\varepsilon\right)G_{3/2},$$
$$-\frac{1}{M_d}\Delta_R H_{3/2} + U_u H_{3/2} + \Delta\varepsilon\left(\frac{\sqrt{5}}{6}G_{3/2} + \frac{1}{6}H_{3/2}\right)$$
$$= \left(\varepsilon + \frac{1}{3}\Delta\varepsilon\right)H_{3/2}, \tag{8}$$

where $U_g(R)$ and $U_u(R)$ are the molecular potentials in the $1s\sigma_g$ and $2p\sigma_u$ states, including dynamical corrections of first order in m_μ/M_d due to nuclear motion.[6] The energy ϵ is measured from the upper hyperfine level; $\Delta\epsilon$ is the hyperfine splitting, Eq. (3).*

Along with G(R) and H(R), it is convenient to introduce the functions L(R) and K(R), which describe the motion of a free deuteron relative to the dμ atom in its upper ($F = 3/2$) and lower ($F = 1/2$) hyperfine states, respectively. For large R, the wave function of the system (5) must be a linear combination of the functions

$$\Phi^{(3/2)}_{3/2,\,M_J} = 2^{-1/2}\{L_{3/2}(R)\,\psi(r_1)\,S^{(3/2)}_{3/2,\,M_J}(1,\ \mu;\ 2)$$
$$+ L_{3/2}(R)\psi(r_2)\,S^{(3/2)}_{3/2,\,M_J}(2,\ \mu;\ 1)\},$$
$$\Phi^{(1/2)}_{3/2,\,M_J} = 2^{-1/2}\{K_{3/2}(R)\,\psi(r_1)\,S^{(1/2)}_{3/2,\,M_J}(1,\mu;\ 2)$$
$$+ K_{3/2}(R)\,\psi(r_2)\,S^{(1/2)}_{3/2,\,M_J}(2,\mu;\ 1)\} \tag{9}$$

[$\psi(r_1)$ and $\psi(r_2)$ are the wave functions of the meson bound to the first and second deuterons, respectively].

By decomposing the spin functions in (6) into the spin functions in (9) and using the fact that, as $R \to \infty$,

$$\Sigma_g \to \{\psi(r_1) + \psi(r_2)\}/\sqrt{2},$$
$$\Sigma_u \to \{\psi(r_1) - \psi(r_2)\}/\sqrt{2}, \tag{10}$$

it is not difficult to find the relations between the functions G(R), H(R), and K(R), L(R), which describe the relative motion of the nuclei:

$$L_{3/2} = \{G_{3/2} + \sqrt{5}H_{3/2}\}/\sqrt{6}, \quad K_{3/2} = \{\sqrt{5}G_{3/2} - H_{3/2}\}/\sqrt{6}. \tag{11}$$

From Eqs. (8) and (11) it is clear that, as $R \to \infty$, L(R) and K(R) satisfy the equation

$$M_d^{-1}\Delta_R L + \varepsilon L = 0, \quad M_d^{-1}\Delta_R K + (\varepsilon + \Delta\varepsilon)\,K = 0. \tag{12}$$

To determine the probability for the transition $F = 3/2 \to 1/2$ in collisions of the type (1), Eq. (8) must be solved with the boundary condition that K(R) (which describes the relative nuclear motion in the lower hyperfine state) is an outgoing wave as $R \to \infty$:

$$K(R) \sim \gamma R^{-1}e^{ik_2R}, \ \ L(R) \sim (\alpha e^{ik_1R} - e^{-ik_1R})/2ik_1R, \tag{13}$$

where

$$k_1 = (M_d\varepsilon)^{1/2},\ k_2 = [M_d(\varepsilon + \Delta\varepsilon)]^{1/2} \approx (M_d\,\Delta\varepsilon)^{1/2}\ (\varepsilon \ll \Delta\varepsilon).$$

The normalization of L is that corresponding to an incoming plane wave of amplitude unity at infinity. Let R_0 be of the order of magnitude of the radius of the potentials $U_g(R)$ and $U_u(R)$ in Eq. (8). The solutions of (12) in the region $R_0 \ll R \ll k_2^{-1} \ll k_1^{-1}$ can be joined to the solutions of Eqs. (8), which in this region have the form

$$G(R) \sim (R - \lambda_g)/R, \quad H(R) \sim (R - \lambda_u)/R. \tag{14}$$

The scattering lengths λ_g and λ_u can be determined by numerical integration[7] or calculated analytically by approximating the potentials by simple functions.[1,6]

---

*Of course, the use of (4) to compute the spin interaction in (8) is not exact, and, generally speaking, is not necessary for what follows, since for small R only the first two terms in (8) are used. The use of (8), however, makes possible a direct derivation of Eq. (12), which is correct for large R.

In the region $k_2R \ll 1$ the solution has the form

$$L_{3/2} = \left\{R - \frac{(\lambda_g + 5\lambda_u) + 6ik_2\lambda_g\lambda_u}{6 + ik_2(5\lambda_g + \lambda_u)}\right\}\frac{1}{R},$$

$$K_{3/2} = -\frac{\sqrt{5}(\lambda_g - \lambda_u)}{6 + ik_2(5\lambda_g + \lambda_u)}\frac{1 + ik_2R}{R}. \quad (15)$$

From this, the transition cross section for the system with spin $3/2$ is obtained directly;

$$\sigma_{3/2} \approx \tfrac{5}{9}\pi(\lambda_g - \lambda_u)^2\, k_2/k_1. \quad (16)$$

2. If the spin, J, of the system is $1/2$, the transition cross section can be calculated in a completely similar manner. The total spin of the two deuterons can be 0 or 1. Thus, the wave function of the system can be written in the form

$$\Psi_{1/2,\,M_J} = G_{1/2}(R)\,\Sigma_g S^{(0)}_{1/2,M_J}(1,2;\mu)$$
$$+ H_{1/2}(R)\,\Sigma_u S^{(1)}_{1/2,M_J}(1,2;\mu), \quad (17)$$

and the wave functions describing the motion of the deuteron and $d\mu$ atom in the upper and lower hyperfine states, respectively, as in (9), have the form

$$\Phi^{(3/2)}_{1/2,\,M_J} = 2^{-1/2}\{L_{1/2}(R)\psi(r_1)S^{(3/2)}_{1/2,\,M_J}(1,\mu;2)$$
$$+ L_{1/2}(R)\psi(r_2)S^{(3/2)}_{1/2,\,M_J}(2,\mu;1)\},$$
$$\Phi^{(1/2)}_{1/2,\,M_J} = 2^{-1/2}\{K_{1/2}(R)\psi(r_1)S^{(1/2)}_{1/2,\,M_J}(1,\mu;2)$$
$$+ K_{1/2}(R)\psi(r_2)S^{(1/2)}_{1/2,\,M_J}(2,\mu;1)\}. \quad (18)$$

Here, the functions $K_{1/2}(R)$ and $L_{1/2}(R)$ are connected to the functions $G_{1/2}(R)$ and $H_{1/2}(R)$ by the equations

$$K_{1/2} = \{-G_{1/2} + \sqrt{2}H_{1/2}\}/\sqrt{3}, \qquad L_{1/2} = \{\sqrt{2}\,G_{1/2} + H_{1/2}\}/\sqrt{3} \quad (19)$$

and satisfy boundary conditions of the form (13) as $R \to \infty$. Matching the functions gives, in the region $R_0 \ll R \ll k_2^{-1}$,

$$K_{1/2} = \frac{\sqrt{2}(\lambda_g - \lambda_u)}{3 + ik_2(\lambda_g + 2\lambda_u)}\frac{(1 + ik_2R)}{R},$$

$$L_{1/2} = \left\{R - \frac{(2\lambda_g + \lambda_u) + 3ik_2\lambda_g\lambda_u}{3 + ik_2(\lambda_g + 2\lambda_u)}\right\}\frac{1}{R}. \quad (20)$$

The transition cross section for the $dd\mu$ system with spin $J = 1/2$ is thus

$$\sigma_{1/2} \approx \tfrac{8}{9}\pi(\lambda_g - \lambda_u)^2 k_2/k_1. \quad (21)$$

With the statistical weights of the $J = 5/2$, $3/2$, and $1/2$ states, we obtain for the transition cross section

$$\sigma_{F=3/2\to 1/2} = \tfrac{1}{3}\sigma_{3/2} + \tfrac{1}{6}\sigma_{1/2} = \tfrac{1}{3}\pi(\lambda_g - \lambda_u)^2\, k_2/k_1. \quad (22)$$

The $F = 3/2 \to 1/2$ transition probability for $d\mu$ in a $d\mu + d$ collision, consequently, is

$$W = N_d\,\sigma_{F=3/2\to 1/2}\,v = \pi(\lambda_g - \lambda_u)^2 N_d v^*/3, \quad (23)$$

where $v^* = 2(\Delta\epsilon/M_d)^{1/2}$ is the velocity of the nucleus after the transition and N_d is the number of deuterons per cc.

It is essential to note that the $F = 3/2 \to 1/2$ transition probability in $d\mu$ is three orders of magnitude smaller than the corresponding $F = 1 \to 0$ transition probability in $p\mu$, which is

$$W_p = \tfrac{1}{4}\pi(\lambda_g^{(p)} - \lambda_u^{(p)})^2 N_p v_p^* \quad (24)$$

[where $v_p^* = 2(\Delta\epsilon_{p\mu}/M_p)^{1/2}$; N_p is the number of protons per cc, $\lambda_g^{(p)}$ and $\lambda_u^{(p)}$ are the analogs of the scattering lengths in (14) for protons]. This change in magnitude comes chiefly from the fact that the scattering lengths $\lambda_g^{(p)}$ and $\lambda_n^{(p)}$ have opposite signs, and $\lambda_g^{(p)}$ is large because of the resonance[1,6] (according to references 5 and 6, $\lambda_g^{(p)} = -17.3\,a_\mu$, $\lambda_u^{(p)} = 5.25\,a_\mu$), while for deuterons λ_g and λ_u have the same sign and are nearly equal. According to references 5 and 6, $\lambda_g = 6.67$, $\lambda_u = 5.73$; the calculations of Cohen et al.[7] give similar values (see Fig. 2 in reference 7), with $\lambda_g = -\lim_{k\to 0}(\delta^+/k)$, $\lambda_u = -\lim_{k\to 0}(\delta^-/k)$. Under the conditions in a liquid-deuterium chamber, the transition to the $F = 1/2$ state is not reversible and its probability is (for $N_d = 3.5 \times 10^{22}\ \text{cm}^{-3}$)

$$W \approx 6 \cdot 10^6\ \text{sec}^{-1} \quad (25)$$

We mention that in real deuterium, the $d\mu$ atoms collide not with atoms, but with D_2 molecules, and the effective cross section may be different for ortho and para deuterium. The calculation for this case can be performed by a method like Fermi's pseudopotential method, which was proposed for the scattering of slow neutrons on molecules. Since, however, the consideration of molecular structure in $p\mu + H_2$ scattering gives an insignificant effect,[8] one may suppose that it is also not essential for $d\mu + D_2$ scattering (see note added in proof).

2. DEPOLARIZATION OF μ MESONS AND CROSS SECTION FOR ELASTIC SCATTERING OF THE $d\mu$ ATOM IN ITS LOWER HYPERFINE STATE

The collision of $d\mu$ atoms with deuterons proceeding with μ exchange gives rise to a supplementary mechanism for the depolarization of μ mesons in the K shell of deuterium.

Let Φ_{F,M_F} be the spin function of a dμ atom with spin F and projection M_F along the direction of the original polarization of the μ meson, and let χ_m be the spin function of the free deuteron. Then, by decomposing $\Phi_{F,M_F}\chi_m$ into the spin functions $S^{(F)}_{J,M_J}(1, \mu; 2)$ of the combined system and using the scattering amplitude in each of the spin states [see (15) and (20); the scattering length in the $J = {}^5\!/_2$ state is obviously λ_g], it is easy to obtain the scattering amplitude for the state $\Phi_{F,M_F}\chi_m$ and thus calculate the change of polarization of the μ meson in the scattering (1).

As an example, we give the scattered wave amplitude for the state $\Phi_{3/2,\,3/2}\chi_{-1}$

$$[\Phi_{3/2,\,3/2}\chi_{-1}] \to -\frac{1}{R}\left\{\frac{1}{2}(\lambda_g + \lambda_u)\Phi_{3/2,\,3/2}\chi_{-1} + \frac{1}{2\sqrt{3}}(\lambda_g - \lambda_u)\Phi_{3/2,-1/2}\,\chi_1\right\} - \frac{1}{\sqrt{6}}\frac{1}{R}e^{ik_2R}(\lambda_g - \lambda_u)\Phi_{1/2,-1/2}\,\chi_1. \tag{26}$$

From Eq. (26) it is clear that depolarization occurs both in the transition to the lower hyperfine state and also in the elastic channel. In both cases, the depolarization is zero for $\lambda_g = \lambda_u$. Since the polarization of the μ meson in the $\Phi_{1/2,-1/2}$ state is $+{}^1\!/_3$, the transition to $F = {}^1\!/_2$ does not give a complete loss of polarization. Consideration, as in (26), of the different hyperfine states of the dμ atom shows that if only $F = {}^3\!/_2 \to {}^1\!/_2$ transitions are taken into account the μ meson could have a polarization of 1 or 2 per cent (if one assumes that the polarization is of the order of 10 or 20 per cent after the μ meson cascades down to the K shell). However, a simple calculation shows that further collisions of the dμ atom in its lower hyperfine state lead to practically complete depolarization.

To calculate the scattering cross section for

$$d\mu\,(F = 1/2) + d \to d\mu\,(F = 1/2) + d \tag{1'}$$

at energies significantly less than the hyperfine splitting $\Delta\epsilon$, one must replace the boundary condition (13) by the condition that there be no exponentially increasing term in the solution for L(R) [see (12); $\epsilon \approx -\Delta\epsilon$] as $R \to \infty$:

$$K \approx (R - \lambda)/R, \qquad L \approx \gamma R^{-1}e^{-\varkappa R} \approx \gamma\,(1 - \varkappa R)/R. \tag{27}$$

(27), along with (11), (19), and (14), gives for the scattering in the states with total spin $J = {}^3\!/_2$ and $J = {}^1\!/_2$

$$K_{3/2} \approx \left\{R - \frac{(5\lambda_g + \lambda_u) + 4\lambda_g\lambda_u\varkappa}{6 - \varkappa(\lambda_g - 5\lambda_u)}\right\}\frac{1}{R},$$

$$K_{1/2} \approx \left\{R - \frac{(\lambda_g + 2\lambda_u) - 3\lambda_g\lambda_u\varkappa}{3 - \varkappa(2\lambda_g + \lambda_u)}\right\}\frac{1}{R}. \tag{28}$$

As in the derivation of (26), the amplitude of the scattered wave for the dμ atom in the $F = {}^1\!/_2$ state can be obtained:

$$[\Phi_{1/2,1/2}\chi_{-1}] \to -\frac{1}{R}\left\{\frac{1}{2}(\lambda_g + \lambda_u)\Phi_{1/2,1/2}\chi_{-1} + \frac{\sqrt{2}}{6}(\lambda_g - \lambda_u)\Phi_{1/2,-1/2}\,\chi_0\right\},$$

$$[\Phi_{1/2,1/2}\chi_0] \to -\frac{1}{R}\left\{\frac{1}{3}(2\lambda_g + \lambda_u)\Phi_{1/2,1/2}\chi_0 + \frac{\sqrt{2}}{6}(\lambda_g - \lambda_u)\Phi_{1/2,-1/2}\,\chi_1\right\},$$

$$[\Phi_{1/2,1/2}\chi_1] \to -\frac{1}{R}\left\{\frac{1}{6}(5\lambda_g + \lambda_u)\Phi_{1/2,1/2}\chi_1\right\}. \tag{29}$$

Thus, the cross section for (1′) with reoriented dμ atom spin is

$$\sigma_e = \tfrac{4}{27}\pi(\lambda_g - \lambda_u)^2. \tag{30}$$

Since the reorientation probability under liquid-deuterium conditions ($N = 3.5 \times 10^{22}$ cm^{-3}; $v \approx 5 \times 10^4$ cm/sec, with λ_g and λ_u from reference 6)

$$W_e = Nv\sigma_e \approx 5\cdot 10^5 \text{ sec}^{-1} \tag{31}$$

is of the order of the decay probability, $\mu \to e + \nu + \bar{\nu}$, one can conclude that in liquid deuterium, as in liquid hydrogen, the μ mesons are practically completely depolarized.

The effective cross section for the scattering (1) for the $F = {}^1\!/_2$ dμ atom is, according to (28),

$$\sigma^{(e)}_{(F=1/2)} = \frac{2}{3}\left(\frac{5\lambda_g + \lambda_u}{6}\right)^2 + \frac{1}{3}\left(\frac{\lambda_g + 2\lambda_u}{3}\right)^2. \tag{32}$$

Note that, since λ_g and λ_u are nearly equal and have the same sign, the inclusion of hyperfine effects in dμ + d scattering does not lead to a significant change in the scattering cross section, while in pμ + p scattering the interference leads to a considerable reduction in the cross section.

3. EFFECT OF $F = {}^3\!/_2 \to {}^1\!/_2$ TRANSITIONS ON CAPTURE IN DEUTERIUM

First it must be mentioned that μ capture in deuterium must take place from the dμ atomic state and not from the ddμ molecular state, since the formation of the molecule (which, by the way, has a small probability) would lead to practically instantaneous catalysis of the nuclear d+d reaction.[10] Thus, the interpretation of the data on μ capture in deuterium is in a certain sense simpler than for capture in hydrogen, where the formation of the molecule complicates the picture.[3,4] The experimental study of these processes in a bubble chamber will become possible, obviously, when a μ-meson beam with a very low π-meson contamination can be obtained.

The capture of μ mesons in deuterium has been discussed previously.[11–13] As Bukhvostov and Shmushkevich[13] have shown, the capture probability depends strongly on the distribution of mesons between the hyperfine states of the dμ atom. In particular, for the V-A interaction there is no capture from the $F = 3/2$ state. Therefore, the completeness of the $F = 3/2 \rightarrow 1/2$ transition increases the capture probability by a factor of three over the value which would be obtained with a statistical distribution in the $F = 3/2$ and $F = 1/2$ states.

If the μ-capture interaction is not V-A, then capture is possible from the $F = 3/2$ state. However, since the final state neutrons are in the triplet state (as can be seen from the work of Überall and Wolfenstein[12]), the $F = 3/2$ capture is always suppressed in comparison with $F = 1/2$ capture. Thus, in this case the $F = 3/2 \rightarrow 1/2$ transition leads to a considerable increase in the capture probability. (The exact value of the capture probability can be obtained from Bukhvostov and Shmushkevich's formula[13] by replacing the $F = 1/2$ probability (p_-) by unity.)

4. EFFECT OF THE $F = 3/2 \rightarrow 1/2$ TRANSITION ON μ CATALYSIS

L. Wolfenstein (private communication) has pointed out a very curious possible consequence of the $F = 3/2 \rightarrow 1/2$ transition in the dμ atom for the catalysis of nuclear reactions in mixtures of hygrogen and deuterium.

The fact is that the nuclear p+d reaction in the pdμ molecule depends strongly on the molecular spin state. The pdμ molecule has states with total spin 2, 1 (two states), and 0 (see, e.g., reference 6); since the spacing of the molecular levels with different spins is significantly greater than the level widths, the nuclear reaction proceeds independently in each of these states. In the spin-2 state, the total spin of the proton and deuteron is $3/2$; in the spin-0 state it is $1/2$. The spin-1 states are superpositions of states in which the total spin of the proton and deuteron is $3/2$ and $1/2$. Since the decisive role in the transition $p+d \rightarrow He^3$ with μ-meson conversion is played by the E0 transition which occurs when the total spin of the proton and deuteron is $1/2$,[14–16] it is clear that the dμ transition ($F = 3/2 \rightarrow 1/2$) occurring before formation of the molecule raises the statistical weight of such states and thus increases the number of regenerated μ mesons.

For a more accurate estimate, one must find the weights of the states with proton deuteron spins $3/2$ and $1/2$ in the pdμ molecular states with total spin 1. The spin functions for the pdμ states with total spin 1 can be represented in the form

$$\chi_{1,M_J} = -C_1 S^{(1/2)}_{1,M_J}(p, d;, \mu) + C_2 S^{(3/2)}_{1,M_J}(p, d; \mu),$$

$$\chi'_{1,M_J} = C_2 S^{(1/2)}_{1,M_J}(p, d; \mu) + C_1 S^{(3/2)}_{1,M_J}(p, d \ \mu) \qquad (33)$$

(where, according to a rough estimate,[6] $C_1 = 0.41$, and $C_2 = 0.91$). If the transition of the dμ atom to the $F = 1/2$ state occurs before formation of the pdμ molecule, then at the instant of formation of the molecule the following spin functions can occur with equal probabilities

$$\Phi_{1/2,1/2}(d, \mu)\,\varphi_{1/2}(p), \quad \Phi_{1/2,-1/2}(d, \mu)\,\varphi_{-1/2}(p),$$

$$\Phi_{1/2,1/2}(d, \mu)\,\dot{\varphi}_{-1/2}(p), \quad \Phi_{1/2,-1/2}(d, \mu)\,\varphi_{1/2}(p).$$

It is not hard to verify that the spin functions of the system which correspond to the above initial functions at $t = 0$ are the following

$$\Sigma_1 = \Theta_{1,1}(t) \underset{t=0}{\rightarrow} \Phi_{1/2,1/2}(d, \mu)\,\varphi_{1/2}(p),$$

$$\Sigma_2 = -\Theta_{1,-1}(t) \underset{t=0}{\rightarrow} \Phi_{1/2,-1/2}(d, \mu)\,\varphi_{-1/2}(p),$$

$$\Sigma_3 = \frac{1}{\sqrt{2}}\{\Theta_{1,0}(t) + \chi_{0,0}e^{-iE_0t}\} \underset{t=0}{\rightarrow} \Phi_{1/2,1/2} \ \varphi_{-1/2},$$

$$\Sigma_4 = \frac{1}{\sqrt{2}}\{\Theta_{1,0}(t) - \chi_{0,0}e^{-iE_0t}\} \underset{t=0}{\rightarrow} \Phi_{1/2,-1/2}(d, \mu)\,\varphi_{1/2}(p), \qquad (34)$$

where

$$\Theta_{1,M_J}(t) = \left(-\tfrac{1}{3}C_1 + \frac{2\sqrt{2}}{3}C_2\right)\chi_{1,M_J}e^{-iE_1t} + \left(\frac{2\sqrt{2}}{3}C_1 + \tfrac{1}{3}C_2\right)\chi'_{1,M_J}e^{-iE'_1t}$$

E_1, E'_1, and E_0 are the energies of the states χ_{1,M_J}, χ'_{1,M_J}, and $\chi_{0,0}$). From (34) it follows that the probabilities that the system is in the states χ_1, χ'_1 and χ_0 are

$$W_{\chi_1} = \tfrac{1}{12}(-C_1 + 2\sqrt{2}C_2)^2 \approx 0.39,$$

$$W_{\chi'_1} = \tfrac{1}{12}(2\sqrt{2}C_1 + C_2)^2 \approx 0.36, \qquad W_{\chi_0} = \tfrac{1}{4}. \qquad (35)$$

Estimates of the nuclear reaction probability based on nuclear models are highly uncertain. However, if we accept Cohen, Judd, and Riddell's result,[7] we can conclude that the M1 transition occurring in the spin $1/2$ p+d state is the most probable γ transition in the $p + d \rightarrow He^3 + \gamma$ reaction. If we let R be the probability for this transition, and A be the probability of the E0 transition with μ-meson conversion, then we obtain for the reaction yields in the pdμ molecule (formed by dμ atoms in the $F = 1/2$ state)

$$Y_\gamma = \left\{ 0.39 \frac{C_1^2 R}{\lambda_0 + C_1^2 (R + A)} + 0.36 \frac{C_2^2 R}{\lambda_0 + C_2^2 (R + A)} + \frac{1}{4} \frac{R}{\lambda_0 + R + A} \right\},$$

$$Y_\mu = \left\{ 0.39 \frac{C_1^2 A}{\lambda_0 + C_1^2 (R + A)} + 0.36 \frac{C_2^2 A}{\lambda_0 + C_2^2 (R + A)} + \frac{1}{4} \frac{A}{\lambda_0 + R + A} \right\}, \tag{36}$$

when Y_μ and Y_γ are the yields of the $p + d \rightarrow He^3$ reaction with μ-meson conversion and γ-ray emission, respectively; $\lambda_0 = 0.45 \times 10^6\ sec^{-1}$ is the decay probability of the μ meson. In Eqs. (36) the M1 and E2 transitions from the spin $3/2$ state and the conversion of the μ meson in the M1 transition are neglected. According to (36), the reaction yield exceeds that from the pdμ molecule formed by dμ atoms with a statistical distribution in the $F = 3/2$ and $F = 1/2$ states. In the latter case (with the assumptions made above) the reaction yield is

$$Y_\mu = \left\{ \frac{1}{4} \frac{C_1^2 A}{\lambda_0 + C_1^2 (R + A)} + \frac{1}{4} \frac{C_2^2 A}{\lambda_0 + C_2^2 (R + A)} + \frac{1}{12} \frac{A}{\lambda_0 + R + A} \right\}. \tag{37}$$

The numerical value of the $F = 3/2 \rightarrow 1/2$ transition probability in the dμ atom, apparently is consistent with Wolfenstein's conjecture that the $3/2 \rightarrow 1/2$ transition does not take place in hydrogen-deuterium mixtures with a deuterium concentration of the order of one per cent, while for larger deuterium concentrations the $3/2 \rightarrow 1/2$ transition takes place before the formation of the pdμ molecule. This effect accounts for some of the increase in the $p + d \rightarrow He^3$ reaction yield at large deuterium concentrations, but is still insufficient to explain the results of Fetkovich et al.[17] if the expressions for the probability of formation of the pdμ molecule calculated in references 7 and 18 are used.

It should be noted that if the nuclear reaction probability from the state with spin $3/2$ for p+d is significantly less than that from the state with spin $1/2$, then the transition of the dμ atom to its lower hyperfine state increases the reaction yield equally for μ-meson conversion and for γ-ray emission, so that the conversion coefficient remains constant. If the $p + d \rightarrow He^3 + \gamma$ reaction were to go mainly from the state with spin $3/2$ for p+d, then the transition of dμ to its lower $F = 1/2$ state would lead to an increase in the E0 transition probability and a decrease in the radiative transition probability. In principle, these effects could be examined experimentally by studying the yield of the $p + d \rightarrow He^3 + \gamma$ reaction in mixtures of hydrogen and deuterium, as in the experiments of Ashmore et al.,[19] but with larger concentrations of deuterium.

In conclusion, I express my deep gratitude to Academician Ya. B. Zel'dovich, who suggested the possibility of exchange transitions and made many valuable remarks, and also to L. I. Lapidus, A. A. Logunov, Ya. A. Smorodinskii, and M. I. Shmushkevich for useful criticisms. The author is deeply grateful to L. Wolfenstein for the interesting ideas expressed in his letter.

Note added in proof (January 12, 1961). A. M. Moskalenko has calculated the $F = 3/2 \rightarrow 1/2$ transition probability for the dμ atom in collisions with D_2 molecules. The transition cross section in collisions with orthodeuterium molecules is $\sigma \approx 0.76\pi(\lambda_g - \lambda_u)^2$ and in collisions with paradeuterium $\sigma \approx 0.93\pi(\lambda_g - \lambda_u)^2$. Thus, the consideration of molecular binding does not lead to a significant change in the transition cross section.

---

[1] S. S. Gershteĭn, JETP **34**, 463 (1958), Soviet Phys. JETP **7**, 318 (1958).

[2] Ya. B. Zel'dovich and S. S. Gershteĭn, JETP **35**, 821 (1958), Soviet Phys. JETP **8**, 570 (1959).

[3] Ya. B. Zel'dovich and S. S. Gershteĭn, JETP **35**, 649 (1958), Soviet Phys. JETP **8**, 451 (1959).

[4] S. Weinberg, Phys. Rev. Lett. **4**, 575 (1960).

[5] S. S. Gershteĭn, Dissertation, Inst. Phys. Prob. Acad. Sci. U.S.S.R., 1958.

[6] Ya. B. Zel'dovich and S. S. Gershteĭn, Usp. Fiz. Nauk **71**, 581 (1960), Soviet Phys.-Uspekhi **3**, 593 (1961).

[7] Cohen, Judd, and Riddell, Phys. Rev. **119**, 397 (1960).

[8] S. S. Gershteĭn, JETP **34**, 993 (1958), Soviet Phys. JETP **7**, 685 (1958).

[9] S. S. Gershteĭn, JETP **36**, 1309 (1959), Soviet Phys. JETP **9**, 927 (1959).

[10] Ya. B. Zel'dovich, Doklady Akad. Nauk SSSR **95**, 493 (1954).

[11] A. P. Rudik, Doklady Akad. Nauk SSSR **92**, 739 (1953).

[12] H. Überall and L. Wolfenstein, Nuovo cimento **10**, 136 (1958).

[13] A. P. Bukhvostov and I. M. Shmushkevich, JETP 37, 1471 (1959), Soviet Phys. JETP 10, 1402 (1960).

[14] Ya. B. Zel'dovich and A. D. Sakharov, JETP 32, 947 (1957), Soviet Phys. JETP 5, 775 (1957).

[15] J. D. Jackson, Phys. Rev. 106, 330 (1957).

[16] T. H. R. Skyrme, Phil. Mag. 2, 910 (1957).

[17] Fetkovich, Fields, Yodh, and Derrick, Phys. Rev. Lett. 4, 570 (1960).

[18] Belyaev, Gershteĭn, Zakhar'ev, and Lomnev, JETP 37, 1652 (1959), Soviet Phys. JETP 10, 1171 (1960).

[19] Ashmore, Nordhagen, Strauch, and Townes, Proc. Phys. Soc. (London) 71, 161 (1958).

Translated by M. Bolsterli
108

Letters to the Editor

*TRANSVERSE POLARIZATION OF Λ HYPERONS, GENERATED BY 2.8-Bev/c PIONS ON XENON NUCLEI**

I. A. IVANOVSKAYA, E. V. KUZNETSOV, A. PROKESH, and I. V. CHUVILO

Joint Institute for Nuclear Research; Institute of Theoretical and Experimental Physics, Academy of Sciences, U.S.S.R.

Submitted to JETP editor December 3, 1960

J. Exptl. Theoret. Phys. (U.S.S.R.) **40**, 708-709 (February, 1961)

THE question of the magnitude and sign of the polarization of Λ hyperons generated in different reactions at different interacting-particle energies, was first studied in detail in an investigation of the reaction $\pi^- + p \rightarrow \Lambda + K^0$ in connection with a verification of the conservation of space parity in neutrinoless decays, a particular case of which is the decay $\Lambda \rightarrow p + \pi^-$.[2-4]

It was shown in references 3 — 4, where negative pions of energy ~ 1 Bev were used, that space parity is not conserved in the decay of Λ particles and that the Λ hyperons are polarized along the direction $\mathbf{p}_{\text{inc}} \times \mathbf{p}_\Lambda$ ($\mathbf{p}_{\text{inc}}$ is the momentum of the incident pion, $\mathbf{p}_\Lambda$ is the momentum of the Λ hyperon).

The angular distribution of the decay pions is proportional to $(1 + \alpha\overline{P} \cos\beta)$, where $\overline{P}$ is the polarization averaged over the creation angles, α a coefficient characterizing the degree of parity nonconservation, and β the angle between the momentum of the decay pion and the vector $\mathbf{p}_{\text{inc}} \times \mathbf{p}_\Lambda$ (in the rest frame of the Λ hyperon).

The results of the measurements of $\alpha\overline{P}$ were summarized by Glaser:[5]

Berkeley (hydrogen bubble chamber):	$\alpha\overline{P} = 0.73 \pm 0.14$
Princeton (multi-plate cloud chamber):	No asymmetry, but statistics scanty
Michigan (xenon bubble chamber):	$\alpha\overline{P} = 0.45 \pm 0.15$

The energy of the incident pions in all the investigations cited by Glaser is close to 1 Bev. It can be seen that at these energies $\alpha\overline{P}$ differs from zero and is positive.

An investigation of the "up-down" asymmetry in the distribution of the decay pions relative to the plane of Λ creation at other values of incident-pion energies and on other nuclei is of interest both from the point of view of determining the value of $\alpha\overline{P}$ and the sign of polarization of the Λ hyperons generated in various processes, and from the purely methodological point of view — for finding possible sources of polarized Λ particles.

We have measured the "up-down" asymmetry in the decay of Λ hyperons generated by negative pions with momentum (2.8 ± 0.3) Bev/c in a xenon bubble chamber[6] in the reaction

$$\pi^- + \text{Xe} \rightarrow \Lambda + K + \text{Xe}' + n\pi.$$

The average multiplicity of the charged pions accompanying the Λ particles is, according to preliminary estimates, $n \approx 1.2$.

The identification of the Λ particles and the determination of the momenta of the decay negative pion and proton were based on the magnitude of the angle of divergence of the π^- and p relative to the direction of $\mathbf{p}_\Lambda$, and also on the measured values of the ranges and ionizing abilities of these particles.

The figure shows the distribution of the decay pion relative to cos β (75 up and 73 down). As can be seen from the plot, there is practically no asymmetry. The coefficient $\alpha\overline{P}$, calculated from the average cosine, is found to be

$$\alpha\overline{P} = 3\Sigma\cos\beta_i/N \pm (3/N)^{1/2} = 0.08\pm0.14.$$

Thus, the Λ hyperons generated by 2.8-Bev/c negative pions on xenon nuclei do not have a polarization component in the direction $\mathbf{p}_{\text{inc}} \times \mathbf{p}_\Lambda$, inasmuch as[7,8] $\alpha \neq 0$. Consequently, the heavy nuclei cannot be used as targets for the production of Λ particles polarized in the direction $\mathbf{p}_{\text{inc}} \times \mathbf{p}_\Lambda$ when the momentum of the incident pions is ~ 3 Bev/c.

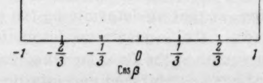

We are continuing to accumulate material in order to improve the statistical accuracy.

---

*A preliminary report was published in the Proceedings of the Rochester Conference of 1960.[1]

---

[1] Proc. of the 1960 Ann. Conf. on High-Energy Physics, Rochester, 1960, p. 382.

[2] Lee, Steinberger, Feinberg, Kabir, and Yang, Phys. Rev. **106**, 1367 (1957).

[3] Crawford, Cresty, Good, Gottstein, Lyman,

Solmitz, Stevenson, and Ticho, Phys. Rev. 108, 1102 (1957).

[4] Eisler, Plano, et al., Phys. Rev. 108, 353 (1957).

[5] D. A. Glaser, Paper delivered at Kiev Conference on High-Energy Physics, 1959.

[6] E. V. Kuznetsov and I. Ya. Timoshin, Приборы и техника эксперимента (Instrum. and Exptl. Techniques), No. 4, 40 (1959).

[7] Boldt, Bridge, Caldwell, and Pall, Phys. Rev. Lett. 1, 256 (1958).

[8] R. W. Birge and W. B. Fowler, Phys. Rev. Lett. 5, 254 (1960).

Translated by J. G. Adashko
109

CIRCULAR POLARIZATION OF GAMMA QUANTA IN THE REACTION $B^{10}(d, p\gamma)B^{11}$

J. ZIMANYI, J. ERÖ, L. POCS, and J. SZENTPETERYI

Central Physics Research Institute, Academy of Sciences, Hungarian People's Republic, Budapest

Submitted to JETP editor November 22, 1960

J. Exptl. Theoret. Phys. (U.S.S.R.) 40, 709-711 (February, 1961)

ZIMANYI has shown in an earlier paper[1] that a reaction that yields polarized products causes the final nucleus to become excited so as to emit a circularly-polarized γ quantum after emission of the nucleon, if the quantum is registered simultaneously with the nucleon. This circular polarization is connected with the polarization of the final nucleus by the known relations of multipole radiation, so that by determining the degree of polarization of the γ quanta we determine the polarization vector of the final nucleus. Satchler[2] and Zimanyi[3] have established recently that measurement of the circular polarization of the γ quanta may be particularly important in the investigation of stripping reactions, since it can yield information on the noncentral part of the interaction.

We have carried out experiments on the determination of the circular polarization of 2.14-Mev γ quanta from the first excited state of B^{11} in the reaction $B^{10}(d, p\gamma)B^{11}$. A thick layer of boron enriched with B^{10} to 90 percent was bombarded with 420-kev deuterons. The stripping mechanism plays an important part even at so low an energy.[4]

The experimental setup is shown in Fig. 1. We detected the protons and γ quanta emitted at 90° to the deuteron beam; the azimuthal angle between the two detectors was also 90°. We used the usual slow and fast coincidence system with resolution $\tau = 2.3 \times 10^{-9}$ sec. The slow part of the circuit consisted of two single-channel pulse-height analyzers to detect the 7.1-Mev protons and 2.14-Mev γ quanta. The polarization analyzer used was a core 8 cm long, made of Armco iron.

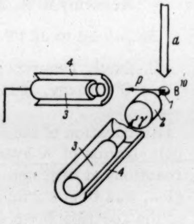

FIG. 1. Diagram of experimental setup: 1 – target, 2 – analyzer, 3 – photomultiplier, 4 – shield.

If we denote by N^+ and N^- the number of γ quanta detected after passage through an analyzer magnetized parallel and antiparallel to the direction of propagation of the γ quanta, then the polarization is

$$P_\gamma = A(N^+ - N^-)/(N^+ + N^-).$$

The constant A depends on the energy of the γ quanta and on the geometry of the analyzer. In our case A = 32.

To prevent the stray field of the magnet from producing an asymmetry that may affect the photomultiplier, we used a permalloy shield and carried out two series of measurements, the geometry of which is shown in Fig. 2. If the magnetic field has axial symmetry, the asymmetry of the setup for cases 2a and 2b will be the same, but the sign of the polarization will be reversed. The effect of instability of the electronic apparatus was eliminated by changing the magnetization direction every 200 sec.

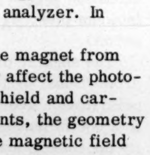

FIG. 2. Paths of deuterons, protons, and γ rays for the two measurements.

The results obtained so far are tentative, since only some 40 000 coincidences were counted. The polarization was found to be $P_\gamma = 37 \pm 19$ percent with the sign of $\mathbf{n} = \mathbf{k}_d \times \mathbf{k}_p$ chosen positive, in accordance with the agreement in Basle. Since the radiation of the 2.14-Mev γ quanta investigated in our experiment is a pure M1 transition[5] and the first excited level of B^{11} has a spin $I = \frac{1}{2}$, the connection between the circular polarization and the polarization of the final nucleus is of the form $P_f = -2P_\gamma$. At the present state of the measurements, the statistical error is considerable, so that we are continuing our measurements to accumulate adequate statistics.

---

[1] J. Zimanyi, Nucl. Phys. 10, 88 (1958-59).

[2] G. R. Satchler, Nucl. Phys. 16, 674 (1960).

[3] J. Zimanyi, Paper delivered at Conference on Low-Energy Nuclear Physics, Balatoneszed, Hungary, 1960.

[4] Paris, Valckx, and Endt, Physica 20, 573 (1954).

[5] D. H. Wilkinson, Phys. Rev. 105, 666 (1957).

Translated by J. G. Adashko
110

CAUSES OF ANOMALOUS BROADENING OF FERROMAGNETIC RESONANCE ABSORPTION LINE IN FERRITES NEAR THE CURIE POINT

K. P. BELOV

Moscow State University

Submitted to JETP editor December 8, 1960

J. Exptl. Theoret. Phys. (U.S.S.R.) 40, 711-713 (February, 1961)

IN measurements of the temperature dependence of ferromagnetic resonance in ferrites (both mono- and polycrystals) it was noted many times that as the Curie point is approached the width of the resonance-absorption line increases anomalously. In the theories of de Gennes, Kittel and Portis[1] and of Skrotskii and Kurbatov[2] this increase is ascribed to the influence of thermal fluctuations of the spontaneous magnetization, which, as is well known, reach a maximum near the Curie point. According to reference 2, this last circumstance leads to inhomogeneities of the internal (exchange) field, causing a spread in the resonance frequencies and consequently a broadening of the resonance line.

Making use of an analysis of the experimental material, we propose here arguments that indicate that the thermal fluctuations of the spontaneous magnetization are not the principal cause of the marked increase in the width of the ferromagnetic-resonance line near the Curie point; the main cause of the anomalous broadening of the resonance line near the Curie point is masked by the influence of structural factors. These arguments are as follows.

1. The quantitative manifestation of the intensity of thermal fluctuations of spontaneous magnetization near the Curie point may be the maximum (see Fig. 1) of the susceptibility of the para process, χ_p (inasmuch as χ_p is measured in a field, the fluctuations of the magnetization are somewhat suppressed by this field). According to the foregoing theories, it might appear that the temperature dependence of the line width $\Delta H(T)$ should essentially duplicate the course of the $\chi_p(T)$ curve, i.e., a maximum should be observed on the $\Delta H(T)$ curve in the vicinity of the Curie point. This, however, is not observed experimentally. Near the Curie temperature, where thermal fluctuations of the spontaneous magnetization take place, ΔH increases continuously (see the figure).

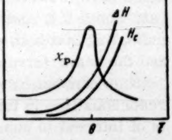

Temperature variation (schematic) of the width ΔH of the resonance curve, the coercive force H_c, and the susceptibility of the para process χ_p in ferrites in the vicinity of the Curie point.

In addition, the maximum increase in ΔH does not coincide with the position of the maximum of χ_p. This suggests that the thermal fluctuations of the spontaneous magnetization influence little the width of the resonance line, if at all.

2. In our opinion, a more influential factor causing the broadening of the resonance line near the Curie point are the structural inhomogeneities in the ferrites, which, in turn, lead to inhomogeneities in the spontaneous magnetization through the body of the specimen (volume fluctuations of the spontaneous magnetization). In ferrites (both mono- and polycrystals) such structural inhomogeneities may be the following: disordered distribution of the magnetic ions over the octohedral and tetrahedral sites,* the presence of atomic vacancies, dislocations, etc. As shown by us in earlier papers,[3] the spontaneous magnetization is particularly sensitive to the structural inhomogeneities in the region of the Curie point, where the

least changes in the atomic distances and locations of the atoms influence the value of the magnetization. This circumstance leads to the formation of "tails" of spontaneous magnetization in the region of the Curie point.[3] For the same reason, an increase in the coercive force[4] is observed in many ferrites near the Curie point (as a result of the magneto-heterogeneous state, caused by the volume fluctuations of spontaneous magnetization). The same factor is responsible for the broadening of the ferromagnetic-resonance line near the Curie point. The volume fluctuations of spontaneous magnetization produce in the ferrite an inhomogeneous internal field and this leads to a spread in the resonance frequencies, and consequently to the broadening of the resonance-absorption line.

It is interesting to note that measurements of ΔH and H_C, made on single crystals of magnesium and magnesium-manganese ferrites,[5] give approximately the same temperature variation of these quantities in the region of the Curie point (see the figure). Naturally, the mechanisms of the phenomena connected with the coercive forces and the width of the ferromagnetic resonance-absorption line are different, and there is hardly any deep meaning in a comparison of the temperature variations of the indicated quantities. It should be noted here, however, that the temperature intervals where ΔH and H_C increase are the same, indicating that both phenomena are caused by one and the same (structural) factor.

3. In connection with the anomalous width of the resonance line in ferrites near the Curie point, it is of interest to consider also the anomalies in the width of the resonance line of ferrites near the points of compensation of magnetic sublattices. As is well known, ΔH broadens greatly (in garnet-ferrite of gadolinium[6] and in chromite-ferrite of lithium[7]) as the point of compensation is approached from the high- and low-temperature sides. At the same time, an anomalous increase in H_C was observed in the same temperature region for the same ferrites.[4] (It should be noted that on approaching the point of compensation the magnetic-anisotropy constant not only fails to increase, but even decreases somewhat in absolute magnitude.[8]) We propose that the anomalous increase in ΔH and H_C on approaching the compensation point is also explained by the occurrence of magneto-heterogeneous state of the ferrite in the vicinity of this point. It should be noted that, unlike the case of the Curie point, there are practically no thermal fluctuations of the spontaneous magnetization in the region of the compensation point (the susceptibility of the para process has no maximum), so that the point of compensation is not a point of second-order magnetic phase transformation. One can therefore speak with assurance of the small role of thermal fluctuations of the spontaneous magnetization in the broadening of the resonance line of ferromagnetic absorption, and that the main cause of the broadening of the resonance line are the magnetic inhomogeneities of the ferrites.

4. Everything said above regarding the causes of the anomalous broadening of the resonance line in ferrites near the Curie point applies probably to metallic ferromagnets, too. An anomalous increase in the width of the ferromagnetic resonance absorption line[9] on approaching the Curie point is observed in many metallic ferromagnets. On the other hand, in the same temperature interval one observes in these ferromagnets "tails" of spontaneous magnetization[3] and, frequently, an increase in the coercive force.[10] The experimental material, however, is too scanty for analysis.

I express my indebtedness to V. N. Lazukin and A. I. Pil'shchikov for a discussion of the problems touched upon in the present article.

---

*The influence of structural inhomogeneities in ferrites on the broadening of the reasonance line in the region of temperatures below the Curie point was recently considered by Clogston, Suhl, Walker, and Anderson [11]

---

[1] de Gennes, Kittle, and Portis, Phys. Rev. **116**, 323 (1959).

[2] G. V. Skrotskii and L. V. Kurbatov, Физика металлов и металловедение (Phys, of Metals and Metallography), **10**, 335 (1960).

[3] K. P. Belov, Магнитные превращения (Magnetic Transformations), Fizmatgiz, 1959.

[4] K. M. Bol'shova and T. A. Elkina, Vestnik, Moscow State Univ. No. 2, 95 (1957), and No. 4, 85 (1959).

[5] K. P. Belov and V. F. Belov, Soviet Phys.-Solid State, in press.

[6] Calhoun, Overmeyer, and Smith, Phys. Rev. **107**, 993 (1959).

[7] J. Pauleve, Compt. rend. **41**, No. 6, 548 (1955).

[8] Smith, Overmeyer, and Calhoun, J. Res. Dev. IBM **3**, 153 (1959).

[9] K. Standley and K. Reich, Proc. Phys. Soc. **A68**, 713 (1955).

[10] A. S. Zaĭmovskii, Bull. All-Union Electrotech. Inst. **2**, 1 (1941). M. V. Dekhtyar, op. cit. ref. 2, **3**, 55 (1956), V. I. Ivanovskii, ibid. **4**, No. 1, 1957.

[11] Clogston, Suhl, Walker, and Anderson, J. Phys. Chem. Solids, **1**, No. 3, 129 (1956).

Translated by J. G. Adashko
111

ENERGY SHIFTS OF GAMMA TRANSITIONS OBSERVED IN RESONANCE ABSORPTION OF GAMMA QUANTA IN CRYSTALS

V. A. BRYUKHANOV, N. N. DELYAGIN, B. ZVENGLINSKII, and V. S. SHPINEL'

Nuclear Physics Institute, Moscow State University.

Submitted to JETP editor December 2, 1960

J. Exptl. Theoret. Phys. (U.S.S.R.) **40**, 713-714 (February, 1961)

In previous notes[1,2] we have reported an investigation of resonance absorption of gamma quanta in crystals (Mössbauer effect) for the 23.8-kev γ transition in Sn^{119}. In particular, it was shown that in a crystal of white metallic tin (β-tin) the emission and absorption lines are split into two components. According to our latest measurements the separation between these two components is $\Delta = (1.10 \pm 0.15) \times 10^{-7}$ ev.

In the present work, using a source of Sn^{119m} (white metallic tin) at liquid nitrogen temperature, we have obtained absorption spectra for absorbers prepared from different crystalline compounds containing tin (in the normal isotopic mixture): SnI_4 (~ 30 mg/cm^2), $SnCl_2$ (~ 60 mg/cm^2) and SnO_2 (5.3 mg/cm^2). For SnI_4 and $SnCl_2$, the measurements were done with the absorber cooled by liquid nitrogen; for the SnO_2 absorber, the cooling was not done since it did not give any significant increase of the effect. The dependence of the effective cross section for resonance absorption on the velocity of the source relative to the absorber was measured with the apparatus described briefly in an earlier report.[1] The absorption spectra obtained are shown in the figure (where N is the total number of pulses).

The spectra have the doublet structure which we also observed earlier for the $SnNb_3$ crystal.[1] This structure is caused by the splitting of the emission of the source, which we mentioned above. In addition to the doublet structure, for SnO_2 and $SnCl_2$ we also observed an energy shift of the absorption line. For the SnO_2 crystal, the energy shift is negative, $\delta_1 = -(2.4 \pm 0.3) \times 10^{-7}$ ev, while for the $SnCl_2$ crystal it is positive, $\delta_2 = +(0.72 \pm 0.10) \times 10^{-7}$ ev (if we choose as our reference point the energy of the absorption line for SnI_4, which corresponds to zero source velocity in the notation used on the figure). Relative shifts of lines in a source and absorber which are not chemically identical and which are at different temperatures may be due to various causes.[3]

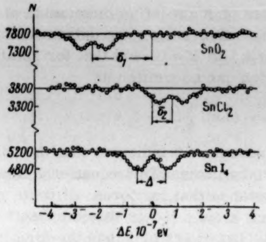

The shifts observed by us can be explained by assuming that the energies of the states between which the transition occurs include an interaction between the nucleus and those electrons which have a nonzero wave function in the region of the nucleus. This interaction depends on the charge distribution in the nucleus, and can differ by an amount ΔE for two different states of the nucleus. Thus the energy of the emitted quantum can be written as $E = E_0 + \Delta E$, and the experimentally observed shifts must be due to the difference in ΔE for the different crystalline compounds. A theoretical computation of such shifts would enable us to obtain additional information concerning the distribution of charge in the nucleus.

---

[1] Delyagin, Shpinel', Bryukhanov, and Zvenglinskii, JETP **39**, 220 (1960), Soviet Phys. JETP **12**, 159 (1961).

[2] Delyagin, Shpinel', Bryukhanov, and Zvenglinskii, JETP **39**, 894 (1960), Soviet Phys. JETP **12**, 619 (1961).

[3] O. C. Kistner and A. W. Sunyar, Phys. Rev. Letters **4**, 412 (1960).

Translated by M. Hamermesh
112

ON THE ENERGY DEPENDENCE OF THE SCATTERING CROSS SECTION AT SMALL ENERGIES

S. M. BILEN'KII

Joint Institute for Nuclear Research

Submitted to JETP editor December 26, 1960

J. Exptl. Theoret. Phys. (U.S.S.R.) **40**, 714-715 (February, 1961)

F. L. Shapiro[1] has shown that the first two terms in the expansion of the total inelastic cross section

σ_r in powers of k (relative momentum of the particles in the initial state) are determined by the value of $(\sigma_r k)$ at $k = 0$, and that for small k the cross section can be written as

$$\sigma_r = (\sigma_r k)_0 \frac{1}{k}\left(1 - \frac{1}{2\pi} k (\sigma_r k)_0 + \ldots\right), \tag{1}$$

where the subscript 0 indicates that the value at $k = 0$ has to be taken. This equation follows from the circumstance that for forces of finite range the expansion of $k \cot \delta$ (δ is the complex s-wave phase shift) in powers of k has the form[1,2]

$$k \operatorname{ctg} \delta = b(k^2) = b(0) + k^2 b'(0) + \ldots. \tag{2}^*$$

We now show that (2), together with unitarity, leads also to a similar form of the expansion of the elastic cross sections in powers of k. Here the first two terms of the series have the form

$$\sigma = \sigma_0 \left(1 - \frac{1}{2\pi} k (\sigma_r k)_0 + \ldots\right), \tag{3}$$

which means that up to terms linear in k the elastic scattering cross section is determined by the quantity $(\sigma_r k)_0$ and by the value of the scattering cross section at $k = 0$.

Since the lowest power with which the partial waves contribute to the power series expansion is k^{4l}, only s waves have to be considered. From (2) we have

$$\sigma = \frac{4\pi}{|b(k^2)|^2 + k^2 - 2k \operatorname{Im} b(k^2)} = \frac{4\pi}{|b(0)|^2}\left(1 + 2k \frac{\operatorname{Im} b(0)}{|b(0)|^2} + \ldots\right). \tag{4}$$

It is easy to see, for example from the optical theorem, that

$$|b(0)|^{-2} \cdot \operatorname{Im} b(0) = -(\sigma_r k)_0 / 4\pi. \tag{5}$$

From this we obtain Eq. (3).

In the case where only elastic scattering occurs, i.e., when $b(k^2)$ is real, the cross section has thus for small k the form

$$\sigma = \sigma_0 + k^2 \sigma_1 + \cdots. \tag{6}$$

If, on the other hand, inelastic processes also occur at $k = 0$ then a term linear in k appears in the power series expansion, and owing to unitarity its coefficient is determined by the total inelastic cross section. The expressions (1) and (3) are applicable for those cases where one can limit oneself to the first term in the expansion (2). We note that when (3) holds the cross section decreases with increasing k. We also note that (3) is correct even if only one of the initial particles has zero spin. Formula (3) can be used in the extrapolation of $\pi^- p$ and $\bar{K}p$ scattering to zero energy.

In conclusion, I express my deep gratefulness to Professor Ya. A. Smorodinskii for interesting discussions.

---

*ctg = cot

---

[1] F. L. Shapiro, JETP **34**, 1648 (1958), Soviet Phys. JETP **7**, 1132 (1958).

[2] H. A. Bethe, Phys. Rev. **76**, 38 (1949).

Translated by M. Danos
113

BEHAVIOR OF THE CROSS SECTION OF ELECTROMAGNETIC PRODUCTION OF PARTICLES AT THE THRESHOLD

V. N. BAǏER and S. A. KHEǏFETS

Submitted to JETP editor December 1, 1960

J. Exptl. Theoret. Phys. (U.S.S.R.) **40**, 715-717 (February, 1961)

As was shown previously,[1] the total cross section of high energy inelastic and elastic scattering of electrons at large angles in the center-of-mass system (c.m.s.), calculated in a doubly logarithmic approximation, can be represented in the form

$$d\sigma = d\sigma_0 \exp\left\{-\frac{8e^2}{\pi} \ln\frac{E}{m} \ln\frac{E}{\Delta E}\right\}. \tag{1}$$

Here $d\sigma_0$ is the scattering cross section computed in the low-order perturbation theory, E the electron energy, m the electron mass, and ΔE the maximum achievable energy of the quanta radiated in the collision process, which defines the threshold sensitivity of the detector of electrons.

If $\Delta E = E$ (i.e., the detector records all electrons, independently of their energy), then the total cross section coincides with the cross section computed in the low-order perturbation theory approximation ($d\sigma = d\sigma_0$). As is known,[2] this is connected with the fact that in this approximation, the decrease of the cross section of the fundamental process, without emission of additional quanta, due to taking the radiation corrections into account, is entirely compensated by the increase of the cross section of processes with multiple additional radiation of hard photons in the case of an arbitrary radiation ($\Delta E = E$).

The same formula also holds for the scattering of electrons on positrons.

In principle, another situation arises in the conversion of an electron-positron pair into a pair of other charged particles with larger mass (for example, $e^+ + e^- \rightarrow \mu^+ + \mu^-$), inasmuch as in this case the maximum energy of the radiated photon cannot be larger than $E - \mu$ (μ is the mass of the particle). Thus, in addition to the limitation imposed by the sensitivity of the apparatus, there arises a physical limitation on the energy of the photon. In this case, the given compensation cannot take place and, independently of the sensitivity of the detector, an account of the radiative corrections seriously changes the character of the dependence of the cross section on energy. It is clear that the effect is greatest close to the threshold of particle production.

As a qualitative example, we consider the production of a pair of fermions with mass μ in the annihilation of an electron-positron pair with energy E in the c.m.s. Calculation can be carried out the same as in reference 1, where it was shown that the contributions of diagrams containing more than one staircase line are mutually compensated, so that it is sufficient to consider only the enveloping virtual lines. This means that we have two "overgrown" vertices, connected by a single virtual photon line. It is evident that for $E \gg \mu$, the difference between fermions with mass μ and electrons becomes insignificant, so that Eq. (1) remains valid, but the maximum $\Delta E \leq E - \mu$. With decrease in energy, the contribution from the virtual quanta with which the heavy fermions are exchanged decreases. As can be shown, at the threshold of the reaction for $E \sim \mu$, their contribution becomes negligible. This is connected with the fact that at threshold the momentum of the fermions produced is very small; therefore, for a description of the interaction between them, the lower orders of perturbation theory are sufficient. Thus, at threshold, only the electron vertex makes a contribution; in this case the cross section of the reaction for arbitrary radiation has the form

$$d\sigma = d\sigma_0 F^2(E^2) \exp\left\{-\frac{4e^2}{\pi} \ln\frac{E}{E-\mu} \ln\frac{E}{m}\right\}, \tag{2}$$

$$d\sigma_0 = \frac{r_0^2}{16\gamma^2}\frac{q}{E}\left[1 + \frac{\mu^2}{E^2} + \frac{q^2}{E^2}\cos^2\theta\right]. \tag{3}$$

Here r_0 is the classical radius of the electron; $\gamma = E/m$; q is the momentum of the fermion; θ is the angle of flight of fermions relative to the direction of motion of the electrons; $F(E^2)$ is the form factor of the electrons.

For nonrelativistic fermions (close to threshold) Eq. (2) can also be written in the form

$$d\sigma = d\sigma_0 F^2(E^2)\,(q/\sqrt{2\mu E})^{(8e^2/\pi)\ln(E/m)}. \tag{4}$$

For μ mesons, the effect under consideration gives (close to threshold) the change in the character of the dependence of the cross section on the momentum of the emerging particles: in place of $d\sigma \sim q$, we have $d\sigma \sim q^{1.1}$ in the case of an arbitrary radiation. The effect will be still greater if we record the energy of the emerging mesons in some energy range.

The authors express their deep gratitude to Academician I. E. Tamm and to A. A. Abrikosov for discussions.

---

[1] V. N. Baĭer and S. A. Kheĭfets, JETP 40, 613 (1961), this issue, p. 428.

[2] A. A. Abrikosov, JETP 30, 96, 386, 544 (1956), Soviet Phys. JETP 3, 71, 474, 379 (1956).

Translated by R. T. Beyer
114

SOVIET PHYSICS JOURNALS

Translations of the 1961 Originals—*Published in English by the American Institute of Physics with the cooperation of the National Science Foundation.*

Publication year July, 1961—June, 1962.

Soviet Physics—JETP

A translation, beginning with 1955 issues of *Zhurnal Eksperimental'noi i Teoreticheskoi Fiziki* of the USSR Academy of Sciences. Leading physics journal of Soviet Union. Similar to "The Physical Review" in quality and range of topics. Outstanding new work is most likely to appear in this journal.

Vols. 13 and 14 comprising twelve issues, approx. 4000 pp.
$75 domestic, $79 foreign
Libraries $50 domestic, $54 foreign. Single copies, $8*

Soviet Physics—SOLID STATE

A translation, beginning with 1959 issues of *Fizika Tverdogo Tela* of the USSR Academy of Sciences. Offers results of theoretical and experimental investigations in the physics of semiconductors, dielectrics, and on applied physics associated with these problems. Also publishes papers on electronic processes taking place in the interior and on the surface of solids.

Vol. 3 comprising twelve issues, approx. 3800 pp.
$70 domestic, $74 foreign
Libraries $45 domestic, $49 foreign. Single copies, $8*

Soviet Physics—TECHNICAL PHYSICS

A translation, beginning with 1956 issues of *Zhurnal Tekhnicheskoi Fiziki* of the USSR Academy of Sciences. Contains work on plasma physics and magnetohydrodynamics, aerodynamics, ion and electron optics, and radio physics. Also publishes articles in mathematical physics, the physics of accelerators, and molecular physics.

Vol. 6 comprising twelve issues, approx. 2000 pp.
$55 domestic, $59 foreign
Libraries $35 domestic, $39 foreign. Single copies, $8*

Soviet Physics—ACOUSTICS

A translation, beginning with 1955 issues of *Akusticheskii Zhurnal* of the USSR Academy of Sciences. Devoted principally to physical acoustics but includes electro-, bio-, and psychoacoustics. Mathematical and experimental work with emphasis on pure research.

Vol. 7 comprising four issues, approx. 500 pp.
$12 domestic, $14 foreign
(No library discounts.) Single copies, $4

Soviet Physics—DOKLADY

A translation, beginning with 1956 issues of the physics sections of *Doklady Akademii Nauk SSSR*, the proceedings of the USSR Academy of Sciences. All-science journal offering four-page reports of recent research in physics and borderline subjects.

Vol. 6 comprising twelve issues, approx. 1500 pp.
$35 domestic, $38 foreign
Libraries $25 domestic, $28 foreign*
Single copies Vols. 1 and 2, $5;
Vol. 3 and later issues, $7

Soviet Physics—CRYSTALLOGRAPHY

A translation, beginning with 1957 issues of the journal *Kristallografiya* of the USSR Academy of Sciences. Experimental and theoretical papers on crystal structure, lattice theory, diffraction studies, and other topics of interest to crystallographers, mineralogists, and metallurgists.

Vol. 6 comprising six issues, approx. 1000 pp.
$25 domestic, $27 foreign
Libraries $15 domestic, $17 foreign. Single copies, $5*

SOVIET ASTRONOMY—AJ

A translation, beginning with 1957 issues of *Astronomicheskii Zhurnal* of the USSR Academy of Sciences. Covers various problems of interest to astronomers and astrophysicists including solar activity, stellar studies, spectroscopic investigations of radio astronomy.

Vol. 5 comprising six issues, approx. 1100 pp.
$25 domestic, $27 foreign
Libraries $15 domestic, $17 foreign. Single copies, $5*

Soviet Physics—USPEKHI

A translation, beginning with September, 1958, issue of *Uspekhi Fizicheskikh Nauk* of the USSR Academy of Sciences. Offers reviews of recent developments comparable in scope and treatment to those carried in *Reviews of Modern Physics.* Also contains reports on scientific meetings within the Soviet Union, book reviews, and personalia.

Vol. 4 comprising six issues, approx. 1700 pp.
(Contents limited to material from Soviet sources)
$45 domestic, $48 foreign
Libraries $30 domestic, $33 foreign. Single copies, $9*

**For libraries of nonprofit academic institutions.*

SOVIET PHYSICS JETP VOLUME 13, NUMBER 2 AUGUST, 1961

CONTENTS

Title	Authors	Page	Russian Reference
Channel Expansion in Small Intense Sparks	B. A. Demidov, Yu. F. Skachkov, and S. D. Fanchenko	263	40, 385
An Investigation of the Paramagnetism of μ-Mesic Atoms	L. B. Egorov, G. V. Zhuravlev, A. E. Ignatenko, Li Hsuang-Ming, M. G. Petrashku, and D. Chultém	268	40, 391
The Interaction of 660-Mev Protons with Carbon, Nitrogen, and Oxygen Nuclei	N. A. Perfilov and Yu. I. Serebrennikov	274	40, 400
Fission of Antimony by High-Energy Protons	A. K. Lavrukhina, É. E. Rakovskii, Su Hung-Kuei, and S. Khoĭnatskii	280	40, 409
Investigation of Nuclear-Active Particles and Electron-Photon Showers with Energies > 10^{12} ev at 3860 m Altitude	E. V. Denisov, V. I. Zatsepin, S. I. Nikol'skii, A. A. Pomanskii, B. V. Subbotin, E. I. Tukish, and V. I. Yakovlev	287	40, 419
Magnetic Spectrum Analyzers	E. K. Zavoĭskii and V. A. Skoryupin	292	40, 426
The Effect of Pressure on the Electrical Resistance and Galvanomagnetic Effect in Chromium Telluride	N. P. Grazhdankina, L. G. Gaĭdukov, K. P. Rodionov, M. I. Oleĭnik, and V. A. Shchipanov	297	40, 433
Resonance of Domain Walls in Cobalt Ferrite	T. M. Perekalina, A. A. Askochinskii, and D. G. Sannikov	303	40, 441
Plasma Confinement in a Trap with a Magnetic Field that Increases toward the Periphery	S. Yu. Luk'yanov, I. M. Podgornyĭ, and V. N. Sumarokov	308	40, 448
Asymmetry in the Angular Distribution of Electrons from $\mu - e$ Decay in Magnetic Fields up to 35,000 Oersted	S. A. Ali-Zade, I. I. Gurevich, and B. A. Nikol'skii	313	40, 452
On the Superconductivity of Tin and Indium under Pressure	L. S. Kan, B. G. Lazarev, and V. I. Makarov	317	40, 457
Production of Charged Mesons by 290-Mev π^- Mesons on Hydrogen	Yu. A. Batusov, S. A. Bunyatov, V. M. Sidorov, and V. A. Yarba	320	40, 459
Production of $\Lambda^0(\Sigma^0)$ Hyperons and K^0 Mesons in π^-p Interactions at 6.8 ± 0.6 Bev/c	Wang Kang-Chang, Wong Ts'u-Tseng, V. I. Veksler, J. Vrana, Ting T'a-Tsao, V. G. Ivanov, E. N. Kladnitskaya, A. A. Kuznetsov, Nguyen Dinh Tu, A. V. Nikitin, M. I. Solov'ev, and Ch'eng Ling-Yen	323	40, 464
Investigation of the Radiation from Zn^{63}	S. S. Vasil'ev, No Hsieng Ch'ang, and L. Ya. Shavtvalov	331	40, 475
Elastic Scattering of 13.6-Mev Deuterons by Nuclei. II	Yu. V. Gofman and O. F. Nemets	333	40, 477
On the 892.4-kev Gamma Transition in W^{182}	V. D. Vitman, N. A. Voinova, B. S. Dzhelepov, and A. A. Karan	335	40, 479
On the Temperature of Lightning and Force of Thunder	Yu. A. Zhivlyuk and S. L. Mandel'shtam	338	40, 483
Recoil Effect for the Two-Particle Interaction in Nonrelativistic Quantum Field Theory	A. V. Tulub	341	40, 488
Neutron Polarization in the Disintegration of Be^9 Nuclei by Circularly Polarized Gamma Quanta	I. Sh. Vashakidze, T. I. Kopaleĭshvili, and G. A. Chilashvili	343	40, 491
Asymptotic Behavior of the Scattering Amplitude at Infinite Energies	L. A. Khalfin	345	40, 493
On the Three-Body Problem with Short-Range Forces	G. S. Danilov	349	40, 498
On the Physical Meaning of Negative Probabilities	J. P. Vigier and Ya. P. Terletskii	356	40, 508
Theory of Molecular Dissociation Induced by Neutrons. I. Diatomic Molecules	Yu. S. Sayasov and G. K. Ivanov	360	40, 513
Attenuation of Magnetohydrodynamic and Magnetoacoustic Waves in a Plasma with Anisotropic Conductivity and Viscosity	R. V. Deutsch	367	40, 524
Instability of Low-Frequency Electromagnetic Waves in a Plasma Traversed by a Beam of Charged Particles	M. S. Kovner	369	40, 527
Determination of the Parities of Strange Particles by Means of Dispersion Relations	Ya. I. Granovskii and V. N. Starikov	375	40, 537
Double Dispersion Relations for Potential Scattering	V. I. Mal'chenko	381	40, 546
On the Mechanism of Photonuclear Reactions	A. M. Badalyan and A. I. Baz'	383	40, 549
Bremsstrahlung from a Longitudinally Polarized Electron with Account of the Finite Size of the Nucleus	B. K. Kerimov and F. S. Sadykhov	387	40, 553
The Doppler Width of Emission and Absorption Lines	M. I. Podgoretskii and A. V. Stepanov	393	40, 561
Theory of Inelastic Scattering of Neutrons by Imperfect Crystals	M. A. Krivoglaz	397	40, 567
Spin-Acoustic Resonance in Paramagnetic Metals	V. I. Gerasimenko	410	40, 585
Dispersion Formulas which Take into Account the Optical Interaction	V. I. Serdobol'skii	413	40, 590
Photoproduction of Pions on Pions	L. D. Solov'ev	418	40, 597
Complete Set of Experiments for Determination of Relations between the Amplitudes for Pion Production by Nucleons in Various Isotopic Spin States	K. S. Marish and L. M. Soroko	423	40, 605
High-Energy Electron-Electron Scattering	V. N. Baĭer and S. A. Kheĭfets	428	40, 613
Electromagnetic Properties of a Relativistic Plasma. II	V. P. Silin	430	40, 616
Relation between the Equations for Partial Amplitudes and for Spectral Functions	Yu. A. Simonov	436	40, 626
Calculation of Some Extensive Air Shower Characteristics with Allowance for Fluctuations	L. G. Dedenko	439	40, 630

(Contents continued on inside back cover)

CONTENTS—continued

Title	Authors	Page	Russian Reference
On the Theory of Fermion Masses	Ya. B. Zel'dovich	444	40, 638
Thermodynamics of Anisotropic Superconductors	V. L. Pokrovskii	447	40, 641
Vortex Lines in an Imperfect Bose Gas	L. P. Pitaevskii	451	40, 646
Antiprotonium Level Shifts for Large Orbital Angular Momenta	A. F. Grashin	455	40, 652
An Investigation of the Properties of Transuranium Elements Based on the Superfluid Model of the Nucleus	V. G. Solov'ev	456	40, 654
Variation of the Adiabatic Invariant of a Particle in a Magnetic Field. II	A. M. Dykhne and A. V. Chaplik	465	40, 666
The Magnetic Properties of Beryllium in the Temperature Range 300 to 4.2°K	B. I. Verkin, I. M. Dmitrenko, and I. V. Svechkarev	468	40, 670
On the Problem of Computing Moments of Inertia of Nuclei	S. T. Belyaev	470	40, 672
Photoproduction of Neutrino-Antineutrino Pairs on Electrons	Wang Jung, J. Fischer, I. Ciulli, and S. Ciulli	473	40, 676
Positions of the Singularities of Certain Feynman Diagrams	V. A. Kolkunov	474	40, 678
Single-Particle Excitations and Superfluidity in Systems Consisting of Fermi Particles with an Arbitrary Interaction. Application to the Nucleus	A. B. Migdal	478	40, 684
Transitions Between Hyperfine Levels in Mesic Deuterium Atoms	S. S. Gershteĭn	488	40, 698

LETTERS TO THE EDITOR

Title	Authors	Page	Russian Reference
Transverse Polarization of Λ Hyperons, Generated by 2.8-Bev/c Pions on Xenon Nuclei	I. A. Ivanovskaya, E. V. Kuznetsov, A. Prokesh, and I. V. Chuvilo	495	40, 708
Circular Polarization of Gamma Quanta in the Reaction B^{10}(d, pγ)B^{11}	J. Zimanyi, J. Erö, L. Pocs, and J. Szentpeteryi	496	40, 709
Causes of Anomalous Broadening of Ferromagnetic Resonance Absorption Line in Ferrites near the Curie Point	K. P. Belov	497	40, 711
Energy Shifts of Gamma Transitions Observed in Resonance Absorption of Gamma Quanta in Crystals	V. A. Bryukhanov, N. N. Delyagin, B. Zvenglinskii, and V. S. Shpinel'	499	40, 713
On the Energy Dependence of the Scattering Cross Section at Small Energies	S. M. Bilen'kii	499	40, 714
Behavior of the Cross Section of Electromagnetic Production of Particles	V. N. Baĭer and S. A. Kheĭfets	500	40, 715